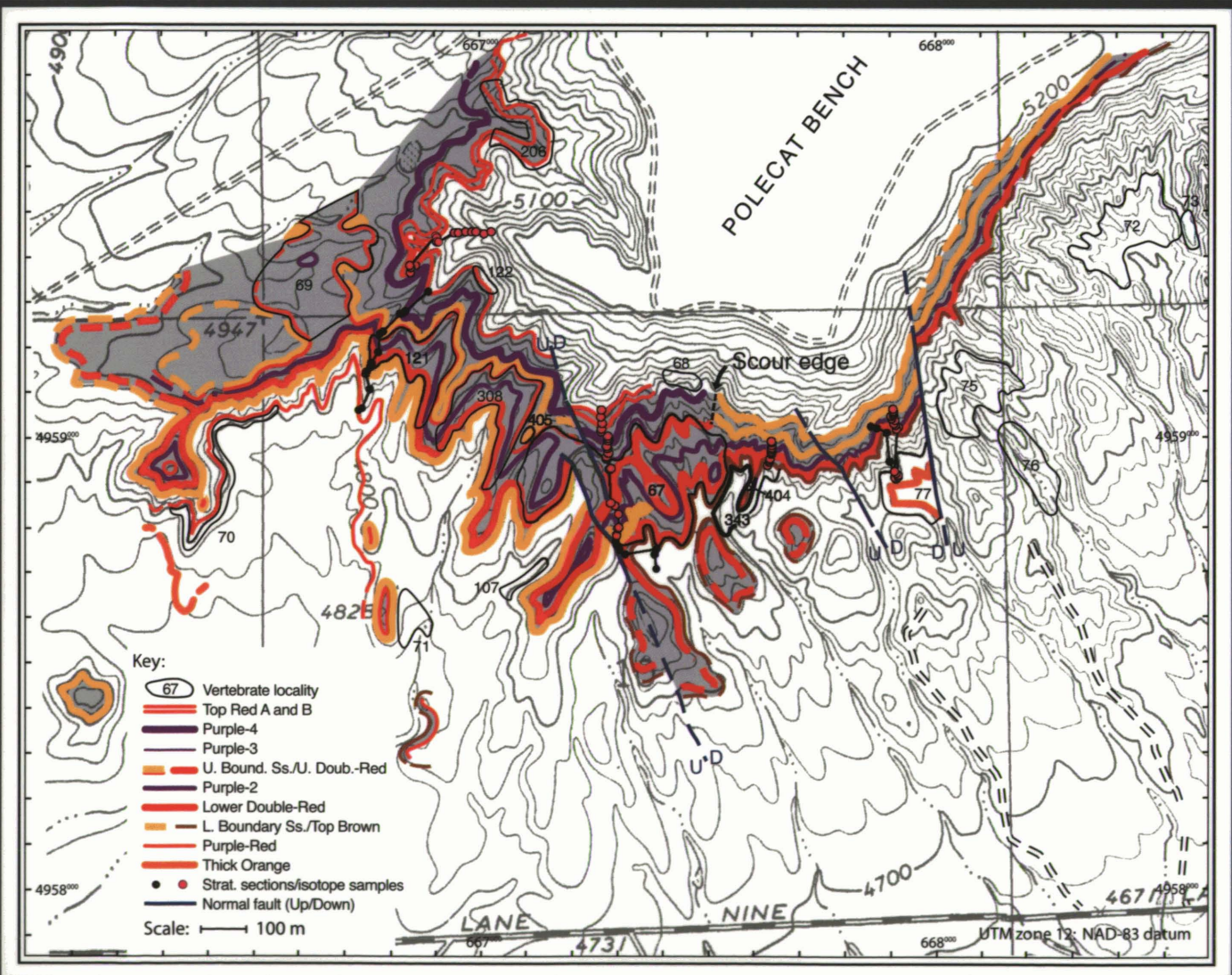


PALEOCENE-EOCENE STRATIGRAPHY AND BIOTIC CHANGE IN THE BIGHORN AND CLARKS FORK BASINS, WYOMING



PAPERS ON PALEONTOLOGY — RECENT NUMBERS

24. Early Cenozoic Paleontology and Stratigraphy of the Bighorn Basin, Wyoming by *Philip D. Gingerich (ed.) and others* (1980)
25. Dimorphic Middle Devonian Paleocopan Ostracoda of the Great Lakes Region by *Robert V. Kesling and Ruth B. Chilman* (1987)
26. The Clarkforkian Land-Mammal Age and Mammalian Faunal Composition across the Paleocene-Eocene Boundary by *Kenneth D. Rose* (1981)
27. The Evolutionary History of Microsypoidea (Mammalia, ?Primates) and the Relationship between Plesiadapiformes and Primates by *Gregg F. Gunnell* (1989)
28. New Earliest Wasatchian Mammalian Fauna from the Eocene of Northwestern Wyoming: Composition and Diversity in a Rarely Sampled High-Floodplain Assemblage by *Philip D. Gingerich* (1989)
29. Evolution of Paleocene and Eocene Phenacodontidae (Mammalia, Condylarthra) by *J. G. M. Thewissen* (1990)
30. Marine Mammals (Cetacea and Sirenia) from the Eocene of Gebel Mokattam and Fayum, Egypt: Stratigraphy, Age, and Paleoenvironments by *Philip D. Gingerich* (1992)
31. Terrestrial Mesonychia to Aquatic Cetacea: Transformation of the Basicranium and Evolution of Hearing in Whales by *Zhexi Lou and Philip D. Gingerich* (1999)
32. Fishes of the Mio-Pliocene Ringold Formation, Washington: Pliocene Capture of the Snake River by the Columbia River by *Gerald R. Smith, Neil Morgan, and Eric Gustafson* (2000)
33. Paleocene-Eocene Stratigraphy and Biotic Change in the Bighorn and Clarks Fork Basins, Wyoming by *Philip D. Gingerich (ed.) and others* (2001)

Museum of Paleontology
The University of Michigan
Ann Arbor, Michigan 48109-1079

**PALEOCENE-EOCENE STRATIGRAPHY AND BIOTIC CHANGE
IN THE BIGHORN AND CLARKS FORK BASINS, WYOMING**



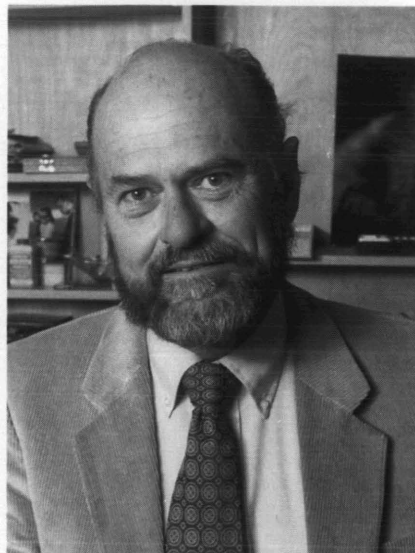
William J. Sinclair



Walter Granger



Glenn L. Jepsen



Elwin L. Simons

Frontispiece: Early expedition leaders who initiated modern studies of biostratigraphy and faunal change focused on Paleocene-Eocene mammals of the Bighorn and Clarks Fork basins. Photographs courtesy of: Archives of the Department of Geosciences, Princeton University (Sinclair and Jepsen); Library of the American Museum of Natural History (Granger); and Duke University Primate Center (Simons).

PALEOCENE-EOCENE STRATIGRAPHY AND BIOTIC CHANGE IN THE BIGHORN AND CLARKS FORK BASINS, WYOMING

A volume summarizing results of ongoing research in the
Bighorn and Clarks Fork basins compiled for
an international conference on

Climate and Biota of the Early Paleogene

held in Powell, Wyoming, July 3-8, 2001

Edited by
PHILIP D. GINGERICH

UNIVERSITY OF MICHIGAN
PAPERS ON PALEONTOLOGY NO. 33

2001

Papers on Paleontology No. 33

Museum of Paleontology
The University of Michigan
Ann Arbor, Michigan 48109-1079

Philip D. Gingerich, Director

Published June 15, 2001

PREFACE

PHILIP D. GINGERICH, EDITOR

The Bighorn and Clarks Fork basins of northwestern Wyoming are world-renowned for their brightly-colored fossil beds yielding mammals and other vertebrates of the Paleocene and early Eocene epochs. The first collections were made by Jacob Wortman in 1880 and 1881 while employed by Edward Drinker Cope of Philadelphia, one of the best known American vertebrate paleontologists of the nineteenth century. Wortman was very successful, and as a result Cope was able to describe many new genera and species based on this collection. William Berryman Scott of Princeton University tried to duplicate Wortman's success in 1884, working with assistants and a military escort, but left with four specimens that fit into a cigar box. Some parts of the Bighorn and Clarks Fork basins are richly fossiliferous, but others are poorly so. And the fossils themselves are, in any case, only part of what makes the basins so important.

The greater importance of the Bighorn and Clarks Fork basins became evident from field studies by William J. Sinclair of Princeton University and Walter Granger of the American Museum of Natural History, from 1910 through 1912. Sinclair and Granger found lots of fossils, but in addition showed that different faunas are represented, and that these can be studied in temporal succession based on superposition of strata in the field. Two of Granger's faunas, the Clarkforkian fauna and the Sandcouleean fauna, named from the Clarks Fork Basin, have long been recognized, respectively, as the land-mammal age preceding and the subage succeeding the Paleocene-Eocene boundary in North America. Glenn L. Jepsen of Princeton University spent a career developing large quarry samples of early, middle, and late Paleocene age on Polecat Bench, on the divide that separates the Bighorn and Clarks Fork basins. Later Elwyn L. Simons of Yale University and Duke University initiated the first field program pioneering collection of Eocene mammals on finer stratigraphic and temporal scales. There are relatively few places in the world where Jepsen's and Simons' research could have been attempted, and when each succeeded they demonstrated further the importance of the Bighorn and Clarks Fork basins for understanding mammalian evolution.

The Bighorn and Clarks Fork basins are important educationally too. Hundreds of undergraduate and graduate students have received field training in paleontology here, and in the process students were largely responsible for making the extraordinary collections we have available for study today. Lessons learned in the Bighorn and Clarks Fork basins have had a wider impact than many realize. In the early days Bighorn Basin collections were exchanged with many museums in Europe. And in 2001 we will remember the late Minchen Chow of China as we scatter his ashes at Princeton Quarry on the northwest side of Polecat Bench. Chow worked at Princeton Quarry as a student in the early 1950s before returning to Beijing to become professor of paleontology. In China he trained many students and was able to develop a similarly extraordinary Paleocene and early Eocene record of mammalian evolution in Asia.

Occasions to showcase Bighorn and Clarks Fork basin field research nationally and internationally come about once every twenty years. The Society of Vertebrate Paleontology sponsored a summer field conference in 1980 to celebrate the centennial anniversary of Jacob Wortman's first trip into the Bighorn Basin in search of fossils (Gingerich, 1980). In 2001 an international group interested in the climate and biota of the Paleocene and Eocene is meeting in Powell in the northern Bighorn Basin. Anticipating the 2001 meeting, this monograph was organized to encourage publication of current reviews and new results on subjects of ongoing research relating to Paleocene-Eocene stratigraphy and biotic change in northwestern Wyoming. Two recent reviews published elsewhere are worthy of note because neither subject is treated in detail here: Hartman and Roth (1998) on Paleocene-Eocene non-marine mollusks, and Wing (1998) on floral and climate change.

What is new here compared to 1980? Computer technology has greatly enhanced our ability to manage large databases, making basin-scale studies feasible. The availability of a standard satellite global positioning system (GPS) facilitates mapping on all scales. Sedimentological research has matured. The first results of paleomagnetic stratigraphy were available in 1980, but these are now much better developed and more informative. Recognition of a distinctive 'Wa-0' land-mammal fauna has enabled close focus on

Paleocene-Eocene change in mammalian evolution. Isotopes of carbon and oxygen now play a crucial role both in global correlation of the Paleocene-Eocene boundary and in studies of climate and climate change. Finally, the mammals that have been the focus of so much research in the Bighorn and Clarks Fork basins are now themselves much better known. Substantial postcranial skeletons enable them to be viewed more clearly as the living animals they once were.

Acknowledgments

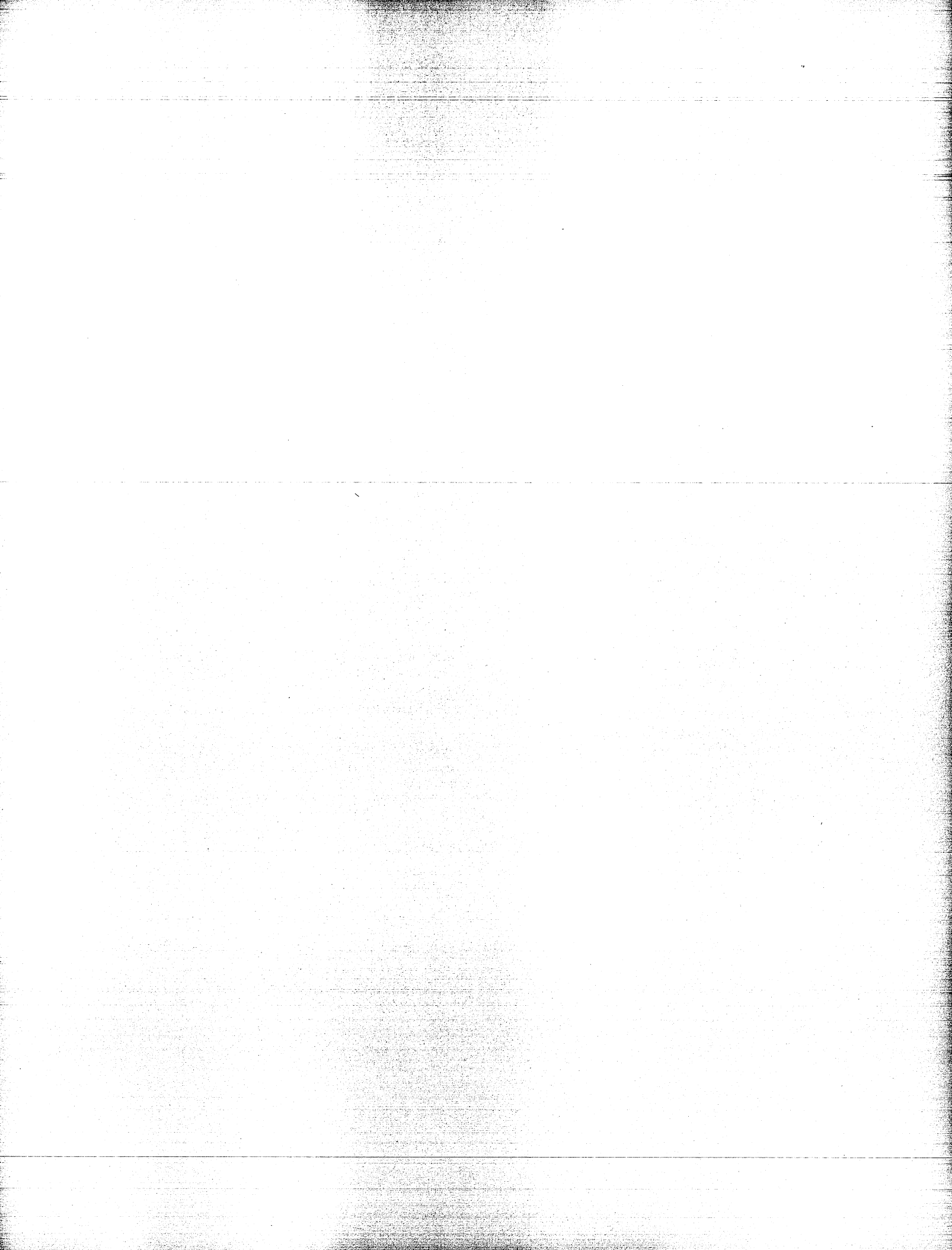
In Ann Arbor, Reynetta Fath was responsible for typesetting, Bonnie Miljour prepared and improved many of the illustrations, and Cindy Stauch helped to ensure timely publication. In Powell, all of us going back to Jepsen are indebted to the Churchill family for a half-century of hospitality and encouragement.

Literature Cited

- GINGERICH, PHILIP D. (ed.). 1980. Early Cenozoic Paleontology and Stratigraphy of the Bighorn Basin, Wyoming 1880-1980. University of Michigan Papers on Paleontology, 24: 1-146.
- HARTMAN, J. H. and B. ROTH. 1998. Late Paleocene and early Eocene nonmarine molluscan faunal change in the Bighorn Basin, northwestern Wyoming and south-central Montana. *In* M.-P. Aubry, S. G. Lucas, and W. A. Berggren (eds.), Late Paleocene-Early Eocene Climatic and Biotic Events in the Marine and Terrestrial Records, Columbia University Press, pp. 323-379.
- WING, S. L. 1998. Late Paleocene-early Eocene floral and climatic change in the Bighorn Basin, Wyoming. *In* M.-P. Aubry, S. G. Lucas, and W. A. Berggren (eds.), Late Paleocene-Early Eocene Climatic and Biotic Events in the Marine and Terrestrial Records, Columbia University Press, New York, pp. 380-400.

TABLE OF CONTENTS

<p>Frontispiece ii</p> <p>Title page iii</p> <p>Preface v</p> <p>Table of Contents vii</p> <p>Overview of Mammalian Biostratigraphy in the Paleocene-Eocene Fort Union and Willwood Formations of the Bighorn and Clarks Fork Basins PHILIP D. GINGERICH and WILLIAM C. CLYDE 1</p> <p>Sedimentology and Depositional Setting of the Willwood Formation in the Bighorn and Clarks Fork Basins MARY J. KRAUS 15</p> <p>Not Just Red Beds: The Occurrence and Formation of Drab Sections in the Willwood Formation of the Bighorn Basin K. SIÂN DAVIES-VOLLUM 29</p> <p>Biostratigraphy of the Continental Paleocene-Eocene Boundary Interval on Polecat Bench in the Northern Bighorn Basin PHILIP D. GINGERICH 37</p> <p>Refined Isotope Stratigraphy Across the Continental Paleocene-Eocene Boundary on Polecat Bench in the Northern Bighorn Basin GABRIEL J. BOWEN, PAUL L. KOCH, PHILIP D. GINGERICH, RICHARD D. NORRIS, SANTO BAINS, and RICHARD M. CORFIELD 73</p>	<p>Pollen Assemblages and Paleocene-Eocene Stratigraphy in the Bighorn and Clarks Fork Basins GUY J. HARRINGTON 89</p> <p>Turtle Diversity and Abundance through the Lower Eocene Willwood Formation of the Southern Bighorn Basin PATRICIA A. HOLROYD, J. HOWARD HUTCHISON, and SUZANNE G. STRAIT 97</p> <p>Mammalian Biostratigraphy of the McCullough Peaks Area in the Northern Bighorn Basin WILLIAM C. CLYDE 109</p> <p>New Wa-0 Mammalian Fauna from Castle Gardens in the Southeastern Bighorn Basin SUZANNE G. STRAIT 127</p> <p>Basin-Margin Vertebrate Faunas on the Western Flank of the Bighorn and Clarks Fork Basins GREGG F. GUNNELL and WILLIAM S. BARTELS 145</p> <p>Compendium of Wasatchian Mammal Postcrania from the Willwood Formation of the Bighorn Basin KENNETH D. ROSE 157</p> <p>Taphonomy of Small Mammals in Freshwater Limestones from the Paleocene of the Clarks Fork Basin JONATHAN I. BLOCH and DOUG M. BOYER 185</p>
---	---



OVERVIEW OF MAMMALIAN BIOSTRATIGRAPHY IN THE PALEOCENE-EOCENE FORT UNION AND WILLWOOD FORMATIONS OF THE BIGHORN AND CLARKS FORK BASINS

PHILIP D. GINGERICH¹ and WILLIAM C. CLYDE²

¹*Department of Geological Sciences and Museum of Paleontology, The University of Michigan,
Ann Arbor, Michigan 48109-1079*

²*Department of Earth Sciences, University of New Hampshire, Durham, New Hampshire 03824-3589*

Abstract. — Some 2200 fossil vertebrate localities are known from the Paleocene Fort Union Formation and from the Paleocene and lower Eocene Willwood Formation of the Bighorn and Clarks Fork basins in northwestern Wyoming. Many localities yield faunas adequate to enable reference to one of the twenty distinct land-mammal zones representing the Puercan, Torrejonian, Tiffanian, Clarkforkian, and Wasatchian land-mammal ages spanning Paleocene and early Eocene time here. These are grouped biostratigraphically and plotted on a map of the two basins combined. Range charts of mammalian genera are compared for (1) the Polecat Bench–Sand Coulee area in the Clarks Fork and northern Bighorn basins, (2) the Foster Gulch–McCullough Peaks area in the northern Bighorn Basin, (3) the central Bighorn Basin, and (4) the southern Bighorn Basin. These show that mammalian biostratigraphy is similar in all four areas, with parts of the stratigraphic record being better developed in some areas than in others. The Paleocene and earliest Eocene are best known from the Clarks Fork Basin and from the northern Bighorn Basin, whereas middle and late early Eocene faunas are principally known from the west side of the northern and central parts of the Bighorn Basin. East-west asymmetry in the distribution of mammalian faunas reflects overthrusting from the west as strata and their contained fossil faunas accumulated and were buried.

INTRODUCTION

The Bighorn and Clarks Fork basins of northwestern Wyoming, drained by the Bighorn and Clarks Fork rivers, respectively (Fig. 1), are distinct parts of a single foreland depositional basin that accumulated continental sedimentary rocks during uplift of the Rocky Mountains. These basins preserve a thick sequence of continental sedimentary rocks representing Paleocene and early Eocene time. Two formations of particular interest, the Fort Union and Willwood formations, together rest conformably or unconformably on marine to continental upper Cretaceous strata. The highest of the Cretaceous strata

belong to the dinosaur-bearing Lance Formation of latest Cretaceous age.

The first formation of interest here, the Fort Union Formation (*Tfu* in Fig. 1), is as much as 1700 m thick in places. It consists of thin-bedded, light-colored fluvial sandstones and conglomerates, with drab to olive-brown shales, carbonaceous shales, and thin beds of lignite and coal. Paleosols are generally hydromorphic and yellow to orange in color. Carbonates are present as thin, laterally-persistent, orange to brown marl or limestone bands. The Fort Union Formation is Paleocene in age and yields a vertebrate fauna dominated by champsosaurs, turtles, crocodylians, and mammals.

The second formation of interest, the Willwood Formation (*Twl* in Fig. 1), can be as much as 1400 m thick. It consists of immature fluvial sandstones and sometimes conglomerates, and conspicuously-varicolored mudstones. Paleosols are highly

In: Paleocene-Eocene Stratigraphy and Biotic Change in the Bighorn and Clarks Fork Basins, Wyoming (P. D. Gingerich, ed.), University of Michigan Papers on Paleontology, 33: 1-14 (2001).

oxidized and often bright orange, red, and purple in color. Carbonates are generally present as dispersed nodules that formed within ancient soils. Carbonaceous shales are relatively rare. The Willwood Formation is predominantly Eocene in age and yields a vertebrate fauna dominated by turtles, crocodylians, and mammals.

The Tatman Formation (*Tta* in Fig. 1) overlying the Fort Union and Willwood formations is a relatively thin lacustrine unit of brown, papery, carbonaceous and calcareous shales interbedded with drab clays and sandstones. Vertebrate fossils are rare, and the Tatman Formation is mentioned here because it covers a substantial area of Willwood Formation along the southwestern margin of the Bighorn Basin. The Tatman Formation is considered early-to-middle Eocene in age.

The Fort Union and Willwood formations together provide evidence of a single major Laramide orogenic cycle. During this cycle there was a subtle change in the balance between basin subsidence and sediment accumulation. Initially, during deposition of the Fort Union Formation, subsidence exceeded accumulation, the water table was generally at or above the land surface, the environment was largely forested and wet, and great masses of vegetation were buried. Later, during deposition of the Willwood Formation, accumulation exceeded subsidence, the land surface was generally higher than the water table, the environment was more open and dryer, and much less organic material was buried.

Cycles are present on finer scales as well. There is always a tectonically-controlled 'alloycyclic' component causing some parts of a basin to subside faster, and hence accumulate sediment faster, than others. The axis, for example, generally subsides faster than a basin margin, and hiatuses in sediment accumulation are more likely to be found on basin margins. There is also a more stochastic 'autocyclic' component that controls architecture on a finer scale (documented in the Fort Union by Gingerich, 1969, and in the Willwood by Neasham and Vondra, 1972, and Bown, 1979). Sediment accumulation in an orogenic setting like the Bighorn and Clarks Fork basins often involves a geometry of bounded wedges and fans rather than simple parallel layering.

The Fort Union and Willwood formations of the Bighorn and Clarks Fork basins have long been known for their mammalian fossils, which are relatively common in thick sequences of superposed strata that can be traced and examined in badland outcrops extending for kilometers with little interruption. These fossils are interesting because they enable evolutionary lineages to be traced through time in unusual detail, and they document episodes of biotic change, sometimes abrupt, that appear to require explanation in terms of broader environmental change. Mammals are particularly useful for evolutionary studies, for study of biotic and environmental change, and for constraining depositional history. This is because mammals evolved rapidly, their teeth and bones preserve well in the fossil record and are informative about the

mammals they represent, and mammalian fossils generally have been more intensively studied than other fossil remains.

Study of mammalian fossils in stratigraphic context means that episodes of faunal change affecting mammals can be related directly to change in other vertebrates, invertebrates, and plants preserved in the same strata. Change affecting mammals can also be related directly to environmental proxies such as stable isotopes of carbon and oxygen. Further, change affecting any of these systems can be constrained in time by interpolation between paleomagnetic polarity reversal events recorded in the strata themselves. In some cases, as at the Paleocene-Eocene boundary where artiodactyls, perissodactyls, and modern primates first appear, faunal change can now be explained in terms of oceanic and atmospheric events altering climate and favoring biogeographic dispersal (see, e.g., Bowen et al., this volume). Finally, it is worth mentioning that the geographic and stratigraphic distribution of faunas in the Bighorn and Clarks Fork basins is the principal evidence we have for interpreting the depositional history and hence the timing of tectonic deformation during development of the combined basins.

The purpose of this contribution is to provide an overview of the geographic distribution of some 2200 known Bighorn and Clarks Fork basin fossil mammal localities (Fig. 1), and to provide an overview of the stratigraphic distribution of mammalian faunas of different ages (Figs. 2-5).

DEVELOPMENT OF A MAMMALIAN BIOSTRATIGRAPHY

The Western Interior basins of North America are rich in late Mesozoic (latest Cretaceous) and early Cenozoic (Paleocene and Eocene) vertebrate fossils. The animals that these fossils represent lived, died, and were buried during the Laramide Orogeny, when the Rocky Mountains were uplifted and thick wedges of fresh sediment accumulated in intervening depositional basins. Explorers in the middle nineteenth century (principally F. V. Hayden) recognized a Laramie formation or series of strata thought to be late Cretaceous in age, a Wasatch Formation thought to be early Eocene, an intermediate Wind River Formation, and a higher Bridger Formation thought to be middle Eocene. There was at the time no intervening Paleocene epoch.

Wortman, Fisher, and Loomis

The first search for vertebrate fossils in the Bighorn Basin was carried out by J. L. Wortman in 1880 and 1881, who was employed privately by E. D. Cope. Wortman entered the Bighorn Basin from the south, from Fort Washakie in the Wind River Basin, and found it to yield abundant fossil mammals. The fossils were described by Cope (1880, 1882). These were found in 'Wasatch beds' characterized by the preponderance of red clay and containing 'small limestone nodules of a rusty

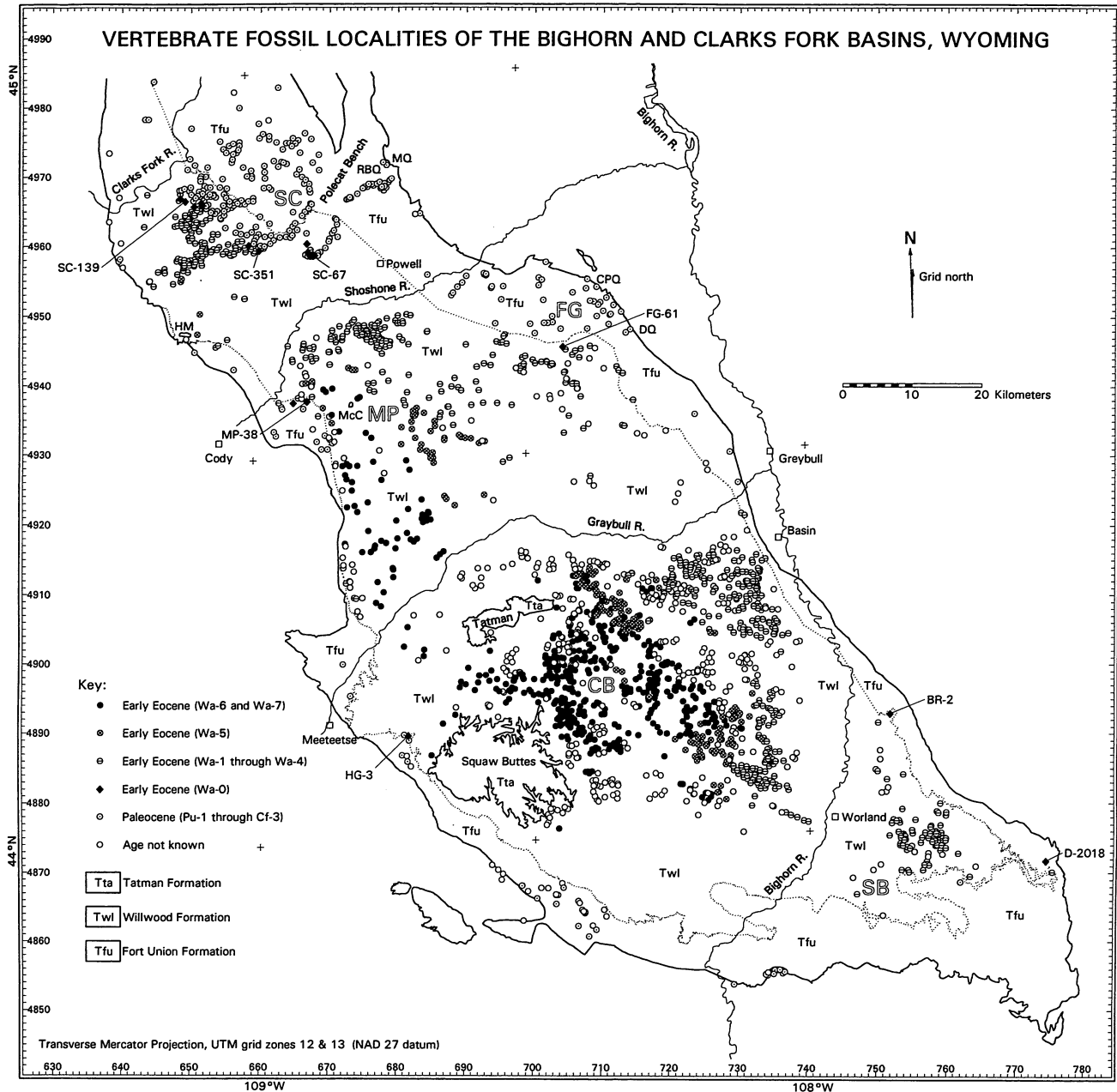


FIGURE 1 — Map of the Bighorn and Clarks Fork basins in northwestern Wyoming showing the distribution of 2224 Paleocene and lower Eocene vertebrate fossil localities in relation to principal rivers and geological formations. Four regions discussed separately here are: (1) the Polecat Bench–Sand Coulee (SC) area in the Clarks Fork and northern Bighorn basins, north of the Shoshone River; (2) the Foster Gulch (FG)–McCullough Peaks (MP) area in the northern Bighorn Basin south of the Shoshone River and north of the Graybull River; (3) the central Bighorn Basin (CB) south of the Graybull River and north and west of the Bighorn River; and (4) the southern Bighorn Basin (SB) east of the Bighorn River. Heart Mountain (HM) and McCullough Peaks (McC) are peaks supported by allochthonous detached blocks of Paleozoic limestone that reached their present positions on top of the Willwood Formation by gravity-sliding. Fossil localities are from Bown (1979), Rose (1981), Gingerich and Klitz (1985), Hartman (1986), Leite (1992), and Bown et al. (1994a), Clyde (1997, this volume), Strait (this volume). Geology is from Love et al. (1978a,b, 1979) and Pierce (1997).

brown appearance' (Wortman, 1882). The perissodactyl *Lambdaotherium* was not found in the Bighorn Basin, and this absence was considered an important distinction from the fauna of the Wind River Formation.

A second field investigation of the Bighorn Basin was carried out by Wortman in 1891, now working for the American Museum of Natural History. This time Wortman entered the Bighorn Basin from the north, from the then-new railhead at Red Lodge. He traversed the Clarks Fork Basin, where he was the first to establish the presence of Wasatchian mammals, and followed the old Bridger Trail on his way to Wasatch exposures south of the Graybull River. The new fossils were described by Osborn (1892) and by Wortman (e.g., 1896). Wortman (1892) concluded: (1) that Puerco and Laramie strata (Paleocene and latest Cretaceous) are absent and do not underlie the Bighorn Wasatch, which lies on older Mesozoic rocks; and (2) that Wind River beds in the Wind River Basin are distinct from those of the Bighorn Wasatch, and were deposited in a later-filling lake.

A third phase of field work in the Bighorn and Clarks Fork basins started in 1904 when C. A. Fisher of the U. S. Geological Survey and F. B. Loomis of Amherst College initiated independent investigations. Fisher's work was carried out in connection with construction of the Buffalo Bill Dam on the Shoshone River and development of the then new Shoshone Irrigation District. Fisher (1906) mapped what we today call Paleocene strata as part of his Cretaceous 'Laramie and succeeding formations' (p. 31), representing 'possibly in its upper portions the Fort Union beds' (p. 32). Absence of distinctive fossils was cited as a cause for some uncertainty about age. Fisher mapped extensive deposits of 'Wasatch Formation' that were already well known to be Wasatch or early Eocene in age. Both Fisher and Loomis concluded that the Wasatch deposits of the Bighorn Basin were fluvial because of: (1) association with erosional truncation of underlying formations around the basin margin (Fisher, 1906, p. 42); (2) the dominance of terrestrial rather than aquatic vertebrates found in them (Loomis, 1907, p. 358); and (3) an abundance of lenticular bedforms, poor sorting, and red color indicating subareal oxidation (Loomis, 1907, p. 361).

Loomis (1907) published the first detailed stratigraphic section of Wasatch deposits in the Bighorn Basin, starting from the Owl Creek Mountains near Meeteetse in the west and carrying the section northward and eastward through the Buffalo Basin area to reach the top of Tatman Mountain, covering a distance of some 27 km. He worked from a camp near the head of Fifteen Mile Creek, possibly in or near Hole-in-the-Ground (e.g., HG-3 on the map in Fig. 1), which was presumably on or near his line of section. Loomis found that the mammalian fauna in the Buffalo Basin area lacked the perissodactyl *Homogalax* ('*Systemodon*') characteristic of the Wasatch fauna, but included the perissodactyls *Heptodon* and *Lambdaotherium* characteristic of the Wind River fauna. Thus he concluded that both faunas, Wasatch and Wind River, are present, one above the other, in the Bighorn Basin.

Sinclair and Granger

The reports on the Bighorn Basin by Fisher and Loomis inspired three extended collecting trips in 1910-1912 led by W. J. Sinclair of Princeton University and W. Granger of the American Museum of Natural History. There was also a followup trip in 1913 when neither leader was present. Sinclair and Granger's first field work focused on Loomis' results, and then took advantage of Fisher's geological map to trace beds of interest around the margin of the Bighorn Basin. In their first report, Sinclair and Granger (1911) subdivided the Bighorn 'Wasatch' into three faunal intervals (numbered 1, 2, and 3), and specified that the *Lambdaotherium* beds of the Bighorn 'Wind River' formation might include both faunal intervals represented in the Wind River Basin (named Lysite and Lost Cabin, respectively; the latter, with *Lambdaotherium*, was known to be present).

After their second season of field work, Sinclair and Granger (1912) changed the name of the 'Wasatch' beds in the Bighorn Basin to 'Knight' formation, and described a new 'Ralston' fauna from the top of the Fort Union Formation. They confirmed the presence of a distinct Lysite fauna with *Heptodon* but lacking *Homogalax* ('*Systemodon*') and *Lambdaotherium*, and they proposed a new Tatman Formation younger than the Bighorn 'Wind River' formations.

Granger (1914) revised stratigraphic nomenclature still further. 'Ralston' was found to have been used elsewhere, and Granger proposed calling these Clark Fork beds, with the Clark Fork fauna being characterized by the predominance of phenacodontid condylarths and an absence of perissodactyls, artiodactyls, rodents, and primates (rodents were later found in these beds). Discovery of *Heptodon* in the type area of the Knight Formation in southwestern Wyoming required that a new name be given to the Bighorn 'Knight' beds, and Granger proposed that these be called Gray Bull beds. Lower, middle, and upper Gray Bull thus replaced Knight faunas 1, 2, and 3. Finally, the name Sand Coulee beds was proposed for an interval of red-banded shales above the Clark Fork beds and below the Gray Bull beds that yield the perissodactyl *Hyracotherium* ('*Eohippus*') but lack *Homogalax* ('*Systemodon*'). Granger (1914, p. 207) assigned the Clark Fork beds to the Paleocene, and Sand Coulee and higher beds to the Eocene. (The earliest references we can find using *Paleocene* for the 'basal Eocene' of Osborn (1910) and others are by Sinclair (1912) and Scott (1913).)

Thus at the end of their effort, Sinclair and Granger recognized the following sequence of mammalian faunas and 'formations' in the Bighorn Basin: (1) a Clark Fork fauna, faunal zone, and 'formation,' lacking perissodactyls, and 'perhaps representing the top of the Paleocene Series' (Granger, 1914, p. 204); (2) a Sand Coulee fauna, faunal zone, and 'formation,' with *Hyracotherium* ('*Eohippus*') but lacking *Homogalax* ('*Systemodon*'), representing the lowest interval

in the lower Eocene; (3) lower, middle, and upper faunas from the Gray Bull faunal zone and 'formation,' with both *Hyracotherium* ('*Eohippus*') and *Homogalax* ('*Systemodon*'); (4) a Lysite fauna, faunal zone, and 'formation,' with *Hyracotherium* ('*Eohippus*') and *Heptodon*, but lacking *Homogalax* ('*Systemodon*') and *Lambdaotherium*; (5) a Lost Cabin fauna, faunal zone, and 'formation,' with *Hyracotherium* ('*Eohippus*'), *Heptodon*, and *Lambdaotherium*, but again lacking *Homogalax* ('*Systemodon*'); and finally (6) a Tatman 'formation' with scraps of bone and with invertebrates suggesting a Bridger middle Eocene age. Sinclair and Granger recognized a sequence of Clark Fork, Sand Coulee, and Graybull faunas, with no Lysite or Lost Cabin fauna, in the Clarks Fork Basin; while all five mammalian faunas were thought to be present in the Bighorn Basin when the northern and central parts are considered together.

Sinclair and Jepsen

W. J. Sinclair of Princeton University started field work in Gray Bull beds of the central Bighorn Basin again in 1927, accompanied this time by graduate student G. L. Jepsen. A new Paleocene fauna had just been discovered from the Fort Union Formation of Bear Creek in southern Montana (Simpson, 1928, 1929a,b), and it is not surprising that in 1928 Jepsen moved northward from the central Bighorn Basin toward Bear Creek and started to investigate the Fort Union Formation on Polecat Bench. There he found the primate *Plesiadapis* and pantodont *Titanoides*, both characteristic of Paleocene faunas.

Jepsen returned to the Bighorn and Clarks Fork basins in 1929, when he found: (1) the type specimen of *Plesiadapis cookei*, which became an important index fossil for the Clarkforkian land-mammal age (latest Paleocene); (2) Princeton Quarry of Tiffanian age (late Paleocene); (3) Rock Bench Quarry of Torrejonian age (middle Paleocene); and (4) Mantua Quarry of Puercan age (early Paleocene)— all in one superposed Polecat Bench–Sand Coulee sequence of strata (Jepsen, 1930, 1940; Gingerich, this volume). Jepsen was a member of the Wood committee on nomenclature and correlation of North American faunas (Wood et al., 1941), and Puercan, Torrejonian, Tiffanian, Clarkforkian, and Wasatchian are the names given to North American provincial land-mammal ages (see Archibald et al., 1987, and Krishtalka et al., 1987, for updates).

Jepsen carried on research in the Bighorn and Clarks Fork basins virtually every year from 1930 until he died in 1974. Many students were trained in the process, and Princeton collections formed the backbone of theses on Paleocene and early Eocene mammals published by Van Houten (1944, 1945), Simons (1960), Wood (1967), Gingerich (1975, 1976b), Rose (1975, 1981), Krause (1980, 1982), Gunnell (1989), and Thewissen (1990).

The Van Houten (1944) paper deserves special mention because this is where the 'Bighorn Wasatch' of earlier authors was described in detail, and the name 'Wasatch' here replaced

by Willwood Formation. Willwood is a small agricultural settlement at the northern edge of the McCullough Peaks badlands in the northern Bighorn Basin, making this de facto the type area of the formation.

Simons, Radinsky, and Ongoing Investigations

E. L. Simons and L. Radinsky of Yale University initiated the present phase of detailed mammalian biostratigraphy in the Bighorn and Clarks Fork basins. The two worked together in Wyoming for Jepsen and Princeton University in 1960, and then initiated the first of a long series of Yale University expeditions to the central Bighorn Basin in 1961. These were carried forward by Simons. The objectives initially were clarification of the temporal successions of Wasatchian species of *Coryphodon* as an extension of Simons' dissertation research on pantodonts, and the temporal succession of the tapiroids *Homogalax* and *Heptodon*, as part of Radinsky's dissertation. Radinsky measured a stratigraphic section documenting a 15 m zone of overlap of *Homogalax* and *Heptodon* (Radinsky, 1963, p. 77) at the base of the Lysitean. Extension of the Radinsky stratigraphic section by G. E. Meyer formed the basis for later evolutionary analyses of *Hyopsodus*, *Cantius* ('*Pelycodus*'), and *Haplomytus* (Gingerich, 1974, 1976a; Gingerich and Simons, 1977).

During the 1960s two other stratigraphic projects were active in the Willwood Formation of the central Bighorn Basin. The first, by Rohrer and Gazin on the Willwood Formation of Tatman Mountain, led to publication of two geological maps (Rohrer (1964a,b) and a brief text (Rohrer and Gazin, 1965). The second, by Neasham and Vondra (1971), is important in demonstrating that red beds in the Willwood Formation are due to soil formation on the higher and better drained parts of alluvial floodplains.

The Bighorn and Clarks Fork basins have been sites of active paleontological investigation from the 1970s to the present, with many of the investigators being students of Simons (or now second- and third-generation students of Simons). Notable theses and publications contributing to our understanding of mammalian biostratigraphy include Gingerich (1975, 1976b, 1982, 1983, 1989, 1991, 2000, this volume), Bown (1979), Schankler (1980, 1981), Rose (1981), Winkler (1983), Hartman (1986), Badgley and Gingerich (1988), Badgley (1990), Leite (1992), Bown et al. (1994a), Gunnell (1998), Clyde (this volume), and Strait (this volume). Results are summarized in the following charts (Figs. 2-5), where Tiffanian land-mammal age zones are abbreviated Ti-1 through Ti-6, Clarkforkian zones are abbreviated Cf-1 through Cf-3, and Wasatchian zones are abbreviated Wa-0 through Wa-7 (following Gingerich, 1983, 1989, 1991, and this volume). In the Wasatchian, Wa-0 through Wa-2 correspond to Granger's Sandcouleean subage, Wa-3 through Wa-5 correspond to Granger's Graybullian subage, Wa-6 is equivalent to Sinclair and Granger's Lysitean subage, and Wa-7 is equivalent to Sinclair and Granger's Lostcabinian subage.

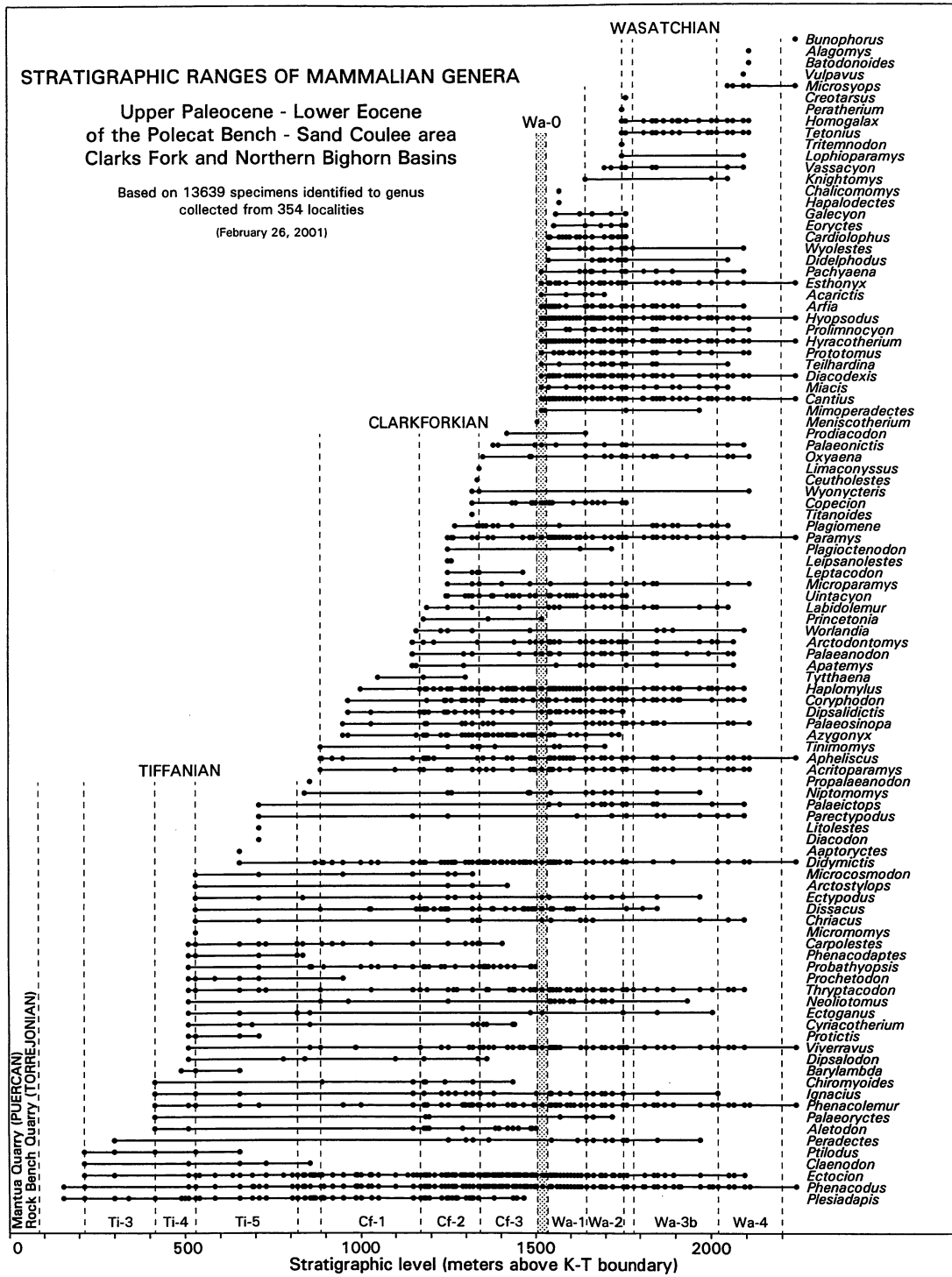


FIGURE 2 — Stratigraphic ranges of late Paleocene and early Eocene mammalian genera in the Polecat Bench–Sand Coulee area of the Clarks Fork and northern Bighorn basins. Dashed lines separate zones of the Tiffanian, Clarkforkian, and Wasatchian land-mammal ages (labeled Ti-3, etc., at the bottom of the chart). Stippled column is Wa-0. Chart is based on a University of Michigan database of stratigraphic occurrences maintained by the senior author.

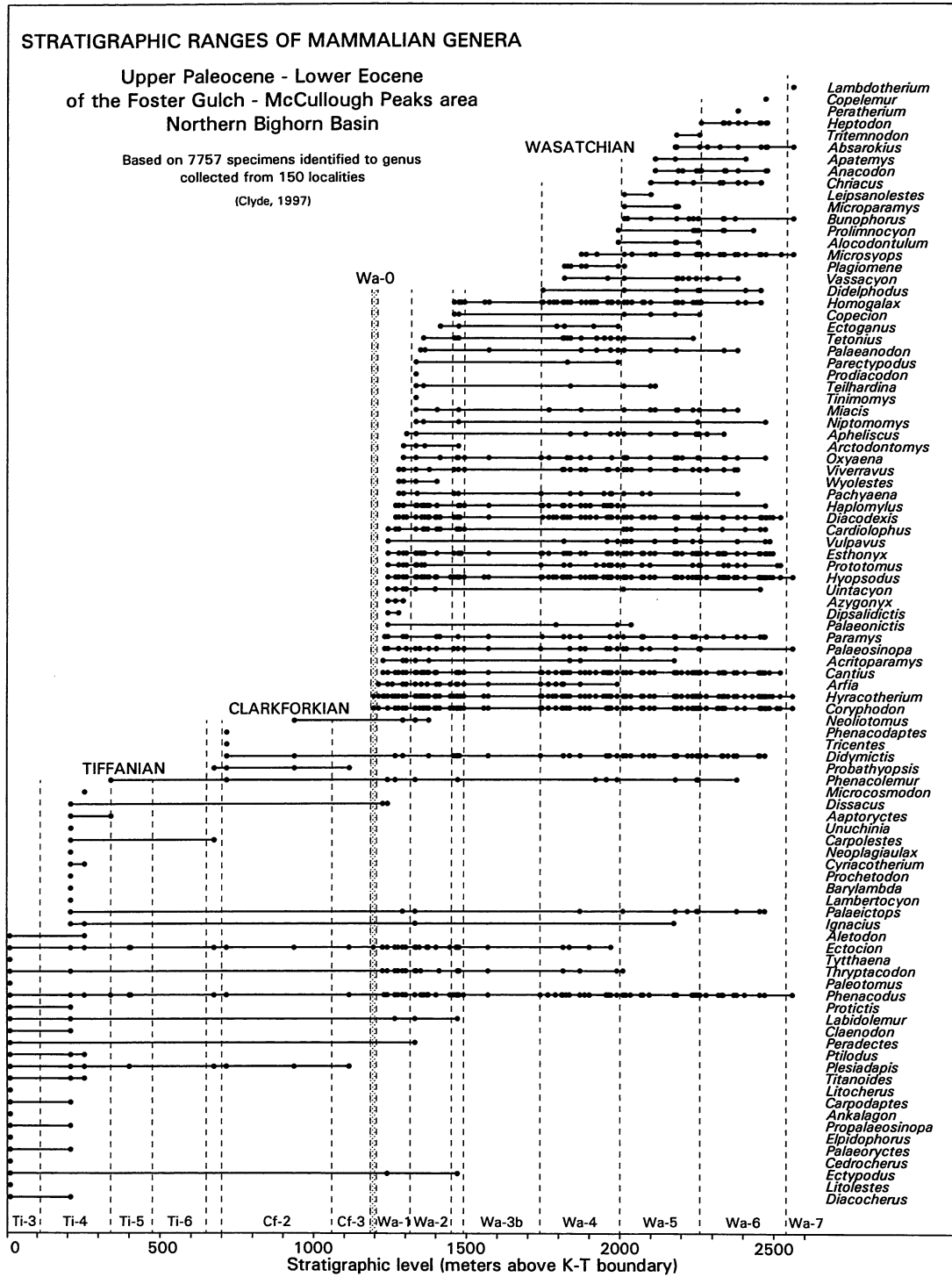


FIGURE 3 — Stratigraphic ranges of late Paleocene and early Eocene mammalian genera in the Foster Gulch–McCullough Peaks area of the northern Bighorn Basin. Dashed lines separate zones of the Tiffanian, Clarkforkian, and Wasatchian land-mammal ages (labeled Ti-3, etc., at the bottom of the chart). Stippled column is Wa-0. Chart is based on the Southeast McCullough Peaks composite stratigraphic section of Clyde (1997, this volume), fossil identifications of Clyde (1997), and the University of Michigan database of stratigraphic occurrences maintained by the senior author.

STRATIGRAPHIC DISTRIBUTION OF PALEOCENE– EOCENE MAMMALS

The combined Clarks Fork and Bighorn basins can be divided into four geographical regions: (1) the Polecat Bench–Sand Coulee area in the Clarks Fork and northern Bighorn Basin north of the Shoshone River (*SC* in Fig. 1); (2) the Foster Gulch–McCullough Peaks area in the northern Bighorn Basin south of the Shoshone River and north of the Graybull River (*FG* and *MP* in Fig. 1); (3) the entire central Bighorn Basin south of the Graybull River and north of the Bighorn River (*CB* in Fig. 1); and (4) the southern Bighorn Basin south and east of the Bighorn River (*SB* in Fig. 1). Each of these regions has yielded an important sequence of mammalian faunas, which are discussed in turn.

Polecat Bench–Sand Coulee Area

The most complete sequence of mammal-bearing Paleocene strata is on Polecat Bench, starting with the Mantua and Rock Bench quarries (Puercan and Torrejonian, respectively; *MQ* and *RBQ* in Fig. 1) discovered and described by Jepsen (1930, 1940). Both are in the lower 60 m of the Fort Union Formation on Polecat Bench (Gingerich, this volume). The remainder of the Polecat Bench–Sand Coulee stratigraphic section, from 150 m to 2240 m, yields Tiffanian to Clarkforkian faunas from the Fort Union Formation, and Clarkforkian to middle Wasatchian faunas from the Fort Union and Willwood formations (the formational boundary here is lower than the Clarkforkian–Wasatchian boundary). A range chart of Tiffanian, Clarkforkian, and Wasatchian genera is shown in Figure 2, based on the University of Michigan database of stratigraphic occurrences maintained by the senior author.

The Tiffanian land-mammal age starts with the appearance of *Plesiadapis* and *Phenacodus*. Tiffanian zones Ti-3 through Ti-6 are well represented in the Polecat Bench–Sand Coulee section, with each being recognized by the presence of distinctive species of *Plesiadapis* (Gingerich, 1975, 1976b, this volume). A new study of all Tiffanian localities in the Clarks Fork and northern Bighorn basins is underway (Secord, in prep.), and a clearer understanding of faunal change through the Tiffanian, and from the late Tiffanian into the early Clarkforkian, will soon be forthcoming.

The Clarkforkian land-mammal age starts with appearance of the first Rodentia (here *Acritoparamys*), which are presently known from as low as the 885 m level. *Apheliscus*, *Azygonyx*, *Coryphodon*, and *Haplomyilus* appear at or near the beginning of the Clarkforkian as well. Clarkforkian zones Cf-1 through Cf-3 correspond to the early, middle, and late Clarkforkian of Rose (1981; see also Gingerich, this volume), with the first two again being characterized by the presence of distinctive species of *Plesiadapis*.

The Wasatchian land-mammal age starts with the first appearance of Perissodactyla (here *Hyracotherium* in zone Wa-0; Granger, 1914; Gingerich, 1989, this volume).

Diacodexis representing Artiodactyla, *Cantius* and *Teilhardina* representing Primates, and *Prototomus* and *Prolimnocyon* representing hyaenodontid Creodonta appear at this time as well. Wasatchian zones Wa-0, Wa-1, and Wa-2 with *Hyracotherium* correspond to the Sandcouleean subage of Granger (1914); while zones Wa-3, Wa-4, and Wa-5 with *Homogalax* correspond to the Graybullian subage of Granger (1914). Wasatchian zones Wa-6 and Wa-7 are missing at the top of the Polecat Bench–Sand Coulee section in the Clarks Fork and northern Bighorn basins.

Foster Gulch–McCullough Peaks Area

The Foster Gulch–McCullough Peaks stratigraphic section is different from the Polecat Bench–Sand Coulee section because 34 km southeast of Mantua Quarry there is no Puercan, Torrejonian, or early Tiffanian at the base of the Fort Union section. Instead zone Ti-3, represented by Cedar Point Quarry 10 m above the base (*CPQ* in Fig. 1), rests disconformably on the upper Cretaceous Lance Formation. Ten km farther to the southeast zone Ti-4, represented by Divide Quarry a few meters above the base (at the 210 m level; *DQ* in Fig. 1), rests disconformably on the Lance Formation. Some 300 m of stratigraphic thickness and about 6 m.y. of geological time have been lost in moving 34 km along strike from Mantua Quarry to Cedar Point Quarry. An additional ca. 200 m of stratigraphic thickness and as much as 1 m.y. more of geological time have been lost in moving the additional 7 km southeast from Cedar Point to Divide Quarry. The Fort Union Formation clearly laps unconformably onto the Lance Formation along the eastern margin of the Bighorn Basin (Gingerich, 1983), showing how an uplifted basin margin bounded Fort Union fans during deposition.

The remainder of the Foster Gulch–McCullough Peaks stratigraphic section, from 210 m to 2560 m, yields Tiffanian and Clarkforkian faunas from the Fort Union Formation, and early-to-late Wasatchian faunas from the Willwood Formation (the formational boundary here coincides with the Clarkforkian–Wasatchian boundary). A range chart of genera is shown in Figure 3, based on the Southeast McCullough Peaks composite stratigraphic section of Clyde (1997, this volume), fossil identifications by Clyde (1997), and the University of Michigan database of stratigraphic occurrences maintained by the senior author.

The lowest zone of the Tiffanian land-mammal age is Ti-3, represented by Cedar Point Quarry, as mentioned above. Cedar Point Quarry has yielded a large mammalian fauna (summarized in Rose, 1981, with additions in Fig. 3 based on later publications). Similarly, Ti-4, represented by Divide Quarry, has yielded a large mammalian fauna (under study by R. Secord). The highest Tiffanian fauna here comes from the 405 m level. There are not as many Tiffanian localities or collecting levels in the McCullough Peaks area, nor is the Ti-3 through Ti-6 thickness as great (ca. 400–500 m vs. ca. 800 m), but the

Tiffanian in the McCullough Peaks area has yielded about the same number of genera as that in the Polecat Bench–Sand Coulee section.

The Clarkforkian land-mammal age starts at the 675 m level in the McCullough Peaks area and continues up to the 1115 m level, which is the highest level yielding *Plesiadapis* here. The Clarkforkian here is about the same thickness (ca. 500–600 m) as it is in the Polecat Bench–Sand Coulee section, but there are many fewer collecting levels and many fewer genera known. The difference is probably due to a difference in depositional environment, directly or indirectly, as there are many fewer sandstones and consequently relatively poor and less productive exposures.

The Wasatchian land-mammal age starts at the 1195 m level and continues to the 2560 m level. Wa-0 is represented by one locality at 1195 m that yields *Hyracotherium sandrae* and *Ectocion parvus* characteristic of the zone. *Homogalax protapirinus* marking the beginning of zone Wa-3 and the beginning of the Graybullian subage comes in at 1455 m, *Bunophorus etsagicus* marking the beginning of zone Wa-5 comes in at 2010 m, *Heptodon calciculus* marking the beginning of zone Wa-6 and the Lysitean subage comes in at 2260 m, and *Lambdaotherium popoagicum* marking the beginning of Wa-7 and the Lostcabinian subage is known from one level at 2560 m above the base of the Foster Gulch–McCullough Peaks section. The Sandcouleean subage here (Wa-0 through Wa-2) is ca. 260 m thick, while the early and middle Gray-bullian subage (Wa-3 through Wa-4) is ca. 555 m thick. These thicknesses are about 25% greater than thicknesses for the same intervals in the Polecat Bench–Sand Coulee section (ca. 210 m and 450 m, respectively).

Central Bighorn Basin

The central Bighorn Basin has Torrejonian, Tiffanian, and Clarkforkian mammal localities, but these are all on the west side of the basin (Leite, 1992; Gingerich, unpublished), separated from late Wasatchian strata by a major unconformity (and in places a distinctly angular unconformity; e.g., Van Houten, 1944, pl. 3, fig. 1). The major stratigraphic sections incorporating mammals all start at the base of the Willwood Formation on the east side of the basin (e.g., those of Meyer and Radinsky, unpublished; Schankler and Wing in Schankler, 1980; and Bown et al., 1994a). There is a narrow band of strata mapped as Fort Union Formation here, but there is no mammalian control on age. The Willwood Formation covers a large area in the central Bighorn Basin and has yielded more than 100,000 fossil mammal specimens from about 1,500 localities (Bown et al., 1994a). The principal analysis of central Bighorn Basin faunas is by Schankler, who published a summary of his results in 1980. A range chart of Wasatchian genera is shown in Figure 4, based on information digitized from Schankler's range charts (Schankler, 1980; reanalyzed too by Bown and Kraus, 1993; see also Bown et al., 1994b).

There are ambiguities in interpretation of Schankler's ranges because he did not publish any systematic descriptions connecting his identifications of taxa to specimens in the Yale University collection. Bown and Kraus (1993) and Bown et al. (1994a) have revised the thicknesses of some of Schankler's zones, and Schankler's biozonation is different in some respects from that advocated by Granger (1914). Nevertheless, Schankler's central Bighorn Basin ranges of mammalian genera (Fig. 4) can be compared with those from the Polecat Bench–Sand Coulee and Foster Gulch–McCullough Peaks areas outlined here (Figs. 2 and 3).

There are almost certainly Wasatchian mammals of the Sandcouleean subage from Wa-1 and/or Wa-2 present in the lower 100 m of the central Bighorn Basin stratigraphic section, but these have not been described carefully enough to enable Wa-1 and Wa-2 to be distinguished. The beginning of zone Wa-3 and the beginning of the Graybullian subage are normally marked by the first appearance of the perissodactyl genus *Homogalax*, a genus missing from Schankler's chart. Stanley (1982) published a revised version of Schankler's chart that shows *Homogalax* originating at the 130 m level. Initiation of Wa-3 at this level appears reasonable in comparison to the Polecat Bench–Sand Coulee and Foster Gulch–McCullough Peaks faunal records, but the resulting thickness of Sandcouleean strata (ca. 130 m) is about one-half that in the Foster Gulch–McCullough Peaks area to the north, and the thickness of early and middle Graybullian strata here (ca. 400 m) is also less.

Continuing up-section, the first appearance of *Bunophorus* marks the beginning of zone Wa-5 in the late part of the Graybullian subage. The first appearance of *Heptodon* indicates the beginning of zone Wa-6 and the Lysitean subage. Finally, the first appearance of *Lambdaotherium* marks the beginning of zone Wa-7 and the beginning of the Lostcabinian subage.

The meaning of Schankler's 'Biohorizon A' at the 200 m level in his central Bighorn Basin section has long been confusing (Badgley and Gingerich, 1988; Badgley, 1990). The clearest evidence on this is given not by Schankler (1980) but by Schankler (1981), who places 'Biohorizon A' at the time of disappearance of *Copecion* ('*Phenacodus*') *brachypternus*. This happens between zones Wa-3a and Wa-3b in the Polecat Bench–Sand Coulee section and in the Foster Gulch–McCullough Peaks section. *Copecion brachypternus* then reappears in Wa-5. Thus 'Biohorizon A' is evidently the faunal turnover separating Wa-3a from Wa-3b. The boundary between Wa-3b and Wa-4 coincides with the well-marked species-level replacement of *Hyracotherium aemulor* by *H. pernix*, noted by Froehlich (1996, p. 414) as being between the 250 and 300 m levels in the Schankler-Wing and Bown et al. sections in the central Bighorn Basin.

Schankler's zonation of the Wasatchian involves a *Haplomylus-Ectocion* range zone, a *Bunophorus* interval zone, and a *Heptodon* range zone. It is different from the zonation advocated by Granger (1914), involving a Sandcouleean subage, a Graybullian subage, a Lysitean subage, and a Lostcabinian

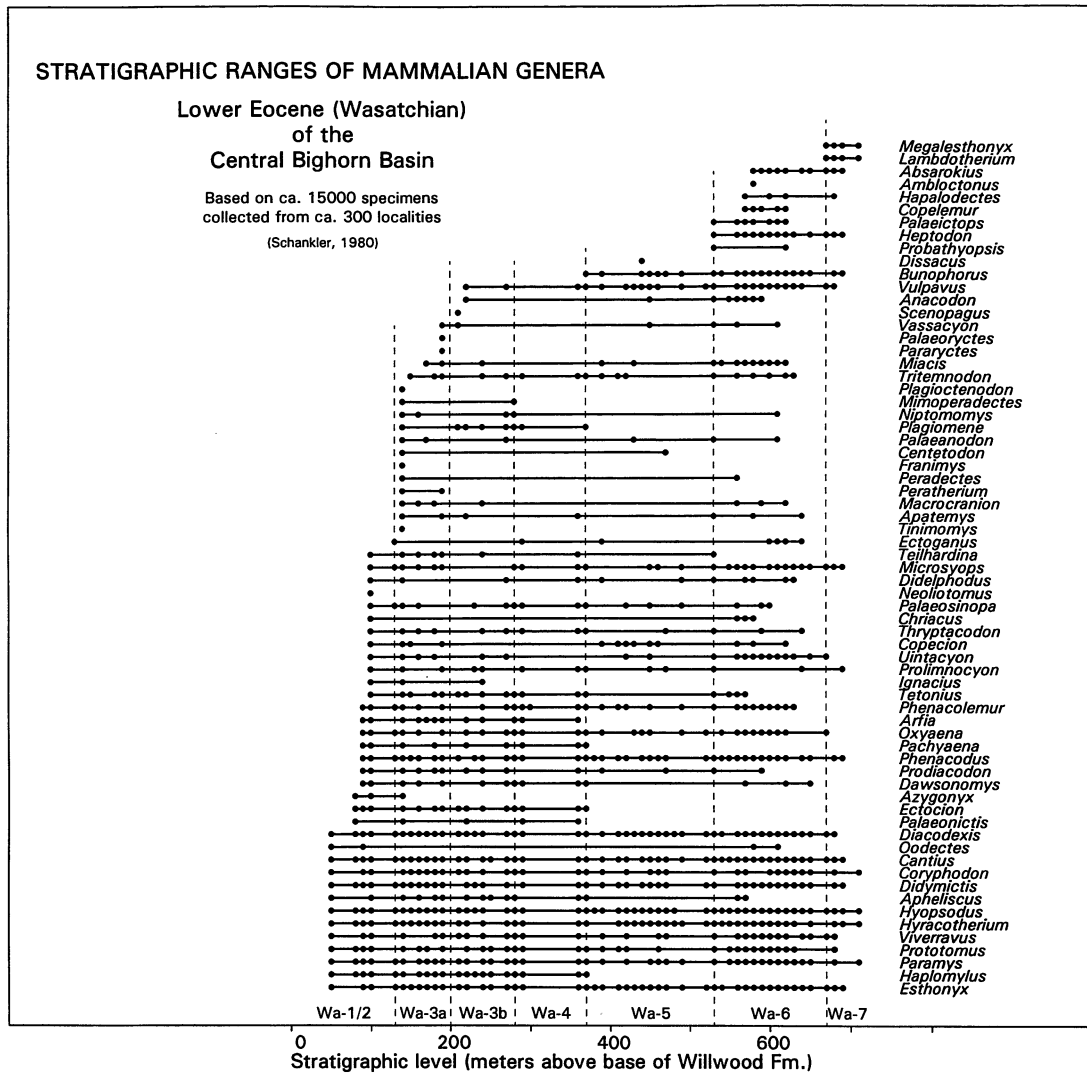


FIGURE 4 — Stratigraphic ranges of early Eocene mammalian genera in the central Bighorn Basin. Dashed lines separate zones of the Wasatchian land-mammal age (labeled Wa-1/2, etc., at the bottom of the chart). Chart is derived from Figure 3 in Schankler (1980). Generic names have been updated when possible; e.g., *Phenacodus brachypternus* is now placed in *Copecion brachypternus* (Gingerich, 1989).

subage, but the two are certainly comparable and probably even compatible. Granger had the advantage of a broader geographic and stratigraphic perspective based on his work in the Polcat Bench–Sand Coulee area and in the Foster Gulch–McCullough Peaks area as well as in the central Bighorn Basin, and his distinction of Sandcouleean from Graybullian faunas appears more representative of the general pattern of faunal evolution in the early Wasatchian than Schankler’s lumping of everything into one or two thick units based on the parallel ranges of *Haplomyilus* and *Ectocion*. Further clarification will come when the stratigraphic distribution of perissodactyls, so important to Granger’s zonation, is studied in more detail in the central Bighorn Basin.

Southern Bighorn Basin

Three studies have been published on Paleocene-Eocene mammals from the southern Bighorn Basin. One deals with Puercan, Torrejonian, and Tiffanian mammals from a cluster of localities along the southern margin of the Fort Union Formation outcrop (Hartman, 1986), while the other two describe Wasatchian mammals at a considerable distance north and east of the Hartman localities (Bown, 1979; see also Bown et al., 1994a, and Strait, this volume). No Clarkforkian mammals have been found as yet in the southern Bighorn Basin, and the Paleocene mammals that have been found cannot be related stratigraphically to the Wasatchian mammals in the southern

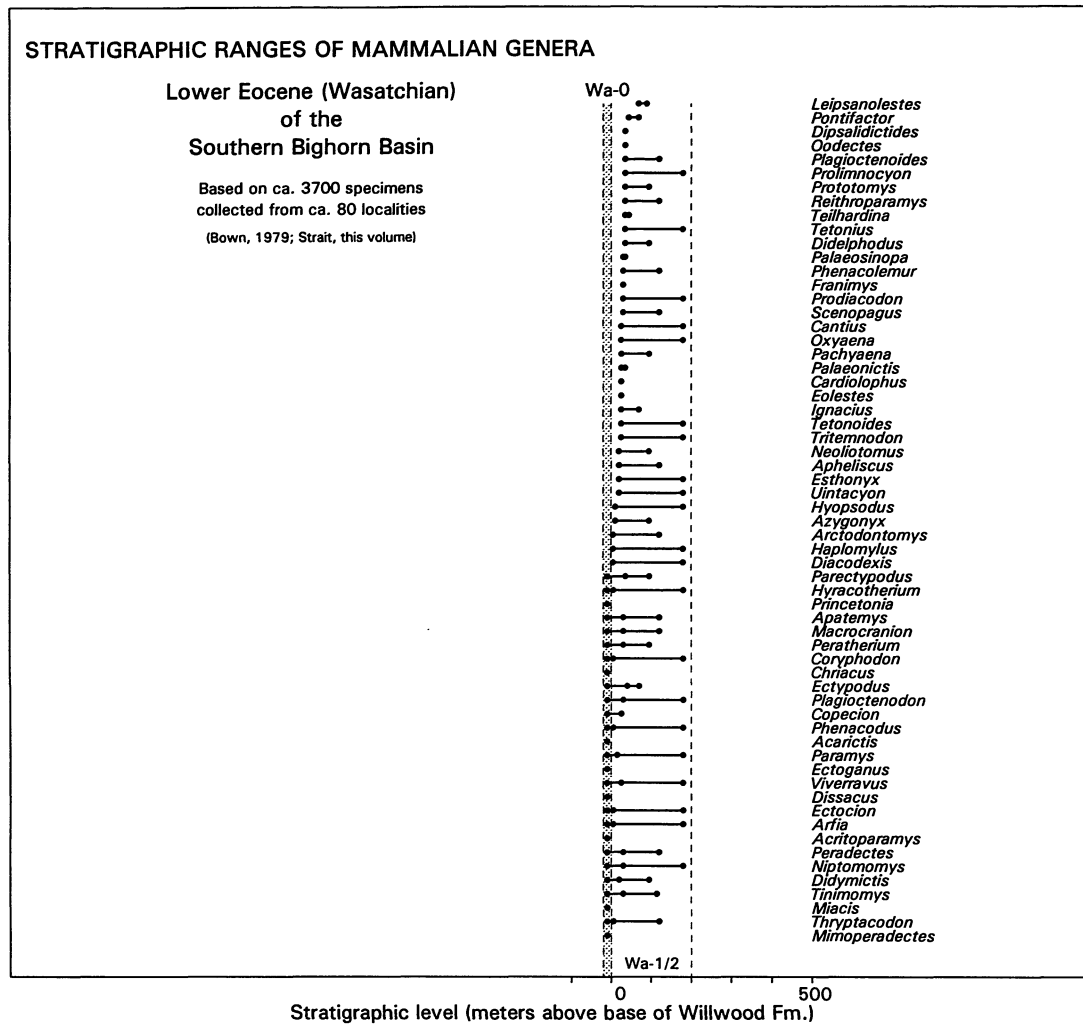


FIGURE 5 — Stratigraphic ranges of early Eocene mammalian genera in the southern Bighorn Basin. Dashed lines separate zones of the Wasatchian land-mammal age (labeled Wa-1/2, representing Wa-1 and/or Wa-2, at the bottom of the chart). Stippled column is Wa-0. Chart is derived from Strait (this volume), and from Bown (1979) and Bown et al. (1994a).

Bighorn Basin. A range chart of Wasatchian genera is shown in Figure 5.

The southern Bighorn Basin stratigraphic section clearly has Wa-0 mammals (Strait, this volume), overlain by Sandcouleean mammals (Bown, 1979), with no evidence of later Graybullian mammals. The total thickness of the Sandcouleean section here (Wa-0 through Wa-2) is ca. 220 m, which is more than double the Sandcouleean section in the central Bighorn Basin, and comparable to Sandcouleean sections farther north in the Polecat Bench–Sand Coulee and Foster Gulch–McCullough Peaks areas.

At the southeastern end of the Bighorn Basin the Fort Union Formation laps unconformably onto and over late Cretaceous formations (Love et al., 1979), and better mammalian age control here would enable estimation of the duration of the hiatus.

GEOGRAPHIC DISTRIBUTION OF PALEOCENE–EOCENE MAMMALS

Figure 1 shows the geographic distribution of Paleocene–Eocene mammals in the Bighorn and Clarks Fork basins. Localities are coded by faunal age, when known, to distinguish Paleocene, early Eocene Wa-0, early Eocene Wa-1 through Wa-4, early Eocene Wa-5, and early Eocene Wa-6 through Wa-7 localities. Paleocene strata are best exposed in the northern end of the depositional trough in the Clarks Fork and northern Bighorn basins, and at the southern end of the trough in the southern Bighorn Basin. There is a narrow band of Fort Union Formation encircling the rest of the basin with some potential to yield Paleocene mammals, though the Paleocene section is sometimes incomplete on the east side of the basin

where it laps onto underlying Cretaceous strata and it is sometimes incomplete on the west side of the basin where it has been removed by erosion and overlapped unconformably by Eocene strata.

The map in Figure 1 also shows an asymmetry in the Foster Gulch–McCullough Peaks area and the central Bighorn basin, where older Wasatchian strata (Wa-0 through Wa-4) occupy the eastern one-third of the basin trough while younger Wasatchian strata (Wa-5 through Wa-7) occupy much of the western two-thirds. This is partly due to topography, because the entire area drains eastward into the Bighorn River, but it is also due to structural deformation of the basin during deposition. The western margin of the Clarks Fork and Bighorn basins is a high-angle overthrust involving basement rocks, and the basin itself is thus deepest along its western margin. The distribution of Wa-5 through Wa-7 strata is approximately the trace of the basin axis.

We hope that this summary of mammalian biostratigraphy in the Bighorn and Clarks Fork basins will encourage research in geographic areas and on geological and paleontological problems that have not been investigated thoroughly, and that development of a basin-wide reference map will encourage presentation and comparison of localized results in this broader context.

ACKNOWLEDGMENTS

This chapter summarizes more than a century of field and laboratory work on mammalian stratigraphy by colleagues mentioned above and listed in the following literature section. J. I. Bloch, G. F. Gunnell, R. Secord, and P. Wilf read the manuscript and provided many suggestions leading to its improvement.

LITERATURE CITED

- ARCHIBALD, J. D., W. A. CLEMENS, P. D. GINGERICH, D. W. KRAUSE, E. H. LINDSAY, and K. D. ROSE. 1987. First North American land mammal ages of the Cenozoic era. In M. O. Woodburne (ed.), *Cenozoic Mammals of North America: Geochronology and Biostratigraphy*, University of California Press, Berkeley, pp. 24-76.
- BADGLEY, C. E. 1990. A statistical assessment of last appearances in the Eocene record of mammals. In T. M. Bown and K. D. Rose (eds.), *Dawn of the age of mammals in the northern part of the Rocky Mountain interior, North America*, Geological Society of America Special Paper, 243: 153-167.
- BADGLEY, C. E. and P. D. GINGERICH. 1988. Sampling and faunal turnover in Early Eocene mammals. *Palaeogeography, Palaeoclimatology, Palaeoecology*, 63: 141-157.
- BOWN, T. M. 1979. Geology and mammalian paleontology of the Sand Creek facies, lower Willwood formation (Lower Eocene), Washakie county, Wyoming. *Geological Survey of Wyoming Memoir*, 2: 1-151.
- BOWN, T. M., P. A. HOLROYD, and K. D. ROSE. 1994b. Mammal extinctions, body size, and paleotemperature. *Proceedings of the National Academy of Sciences USA*, 91: 10403-10406.
- BOWN, T. M. and M. J. KRAUS. 1993. Time-stratigraphic reconstruction and integration of paleopedologic, sedimentologic, and biotic events (Willwood Formation, lower Eocene, northwest Wyoming, U.S.A.). *Palaios*, 8: 68-80.
- BOWN, T. M., K. D. ROSE, E. L. SIMONS, and S. L. WING. 1994a. Distribution and stratigraphic correlation of upper Paleocene and lower Eocene fossil mammal and plant localities of the Fort Union, Willwood, and Tatman Formations, southern Bighorn Basin, Wyoming. *U.S. Geological Survey Professional Paper*, 1540: 1-103.
- CLYDE, W. C. 1997. Stratigraphy and mammalian paleontology of the McCullough Peaks, northern Bighorn Basin, Wyoming: implications for biochronology, basin development, and community reorganization across the Paleocene-Eocene boundary. Ph.D. dissertation, University of Michigan 270 pp.
- COPE, E. D. 1880. The northern Wasatch fauna. *American Naturalist*, 1880: 908-909.
- COPE, E. D. 1882. Contributions to the history of the Vertebrata of the lower Eocene of Wyoming and New Mexico. *Proceedings of the American Philosophical Society*, 20: 139-197.
- FISHER, C. A. 1906. Geology and water resources of the Bighorn Basin, Wyoming. *U.S. Geological Survey Professional Paper*, 53: 1-72.
- FROEHLICH, D. J. 1996. The systematics of basal perissodactyls and the status of North American early Eocene equids. Ph.D. dissertation, University of Texas, Austin, 485 pp.
- GINGERICH, P. D. 1969. Markov analysis of cyclic alluvial sediments. *Journal of Sedimentary Petrology*, 39: 330-332.
- GINGERICH, P. D. 1974. Stratigraphic record of early Eocene *Hyopsodus* and the geometry of mammalian phylogeny. *Nature*, 248: 107-109.
- GINGERICH, P. D. 1975. New North American Plesiadapidae (Mammalia, Primates) and a biostratigraphic zonation of the middle and upper Paleocene. *Contributions from the Museum of Paleontology, University of Michigan*, 24: 135-148.
- GINGERICH, P. D. 1976a. Paleontology and phylogeny: patterns of evolution at the species level in early Tertiary mammals. *American Journal of Science*, 276: 1-28.
- GINGERICH, P. D. 1976b. Cranial anatomy and evolution of early Tertiary Plesiadapidae (Mammalia, Primates). *University of Michigan Papers on Paleontology*, 15: 1-140.
- GINGERICH, P. D. 1982. Time resolution in mammalian evolution: sampling, lineages and faunal turnover. In B. Mamet and M. J. Copeland (eds.), *Proceedings of the Third North American Paleontological Convention, Montreal*, 1: 205-210.
- GINGERICH, P. D. 1983. Paleocene-Eocene faunal zones and a preliminary analysis of Laramide structural deformation in the Clarks Fork Basin, Wyoming. *Wyoming Geological Association Guide Book*, 34: 185-195.
- GINGERICH, P. D. 1989. New earliest Wasatchian mammalian fauna from the Eocene of northwestern Wyoming: composition and diversity in a rarely sampled high-floodplain assemblage. *University of Michigan Papers on Paleontology*, 28: 1-97.

- GINGERICH, P. D. 1991. Systematics and evolution of early Eocene Perissodactyla (Mammalia) in the Clarks Fork Basin, Wyoming. *Contributions from the Museum of Paleontology, University of Michigan*, 28: 181-213.
- GINGERICH, P. D. 2000. Paleocene-Eocene boundary and continental vertebrate faunas of Europe and North America. In B. Schmitz, B. Sundquist, and F. P. Andreasson (eds.), *Early Paleogene Warm Climates and Biosphere Dynamics*, Uppsala, Geological Society of Sweden, GFF [Geologiska Föreningens Förhandlingar], 122: 57-59.
- GINGERICH, P. D. and K. KLITZ. 1985. Paleocene and early Eocene fossil localities in the Fort Union and Willwood Formations, Clarks Fork Basin, Wyoming. *Miscellaneous Contributions, Museum of Paleontology, University of Michigan*, 1 sheet (map).
- GINGERICH, P. D. and E. L. SIMONS. 1977. Systematics, phylogeny, and evolution of early Eocene Adapidae (Mammalia, Primates) in North America. *Contributions from the Museum of Paleontology, University of Michigan*, 24: 245-279.
- GRANGER, W. 1914. On the names of lower Eocene faunal horizons of Wyoming and New Mexico. *Bulletin of the American Museum of Natural History*, 33: 201-207.
- GUNNELL, G. F. 1989. Evolutionary history of Microsypoidea (Mammalia, ?Primates) and the relationship between Plesiadapiformes and Primates. *University of Michigan Papers on Paleontology*, 27: 1-157.
- GUNNELL, G. F. 1998. Mammalian faunal composition and the Paleocene-Eocene epoch/series boundary: evidence from the northern Bighorn Basin, Wyoming. In M.-P. Aubry, S. G. Lucas, and W. A. Berggren (eds.), *Late Paleocene-Early Eocene Climatic and Biotic Events in the Marine and Terrestrial Records*, Columbia University Press, New York, pp. 409-427.
- HARTMAN, J. E. 1986. Paleontology and biostratigraphy of lower part of Polecat Bench Formation, southern Bighorn Basin, Wyoming. *Contributions to Geology, University of Wyoming*, 24: 11-63.
- JEPSEN, G. L. 1930. Stratigraphy and paleontology of the Paleocene of northeastern Park County, Wyoming. *Proceedings of the American Philosophical Society*, 69: 463-528.
- JEPSEN, G. L. 1940. Paleocene faunas of the Polecat Bench Formation, Park County, Wyoming. Part I. *Proceedings of the American Philosophical Society*, 83: 217-340.
- KRAUSE, D. W. 1980. Multituberculates from the Clarkforkian Land-Mammal age, late Paleocene-early Eocene of western North America. *Journal of Paleontology*, 54: 1163-1183.
- KRAUSE, D. W. 1982. Multituberculates from the Wasatchian land-mammal age, early Eocene, of western North America. *Journal of Paleontology*, 56: 271-294.
- KRISHNALKA, L., R. K. STUCKY, R. M. WEST, M. C. MCKENNA, C. C. BLACK, T. M. BOWN, M. R. DAWSON, D. J. GOLZ, J. J. FLYNN, J. A. LILLEGRAVEN, and W. D. TURNBULL. 1987. Eocene (Wasatchian through Duchesnean) biochronology of North America. In M. O. Woodburne (ed.), *Cenozoic Mammals of North America: Geochronology and Biostratigraphy*, University of California Press, Berkeley, pp. 77-117.
- LEITE, M. B. 1992. Vertebrate biostratigraphy and taphonomy of the Fort Union Formation (Paleocene) east of Grass Creek Basin, southwestern Bighorn Basin, Wyoming. Ph.D. dissertation, University of Wyoming, Laramie, 236 pp.
- LOOMIS, F. B. 1907. Origin of the Wasatch deposits. *American Journal of Science, Series 4*, 23: 356-364.
- LOVE, J. D., A. C. CHRISTIANSEN, and J. L. EARLE. 1978a. Preliminary geologic map of the Sheridan 1° × 2° quadrangle, northern Wyoming (1:250,000). U.S. Geological Survey Open-File Report, 78-456: 1 sheet.
- LOVE, J. D., A. C. CHRISTIANSEN, J. L. EARLE, and R. W. JONES. 1978b. Preliminary geologic map of the Arminto 1° × 2° quadrangle, central Wyoming (1:250,000). U.S. Geological Survey Open-File Report, 78-1089: 1 sheet.
- LOVE, J. D., A. C. CHRISTIANSEN, T. M. BOWN, and J. L. EARLE. 1979. Preliminary geologic map of the Thermopolis 1° × 2° quadrangle, central Wyoming (1:250,000). U.S. Geological Survey Open-File Report, 79-962: 1 sheet.
- NEASHAM, J. W. and C. F. VONDRA. 1972. Stratigraphy and petrology of the lower Eocene Willwood Formation, Bighorn Basin, Wyoming. *Bulletin of the Geological Society of America*, 83: 2167-2180.
- OSBORN, H. F. 1892. Fossil mammals of the Wahsatch and Wind River Beds. Collection of 1891. Taxonomy and morphology of the primates, creodonts, and ungulates. *Bulletin of the American Museum of Natural History*, 1: 101-134.
- OSBORN, H. F. 1910. *The Age of Mammals in Europe, Asia, and North America*. MacMillan Company, New York, 635 pp.
- PIERCE, W. G. 1997. Geologic map of the Cody 1° × 2° quadrangle, northwestern Wyoming (1:250,000). U.S. Geological Survey Miscellaneous Investigations Series, I-2500: 1 sheet.
- RADINSKY, L. B. 1963. Origin and early evolution of North American Tapiroidea. *Bulletin of the Peabody Museum Natural History, Yale University*, 17: 11-106.
- ROHRER, W. L. 1964a. Geology of the Sheep Mountain Quadrangle, Wyoming. U. S. Geological Survey map GQ-310, 1 sheet.
- ROHRER, W. L. 1964b. Geology of the Tatman Mountain Quadrangle, Wyoming. U. S. Geological Survey map GQ-311, 1 sheet.
- ROHRER, W. L. and C. L. GAZIN. 1965. Gray Bull and Lysite faunal zones of the Willwood Formation in the Tatman Mountain area, Bighorn Basin, Wyoming. U.S. Geological Survey Professional Paper, 525D: 133-138.
- ROSE, K. D. 1975. The Carpolestidae: early Tertiary primates from North America. *Bulletin of the Museum of Comparative Zoology, Harvard University*, 147: 1-74.
- ROSE, K. D. 1981. The Clarkforkian land-mammal age and mammalian faunal composition across the Paleocene-Eocene boundary. *University of Michigan Papers on Paleontology*, 26: 1-197.
- SCHANKLER, D. M. 1980. Faunal zonation of the Willwood formation in the central Bighorn Basin, Wyoming. In P. D. Gingerich (ed.), *Early Cenozoic Paleontology and Stratigraphy of the Bighorn Basin, Wyoming*, University of Michigan Papers on Paleontology, 24: 99-114.
- SCHANKLER, D. M. 1981. Local extinction and ecological re-entry of early Eocene mammals. *Nature*, 293: 135-138.
- SCOTT, W. B. 1913. *A History of Land Mammals in the Western Hemisphere*. Macmillan Company, New York, 693 pp.

- SIMONS, E. L. 1960. The Paleocene Pantodonta. Transactions of the American Philosophical Society, 50: 1-81.
- SIMPSON, G. G. 1928. A new mammalian fauna from the Fort Union of southern Montana. American Museum Novitates, 297: 1-15.
- SIMPSON, G. G. 1929a. A collection of Paleocene mammals from Bear Creek, Montana. Annals of Carnegie Museum, 19: 115-122.
- SIMPSON, G. G. 1929b. Third contribution to the Fort Union fauna at Bear Creek, Montana. American Museum Novitates, 345: 1-12.
- SINCLAIR, W. J. 1912. Contributions to geologic theory and method by American workers in vertebrate paleontology. Bulletin of the Geological Society of America, 23: 262-266.
- SINCLAIR, W. J. and W. GRANGER. 1911. Eocene and Oligocene of the Wind River and Bighorn Basins. Bulletin of the American Museum of Natural History, 30: 83-117.
- SINCLAIR, W. J. and W. GRANGER. 1912. Notes on the Tertiary deposits of the Bighorn Basin. Bulletin of the American Museum of Natural History, 31: 57-67.
- STANLEY, S. M. 1982. Macroevolution and the fossil record. Evolution, 36: 460-473.
- THEWISSEN, J. G. M. 1990. Evolution of Paleocene and Eocene Phenacodontidae (Mammalia, Condylarthra). University of Michigan Papers on Paleontology, 29: 1-107.
- VAN HOUTEN, F. B. 1944. Stratigraphy of the Willwood and Tatman Formations in northwestern Wyoming. Geological Society of America Bulletin, 55: 165-210.
- VAN HOUTEN, F. B. 1945. Review of the latest Paleocene and early Eocene mammalian faunas. Journal of Paleontology, 19: 421-461.
- WINKLER, D. A. 1983. Paleocology of an early Eocene mammalian fauna from paleosols in the Clarks Fork Basin, northwestern Wyoming (U. S. A.). Palaeogeography, Palaeoclimatology, Palaeoecology, 43: 261-298.
- WOOD, H. E., R. W. CHANEY, J. CLARK, E. H. COLBERT, G. L. JEPSEN, J. B. REESIDE, and C. STOCK. 1941. Nomenclature and correlation of the North American continental Tertiary. Bulletin of the Geological Society of America, 52: 1-48.
- WOOD, R. C. 1967. A review of the Clark Fork vertebrate fauna. Breviora, Museum of Comparative Zoology, Harvard University, 257: 1-30.
- WORTMAN, J. L. 1882. The geology of the Big-Horn Basin. Proceedings of the American Philosophical Society, 34: 139-142.
- WORTMAN, J. L. 1892. Geological and geographical sketch of the Big Horn Basin. Bulletin of the American Museum of Natural History, 1: 135-147.
- WORTMAN, J. L. 1896. Species of *Hyracotherium* and allied Perissodactyla from the Wasatch and Wind River beds of North America. Bulletin of the American Museum of Natural History, 8: 81-110.

SEDIMENTOLOGY AND DEPOSITIONAL SETTING OF THE WILLWOOD FORMATION IN THE BIGHORN AND CLARKS FORK BASINS

MARY J. KRAUS

Department of Geological Sciences, The University of Colorado, Boulder, CO 80309-0399

Abstract.— The fluvial sedimentology and paleosols of the Willwood Formation have been analyzed in three parts of the Bighorn Basin. The three areas show a consistent alluvial architecture that consists of three components: major sheet sandstones, mudrocks with more strongly developed paleosols, and heterolithic deposits with weakly-developed paleosols. The major sheet sandstones are 10-30 m thick and laterally extensive (1-2 km wide in a direction perpendicular to paleoflow). They were deposited by trunk rivers, which were mixed-load, meandering rivers. The channels were confined to their meander belts long enough to produce amalgamated sandstones with as many as 6 vertically stacked stories.

Overbank deposition of the trunk rivers produced mudrocks that are several meters thick and on which moderately-to well-developed paleosols formed. The degree of pedogenic development indicates that the mudrocks accumulated slowly on the floodplain and at some distance from the active channel. Paleosols in the three study areas differ in their degree of soil hydromorphy or wetness. One control on hydromorphy appears to be grain size, which varies among the study areas. Where sediment was coarser, the soils were better drained, and where sediment was clay-rich, the soils show evidence for strong gleying.

Interbedded with the well-developed paleosols are heterolithic intervals that consist of mudrocks and ribbon sandstones. The heterolithic intervals are 3-7 m thick and can be traced laterally for as much as 5 km both parallel and perpendicular to paleoslope. Here mudrocks show only weak pedogenic modification, indicating that the heterolithic intervals were deposited very rapidly. Based on their similarity to modern avulsion deposits, the heterolithic intervals are attributed to deposition on the floodplain by extensive crevasse splay systems that developed as the trunk channel underwent avulsion. The ribbon sandstones represent the crevasse splay channels that fed the developing avulsion belt. Weakly developed paleosols provide an easy means of recognizing avulsion deposits in the Willwood Formation. These avulsion deposits form a significant part of the Willwood Formation and demonstrate the importance of avulsion in constructing the floodplains of some meandering river systems. Furthermore, rapid aggradation of avulsion deposits on top of overbank deposits was instrumental in preserving the more strongly developed paleosols characteristic of the latter.

INTRODUCTION

The Willwood Formation is one of many thick alluvial units deposited by meandering rivers in an intermontane basin.

In: Paleocene-Eocene Stratigraphy and Biotic Change in the Bighorn and Clarks Fork Basins, Wyoming (P. D. Gingerich, ed.), University of Michigan Papers on Paleontology, 33: 15-28 (2001).

Despite its rather typical origins and the fact that it shares characteristics with many other alluvial deposits, the sedimentology of the Willwood Formation has been well studied because of its distinctive and well-exposed floodplain paleosols. The Willwood paleosols have proved important for understanding the processes by which floodplains are constructed as well as the larger scale controls (e.g., climate,

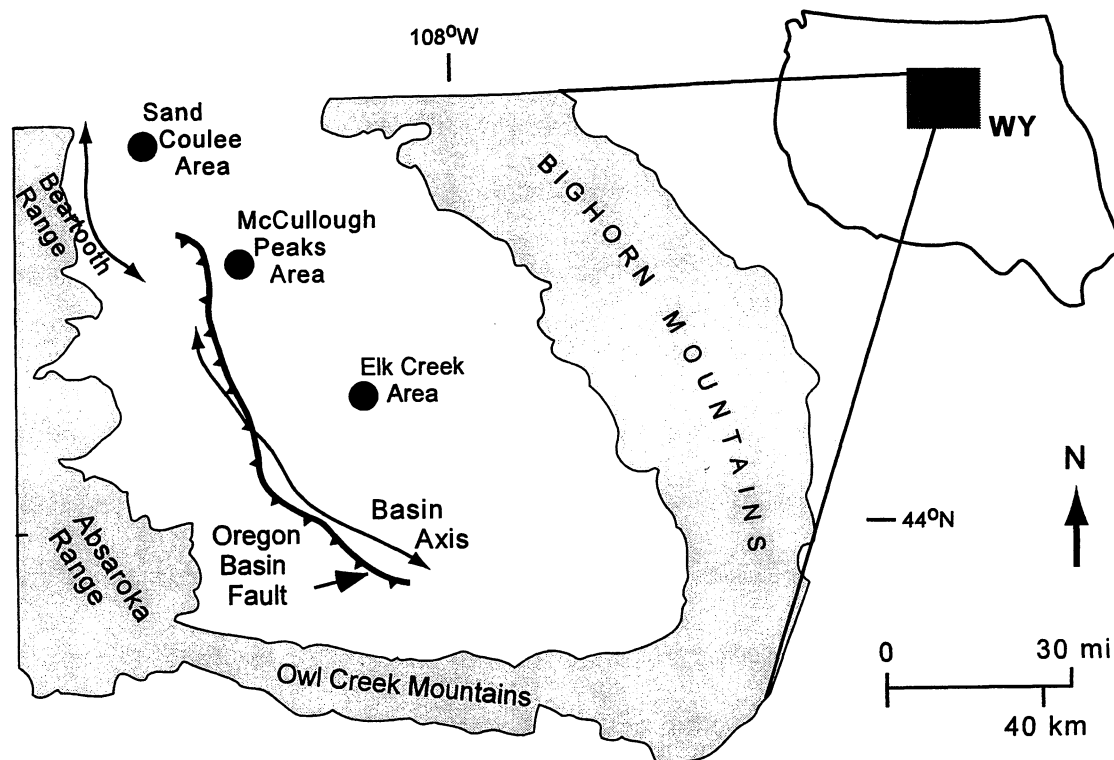


FIGURE 1 — Map of the greater Bighorn Basin, Wyoming, showing major mountain ranges surrounding the basin, and location of study areas in Sand Coulee in the Clarks Fork Basin, McCullough Peaks in northern Bighorn Basin, and along Elk Creek in the central Bighorn Basin.

basin subsidence) that influence the alluvial stratigraphy that develops over time.

Willwood paleosols are variable at different spatial scales ranging from the local to basin-wide. Studies on the Willwood paleosols have shown, at the local scale, that paleosols change laterally in response to variations in grain size and topography, which are commonly related to position on the ancient floodplain (e.g., Bown and Kraus, 1987; Kraus and Aslan, 1993; Kraus, 1997). In particular, areas of the floodplain that were close to the coeval channel have more weakly developed and better drained paleosols; areas that were more distant from the channel have more strongly developed and more poorly drained paleosols. At the scale of the sedimentary basin, Willwood paleosols in different locations differ because of basal variations in topography, grain size, climate, and subsidence rate (e.g., Kraus and Gwinn, 1997; Kraus and Aslan, 1999).

Recent studies (e.g., Kraus and Aslan, 1993; Kraus, 1996) have shown that avulsion of the trunk rivers also had a major impact on Willwood paleosols. Much of the Willwood Formation consists of stratigraphic intervals that are meters thick and consist of two parts: (1) fine-grained deposits that are characterized by well-developed paleosols and (2) interbedded mudstones and sandstones characterized by weakly developed paleosols. The fine-grained deposits have been attributed to

overbank flooding of the trunk channel; the heterolithic deposits have been attributed to avulsion of the trunk channel.

This paper synthesizes past studies and ongoing analyses of the sedimentology of the Willwood Formation in the Bighorn Basin, Wyoming. The major goals are to describe the alluvial architecture of the Willwood Formation and outline its general depositional setting. Of special interest are the fine-grained deposits with well-developed paleosols and the heterolithic intervals with weakly developed paleosols. Well developed paleosols are described and their genesis as overbank deposits is discussed. In addition, paleosols from three parts of the Bighorn Basin are compared and contrasted to show paleosol variability at several different scales and the significance of that variability. The sedimentologic and pedogenic properties of the heterolithic deposits are described, their interpretation as avulsion deposits is explained, and their importance to the alluvial stratigraphy is discussed.

GEOLOGICAL SETTING

The alluvial Willwood Formation was deposited throughout the Bighorn Basin of Wyoming during latest Paleocene and early Eocene time (Fig. 1). Deposition accompanied Laramide structural development of the basin, which is part of the Rocky

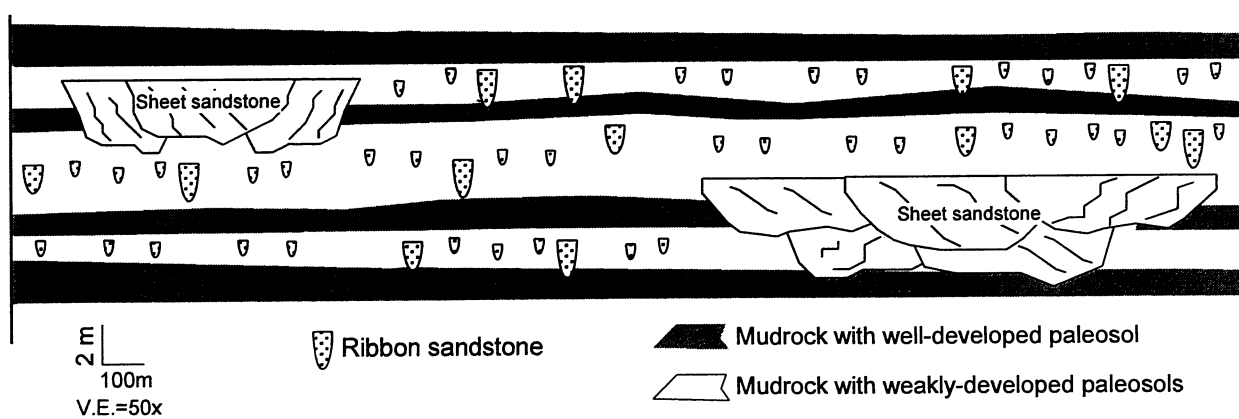


FIGURE 2 — Schematic cross-section showing alluvial architecture of the Willwood Formation. Most of the Willwood Formation consists of either mudrocks, on which well-developed soils formed, or lithologically heterogeneous strata. The heterolithic strata consist of ribbon sandstones and mudrocks on which weakly developed soils formed. Major sheet sandstones locally scour those two elements. Vertical exaggeration is $\times 50$.

Mountain foreland. The deep, westwardly asymmetric basin is adjacent to mountain ranges with Precambrian crystalline rocks at their cores (e.g., Blackstone, 1986). The Bighorn, Beartooth, and Owl Creek mountains have been attributed to compression in a northeast-southwest horizontal thrust field (Brown, 1993), and basin subsidence resulted from loading by the basin-margin uplifts (e.g., Hagen, et al., 1985). The Absaroka Mountains were created by volcanic activity that post-dated the deposits described here.

Study Areas

This paper includes information from three stratigraphic intervals in different areas of the greater Bighorn Basin (Fig. 1). The oldest interval, which has been assigned to the middle of the Clarkforkian (e.g., Rose, 1981), is present in the Sand Coulee area of the Clarks Fork Basin. To the south is the McCullough Peaks study area in the northern Bighorn Basin proper. Clyde's (1997) sections show that the study interval there spans the boundary between the Wasatchian-4 and Wasatchian-5 biozones. In the central part of the Bighorn Basin, Willwood strata have been studied along Elk Creek. These strata are approximately time-equivalent to the section in McCullough Peaks (Bown et al., 1994; Clyde, 1997).

Alluvial Architecture

The alluvial architecture of the Willwood Formation is characterized by three major elements (Figs. 2 and 3): Intervals consisting of (1) mudrocks on which moderately to well developed paleosols formed alternate vertically with (2) heterolithic intervals consisting of ribbon and thin sheet sandstones together with mudrocks on which weakly developed paleosols formed. These two components of the Willwood system are locally truncated by (3) laterally extensive,

amalgamated sandstone bodies. The following sections describe each of these elements and interpret the depositional settings, treating first the amalgamated sandstones, then the mudstones with well-developed paleosols, and finally the heterolithic intervals.

MAJOR SANDSTONE BODIES

The major sandstone bodies range from ca. 1 to 2 km wide and 10 to 30 m thick. They are classified as sheet sandstones because they have width/thickness (W/T) ratios that generally exceed 100. The major sandstones are multi-storied with up to six vertically stacked stories (Fig. 2). The preserved thickness of individual stories averages 3 to 5 m depending on the study area, and stories can be up to several hundred meters wide. The bases of most stories contain mudstone intraclasts and carbonate nodules, which were eroded from coeval soils.

Grain size of the sheets varies from very fine to coarse sand. Individual stories commonly consist of sandy inclined strata with a stratigraphic dip that is generally less than 20° . Internally, the inclined deposits show sedimentary structures that include medium (up to 10 cm thick and 10 cm wide) to large-scale (m-scale) sets of planar and trough cross-stratification. Paleocurrent directions, taken from large-scale cross-stratification, are generally ca. 90° to the dip directions of associated inclined strata. The paleocurrent trends also change vertically and laterally within individual stories.

Interpretation

The major sandstone bodies are interpreted as the deposits of the trunk rivers based on their thickness and lateral extent. Because the inclined beds within individual stories trend nearly 90° to the dip directions of associated large scale cross-bedding, they are interpreted as lateral accretion deposits that

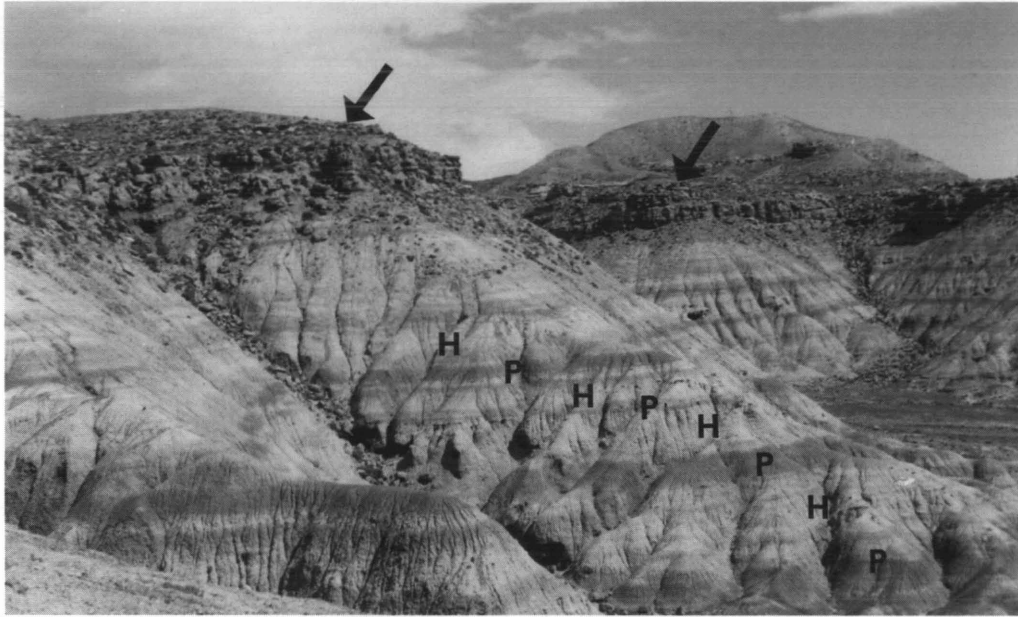


FIGURE 3 — Field view showing alluvial architecture in the Sand Coulee study area. A major sheet sandstone (arrows) caps the ridge. Cumulative paleosols (*P*) form the darker bands and are attributed to overbank deposition. The cumulative paleosols alternate with lighter-colored heterolithic intervals (*H*). Weakly developed paleosols and ribbon sandstones characterize the heterolithic deposits. They are interpreted as avulsion deposits. Sloping ridge in foreground of photo is 75 m high.

formed in point bars. The presence of lateral accretion deposits, highly variable paleoflow directions in vertically successive stories, and the overall upward-fining trend of individual stories are consistent with deposition in meandering channels (e.g., Thomas et al., 1987). The mudrock-dominated lithology of the surrounding strata indicates that the trunk rivers were mixed load channels that carried abundant clay and silt in addition to sand. This too is consistent with meandering channels.

The trunk channels varied from approximately 150 m to 450 m wide, and from about 3 m to 10 m deep at bankfull, based on story thicknesses. The widths of the major sandstone bodies indicate that the channels were flanked by meander-belts that ranged from ca. 1 to 2 km wide. As is the case with the modern South Saskatchewan system (Morozova and Smith, 2000), each of the major channel belts in the Willwood system may have had more than one channel, although one of those channels probably dominated the system. Paleoflow for the fluvial systems in all three areas was to the northwest, paralleling the structural axis of the basin (Fig. 1).

MUDROCKS WITH WELL-DEVELOPED PALEOSOLS

The second architectural element in the Willwood Formation is intervals of mudrock that show significant pedogenic modification (Figs. 2 and 3). The fine-grained

deposits represent the parent material on which formed paleosols of varying degrees of soil development and soil drainage. The following sections describe the parent material, key soil properties, and representative soil profiles. Interpretation of the paleosols follows.

Parent Material

The grain size distributions of representative fine-grained deposits from the various study areas were determined quantitatively. The fine-grained deposits in the McCullough Peaks area tend to be somewhat coarser than those in Sand Coulee (Table 1). The Elk Creek deposits are considerably finer-grained. Most dramatic is the average clay content of the Elk Creek samples, which is 78%. Using the classification of Blatt et al. (1972), the fine-grained deposits are classified as mudrocks. The term mudrock includes siltstones, with greater than 67% silt; mudstones, with less than 67% silt and less than 67% clay; and claystones, which have greater than 67% clay.

Mudrocks from the study areas show similar clay mineralogy. The dominant clay mineral is mixed-layer illite/smectite with approximately 40% illite and 60% smectite (averaging 50% of all samples). It is accompanied by illite (38%) and kaolinite (9%). Within individual profiles, the clay minerals show no distinct trends.

TABLE 1 — Quantitative size summary of clay content and claystone in Willwood deposits.

Location	No. of samples	Average clay content	Proportion of claystones
Sand Coulee	61	64%	21%
McCullough P	49	55%	51%
Elk Creek	83	78%	82%

Paleosol Properties and their Significance

Matrix and mottle colors

Willwood mudrocks are dominated by gray, red, purple, and yellow-brown as matrix and mottle colors (Fig. 4). Thin sections show that small (less than 0.1 mm) flecks of red hematite are scattered throughout the yellow-brown matrix and mottles. Red matrix and mottles are densely impregnated with red, but also contain small areas that are stained yellow-brown. These observations are consistent with modern soils, in which a mix of hematite and goethite produces yellow-brown and red colors, and, as hematite increases, soils get redder (e.g., Bigham, et al., 1978; Torrent et al., 1980; Schwertmann, 1993). In contrast, gray matrix and mottles are nearly devoid of hematite and goethite, suggesting that their gray color resulted from the removal of iron oxides. Purple areas are intermediate in terms of their iron oxide content. They are characterized by the presence of red, hematite microspheres (less than 5 μ m in diameter) but the hematite particles are sparse and widely distributed compared to red matrix. Purple matrix also shows no yellow-brown stain, except as discrete mottles or nodules, indicating that the purple color is not due to a mix of hematite and goethite as it is in red matrix and mottles.

Colors in the Willwood paleosols are judged to be of pedogenic rather than burial diagenetic origin. Not only do red (hematite-bearing) and yellow-brown (goethite-bearing) coexist in mottled Willwood mudrocks, but also red mudrocks overlie and underlie yellow-brown mudrocks. It seems improbable that diagenetic modification would have produced such mixes of hematite and goethite. In addition, the mottling patterns are similar to those in modern soils that have undergone either groundwater gleying or surface-water gleying (Pipujol and Buurman, 1994).

Redoximorphic features

Soils that are saturated for several months of the year can undergo gleying, in which iron and manganese are reduced and mobilized (e.g., Duchaufour, 1982; Vepraskas, et al., 1992; Vepraskas, 1994). As water table levels fall and the soil dries, the iron and manganese may be leached from the soil or concentrated in more oxidized areas, either within peds or along ped faces and soil channels as mottles and/or nodules (e.g. Duchaufour, 1982; Fanning and Fanning, 1989). These pro-

cesses produce distinctive features, termed redoximorphic features, which can be observed in the field or in thin section (Vepraskas, 1994). Redox depletions show areas where iron was reduced and from which it moved away; redox concentrations indicate where iron moved and was oxidized (e.g., Vepraskas et al., 1992; Vepraskas, 1994).

Gray mottles are the most common kind of iron depletion in the Willwood paleosols. The gray zones are irregular to elongate in shape and are generally surrounded by thin (less than 0.1 mm thick) red rims, which are a kind of iron enrichment zone (Fig. 5A). Many of the gray mottles probably represent root channels, which, because of the presence of organic matter, are especially prone to the reduction and removal of iron oxides (e.g. Schwertmann, 1993).

Redox concentration features include the red rims around gray mottles, iron-oxide mottles, and iron-oxide nodules (Fig. 5A, B). The mottles are yellow-brown or red, and the mottles grade into nodules that are more heavily impregnated with iron oxides. In thin section, most nodules include dispersed detrital grains of the same size and shape as grains in the surrounding matrix (Fig. 5B). Some nodules are ring nodules with both red and yellow-brown rings, indicating fluctuations in soil moisture (Fig. 5C).

Calcite accumulations

Small (usually less than 100 μ m in diameter) carbonate nodules are locally present in small quantities, usually in red mudstones. The nodules range from ovoid to irregular in shape. In thin section, micro-accumulations of calcite are found, typically in gray depletion zones (Fig. 5D). Most consist of micrite or microspar with crystal sizes of ca. 0.05 mm; however, some examples have coarser spar in the center of the accumulation.

The microscopic calcite appears primarily within gray depletion channels with red rims. Following Pipujol and Buurman (1997), the calcite is attributed to gleying as a result of impeded drainage. Water moving through soil channels first removes iron from the channel. Later, micrite precipitates from water containing calcium carbonate in the channels.

Pedogenic slickensides

In the field, slickensides are shiny, clay-lined planar fractures that intersect to form concave-up, dish-shaped structures.

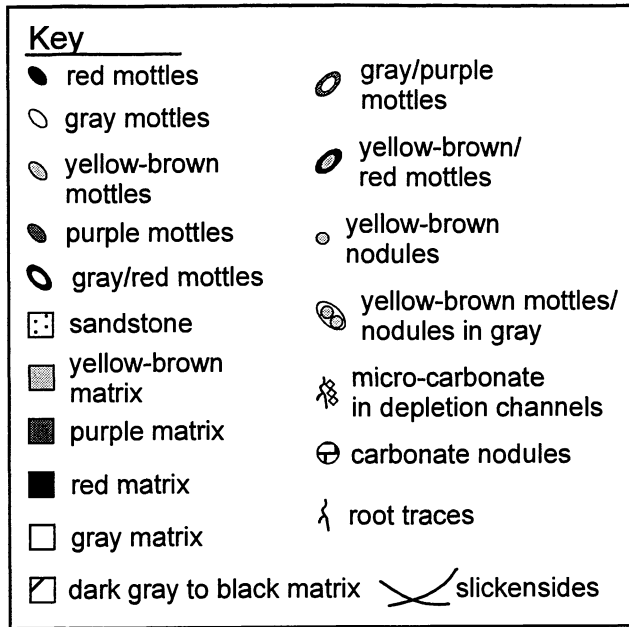


FIGURE 4 — Key to stratigraphic sections of paleosols.

slickensides are common in modern soils that are rich in smectitic clays and that undergo shrinking and swelling as a result of seasonal wetting and drying (Yaalon and Kalmar, 1978; Schumacher et al., 1988; Aslan and Autin, 1998).

In the Willwood paleosols, the presence of large slickensides appears to depend partly on grain size. Purple and red mudrocks containing less than ca. 60% clay do not have large slickensides, whereas, approximately half of the red and purple mudrocks with greater than 60% clay show large slickensides. As noted above, most of the Willwood clay is smectitic in composition, which favors slickenside formation.

Paleosol Profiles

Paleosol profiles in the Willwood Formation are recognized on the basis of vertical grain size trends and color patterns (e.g., Kraus and Aslan, 1993; Kraus, 1997). Paleosols that are termed cumulative paleosols commonly show a gradual upward increase in clay content or a relatively high but uniform clay content until the top of the profile, which is placed at a bed that is coarser or a series of beds that show erratic grain size changes (Fig. 6). The term cumulative indicates that pedogenesis was concurrent with the gradual accumulation of the parent material. Cumulative paleosols are of several different kinds primarily because of local and temporal variations in sediment accumulation rates and drainage. Red paleosols are characteristic of both Sand Coulee and McCullough Peaks (Kraus, 1997). Red/purple paleosols are found in McCullough Peaks and are the dominant paleosol type in Elk Creek (Kraus and Aslan, 1993; Kraus and Gwinn, 1997). Purple paleosols

are also present in Elk Creek but have not been found in the other study areas.

Red paleosols

Red paleosols generally consist of gray mudrock underlain by red mudrock (Fig. 6). The gray mudstone has yellow-brown mottles and gray depletion zones with red rims. The red mudrock has common, although not abundant, yellow-brown mottles. In some examples, a yellow-brown mudrock with red mottles is present between the gray and red beds (Fig. 6A). Gray mottles, many of which are probably root traces, are abundant through the profile. Slickensides are present locally, especially in the more clay-rich beds. The base of the profile is a coarser unit, generally greenish-grey siltstone mottled with red and yellow-brown or sandstone.

Clay weight % decreases down into the C horizon, as does TOC weight %, except for a jump in the lower part of the red horizon (Fig. 6B). Fe_2O_3 wt% increases downward from the gray into the red beds, as does the Fe/clay ratio. Those trends indicate some downward movement of both clay and iron.

The gray bed is interpreted as an A horizon on the basis of its relatively high TOC content and lower iron and clay compared to the underlying red mudrock. The underlying red bed is interpreted as the B horizon. The B horizon underwent rubification or reddening, a soil process that is favored by a subtropical climate with a distinct dry season (Duchaufour, 1982). Duchaufour (1982) argued for classifying soils of subtropical and tropical climates on the basis of how intensely they have been weathered. Following his classification, the red paleosols are Fersiallitic soils, which are usually characterized by red B horizons due to rubification. Fersiallitic soils typically contain smectite and, especially if that smectite is abundant, they contain slickensides. Such soils commonly form in climates with MAT between 13 and 20°C and seasonally spaced rainfall (Duchaufour, 1982). During the wet season, iron is reduced and mobilized causing downward translocation. The warm dry season is critical for rubification of the iron in the B horizon.

The red color indicates that the B horizon was at least moderately well drained and oxidizing (e.g., Kampf and Schwertmann, 1982). The yellow-brown mudrock found in some of the red paleosols probably formed in the lower part of the A horizon because of mild reducing conditions related to organic material (e.g., Macedo and Bryant, 1987; 1989). Red soils in the tropics and subtropics commonly have a yellow A horizon above a red B horizon (e.g. Kampf and Schwertmann, 1982).

Purple paleosols

A typical purple paleosol profile consists of gray mudrock above purple and yellow-brown mudrocks (Fig. 7). The gray beds generally have yellow-brown mottles. The purple beds contain gray as well as yellow-brown mottles and nodules. Large slickensides are common in the clay-rich purple mudrocks, whereas carbonate accumulations are absent.

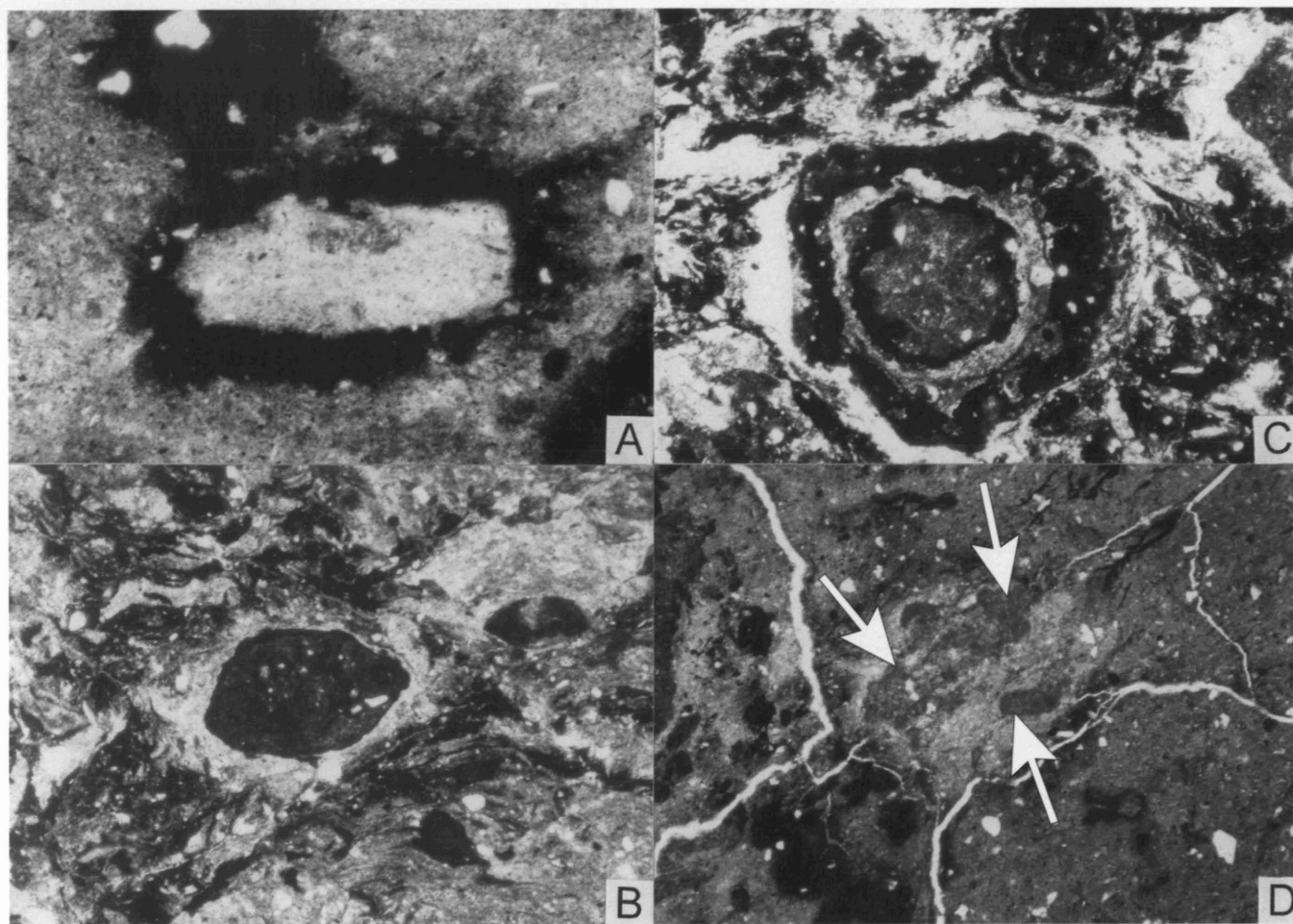


FIGURE 5 — Photomicrographs of paleosol features. A, gray depletion channel (redox depletion) with thick red rim (redox concentration). Width of view is 1.35 mm; plane-polarized light. B, yellow-brown nodule (redox concentration) surrounded by a gray depletion zone. Width of view is 1.35 mm; plane-polarized light. C, ring nodule with red and yellow-brown rings. Width of view is 1.25 mm; plane polarized light. D, gray depletion channel with small, micrite accumulations (arrows) present in the depletion. Width of view is 3.4 mm; plane-polarized light.

Typically, TOC decreases downward into the purple unit, where it remains low (Fig. 7). Clay weight percent decreases downward through profiles and no discernible Bt horizon can be identified. In most examples, the upper gray bed is depleted in Fe_2O_3 compared to the underlying purple and yellow-brown units, which are relatively enriched.

On the basis of their high clay content, dominance of smectite, and large slickensides, the purple paleosols are interpreted as Vertisols (e.g., Soil Survey Staff, 1975, 1998; Duchaufour, 1982). Vertisol formation requires abundant smectite and seasonal wetting and drying to produce the slickensides (e.g., Yaalon and Kalmar, 1978; Wilding and Tessier, 1988). Although marked dry and rainy seasons are needed for the shrink/swell processes, Vertisols develop under a wide range of moisture conditions. The prominent redoximorphic features

seen in the purple paleosols are characteristic of Aquerts, which may be dry for only a few weeks each year (e.g., Buol et al., 1997). Not only climate, but also the high clay content of Aquerts can contribute to their poor drainage.

The down-profile trends in clay and $\text{Fe}_2\text{O}_3/\text{clay}$ ratios (Fig. 7) show modest downward movement of iron but little if any downward movement of clays (e.g. Blume and Schwertmann, 1969). Clay movement was probably impeded by the impermeable nature of the clay-rich parent material (e.g., Duchaufour, 1982). More importantly, the impermeable parent material probably impeded downward drainage and resulted in surface-water gleying (e.g., Blume and Schwertmann, 1969).

The gray matrix with yellow-brown mottles in the upper unit is typical of a gleyed A horizon. The yellow A horizon observed in some profiles probably resulted from weak

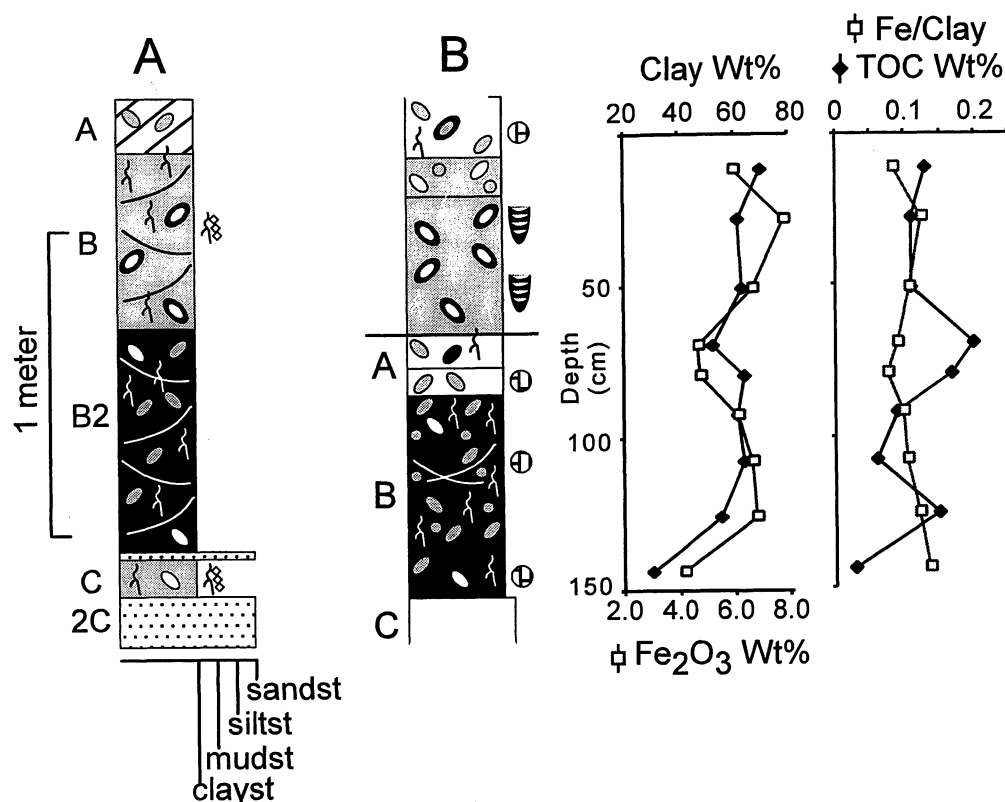


FIGURE 6 — Representative stratigraphic McCullough Peaks. Profile B shows grain size and chemical data as well as morphological data. A, A horizon; B, B horizon; C, C horizon; B1 and B2 indicate subdivisions of the B horizon based on different morphologic properties. Above profile B are fine-grained deposits showing weak pedogenic development and interpreted as avulsion deposits. See Figure 4 for key to symbols.

reduction caused by wetness and the higher organic content of the A horizon (Macedo and Bryant, 1987, 1989). The purple beds are interpreted as gleyed B (Bg) horizons on the basis of pervasive yellow-brown mottling and iron oxide nodules. The purple B horizons of the Vertisols have attributes that are typical of a strong stage of gley development (i.e., poor drainage) as defined by Pipujul and Buurman (1997). The lowermost part of the profile, where grain size increases, is interpreted as a C horizon. Because it too shows gleyed features, it is delimited as a Cg horizon.

Red/purple paleosols

Red/purple paleosols are distinguished by the presence of a purple/red mudrock couplet or red/purple/red sequence (Fig. 8). In the example shown, the uppermost unit is a yellow-brown mudstone with gray depletion zones (probably root traces) surrounded by red, iron oxide concentrations. In other examples, the uppermost bed has gray matrix with yellow-brown mottles. Yellow-brown mottles and nodules as well as gray depletion zones with rims of a deeper red than the matrix characterize the red mudrocks. Carbonate nodules or

micro-accumulations are common, primarily in depletion channels. The clay-rich red beds (greater than 60% clay) commonly show large slickensides. The purple beds resemble those in the purple paleosols; however, micrite accumulations are locally present in gray depletion channels, whereas they are absent from the purple paleosols.

Many of the uppermost gray or yellow-brown beds show higher TOC contents than the remainder of the profile, suggesting that they represent A horizons. The red and purple beds are interpreted as the B horizon. Although clay weight percent increases downward from the A horizon into the underlying red and purple mudrocks, no Bt horizon can be identified. Where the grain size increases in the lowermost part of the profile, a C horizon is recognized. Fe₂O₃ usually shows only weak downward increases, as do Fe/clay ratios (Fig. 8). Thus, the red/purple paleosols resemble the purple paleosols in that they show little evidence for downward movement of iron or clay.

Like the purple paleosols, the red/purple paleosols are interpreted as Vertisols; however they differ from the purple paleosols in features of the B horizon. Although the purple part of the B horizon shows strong surface-water gleying

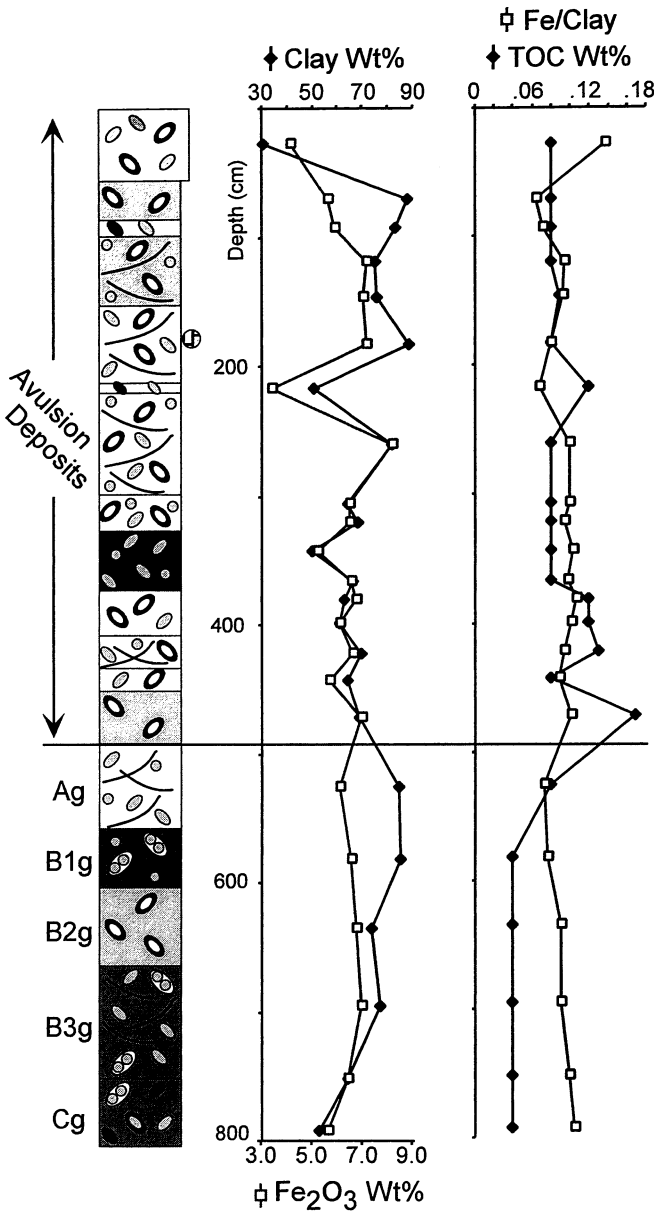


FIGURE 7 — Morphologic, textural, and chemical data for a representative purple paleosol from Elk Creek. Above the strongly developed profile are fine-grained deposits showing weak pedogenic development and interpreted as avulsion deposits. Ag and Bg, gleyed A and B horizons; B1, B2, etc. indicate subdivisions of the B horizon based on different morphologic properties. See Figure 4 for key to symbols.

(hydromorphy), the red bed reflects less intense gleying because of the presence of abundant hematite and fewer redoximorphic features. Consequently, the red/purple paleosols are interpreted to have been of intermediate drainage

conditions. They were wetter soils than the red paleosols but better drained than the purple paleosols.

Depositional Interpretation of Overbank Deposits

The fine-grained deposits on which the red, red/purple, and purple paleosols formed are interpreted as overbank deposits that resulted from episodic flooding over the channel levees (e.g., Kraus and Aslan, 1993; Kraus, 1996). The fine-grained nature of the sediment on which the paleosols formed suggests that it was deposited at least a moderate distance from the channel. The paleosols are all moderately to well developed as indicated by the absence of any relict stratification and the presence of abundant soil features and distinct soil horizons. The degree of pedogenic development implies that sediment accumulation was relatively slow (e.g., Marriott and Wright, 1993). This is consistent with deposition of the parent material at some distance from the channel.

Significance of Different Paleosols

Various morphologic features suggest that the different kinds of paleosols reflect variable drainage conditions. The red (fersiallitic) paleosols were the best drained based on the presence of a red B horizon. Although yellow-brown mottles indicate seasonal wetting of the soil, mottles are not abundant. The intense mottling and presence of iron oxide nodules in the purple paleosols are characteristic of poorly drained soils. The red/purple paleosols were of intermediate drainage based on the presence of both purple and red parts of the B horizon.

Several different kinds of paleosols are found within each study area and the paleosols among the study areas differ. McCullough Peaks has red and red/purple paleosols; Elk Creek has red/purple and purple paleosols but only sparse red paleosols. Sand Coulee is dominated by red paleosols but also has some more poorly drained, gray and yellow-brown paleosols (Kraus, 1997). A variety of factors can influence the wetness of floodplain soils including the parent material, which controls permeability; landscape position (topography); and climate. These factors operate at different spatial and temporal scales.

Differences within each study area are attributed to position on the local floodplain. Various workers have shown that floodplain paleosols that formed closer to the active channel and, thus, on coarser and more permeable sediment and in a more elevated position tend to be better drained (e.g., Fastovsky and McSweeney, 1987; Arndorff, 1993; Kraus and Aslan, 1999). In contrast, floodplain paleosols are more poorly drained if they formed more distal to the channel where the parent material was finer-grained and less permeable and the floodplain was lower and closer to the water table.

The differences among the three study areas occur at a larger, regional scale. Because of their approximate time-equivalence and relative proximity in the basin, climate is not an obvious factor in paleosol differences between McCullough Peaks and Elk Creek. Climate might have played a role in the drier paleosols found in Sand Coulee. The topographic relief of each

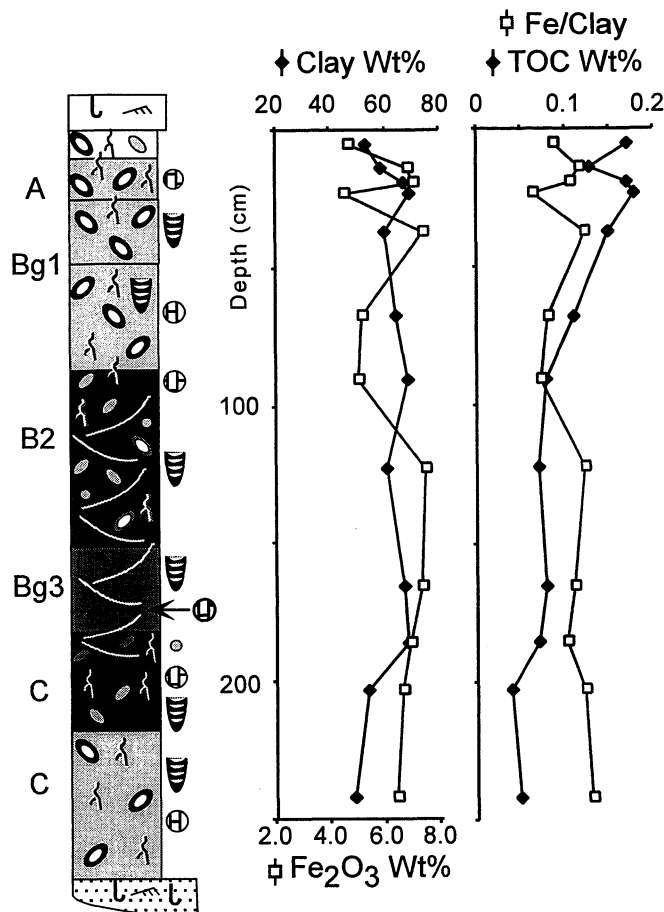


FIGURE 8 — Morphologic, textural, and chemical data for a red/purple paleosol from McCullough Peaks. A, A horizon; Bg, gleyed B horizons; C, C horizon; B1, B2, etc. indicate subdivisions of the B horizon based on different morphologic properties. See Figure 4 for key to symbols.

of the three areas is difficult to assess. Yet, all three areas were situated towards the middle of the basin, not far from the basin axis, suggesting no major differences among the three (Fig. 1).

Grain size variations (across both space and time) do appear to have influenced variations in soil wetness. The average clay content of the Elk Creek mudrocks is 78% (Table 1), and 86% of the samples analyzed have 67% clay or more. In fact, 50% of the samples exceed 79% clay content. More importantly, the purple paleosols, especially their upper parts, are developed on material that is 80-90% clay. The clay content of paleosols in both Sand Coulee and McCullough Peaks is much less (Table 1). The surface-water gleying features that are so characteristic of the Elk Creek paleosols are consistent with the clay rich parent material and the development of perched water tables. The siltier nature of the paleosols in McCullough Peaks and Sand Coulee is reflected in the absence of significant surface-water gley attributes.

Thus, depositional factors appear to have influenced paleosol morphology at the scale of the basin. Grain size differences contributed to more poorly drained paleosols in Elk Creek and better-drained paleosols in Sand Coulee and McCullough Peaks.

HETEROLITHIC INTERVALS

In all three study areas, the cumulative paleosols are interbedded with stratigraphic intervals that consist of fine-grained deposits and ribbon sandstones (Fig. 2). These heterolithic intervals have a sheet-like geometry. The best-exposed examples can be traced for more than 5 km both parallel and perpendicular to paleoslope; thickness ranges from ca. 3 to 7 m. Wherever a major sheet sandstone is present, it overlies and locally truncates a heterolithic interval (Fig. 2).

Fine-grained Deposits

Fine-grained deposits in the heterolithic intervals range from claystone to siltstone (Figs. 6 and 7). Some of the fine-grained beds show relict stratification, indicating minimal post-depositional modification of the sediment. Most of the mudrocks show evidence for pedogenic modification, including mottling, root traces and burrows, and slickensides (Figs. 6 and 7). But these features are not abundant and soil horizons are only faint, indicating that pedogenic development was only weak. Vertical sequences show erratic downward changes in grain size and geochemical properties (e.g., iron, manganese, and total organic carbon content), which is also characteristic of alluvial sediments that have undergone only weak pedogenesis (e.g., Duchaufour, 1982). Because soil horizons are typically faint, delimiting soil profiles is difficult. Those profiles that can be recognized are thin (less than 1 m thick) and vertically stacked, indicating that these are compound paleosols. These form when sedimentation is rapid and unsteady (e.g., Marriott and Wright, 1993).

Ribbon and Thin Sheet Sandstones

Most of the sandstones within the heterolithic intervals are channel sandstones that are classified as ribbons because they are narrow with width/thickness ratios that are generally less than 10. The ribbon sandstones have been well documented throughout the Willwood Formation (Kraus 1996; Kraus and Gwinn, 1997; Dykstra, 1999; Davies-Vollum and Kraus, in press). They have scoop-shaped bases that cut down as much as 5 m into underlying mudrocks. In some cases, they cut down into the well-developed paleosol below the heterolithic interval in which they sit (Fig. 2). Although ribbons range from 0.3 to 9 m thick, the great majority (ca. 75%) of those described are less than 3 m thick. Those that are well exposed and can be mapped are slightly sinuous to straight in plan view.

Although internal stratification in the ribbons is usually poorly preserved, where bedding is present, most structures are generally small-scale and large-scale trough cross-stratification. Where ribbon margins are preserved, many have thin

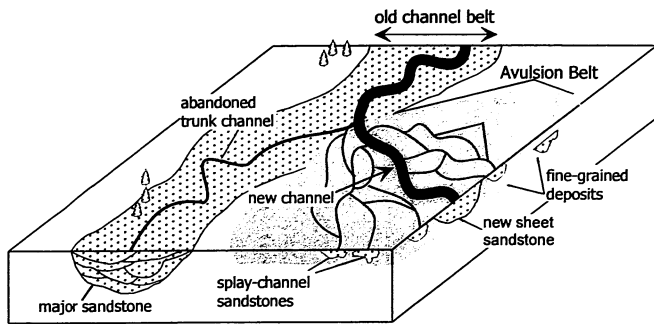


FIGURE 9 — Schematic diagram showing avulsion belt deposits that formed as the trunk river avulsed. Networks of small crevasse splay channels, which produce ribbon sandstones, feed the avulsion belt. Most of the avulsion belt consists of fine-grained deposits, and these encase the ribbon sandstones. The now abandoned trunk channel produced the major sandstone. A new trunk channel has formed but covers only a small part of the laterally extensive avulsion belt. The new channel has begun to create another sheet sandstone. Modified from Smith et al. (1989).

(0.3 to 1 m thick) sandstone or siltstone wings extending from the top. The sheets become thinner and finer-grained away from their associated ribbon sandstone and eventually grade into mudstones and claystones. Many of the larger ribbons show paleoflow parallel to flow in the major sheet sandstones in a particular study area. Smaller ribbons show paleocurrent trends that differ more from the trend of the associated major sandstone bodies. Field mapping shows that several ribbon sandstones can be present at the same stratigraphic level, suggesting that the channels were active at the same time and, thus, may have formed channel networks (Kraus and Gwinn, 1997; Davies-Vollum and Kraus, in press).

Interpretation of Avulsion Deposits

The heterolithic intervals have been interpreted as ancient avulsion belt deposits (e.g., Kraus and Aslan, 1993; Kraus, 1996; Kraus and Wells, 1999). In the modern fluvial record, avulsion deposits have been described from the Saskatchewan River in Canada (e.g., Smith et al., 1989, Perez-Arlucea and Smith, 1999). These deposits form as the trunk river avulses or is abandoned (Fig. 9). In the abandonment process, a network of splay channels takes up the flow from the old channel and those networks spread water and sediment onto low parts of the surrounding floodplain. The avulsion deposits consist of ribbon sands, representing deposits of the splay channels, and fine-grained deposits, representing overbank deposits from the splay channels. Eventually a new trunk channel develops, and the old channel is abandoned. Locally, the new channel that was established following avulsion truncates the avulsion deposits.

The mix of fine-grained deposits and sandstone as well as the arrangement of those two lithologies in the Willwood heterolithic intervals are similar to those described from the Saskatchewan River avulsion belt (Figs. 2 and 9). The weak pedogenic modification of the fine-grained Willwood deposits shows that sedimentation was very rapid, which is consistent with the modern example where the 2-3 m thick avulsion belt has been deposited in only 100 years (e.g., Smith et al., 1989). The ribbon sands also show similarities. Most ribbon sandstones in the Willwood Formation have W/T ratios similar to those observed from ribbon sands in the Saskatchewan system. Paleoflow trends of the Willwood ribbons, which are subparallel to or in the same direction as paleoflow in the trunk channel, resemble the trends of splay channels in the Saskatchewan system. Finally, the new Saskatchewan channel locally truncates its associated avulsion belt, and, in the Willwood Formation, major channel sandstones regularly overlie and scour into heterolithic intervals.

The ribbon sandstones are interpreted as ancient splay channels that fed the developing avulsion belt; the thin sheets probably formed as sheet floods or overbank deposits from the splay channels (Fig. 9). The presence of ribbons at the same stratigraphic level indicates that small channels coexisted on a particular area of the floodplain. The weakly developed paleosols that formed on the fine-grained parts of the heterolithic intervals indicate that this sediment was deposited very rapidly and that it had a depositional history distinct from the mudrocks on which the more strongly developed paleosols formed. These mudrocks were probably deposited in interchannel areas as overbank deposits from the splay channels, not from the trunk river.

Significance of Avulsion Deposits

The process of avulsion was important to the Willwood depositional system. First, because avulsion quickly deposited a relatively thick (several meters) interval of sediment on the floodplain, it buried and, thus, preserved, the underlying cumulative soil. This may be one reason paleosols are so distinct and well preserved in the Willwood Formation. Second, measured stratigraphic sections in the three study areas show that avulsion deposits make up approximately 50% of the fine-grained deposits in the Willwood Formation (Fig. 10). That fact emphasizes the fact that two processes - overbank flooding and channel avulsion - were responsible for construction of the Willwood floodplain deposits. This is in contrast to the traditional model of meandering river systems in which all of the non-channel deposits are attributed to overbank flooding. The volumetric significance of the avulsion deposits in the Willwood Formation probably reflects the fact that, by analogy to the modern example, an individual avulsion belt covered a very large area on the ancient floodplain. The Saskatchewan avulsion complex, which is still undergoing development, covers 500 km². Finally, the fact that fine-grained sediment resulted from two depositional processes led to two major groups of paleosols (Fig. 10). Weakly developed

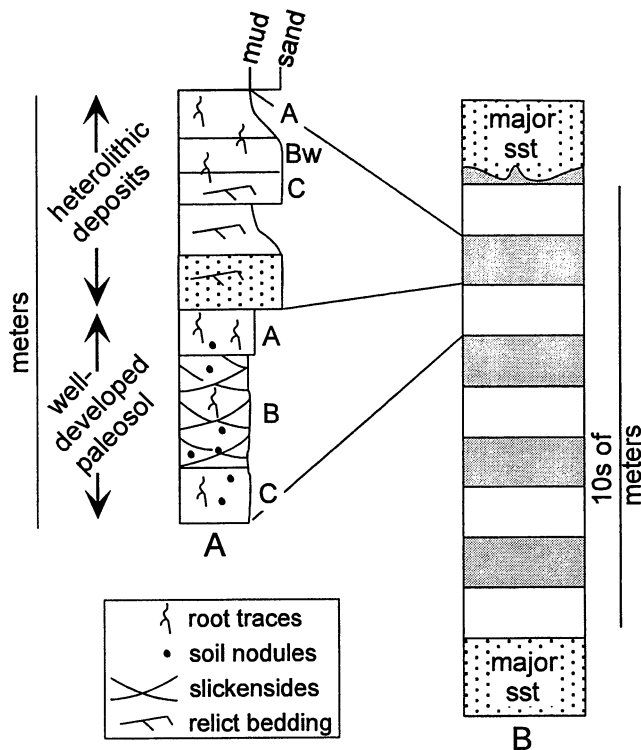


FIGURE 10 — Schematic diagram of Willwood floodplain deposits. A, two kinds of floodplain deposit are recognized based on their paleosol properties: fine-grained deposits with well-developed paleosols are interpreted as overbank deposits, while heterolithic deposits with weakly developed paleosols are interpreted as avulsion deposits. B, at the scale of tens of meters, those two genetically different kinds of floodplain deposit are interbedded to form cycles of weak/strong pedogenesis. Major channel sandstones form the top and bottom of the vertical section of floodplain deposits. Those sandstones appear and disappear because of channel avulsion. Letters to the side of column A indicate soil horizons. Bw, weakly differentiated B horizon.

paleosols formed on avulsion deposits because net sediment accumulation rates exceeded local rates of pedogenesis. Cumulative paleosols formed on the gradually accumulating overbank deposits.

SUMMARY: DEPOSITIONAL SETTING AND ALLUVIAL STRATIGRAPHY

The Willwood Formation was deposited across the Bighorn Basin by meandering trunk rivers that were on the order of 4 to 10 meters deep. The mudrock-dominated lithology of the study

section indicates that the trunk rivers were mixed load channels that carried abundant clay and silt in addition to sand. The river channels would have been surrounded by a meanderbelt that was ca. 1 to 2 km wide, which is the width of the sheet sandstones that are the depositional product of the trunk rivers. The multi-story and multi-lateral nature of the sandstone bodies resulted from amalgamation of point bar deposits within the channel belt. The channels were confined to their meander belts for a period of time sufficient to produce up to 6 vertically stacked stories.

Overbank flooding of the trunk channel, which may have taken place on a yearly basis, produced thin increments (mm) of fine-grained sediment on the floodplain. Because this sediment accumulated very slowly, pedogenesis was concurrent with deposition and yielded cumulative paleosols. The paleosols vary in terms of their drainage both within a particular part of the basin and among different parts of the basin. The local differences reflect distance from the sediment-producing channel. Quantitative grain size analyses suggest that the larger scale differences were at least partly controlled by regional differences in grain size. Coarser sediment produced better-drained soils; finer sediment produced more poorly drained soils.

Episodic avulsion of the trunk channel also contributed to construction of the Willwood floodplain. Avulsion proceeded by the progradation of crevasses-splay systems onto the floodplain. A network of splay channels took up flow from the channel undergoing abandonment. This process produced avulsion deposits, which are several meters thick and consist of fine-grained deposits that surround sandbodies deposited in the splay channels. Eventually the old channel was completely abandoned. A new trunk channel was established and locally truncates the avulsion belt. Because of rapid deposition rates, the fine-grained deposits in the avulsion belt show only weak pedogenic modification.

The three components documented for the Willwood alluvial system differ from the two components accepted by most meandering river models. Most models recognize sandstones deposited by the major channels and fine-grained deposits produced by overbank flooding of those trunk rivers. In the Willwood Formation, only about half of the fine-grained deposits appear to have been produced by overbank flooding of the trunk channels. The other half of the fine-grained deposits were the result of deposition on the floodplain as the trunk river underwent avulsion. Recognizing these two kinds of fine-grained deposits in the Willwood Formation is important for correctly reconstructing how the floodplain developed over time. Furthermore, these two styles of floodplain construction - slow, steady overbank deposition and rapid, unsteady avulsion deposition - have had a significant impact on paleosol formation in the Willwood Formation. First, the two processes produced paleosol cycles with more strongly developed paleosols alternating vertically with intervals showing only weak pedogenesis (Fig. 10). Second, the rapid deposition of the avulsion deposits was instrumental in preserving the more strongly developed paleosols that were buried.

ACKNOWLEDGMENTS

This research was supported by National Science Foundation Grants EAR-9303959 and 9706115 to MJK. Research on the sedimentology of Paleogene deposits in the Bighorn Basin has included Andres Aslan, Mason Dykstra, Brian Gwinn, Andy Pulham, and Tina Wells.

LITERATURE CITED

- ARNDORFF, L. 1993. Lateral relations of deltaic palaeosols from the Lower Jurassic Ronne Formation on the island of Bornholm, Denmark. *Palaeogeography, Palaeoclimatology, Palaeoecology*, 100: 235-250.
- ASLAN, A., and W. J. AUTIN. 1998. Holocene flood-plain soil formation in the southern lower Mississippi Valley: implications for interpreting alluvial paleosols. *Geological Society of America Bulletin*, 110: 433-449.
- BLACKSTONE, D. L., Jr. 1986. Foreland compressional tectonics: southern Bighorn Basin and adjacent areas, Wyoming. *Geological Survey of Wyoming, Report of Investigations*, 34: 1-32.
- BIGHAM, J. M., D. C. GOLDEN, S. W. BUOL, S. B. WEED, and L. H. BOWEN. 1978. Iron oxide mineralogy of well-drained Ultisols and Oxisols: II. Influence on color, surface, and phosphate retention. *Soil Science Society of America Journal*, 42: 825-830.
- BLATT, H., G. MIDDLETON, and R. MURRAY. 1972. *Origin of Sedimentary Rocks*. Prentice-Hall, Inc., Englewood Cliffs, New Jersey, 634 pp.
- BLUME, H. P. and U. SCHWERTMANN. 1969. Genetic evaluation of profile distributions of aluminum, iron, and manganese oxides. *Soil Science Society of America Proceedings*, 33: 438-444.
- BOWN, T. M., and M. J. KRAUS. 1987. Integration of channel and floodplain suites, I. Developmental sequence and lateral relations of alluvial paleosols. *Journal of Sedimentary Petrology*, 57: 587-601.
- BOWN, T. M., K. D. ROSE, E. L. SIMONS, and S. L. WING. 1994. Distribution and stratigraphic correlation of fossil mammal and plant localities of the Fort Union, Willwood, and Tatman Formations (upper Paleocene-lower Eocene), central and southern Bighorn Basin, Wyoming. *U. S. Geological Survey Professional Paper*, 1540: 1-103.
- BROWN, W. G. 1993. Structural style of Laramide basement-cored uplifts and associated folds. *In: A. W. Snoke, J. R. Steidtmann, and S. M. Roberts (eds.), Geology of Wyoming. Geological Survey of Wyoming Memoir*, 5: 312-371.
- BUOL, S. W., F. D. HOLE, R. J. McCracken, and R. J. SOUTHARD. 1997. *Soil Genesis and Classification*, 4th Edition, Iowa State University Press, Ames, 527 pp.
- CLYDE, W. C. 1997. Stratigraphy and mammalian paleontology of the McCullough Peaks, northern Bighorn Basin, Wyoming: implications for biochronology, basin development, and community reorganization across the Paleocene-Eocene boundary. Unpublished Ph. D. thesis, University of Michigan, Ann Arbor, 271 pp.
- DAVIES-VOLLUM, S., and M. J. KRAUS. 2001. The relationship between alluvial backswamps and avulsion cycles: an example from the Willwood Formation of the Bighorn Basin, Wyoming. *Sedimentary Geology*, in press.
- DUCHAUFOR, P. 1982. *Pedology*. Allen and Unwin, London, 448 pp.
- DYKSTRA, M. 1999. Fluvial architecture in the lower Eocene Willwood Formation, northwestern Wyoming as an indicator of avulsion style. Unpublished M.S. thesis, University of Colorado, Boulder, 60 pp.
- FANNING, D. S., M. C. B. FANNING. 1989. *Soil: Morphology, Genesis, and Classification*. Wiley and Sons, New York, 395 pp.
- FASTOVSKY, D. E., and K. McSWEENEY. 1987. Paleosols spanning the Cretaceous-Paleogene transition, eastern Montana and western North Dakota. *Geological Society of America Bulletin*, 99: 66-77.
- HAGEN, E. S., M. W. SHUSTER, and K. P. FURLONG. 1985. Tectonic loading and subsidence of intermontaine basins: Wyoming foreland province. *Geology*, 13: 585-588.
- KAMPF, N., U. SCHWERTMANN. 1982. Goethite and hematite in a climosequence in southern Brazil and their application in classification of kaolinitic soils. *Geoderma*, 29: 27-39.
- KRAUS, M. J. 1996. Avulsion deposits in lower Eocene alluvial rocks, Bighorn Basin, Wyoming. *Journal of Sedimentary Research*, 66B: 354-363.
- KRAUS, M. J. 1997. Early Eocene alluvial paleosols: pedogenic development, stratigraphic relationships, and paleosol/landscape associations. *Palaeogeography, Palaeoclimatology, Palaeoecology*, 129: 387-406.
- KRAUS, M. J., and A. ASLAN. 1993. Eocene hydromorphic paleosols: significance for interpreting ancient floodplain processes. *Journal of Sedimentary Petrology*, 63: 453-463.
- KRAUS, M. J., and A. ASLAN. 1999. Paleosol sequences in floodplain environments: a hierarchical approach. *In: M. Thiry and S. Coincon (eds.), Palaeoweathering, Palaeosurfaces and Related Continental Deposits, International Association of Sedimentologists Special Publication*, 27: 303-321.
- KRAUS, M. J., and B. M. GWINN. 1997. Controls on the development of early Eocene avulsion deposits and floodplain paleosols, Willwood Formation, Bighorn Basin. *Sedimentary Geology*, 114: 33-54.
- KRAUS, M. J., and T. M. WELLS. 1999. Recognizing avulsion deposits in the ancient stratigraphical record. *In: N. D. Smith and J. Rogers (eds.), Fluvial Sedimentology VI, International Association of Sedimentologists Special Publication*, 28: 251-268.
- MACEDO, J., and R. B. BRYANT. 1987. Morphology, mineralogy, and genesis of a hydrosequence of Oxisols in Brazil. *Soil Science Society of America Journal*, 51: 690-698.
- MACEDO, J., and R. B. BRYANT. 1989. Preferential microbial reduction of hematite over goethite in a Brazilian Oxisol. *Soil Science Society of America Journal*, 53: 1114-1118.
- MARRIOTT, S. B., and V. P. WRIGHT. 1993. Palaeosols as indicators of geomorphic stability in two Old Red Sandstone alluvial suites, South Wales. *Journal of the Geological Society, London*, 150: 1109-1120.

- MOROZOVA, G. S., and N. D. SMITH. 2000. Holocene avulsion styles and sedimentation patterns of the Saskatchewan River, Cumberland Marshes, Canada. *Sedimentary Geology*, 130: 81-105.
- PEREZ-ARLUCEA, M., and N. D. SMITH. 1999. Depositional patterns following the 1870s avulsion of the Saskatchewan (Cumberland Marshes, Saskatchewan, Canada). *Journal of Sedimentary Research*, 69: 62-73.
- PiPUJOL, M. D., and P. BUURMAN. 1994. The distinction between ground-water gley and surface water gley phenomena in Tertiary paleosols of the Ebro basin, NE Spain. *Palaeogeography, Palaeoclimatology, Palaeoecology*, 110: 103-113.
- PiPUJOL, M. D., and P. BUURMAN. 1997. Dynamics of iron and calcium carbonate redistribution and palaeohydrology in middle Eocene alluvial paleosols of the southeast Ebro Basin margin (Catalonia, northeast Spain). *Palaeogeography, Palaeoclimatology, Palaeoecology*, 134: 87-107.
- ROSE, K. D. 1981. The Clarkforkian land-mammal age and mammalian faunal composition across the Paleocene-Eocene boundary. *University of Michigan Papers on Paleontology*, 26: 1-196.
- SCHUMACHER, B. A., W. J. DAY, M. C. AMACHER, and B. J. MILLER. 1988. Soils of the Mississippi River alluvial plain in Louisiana. *Louisiana Agricultural Experiment Station Bulletin*, 796: 1-275.
- SCHWERTMANN, U. 1993. Relations between iron oxides, soil color, and soil formation. *Soil Science Society of America Special Publication*, 31: 51-69.
- SMITH, N. D., T. A. CROSS, J. P. DUFFICY, and S. R. CLOUGH. 1989. Anatomy of an avulsion. *Sedimentology*, 36: 1-24.
- SOIL SURVEY STAFF. 1975. *Soil Taxonomy*. U. S. Department of Agriculture Handbook 436: 1-754.
- SOIL SURVEY STAFF. 1998. *Keys to Soil Taxonomy*, 8th Edition. U. S. Department of Agriculture Natural Resource Conservation Service, 327 pp.
- THOMAS, R. G., D. G. SMITH, J. M. WOOD, J. VISSER, E. A. CALVERLEY-RANGE, and E. H. KOSTER. 1987. Inclined heterolithic stratification terminology, description, interpretation and significance. *Sedimentary Geology*, 53:123-179.
- TORRENT, J., U. SCHWERTMANN, and D. G. SCHULZE. 1980. Iron mineralogy of some soils in two river terrace sequences in Spain. *Geoderma*, 23: 191-208.
- VEPRASKAS, M. J. 1994. Redoximorphic features for identifying aquic conditions. *North Carolina Agricultural Research Service, Technical Bulletin*, 301: 1-74.
- VEPRASKAS, M. J., L. P. WILDING, and L. R. DREES. 1992. Aquic conditions for soil taxonomy: concepts, soil morphology and micromorphology. *In: A. J. Ringrose-Voase and G. S. Humphreys (eds.), Soil Micromorphology: Studies in Management and Genesis*. Elsevier, pp. 117-131.
- WILDING, L. P., and D. TESSIER. 1988. Genesis of Vertisols: shrink-swell phenomena. *In: L. P. Wilding and R. Puentes (eds.), Vertisols: Their Distribution, Properties, Classification, and Management*. Texas A&M Technical Monograph, 18: 205-225.
- YAALON, D. H., D. KALMAR. 1978. Dynamics of cracking and swelling clay soils: displacement of skeletal grains, optimum depth of slickensides, and rate of intra-pedonic turbation. *Earth Surface Processes*, 3: 31-42.

NOT JUST RED BEDS: THE OCCURRENCE AND FORMATION OF DRAB SECTIONS IN THE WILLWOOD FORMATION OF THE BIGHORN BASIN

K. SIÂN DAVIES-VOLLUM

Geology Department, Pomona College, 609 North College Avenue, Claremont, California 91711

Abstract.— The lower Eocene Willwood Formation of the Bighorn Basin is predominantly bright colored, but it does preserve drab-colored intervals composed of carbonaceous shales, low-chroma paleosols and sandstones. These drab intervals are found throughout the basin but are stratigraphically limited to approximately the upper and lower 200 m of the Willwood Formation. Drab intervals on Fifteenmile Creek and on the South Fork of Elk Creek have a characteristic stratigraphic sequence of (1) basal hydromorphic soil; (2) carbonaceous shale; (3) cumulative, immature paleosols that enclose ribbon sandstones; capped by (4) an orange-brown paleosol. This is similar to avulsion sequences that have been described from other parts of the Willwood Formation, except that the drab intervals have hydromorphic paleosols and carbonaceous shales at their base instead of more mature paleosols. The drab intervals have been interpreted as forming in distal alluvial environments that experienced trunk channel avulsions and they provide a previously undocumented link between trunk channel processes and distal floodplain environments. The limited stratigraphic distribution of drab intervals in the Willwood Formation is probably related to drainage, with poor drainage dominating those intervals. Drainage is controlled by local variation in climate and accommodation space associated with regional uplift. Uplift of the Owl Creek Mountains is probably an important factor explaining the absence of drab intervals in the middle part of the Willwood Formation.

INTRODUCTION

The Willwood Formation of the Bighorn Basin is distinguished from the underlying Fort Union Formation by its predominantly red, purple, and yellow-brown beds that give outcrops a striking appearance (Van Houten, 1944). These bright colors reflect the predominance of well-developed paleosols that formed on alluvial floodplains during the early Eocene (Wing and Bown, 1985, Kraus, 1992). However, there are some stratigraphic sections in the Willwood Formation that are predominantly drab in color. Laterally extensive carbonaceous shales, low-chroma paleosols, and sandstones characterize these drab intervals (Fig. 1). The carbonaceous shales are the only beds with significant amounts of organic carbon in the Willwood Formation. This is unlike other Eocene conti-

mental rocks of Western Interior basin, such as those of the Powder River Basin that contain extensive coal deposits (Flores and Warwick, 1984).

Drab intervals in the Willwood Formation occur at a variety of locations in the Bighorn Basin (Fig. 2). However their stratigraphic distribution is confined to only two parts of the 780 m thickness of the Willwood Formation (Wing, 1984), the lowermost 200 m and uppermost 180 m (Fig. 3). In the lower part of the Willwood Formation drab sections with laterally continuous carbonaceous shales are found in the following areas:

1. Elk Creek, Antelope Creek, and Three Sisters area west of Greybull: drab sections are most abundant in the basal 150 m but some drab intervals are found up into the basal 350 m.
2. Foster Gulch: drab sections are scattered in the lower 100-200 m.

In: Paleocene-Eocene Stratigraphy and Biotic Change in the Bighorn and Clarks Fork Basins, Wyoming (P. D. Gingerich, ed.), University of Michigan Papers on Paleontology, 33: 29-35 (2001).

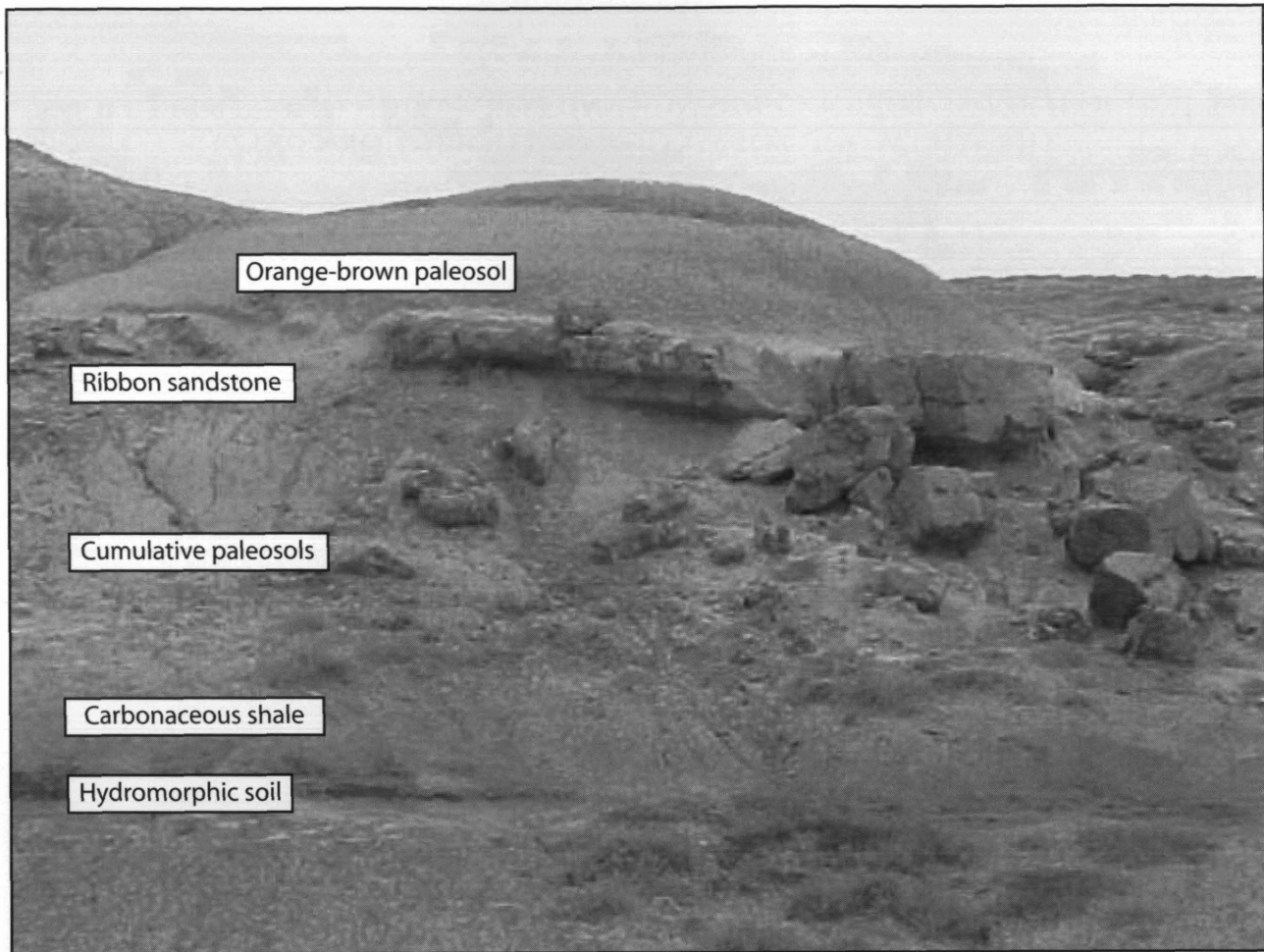


FIGURE 1 — Drab interval on the South Fork of Elk Creek showing lithologies described in the text. The section here is approximately 6 m thick.

3. North and east side of McCullough Peaks: some drab intervals found above 200 m.
4. Flanks of Oregon Basin north of Meeteetse: drab sections occupy the lower 100 m.

In the upper part of the Willwood Formation, drab intervals are found:

5. South side of Fifteenmile Creek drainage (Bobcat Ridge/Squaw Buttes Divide): between about 620 m and the top of the formation.
6. North and south sides of Tatman Mountain: between about 620 m and the top of the formation.

Here I will focus on the lithology and depositional environments of drab intervals in two of these areas: the upper part of the Willwood Formation on Fifteenmile Creek, and the lower part of the Willwood Formation along the South Fork of Elk

Creek (Figs. 2-3). Carbonaceous shales in these sections are the same as those originally described as WCS 15 (Fifteenmile Creek) and WCS 7 (South Fork of Elk Creek) (Wing, 1984). In addition, Farley (1990) described the palynology of five facies in the drab interval on the South Fork of Elk Creek.

DRAB SECTIONS ON ELK CREEK AND FIFTEENMILE CREEK

Drab intervals are defined by the presence of laterally continuous carbonaceous shales that compose up to 20% of stratal thickness in the lower- and uppermost portions of the Willwood formation (Wing, 1984). The shales can be traced significant distances along strike in outcrop. On Elk Creek the carbonaceous shale can be traced for 3 km in a north-south direction and on Fifteenmile Creek for 18 km in an east-west direction. This is in contrast to carbonaceous shales in the middle part of the Willwood Formation (approximately 200-680 m) where

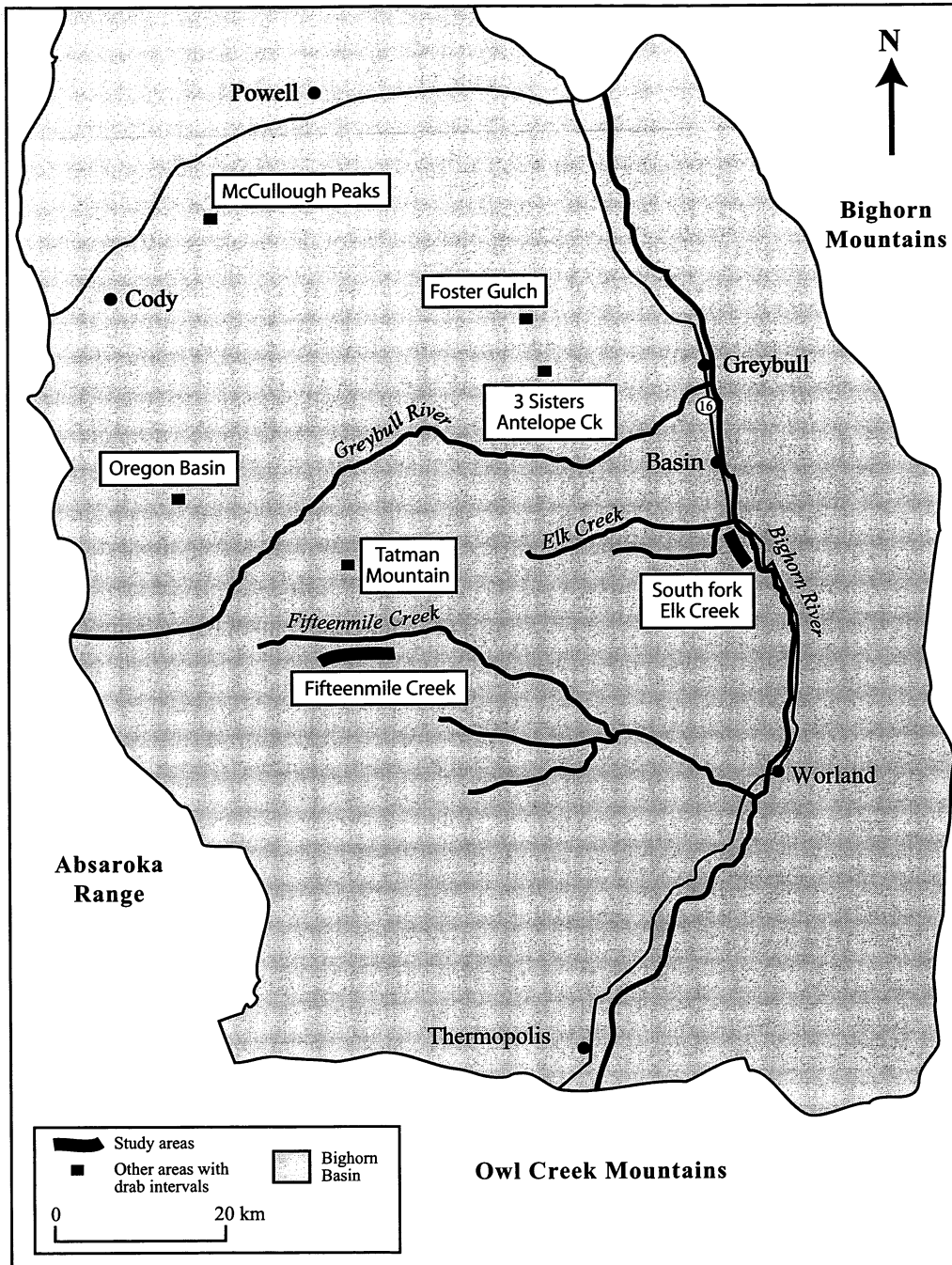
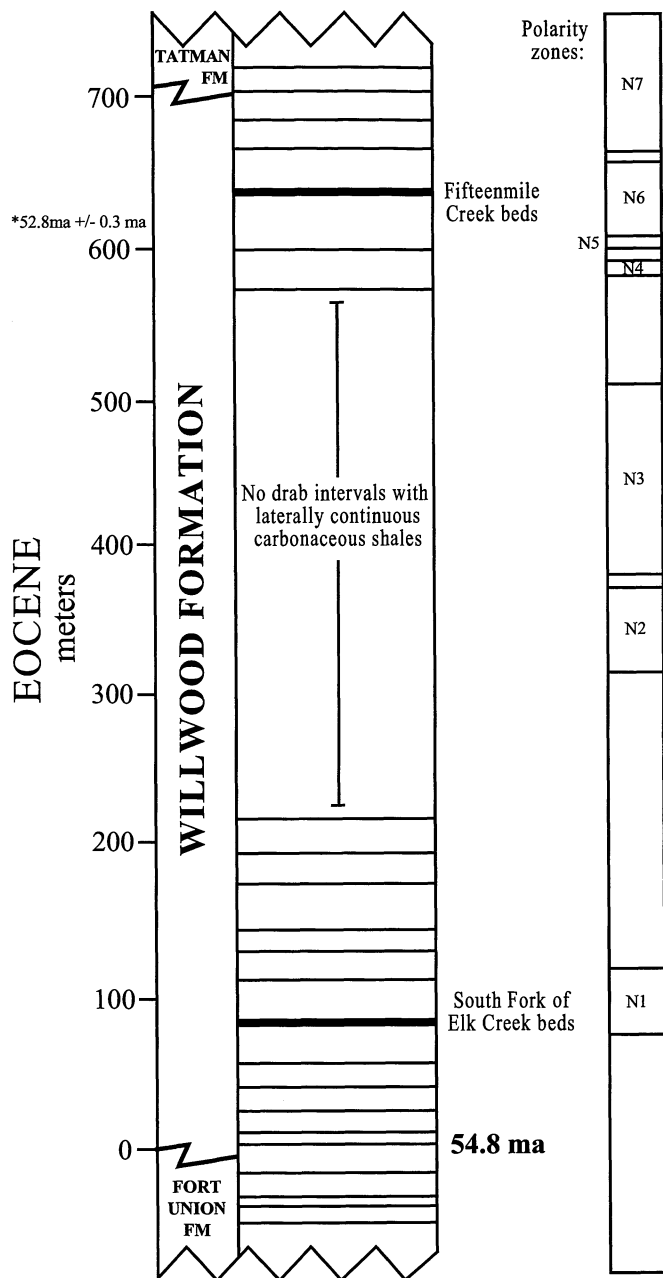


FIGURE 2 — Map of the Bighorn basin showing geographic locations of drab intervals containing laterally extensive carbonaceous shales. The two areas described in this paper are highlighted in bold type.

organic-rich deposits are confined to lenticular shale units interpreted as channel fill deposits (Wing, 1984). It should be noted, however, that channel fills occurring throughout the Willwood Formation are not limited to carbonaceous shales

but also comprise paleosols, laminated claystones, and siltstones.

In addition to laterally continuous carbonaceous shales, drab intervals contain low-chroma paleosols and sandstones that can



* Tauxe et al, 1994

FIGURE 3 — Section through the Willwood Formation showing the stratigraphic positions of drab intervals containing laterally extensive carbonaceous shales. The radiometric calibration and polarity zones are from Tauxe et al. (1994).

have ribbon, tabular, and massive geometries. These lithologies occur in a common sequence of: (1) basal thick gray paleosol, (2) carbonaceous shale, (3) a series of drab paleosols that encloses the sandstone bodies, and (4) an orange-brown paleosol that caps the sequence (Fig. 4).

Carbonaceous shales: general characteristics and depositional environment

Carbonaceous shales are drab brown, often occurring as friable ledges in outcrop that stand out from surrounding paleosols. Despite their lateral continuity the shales are commonly not thick (maximum bed thickness is approximately 0.75 m along the South Fork of Elk Creek and approximately 3 m on Fifteenmile Creek). In both cases the bed can thin to as little as ten cm and at the western end of the Fifteenmile Creek outcrop the carbonaceous shale grades laterally into a gray mudrock. There is considerable lateral variability in organic content, occurrence of plant fossils, clastic content, and preservation of bedding. Davies-Vollum and Wing (1998) identified six sub-facies within carbonaceous shale beds based largely on these criteria.

The most striking vertical variation within carbonaceous shale beds is an upward increase in clastic material accompanied by a decrease in total organic carbon [TOC]. TOC content at the middle and top of the beds varies from 5-10%. However, at the base of the shale are mats of plant fossils and rare, thin stringers of lignite with TOC content of over 65%. Although basal organic content is high, the best preserved plant fossils are found in the middle and upper parts of the bed where they are preserved in clastic-rich lenses. These carbonaceous shales are one of the few lithologies in which abundant plant fossil material can be found in the Willwood Formation. This material comprises gypsified wood, carbonaceous mats and well-preserved singular angiosperm fossils that are found in the more clastic-rich parts of the shale. Throughout the shale yellow-colored natrojarosite is present and gypsum is common. Particularly well-formed crystals of gypsum, up to 5 cm in length, are found in association with the more organic-rich portions of the shales.

These carbonaceous shales are interpreted as having formed in topogeneous backswamps that developed in low-lying distal environments on the alluvial floodplain (Davies-Vollum and Wing, 1998). The observed vertical and lateral variations reflect subtle spatial and temporal changes in drainage, redox conditions, bioturbation, and clastic inputs in the backswamp environment. Natrojarosite and gypsum are derived from original pyrite that indicates anoxia and waterlogging during the accumulation of organic material. The limited fine-grained clastic component at the base of the shale reflects a period where distal areas of the floodplain were cut-off from sediment source. The increase in clastic content toward the top of the shale reflects a reintroduction of sediment into distal areas of the floodplain.

Drab paleosols: general characteristics and depositional environment

Paleosols within the drab sections are of low-chroma and although superficially similar, three types can be identified. The first type of paleosol, type-1, was described by Davies-Vollum (1999). It underlies the carbonaceous shale along the whole length of outcrop and has well defined upper contact

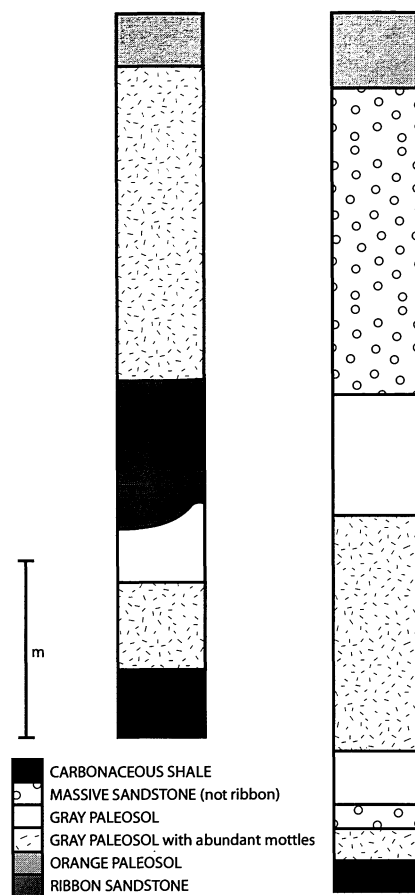


FIGURE 4 — Representative lithologic sections of the drab interval on the South Fork of Elk Creek. These sections illustrate some of the lateral and vertical changes within the drab interval on the South Fork of Elk Creek. Scale = 1 meter.

with the shale. The paleosol is homogeneous and generally fine grained, although it does contain rare sand. It has a blue-gray color, mottled orange with goethite. Unlike the overlying carbonaceous shale the only organic materials it preserves are thin (mm scale) rootlets.

The second type of paleosol, type-2, occurs as multiple soil units above the carbonaceous shale. It contains primary bedding structures, but no soil horizons. It is gray in color, with red and orange mottles. Like type-1 paleosols, type-2 paleosols contain small rootlets.

The third type of paleosol that occurs in drab intervals, type-3, is yellow-brown, rather than gray, and caps the sequence of beds characteristic of drab sections. Type-2 and type-3 paleosols are described in greater detail in Davies-Vollum and Kraus (2001)

Differences between paleosols reflect their mode of formation, drainage, and sediment accumulation rates. The color and mottling of the type-1 paleosol suggest that it formed as a

hydromorphic soil dominated by gley processes that inhibited the development of a more mature soil. However, the presence of root structures suggests that this hydromorphic soil periodically experienced dry conditions (Davies-Vollum, 1999). The varied mottling of type-2 paleosol indicates better drainage than type-1 paleosols. However, the presence of primary sedimentary structures shows that these soils were immature. Deposition and pedogenesis were concurrent. Weak pedogenic modification suggests that sedimentation was rapid, and accommodation space was high (Davies-Vollum and Kraus, 2001). Type-2 soils are cumulative; incorporating rapidly deposited sediment on the distal floodplain. However, they are immature, unlike cumulative soils described by Kraus and Aslan (1993). The orange color of the type-3 paleosols indicates a more mature soil, reflecting both better-drained substrate and lower rates of sediment accumulation (Davies-Vollum and Kraus, 2001).

Sandstones: characteristics and depositional environment

Sandstones within the drab intervals occur enclosed by cumulative (type-2) paleosols above the carbonaceous shales (Fig. 1). The most distinctive sandstone geometry is ribbon-like in form, with an erosive base. However, there are also massive beds that are indistinct from the paleosols, and (in the Fifteenmile Creek section) some thin, tabular sand bodies.

Ribbon sandstone outcrops influence the local topography; they tend to outcrop along the top of ridges in both areas because they are more resistant to erosion than the carbonaceous shales and paleosols. This outcrop pattern enables them to be mapped and it is possible to distinguish channel networks. On the South Fork of Elk Creek, sandstone ribbons cluster at particular stratigraphic levels within the sequence of cumulative paleosols (Davies-Vollum and Kraus, 2001). Although the width and height of the ribbons is greater on Fifteenmile Creek, and some ribbons occur in nested sets, networks can also be identified.

Ribbon sandstones locally incise the cumulative paleosols (Fig. 4), and some of them cut down far enough to scour the carbonaceous shale. Some ribbon sandstones in the Fifteenmile Creek area have a basal lag of poorly sorted, matrix-supported clasts up to a centimeter in diameter. Here and on the South Fork of Elk Creek convolute bedding is common, and there is evidence for loading and squeezing of the underlying carbonaceous shale. Despite convolutions, planar and trough cross beds are preserved in some outcrops. On the South Fork of Elk Creek these have yielded paleocurrent data (Davies-Vollum and Kraus, 2001). These paleocurrent data, together with mapping of the sandstone networks, indicate that channels depositing the ribbon sandstones formed anastomosed networks.

Convolute bedding within the ribbon sandstones, together with the loading and squeezing of carbonaceous shales, indicates a high water table and rapid deposition at the time of sandstone influx. Basal lags within some sandstone ribbons also indicate rapid, high-energy influxes of sediment. The anastomosing networks of sandstone ribbons are similar to those that develop during channel avulsion, feeding crevasse-splay

networks that can move rapidly out onto distal parts of a floodplain.

Sequence of events recorded by drab intervals

Drab intervals containing laterally continuous carbonaceous shales on Fifteenmile Creek and on the South Fork of Elk Creek have been interpreted as distal alluvial environments that record trunk channel avulsions (Davies-Vollum and Kraus, 2001). Hydromorphic soils at the bases of these intervals formed in periodically dry swamps. A high water table caused gleying within the soil, but periodic drying degraded organic material. Organic material began to accumulate when clastic input to distal areas became restricted and waterlogging caused anoxia. The waterlogging is marked by the switch from hydromorphic paleosol to carbonaceous shale.

Lack of sediment accumulation contributed to poor drainage in the distal backswamp, as this area became one of the lowest areas on the floodplain. Restriction of clastic material was probably due to an elevated trunk channel that had built up its alluvial ridge. When an alluvial ridge was finally breached, the trunk channel avulsed and crevasse-splay complexes rapidly filled in the distal low-lying topography. Avulsion of the trunk channel provided the mechanism by which carbonaceous shales were preserved. Pedogenesis resumed, with frequent clastic input to the distal floodplain and a lower water table. This is marked by the switch from carbonaceous shale to cumulative paleosols.

The mix of ribbon sandstones and cumulative paleosols, and their rapid rates of deposition, suggest that the stratigraphic interval directly above the carbonaceous shale was deposited on an avulsion belt. Establishment of a new trunk channel is marked by the disappearance of channel networks. The avulsion deposits filled in the topographic depression where the carbonaceous shale had developed, so the water table was lowered and the substrate was better drained. Reduced accommodation space slowed the rate of accumulation of clastic material, which, together with improved drainage, promoted the development of the more strongly developed, but still relatively drab, orange-brown paleosols. Pedogenesis in a relatively well-drained substrate prevailed until the sequence was repeated, the water table rose, and paleosols became increasingly hydromorphic in character.

SIGNIFICANCE AND DISTRIBUTION OF DRAB INTERVALS

Drab intervals, despite being deposited in distal alluvial environments, record changes in both sediment accumulation rate and drainage that can be linked to trunk channel processes. This is significant because it is the first recognized link between trunk channel processes and distal alluvial environments.

The lithology and stratigraphy of drab sections are similar to avulsion intervals that have previously been described from other parts of the Willwood Formation (Kraus, 1996; Kraus

and Wells, 1999). The only difference is that the avulsion sections within drab intervals are underlain by a carbonaceous shale and a hydromorphic paleosol instead of well-developed paleosols. The general similarity between avulsion intervals suggests that similar trunk channel processes were active throughout deposition of the Willwood Formation, but that the areas that received avulsion belt sediments must have varied between more distal, poorly drained environments and proximal, better-drained environments. Well-drained areas that underlie avulsion deposits are characterized by well-developed paleosols, whereas poorly-drained areas are characterized by carbonaceous shales and hydromorphic paleosols.

Drainage on the alluvial floodplain is largely influenced by two factors: tectonics and climate. Local and regional tectonics control the availability of accommodation space in a basin. When accommodation space is created at a faster rate than sediment can fill it, low-lying, poorly drained areas prevail. Wing (1984) equated the lack of laterally continuous carbonaceous run on shales associated with drab intervals in the middle part of the Willwood Formation to rapid elevation of the Owl Creek Mountains (Fig. 2) at this time. Uplift occurred in association with a shift in accommodation space and drainage patterns within the basin (Bown, 1980). In addition, if weather systems were predominantly from the south and east, uplift of the Owl Creek Mountains could have had an effect on local precipitation and drainage patterns through development of an orographic effect. This would have cast a rain shadow over the basin. Although this scenario could explain the lack of drab intervals and laterally continuous carbonaceous shales in the middle part of the Willwood Formation, it is not clear why these lithologies reappear in the upper 200 m of the Willwood Formation.

Humidity and the temporal and spatial distribution of precipitation are the most important climatic factors controlling drainage. During the early Eocene the interior of North America experienced equable climates (Wing and Greenwood, 1993). However, this warm period is punctuated by a strong temperature decline during the first million years of the epoch (Wing et al., 2000). It is unclear what effect such a temperature decrease would have had on humidity and precipitation patterns, but the timing does coincide with the formation of drab intervals in the lower part of the Willwood Formation. However, here again, this does not explain the reoccurrence of laterally continuous shales and drab intervals in the upper part of the Willwood Formation.

SUMMARY

Drab intervals in the Willwood Formation are confined to approximately the lower- and uppermost 200 m of the formation. These intervals are largely composed of hydromorphic paleosols, laterally extensive carbonaceous shales, immature cumulative paleosols, ribbon sandstones, and orange-brown paleosols. Such sequences developed on a distal alluvial floodplain just prior to and during avulsion of a trunk channel, and they represent a link between trunk channel processes and dis-

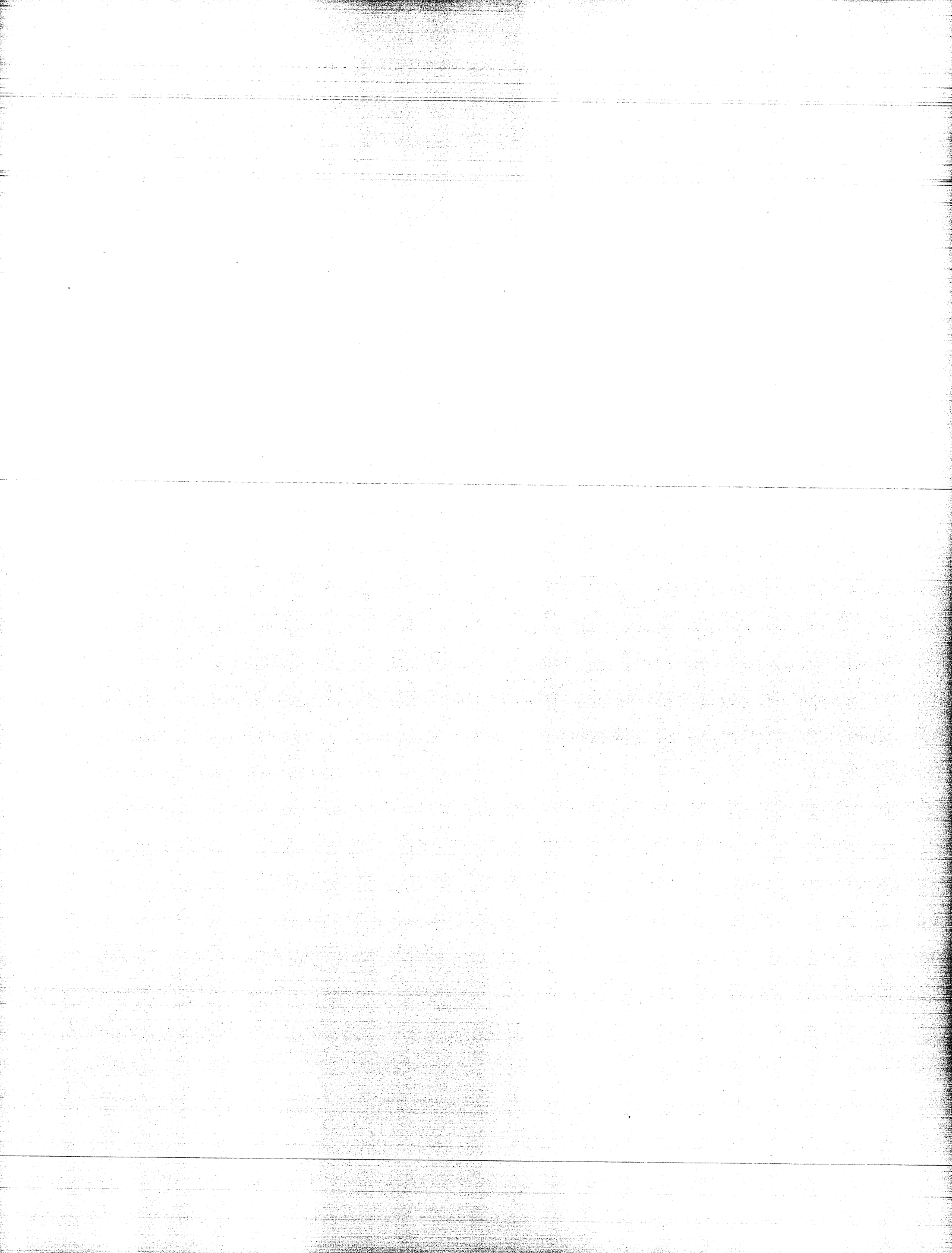
tal floodplain environments. The distribution of carbonaceous shales overlain by drab avulsion intervals rather than more mature paleosols is probably drainage-related. It is hard to distinguish between climate and tectonics as causative factors for drainage variation and the resulting distribution of drab intervals in the Willwood Formation. Development of drab intervals was certainly influenced by both variations in local climate and changing accommodation space related to regional uplift.

ACKNOWLEDGMENTS

I thank Scott Wing for advice on the location of carbonaceous shales, Mary Kraus for insight into avulsions, and Ian Vollum for assistance in the field.

LITERATURE CITED

- BOWN, T. M. 1980. The Willwood Formation (lower Eocene) of the southern Bighorn Basin, Wyoming, and its mammalian fauna. In P. D. Gingerich (ed.), *Early Cenozoic Paleontology and Stratigraphy of the Bighorn Basin, Wyoming*, University of Michigan Papers on Paleontology, 24: 127-138.
- DAVIES-VOLLUM, K. S. 1999. The formation of beds underlying carbonaceous shales as aquatic paleosols: examples from the Bighorn Basin of Wyoming. *International Journal of Coal Geology*, 41: 239-255.
- DAVIES-VOLLUM, K. S., and M. J. KRAUS. 2001. A relationship between alluvial backswamps and avulsion cycles: an example from the Willwood Formation of the Bighorn Basin. *Sedimentary Geology*, in press.
- DAVIES-VOLLUM, K. S., and S. L. WING. 1998. Sedimentological, taphonomic, and climatic aspects of Eocene swamp deposits (Willwood Formation, Bighorn Basin, Wyoming). *Palaios*, 13: 28-40.
- FARLEY, M. B. 1990. Palynological facies fossils in nonmarine environments in the Paleogene of the Bighorn Basin. *Palaios*, 4: 565-573.
- FLORES, R. M., and P. D. WARWICK. 1984. Dynamics of coal deposition in intermontane alluvial paleoenvironments, Eocene Wasatch Formation, Power River Basin, Wyoming. In R. L. Houghton and E. N. Clausen (eds.), *Symposium on the Geology of Rocky Mountain Coal*, North Dakota Geological Society Publication 84-1, pp. 184-199.
- KRAUS, M. J. 1992. Alluvial response to differential subsidence: sedimentologic analysis aided by remote sensing, Willwood Formation (Eocene), Bighorn Basin, Wyoming, USA. *Sedimentology*, 39: 455-470.
- KRAUS, M. J. 1996. Avulsion deposits in lower Eocene alluvial rocks, Bighorn Basin, Wyoming. *Journal of Sedimentary Research*, 66: 354-363.
- KRAUS, M. J., and A. ASLAN. 1993. Eocene hydromorphic paleosols: significance for interpreting ancient floodplain processes. *Journal of Sedimentary Petrology*, 63: 453-463.
- KRAUS, M. J., and T. M. WELLS. 1999. Recognizing avulsion deposits in the ancient stratigraphical record. In N. D. Smith and J. Rogers (eds.), *Fluvial Sedimentology VI, Special Publication of the International Association of Sedimentologists*, 28: 251-268.
- TAUXE, L., J. GEE, Y. GALLET, T. PICK, and T. M. BOWN. 1994. Magnetostratigraphy of the Willwood Formation, Bighorn Basin, Wyoming: new constraints on the location of the Paleocene/Eocene boundary. *Earth and Planetary Science Letters*, 125: 159-172.
- VAN HOUTEN, F. B. 1944. Stratigraphy of the Willwood and Tatman Formations in northwestern Wyoming. *Geological Society of America Bulletin*, 55: 165-210.
- WING, S. L. 1984. Relation of paleovegetation to geometry and cyclicity of some fluvial carbonaceous deposits. *Journal of Sedimentary Petrology*, 54: 52-66.
- WING, S. L., H. BAO, and P. L. KOCH. 1999. An early Eocene cool period? Evidence for continental cooling during the warmest part of the Cenozoic. In B. T. Huber, G. K. MacLeod, and S. L. Wing (eds.), *Warm Climates in Earth History*, Cambridge University Press, Cambridge, pp. 197-237.
- WING, S. L., and T. M. BOWN. 1985. Fine scale reconstruction of late Paleocene-early Eocene paleogeography in the Bighorn Basin of northern Wyoming. In R. M. Flores and S. S. Kaplan (eds.), *Cenozoic Paleogeography of the West-Central United States*, Rocky Mountain Section, SEPM, Denver, pp. 93-105.
- WING, S. L., and D. R. GREENWOOD. 1993. Fossils and fossil climate: the case for equable continental interiors in the Eocene. *Philosophical Transactions of the Royal Society of London, Series B*, 341: 243-252.



BIOSTRATIGRAPHY OF THE CONTINENTAL PALEOCENE-EOCENE BOUNDARY INTERVAL ON POLECAT BENCH IN THE NORTHERN BIGHORN BASIN

PHILIP D. GINGERICH

*Department of Geological Sciences and Museum of Paleontology, The University of Michigan,
Ann Arbor, Michigan 48109-1079*

Abstract.— The Paleocene-Eocene boundary interval in land-mammal evolution is best documented at the south end of Polecat Bench, in the northern Bighorn Basin of Wyoming. Faunas of the late Paleocene Tiffanian and Clarkforkian land-mammal ages and the succeeding early Eocene Wasatchian land-mammal age are all well represented here. Strata on Polecat Bench and in the contiguous Sand Coulee area of the Clarks Fork Basin include type sections of thirteen successive mammalian zones, abbreviated Ti-4 to Ti-6, Cf-1 to Cf-3, Wa-0?, and Wa-0 to Wa-4 (with Wa-3 subdivided) that together span much of the upper Paleocene and lower Eocene. University of Michigan locality SC-67 at the south end of Polecat Bench has yielded the largest and most diverse fauna of earliest Wasatchian age (Wa-0), but facies changes, channel scouring-and-filling, faulting, and topography have long combined to make a clear understanding of physical stratigraphy difficult. This has been clarified now by detailed differential GPS mapping of a critical area covering several square kilometers. In the western part of the study area the early Eocene Wa-0 mammalian faunal interval is composed of unusually mature red and purple stage-3 and stage-4 cumulative paleosols, underlain and overlain by sheet-like 'boundary' channel sandstone complexes. However, from SC-67 eastward there are no bounding channel sandstones. A ribbon sandstone near the base of SC-67 has been mistaken for a lower boundary sandstone in the past, and a major scour-and-fill sequence just east of SC-67 has been mistaken for an upper boundary sandstone.

The Wa-0 faunal zone is about 25 m thick, and the transition from underlying to overlying zones appears to be virtually continuous in fine-grained mudstones. A ca. 4-5 m thick interval of brown paleosols below Wa-0, in what were previously thought to be Clarkforkian strata, is now included in the lower Wasatchian as a new zone. The new zone, abbreviated Wa-0?, has yielded numerous endocarps of the elm-related dicot *Celtis* (hackberry) and a dentary of the mammalian condylarth *Meniscotherium* (but no other Wasatchian mammals). Early appearance of the *Celtis-Meniscotherium* association and an average rate of sediment accumulation of 470 to 475 m/m.y. suggest that Wasatchian floral and faunal change started some 9-10 k.y. earlier than previously recognized. The thickness of the Wa-0 zone proper indicates that it probably represents only about 50 k.y. of geological time.

INTRODUCTION

Polecat Bench is a northeast-to-southwest-trending Pleistocene river terrace in the northern Bighorn Basin, north

and west of the town of Powell, Wyoming (Fig. 1). It stands some 150 m above the surrounding 'flats' or plains, forming a watershed that separates the Clarks Fork Basin to the northwest from the northern part of the Bighorn Basin to the southeast. The surface of Polecat Bench slopes downward at a low gradient toward the northeast, falling from an elevation of 1580 m to an elevation of 1460 m in a distance of twenty kilometers.

In: Paleocene-Eocene Stratigraphy and Biotic Change in the Bighorn and Clarks Fork Basins, Wyoming (P. D. Gingerich, ed.), University of Michigan Papers on Paleontology, 33: 37-71 (2001).

Alignment with the Shoshone River canyon west of Cody, Wyoming, indicates that the river that formed Polecat Bench was a precursor of the present-day Shoshone River and part of the greater Bighorn River drainage excavating the Bighorn Basin.

Polecat Bench is important geologically because its resistant gravel surface supports a virtually continuous sequence of finer-grained, softer, and older continental sedimentary rocks spanning the uppermost Cretaceous through lower Eocene. Cretaceous and Paleogene strata form a southwesterly-dipping monocline well exposed in badlands along the west and southeast sides of the bench (Figs. 2-3). The Paleocene part of the sequence is some 1500 m thick (Fig. 3), making it one of the thickest and most continuous records of continental Paleocene strata known anywhere. Most of this thickness is upper Paleocene, with localities yielding mammalian fossils of the Tiffanian and Clarkforkian land-mammal ages (open diamonds and open circles, respectively, in Fig. 1). In addition, there is a 100 m thick wedge of lower Eocene strata at the south end of Polecat Bench with localities that yield Wasatchian land mammals (open squares and solid squares in Fig. 1).

Biozones reflecting faunal change through the middle-late Paleocene and early Eocene in northwestern Wyoming are summarized in Table 1. Zones and subzones can be recognized where strata of suitable age are exposed throughout the Bighorn-Clarks Fork-Crazy Mountain region of Wyoming and Montana, and some zones undoubtedly have broader geographic extent. Stages and ages of higher rank are recognized by the biozones (zones and subzones) included within them: the Clarkforkian land-mammal stage/age, named for the Clarks Fork Basin on the west side of Polecat Bench (Granger, 1914; Wood et al., 1941) includes the Rodentia interval zone, the *Plesiadapis cookei* taxon range zone, and the *Phenacodus-Ectocion* acme zone. Wa-3 as a whole includes both the *Homogalax protapirinus* and *Hyracotherium aemulor* interval subzones. The Sandcouleean substage/age of Granger (1914) and Wood et al. (1941) includes Wa-0 through Wa-2. The Graybullian substage/age of Granger (1914) and Wood et al. (1941) includes Wa-3 through Wa-5. The zones described here differ conceptually from the ages and 'zones' (biochrons) of Archibald et al. (1988) in being explicitly based on type sections, providing a tangible stratigraphic basis for recognition of corresponding ages and biochrons. Some or all biozones will undoubtedly require modification as new fossils are found, but superpositional relationships will not change and the utility of such a system of biozones for studying the Paleocene-Eocene transition in the Bighorn-Clarks Fork-Crazy Mountain region is amply demonstrated. Each biozone is distinctive as a faunal assemblage, and the index taxa listed in Table 1 are those perceived to be most useful for recognizing broader faunal changes.

The Clarkforkian-Wasatchian transition at the south end of Polecat Bench has proven particularly interesting and important in recent years because of its distinctive basal Wasatchian or Wa-0 mammalian fauna (Gingerich, 1989, 2000; Clyde and Gingerich, 1998; open squares in Fig. 1). The Wa-0 fauna includes the first North American representatives of colonizing

Perissodactyla, Artiodactyla, Primates, and hyaenodontid Creodonta that mark the beginning of the Eocene on northern continents, and it includes many seemingly-dwarfed taxa smaller than those that preceded and/or succeeded them. Such distinctive faunas deserve special attention because they may presage, as Wa-0 has done, unusual conditions of great interest for understanding environmental change.

The Wa-0 fauna at the south end of Polecat Bench is associated with unusually mature paleosols for the northern Bighorn and Clarks Fork basins (Kraus, 1987), a large negative carbon isotope excursion (decrease in the ratio of $\delta^{13}\text{C}$ to $\delta^{12}\text{C}$) that can be correlated worldwide (Koch et al., 1992, 1995; Bains et al., submitted; Bowen et al., this volume), and coincides with benthic marine extinctions and global climatic warming thought to result from melting of hydrated methane on continental shelves (Kennett and Stott, 1991; Zachos et al., 1994; Dickens et al., 1995; Bains et al., 1999; Norris and Röhl, 1999).

The importance of the south end of Polecat Bench is now well established, both for studying the Clarkforkian-Wasatchian transition locally, and for understanding the impact of global Paleocene-Eocene environmental change on continental climates and biotas more generally. Diverse investigations are being carried out by scholars from different institutions, and this will continue in the future. To be comparable, independent studies must be carried out and reported in a common reference frame, which prompted a new effort in 2000 to map the south end of Polecat Bench and clarify its stratigraphy. The map and stratigraphic sections that follow will help in providing a better understanding of the Clarkforkian-Wasatchian transition and its relationship to Paleocene-Eocene environmental change.

HISTORY OF STUDY

Recognition of Wa-0 as a distinctive faunal interval has taken a long time. The first Wa-0 mammals, *Dipsalidictis platypus* and *Ectocion parvus*, were collected by Princeton University professor William J. Sinclair on August 12 and 13, 1911, from red-banded beds in the bluff three miles north of Ralston, Wyoming [i.e., Polecat Bench], while working with an American Museum of Natural History field party. *Meniscotherium priscum* was collected in the same area at the same time. These were part of a fauna from the Clarks Fork Basin first described as being Clarkforkian in age (Sinclair and Granger, 1912, p. 59; Granger, 1914, p. 204). A few additional specimens were collected over the years by Princeton University field parties but these were not considered interesting enough to warrant publication at the time.

University of Michigan research on the Paleocene-Eocene transition started in 1975, when the existence of a Clarkforkian land-mammal age was in doubt because the Clarkforkian fauna was considered artificial, possibly resulting from inadvertent mixing of Tiffanian and Wasatchian fossils (Wood, 1967). In our first summer of field work, 64 localities (SC-1 through SC-64) were established in the Sand Coulee area of the Clarks Fork

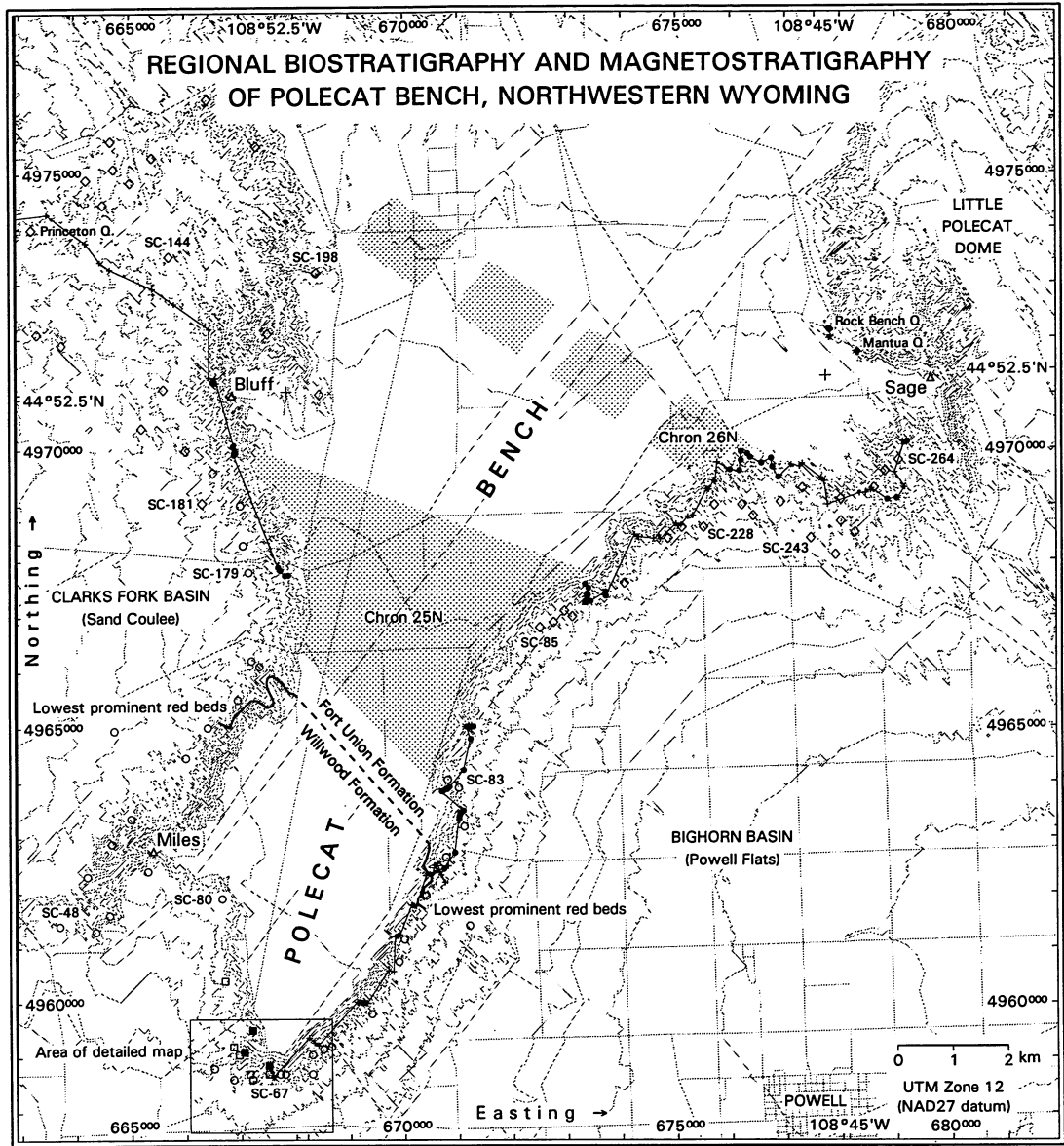


FIGURE 1 — Regional biostratigraphy and magnetostratigraphy of Polecat Bench in northwestern Wyoming. Fossil localities yielding mammals of successive land-mammal ages are coded by age, using the following symbols: Torrejonian (solid diamonds), Tiffanian (open diamonds), Clarkforkian (open circles), earliest Wasatchian Wa-0 (open squares), and later early Wasatchian (solid squares). Some of the more important localities are labeled (SC-67, etc.). National Geodetic Survey stations Bluff, Miles, and Sage are shown as open triangles. Paleomagnetic traverses of Butler et al. (1981) are shown as connected lines on both the west and southeast sides of Polecat Bench, where plus signs mark sites of reversed polarity and solid circles mark sites of normal polarity; stippled bands show inferred traces of magnetozones across Polecat Bench. Stratigraphic sections on the west and southeast sides of Polecat Bench are illustrated in Figs. 2 and 3, respectively; these sections are tied together at the top by a prominent purple mudstone (Purple-4) that can be traced from a point above SC-67 to a point stratigraphically above SC-80. A detailed map of upper Clarkforkian and lower Wasatchian strata at the south end of Polecat Bench is illustrated in Fig. 6.

Basin, and we were able to draw a line on a map separating localities yielding the archaic primate *Plesiadapis* from those yielding the dawn horse *Hyracotherium* and other characteristic Wasatchian mammals.

In 1976 we devoted special attention first to Polecat Bench, and then to identification of the line of separation of Clarkforkian and Wasatchian faunas in Clarks Fork Basin. The line on our initial map proved to coincide with a sheet-like

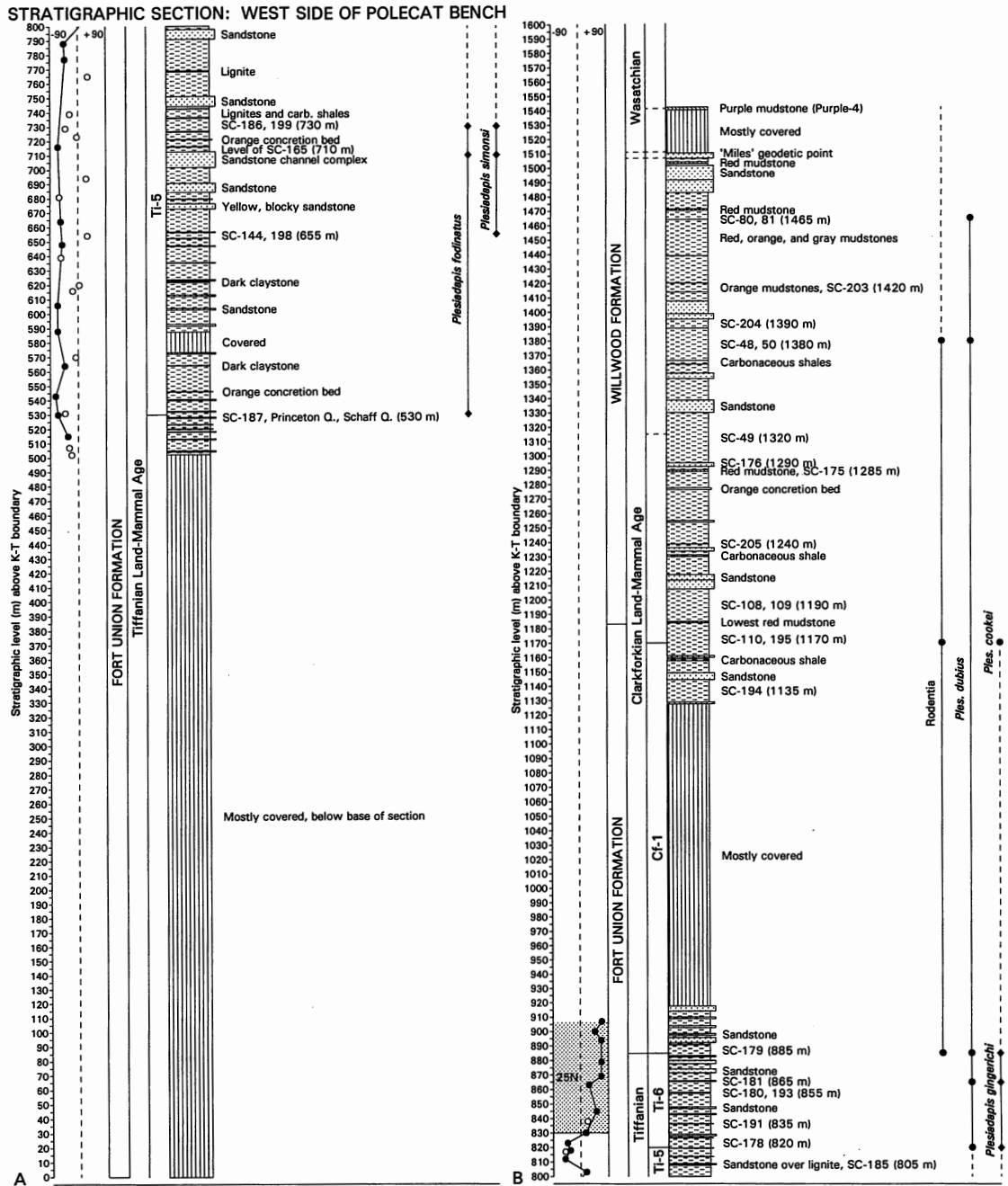


FIGURE 2 — Stratigraphic section of Tiffanian, Clarkforkian, and lower Wasatchian strata in the Fort Union and Willwood formations on the west side of Polecat Bench. Lithologies for the lower part of the section (column A and lower part of B) were recorded by E. H. Lindsay in connection with paleomagnetic sampling (Butler et al., 1981). Lithologies for the upper part of the section (upper part of column B) were recorded by the author and D. W. Krause. Stratigraphic ranges of index taxa are shown to the right of both columns, where solid figures indicate occurrences in this section: diamonds mark type sections for zones (see Table 1). Correlation to the southeast side of Polecat Bench (Fig. 3) is based on: (1) the base of magnetochron 25N; (2) the level of the lowest prominent red mudstone marking the base of the Willwood Formation; and (3) the level of the Purple-4 mudstone, which can be traced from the south end of the bench above SC-67 to a level above SC-80. Meter levels correspond to those in Fig. 3.

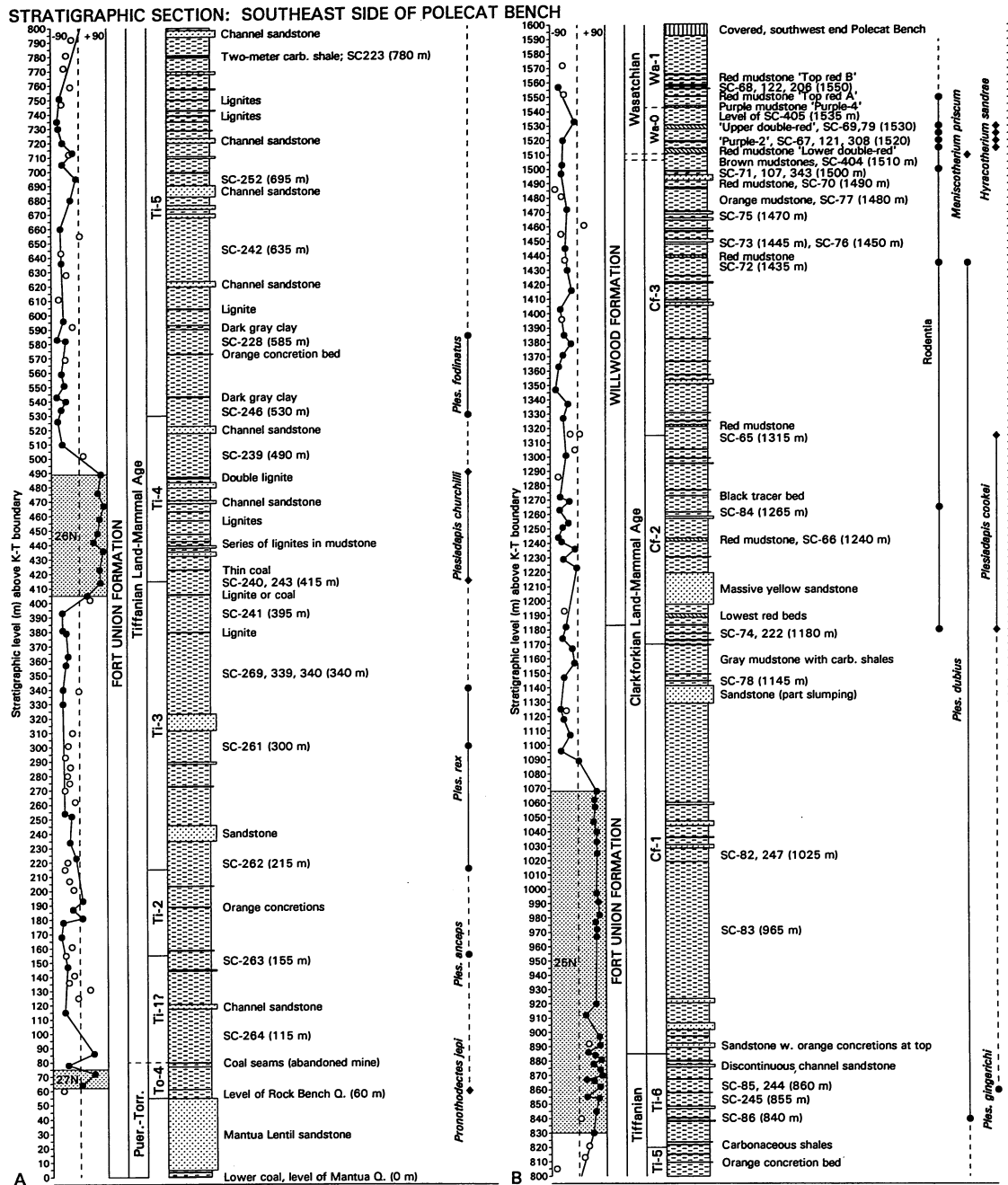


FIGURE 3 — Stratigraphic section of Puercan, Torrejonian, Tiffanian, Clarkforkian, and lower Wasatchian strata in the Fort Union and Willwood formations on the southeast side of Polecat Bench. Lithologies in both columns (A and B) were recorded by E. H. Lindsay and Y. Tomida in connection with paleomagnetic sampling (Butler et al., 1981). Stratigraphic ranges of index taxa are shown to the right of both columns, where solid figures indicate occurrences in this section: diamonds mark type sections for zones (see Table 1). Meter levels are measured above the Cretaceous-Tertiary (K-T) boundary. Thickness of the Fort Union part of the section here was measured by the author (Gingerich, 1968, 1976). Thickness of the Willwood part of the section was measured by the author and K. D. Rose.

TABLE 1 — Formal stratigraphic nomenclature of mammalian biozones spanning the Paleocene-Eocene boundary in northwestern Wyoming (following NACSN, 1983). Abbreviations: *LRD*, lowest range datum (equivalent to first appearance datum or FAD in type section); *HRD*, highest range datum (equivalent to last appearance datum or LAD in type section). Beginnings and ends of zones are defined by LRDs unless otherwise noted. Some ranges reported here differ slightly from those of Gingerich (2000) due to newly improved correlation across Polecat Bench.

Biozone Stratotype section	Author	LRD marking beginning of zone	LRD marking end of zone	Abbr.
Wasatchian land-mammal age (in part)				
<i>Bunophorus etsagicus</i> interval zone 380-530 m interval in Elk Creek section of Schankler, central Bighorn Basin [see Schankler, 1980, p. 103; <i>B. etsagicus</i> is present at the 2240 m level (locality SC-295) in South Rim section of Gingerich (1982a; for map see Gingerich and Klitz, 1985)]	Schankler (1980)	<i>Bunophorus etsagicus</i>	<i>Heptodon calciculus</i>	Wa-5
<i>Hyracotherium permix</i> interval zone 2020-ca. 2200 m interval (localities SC-112, 113, 148, 255, 297, 253, 256, 265, 299, and 303) in South Rim section of Gingerich (1982a; for map see Gingerich and Klitz, 1985)	Gingerich (1983a, 1991)	<i>Hyracotherium permix</i>	<i>Bunophorus etsagicus</i>	Wa-4
<i>Hyracotherium aemulor</i> interval subzone 1780-2020 m interval (localities SC-32, 224, 290, 33, 225, 236, 34, 314, 35, 36, 232, 63, 114, 3, 64, 111, and 254) in South Rim section of Gingerich (1982a; for map see Gingerich and Klitz, 1985)	Gingerich (1991)	<i>Hyracotherium aemulor</i>	<i>Hyracotherium permix</i>	Wa-3b
<i>Homogalax protapirinus</i> interval subzone 1750-1780 m interval (localities SC-5, 309, 310, 87, 213, and 221) in Sand Coulee Divide section of Gingerich (1982a; for map see Gingerich and Klitz, 1985); also present (locality SC-133) in South Rim section of Gingerich (1982a; for map see Gingerich and Klitz, 1985)	Gingerich (1991)	<i>Homogalax protapirinus</i>	<i>Hyracotherium aemulor</i>	Wa-3a
<i>Arfia shoshoniensis</i> interval zone 1645-1750 m interval (localities SC-210, 54, 2, and 12) in Sand Coulee Divide section of Gingerich (1982a; for map see Gingerich and Klitz, 1985); also present (localities SC-47 and 46) in South Rim section of Gingerich (1982a; for map see Gingerich and Klitz, 1985)	Gingerich (1991)	<i>Arfia shoshoniensis</i>	<i>Homogalax protapirinus</i>	Wa-2
<i>Cardiolphus radinskyi</i> interval zone 1543-1645 m interval (localities SC-40, 142, 44, 17, 18, 16, and 37) in Sand Coulee Divide section of Gingerich (1982a; for map see Gingerich and Klitz, 1985); also present (localities SC-6, 4, and 129) in South Rim section of Gingerich (1982a; for map see Gingerich and Klitz, 1985)	Gingerich (1991)	<i>Cardiolphus radinskyi</i>	<i>Arfia shoshoniensis</i>	Wa-1
<i>Hyracotherium sandrae</i> interval zone 5-35 m interval in South Polecat Bench SC-67 section of this paper (ca. 1510-1543 m interval in Fig. 10; for map see Fig. 6)	Gingerich (1991)	<i>Hyracotherium sandrae</i>	<i>Cardiolphus radinskyi</i>	Wa-0
<i>Meniscotherium priscum</i> interval zone 6-10 m interval in South Polecat Bench SC-343 section of this paper (ca. 1506-1510 m interval in Fig. 9; for map see Fig. 6)	New	<i>Meniscotherium priscum</i>	<i>Hyracotherium sandrae</i>	Wa-0?
Clarkforkian land-mammal stage/age				
<i>Phenacodus-Ectocion</i> acme zone 1315-1506 m interval (localities SC-72, 73, 76, 75, 77, 70, 71, 107, 343) in Figure 3 (for maps Fig. 1 and Gingerich and Klitz, 1985)	Rose (1981)	<i>Plesiadapis cookei</i> (HRD)	<i>Meniscotherium priscum</i>	Cf-3
<i>Plesiadapis cookei</i> taxon range zone 1180-1315 m interval (localities SC-74, 65) in Figure 3 (for maps see Fig. 1 and Gingerich and Klitz, 1985)	Gingerich (1975, 1983a)	<i>Plesiadapis cookei</i>	<i>Plesiadapis cookei</i> (HRD)	Cf-2
Rodentia interval zone 885-1180 m interval (locality SC-179) in Figure 2 (for maps see Fig. 1 and Gingerich and Klitz, 1985)	Rose (1981)	Rodentia	<i>Plesiadapis cookei</i>	Cf-1

multistory sandstone interval, soon called the 'boundary sandstone,' that could be traced across much of the Clarks Fork Basin. The boundary sandstone was studied in detail by Kraus (1979, 1980), who found it to be 12-31 m thick and deposited by a meandering stream system, with paleocurrent directions indicating that the stream system flowed nearly due north. Kraus interpreted the boundary sandstone as indicating extensive reworking and selective preservation of coarser sediments, due to decreased basin subsidence and decreased rates of sediment accumulation at the end of the Clarkforkian and beginning of Wasatchian time.

Locality SC-67 was established in 1976, and the initial SC-67 collection included a specimen of *Hyracotherium* that

showed the locality to be Wasatchian, but the species represented, *H. sandrae*, was not recognized as distinctive until later when a larger sample was available. The fauna at SC-67 was first recognized to be unusual because of the relative abundance of *Ectocion parvus*, a small species named by Granger (1915). Another species named by Granger, *Meniscotherium priscum*, was considered to be part of this fauna as well (Gingerich, 1982b). However, it was not until later, after the Wasatchian had been subdivided into zones Wa-1 through Wa-7 (Gingerich, 1983a), that the distinctiveness and importance of the SC-67 fauna were recognized (Gingerich, 1989). This required addition of a zone at the beginning of the Wasatchian sequence: hence the designation Wa-0.

TABLE 1 (cont.) — Formal stratigraphic nomenclature of mammalian biozones spanning the Paleocene-Eocene boundary in northwestern Wyoming (following NACSN, 1983). Abbreviations: *LRD*, lowest range datum (equivalent to first appearance datum or FAD in type section); *HRD*, highest range datum (equivalent to last appearance datum or LAD in type section). Beginnings and ends of zones are defined by LRDs unless otherwise noted. Some ranges reported here differ slightly from those of Gingerich (2000) due to newly improved correlation across Polecat Bench.

Biozone Stratotype section	Author	LRD marking beginning of zone	LRD marking end of zone	Abbr.
Tiffanian land-mammal stage/age				
<i>Plesiadapis gingerichi</i> interval zone 820-885 m interval (localities SC-178 and 181) in Figure 2 (for maps see Fig. 1 and Gingerich and Klitz, 1985)	Rose (1981)	<i>Plesiadapis gingerichi</i>	Rodentia	Ti-6
<i>Plesiadapis simonsi</i> lineage zone 655-820 m interval (localities SC-198, 165, 186) in Figure 2 (for maps see Fig. 1 and Gingerich and Klitz, 1985)	Gingerich (1975)	<i>Plesiadapis simonsi</i>	<i>Plesiadapis gingerichi</i>	
<i>Plesiadapis fodinatus</i> lineage zone 530-820 m interval (localities SC-187, 165, 186, 198) in Figure 2 (for maps see Fig. 1 and Gingerich and Klitz, 1985)	New	<i>Plesiadapis fodinatus</i>	<i>Plesiadapis dubius</i>	Ti-5
<i>Plesiadapis churchilli</i> lineage zone 415-530 m interval (localities SC-240, 243, 239) in Figure 3 (for maps see Fig. 1 and Gingerich and Klitz, 1985)	Gingerich (1975)	<i>Plesiadapis churchilli</i>	<i>Plesiadapis fodinatus</i>	Ti-4
<i>Plesiadapis rex</i> lineage zone Ca. 1500 m interval (locality GGS-13) of Hartman and Krause (1993): table 2 (for map see fig. 1, loc. cit.). Reference section: 215-415 m interval (localities SC-262, 261, 339) in Figure 3 (for maps see Fig. 1 and Gingerich and Klitz, 1985)	Gingerich (1975)	<i>Plesiadapis rex</i>	<i>Plesiadapis churchilli</i>	Ti-3
<i>Plesiadapis anceps</i> lineage zone Ca. 1170-1500 m interval (Scarritt Quarry) of Hartman and Krause (1993): table 2 (for map see fig. 1, loc. cit.). Reference section: 155-215 m interval (locality SC-263) in Figure 3 (for maps see Fig. 1 and Gingerich and Klitz, 1985)	Gingerich (1975)	<i>Plesiadapis anceps</i>	<i>Plesiadapis rex</i>	Ti-2
<i>Plesiadapis praecursor</i> lineage zone Ca. 1000-1170 m interval (Douglass Quarry) of Hartman and Krause (1993): table 2 (for map see fig. 1, loc. cit.)	Gingerich (1975)	<i>Plesiadapis praecursor</i>	<i>Plesiadapis anceps</i>	Ti-1
Torrejonian land-mammal age (in part)				
<i>Pronothodectes jepi</i> lineage zone Ca. 60 m interval (Rock Bench Quarry) in Figure 3 (for maps see Fig. 1 and Gingerich and Klitz, 1985)	Gingerich (1975)	<i>Pronothodectes jepi</i>	<i>Plesiadapis praecursor</i>	To-4
<i>Pronothodectes gidleyi</i> lineage zone Ca. 560 m interval (Gidley Quarry) of Hartman and Krause (1993): table 2 (for map see fig. 1, loc. cit.)	Gingerich (1975)	<i>Pronothodectes gidleyi</i>	<i>Pronothodectes jepi</i>	To-3

Meniscotherium has proven particularly interesting and, as outlined below, suggests that there is still more to learn about the Clarkforkian-Wasatchian transition.

PALEOCENE-EOCENE STRATIGRAPHY IN MAP VIEW

The stratigraphy of the south end of Polecat Bench is surprisingly complex when studied in detail, which has led at different times to confusion and error in labeling of stratigraphic units, in mapping of localities, in recording the total thickness of the earliest Wasatchian Wa-0 interval, and in tracing beds laterally (Gingerich, 1989). Development of a consistent interpretation enabling such errors to be corrected has required detailed mapping of a 2 km² study area. This is in a region of hilly topography with limited visibility from valley to valley, making accurate recognition of map positions difficult. Consequently, field mapping was carried out with a portable

differential global positioning system offering meter- to near meter-scale precision and accuracy.

Mapping methods

The Differential global positioning system [DGPS] used here included a battery-powered Starlink Invicta® 210S ten-channel GPS receiver attached to a Starlink MBA-4 GPS/L-band helix antenna on a 2.5 m pole, with an At Work Computers® portable Ranger computer running Tripod Data Systems® SoloField-for-Windows-CE software (Version 2.1 beta). The differential signal was provided by OmniStar® satellite.

The GPS unit was calibrated using the U. S. National Geodetic Survey [NGS] Miles triangulation station approximately 4.5 km NW of the study area (44° 48' 04.88685" N latitude, 108° 54' 33.70222" W longitude, and 1596.7 m elevation; *vide* U.S. National Geodetic Survey at <http://>

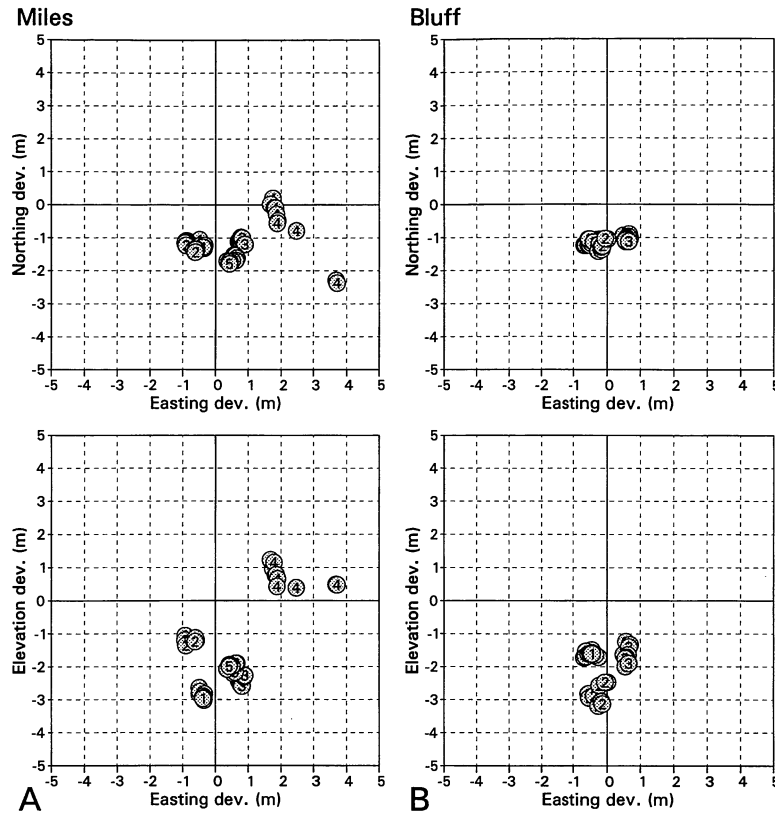


FIGURE 4 — Test of precision and accuracy of the differential global position system (DGPS) used to map strata at the south end of Polecat Bench. A, results for National Geodetic Survey station Miles (open triangle in Fig. 1): this is the point used for calibration of the DGPS unit. B, results for National Geodetic Survey station Bluff (open triangle in Fig. 1). All panels are ten meters on a side, with the known (and hence, here, expected) value of the easting, northing, and/or elevation of a recording falling at the center of the panel (known values are taken from http://www.ngs.noaa.gov/cgi-bin/ds_quads.prl). The upper panel in each test shows recorded points plotted in map view, with north at the top. Lower panel in each test shows recorded points plotted in a corresponding elevation view. Each record plotted here mimics a station used in mapping in being the average of 10 or more successive DGPS measurements ('epochs'), and each test included 10 records spaced about a minute apart (each cluster includes 10 records). Cluster 1 was recorded on 28 June 2000; 2 was recorded on 30 June 2000; 3 was recorded on 12 July 2000; 4 was recorded on 17 September 2000 (Miles only); and 5 was recorded on 20 September 2000 (Miles only). Note that clusters 1, 2, 3, and 5 together fall within a cube about two meters on a side, indicating near meter-scale precision, both at the calibration site and at the independent site. Cluster 4 fills a larger 3 or 4-meter volume centered several meters from the tighter clusters, showing that there are times when DGPS exceeds meter-scale precision. All of the more precise results are about 1 m south and 2-3 m lower in elevation than expected, indicating a systematic inaccuracy of unknown cause.

www.ngs.noaa.gov/cgi-bin/ds_quads.prl). Zone file settings included NADCON projection, NAD83 horizontal datum, ellipsoid elevation, and WGS84 vertical datum. The study area is in Universal Transverse Mercator zone 12, and all coordinates were recorded in meters on orthogonal UTM easting, northing, and elevation axes. Note that the horizontal datum used here, NAD83, is *not* the NAD27 datum of available USGS topographic maps (see below). Minimally 10 measurements (epochs) were averaged for each map station recorded, and the maximum acceptable horizontal dilution of precision (HDOP) was 2.0.

DGPS accuracy and precision

Differential GPS accuracy and precision were tested by recording three-dimensional coordinates of known points 10 times each during three successive visits spanning the duration of field work. Known points used were (1) the original Miles calibration point 4.5 km NW of the study area, and (2) the Bluff calibration point 12 km N of the study area, both on the west side of Polecat Bench (Fig. 1). Known coordinates of these points are provided at the NGS web site mentioned above. Results of the successive tests are shown graphically in Figure 4.

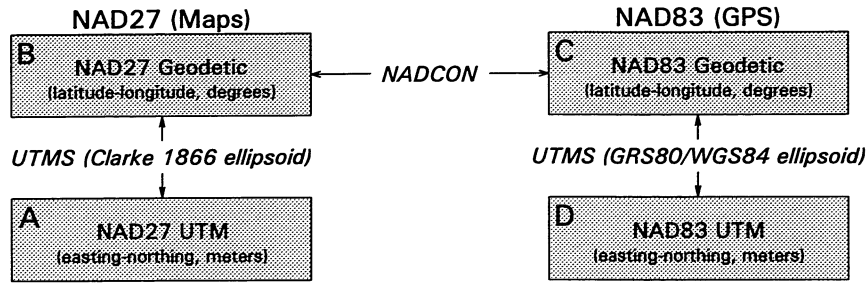


FIGURE 5 — Protocols required for transformation of North American Datum NAD27 geographic coordinates to NAD83 and vice versa. Geodetic coordinates (latitude and longitude recorded in degrees) can be converted from NAD27 to NAD83 or NAD83 to NAD27 in a single transformation step using publically-available NADCON software (Dewhurst et al., 1992; NADCON is the U.S. Federal standard for NAD27 to NAD83 transformations). Transformation of UTM coordinates is more complicated, with three steps required to convert NAD27 UTM to NAD83 UTM or vice versa. Transformation of datums can only be done in a geodetic framework, which means that NAD27 UTM must be converted to NAD27 Geodetic or NAD83 UTM must be converted to NAD83 Geodetic to start this transformation. Recovery of UTM coordinates following transformation of datums requires conversion from Geodetic to UTM. UTM-Geodetic conversions can be made using publically-available UTMS software (Carlson and Vincenty (1993). UTMS works on either ellipsoid (Clarke 1866 ellipsoid of NAD27 or GRS80/WGS84 ellipsoid of NAD83) and it works in both directions (from UTM to Geodetic and vice versa). Stated simply with reference to the diagram here, B and C can be transformed in one step using NADCON. Transformation from A to D (or D to A) requires three steps passing through B and C, using UTMS, then NADCON, then UTMS again.

In each panel of Figure 4, coordinates for a particular series of ten measurements are represented by spheres labeled 1, 2, 3, 4, or 5, representing the visit number. Short-term precision is high and in most cases spheres of the same number in a panel generally fall within a meter of each other (with the exception of visit 4 at Miles). Short-term accuracy is a little lower and eastings vary within about ± 1 m of expectation, northings are generally 1.0-1.5 m less than expectation, and elevations vary from about 1.0 to 3.0 m below expectation (again excepting visit 4 at Miles). Long-term precision is lower as all spheres in a panel taken together appear to fall within about two to three meters of each other. Long-term accuracy is approximately the same as short-term accuracy: at both test localities eastings appear unbiased, northings are generally about 1 m less than expectation, and elevations are generally about 1 to 3 m less than expectation.

In this study, such near meter-scale accuracy is comparable to the accuracy or inaccuracy of determining horizontal outcrop limits of strata to be measured. However, meter- or near meter-scale accuracy is comparable to the vertical thickness of many of the stratigraphic units of interest here, and DGPS is not an adequate substitute for direct measurement of bed thicknesses in stratigraphic sections (note that use of DGPS to determine bed spacing in Figure 12 is constrained by the thickness of a comparable interval in an adjacent section).

NAD27 and NAD83 conversion

Simultaneous use of two different geodetic datums means that information registered on U. S. Geological Survey

topographic maps (using the NAD27 geodetic datum) cannot be combined with information derived from the global positioning system (GPS or DGPS, using the NAD83 datum) without transformation. This is true for information recorded in geodetic coordinates (latitude and longitude), which require a single transformation step, as well as UTM zone coordinates (easting and northing in meters), which require three distinct transformation steps. The conversion procedure is illustrated in Figure 5. Software in the public domain is available to carry out the transformations. The two programs required are NADCON (Dewhurst et al., 1992; the NADCON algorithm is a U.S. government standard for NAD27 to NAD83 transformations), and UTMS (Carlson and Vincenty, 1993).

Registration on topography

Registration on topography provides an alternative to transformation of NAD83 GPS coordinates and NAD27 map coordinates. Fossil localities, distinctive geological strata, faults, and other features of interest were recorded in the field using DGPS (NAD83). These were then plotted at the same scale as the topographic base map being used (NAD27), and the two maps were superimposed and registered using topography. Outcrop limits encircling hills are particularly useful for registration.

Marker beds used for mapping were chosen on the basis of their identifiability, visibility, and to some extent their accessibility. Then an attempt was made to map marker beds using as many control points as possible. However, paleosols at the south end of Polecat Bench are commonly covered with spherical calcareous nodules, making them slippery, and many outcrop slopes are simply too steep to climb. Marker beds could

TABLE 2 — Bedding-plane orientation of key marker beds in the Paleocene-Eocene transition at the south end of Polecat Bench. Orientations were computed separately for seven local areas: SC-80, SC-206, etc., here listed from north to southwest to east, wrapping around the end of the bench. Within areas, beds are listed in stratigraphic sequence. Note: (1) systematic change of strike from east to west here (ignoring the bed above SC-80), circumscribing a shallow syncline at the southwest corner of Polecat Bench; (2) substantial variation in computed strike values, even within the same area, due to error associated with low dips (and possibly differential compaction of anisotropic sediments); and (3) consistently low dip values in the range of 1.5° to 3.2° (median at SC-67 is ca. 2.0° SW). Purple-4 bed near SC-80 was used to link the tops of the stratigraphic sections shown in Figs. 2 and 3.

Bed	Number of points	b_0	b_1	b_2	Strike	Dip
<i>Above SC-80</i>						
Purple-4	10	-129.2460	0.0140	0.0261	N 61.8° W	1.7° SW
<i>SC-206 and vicinity</i>						
Top Red-B	41	-176.3453	-0.0208	0.0253	N 50.5° E	1.9° SE
Top Red-A	43	-265.9125	-0.0341	0.0342	N 45.0° E	2.8° SE
Purple-4	18	-107.5272	-0.0284	0.0307	N 47.2° E	2.4° SE
<i>Above SC-70</i>						
Lower Boundary Sandstone	14	24.0704	-0.0264	0.0277	N 46.4° E	2.2° SE
<i>SC-121 and vicinity</i>						
Lower Boundary Sandstone	30	-167.7362	-0.0097	0.0291	N 71.5° E	1.8° SSE
<i>SC-308 and vicinity</i>						
Lower Boundary Sandstone	32	-782.2860	0.0295	0.0349	N 49.8° W	2.6° SW
<i>SC-67 and vicinity</i>						
Purple-4	13	166.3733	0.0239	0.0198	N 39.6° W	1.8° SW
Upper Double-Red (top)	23	490.5610	0.0283	0.0135	N 25.5° W	1.8° SW
Upper Double-Red (base)	20	119.2739	0.0262	0.0200	N 37.3° W	1.9° SW
Purple-2	44	-751.3870	0.0242	0.0349	N 55.3° W	2.4° SW
Lower Double-Red (top)	14	-1840.5437	0.0110	0.0550	N 78.7° W	3.2° SW
Lower Double-Red (base)	23	228.0517	0.0332	0.0170	N 27.1° W	2.1° SW
Brown mudstone series (top)	16	-132.6727	0.0333	0.0231	N 34.8° W	2.3° SW
Ledge sandstone	80	2.4455	0.0133	0.0233	N 60.3° W	1.5° SW
<i>SC-343 and vicinity</i>						
Brown mudstone series (top)	23	-324.9102	0.0179	0.0284	N 57.8° W	1.9° SW
Purple-0	29	-121.5387	0.0462	0.0211	N 24.6° W	2.9° SW

only be mapped in the field where they could be reached. Mapping was necessarily completed in the laboratory by interpolation after known points on each bed were superimposed and registered on the topographic base map. Interpolation could then be constrained by following contour lines on the underlying topography.

Map of the South End of Polecat Bench

A detailed map of Paleocene-Eocene stratigraphy at the south end of Polecat Bench is shown in Figure 6. The principal area

of interest is in Section 10, T55N, R100W, Park County, Wyoming, on U.S. Geological Survey 1:24,000 scale Elk Basin SW and Elk Basin SE 7.5-minute topographic quadrangles. Both were published in 1966. Stratigraphic mapping was plotted on topography at a scale of 1:12,500, and the map in Figure 6 is reproduced at a scale of ca. 1:15,000. Topography ranges in elevation from about 4700 to 5200 ft (1430 to 1580 m) above sea level, with a 20 ft contour interval on the base map. Vertebrate fossil localities numbered on the map are all University of Michigan 'Sand Coulee' localities: e.g., 67 represents locality SC-67, etc.

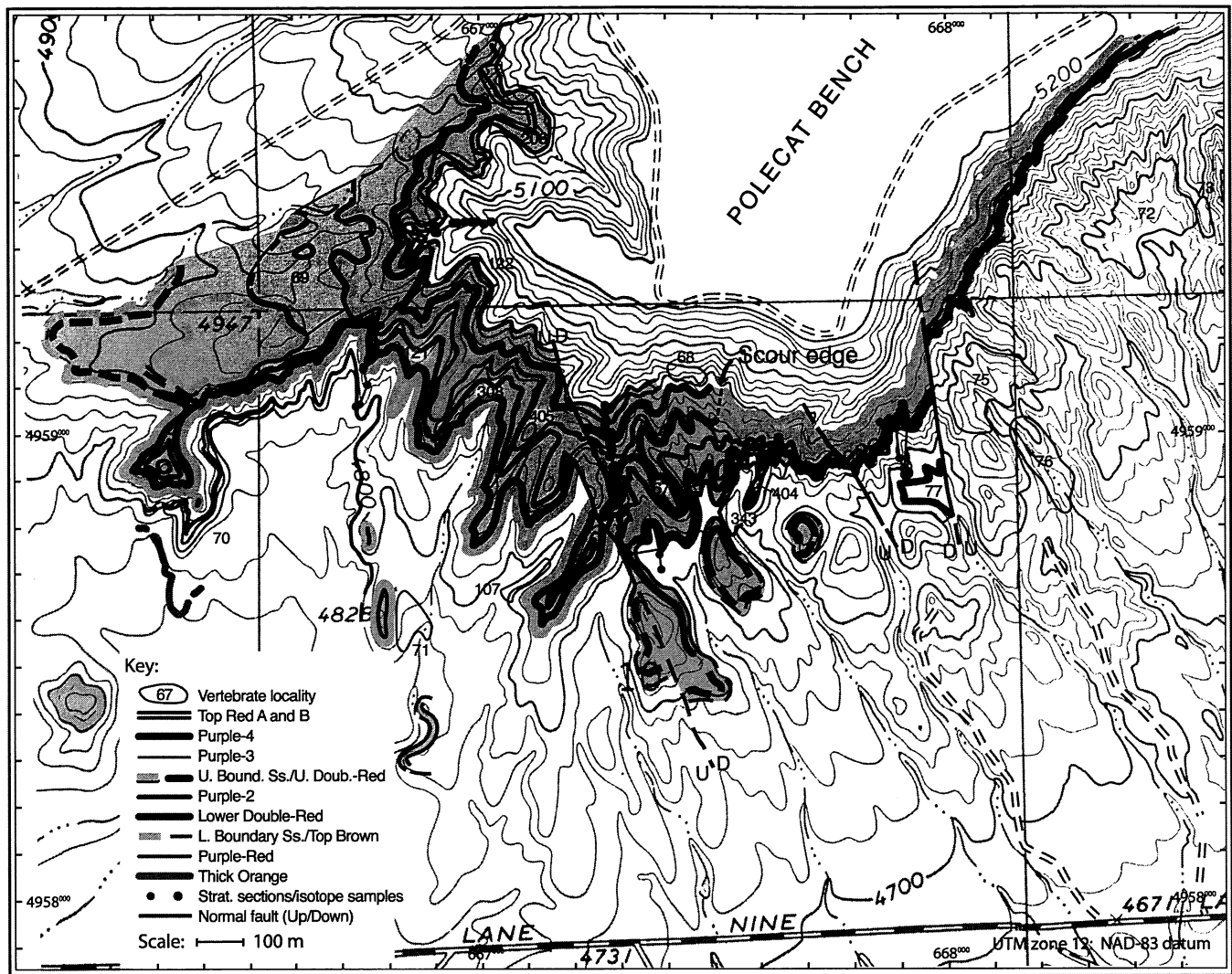


FIGURE 6 — Detailed geological map of the south end of Polecat Bench showing the positions of mammal-bearing fossil localities, the principal marker beds of interest here, the traces of measured stratigraphic sections, the locations of isotope samples, and normal faults displacing strata. All were mapped using a differential global positioning system and are registered on topography of U. S. Geological Survey 7.5' topographic quadrangles Elk Basin SE and Elk Basin SW. Note the presence of Lower and Upper Boundary Sandstones enclosing Wa-0 localities SC-69, SC-121, SC-308, and the western part of SC-67 on the west half of the map. These boundary sandstones are missing east of the western pair of faults in the middle of the map. A distinct ribbon sandstone near the base of SC-67 just east of the western pair of faults has long been confused with the Lower Boundary Sandstone. Two thick scour-fill sandstones in the upper part of the section east of the point labeled scour edge have long been confused with the Upper Boundary Sandstone.

Faults

Four faults were mapped that disturb strata to a significant degree (Fig. 6). These are all normal faults trending NNW-SSE. The two westernmost faults are approximately aligned and undoubtedly developed together. Both dip steeply to the ENE. Vertical displacement is minimal where the two overlap, and displacement increases to some 5-10 m both north and south of this. Hence the two are possibly manifestations

of a single NNW-SSE-trending scissors fault. Neither has been traced farther than is shown on the map, and the northern of the two faults appears not to cut strata in the vicinity of locality SC-206. The third fault, more centrally located, dips steeply to the ENE and has a displacement of ca. 10 m. The easternmost fault is the most conspicuous. It dips steeply to the WSW and has a displacement of ca. 20 m. Taken together the four faults indicate development of a 0.7-0.8 km wide, shallowly

down-dropped block or graben directly south of the south end of Polecat Bench.

Folding

All strata at the south end of Polecat Bench are shallowly dipping, with dips ranging from 1.5 to 3.2° relative to horizontal. Dips such as these are too great to ignore, but are very difficult to measure with handheld instruments in the field. DGPS mapping of the outcrop traces of strata in an area yields a set of points that can be used to determine bedding planes. Here equations of best-fit planes were determined by least-squares (Davis, 1986, p. 406), using differentially-corrected, three-dimensional, metric GPS coordinates of points recorded in the field for each bed in each area. Beta values (b) are the constant, easting coefficient, and northing coefficient, respectively, where $Z = b_0 + b_1 \cdot X + b_2 \cdot Y$ is the equation of the plane (planes were fit to UTM easting and northing coordinates stripped of their leading 66 and 49, respectively, to simplify computation). Strike and dip were calculated analytically from the beta values. Results are listed in Table 2. Note that there is a systematic change of strike from west to east across the study area, starting with a strike of ca. N 45° E at SC-70 and SC-206 in the west and ending with strikes of ca. N 45° W at SC-343 in the east, circumscribing a shallow syncline at the southwest corner of Polecat Bench just west of the faulted graben.

Boundary sandstones

As outlined above, our efforts in the 1970s to clarify the existence and meaning of the Clarkforkian land-mammal age (Rose, 1981) led us to focus attention on the major multistory sheet sandstone marking the boundary between the Clarkforkian and Wasatchian land-mammal ages in the Clarks Fork Basin. Simultaneous discovery of the dawn horse *Hyracotherium* at locality SC-67 at the southwestern end of Polecat Bench, above strata yielding *Plesiadapis* and other typically Clarkforkian taxa, suggested the presence of a Clarkforkian-Wasatchian boundary sandstone at the base of SC-67. As Wa-0 mammals were found at other localities in the Clarks Fork Basin it became clear that these were coming from mudstones *within* the boundary sandstone unit. However, extension of this idea to the most productive Wa-0 locality, SC-67, led to confusion. The conspicuous sandstones at the base and top of SC-67 are now demonstrably not the same as the lower and upper boundary sandstone units exposed below and above a western extension of SC-67, below and above localities SC-308 and SC-121 to the north and west of SC-67, and below and above Wa-0 localities in the Clarks Fork Basin proper even farther to the north and west.

The lower boundary sandstone west of SC-67 is a major ridge-forming, 2-3 m thick, yellow, medium-to-coarse-grained sandstone (see SC-121 stratigraphic section below). The lower boundary sandstone is well exposed above late Clarkforkian localities SC-70, SC-71, and SC-107, and it is well exposed below Wa-0 localities SC-121 and SC-308. It is the lower channel sandstone in figure 6B of Kraus (1987, p. 608). The lower

boundary sandstone is not found south of SC-71, nor is it found in SC-67 proper east of the western pair of faults in Figure 6.

The upper boundary sandstone west of SC-67 is also a major ridge-forming sandstone. It is a ca. 7 m thick, yellow, fine-to-medium-grained sandstone (see SC-121 stratigraphic section below). The upper boundary sandstone is well exposed above the western extension of SC-67, and above SC-121 and SC-308. Locality SC-405 is developed within the upper boundary sandstone, near its base where there is a lag of coprolites, reptilian and mammalian bones, and occasional mammalian teeth. The upper boundary sandstone is the upper channel sandstone in figure 6B of Kraus (1987, p. 608). This unit is not found east of the western pair of faults in Figure 6, and it appears to thin and disappear where it is exposed above locality SC-69.

The lower and upper boundary sandstones are correctly labeled in Figure 7 of Gingerich (1989, p. 14). They are parts of the major sheet sandstone complex described by Kraus (1980; for more on sheet sandstones see Kraus 1996, 1997, and this volume), and they appear to have been deposited by meandering channels of trunk rivers, which generally flowed to the north paralleling the structural axis of the developing basin (Kraus, this volume). It may be fortuitous that the eastern edge of both sheet sandstones coincides with the line formed by the western pair of faults mapped in Figure 6, or faulting may have been controlled by the edge of the sheet sandstones.

Ribbon sandstones

Ribbon sandstones may be similar in thickness to major sheet sandstones, but these are less extensive laterally and they are generally finer-grained. One ribbon sandstone at the southwestern corner of SC-67 (Fig. 6) is of particular interest because it has long been misidentified as representing an eastward extension of the lower boundary sandstone. The sandstone is 0.8 to 2.6 m thick, counting 1.8 m of thickness cut into the underlying red mudstone of Lower Double-Red A (see SC-67 stratigraphic section below). It is yellow, and very-fine-grained. The ribbon-like geometry of the unit is masked because it is principally exposed where it is cut longitudinally by erosion. This sandstone is labeled 'top of boundary sandstone' at the base of the SC-67 stratigraphic section of Badgley (Gingerich, 1989, p. 13). However, the ribbon sandstone is separated from the lower boundary sandstone by the westernmost of the western pair of faults mapped in Figure 6. It is transected by a valley, revealing that it is ribbon-like rather than sheet-like in cross-section. Further, it is stratigraphically above the Top Brown Mudstone to sandstone to Lower Double-Red A sequence that marks the lower boundary of Wa-0 here and elsewhere (see SC-67 stratigraphic section below). This particular ribbon sandstone cuts across a sequence of mudstones with well-developed, brightly-colored paleosols (see below).

Scour-fill sandstones

The sandstone taken to be the upper boundary sandstone north and east of locality SC-67 (marked by arrows in figure 5 of Gingerich, 1989, p. 12) is now recognized to be the higher



FIGURE 7 — Photograph of the South Polcat Bench SC-77 stratigraphic section at and just above locality SC-77. The Thick Orange marker bed occurs near the base of the section. The purplish red mudstones, red mudstones, Purple-0, and Lower Double-Red marker beds are present in the lower part of the section, capped by sandstones and drab mudstones of the scour-fill sequence higher up on the side of Polcat Bench. The Paleocene-Eocene boundary marked by the beginning of the carbon isotope excursion (ca. 1500 m level in the Polcat Bench master section) occurs in the interval marked P-E7.

Key marker beds

Most of the distinctive bright-colored sediments exposed at the south end of Polcat Bench are what Kraus (1996, 1997, this volume) terms mature cumulative paleosols, meaning that they were built up (accumulated) slowly in a long succession of many flooding episodes. This contrasts with the immature avulsive paleosols in the scour fill just mentioned, which were deposited much more rapidly in relatively few events. Key marker beds used for mapping are listed in the key to Figure 6, and all of the key marker beds (including some not mapped in Fig. 6) are described here from stratigraphically lowest to highest (oldest to youngest). Sections including these marker beds are described and illustrated below.

Thick Orange mudstones. The lowest marker bed mapped here is a distinctive 2-m thick sequence of orange mudstones. These are best exposed at the base of the SC-77 section in locality SC-77 itself at the eastern margin of the mapped area (Fig. 7). The Thick Orange mudstones are also well exposed just west and south of SC-70 at the western margin of the mapped area. The lower beds in the sequence of

of two sheet-like sandstones in a sequence of drab sediments filling a major erosional scour. The scour surface extends eastward and northeastward for a kilometer from the mapped scour edge shown in Figure 6. The lower of the sheet-like sandstone units is a 7-14 m thick, fine-to-medium-grained, yellow sandstone (see top of SC-77 stratigraphic section below). It has an erosional base, with a ca. 50 cm thick lag of reworked soil nodules in many places. Paleosols in the scour fill sequence are immature, and the whole scour appears to have been filled rapidly, probably during a sequence of channel avulsions (see Kraus, 1996, this volume).

The depth of this major erosional scour can be estimated by comparing the SC-77 and SC-67 stratigraphic sections shown below. The base of the scour-fill sandstone at the top of the SC-77 section lies some 2 m above the top of marker bed Purple-2. The lowest bed in the SC-67 section that can be traced across all beds between the 15 and 40 m levels in the SC-67 section were removed by erosion. Thus the depth of the scour was approximately 25 m, which provides an estimate of local relief before the scour was filled.

interest here are mostly covered and the orange mudstones have not been observed between SC-77 and SC-70.

Purple-Red mudstone. The Purple-Red mudstone mapped here marks the top of locality SC-70. This can be traced eastward to the base of the SC-121 section, and then southward to a level below SC-71 where it disappears. The Purple-Red mudstone may correspond to the red mudstones at the 14-16 m level in the SC-77 section, but this cannot be confirmed by tracing beds.

Purple-0. Purple-0 is a red to purple marker bed (Fig. 7) that can be traced from the SC-77 section westward to the SC-343 section. It occurs at the base of a sequence of 4-5 predominantly brown paleosols that were formerly thought to be Clarkforkian in age but yield abundant endocarps of characteristically Wasatchian *Celtis phenacodorum* and the mammalian condylarth *Menisotherium priscum*.

Top Brown mudstone. The Top Brown mudstone is the highest of the 4-5 predominantly brown paleosols just mentioned. This can be traced from the SC-77 section westward to the SC-343 section and on to the SC-67 section. North and west of SC-67 the Top Brown mudstone (and possibly some of the other brown mudstones underlying this) are removed by erosion and replaced by the Lower Boundary Sandstone described above.

Lower Double-Red mudstones. Some 2 m above the Top Brown mudstone is a much thicker pair of reddish orange to red mudstones (Fig. 7). The lower of these is called Lower Double-Red A and the higher Lower Double-Red B. The top of Lower Double-Red B is sometimes purple and represents a Purple-1 marker bed (not used here). Both of the lower double red mudstones can be traced from SC-77 westward to SC-343. The higher of the lower double reds is cut out by the ribbon sandstone at SC-67 described above, but the lower part of the unit is present. The lower double red mudstones are represented as a single thick red mudstone unit at SC-121. This single thick red mudstone unit is the lower of the stage-4 paleosols in the figure 6B stratigraphic section described by Kraus (1987, p. 608).

Purple-2 mudstone. The most laterally-extensive marker bed at the south end of Polecat Bench is the Purple-2 marker bed. This can be traced continuously from the eastern edge of the mapped area, where it occurs just below the major scour surface, to the western edge of the mapped area, where it encircles the low peak above locality SC-70. There are other purple beds that can be confused with Purple-2, but it is the only prominent purple bed lying in between the Lower Double-Red and the Upper Double-Red marker beds. Purple-2 illustrates too the importance of physically tracing marker beds because it was earlier thought to be three distinct beds and it is represented at three levels in the stratigraphic section previously published for SC-67 (Gingerich, 1989, p. 13). The lower 'maroon brown' unit at the 1-m level, the wash site at the 7-m level, and the *Coryphodon* at the 13-m level all represent the same Purple-2 marker bed at different places in SC-67. This reddish-purple to purple mudstone unit is the middle stage-4

paleosol in the figure 6B stratigraphic section described by Kraus (1987, p. 608).

Upper Double-Red mudstones. The Upper Double-Red mudstones are similar in appearance to the Lower Double-Red mudstones described above, and the two are easily confused if not traced carefully and considered in relation to Purple-2. Here again, the lower unit is called Upper Double-Red A and the higher is called Upper Double-Red B. Both Upper Double-Red mudstones were completely removed by the major scour above and to the east of SC-67. The higher part of the Upper Double-Red mudstones is replaced by the Upper Boundary Sandstone west of the western pair of faults running through SC-67, and Upper Double-Red A is mapped as a unit with the upper boundary sandstone where the two occur together. Upper Double-Red A is the highest of the stage-4 paleosols in the figure 6B stratigraphic section described by Kraus (1987, p. 608).

Purple-3 mudstone. Purple-3 is a thin but conspicuous purple mudstone overlying the Upper Double-Red mudstones above SC-67. This unit marks the upper limit of the locality both geographically and stratigraphically. It is probably more or less correlative with the SC-405 level in the upper boundary sandstone, and together these appear to mark the stratigraphic upper limit of the Wa-0 mammalian fauna and the transition to a Wa-1 fauna. Purple-3 is truncated by the major scour surface east of SC-67, and it is replaced by the upper boundary sandstone west of SC-67.

Purple-4 mudstone. The thickest and most conspicuous purple mudstone at the south end of Polecat Bench is the Purple-4 mudstone. It is missing east of SC-67, where it was removed by the major scour event. Above SC-67 the unit is on the order of 1 m thick, and the color is a genuine grayish-red purple on a freshly fractured surface, as contrasted with the grayish red mudstones that weather purple found lower in the section. This bed can be traced from the scour edge above SC-67 westward to the western pair of faults, where it is offset. Then it can be traced northward above SC-405, SC-308, and SC-121, and then to a position below SC-206 (Fig. 6). Purple-4 can be traced farther northward on the west side of Polecat Bench to a point east of SC-80 (Fig. 1), where it provides an important tie at the 1541-1542 m level between stratigraphic sections on the west and east sides of Polecat Bench (Figs. 2-3).

Purple-4 is interesting too because it appears to line up stratigraphically with the top of the upper of the two sheet-like sandstones in the scour fill sequence east of SC-67. Hence the unusual maturity of Purple-4 as a paleosol may reflect oxidation during the time the section east of SC-67 was scoured and filled. Details of bedding contact between laterally-equivalent cumulative and avulsion facies at the scour edge are unfortunately obscured by erosion and slumping.

Top Red A mudstone. The Top Red A mudstone is the first prominent red bed above Purple-4. It is well exposed above SC-67 and it is important because it can be traced eastward across the top of the scour and fill sequence east of SC-67. This constrains the time of scouring and filling to lie between

the time of deposition of the Purple-4 and the Top Red A mudstones. Top Red A can be traced westward to the western pair of faults, where it is offset, and then it can be traced north and east around the south end of Polecat Bench to SC-206 where it is one of the lower beds yielding fossils in that locality. SC-68 and SC-122 were not located precisely relative to marker beds when they were first collected, but their mapped positions suggest that they were developed on Top Red A. SC-68, SC-122, and SC-206 all yield Wa-1 faunas (see below).

Top Red B mudstone. The Top Red B mudstone is a slightly thinner red mudstone, also prominent, that is found above SC-67. Tracing this eastward, it is replaced by a thin channel or ribbon sandstone that is at approximately the same level as a carbonaceous shale above the scour and fill sequence farther to the east. Tracing Top Red B westward, it parallels Top Red A all the way to SC-206, where it is one of the higher beds yielding Wa-1 fossils.

Fossil localities

Eighteen mammal-bearing fossil localities are shown in Figure 6. Four of these (SC-72, SC-73, SC-75, and SC-76) are late Clarkforkian localities east of the study area and older than any considered in detail here (see Fig. 3). Five Clarkforkian localities are of interest here: SC-70, SC-71, SC-77, SC-107, and SC-343. Earliest Wasatchian localities include SC-404 that is stratigraphically lower than most Wa-0 localities, and SC-67, SC-69, SC-121, and SC-308 that yield a typical Wa-0 fauna. SC-405 may be the lowest Wa-1 locality, although it has not yielded a large fauna. SC-68, SC-122, and SC-206 all yield typical Wa-1 mammals. Faunas from the latter fourteen fossil localities are discussed in a following section on biotic change.

PALEOCENE-EOCENE STRATIGRAPHY IN VERTICAL SECTIONS

Five stratigraphic sections were measured at the south end of Polecat Bench, and stable isotopes were sampled from four of these (Bowen et al., this volume). Colored circles in Figure 6 show the positions of isotope samples, while solid circles show the trace of lithological sections (where these are different). The easternmost and lowest stratigraphic section was measured in the vicinity of locality SC-77. A second stratigraphic section was measured in the vicinity of SC-343. It duplicates part of the SC-77 section, and both are capped by the same scour-and-fill interval of drab avulsion sediment. The third stratigraphic section starts below and ends above locality SC-67. This supercedes and replaces the SC-67 section published previously (Gingerich, 1989, p. 13), with notable improvements due to more careful mapping and tracing of marker beds. The fourth stratigraphic section was measured in the vicinity of SC-121. This is a lateral equivalent of the SC-67 section, but no isotope samples were taken in the SC-121 section. The stratigraphic section in figure 6B of Kraus (1987, p. 608) was measured on the west side of locality SC-405, about

half way between the SC-67 and SC-121 sections described here. Finally, the fifth stratigraphic section is effectively a continuation of the SC-121 section, and consists of a series of superposed isotope samples taken at the SC-206 end of the study area to extend sampling higher than is possible above SC-67.

The SC-77, SC-343, SC-67, and SC-121 sections were measured with a Jacob's staff and Abney level, starting at the base of the section and working up to the top. Lithological descriptions and colors were recorded as each section was measured. In the SC-206 section only the lithologies and colors of sampled paleosol horizons were recorded. The spacing of beds in the SC-206 section is based on positions and elevations determined by differential GPS and the calculated perpendicular height of each isotope site above the plane of the Purple-4 mudstone (rescaled slightly to match the Purple-4 to Top Red B thickness measured by leveling in the SC-67 section).

SC-77 Stratigraphic Section

The SC-77 stratigraphic section is illustrated diagrammatically in Figure 8. It is 50 m thick, starting in upper Clarkforkian strata and ending in lower Wasatchian strata. The predominant 'background' lithology is gray mudstone (colors are described in appendix Table A1). The Thick Orange mudstones mentioned above as key marker beds are exposed in locality SC-77 in the 2-4 m interval near the base of the section. Red mudstones possibly correlative with the Purple-Red mudstone marker bed exposed above SC-70 are found 14-16 m above the base of the section. Purple-0 lies in the 25-26 m interval here. This is overlain by the brown paleosol sequence in the interval from 27-31 m, with the Top Brown marker bed present at the top of the sequence. Lower Double-Red beds A and B are well exposed in the interval from 32-35 m above the base of the section. Purple-2 is thick here, spanning the interval from about 39-41 m. The section is truncated by the major scour-and-fill sequence, beginning at 43 m above the base of the section. Descriptions of these key marker beds and other notable beds are recorded in Figure 8, with their corresponding fresh colors. The positions of in situ paleosol soil nodules sampled for carbon and oxygen isotopes are shown at the right of the lithological column in Figure 8, yielding samples numbered from 2-8 and from 10-24 (see Bowen et al., this volume).

One mammal-bearing fossil locality, SC-77 itself, lies within the SC-77 section. This yields a late Clarkforkian fauna (Cf-3; see below), principally from gray mudstones just below the Thick Orange mudstone interval. The levels of two other nearby fossiliferous localities, SC-343 and SC-404, can be correlated with this section by tracing beds laterally. The base of the SC-77 section shown in Figure 8 is at about 1479.5 m above the Cretaceous-Tertiary boundary in the master Polecat Bench section, as measured on the southeast side of Polecat Bench (Fig. 3). This means that Purple-0 is at about the 1505 m level, the base of the Wa-0 interval is at about the 1510 m level, Purple-2 is at about the 1520 m level, and the base of the

South Polecat Bench SC-77 section

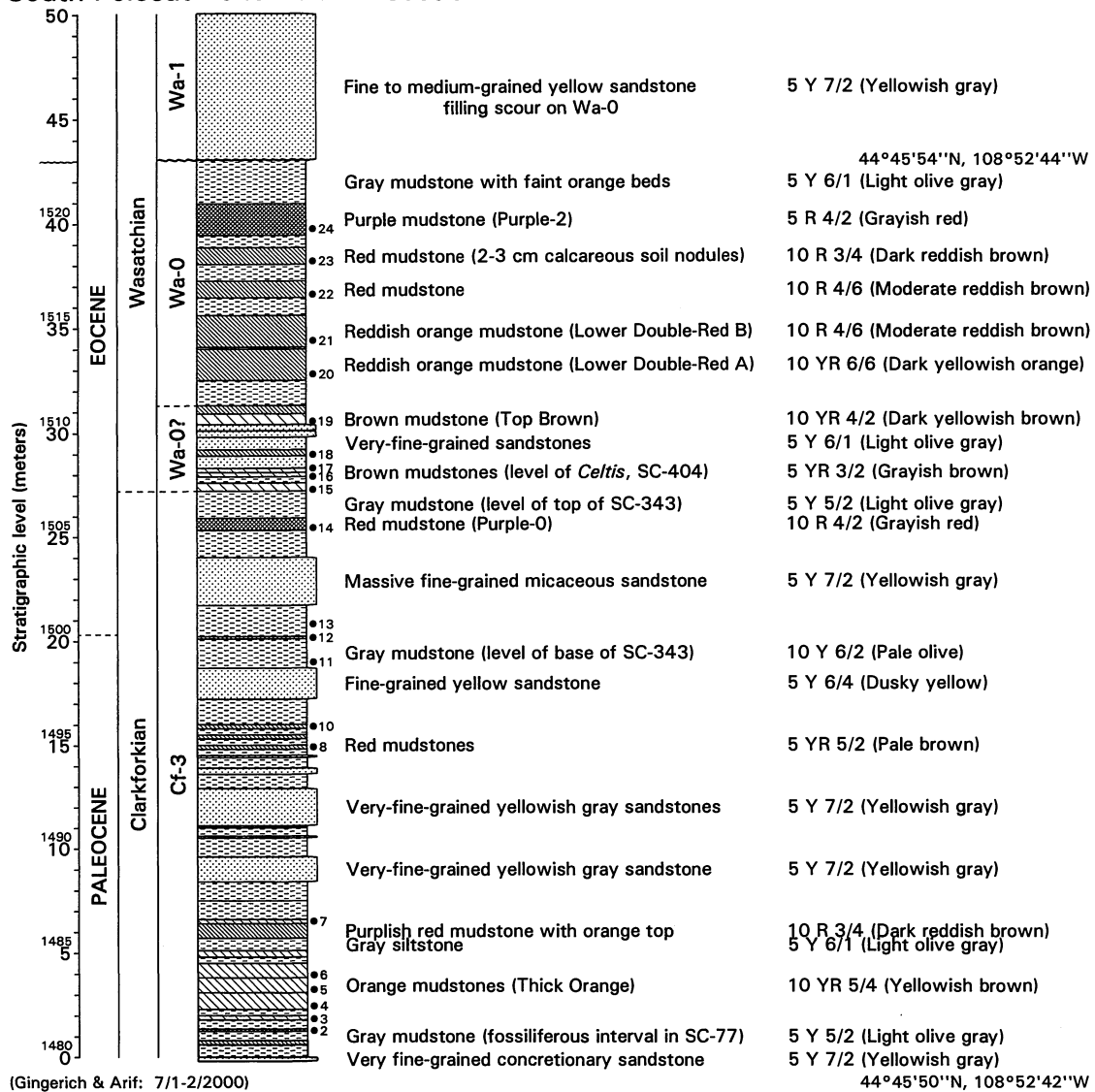


FIGURE 8 — South Polecat Bench SC-77 stratigraphic section. Ordinate is in meters above the base of the section (inset numbers on the ordinate are meter levels in the Polecat Bench master section). Lithologies include standard descriptions in the middle column and fresh colors in the right-hand column. Solid circles show stratigraphic positions of isotope samples (see Bowen et al., this volume). Paleocene-Eocene boundary marked by the beginning of the negative $\delta^{13}\text{C}$ isotope excursion is at about the 20 m level here (1500 m in Polecat Bench master section; Bowen et al., this volume). This is about 7 m lower than the beginning of Wasatchian zone Wa-0? marked by the appearance of *Celtis* and *Meniscotherium*, and about 11 m lower than the beginning of Wasatchian zone Wa-0 marked by the appearance of *Perissodactyla*, *Artiodactyla*, and *Primates*. Note the disconformity near the top of the section where sandstone of the scour-fill sequence overlies mudstone above the Purple-2 marker bed.

scour-and-fill sequence is at about the 1522 m level in the Polecat Bench section.

SC-343 Stratigraphic Section

The SC-343 stratigraphic section is illustrated in Figure 9. It is 25 m thick, starting in upper Clarkforkian strata and end-

ing in lower Wasatchian strata. Lithologies, thicknesses, and colors match those in the SC-77 section very closely. Purple-0 lies in the 4-5 m interval here. This is overlain by the brown paleosol sequence in the interval from 6-10 m, with the Top Brown marker bed present at the top of the sequence. Lower Double Red beds A and B are well exposed in the interval from 11-14 m above the base of the section. Purple-2 is thick here,

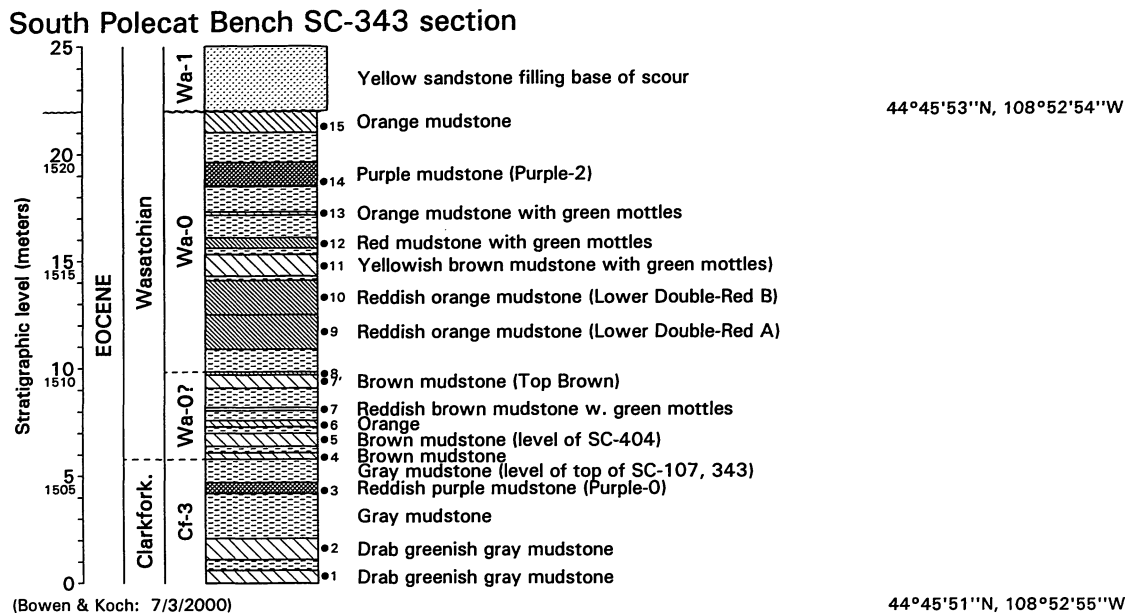


FIGURE 9 — South Polecat Bench SC-343 stratigraphic section. Ordinate is in meters above the base of the section (inset numbers on the ordinate are meter levels in the Polecat Bench master section). Lithologies include standard descriptions in the middle column. Colors here were not recorded systematically (see SC-77 section above). Solid circles show stratigraphic positions of isotope samples (see Bowen et al., this volume). Locality SC-404 yielding *Meniscotherium* occurs just above the level of SC-343 and other latest Clarkforkian Cf-3 localities, and just below the level of SC-67 and other earliest Wasatchian Wa-0 localities. Again note the disconformity near the top of the section where sandstone of the scour-fill sequence overlies mudstone above the Purple-2 marker bed.

spanning the interval from about 18.5-19.5 m. The section is truncated by the major scour-and-fill sequence, beginning at 22 m above the base of the section. The positions of in situ paleosol soil nodules sampled for carbon and oxygen isotopes are shown at the right of the lithological column in Figure 9, yielding samples numbered from 1-15 (see Bowen et al., this volume).

Two mammal-bearing fossil localities, SC-343 itself and SC-404, lie within the SC-343 section. SC-343 yields a late Clarkforkian fauna (Cf-3; see below), principally from gray mudstones below the Purple-0 level (and extending several meters below the base of the measured section). The level of one other fossil locality, SC-107, can be correlated with this section by tracing beds laterally. The base of the SC-343 section shown in Figure 9 is at about 1500.5 m above the Cretaceous-Tertiary boundary in the master Polecat Bench section, as measured on the southeast side of Polecat Bench (Fig. 3). This means, as in the SC-77 section, that Purple-0 is at about the 1505 m level, the base of the Wa-0 interval is at about the 1510 m level, Purple-2 is at about the 1520 m level, and the base of the scour-and-fill sequence is at about the 1522 m level in the Polecat Bench section.

SC-67 Stratigraphic Section

The SC-67 stratigraphic section is illustrated diagrammatically in Figure 10. It is 53 m thick, and is entirely in lower

Wasatchian strata. The predominant 'background' lithology is again gray mudstone (colors are described in appendix Table A2). The section starts in the brown paleosol sequence, with the Top Brown marker bed present at about 4.5 m above the base of the section. Lower Double-Red A is exposed in the interval from 6-8 m above the base of the section, but Lower Double-Red B has been cut out by erosion and replaced by the ribbon sandstone described above. Purple-2 is thick, spanning the interval from about 12-13 m. The section continues uninterrupted by the major scour-and-fill sequence found east of SC-67. Upper Double-Red A is thin here, at the 18 m level, but Upper Double-Red B is a thick red bed spanning the interval from about 19.5-21.5 m. Purple-4 is found at about 34 m above the base of the section. Top Red A lies at about the 42 m level, and Top Red B lies at about the 47 m level. Descriptions of these key marker beds and other notable beds are recorded in Figure 10, with their corresponding fresh colors. The positions of in situ paleosol soil nodules sampled for carbon and oxygen isotopes are shown at the right of the lithological column in Figure 10, yielding samples numbered from 1-15 and from 17-23 (see Bowen et al., this volume).

Two mammal-bearing fossil localities, SC-67 itself and SC-68, lie within the SC-67 section. SC-67 has yielded a large earliest Wasatchian fauna (Wa-0; see below), principally from the interval including the Lower Double-Red beds, Purple-2, and the Upper Double-Red beds. SC-68 has yielded a tooth of *Diacodexis metsiacus* and a dentary of *Copecion*

South Polecat Bench SC-67 section

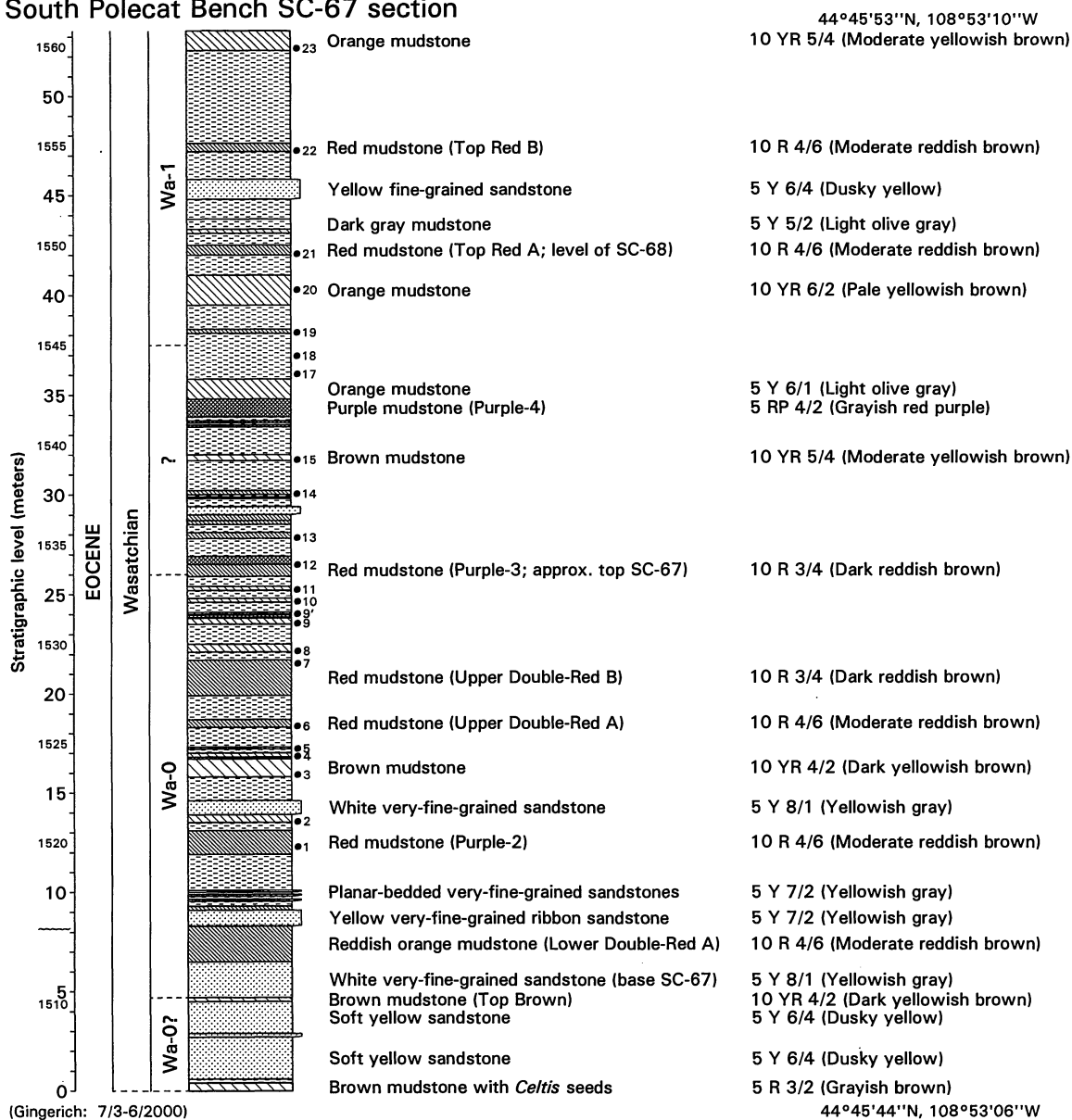


FIGURE 10 — South Polecat Bench SC-67 stratigraphic section. Ordinate is in meters above the base of the section (inset numbers on the ordinate are meter levels in the Polecat Bench master section). Lithologies include standard descriptions in the middle column and fresh colors in the right-hand column. Solid circles show stratigraphic positions of isotope samples (see Bowen et al., this volume). Note the disconformity near the base of the section where a ribbon sandstone replaces the Lower Double-Red B marker bed. There is no scour-fill sequence replacing strata above the Purple-2 marker bed as there is in the SC-77 and SC-343 sections above.

brachypternus indicative of a post-Wa-0 fauna. The base of the SC-67 section shown in Figure 10 is at about 1505.5 m above the Cretaceous-Tertiary boundary in the master Polecat Bench section, as measured on the southeast side of Polecat Bench (Fig. 3). This means that the Top Brown mudstone and

the base of the Wa-0 interval are at about the 1510 m level, Lower Double-Red A is in the interval from 1512-1514 m, the base of the ribbon sandstone scour-and-fill is at about 1514 m, Purple-2 is at about the 1520 m level, Upper Double-Red beds A and B are in the interval from 1526-1529 m, Purple-3 is at

South Polecat Bench SC-121 section

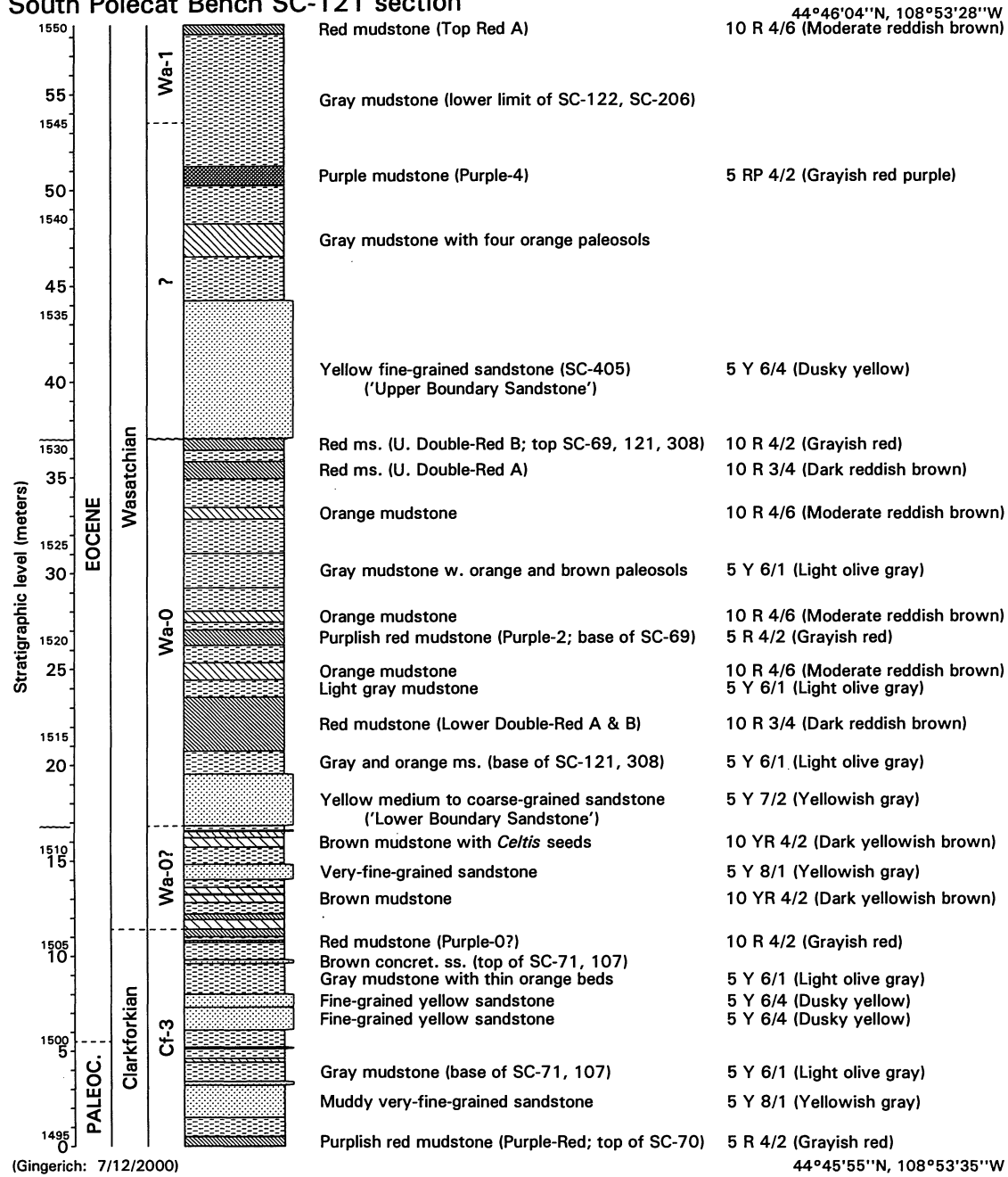


FIGURE 11 — South Polecat Bench SC-121 stratigraphic section. Ordinate is in meters above the base of the section (inset numbers on the ordinate are meter levels in the Polecat Bench master section). Lithologies include standard descriptions in the middle column and fresh colors in the right-hand column. No isotope samples were taken from this section. Paleocene-Eocene boundary marked by the beginning of the negative $\delta^{13}C$ isotope excursion is at about the 5 m level here (1500 m in Polecat Bench master section; Bowen et al., this volume). This is about 6 m lower than the beginning of Wasatchian zone Wa-0? marked by the appearance of *Celtis* and *Meniscotherium*, and about 11 m lower than the disconformity at the base of the Lower Boundary Sandstone that underlies earliest Wasatchian zone Wa-0. There is a second disconformity higher in the section at the base of the Upper Boundary Sandstone. This section enables comparison with a similar section lacking lower and upper boundary sandstones (e.g., SC-67 section above). The middle part of the section here is equivalent to that in figure 6B of Kraus (1987) with its stage 3 and stage 4 paleosols, which was measured and studied nearby.

about 1534 m, Purple-4 is at about 1542 m, Top Red A is at 1550 m, and Top Red B is at about 1555 m in the Polecat Bench section.

SC-121 Stratigraphic Section

The SC-121 stratigraphic section is illustrated diagrammatically in Figure 11. It is 58 m thick, starting in upper Clarkforkian strata and ending in lower Wasatchian strata. The predominant 'background' lithology is gray mudstone (colors are described in appendix Table A3). The section starts at the Purple-Red mudstone that marks the top of locality SC-70 and continues through a red mudstone that may represent Purple-0 at about 11 m above the base. The brown paleosol succession is in the interval from 11-17 m, but the Top Brown marker bed appears to have been removed by erosion during emplacement of the Lower Boundary Sandstone. This occupies the interval from about 17 to 20 m. Lower Double-Red A and B are exposed in the interval from about 20.5 to 23.5 m above the base of the section. Purple-2 spans the interval from about 26-27 m. Upper Double-Red A is thin here, at the 35-36 m level, and Upper Double-Red B at the 1530 m level is thin because most of it has been removed during deposition of the Upper Boundary Sandstone. The latter fills the interval from about 37-44 m above the base of the section. Purple-4 is found at about 50.5-51.5 m above the base of the section. Top Red A caps the section at about 58.0-58.5 m above the base. Descriptions of these key marker beds and other notable beds are recorded in Figure 11, with their corresponding fresh colors. No paleosol soil nodules were sampled for isotopes from this section.

The SC-121 section is important in tying together a number of important mammal-bearing fossil localities. First, the section starts with the Purple-Red bed marking the top of late Clarkforkian locality SC-70. Two late Clarkforkian localities, SC-71 and SC-107, lie in the interval between the Purple-Red marker bed and the red mudstone possibly representing Purple-0. Wa-0 localities SC-121 and SC-308 are lateral equivalents of SC-67, spanning the full stratigraphic interval between the Lower Boundary Sandstone and the Upper Boundary Sandstone. Wa-0 locality SC-69 has Purple-2 at its base and extends to the Upper Boundary Sandstone. Locality SC-405 is developed near the base of the Upper Boundary Sandstone on a long narrow ridge where the top of the unit has been removed by erosion. Finally, two Wa-1 localities, SC-122 and SC-206, have their bases above the Purple-4 mudstone. The base of the SC-121 section shown in Figure 11 is at about 1495 m above the Cretaceous-Tertiary boundary in the master Polecat Bench section, as measured on the southeast side of Polecat Bench (Fig. 3). This means that the brown paleosol sequence lies in the interval from 1506 to 1511 m, the Lower Boundary Sandstone is in the interval from 1511 to 1513 m. Lower Double-Red A and B are in the interval from 1514-1517 m, Purple-2 is at about the 1520 m level, Upper Double-Red beds A and B are in the interval from 1528-1530 m, the Upper Boundary Sandstone fills the interval

from 1530-1536 m, Purple-4 is at about 1542 m, and Top Red A is at 1550 m.

SC-206 Stratigraphic Section

The SC-206 stratigraphic section is illustrated diagrammatically in Figure 12. It is 53.5 m thick, and is entirely in lower Wasatchian strata. The predominant 'background' lithology is gray mudstone (colors of paleosol horizons are described in appendix Table A4). The section starts at the Purple-4 marker bed. Top Red A is in the interval between about 8-9 m above the base of the section. Top Red B is at about the 13 m level. Descriptions of these key marker beds and other notable beds are recorded in Figure 11, with their corresponding fresh colors. The positions of in situ paleosol soil nodules sampled for carbon and oxygen isotopes are shown at the right of the lithological column in Figure 12, yielding samples numbered 1, 3-6 and 8-16 (see Bowen et al., this volume).

The SC-206 section includes mammal-bearing fossil locality SC-206 itself in the interval between about 2 and 17 m above the base of the section. This locality yields Wa-1 mammals, and the productive levels include Top Red A and Top Red B and the gray mudstones just below, between, and just above these marker beds. The base of the SC-206 section shown in Figure 12 is at about 1542 m above the Cretaceous-Tertiary boundary in the master Polecat Bench section, as measured on the southeast side of Polecat Bench (Fig. 3). This is the level of Purple-4, meaning, as before, that Top Red A is at about 1550 m and Top Red B is at about 1555 m in the Polecat Bench section.

BIOTIC CHANGE ACROSS THE PALEOCENE-EOCENE BOUNDARY

Mammalian faunas are known from fourteen localities representing seven distinctive, successive, stratigraphic intervals in the area studied here (not considering the four localities east of the easternmost fault in Fig. 6). Three of these intervals yield upper Clarkforkian faunas of late Clarkforkian age (Cf-3). One yields a new stratigraphically-intermediate fauna that is probably earliest Wasatchian in age (Wa-0?). One yields a basal Wasatchian fauna of earliest Wasatchian age (the original Wa-0 fauna). One yields a lower Wasatchian fauna that is Wa-0 or Wa-1 in age. Finally, one yields a lower Wasatchian fauna that is definitely Wa-1 in age.

Clarkforkian Biota

The lowest stratigraphic interval considered here is the Thick Orange mudstone interval centered at the 1480 m level in the Polecat Bench stratigraphic section. All fossils in this interval come from locality SC-77 at the base of the SC-77 stratigraphic section (Fig. 8). Four identifiable mammalian specimens are known (Table 3), of which *Haplomylus simpsoni* is indicative of Clarkforkian age. Superposition well above the highest range datum of *Plesiadapis cookei* in the Polecat

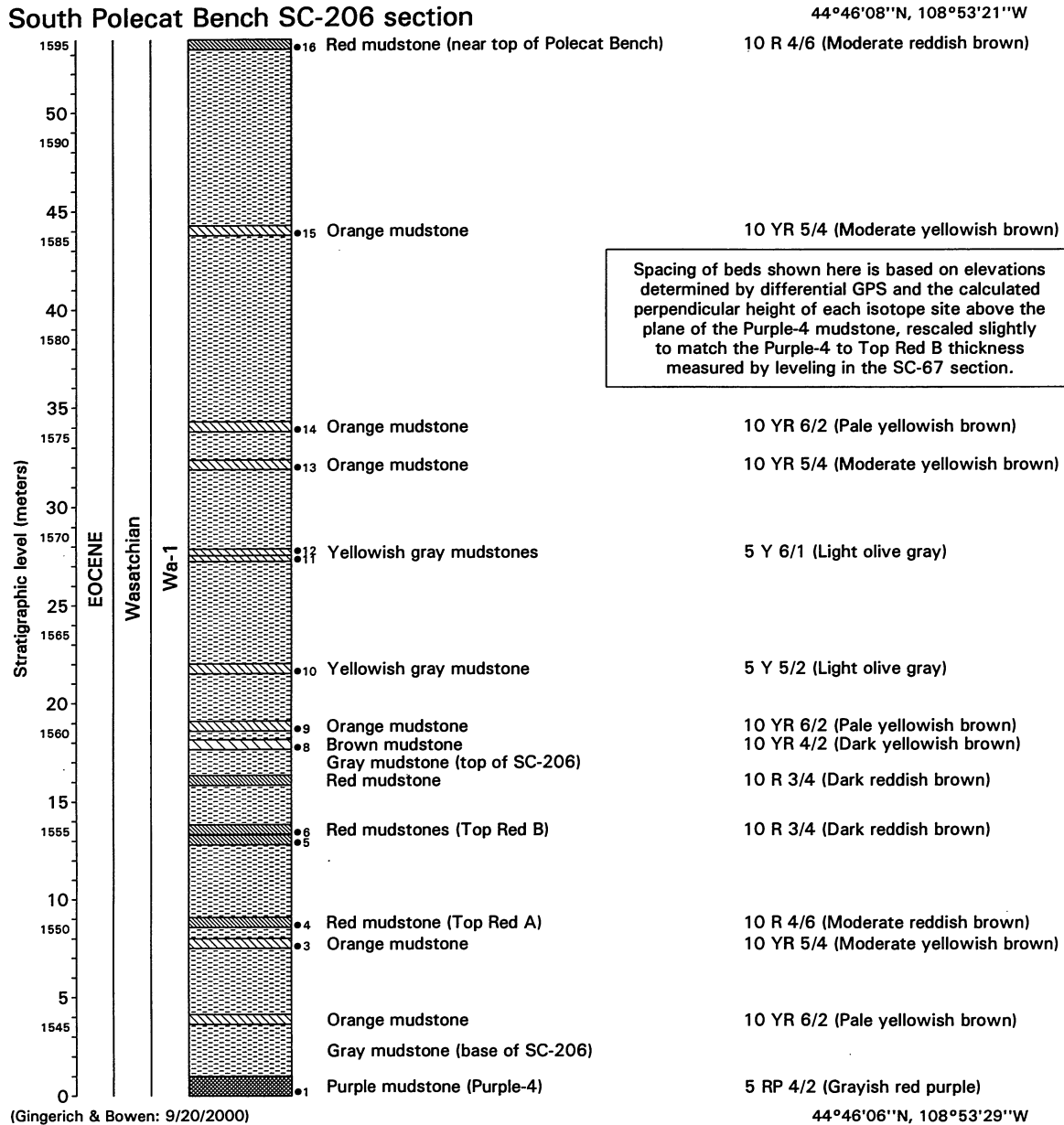


FIGURE 12 — South Polecat Bench SC-206 stratigraphic section. Ordinate is in meters above the base of the section (inset numbers on the ordinate are meter levels in the Polecat Bench master section). Lithologies include standard descriptions in the middle column and fresh colors of sampled intervals in the right-hand column. Solid circles show stratigraphic positions of isotope samples (see Bowen et al., this volume). Isotopes were sampled from this section because it includes strata some 35 m higher in the Polecat Bench master section than those sampled in the SC-67 section.

Bench section indicates that the age is late Clarkforkian (Cf-3; Fig. 3).

The second fossiliferous interval in the Clarkforkian part of the section is found on the opposite side of the mapped area at locality SC-70. The base of SC-70 overlies the Thick Orange

mudstone interval, while the top of SC-70 can be traced to the base of the SC-121 section. Thus the SC-70 fossiliferous interval is centered at the 1490 m level in the Polecat Bench stratigraphic section. Thirteen identifiable mammalian specimens are known (Table 4), with *Probathyopsis praecursor*,

TABLE 3 — Mammalian fauna from late Clarkforkian locality SC-77 in a collecting interval centered on 1480 m in the Polecat Bench stratigraphic section. The presence of *Haplomylus simpsoni* indicates a Clarkforkian age, and superposition above the highest range datum of *Plesiadapis cookei* narrows this to Cf-3. UM, University of Michigan Museum of Paleontology; m, lot number for miscellaneous teeth.

Genus and species	Specimen count	Voucher specimen(s)	Reference(s)
<i>Niptomomys dorenae</i>	1	UM 66176	Rose (1981: 53)
<i>Azygonyx grangeri</i>	1	UM 108656	
<i>Haplomylus simpsoni</i>	1	UM 66177m	Rose (1981: 78)
<i>Dissacus praenuntius</i>	1	UM 66175	Rose (1981: 86)

TABLE 4 — Mammalian fauna from late Clarkforkian locality SC-70 in a collecting interval centered on 1490 m in the Polecat Bench stratigraphic section. The presence of *Probathyopsis praecursor*, *Aletodon gunnelli*, *Apheliscus nitidus*, and *Haplomylus simpsoni* indicates a Clarkforkian age, and superposition above the highest range datum of *Plesiadapis cookei* narrows this to Cf-3. UM, University of Michigan Museum of Paleontology; m, lot number for miscellaneous teeth.

Genus and species	Specimen count	Voucher specimen(s)	Reference(s)
<i>Azygonyx grangeri</i>	1	UM 76859	
<i>Probathyopsis praecursor</i>	1	UM 66146	Rose (1981: 93), Thewissen and Gingerich (1987: 209)
<i>Oxyaena transiens</i>	1	UM 66148m	Rose (1981: 105)
<i>Viverravus politus</i>	1	UM 66853	Rose (1981: 101), Polly (1997: 4)
<i>Aletodon gunnelli</i>	1	UM 66850	Gingerich (1977: 240)
<i>Apheliscus nitidus</i>	1	UM 66147	Rose (1981: 83)
<i>Copecion brachypternus</i>	1	UM 66852	Rose (1981: 73), Thewissen (1990: 68)
<i>Ectocion osbornianus</i>	4	UM 66846, etc.	Rose (1981: 73)
<i>Haplomylus simpsoni</i>	1	UM 66847	Rose (1981: 78)
<i>Dissacus praenuntius</i>	1	UM 66854	Rose (1981: 86)

Aletodon gunnelli, *Apheliscus nitidus*, and *Haplomylus simpsoni* all indicating Clarkforkian age.

The highest fossiliferous interval in the Clarkforkian part of the section is represented by three localities, SC-71, SC-107, and SC-343, distributed across the middle part of the study area. These are above the level of the Red-Purple bed overlying SC-70 (possibly equivalent to the red mudstones in the SC-77 stratigraphic section; Fig. 8), and just above or at the level of Purple-0 in the SC-77 and SC-343 stratigraphic sections (Figs. 8 and 9). Thus this highest Clarkforkian interval is centered at the 1502 m level in the Polecat Bench stratigraphic section. Eighteen identifiable mammalian specimens are known (Table 5), with *Aletodon gunnelli* being the only taxon clearly diagnostic of Clarkforkian age. Another characteristic of late Clarkforkian faunas is the relative abundance of *Phenacodus* and *Ectocion* (Rose, 1981), and 7 of the 18 identifiable specimens (39%) are *Ectocion osbornianus*.

Most specimens were found below Purple-0, but a typically Clarkforkian-looking dark-colored specimen of *Ectocion osbornianus* was found by I. Zalmout in 2000 just above the level of Purple-0 (UM 108647 from SC-343), which is the principal indication that Purple-0 lies within the uppermost Clarkforkian faunal interval.

Meniscotherium priscum Biota

It is generally recognized that stony endocarps of the elm-related shrub or tree *Celtis phenacodorum* are found in Wasatchian but not Clarkforkian strata in the Bighorn Basin (e.g., Rose, 1981, p. 138). In 1989 I described *Celtis* endocarps from several 'latest Clarkforkian' localities where there is no possibility of contamination from overlying sediments (Gingerich, 1989, p. 15). In present terms, the 4-m-thick brown mudstone sequence between 1506 and 1510 m in the Polecat

TABLE 5 — Mammalian fauna from late Clarkforkian localities SC-71, SC-107, and SC-343 in a collecting interval centered on 1502 m in the Polecat Bench stratigraphic section. The presence of *Aletodon gunnelli* indicates a Clarkforkian age, and superposition above the highest range datum of *Plesiadapis cookei* narrows this to Cf-3. *UM*, University of Michigan Museum of Paleontology; *m*, lot number for miscellaneous teeth.

Genus and species	Specimen count	Voucher specimen(s)	Reference(s)
<i>Arctodontomys</i> cf. <i>A. wilsoni</i>	1	UM 80851	Gunnell (1989: 92)
<i>Ignacius</i> sp.	1	UM 102531	
<i>Palaeonodon</i> sp.	1	UM 97883	
Paramyid sp.	1	UM 102532	
<i>Uintacyon rudis</i>	1	UM 76861	Gingerich (1983b: 203)
<i>Viverravus politus</i>	1	UM 66618	Rose (1981: 101), Polly (1997: 4)
<i>Aletodon gunnelli</i>	2	UM 83649, etc.	
<i>Copecion brachypternus</i>	1	UM 83648	Thewissen (1990: 68)
<i>Ectocion osbornianus</i>	7	UM 66619, etc.	Rose (1981: 73), Thewissen (1990: 40)
<i>Phenacodus intermedius</i>	1	UM 83619, etc.	Thewissen (1990: 40)
<i>Thryptacodon antiquus</i>	1	UM 103073	

TABLE 6 — Mammalian fauna from transitional highest Clarkforkian to lowest Wasatchian locality SC-404 in a collecting interval centered on 1507 m in the Polecat Bench stratigraphic section. *Meniscotherium* has only been found in this transitional zone in the Bighorn Basin. It is known from later Wasatchian faunas in southern Wyoming and New Mexico. Association with endocarps of *Celtis phenacodorum* suggests that the biota is probably earliest Wasatchian (early Wa-0) in age. *UM*, University of Michigan Museum of Paleontology; *m*, lot number for miscellaneous teeth.

Genus and species	Specimen count	Voucher specimen(s)	Reference(s)
<i>Meniscotherium priscum</i>	1	UM 108645	This paper (see Fig. 13)

Bench section, centered on 1507 m, yields *Celtis* endocarps by the hundreds if not thousands. These are most easily found lying on a weathered outcrop, but they can also be found in situ in the brown paleosols. The 1506-1510 m interval ranges from just above Purple-0 up to and including the Top Brown mudstone unit just below the base of beds yielding the original Wa-0 fauna. A small area of the 1506-1510 m brown mudstones, what is now locality SC-404, was prospected carefully in 2000 by M. Arif. This locality is exposed on a saddle where it cannot be contaminated from above. *Celtis* endocarps are common, and one mammalian specimen found here in 2000 is a small, light-colored, left dentary with worn M_{1-2} (University of Michigan [UM] 108645; Fig. 13G-H; Table 6). The molars, though worn, show the distinctive lophoselenodont pattern of shearing crests that is only found in *Meniscotherium* among North American late Paleocene to early Eocene mammals (Granger, 1915; Gazin, 1965; Williamson and Lucas, 1992).

Granger (1915, p. 360) named *Meniscotherium priscum* based on a small, light-colored dentary found by W. J. Sinclair in 1911 (American Museum of Natural History [AMNH] 16145), and described it as coming from Clarkforkian strata at the head of Big Sand Coulee in the Clarks Fork Basin. Unfortunately the specimen does not have an entry in Sinclair and Granger's field book for 1911, so it is impossible to be certain where it came from geographically or stratigraphically. Rose (1981, p. 76), following Granger, considered it to be Clarkforkian. I argued in 1982 and again in 1989 that *Meniscotherium priscum* probably came from the vicinity of locality SC-67 at the south end of Polecat Bench (Gingerich, 1982b, p. 490; 1989, p. 55— we know that Sinclair collected here for two days in 1911 while Granger collected at the head of Big Sand Coulee).

The second specimen of *Meniscotherium priscum* to be found in the Bighorn Basin was found in 1987 (UM 91419 from locality MP-71; Fig. 13A-F). It came from a fauna thought

TABLE 7 — Mammalian fauna from early Wasatchian localities SC-67, SC-121, and SC-308 in a collecting interval centered on 1520 m in the Polecat Bench stratigraphic section. The presence of *Cantius torresi*, *Arfia junnei*, *Copecion davisii*, *Diacodexis ilicis*, and *Hyracotherium sandrae* indicates an earliest Wasatchian Wa-0 age. UM, University of Michigan Museum of Paleontology; m, lot number for miscellaneous teeth.

Genus and species	Specimen count	Voucher specimen(s)	Reference(s)
<i>Ectypodus tardus</i>	1	UM 86572m	Gingerich (1989: 22)
<i>Mimoperadectes labrus</i>	3	UM 92347, etc.	Gingerich (1989: 22)
Apatemyid	1	UM 97900	
<i>Macrocranium</i> n. sp.	1	UM 93378	
<i>Arctodontomys wilsoni</i>	1	UM 86572m	Gingerich (1989: 23)
<i>Niptomomys</i> (cf.) sp.	1	UM 85591	Gingerich (1989: 23)
<i>Phenacolemur praecox</i>	1	UM 79890m	Gingerich (1989: 23)
<i>Cantius torresi</i>	10	UM 83467, etc.	Gingerich (1986: 319; 1989: 23; 1995: 188)
<i>Ectoganus bighornensis</i>	12	UM 66617m, etc.	Gingerich (1989: 30)
<i>Azygonyx gunnelli</i>	9	UM 71768m, etc.	Gingerich (1989: 26)
<i>Azygonyx</i> sp.	3	UM 66616m, etc.	Gingerich (1989: 28)
<i>Esthonyx spatularius</i>	1	UM 87354m	Gingerich (1989: 24)
<i>Coryphodon</i> sp.	10	UM 79890m, etc.	Gingerich (1989: 29)
<i>Palaeonodon nievelti</i>	7	UM 83464m, etc.	Gingerich (1989: 63)
<i>Palaeonodon parvulus</i>	1	UM 101141	
<i>Acritoparamys atwateri</i>	7	UM 76237m, etc.	Gingerich (1989: 40)
<i>Acritoparamys</i> (cf.) <i>atavus</i>	1	UM 86003m	Gingerich (1989: 40)
<i>Paramys taurus</i>	6	UM 66617m, etc.	Gingerich (1989: 40)
<i>Acarictis ryani</i>	2	UM 86572m, etc.	Gingerich (1989: 33)
<i>Arfia junnei</i>	20	UM 67664, etc.	Gingerich (1989: 33)
<i>Dipsalidictis platypus</i>	11	UM 66137, etc.	Gingerich (1989: 31), Gunnell and Gingerich (1991: 158)
<i>Dipsalidictis transiens</i>	1	UM 82387m	Gingerich (1989: 32)
<i>Palaeonictis</i> sp.	1	UM 92889	Gingerich (1989: 33)
<i>Prolimnocyon eerius</i>	1	UM 87353	Gingerich (1989: 36)
<i>Prototomus deimos</i>	3	UM 66140m	Gingerich (1989: 33)
<i>Didymictis proteus</i>	14	UM 71765, etc.	Gingerich (1989: 39), Polly (1997: 4)
<i>Miacis winkleri</i>	1	UM 77203m	Gingerich (1989: 39)
<i>Viverravus acutus</i>	1	UM 87339	Gingerich (1989: 37), Polly (1997: 2)
<i>Viverravus politus</i>	1	UM 87857	Gingerich (1989: 36), Polly (1997: 4)
<i>Chriacus badgleyi</i>	6	UM 79887, etc.	Gingerich (1989: 41)
<i>Copecion davisii</i>	35	UM 66611, etc.	Gingerich (1989: 53), Thewissen (1990: 69)
<i>Ectocion osbornianus</i>	1	UM 66612	Gingerich (1989: 52), Thewissen (1990: 40)
<i>Ectocion parvus</i>	67	UM 66138, etc.	Gingerich (1989: 49), Thewissen (1990: 43)
<i>Hyopsodus loomisi</i>	48	UM 66614, etc.	Gingerich (1989: 47)
<i>Phenacodus vortmani</i>	6	UM 77203m, etc.	Gingerich (1989: 52), Thewissen (1990: 59)
<i>Thryptacodon barae</i>	1	UM 85669	Gingerich (1989: 40)
<i>Dissacus praenuntius</i>	6	UM 83477, etc.	Gingerich (1989: 44)
<i>Diacodexis ilicis</i>	11	UM 66613, etc.	Gingerich (1989: 56)
<i>Hyracotherium grangeri</i>	2	UM 66615, etc.	Gingerich (1989: 62)
<i>Hyracotherium sandrae</i>	33	UM 66139, etc.	Gingerich (1989: 58)

to be at the Clarkforkian-Wasatchian boundary, where *Phenacodus* and *Ectocion* are again associated with an endocarp of *Celtis* (Gingerich, 1989, p. 56). Consideration of the newly discovered third specimen in this light suggests a pattern: (1)

Meniscotherium is very rare in the Bighorn Basin, indicating that it comes from an age or environment that is rarely sampled; (2) two of the three *Meniscotherium* found to date in the Bighorn Basin come from strata first thought to be latest

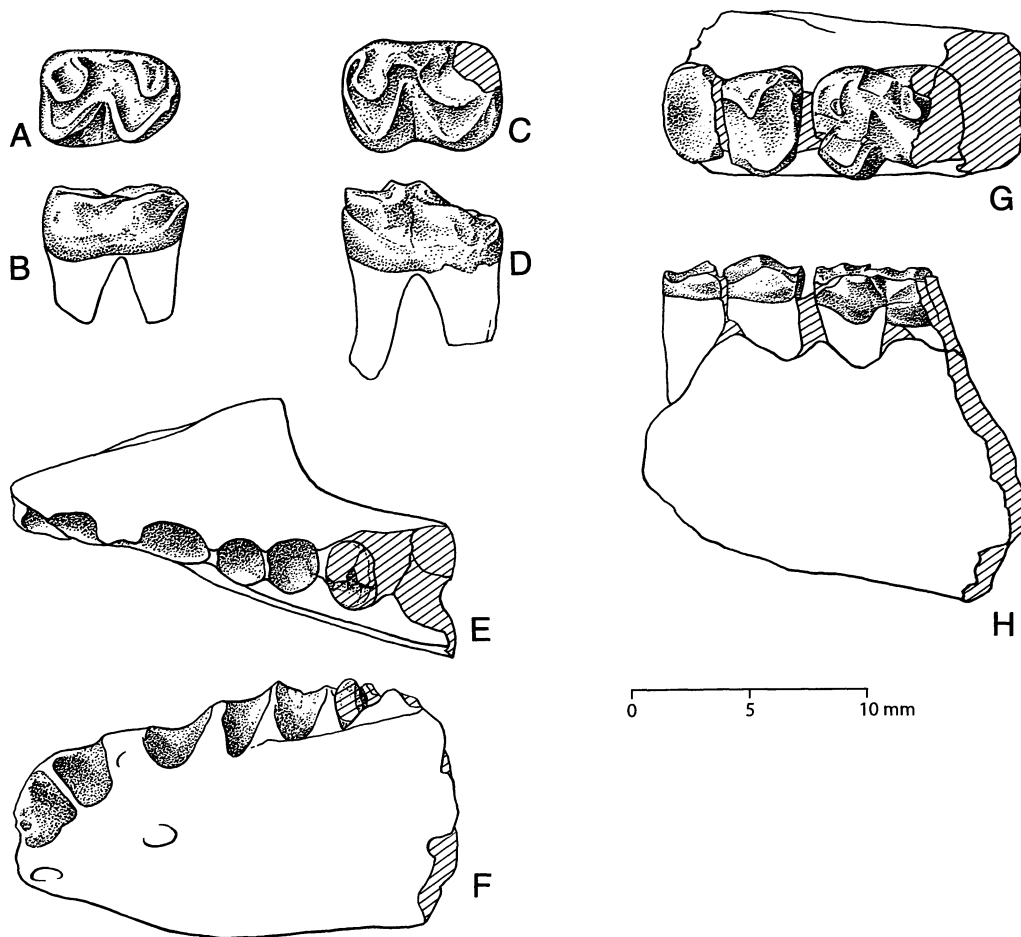


FIGURE 13 — New specimens of *Meniscotherium priscum* from transitional Clarkforkian-Wasatchian strata (Wa-0? interval here) that have *Celtis* but lack Wasatchian Perissodactyla, Artiodactyla, and Primates marking the beginning of Wa-0 time. A-F, University of Michigan [UM] 91419 from locality MP-71 (A-B, right M_1 in occlusal and lateral view; C-D, left M_2 in occlusal and lateral view; E-F, left dentary with alveoli for $I_{2,3}$, C_1 , and P_{1-2}). G-H, UM 108645, left dentary with M_{1-2} in occlusal and lateral view. Lower molars of *Meniscotherium* are distinctive in having a cristid obliqua that joins the protocristid near the metaconid, yielding a more lophoselenodont tooth than is seen in other condylarths.

Clarkforkian but associated with endocarps of *Celtis* (and the provenance of the exception, the type, is not known). I propose as a working hypothesis that *Meniscotherium priscum* and *Celtis phenacodorum* made their first appearance in the Bighorn Basin during the narrow interval of time represented by the brown mudstone sequence spanning the 1506-1510 m interval in the Polecat Bench stratigraphic section. They almost certainly represent a new pre-Wa-0 biota, here called, tentatively, Wa-0?, pending further discoveries that will clarify its composition. Wa-0? is included in the Wasatchian because both *Celtis* and *Meniscotherium* are known from later Wasatchian biotas (*Celtis* is abundant in overlying Wasatchian strata of the Bighorn and Clarks Fork Basins, while *Meniscotherium* is common in later Wasatchian strata of

southern Wyoming and New Mexico; this age interpretation is queried because the zone is still poorly known faunally).

It should be noted that locality SC-404 was previously part of latest Clarkforkian SC-343 discussed above, and the beds sampled in SC-404 are exposed at the top of SC-343 in many places. There are *Celtis phenacodorum* endocarps included with some lots of miscellaneous teeth and bone collected from SC-343, but these are regarded, as before (Gingerich, 1989, p. 15), as contaminants from strata of the SC-404 interval.

Early Wasatchian Wa-0 Biota

The lowest part of the Wasatchian that is well known faunally is the stratigraphic interval including Lower Double-

TABLE 8 — Mammalian fauna from early Wasatchian locality SC-69 in a collecting interval centered on 1530 m in the Polecat Bench stratigraphic section. The presence of *Cantius torresi*, *Copecion davisii*, *Arfia junnei*, and *Hyracotherium sandrae* indicates an earliest Wasatchian (Wa-0) age. *UM*, University of Michigan Museum of Paleontology; *m*, lot number for miscellaneous teeth.

Genus and species	Specimen count	Voucher specimen(s)	Reference(s)
<i>Mimoperadectes labrus</i>	1	UM 66144	Bown and Rose (1979: 93), Gingerich (1989: 22)
<i>Cantius torresi</i>	2	UM 66143, etc.	Gingerich (1989: 23)
<i>Arfia junnei</i>	1	UM 86135	Gingerich (1989: 33)
<i>Copecion davisii</i>	5	UM 83822, etc.	Gingerich (1989: 53), Thewissen (1990: 69)
<i>Ectocion parvus</i>	1	UM 83824	Gingerich (1989: 49), Thewissen (1990: 44)
<i>Hyopsodus loomisi</i>	2	UM 86130, etc.	Gingerich (1989: 47)
<i>Hyracotherium sandrae</i>	1	UM 86137m	Gingerich (1989: 58)

TABLE 9 — Mammalian fauna from early Wasatchian locality SC-405 in a collecting interval centered on 1535 m in the Polecat Bench stratigraphic section. Specimens listed here were previously considered to have come from locality SC-67 (Gingerich, 1989), but enclosure within the Upper Boundary Sandstone, absence of any distinctively Wa-0 taxon, brown-to-black color of bones and teeth, and presence of *Hyracotherium grangeri* suggests an early Wasatchian Wa-1 age. *UM*, University of Michigan Museum of Paleontology; *m*, lot number for miscellaneous teeth.

Genus and species	Specimen count	Voucher specimen(s)	Reference(s)
<i>Coryphodon</i> sp.	2	UM 79892, etc.	Gingerich (1989: 29)
<i>Hyracotherium grangeri</i>	1	UM 83637m	Gingerich (1989: 62; 1991: 187)

TABLE 10 — Mammalian fauna from early Wasatchian localities SC-68, SC-122, and SC-206 in a collecting interval centered on 1550 m in the Polecat Bench stratigraphic section. Superposition, close proximity to beds yielding a Wa-0 fauna, and the presence of *Cantius ralstoni*, *Haplomylys speirianus*, and *Diacodexis metsiacus* combine to indicate an early Wasatchian Wa-1 age. *UM*, University of Michigan Museum of Paleontology; *m*, lot number for miscellaneous teeth.

Genus and species	Specimen count	Voucher specimen(s)	Reference(s)
<i>Cantius ralstoni</i>	2	UM 69421, etc.	
<i>Paramys taurus</i>	1	UM 69419	Ivy (1990: 35)
<i>Didymictis leptomylys</i>	1	UM 69417	Polly (1997: 5)
<i>Copecion brachypternus</i>	1	UM 77014	Thewissen (1990: 68)
<i>Haplomylys speirianus</i>	3	UM 69418, etc.	
<i>Hyopsodus loomisi</i>	5	UM 69416, etc.	
<i>Diacodexis metsiacus</i>	2	UM 71771, etc.	
<i>Hyracotherium grangeri</i>	4	UM 66857, etc.	Gingerich (1991: 187)

Red A and B, Purple-2, and Upper Double-Red A and B marker beds. This interval is distinctive lithologically in having conspicuously thick and brightly colored orange-red and purple

mudstones representing paleosols that are thicker and more mature than those found in adjacent stratigraphic intervals. This interval is distinctive paleontologically in yielding the classic

South Polecat Bench section (composite)

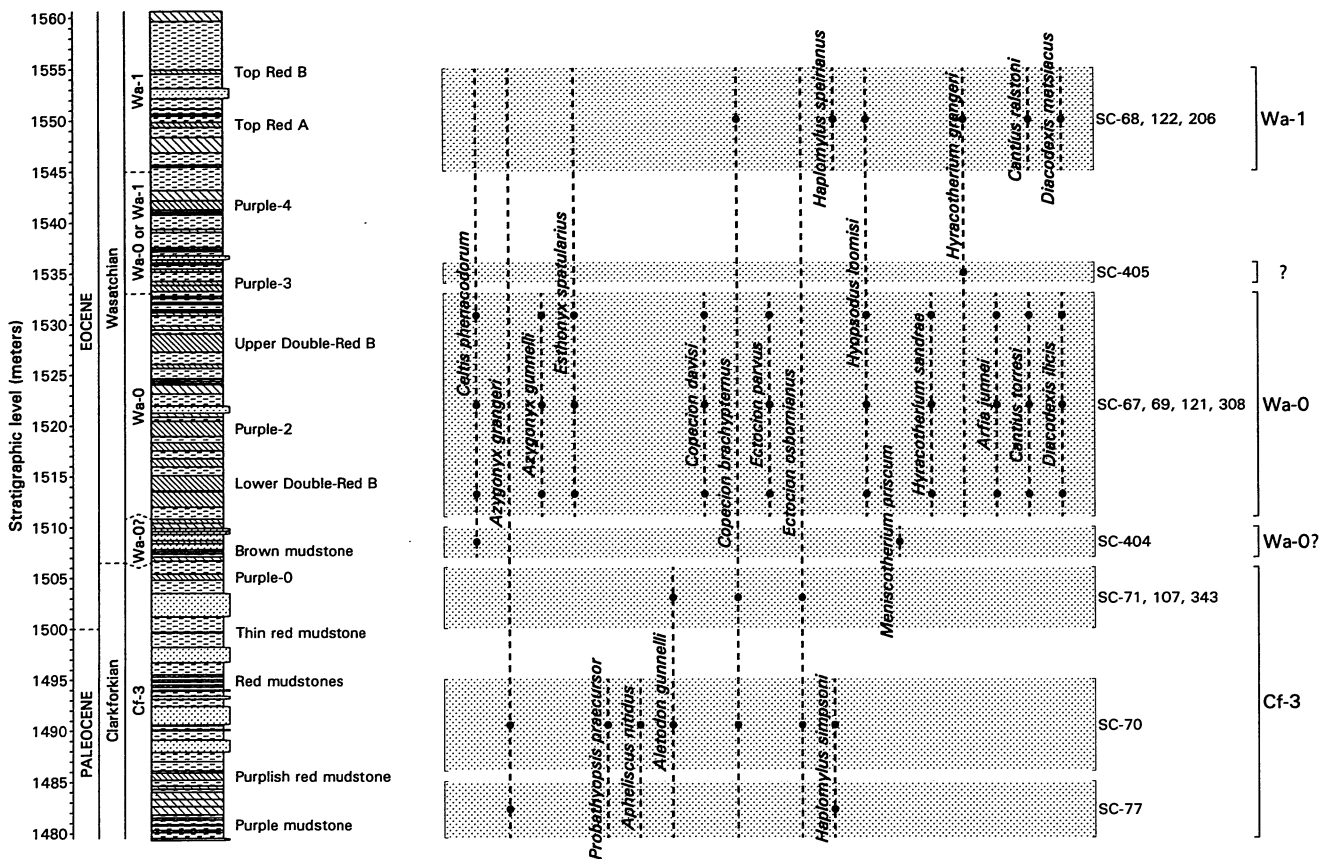


FIGURE 14 — Stratigraphic range chart of *Celtis* and the principal mammalian taxa crossing the Paleocene-Eocene boundary at the south end of Polecat Bench. Composite is based on individual sections shown in detail in Figures 8-11. Fourteen mammal-bearing fossil localities are known, representing seven distinct stratigraphic intervals (shaded). These can be grouped into four notable time-successive associations based on their biota. The first, a Cf-3 association, includes five localities in the lowest three intervals, which have one or more of the distinctively Clarkforkian taxa *Probathyopsis praecursor*, *Apheliscus nitidus*, *Aletodon gunnelli*, and/or *Haplomyilus simpsoni*. The second association, here labeled Wa-0?, includes one locality from the fourth interval, with *Celtis phenacodorum* and *Meniscotherium priscum*. The third, a Wa-0 association, includes four localities from the fifth interval, with *Copecion davisi*, *Hyracotherium sandrae*, *Arfia junnei*, *Cantius torresi*, and *Diacodexis ilicis* as diagnostic taxa. This is followed by a poorly-sampled interval, labeled Wa-0 or Wa-1, with one locality yielding *Hyracotherium grangeri* that could be either Wa-0 or Wa-1 in age. Finally, the fourth association, representing Wa-1, includes three localities from the seventh stratigraphic interval, with *Haplomyilus speirianus*, *Cantius torresi*, and *Diacodexis metsiacus* as diagnostic taxa.

Wa-0 mammalian fauna, which is unusual both in terms of taxonomic composition and in terms of the size of the animals represented (Gingerich, 1989; Clyde and Gingerich, 1998). The Wa-0 fauna includes the first representatives of cosmopolitan Artiodactyla, Perissodactyla, Primates, and hyaenodontid Creodonta that make the Eocene so different from the Paleocene on northern continents. The Wa-0 fauna also has many taxa that are conspicuously smaller in tooth size and overall body size than their congeners before and/or after Wa-0 time.

The Wa-0 fauna has been sampled in two overlapping intervals at the south end of Polecat Bench. Three of the four Wa-0

localities, SC-67, SC-121, and SC-308, span the full thickness of the interval, which is centered on the 1520 m level in the Polecat Bench section. These localities have yielded most of the mammals known from the Wa-0 interval (Table 7). The remaining Wa-0 locality at the south end of Polecat Bench, SC-69, spans the interval from Purple-2 to Upper Double-Red A, which is centered on the 1530 m level in the Polecat Bench section. The faunal sample from SC-69 is listed in Table 8. There is nothing about the fauna from SC-69 to suggest that it is anything other than a smaller subset of the fauna from SC-67, SC-121, and SC-308. Hence all are treated as a single Wa-0 faunal interval (*Meniscotherium*, in contrast,

has not been found at any of these localities in spite of intensive collecting and careful scrutiny of all fossils found).

The taxa restricted to Wa-0 are *Cantius torresi*, *Arfia junnei*, *Copecion davisii*, *Diacodexis ilicis*, and *Hyracotherium sandrae*. The two most common taxa are *Ectocion parvus* and *Hyopsodus loomisi*. *Ectocion parvus* is characteristic of Wa-0, but not diagnostic as a few specimens are known from Clarkforkian and later Wasatchian faunas (Thewissen 1990, p. 42). *Hyopsodus loomisi* in Wa-0 is indistinguishable from *H. loomisi* in Wa-1.

In addition, locality SC-405 (Table 9; this locality was only recently separated from SC-67) is developed in a channel lag deposit within the Upper Boundary Sandstone. The Upper Boundary Sandstone here has cut into and removed much of the Upper Double-Red B marker bed, and it is overlain some 7 m up section by Purple-4. SC-405 is considered to lie at about the 1535 m level in the Polecat Bench stratigraphic section. The lag at SC-405 includes numerous coprolites, bones of turtles and crocodiles, bones of *Coryphodon* (including parts of the skeleton of a developmentally immature individual), and the crown of a molar of *Hyracotherium grangeri*. There are no distinctively Wa-0 taxa present, and bones and teeth are dark brown in color like those of overlying Wa-1 fossils. It is uncertain whether SC-405 taxa are part of the Wa-0 fauna, in which case the locality represents an unusual depositional environment not sampled elsewhere, or whether these are the lowest representatives of the overlying Wa-1 fauna.

Early Wasatchian Wa-1 Biota

The early Wasatchian Wa-1 biota is known with certainty from one interval at the south end of Polecat Bench. Three localities, SC-68, SC-122, and SC-206, have yielded a substantial fauna with taxa that clearly represent Wa-1 rather than Wa-0 (Table 10). These localities lie above Purple-4 in the stratigraphic interval including Top Red A and Top Red B. This is centered at the 1550 m level in the Polecat Bench stratigraphic section. *Cantius ralstoni*, *Copecion brachypternus*, and *Diacodexis metsiacus* are all larger and more advanced than congeners from Wa-0. *Haplomylys speirianus* is common in Wa-1 and Wa-2, but *Haplomylys* has not been found in Wa-0 faunas. In addition, *Hyracotherium grangeri* is common in this interval while it appears to be a very rare component of Wa-0 faunas.

Summary of Biotic Change

Detailed mapping of conspicuous marker beds, faults, and a major scour-and-fill feature at the south end of Polecat Bench has yielded a more complicated but clearer picture of the stratigraphy here. This enables recognition of seven distinct collecting units, as illustrated by stippling in Figure 14. These represent four faunal units (Cf-3, Wa-0?, Wa-0, and Wa-1). The first three collecting units are placed in Cf-3, following Rose (1981), because their faunas do not differ in any way from earlier late Clarkforkian faunas. The fourth

collecting unit, Wa-0? in the brown mudstone sequence just below Wa-0, is the newly recognized *Meniscotherium* zone that includes the lowest range datum of *Celtis*. As noted above, Wa-0? is included in the Wasatchian because both *Celtis* and *Meniscotherium* are known from later Wasatchian biotas (*Celtis* are abundant in overlying Wasatchian strata of the Bighorn and Clarks Fork Basins, while *Meniscotherium* is common in later Wasatchian strata of southern Wyoming and New Mexico; this assignment is queried because the zone is still poorly known faunally). The fifth collecting unit yields the original Wa-0 mammalian fauna (Gingerich, 1989). The sixth collecting unit has too small a fauna to be diagnostic of Wa-0 or Wa-1. Finally, the seventh collecting unit, Wa-1, has a typical Sand Couleean or early Wasatchian fauna.

The average rate of sediment accumulation for the Clarkforkian and early Wasatchian of the Polecat Bench master section is about 470 to 475 m/m.y. (Gingerich, 2000; Bowen et al., this volume), meaning that each meter of sediment represents, on average, about 2.1 k.y. of geological time. Appearance of the *Celtis-Meniscotherium* association in Wa-0?, some 4-5 m below the beginning of Wa-0 proper, suggests that the Wasatchian biota appeared about 9-10 k.y. earlier than previously recognized. The thickness of the classic Wa-0 zone indicates that it probably represents only about 50 k.y. of geological time, which is much less than my previous estimate of 250 k.y. (Gingerich, 1989, p. 77).

PROSPECTUS

Detailed mapping of marker beds in the continental Paleocene-Eocene transition at the south end of Polecat Bench shows both what is possible, and what is required for future high-resolution studies. Initial discovery of the Wa-0 mammalian fauna and recognition of its distinctiveness resulted from a broad stratigraphic survey of the Clarkforkian-Wasatchian transition in the northern Bighorn Basin and in the Clarks Fork Basin, where fossil localities are generally bounded by sheet sandstones defining natural collecting intervals on the order of 10 m thick. The Wa-0 interval is often even thicker. There are some ongoing questions of contamination, involving, as examples, the presence of *Ectocion osbornianus* and the presence of *Hyracotherium grangeri* in the Wa-0 fauna, that could have been avoided if the precise meter level of all specimens had been recorded when they were collected. However, such uncertainty is unavoidable in any broad survey effort, and our earlier survey was carried out knowing that we would later focus more detailed attention on intervals that proved to be particularly interesting.

Now that the Wa-0 fauna is known, it is clear that meter-scale stratigraphic sampling, involving resolution an order of magnitude finer than that used in the initial surveying, will be required to resolve the transitions from Cf-3 to Wa-0 and from Wa-0 to Wa-1. Mammalian faunas documenting these transitions need to be collected anew in a high-resolution framework. Meter-scale stratigraphic sampling

is literally paleosol- scale sampling. Similarly, such meter-scale stratigraphic resolution, corresponding to ca. 2-3 k.y. temporal resolution, will be required to correlate events and intervals in the Paleocene-Eocene transition accurately, both within and outside the Bighorn and Clarks Fork basins. Now that we know where to focus attention, such resolution is possible.

ACKNOWLEDGMENTS

This summary builds on field work carried out in the Bighorn and Clarks Fork basins for almost a century, beginning with an American Museum effort in 1910-1912, a long-term Princeton University commitment from 1927-1974, and our own ongoing University of Michigan work from 1975-2000. The University of Michigan effort has involved more than one hundred colleagues and students over the years, of whom K. D. Rose, D. W. Krause, G. F. Gunnell, D. A. Winkler, M. J. Kraus, C. E. Badgley, J. G. M. Thewissen, W. C. Clyde, G. H. Junne, and B. H. Smith deserve particular mention. R. F. Butler and E. H. Lindsay developed the paleomagnetic stratigraphy. P. L. Koch, J. C. Zachos, S. Bains, R. D. Norris, and G. J. Bowen, developed the isotope stratigraphy, providing added impetus for the detailed mapping and stratigraphy presented here. I thank Muhammad Arif and Iyad Zalmout for help in the field in 2000. J. I. Bloch, G. F. Gunnell, and R. Secord read and improved the manuscript. Research on mammalian faunal evolution across the Paleocene-Eocene boundary has been supported by a series of grants from the National Science Foundation: DEB-7713465, DEB-8010846, DEB-8206242, EAR-8408647, BSR-8607481, EAR-8918023, and EAR-9105147. Research reported here was funded by the University of Michigan College of Literature, Science, and Arts; and by the University of Michigan Museum of Paleontology.

LITERATURE CITED

- ARCHIBALD, J. D., W. A. CLEMENS, P. D. GINGERICH, D. W. KRAUSE, E. H. LINDSAY, and K. D. ROSE. 1988. First North American land mammal ages of the Cenozoic era. In M. O. Woodburne (ed.), *Cenozoic Mammals of North America: Geochronology and Biostratigraphy*, University of California Press, Berkeley, pp. 24-76.
- BAINS, S., R. M. CORFIELD, and R. D. NORRIS. 1999. Mechanisms of climate warming at the end of the Paleocene. *Science*, 285: 724-727.
- BOWN, T. M. and K. D. ROSE. 1979. *Mimoperadectes*, a new marsupial, and *Worlandia*, a new dermopteran, from the lower part of the Willwood Formation (early Eocene), Bighorn Basin, Wyoming. Contributions from the Museum of Paleontology, University of Michigan, 25: 89-104.
- BUTLER, R. F., P. D. GINGERICH, and E. H. LINDSAY. 1981. Magnetic polarity stratigraphy and biostratigraphy of Paleocene and lower Eocene continental deposits, Clarks Fork Basin, Wyoming. *Journal of Geology*, 89: 299-316.
- CARLSON, E. E. and T. VINCENTY. 1993. UTMS (Version 2.0). Information Services Branch, National Geodetic Survey, Silver Spring, Maryland (www.ngs.noaa.gov/PC_PROD/pc_prod.shtml), 96 kb + 6 pp.
- CLYDE, W. C. and P. D. GINGERICH. 1998. Mammalian community response to the latest Paleocene thermal maximum: an isotaphonomic study in the northern Bighorn Basin, Wyoming. *Geology*, 26: 1011-1014.
- DAVIS, J. C. 1986. *Statistics and Data Analysis in Geology*, Second Edition. John Wiley and Sons, New York, 646 pp.
- DEWHURST, W. T., A. R. DREW, and J. M. BENGSTON. 1992. NADCON (Version 2.10). Information Services Branch, National Geodetic Survey, Silver Spring, Maryland (www.ngs.noaa.gov/PC_PROD/pc_prod.shtml), 105 kb + 11 pp.
- DICKENS, G. R., J. R. O'NEIL, D. K. REA, and R. M. OWEN. 1995. Dissociation of oceanic methane hydrate as a cause of the carbon isotope excursion at the end of the Paleocene. *Paleoceanography*, 10: 965-971.
- GAZIN, C. L. 1965. A study of the early Tertiary condylarthran mammal *Meniscotherium*. *Smithsonian Miscellaneous Collections*, 149 (2): 1-98.
- GINGERICH, P. D. 1968. Pollen stratigraphy of the Polecat Bench Formation, Paleocene, Park County, Wyoming. A. B. thesis, Princeton University, 81 pp.
- GINGERICH, P. D. 1975. New North American Plesiadapidae (Mammalia, Primates) and a biostratigraphic zonation of the middle and upper Paleocene. *Contributions from the Museum of Paleontology, University of Michigan*, 24: 135-148.
- GINGERICH, P. D. 1976. Cranial anatomy and evolution of early Tertiary Plesiadapidae (Mammalia, Primates). *University of Michigan Papers on Paleontology*, 15: 1-140.
- GINGERICH, P. D. 1977. *Aletodon gunnelli*, a new Clarkforkian hyposodontid (Mammalia, Condylarthra) from the early Eocene of Wyoming. *Contributions from the Museum of Paleontology, University of Michigan*, 24: 237-244.
- GINGERICH, P. D. 1982a. Time resolution in mammalian evolution: sampling, lineages and faunal turnover. In B. Mamet and M. J. Copeland (eds.), *Proceedings of the Third North American Paleontological Convention*, Montreal, 1: 205-210.
- GINGERICH, P. D. 1982b. Paleocene '*Meniscotherium semicingulatum*' and the first appearance of Meniscotheriidae (Condylarthra) in North America. *Journal of Mammalogy*, 63: 488-491.
- GINGERICH, P. D. 1983a. Paleocene-Eocene faunal zones and a preliminary analysis of Laramide structural deformation in the Clark's Fork Basin, Wyoming. *Wyoming Geological Association Guide Book*, 34: 185-195.
- GINGERICH, P. D. 1983b. Systematics of early Eocene Miacididae (Mammalia, Carnivora) in the Clark's Fork Basin, Wyoming. *Contributions from the Museum of Paleontology, University of Michigan*, 26: 197-225.
- GINGERICH, P. D. 1986. Early Eocene *Cantius torresi*— oldest primate of modern aspect from North America. *Nature*, 320: 319-321.
- GINGERICH, P. D. 1989. New earliest Wasatchian mammalian fauna from the Eocene of northwestern Wyoming: composition and diversity in a rarely sampled high-floodplain assemblage. *University of Michigan Papers on Paleontology*, 28: 1-97.

- GINGERICH, P. D. 1991. Systematics and evolution of early Eocene Perissodactyla (Mammalia) in the Clarks Fork Basin, Wyoming. Contributions from the Museum of Paleontology, University of Michigan, 28: 181-213.
- GINGERICH, P. D. 1995. Sexual dimorphism in earliest Eocene *Cantius torresi* (Mammalia, Primates, Adapoidea). Contributions from the Museum of Paleontology, University of Michigan, 29: 185-199.
- GINGERICH, P. D. 2000. Paleocene-Eocene boundary and continental vertebrate faunas of Europe and North America. In B. Schmitz, B. Sundquist, and F. P. Andreasson (eds.), Early Paleogene Warm Climates and Biosphere Dynamics, Uppsala, Geological Society of Sweden, GFF Geologiska Föreningens Förhandlingar, Geological Society of Sweden, Uppsala, 122: 57-59.
- GINGERICH, P. D. and K. KLITZ. 1985. Paleocene and early Eocene fossil localities in the Fort Union and Willwood Formations, Clarks Fork Basin, Wyoming. Miscellaneous Contributions, Museum of Paleontology, University of Michigan, 1 sheet (map).
- GODDARD, E. N., P. D. TRASK, R. K. DE FORD, O. N. ROVE, J. T. SINGEWALD, and R. M. OVERBECK. 1948. Rock-color chart. Geological Society of America, Boulder, Colorado, 16 pp.
- GRANGER, W. 1914. On the names of lower Eocene faunal horizons of Wyoming and New Mexico. Bulletin of the American Museum of Natural History, 33: 201-207.
- GRANGER, W. 1915. A revision of the lower Eocene Wasatch and Wind River faunas. Part III. Order Condylarthra, families Phenacodontidae and Meniscotheriidae. Bulletin of the American Museum of Natural History, 34: 329-361.
- GUNNELL, G. F. 1989. Evolutionary history of Microsypoidea (Mammalia, ?Primates) and the relationship between Plesiadapiformes and Primates. University of Michigan Papers on Paleontology, 27: 1-157.
- GUNNELL, G. F. and P. D. GINGERICH. 1991. Systematics and evolution of late Paleocene and early Eocene Oxyaenidae (Mammalia, Creodonta) in the Clarks Fork Basin, Wyoming. Contributions from the Museum of Paleontology, University of Michigan, 28: 141-180.
- HARTMAN, J. H. and D. W. KRAUSE. 1993. Cretaceous and Paleocene stratigraphy and paleontology of the Shawmut Anticline and the Crazy Mountains Basin, Montana: road log and overview of recent investigations. Montana Geological Society Field Conference Guidebook, 1993: 71-84.
- IVY, L. D. 1990. Systematics of late Paleocene and early Eocene Rodentia (Mammalia) from the Clarks Fork Basin, Wyoming. Contributions from the Museum of Paleontology, University of Michigan, 28: 21-70.
- KENNETT, J. P. and L. D. STOTT. 1991. Abrupt deep-sea warming, palaeoceanographic changes and benthic extinctions at the end of the Paleocene. Nature, 353: 225-229.
- KOCH, P. L., J. C. ZACHOS, and D. L. DETTMAN. 1995. Stable isotope stratigraphy and paleoclimatology of the Paleogene Bighorn Basin (Wyoming, USA). Palaeogeography, Palaeoclimatology, Palaeoecology, 115: 61-89.
- KOCH, P. L., J. C. ZACHOS, and P. D. GINGERICH. 1992. Correlation between isotope records in marine and continental carbon reservoirs near the Palaeocene-Eocene boundary. Nature, 358: 319-322.
- KRAUS, M. J. 1979. The petrology and depositional environments of a continental sheet sandstone: the Willwood Formation Bighorn Basin, Wyoming. Master of Science thesis, University of Wyoming, 1-102.
- KRAUS, M. J. 1980. Genesis of a fluvial sheet sandstone, Willwood Formation, northwest Wyoming. In P. D. Gingerich (ed.), Early Cenozoic Paleontology and Stratigraphy of the Bighorn Basin, Wyoming, University of Michigan Papers on Paleontology, 24: 87-94.
- KRAUS, M. J. 1987. Integration of channel and floodplain suites, II. Vertical relations of alluvial paleosols. Journal of Sedimentary Petrology, 57: 602-612.
- KRAUS, M. J. 1996. Avulsion deposits in lower Eocene alluvial rocks, Bighorn Basin, Wyoming. Journal of Sedimentary Research, 66: 354-363.
- KRAUS, M. J. 1997. Lower Eocene alluvial paleosols: Pedogenic development, stratigraphic relationships, and paleosol/landscape associations. Palaeogeography, Palaeoclimatology, Palaeoecology, 129: 387-406.
- NACSN [NORTH AMERICAN COMMISSION ON STRATIGRAPHIC NOMENCLATURE]. 1983. North American Stratigraphic Code. American Association of Petroleum Geologists Bulletin, 67: 841-875.
- NORRIS, R. D. and U. RÖHL. 1999. Carbon cycling and chronology. Nature, 401: 775-778.
- POLLY, P. D. 1997. Ancestry and species definition in paleontology: a stratocladistic analysis of Paleocene-Eocene Viverravidae (Mammalia, Carnivora) from Wyoming. Contributions from the Museum of Paleontology, University of Michigan, 30: 1-53.
- ROSE, K. D. 1981. The Clarkforkian land-mammal age and mammalian faunal composition across the Paleocene-Eocene boundary. University of Michigan Papers on Paleontology, 26: 1-197.
- SCHANKLER, D. M. 1980. Faunal zonation of the Willwood formation in the central Bighorn Basin, Wyoming. In P. D. Gingerich (ed.), Early Cenozoic Paleontology and Stratigraphy of the Bighorn Basin, Wyoming. University of Michigan Papers on Paleontology, 24: 99-114.
- SINCLAIR, W. J. and W. GRANGER. 1912. Notes on the Tertiary deposits of the Bighorn Basin. Bulletin of the American Museum of Natural History, 31: 57-67.
- THEWISSEN, J. G. M. 1990. Evolution of Paleocene and Eocene Phenacodontidae (Mammalia, Condylarthra). University of Michigan Papers on Paleontology, 29: 1-107.
- THEWISSEN, J. G. M. and P. D. GINGERICH. 1987. Systematics and evolution of *Proathyopsis* (Mammalia, Dinocerata) from late Paleocene and early Eocene of western North America. Contributions from the Museum of Paleontology, University of Michigan, 27: 195-219.

- WILLIAMSON, T. E. and S. G. LUCAS. 1992. *Meniscotherium* (Mammalia, 'Condylarthra') from the Paleocene-Eocene of western North America. *New Mexico Museum of Natural History and Science*, 1: 1-75.
- WOOD, H. E., R. W. CHANEY, J. CLARK, E. H. COLBERT, G. L. JEPSEN, J. B. REESIDE, and C. STOCK. 1941. Nomenclature and correlation of the North American continental Tertiary. *Bulletin of the Geological Society of America*, 52: 1-48.
- WOOD, R. C. 1967. A review of the Clark Fork vertebrate fauna. *Breviora*, Museum of Comparative Zoology, Harvard University, 257: 1-30.
- ZACHOS, J. C., L. D. STOTT, and K. C. LOHMANN. 1994. Evolution of early Cenozoic marine temperatures. *Paleoceanography*, 9: 353-387.

APPENDIX

TABLE A1 — South Polecat Bench SC-77 stratigraphic section. Beds are listed in stratigraphic order from bottom to top. Color codes are from Goddard et al. (1948). Bed thickness is in meters.

Bed	Thick.	Description	Fresh color		Mottling color		Weathered color	
65	7.00	Fine to medium-grained yellow sandstone	5 Y 7/2	Yellowish gray			10YR 6/2	Pale yellowish brown
64	2.10	Gray mudstone with faint orange beds	5 Y 6/1	Light olive gray			N 7	Light gray
63	1.50	Purple mudstone (Purple-2)	5 R 4/2	Grayish red			5 YR 6/1	Light brownish gray
62	0.60	Gray mudstone	5 GY 6/1	Greenish gray			5 Y 8/1	Yellowish gray
61	0.80	Red mudstone (2-3 cm calc. soil nodules)	10 R 3/4	Dark reddish brown	5 Y 6/1	Light olive gray	10 R 6/6	Moderate reddish orange
60	0.80	Gray mudstone	5 Y 8/1	Yellowish gray			5 Y 8/1	Yellowish gray
59	0.80	Red mudstone	10 R 4/6	Moderate reddish brown			10 R 5/4	Pale reddish brown
58	0.85	Gray mudstone	5 Y 8/1	Yellowish gray			5 Y 8/1	Yellowish gray
57	1.50	Reddish orange ms. (Lower Double-Red B)	10 R 4/6	Moderate reddish brown			10 R 6/6	Moderate reddish orange
56	0.10	Gray mudstone	5 Y 8/1	Yellowish gray			5 Y 6/1	Light olive gray
55	1.50	Reddish orange ms. (Lower Double-Red A)	10 YR 6/6	Dark yellowish orange			10 R 6/6	Moderate reddish orange
54	1.20	Gray mudstone	5 GY 6/1	Greenish gray			5 Y 8/1	Yellowish gray
53	0.40	Red mudstone	10 R 4/2	Dark grayish red	N 6	Medium light gray	10 R 6/2	Pale red
52	0.50	Brown mudstone (Top Brown)	10 YR 4/2	Dark yellowish brown			5 YR 6/1	Light brownish gray
51	0.30	Very fine-grained sandstone	5 Y 6/1	Light olive gray			5 YR 5/2	Pale brown
50	0.30	Very fine-grained sandstone	5 Y 6/1	Light olive gray			5 YR 5/2	Pale brown
49	0.60	Very fine-grained sandstone	5 Y 6/1	Light olive gray			5 Y 7/2	Yellowish gray
48	0.30	Red mudstone	5 R 4/2	Grayish red			10 R 6/2	Pale red
47	0.60	Very fine-grained sandstone	5 Y 6/1	Light olive gray			5 Y 7/2	Yellowish gray
46	0.20	Brown mudstone	5 YR 3/2	Grayish brown			10 YR 6/2	Pale yellowish brown
45	0.20	Brown mudstone	5 YR 3/2	Grayish brown			10 YR 6/2	Pale yellowish brown
44	0.30	Gray mudstone	5 Y 6/1	Light olive gray			5 Y 7/2	Yellowish gray
43	0.40	Brown mudstone	5 R 4/2	Grayish red			10 YR 6/2	Pale yellowish brown
42	1.30	Gray mudstone	5 Y 5/2	Light olive gray			5 Y 6/1	Light olive gray
41	0.60	Red mudstone (Purple-0)	10 R 4/2	Grayish red			10 R 6/2	Pale red
40	1.30	Gray mudstone	5 Y 5/2	Light olive gray			5 Y 8/1	Yellowish gray
39	2.30	Massive fine-grained micaceous sandstone	5 Y 7/2	Yellowish gray			10 YR 4/2	Dark yellowish brown
38	1.50	Gray mudstone	5 Y 5/2	Light olive gray			5 Y 8/1	Yellowish gray
37	0.10	Red mudstone	5 R 4/2	Grayish red			10 R 6/2	Pale red
36	1.40	Gray mudstone	10 Y 6/2	Pale olive			5 Y 7/2	Yellowish gray
35	1.50	Fine-grained yellow sandstone	5 Y 6/4	Dusky yellow			10 YR 4/2	Dark yellowish brown
34	1.20	Gray mudstone	5 Y 5/2	Light olive gray				
33	0.20	Red mudstone	5 YR 5/2	Pale brown			10 R 6/2	Pale red
32	0.30	Gray mudstone	5 Y 5/2	Light olive gray				
31	0.20	Red mudstone	5 YR 5/2	Pale brown			10 R 6/2	Pale red
30	0.30	Gray mudstone	5 Y 5/2	Light olive gray				
29	0.20	Red mudstone	5 YR 5/2	Pale brown			10 R 6/2	Pale red
28	0.30	Gray mudstone	5 Y 5/2	Light olive gray				
27	0.10	Very fine-grained friable sandstone	10 YR 4/2	Dark yellowish brown			10 Y 6/2	Pale olive
26	0.50	Gray mudstone	5 GY 6/1	Greenish gray			5 Y 6/1	Light olive gray
25	0.30	Fine-grained flaggy micaceous sandstone	5 Y 8/1	Yellowish gray			10 YR 6/2	Pale yellowish brown
24	0.70	Gray mudstone	5 Y 7/2	Yellowish gray			5 Y 6/1	Light olive gray
23	1.80	Very fine-grained yellowish gray sandstones	5 Y 7/2	Yellowish gray			5 Y 6/1	Light olive gray
22	0.10	Orange mudstone	10 YR 4/2	Dark yellowish brown				
21	0.40	Gray mudstone	5 Y 6/1	Light olive gray				
20	0.10	Sandstone						
19	0.90	Gray mudstone	5 Y 6/1	Light olive gray				
18	1.20	Very fine-grained yellowish gray sandstone	5 Y 7/2	Yellowish gray			5 Y 6/1	Light olive gray
17	0.90	Gray mudstone	5 Y 4/1	Olive gray			5 Y 6/1	Light olive gray
16	0.90	Gray mudstone	5 Y 5/2	Light olive gray			5 Y 6/1	Light olive gray
15	0.20	Orange mudstone	10 YR 5/4	Yellowish brown	10 YR 6/2	Pale yellowish brown	10 YR 7/4	Grayish orange
14	0.70	Purplish red mudstone	10 R 3/4	Dark reddish brown			10 R 5/4	Pale reddish brown
13	0.60	Gray siltstone	5 Y 6/1	Light olive gray			5 Y 8/1	Yellowish gray
12	0.30	Orange mudstone	10 YR 5/4	Yellowish brown	10 YR 6/2	Pale yellowish brown	10 YR 7/4	Grayish orange
11	0.30	Gray mudstone	5 Y 6/1	Light olive gray			5 Y 8/1	Yellowish gray
10	0.70	Orange mudstone	10 YR 5/4	Yellowish brown	10 YR 6/2	Pale yellowish brown	10 YR 7/4	Grayish orange
9	0.70	Orange mudstone (Thick Orange)	10 YR 5/4	Yellowish brown	10 YR 6/2	Pale yellowish brown	10 YR 7/4	Grayish orange
8	0.80	Orange mudstone	10 YR 5/4	Yellowish brown	10 YR 6/2	Pale yellowish brown	10 YR 7/4	Grayish orange
7	0.30	Finely laminated gray silty clay	5 Y 6/1	Light olive gray			5 Y 8/1	Yellowish gray
6	0.20	Brown mudstone	10 YR 4/2	Dark yellowish brown			10 YR 6/2	Pale yellowish brown
5	0.45	Gray mudstone	5 Y 4/1	Olive gray			5 Y 6/1	Light olive gray
4	0.10	Purple mudstone	10 R 4/2	Grayish red			10 R 6/2	Pale reddish brown
3	0.45	Gray mudstone	5 Y 5/2	Light olive gray			5 Y 6/1	Light olive gray
2	0.20	Red mudstone	10 R 3/4	Dark reddish brown	5 Y 5/2	Light olive gray	10 R 6/2	Pale reddish brown
1	0.60	Gray mudstone	5 GY 7/2	Grayish yellow green			5 Y 8/1	Yellowish gray
0	0.20	Very fine-grained concretionary sandstone	5 Y 7/2	Yellowish gray			5 YR 5/2	Pale brown

TABLE A2 — South Polecat Bench SC-67 stratigraphic section. Beds are listed in stratigraphic order from bottom to top. Color codes are from Goddard et al. (1948). Bed thickness is in meters.

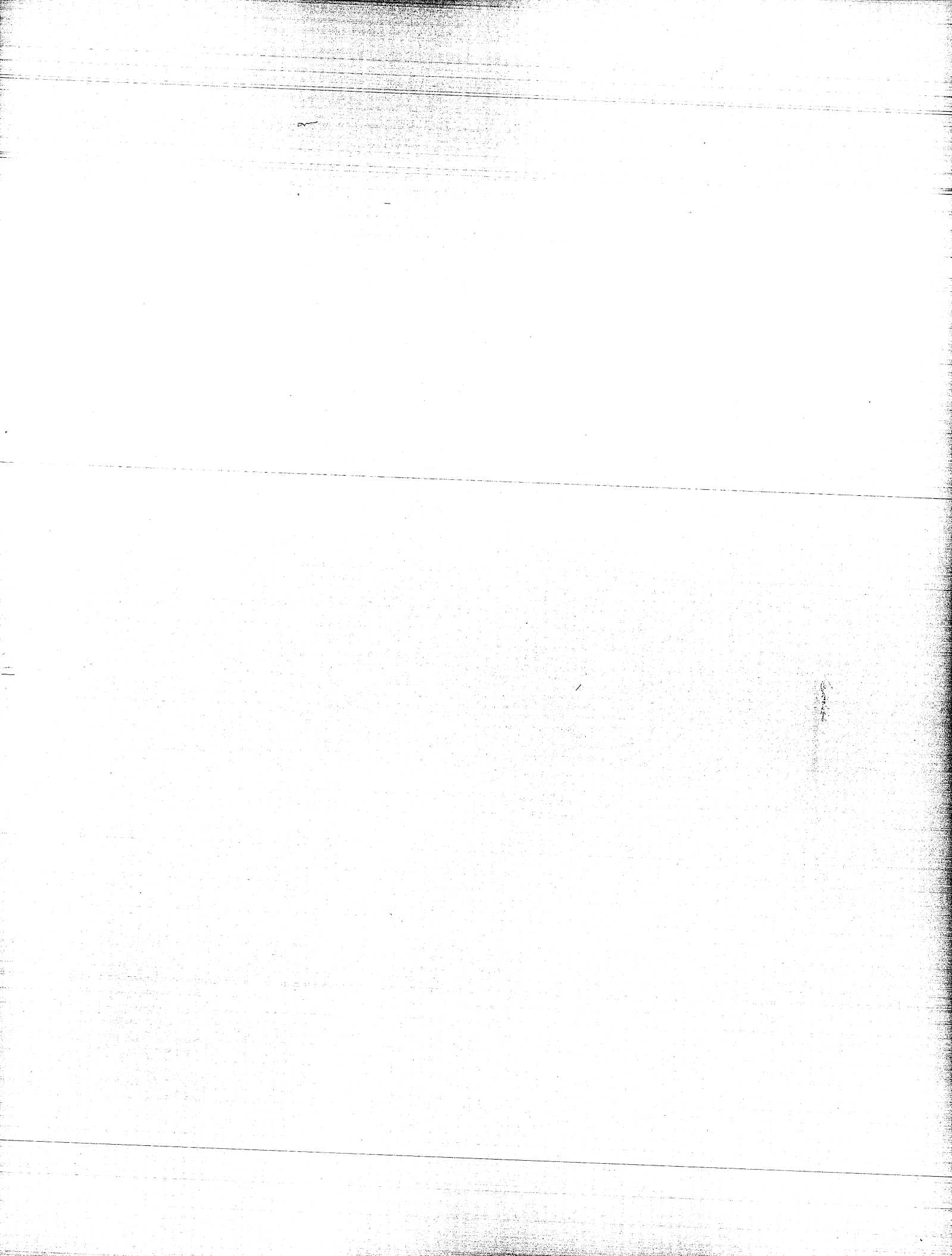
Bed	Thick.	Description	Fresh color	Mottling color	Weathered color			
80	1.00	Orange mudstone	10 YR 5/4	Moderate yellowish brown	5 Y 6/1	Light olive gray	5 Y 6/4	Dusky yellow
79	4.70	Gray mudstone	5 Y 6/1	Light olive gray			10 Y 8/1	Yellowish gray
78	0.40	Red mudstone (Top Red B)	10 R 4/6	Moderate reddish brown	5 Y 6/1	Light olive gray	10 R 6/6	Moderate reddish orange
77	1.40	Gray mudstone	5 Y 6/1	Light olive gray			10 Y 8/1	Yellowish gray
76	1.00	Yellow fine-grained sandstone	5 Y 6/4	Dusky yellow			5 Y 7/2	Yellowish gray
75	1.00	Gray mudstone	5 Y 6/1	Light olive gray			10 Y 8/1	Yellowish gray
74	0.50	Dark gray mudstone	5 Y 5/2	Light olive gray			5 Y 6/1	Light olive gray
73	0.20	Yellow mudstone	5 Y 5/2	Light olive gray	10 YR 5/4	Moderate yellowish brown	5 Y 7/2	Yellowish gray
72	0.60	Gray mudstone	5 Y 6/1	Light olive gray			10 Y 8/1	Yellowish gray
71	0.50	Red mudstone (Top Red A)	10 R 4/6	Moderate reddish brown	5 Y 6/1	Light olive gray	10 R 5/4	Pale reddish brown
70	1.00	Gray mudstone	5 Y 6/1	Light olive gray			5 Y 8/1	Yellowish gray
69	1.50	Orange mudstone	10 YR 6/2	Pale yellowish brown			10 YR 7/4	Grayish orange
68	1.20	Gray mudstone	5 Y 6/1	Light olive gray			10 Y 8/1	Yellowish gray
67	0.20	Red mudstone	10 R 4/2	Grayish red	5 Y 5/2	Light olive gray	10 R 6/2	Pale red
66	2.30	Gray mudstone	5 Y 6/1	Light olive gray			10 Y 8/1	Yellowish gray
65	1.00	Orange mudstone	5 Y 6/1	Light olive gray	5 R 4/2	Grayish red	10 R 5/4	Pale reddish brown
64	0.90	Purple mudstone (Purple-4)	5 RP 4/2	Grayish red purple			5 RP 6/2	Pale red purple
63	0.20	Gray mudstone	5 GY 6/1	Greenish gray			5 GY 8/1	Light greenish gray
62	0.10	Red mudstone	10 R 4/6	Moderate reddish brown				Covered
61	0.10	Gray mudstone	5 GY 6/1	Greenish gray			5 GY 8/1	Light greenish gray
60	0.10	Red mudstone	10 R 4/6	Moderate reddish brown				Covered
59	1.40	Gray mudstone	5 GY 6/1	Greenish gray			5 GY 8/1	Light greenish gray
58	0.30	Brown mudstone	10 YR 5/4	Moderate yellowish brown			10 YR 6/2	Pale yellowish brown
57	1.50	Gray mudstone	10 Y 8/1	Yellowish gray			10 Y 8/1	Yellowish gray
56	0.20	Red mudstone	10 R 4/2	Grayish red	10 R 6/6	Moderate reddish orange	10 R 6/2	Pale red
55	0.12	Gray mudstone	5 Y 6/1	Light olive gray			5 Y 8/1	Yellowish gray
54	0.08	Brown mudstone	10 YR 7/4	Grayish orange			10 R 6/2	Pale red
53	0.40	Gray mudstone	5 Y 6/1	Light olive gray			5 Y 8/1	Yellowish gray
52	0.40	Gray sandstone	5 Y 8/1	Yellowish gray			5 Y 8/1	Yellowish gray
51	0.30	Red mudstone	10 R 4/2	Grayish red			10 R 5/4	Pale reddish brown
50	0.20	Red mudstone	10 YR 6/2	Pale yellowish brown			10 R 6/2	Pale red
49	0.40	Gray mudstone	5 Y 6/1	Light olive gray			5 Y 8/1	Yellowish gray
48	0.30	Red mudstone	10 YR 6/2	Pale yellowish brown			10 R 6/2	Pale red
47	0.90	Gray mudstone	5 Y 8/1	Yellowish gray			5 Y 8/1	Yellowish gray
46	0.40	Purple mudstone (Purple-3)	5 R 4/2	Grayish red	5 Y 5/2	Light olive gray	5 RP 6/2	Pale red purple
45	0.60	Red mudstone (Purple-3 at top)	10 R 3/4	Dark reddish brown			10 R 5/4	Pale reddish brown
44	0.50	Gray mudstone	5 Y 6/1	Light olive gray			5 Y 8/1	Yellowish gray
43	0.20	Orange mudstone	10 R 4/2	Grayish red			10 R 6/6	Moderate reddish orange
42	0.40	Orange mudstone	5 GY 6/1	Greenish gray			5 Y 8/1	Yellowish gray
41	0.20	Orange mudstone	10 R 4/2	Grayish red			10 R 6/6	Moderate reddish orange
40	0.50	Gray mudstone	5 Y 6/1	Light olive gray			5 Y 8/1	Yellowish gray
39	0.10	Orange mudstone	10 R 4/2	Grayish red	10 YR 5/4	Moderate yellowish brown	10 YR 7/4	Grayish orange
38	0.05	Gray mudstone	5 Y 6/1	Light olive gray			5 Y 8/1	Yellowish gray
37	0.10	Red mudstone	10 R 4/6	Moderate reddish brown			10 R 5/4	Pale reddish brown
36	0.05	Gray mudstone	5 Y 6/1	Light olive gray			5 Y 8/1	Yellowish gray
35	0.30	Orange mudstone	10 YR 4/4	Moderate brown			5 YR 6/4	Light brown
34	1.00	Gray mudstone	5 Y 6/1	Light olive gray			5 Y 8/1	Yellowish gray
33	0.40	Orange mudstone	10 R 4/6	Moderate reddish brown	10 YR 5/4	Moderate yellowish brown	10 R 5/4	Pale reddish brown
32	0.40	Gray mudstone	5 Y 6/1	Light olive gray			5 Y 8/1	Yellowish gray
31	1.80	Red mudstone (Upper Double-Red)	10 R 3/4	Dark reddish brown			10 R 5/4	Pale reddish brown
30	1.20	Gray mudstone	5 Y 6/1	Light olive gray			5 Y 8/1	Yellowish gray
29	0.40	Red mudstone	10 R 4/6	Moderate reddish brown			10 R 5/4	Pale reddish brown
28	1.00	Gray mudstone	5 Y 8/1	Yellowish gray			5 Y 8/1	Yellowish gray
27	0.10	Orange mudstone	10 YR 5/4	Moderate yellowish brown	5 Y 6/1	Light olive gray	5 GY 6/1	Greenish gray
26	0.20	Gray mudstone	5 Y 8/1	Yellowish gray			5 Y 8/1	Yellowish gray
25	0.20	Orange mudstone	10 YR 6/2	Pale yellowish brown			10 YR 8/2	Very pale orange
24	0.10	Red mudstone	10 R 4/6	Moderate reddish brown	10 YR 5/4	Moderate yellowish brown	10 R 5/4	Pale reddish brown
23	0.90	Orange mudstone	10 YR 4/2	Dark yellowish brown			10 YR 6/2	Pale yellowish brown
22	1.20	Gray mudstone	5 Y 5/2	Light olive gray			5 Y 6/1	Light olive gray
21	0.70	White very-fine-grained sandstone	5 Y 8/1	Yellowish gray			5 Y 8/1	Yellowish gray
20	0.40	Orange mudstone	10 R 4/6	Moderate reddish brown	5 Y 8/1	Yellowish gray	5 Y 8/1	Yellowish gray
19	0.40	Gray mudstone	5 GY 5/2	Dusky yellow green			5 Y 6/1	Light olive gray
18	1.20	Red mudstone (Purple-2)	10 R 4/6	Moderate reddish brown			10 R 6/2	Pale red
17	1.80	Gray mudstone	5 Y 6/1	Light olive gray			5 Y 8/1	Yellowish gray
16	0.10	Planar-bedded very-fine-grained sandstone	5 Y 7/2	Yellowish gray			5 YR 5/2	Pale brown
15	0.10	Gray mudstone	5 Y 6/1	Light olive gray			5 Y 8/1	Yellowish gray
14	0.10	Planar-bedded very-fine-grained sandstone	5 Y 7/2	Yellowish gray			5 YR 5/2	Pale brown
13	0.15	Gray mudstone	5 Y 6/1	Light olive gray			5 Y 8/1	Yellowish gray
12	0.10	Planar-bedded very-fine-grained sandstone	5 Y 7/2	Yellowish gray			5 YR 5/2	Pale brown
11	0.25	Gray mudstone	5 Y 6/1	Light olive gray			5 Y 8/1	Yellowish gray
10	0.20	Red mudstone	10 R 3/4	Dark reddish brown				
9	0.80	Yellow very-fine-grained channel sandstone	5 Y 7/2	Yellowish gray			5 YR 5/2	Pale brown
8	1.80	Reddish orange ms. (Lower Double-Red)	10 R 4/6	Moderate reddish brown			10 R 6/6	Moderate reddish orange
7	1.80	White very-fine-grained sandstone	5 Y 8/1	Yellowish gray			5 Y 8/1	Yellowish gray
6	0.20	Brown mudstone (Top Brown)	10 YR 4/2	Dark yellowish brown			10 YR 6/2	Pale yellowish brown
5	1.60	Soft yellow sandstone	5 Y 6/4	Dusky yellow			5 Y 7/2	Yellowish gray
4	0.20	Fine-grained ledge-forming sandstone	5 Y 6/4	Dusky yellow			10 R 4/2	Dark yellowish brown
3	2.10	Soft yellow sandstone	5 Y 6/4	Dusky yellow			5 Y 7/2	Yellowish gray
2	0.20	Gray mudstone	5 Y 6/1	Light olive gray			5 Y 8/1	Yellowish gray
1	0.40	Brown mudstone with <i>Celtis</i>	5 R 3/2	Grayish brown			10 YR 6/2	Pale yellowish brown

TABLE A3 — South Polecat Bench SC-121 stratigraphic section. Beds are listed in stratigraphic order from bottom to top. Color codes are from Goddard et al. (1948). Bed thickness is in meters.

Bed	Thick.	Description	Fresh color		Mottling color		Weathered color	
54	0.50	Red mudstone (Top Red A)						
53	6.90	Gray mudstone						
52	1.00	Purple mudstone (Purple-4)	5 RP 4/2	Grayish red purple			5 RP 6/2	Pale red purple
51	2.00	Gray mudstone						
50	1.70	Gray mudstone with four orange paleosols						
49	2.30	Gray mudstone						
48	7.20	Yellow fine-grained sandstone	5 Y 6/4	Dusky yellow	5 Y 7/2	Yellowish gray	10 YR 6/2	Pale yellowish brown
47	0.60	Red mudstone (Upper Double-Red B)	10 R 4/2	Grayish red			10 R 5/4	Pale reddish brown
46	0.60	Gray mudstone	5 Y 6/1	Light olive gray			5 Y 8/1	Yellowish gray
45	0.90	Red mudstone (Upper Double-Red A)	10 R 3/4	Dark reddish brown			10 R 5/4	Pale reddish brown
44	1.50	Gray mudstone	5 Y 6/1	Light olive gray			5 Y 8/1	Yellowish gray
43	0.60	Orange mudstone	10 R 4/6	Moderate reddish brown			5 YR 6/4	Light brown
42	1.80	Gray mudstone	5 Y 6/1	Light olive gray			5 Y 8/1	Yellowish gray
41	1.80	Gray ms. w. orange and brown paleosols	5 Y 6/1	Light olive gray			5 Y 8/1	Yellowish gray
40	1.20	Gray mudstone	5 Y 6/1	Light olive gray			5 Y 8/1	Yellowish gray
39	0.60	Orange mudstone	10 R 4/6	Moderate reddish brown	10 YR 5/4	Moderate yellowish brown	5 YR 6/4	Light brown
38	0.40	Gray mudstone	5 Y 6/1	Light olive gray			5 Y 8/1	Yellowish gray
37	0.80	Purplish red mudstone (Purple-2)	5 R 4/2	Grayish red			5 RP 6/2	Pale red purple
36	0.90	Gray mudstone	5 GY 6/1	Greenish gray			5 Y 8/1	Yellowish gray
35	0.90	Orange mudstone	10 R 4/6	Moderate reddish brown	10 YR 5/4	Moderate yellowish brown	10 R 5/4	Pale reddish brown
34	0.90	Light gray mudstone	5 Y 6/1	Light olive gray			5 Y 8/1	Yellowish gray
33	2.80	Red mudstone (Lower Double-Red A & B)	10 R 3/4	Dark reddish brown			10 R 5/4	Pale reddish brown
32	1.20	Gray and orange mudstone	5 Y 6/1	Light olive gray			5 Y 8/1	Yellowish gray
31	2.70	Yellow medium to coarse-grained sandstone	5 Y 7/2	Yellowish gray			10 YR 6/2	Pale yellowish brown
30	0.25	Gray mudstone	5 Y 6/1	Light olive gray			5 Y 8/1	Yellowish gray
29	0.05	Brown marl	10 YR 7/4	Grayish orange			5 YR 4/4	Moderate brown
28	0.32	Orange mudstone	10 YR 5/4	Moderate yellowish brown			5 YR 6/4	Light brown
27	0.50	Brown mudstone with <i>Celtis</i> endocarps	10 YR 4/2	Dark yellowish brown			10 YR 6/2	Pale yellowish brown
26	0.90	Gray mudstone	5 Y 6/1	Light olive gray			5 Y 8/1	Yellowish gray
25	0.80	Very-fine-grained sandstone	5 Y 8/1	Yellowish gray			10 YR 6/2	Pale yellowish brown
24	0.40	Gray mudstone	5 Y 6/1	Light olive gray			5 Y 8/1	Yellowish gray
23	0.35	Brown mudstone	10 YR 4/2	Dark yellowish brown			10 YR 6/2	Pale yellowish brown
22	0.05	Gray mudstone	5 Y 6/1	Light olive gray			5 Y 8/1	Yellowish gray
21	0.40	Brown mudstone	10 YR 4/2	Dark yellowish brown			10 YR 6/2	Pale yellowish brown
20	0.60	Gray mudstone	5 Y 6/1	Light olive gray			5 Y 8/1	Yellowish gray
19	0.30	Orangish red mudstone	10 R 4/2	Grayish red			10 R 6/2	Pale red
18	0.50	Brown mudstone	5 YR 3/2	Grayish brown			10 R 6/2	Pale red
17	0.40	Orangish red mudstone	10 YR 5/4	Moderate yellowish brown			10 R 6/2	Pale red
16	0.20	Gray mudstone	5 Y 6/1	Light olive gray			5 Y 8/1	Yellowish gray
15	0.10	Red mudstone (level of Purple-0?)	10 R 4/2	Grayish red				
14	0.90	Gray mudstone	5 Y 6/1	Light olive gray			5 Y 8/1	Yellowish gray
13	0.20	Brown concretionary sandstone						
12	1.60	Gray mudstone with thin orange beds	5 Y 6/1	Light olive gray			5 Y 8/1	Yellowish gray
11	0.70	Fine-grained yellow sandstone	5 Y 6/4	Dusky yellow			5 Y 7/2	Yellowish gray
10	1.20	Fine-grained yellow sandstone	5 Y 6/4	Dusky yellow			5 Y 7/2	Yellowish gray
9	0.90	Gray mudstone	5 Y 6/1	Light olive gray			5 Y 8/1	Yellowish gray
8	0.10	Platy sandstone	5 Y 7/2	Yellowish gray			10 YR 6/2	Pale yellowish brown
7	0.50	Gray mudstone	5 Y 6/1	Light olive gray			5 Y 8/1	Yellowish gray
6	0.20	Orange mudstone	5 Y 5/2	Light olive gray	10 YR 4/2	Dark yellowish brown	10 YR 6/2	Pale yellowish brown
5	1.00	Gray mudstone	5 Y 6/1	Light olive gray			5 Y 8/1	Yellowish gray
4	0.20	Planar-bedded very-fine-grained sandstone	5 Y 7/2	Yellowish gray			10 YR 6/2	Pale yellowish brown
3	1.70	Muddy very-fine-grained sandstone	5 Y 8/1	Yellowish gray	5 Y 6/1	Light olive gray	5 Y 8/1	Yellowish gray
2	1.00	Gray mudstone	5 Y 4/1	Olive gray			5 Y 8/1	Yellowish gray
1	0.50	Purplish red mudstone	5 R 4/2	Grayish red			10 R 6/2	Pale red

TABLE A4 — South Polecat Bench SC-206 stratigraphic section. Beds are listed in stratigraphic order from bottom to top. Color codes are from Goddard et al. (1948). Spacing of paleosols is based on elevations determined by differential GPS. Bed thickness is in meters.

Bed	Thick.	Description	Fresh color		Mottling color		Weathered color	
31	0.50	Red mudstone (near top of Polecat Bench)	10 R 4/6	Moderate reddish brown				
30	8.98	Gray mudstone						
29	0.50	Orange mudstone	10 YR 5/4	Moderate yellowish brown				
28	9.47	Gray mudstone						
27	0.50	Orange mudstone	10 YR 6/2	Pale yellowish brown				
26	1.42	Gray mudstone						
25	0.50	Orange mudstone	10 YR 5/4	Moderate yellowish brown				
24	4.01	Gray mudstone						
23	0.13	Yellowish gray mudstone	5 Y 6/1	Light olive gray				
22	0.00	Gray mudstone						
21	0.50	Yellowish gray mudstone	5 Y 6/1	Light olive gray				
20	5.23	Gray mudstone						
19	0.50	Yellowish gray mudstone	5 Y 5/2	Light olive gray				
18	2.42	Gray mudstone						
17	0.50	Orange mudstone	10 YR 6/2	Pale yellowish brown				
16	0.44	Gray mudstone						
15	0.50	Brown mudstone	10 YR 4/2	Dark yellowish brown				
14	1.32	Gray mudstone (top of SC-206)						
13	0.50	Red mudstone	10 R 3/4	Dark reddish brown				
12	2.00	Gray mudstone						
11	0.50	Red mudstone (middle part of Top Red B)	10 R 3/4	Dark reddish brown				
10	0.03	Gray mudstone						
9	0.50	Red mudstone (lower part of Top Red B)	10 YR 4/2	Dark yellowish brown				
8	3.73	Gray mudstone						
7	0.50	Red mudstone (Top Red A)	10 R 4/6	Moderate reddish brown				
6	0.58	Gray mudstone						
5	0.50	Orange mudstone	10 YR 5/4	Moderate yellowish brown				
4	3.37	Gray mudstone						
3	0.50	Orange mudstone	10 YR 6/2	Pale yellowish brown				
2	2.62	Gray mudstone (base of SC-206)						
1	1.00	Purple mudstone (Purple-4)	5 RP 4/2	Grayish red purple	5 Y 8/1	Yellowish gray	5 RP 6/2	Pale red purple



REFINED ISOTOPE STRATIGRAPHY ACROSS THE CONTINENTAL PALEOCENE-EOCENE BOUNDARY ON POLECAT BENCH IN THE NORTHERN BIGHORN BASIN

GABRIEL J. BOWEN¹, PAUL L. KOCH¹, PHILIP D. GINGERICH², RICHARD D. NORRIS³
SANTO BAINS⁴, and RICHARD M. CORFIELD⁴

¹*Department of Earth Sciences, The University of California, Santa Cruz, California 95062*

²*Department of Geological Sciences and Museum of Paleontology, The University of Michigan, Ann Arbor, Michigan 48109-1079*

³*Woods Hole Oceanographic Institution, Woods Hole, Massachusetts 02543-1541*

⁴*Department of Earth Sciences, University of Oxford, Oxford OX1 3PR*

Abstract.— One of the most continuous and best studied continental stratigraphic sections spanning the Paleocene-Eocene boundary is preserved on Polecat Bench in the northern Bighorn Basin. The mammalian biostratigraphy of Polecat Bench sediments has been well documented, and includes a major reorganization of faunas at or near the P-E boundary. To complement the existing biostratigraphy, we measured the isotopic composition of paleosol carbonate nodules at soil-by-soil temporal resolution through the P-E boundary interval. These measurements provide a detailed record of the abrupt, transient, carbon isotope excursion that affected atmospheric and oceanic carbon reservoirs at ca. 55 million years before present [Ma]. Tests of soil thickness and diagenesis indicate that trends in the record are primary, and reflect syndepositional changes in the $\delta^{13}\text{C}$ value of atmospheric CO_2 . The carbon isotope record suggests that the $\delta^{13}\text{C}$ value of atmospheric CO_2 dropped by ca. 8‰ during this interval, and then rebounded. The pattern of change is very similar to that of an independent high-resolution record of Bains et al. (submitted). Changes in the $\delta^{18}\text{O}$ of paleosol carbonates are consistent with a significant increase in local mean annual temperature during the P-E boundary event. Comparison of biotic and isotopic stratigraphies on Polecat Bench shows that faunal changes at the P-E boundary lag behind major events in the carbon and oxygen isotope records by about 10 thousand years [k.y.].

INTRODUCTION

The isotopic chemistry of authigenic soil minerals can be a sensitive recorder of climatic and environmental conditions. Authigenic carbonate from fossil soils (paleosols) is a valuable and widely used source of paleoclimatic and paleoenvironmental proxy information, and the isotope systematics of soil carbonate formation have been documented and modeled (Cerling, 1984). Fossil soils are often developed many times in a stratigraphic section and thus very useful

time series can be derived from the oxygen and carbon isotope composition of paleosol carbonates, with $\delta^{18}\text{O}$ recording primarily changes in paleoclimatic variables, and $\delta^{13}\text{C}$ responding to more general paleoenvironmental shifts. Here delta values express deviations in per mil (‰) units. For example, $\delta^{18}\text{O}$ is the deviation of the oxygen isotope ratio R of a sample from that for a standard (V-PDB). This is calculated as:

$$\delta^{18}\text{O} = 1000 \times (R_{\text{sample}} - R_{\text{standard}})/R_{\text{standard}}$$

where $R = {}^{18}\text{O}/{}^{16}\text{O}$. Similarly, $\delta^{13}\text{C}$ is the deviation (in ‰) of the carbon isotope ratio of a sample from that of a standard (V-PDB), where $R = {}^{13}\text{C}/{}^{12}\text{C}$.

In: Paleocene-Eocene Stratigraphy and Biotic Change in the Bighorn and Clarks Fork Basins, Wyoming (P. D. Gingerich, ed.), University of Michigan Papers on Paleontology, 33: 73-88 (2001).

Extreme transient climate and carbon cycle events at the Paleocene-Eocene boundary have been documented in isotopic proxy records from a number of sources, including marine carbonates (Kennett and Stott, 1991; Zachos et al., 1993; Bains et al., 1999; Katz et al., 1999; Norris and Röhl, 1999), fossil pollen (Beerling and Jolley, 1998), and paleosol carbonates (Koch et al., 1992, 1995; Bowen et al., 2000; Bains et al., submitted). During the Paleocene-Eocene transition, marine bottom waters and high-latitude surface waters warmed dramatically (Kennett and Stott, 1991; Zachos et al., 1993), and substantial warming is indicated in terrestrial settings (Koch et al., 1995; Fricke et al., 1998). This transient climate event is associated with a large change in the carbon isotope composition of earth-surface carbon reservoirs. In the oceans, the $\delta^{13}\text{C}$ values of planktonic foraminifera dropped by ca. 2.5 to 4.5‰, while those of benthic species decreased by ca. 2.5‰ (Kennett and Stott, 1991; Zachos et al., 1993). Proxy records for atmospheric CO_2 show an abrupt decrease in $\delta^{13}\text{C}$ values of as much as 7‰ (Koch et al., 1992, 1995; Bowen et al., 2000; Cojan et al., 2000). This short-lived change in the isotopic composition of carbon at the earth's surface is best explained by the release and oxidation of at least 1500 gigatons of carbon from sea-floor methane hydrate reservoirs, followed by sequestration of this excess carbon during carbon cycle re-equilibration (Dickens et al., 1997; Bains et al., 1999; Beerling, 2000).

The stratigraphic sequence on Polecat Bench in the northern Bighorn Basin of Wyoming preserves a nearly continuous series of carbonate-bearing paleosols (e.g., Fig. 1) that represent late Paleocene and early Eocene time (Gingerich, 1983). These same soils preserve fossil mammals that have been collected and studied by paleomammalogists since the late nineteenth century. Previous study of paleosol carbonates from Polecat Bench and adjacent regions of the Clarks Fork Basin indicated that the Paleocene-Eocene boundary isotope excursion is recorded as a 6 to 7‰ drop in the $\delta^{13}\text{C}$ of soil carbonate nodules (Koch et al., 1992, 1995). Here we exploit recent advances in understanding of the stratigraphy on Polecat Bench (Gingerich, this volume) to present a detailed paleosol-by-paleosol analysis of isotopic change across the Paleocene-Eocene boundary interval on Polecat Bench.

ISOTOPIC SIGNATURE OF SOIL CARBONATE

Processes that affect the isotopic composition of soil carbonate have been well documented in modern settings (Cerling, 1984; Quade et al., 1989; Cerling et al., 1991). Carbon in soil carbonate is derived from soil CO_2 , which is a mixture of carbon dioxide from the atmosphere, and from organic decomposition and root respiration within the soil. The mixing of CO_2 from these sources has been modeled (Cerling, 1984; Cerling et al., 1991), and in soils with moderate to high productivity, minimal influence of atmospheric CO_2 is observed below ca. 30 cm depth. Below this depth, soil CO_2 is enriched in ^{13}C by ca. 4.4‰ relative to plant tissues and respired CO_2 , due to the effects of diffusion (Cerling et al., 1991). This offset, along with consistent fractionations associated with carbonate pre-

cipitation (ca. 10.5‰) add to produce soil carbonate with a $\delta^{13}\text{C}$ value ca. 15‰ greater than that of overlying vegetation (Cerling, 1984). The isotopic composition of vegetation should track the $\delta^{13}\text{C}$ of atmospheric CO_2 with a consistent fractionation of approximately -19‰ for Paleocene-Eocene plants using a C3 photosynthetic pathway (Bocherens et al., 1993; Arens et al., 2000). Therefore, changes in the carbon isotope composition of the atmosphere are propagated and recorded in the $\delta^{13}\text{C}$ of soil carbonate CO_2 .

Oxygen in soil carbonate is derived from soil water, which is derived from rain and snow (Cerling, 1984). Temporal variation in the $\delta^{18}\text{O}$ value of precipitation has commonly been interpreted to reflect variation in mean annual temperature, following the relationship developed by Dansgaard (1964). Recent work, however, has shown that this relationship is not quantitatively applicable on geological time scales (e.g., Boyle, 1997; Fricke and O'Neil, 1999). Study of modern soil carbonates has demonstrated that their oxygen isotope composition is not typically affected by rock-water interactions in the soil zone, but may reflect significant evaporative enrichment of soil waters (Quade et al., 1989).

MATERIALS AND METHODS

Fossil soil development is nearly ubiquitous within fine-grained sediments on Polecat Bench, and paleosols in this study were recognized as brown, green, orange, red, or purple mudstone horizons. Colored mudstones typically represent the B-horizons of ancient soils, and commonly contain pedogenic carbonate nodules as well as other pedogenic minerals (Bown and Kraus, 1981, 1987; Kraus, 1987). Paleosol carbonates were sampled near the base of paleosol B-horizons in freshly-exposed outcrops where there is no evidence of modern soil development (e.g., modern roots). Samples were collected at multiple stratigraphic levels within some of the thicker paleosols. Paleosols were sampled in situ in four local sections, which were mapped concurrently (Gingerich, this volume). Stratigraphic thicknesses were measured by hand leveling using a 1.5-meter Jacob's staff and by differential GPS, and detailed stratigraphic sections can be found elsewhere in this volume. Local sections were correlated by tracing marker beds (Gingerich, this volume), and results are presented on a composite stratigraphic scale. A similar record, generated independently, is presented in Bains et al. (submitted).

In the laboratory, carbonate nodules were polished flat on a lapidary wheel using 600-grit silica carbide powder, washed, then dried in a low temperature oven. Samples (ca. 100 μg) were drilled from the polished surfaces under a binocular microscope using a mounted dental drill. Primary micritic carbonate and secondary diagenetic spar were sampled independently, and, where possible, two samples were drilled from each of two nodules from every soil in each local section. Samples were roasted *in vacuo* at 400° C for 1 hour to remove organic contaminants. These were analyzed using a Micromass Optima or Prism gas-source mass spectrometer, following reaction with 100% phosphoric acid at 90° C, with the aid of an

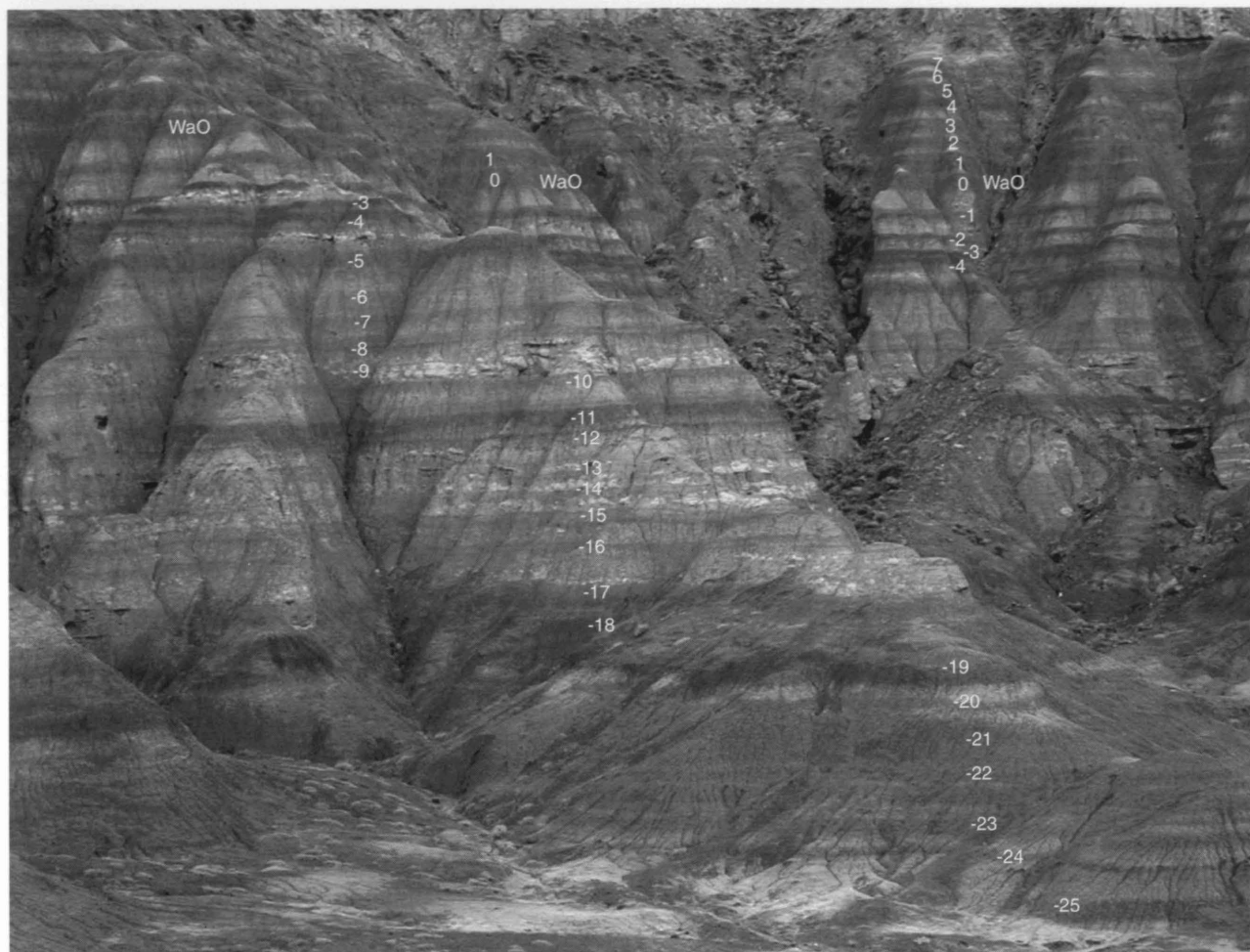


FIGURE 1 — Orange, red, and purple paleosol horizons (numbered darker bands) at the base of the carbon isotope excursion on Polecat Bench (Bains and Norris numbering system is shown here). Principal marker beds of Gingerich (Gingerich, this volume: figs. 7 and 8) are equivalent to beds numbered here, as follows: Thick Orange = beds -23 through -21; Purplish red mudstone = bed -19; Red mudstones = bed -11; Purple-0 = bed -5; Top Brown = bed -1; Lower Double-Red A and B = beds 0 and 1; and Purple-2 = bed 4. The carbon isotope excursion begins at the thin red mudstone represented by bed -8 here. University of Michigan vertebrate locality SC-404 with *Meniscotherium priscum* is at the level of beds -3 and -4. The Wa-0 faunal zone begins at bed 0. In this section the top of Wa-0 and the top of the carbon isotope excursion are missing due to truncated by the scour-and-fill sequence starting above bed 7.

automated Isocarb device. Analytical precision, based on repeated analysis of an in-house standard, was better than 0.1‰ for both carbon and oxygen.

RESULTS

Carbon and oxygen isotope measurements of micrite sampled from Polecat Bench paleosol are listed in Table 1. Ancillary measurements of the thickness of the B-horizons from which soil carbonates were collected are listed in Table 2. In addition, analyses of diagenetic spar from 10 carbonate nodules are presented in Table 3.

Within-Soil Variation and Variation through Time

A minimum of 57 distinct soils are represented in this study, spanning ca. 115 meters of stratigraphic section. The measured carbon isotope compositions span a range of -16.7‰ to -7.2‰, while $\delta^{18}\text{O}$ values were between -17.5‰ and -7.4‰. Both are plotted by stratigraphic level in Figure 2. These data show fairly tight grouping (total range of ca. 1 to 3‰) of carbon and oxygen isotope values at most stratigraphic levels. Notable exceptions occur at the base of the composite section, and at the 1519 m level (carbon and oxygen) and 1544 m level (oxygen). Also apparent is a distinct stratigraphic interval

TABLE 1 — Carbon and oxygen isotope values of micritic carbonate from the Paleocene-Eocene boundary interval on Polecat Bench. Samples in italics were culled and not used in interpretation of $\delta^{13}\text{C}$ excursion.

Soil	Sample	Level	$\delta^{13}\text{C}$	$\delta^{18}\text{O}$	Soil	Sample	Level	$\delta^{13}\text{C}$	$\delta^{18}\text{O}$
PB-00-04-16	1A	1594.2	-8.1	-8.3	PB-00-02-14	2A	1537.0	-12.8	-9.1
PB-00-04-16	1B	1594.2	-8.7	-8.6	PB-00-02-14	2B	1537.0	-12.5	-9.4
PB-00-04-16	2A	1594.2	-9.3	-8.4	PB-00-02-13	1A	1534.8	-13.3	-8.1
PB-00-04-16	2B	1594.2	-9.3	-8.3	PB-00-02-13	1B	1534.8	-13.2	-8.2
PB-00-04-15	1A	1584.7	-8.8	-8.4	PB-00-02-12	12A-1A	1533.5	-14.3	-10.0
PB-00-04-15	1B	1584.7	-8.5	-8.3	PB-00-02-12	12A-1B	1533.5	-14.1	-9.3
PB-00-04-15	2A	1584.7	-8.7	-8.4	PB-00-02-12	12A-2A	1533.5	-14.2	-9.4
PB-00-04-15	2B	1584.7	-8.7	-8.4	PB-00-02-12	12A-2B	1533.5	-14.2	-9.4
PB-00-04-14	1A	1574.7	-8.9	-9.2	PB-00-02-12	12B-1A	1533.0	-12.9	-8.8
PB-00-04-14	1B	1574.7	-8.7	-8.6	PB-00-02-12	12B-1B	1533.0	-13.2	-8.6
PB-00-04-14	2A	1574.7	-9.2	-8.8	PB-00-02-12	12B-2A	1533.0	-12.3	-8.9
PB-00-04-14	2B	1574.7	-8.3	-8.5	PB-00-02-12	12B-2B	1533.0	-12.5	-9.1
PB-00-04-13	1A	1572.8	-8.5	-9.3	PB-00-02-11	1A	1532.2	-13.8	-9.0
PB-00-04-13	1B	1572.8	-8.9	-8.9	PB-00-02-11	1B	1532.2	-14.5	-9.8
PB-00-04-13	2A	1572.8	-9.2	-9.4	PB-00-02-11	1C	1532.2	-13.7	-7.9
PB-00-04-13	2B	1572.8	-8.7	-8.7	PB-00-02-11	2A	1532.2	-13.8	-8.0
PB-00-04-12	1A	1568.6	-9.1	-8.7	PB-00-02-11	2B	1532.2	-13.8	-8.2
PB-00-04-12	1B	1568.6	-9.3	-8.7	PB-00-02-10	1A	1531.6	-13.9	-8.0
PB-00-04-12	2A	1568.6	-7.2	-9.4	PB-00-02-10	1B	1531.6	-13.7	-8.2
PB-00-04-12	2B	1568.6	-7.7	-9.3	PB-00-02-10	2A	1531.6	-13.8	-8.1
PB-00-04-11	1A	1568.2	-9.0	-9.0	PB-00-02-10	2B	1531.6	-14.0	-8.2
PB-00-04-11	1C	1568.2	-8.8	-8.2	PB-00-02-09U	1A	1531.0	-13.9	-8.9
PB-00-04-11	2B	1568.2	-9.1	-8.3	PB-00-02-09U	1B	1531.0	-13.9	-8.8
PB-00-04-11	2C	1568.2	-9.2	-7.8	PB-00-02-09U	2A	1531.0	-13.4	-8.8
PB-00-04-10	1A	1562.4	-9.9	-8.2	PB-00-02-09U	2B	1531.0	-13.8	-8.9
PB-00-04-10	1B	1562.4	-8.9	-8.2	PB-00-02-09	1A	1530.5	-13.6	-9.2
PB-00-04-10	2A	1562.4	-8.9	-7.9	PB-00-02-09	1B	1530.5	-13.7	-8.7
PB-00-04-10	2B	1562.4	-9.6	-8.7	PB-00-02-09	2A	1530.5	-13.7	-9.5
PB-00-04-09	1A	1559.5	-8.7	-9.0	PB-00-02-09	2B	1530.5	-12.9	-10.7
PB-00-04-09	1B	1559.5	-8.8	-9.1	PB-00-02-08	2C	1530.5	-12.7	-8.4
PB-00-04-09	2A	1559.5	-7.4	-9.2	PB-00-02-08	1A	1529.1	-13.9	-9.1
PB-00-04-09	2B	1559.5	-7.2	-8.9	PB-00-02-08	1B	1529.1	-13.7	-9.0
PB-00-02-23	1A	1559.4	-9.4	-8.7	PB-00-02-08	2A	1529.1	-13.8	-8.3
PB-00-02-23	1B	1559.4	-9.4	-8.6	PB-00-02-08	2B	1529.1	-13.9	-8.4
PB-00-02-23	2A	1559.4	-8.2	-9.0	PB-00-02-07	07A-1A	1528.5	-12.8	-9.6
PB-00-02-23	2B	1559.4	-8.3	-9.2	PB-00-02-07	07A-1B	1528.5	-12.4	-9.8
PB-00-04-08	1A	1558.6	-9.1	-8.4	PB-00-02-07	07A-2A	1528.5	-13.1	-8.8
PB-00-04-08	1B	1558.6	-8.5	-9.8	PB-00-02-07	07A-2B	1528.5	-13.1	-9.1
PB-00-04-08	2A	1558.6	-8.4	-9.7	PB-00-02-07	07B-1A	1528.0	-13.4	-8.4
PB-00-04-08	2B	1558.6	-8.2	-9.5	PB-00-02-07	07B-1B	1528.0	-13.6	-8.4
PB-00-04-06	1A	1554.3	-9.3	-8.4	PB-00-02-07	07B-2A	1528.0	-12.4	-8.7
PB-00-04-06	1B	1554.3	-9.1	-8.3	PB-00-02-07	07B-2B	1528.0	-12.4	-10.5
PB-00-02-22	1A	1554.2	-9.2	-9.0	PB-00-02-07	07B-2C	1528.0	-12.6	-8.2
PB-00-02-22	1B	1554.2	-8.8	-8.9	PB-00-02-07	07C-1A	1527.0	-13.5	-8.3
PB-00-02-22	2A	1554.2	-9.6	-9.3	PB-00-02-07	07C-1B	1527.0	-13.5	-8.2
PB-00-02-22	2B	1554.2	-8.8	-8.9	PB-00-02-07	07C-2A	1527.0	-13.5	-8.2
PB-00-04-05	1A	1553.7	-9.2	-8.7	PB-00-02-07	07C-2B	1527.0	-14.2	-8.5
PB-00-04-05	1B	1553.7	-8.9	-8.5	PB-00-02-07	07D-1A	1526.3	-14.3	-8.6
PB-00-04-05	2A	1553.7	-9.5	-8.5	PB-00-02-07	07D-1B	1526.3	-14.3	-8.8
PB-00-04-05	2B	1553.7	-9.5	-8.9	PB-00-02-07	07D-2A	1526.3	-14.5	-8.7
PB-00-04-04	1A	1549.5	-9.6	-9.3	PB-00-02-07	07D-2B	1526.3	-14.4	-8.8
PB-00-04-04	1B	1549.5	-9.9	-9.1	PB-00-02-06	1A	1525.3	-13.2	-9.0
PB-00-04-04	2A	1549.5	-9.9	-8.4	PB-00-02-06	1B	1525.3	-12.8	-8.9
PB-00-04-04	2B	1549.5	-9.9	-9.3	PB-00-02-06	2A	1525.3	-14.0	-8.9
PB-00-02-21	1A	1549.0	-9.7	-10.1	PB-00-02-06	2B	1525.3	-14.4	-8.4
PB-00-02-21	1B	1549.0	-9.7	-9.8	PB-00-02-05	1A	1524.2	-14.0	-8.8
PB-00-02-21	2B	1549.0	-9.6	-9.7	PB-00-02-05	1B	1524.2	-13.7	-8.6
PB-00-02-21	2C	1549.0	-9.7	-8.9	PB-00-02-05	2A	1524.2	-13.9	-8.9
PB-00-04-03	1A	1548.4	-9.8	-8.6	PB-00-02-05	2B	1524.2	-13.9	-8.8
PB-00-04-03	1B	1548.4	-9.9	-8.4	PB-00-02-04	1A	1523.8	-15.6	-8.0
PB-00-04-03	2A	1548.4	-9.9	-8.5	PB-00-02-04	1B	1523.8	-13.9	-8.2
PB-00-04-03	2B	1548.4	-9.9	-8.4	PB-00-02-04	2A	1523.8	-14.0	-8.3
PB-00-02-20	1A	1547.2	-9.5	-9.6	PB-00-02-04	2B	1523.8	-14.0	-8.2
PB-00-02-20	1B	1547.2	-9.6	-9.6	PB-00-02-03	1A	1522.9	-14.2	-7.9
PB-00-02-20	2A	1547.2	-9.8	-9.7	PB-00-02-03	1B	1522.9	-14.3	-7.8
PB-00-02-20	2B	1547.2	-9.8	-9.7	PB-00-02-03	2A	1522.9	-14.1	-8.0
PB-00-02-19	1A	1545.1	-10.1	-8.7	PB-00-02-03	2B	1522.9	-14.2	-8.1
PB-00-02-19	1B	1545.1	-9.7	-8.8	PB-00-01-15	15A-1A	1521.9	-13.3	-7.8
PB-00-02-19	2A	1545.1	-10.4	-9.4	PB-00-01-15	15A-1B	1521.9	-13.4	-7.6
PB-00-02-19	2B	1545.1	-10.2	-9.3	PB-00-01-15	15B-1A	1521.2	-13.7	-8.3
PB-00-04-02	1A	1544.5	-11.5	-15.9	PB-00-01-15	15B-1B	1521.2	-13.8	-8.5
PB-00-04-02	1B	1544.5	-10.7	-17.2	PB-00-01-15	15B-2A	1521.2	-14.3	-8.3
PB-00-04-02	2A	1544.5	-11.5	-17.4	PB-00-01-15	15B-2B	1521.2	-14.3	-8.1
PB-00-04-02	2B	1544.5	-11.4	-17.5	PB-00-02-02	1A	1520.5	-13.8	-7.8
PB-00-02-18	1A	1543.9	-10.2	-9.3	PB-00-02-02	1B	1520.5	-13.7	-7.9
PB-00-02-18	1B	1543.9	-10.1	-8.9	PB-00-02-02	2A	1520.5	-13.7	-8.0
PB-00-02-18	2A	1543.9	-10.2	-9.1	PB-00-02-02	2B	1520.5	-13.1	-8.3
PB-00-02-18	2B	1543.9	-10.2	-9.3	PB-00-01-14	14A-1A	1519.7	-13.9	-8.3
PB-00-02-17	1A	1543.0	-10.3	-8.7	PB-00-01-14	14A-1B	1519.7	-13.9	-8.6
PB-00-02-17	1B	1543.0	-10.1	-8.4	PB-00-01-14	14A-2A	1519.7	-12.9	-9.9
PB-00-02-17	2A	1543.0	-11.2	-8.6	PB-00-01-14	14A-2B	1519.7	-13.1	-9.9
PB-00-02-17	2B	1543.0	-10.9	-8.1	PB-00-01-14	14B-1A	1519.3	-13.7	-10.2
PB-00-04-01	1A	1541.0	-10.6	-8.5	PB-00-01-14	14B-1B	1519.3	-12.0	-13.5
PB-00-04-01	1B	1541.0	-10.6	-8.5	PB-00-01-14	14B-2A	1519.3	-11.4	-15.0
PB-00-04-01	2A	1541.0	-11.9	-8.9	PB-00-01-14	14B-2B	1519.3	-11.1	-15.2
PB-00-04-01	2B	1541.0	-11.3	-9.9	PB-00-02-01	1A	1519.3	-14.9	-9.2
PB-00-02-15	1A	1538.7	-12.8	-9.9	PB-00-02-01	1B	1519.3	-13.6	-11.8
PB-00-02-15	1B	1538.7	-13.4	-10.0	PB-00-02-01	1C	1519.3	-12.3	-11.8
PB-00-02-15	2A	1538.7	-13.3	-9.2	PB-00-02-01	2A	1519.3	-12.6	-13.1
PB-00-02-15	2B	1538.7	-13.5	-9.7	PB-00-02-01	2B	1519.3	-12.9	-12.4
PB-00-02-14	1A	1537.0	-13.1	-8.6	PB-00-03-24	1A	1519.3	-14.0	-8.9
PB-00-02-14	1B	1537.0	-13.6	-8.8	PB-00-03-24	1B	1519.3	-13.9	-9.2

TABLE 1 (cont.) — Carbon and oxygen isotope values of micritic carbonate from the Paleocene-Eocene boundary interval on Polecat Bench. Samples in italics were culled and not used in interpretation of $\delta^{13}\text{C}$ excursion.

Soil	Sample	Level	$\delta^{13}\text{C}$	$\delta^{18}\text{O}$	Soil	Sample	Level	$\delta^{13}\text{C}$	$\delta^{18}\text{O}$
PB-00-03-24	2A	1519.3	-14.3	-8.7	PB-00-01-06	3B	1508.0	-14.6	-8.8
PB-00-03-24	2B	1519.3	-14.9	-7.7	PB-00-01-06	4A	1508.0	-14.6	-8.8
<i>PB-00-01-13</i>	<i>1A</i>	<i>1517.8</i>	<i>-12.3</i>	<i>-11.4</i>	PB-00-01-06	4B	1508.0	-13.9	-8.5
<i>PB-00-01-13</i>	<i>1B</i>	<i>1517.8</i>	<i>-12.5</i>	<i>-10.4</i>	PB-00-03-17	1A	1507.8	-15.5	-9.2
PB-00-01-13	2A	1517.8	-14.1	-7.9	PB-00-03-17	1B	1507.8	-15.5	-9.3
PB-00-01-13	2B	1517.8	-14.0	-7.8	PB-00-03-17	2A	1507.8	-15.6	-9.3
PB-00-03-23	1A	1517.7	-14.4	-8.6	PB-00-03-17	2B	1507.8	-15.4	-9.0
PB-00-03-23	1B	1517.7	-14.3	-8.7	PB-00-03-16	1A	1507.4	-14.1	-8.2
PB-00-03-23	2A	1517.7	-13.6	-8.8	PB-00-03-16	1B	1507.4	-14.1	-7.9
PB-00-03-23	2B	1517.7	-13.5	-8.8	PB-00-03-16	2A	1507.4	-14.5	-8.5
PB-00-01-12	1A	1516.4	-13.9	-9.1	PB-00-03-16	2B	1507.4	-14.4	-8.3
PB-00-01-12	1B	1516.4	-13.8	-9.0	PB-00-01-05	1A	1507.3	-15.7	-8.7
PB-00-01-12	2A	1516.4	-14.8	-8.2	PB-00-01-05	1B	1507.3	-15.9	-8.7
PB-00-01-12	2B	1516.4	-15.2	-8.7	PB-00-01-05	2A	1507.3	-16.7	-8.9
PB-00-03-22	1A	1516.1	-12.9	-8.7	PB-00-01-05	2B	1507.3	-16.6	-8.8
PB-00-03-22	1B	1516.1	-13.8	-8.3	PB-00-01-05	3A	1507.3	-15.0	-8.4
PB-00-03-22	2A	1516.1	-13.2	-9.1	PB-00-01-05	3B	1507.3	-15.1	-8.2
PB-00-03-22	2B	1516.1	-13.7	-8.7	PB-00-01-05	4A	1507.3	-16.0	-8.1
PB-00-01-11	1A	1515.4	-13.2	-8.5	PB-00-01-05	4B	1507.3	-16.0	-8.1
PB-00-01-11	1B	1515.4	-13.3	-8.3	PB-00-03-15	1A	1506.8	-14.3	-7.9
PB-00-01-11	2A	1515.4	-13.2	-9.1	PB-00-03-15	1B	1506.8	-14.5	-7.7
PB-00-01-11	2B	1515.4	-13.0	-9.2	PB-00-03-15	2A	1506.8	-14.5	-8.2
PB-00-01-10	10A-1A	1514.3	-15.0	-7.8	PB-00-03-15	2B	1506.8	-14.2	-7.7
PB-00-01-10	10A-1B	1514.3	-14.9	-7.7	PB-00-01-04	1A	1506.5	-14.2	-9.0
PB-00-01-10	10A-2A	1514.3	-14.6	-8.1	PB-00-01-04	1B	1506.5	-14.2	-8.9
PB-00-01-10	10A-2B	1514.3	-14.5	-8.2	PB-00-01-04	2A	1506.5	-13.5	-9.0
PB-00-01-10	10B-1A	1514.1	-14.7	-7.5	PB-00-01-04	2B	1506.5	-13.6	-8.9
PB-00-01-10	10B-1B	1514.1	-14.7	-7.6	PB-00-01-03	1A	1504.9	-14.2	-8.6
PB-00-01-10	10B-2A	1514.1	-15.1	-8.0	PB-00-01-03	1B	1504.9	-14.1	-8.5
PB-00-01-10	10B-2B	1514.1	-15.0	-8.1	PB-00-03-14	1A	1504.9	-12.9	-8.6
PB-00-03-21	1A	1513.9	-15.2	-8.6	PB-00-03-14	1B	1504.9	-12.9	-8.7
PB-00-03-21	1B	1513.9	-15.2	-8.4	PB-00-03-14	2A	1504.9	-12.7	-8.0
PB-00-03-21	2A	1513.9	-15.1	-8.8	PB-00-03-14	2B	1504.9	-13.0	-8.8
PB-00-03-21	2B	1513.9	-15.2	-8.3	PB-00-01-02	1A	1502.2	-12.9	-8.2
PB-00-01-10	10C-1A	1513.6	-14.9	-8.5	PB-00-01-02	1B	1502.2	-12.5	-8.1
PB-00-01-10	10C-1B	1513.6	-15.0	-8.4	PB-00-01-02	2A	1502.2	-12.3	-8.2
PB-00-01-10	10C-2A	1513.6	-15.6	-8.9	PB-00-01-02	2B	1502.2	-12.3	-8.2
PB-00-01-10	10C-2B	1513.6	-15.7	-9.0	PB-00-01-01	1A	1500.9	-12.3	-9.1
PB-00-01-10	10D-1A	1513.2	-14.7	-7.9	PB-00-01-01	1B	1500.9	-12.3	-9.3
PB-00-01-10	10D-1B	1513.2	-14.6	-7.8	PB-00-01-01	2A	1500.9	-12.4	-9.1
PB-00-01-09	09A-1A	1512.8	-14.4	-7.8	PB-00-01-01	2B	1500.9	-12.6	-8.8
PB-00-01-09	09A-1B	1512.8	-14.5	-8.7	PB-00-03-13	1A	1500.3	-10.5	-8.9
PB-00-01-09	09A-2A	1512.8	-14.9	-8.1	PB-00-03-13	1B	1500.3	-10.2	-8.9
PB-00-01-09	09A-2B	1512.8	-15.0	-8.1	PB-00-03-13	2A	1500.3	-10.0	-8.3
PB-00-01-09	09B-1A	1512.4	-14.9	-8.6	PB-00-03-13	2B	1500.3	-10.1	-8.5
PB-00-01-09	09B-1B	1512.4	-14.8	-8.6	PB-00-03-12	1A	1499.7	-10.0	-7.9
PB-00-01-09	09B-2A	1512.4	-14.5	-8.7	PB-00-03-12	1B	1499.7	-9.9	-7.6
PB-00-01-09	09B-2B	1512.4	-14.7	-9.0	PB-00-03-12	2A	1499.7	-11.3	-8.3
PB-00-03-20	1A	1512.3	-14.9	-9.9	PB-00-03-12	2B	1499.7	-11.2	-8.3
PB-00-03-20	1B	1512.3	-14.9	-8.8	PB-00-03-11	1A	1498.5	-10.1	-9.7
PB-00-03-20	2A	1512.3	-14.9	-8.6	PB-00-03-11	1B	1498.5	-10.0	-9.7
PB-00-03-20	2B	1512.3	-14.8	-8.7	PB-00-03-11	2A	1498.5	-9.8	-9.6
PB-00-01-09	09C-1A	1512.1	-14.9	-8.8	PB-00-03-11	2B	1498.5	-9.6	-9.6
PB-00-01-09	09C-1B	1512.1	-15.1	-8.6	PB-00-03-10	1A	1495.4	-9.8	-8.7
PB-00-01-09	09C-2A	1512.1	-15.1	-8.6	PB-00-03-10	1B	1495.4	-9.4	-9.0
PB-00-01-09	09C-2B	1512.1	-15.1	-9.0	PB-00-03-10	2A	1495.4	-9.4	-7.9
PB-00-01-09	09D-1A	1511.7	-14.8	-8.2	PB-00-03-10	2B	1495.4	-9.1	-8.1
PB-00-01-09	09D-1B	1511.7	-14.4	-8.4	PB-00-03-08	1A	1494.4	-9.9	-8.9
PB-00-01-09	09D-2A	1511.7	-14.7	-8.4	PB-00-03-08	1B	1494.4	-9.9	-8.9
PB-00-01-09	09D-2B	1511.7	-14.5	-8.6	PB-00-03-08	2A	1494.4	-9.7	-9.2
PB-00-01-08	1A	1510.3	-14.3	-8.2	PB-00-03-08	2B	1494.4	-9.7	-9.4
PB-00-01-08	1B	1510.3	-14.5	-8.2	PB-00-03-07	1A	1486.0	-11.2	-9.7
PB-00-01-08	2A	1510.3	-13.3	-8.3	PB-00-03-07	1B	1486.0	-10.3	-9.9
PB-00-01-08	2B	1510.3	-13.7	-8.6	PB-00-03-07	2A	1486.0	-10.8	-9.8
PB-00-03-19	1A	1510.1	-14.0	-9.3	PB-00-03-07	2B	1486.0	-11.4	-9.8
PB-00-03-19	1B	1510.1	-14.6	-9.2	PB-00-03-06	1A	1483.4	-9.5	-9.2
PB-00-03-19	2A	1510.1	-14.6	-8.4	PB-00-03-06	1B	1483.4	-9.5	-8.8
PB-00-03-19	2B	1510.1	-14.8	-8.5	PB-00-03-06	2A	1483.4	-9.3	-9.0
PB-00-01-07.5	1A	1510.0	-13.9	-8.3	PB-00-03-06	2B	1483.4	-9.3	-9.2
PB-00-01-07.5	1B	1510.0	-13.8	-8.2	<i>PB-00-03-05</i>	<i>1A</i>	<i>1482.7</i>	<i>-7.2</i>	<i>-10.5</i>
PB-00-01-07.5	2A	1510.0	-14.7	-8.2	PB-00-03-05	1B	1482.7	-9.2	-8.9
PB-00-01-07.5	2B	1510.0	-14.7	-8.2	PB-00-03-05	1C	1482.7	-7.7	-8.2
PB-00-01-07	1A	1508.7	-14.5	-7.9	PB-00-03-05	2A	1482.7	-8.5	-9.4
PB-00-01-07	1B	1508.7	-14.7	-7.9	PB-00-03-05	2B	1482.7	-8.7	-9.4
PB-00-01-07	2A	1508.7	-14.3	-8.1	PB-00-03-04	1A	1482.0	-8.8	-9.2
PB-00-01-07	2B	1508.7	-14.0	-8.1	PB-00-03-04	1B	1482.0	-8.9	-9.3
PB-00-03-18	1A	1508.5	-13.6	-7.6	<i>PB-00-03-04</i>	<i>2A</i>	<i>1482.0</i>	<i>-10.0</i>	<i>-10.0</i>
PB-00-03-18	1B	1508.5	-13.5	-7.4	PB-00-03-04	2B	1482.0	-9.3	-8.4
PB-00-03-18	2A	1508.5	-14.1	-7.6	<i>PB-00-03-03</i>	<i>1A</i>	<i>1481.3</i>	<i>-11.7</i>	<i>-10.4</i>
PB-00-03-18	2B	1508.5	-14.3	-7.9	<i>PB-00-03-03</i>	<i>1B</i>	<i>1481.3</i>	<i>-11.8</i>	<i>-10.6</i>
PB-00-01-06	1A	1508.0	-14.2	-8.9	<i>PB-00-03-03</i>	<i>2A</i>	<i>1481.3</i>	<i>-13.0</i>	<i>-10.9</i>
PB-00-01-06	1B	1508.0	-14.2	-8.9	PB-00-03-03	2B	1481.3	-12.4	-9.1
PB-00-01-06	2A	1508.0	-14.0	-8.7	PB-00-03-02	1A	1480.8	-9.2	-9.6
PB-00-01-06	2B	1508.0	-14.0	-8.7	PB-00-03-02	2A	1480.8	-8.8	-9.6
PB-00-01-06	3A	1508.0	-14.4	-8.6	PB-00-03-02	3A	1480.8	-9.3	-9.8

characterized by markedly lower $\delta^{13}\text{C}$ values than are observed elsewhere within the section. This interval represents the Pale-

ocene-Eocene boundary carbon isotope excursion, which is discussed in more detail below.

TABLE 2 — Measured thickness of paleosol B-horizons in the Paleocene-Eocene boundary interval on Polecat Bench.

Soil	Thickness (m)	Soil	Thickness (m)
PB-00-01-01	0.6	PB-00-03-01	0.3
PB-00-01-02	1.0	PB-00-03-02	0.2
PB-00-01-03	0.5	PB-00-03-03	0.1
PB-00-01-04	0.3	PB-00-03-04	0.6
PB-00-01-05	0.6	PB-00-03-05	0.6
PB-00-01-06	0.3	PB-00-03-06	0.6
PB-00-01-07	0.2	PB-00-03-07	0.6
PB-00-01-07.5	0.6	PB-00-03-08	0.2
PB-00-01-08	0.2	PB-00-03-09	0.3
PB-00-01-09	1.6	PB-00-03-10	0.2
PB-00-01-10	1.6	PB-00-03-11	0.2
PB-00-01-11	1.0	PB-00-03-12	0.2
PB-00-01-12	0.5	PB-00-03-13	0.3
PB-00-01-13	0.1	PB-00-03-14	0.5
PB-00-01-14	1.1	PB-00-03-15	0.3
PB-00-01-15	1.0	PB-00-03-16	0.2
PB-00-02-01	1.5	PB-00-03-17	0.2
PB-00-02-02	0.5	PB-00-03-18	0.3
PB-00-02-03	2.0	PB-00-03-19	0.5
PB-00-02-04	0.3	PB-00-03-20	1.6
PB-00-02-05	0.2	PB-00-03-21	1.6
PB-00-02-06	0.3	PB-00-03-22	0.6
PB-00-02-07	2.9	PB-00-03-23	0.5
PB-00-02-08	0.3	PB-00-03-24	0.5
PB-00-02-09	1.1	PB-00-04-01	1.4
PB-00-02-09U	0.2	PB-00-04-02	0.4
PB-00-02-10	0.2	PB-00-04-03	0.4
PB-00-02-11	0.4	PB-00-04-04	0.6
PB-00-02-12	1.0	PB-00-04-05	0.4
PB-00-02-13	0.6	PB-00-04-06	0.4
PB-00-02-14	0.2	PB-00-04-07	0.3
PB-00-02-15	0.5	PB-00-04-08	0.2
PB-00-02-16	1.5	PB-00-04-09	0.7
PB-00-02-17	0.2	PB-00-04-10	1.4
PB-00-02-18	0.1	PB-00-04-11	1.2
PB-00-02-19	0.4	PB-00-04-12	0.4
PB-00-02-20	0.3	PB-00-04-13	0.5
PB-00-02-21	0.3	PB-00-04-14	0.5
PB-00-02-22	0.5	PB-00-04-15	0.5
PB-00-02-23	1.2	PB-00-04-16	0.5

The characteristic variation of paleosol carbonate carbon and oxygen isotope compositions was investigated at several levels. The average range for $\delta^{13}\text{C}$ and $\delta^{18}\text{O}$ within individual nodules is 0.23‰ and 0.24‰, respectively ($n = 168$). Nodule averages from single sampling localities have an average range of 0.45‰ for $\delta^{13}\text{C}$ and 0.32‰ for $\delta^{18}\text{O}$ ($n = 86$). Five paleosols were sampled at multiple depths. The average range of mean carbon and oxygen isotope compositions from multiple levels within individual paleosols is 0.97‰ and 0.76‰, respectively. Additionally, four easily identifiable and laterally persistent soils were sampled in two or more local sections. The average range of mean $\delta^{13}\text{C}$ and $\delta^{18}\text{O}$ values at these laterally separated sites was 0.57‰ and 0.39‰. Overall, isotopic variability is greater at larger spatial (lateral and vertical) scales, suggesting that conditions governing the isotopic composition of the paleosol carbonate nodules

were spatially variable within soils. The average range of compositions within individual paleosols, however, is minor in comparison to the temporal trends observed in our data set.

Depth to Carbonate

The paleosol B-horizons from which soil carbonates were collected varied from 10 cm to 3 m in thickness, with an average thickness of 74 cm (Table 2). These colored horizons alternate with white or gray mudstones and sandy mudstones. The contact between colored mudstones and overlying drab mudstones is often marked by an abrupt change in grain size or color, probably representing erosional truncation of the soil following soil development. In addition, these soils must undergo some post-depositional

TABLE 3 — Carbon and oxygen isotope values of paleosol carbonate spar from the Paleocene-Eocene boundary interval on Polecat Bench.

Soil	Sample	Level	$\delta^{13}\text{C}$	$\delta^{18}\text{O}$
PB-00-04-11	1SPAR	1568.2	-6.8	-16.4
PB-00-04-04	2SPAR	1549.5	-7.5	-14.7
PB-00-04-03	2SPAR	1548.4	-11.5	-13.9
PB-00-02-19	1SPAR	1545.1	-11.3	-8.6
PB-00-02-11	1SPAR	1532.2	-14.8	-15.1
PB-00-02-10	2SPAR	1531.6	-15.4	-15.5
PB-00-02-09	2SPAR	1530.5	-14.4	-14.6
PB-00-02-07	07D-1SPAR	1526.3	-13.2	-16.3
PB-00-01-12	SPAR	1516.4	-12.5	-12.5
PB-00-03-08	1SPAR	1494.4	-11.2	-9.1

compaction. Our measurements, then, provide a minimum estimate of B-horizon thickness, and place conservative bounds on total soil thickness. Nodules sampled from at least 30 cm below the top of preserved B-horizons should have formed at sufficient depth within the soils to have $\delta^{13}\text{C}$ values that are minimally affected by the penetration of atmospheric CO_2 .

Where the preserved B-horizon is less than 30 cm thick (20 of the 57 soils sampled), we have no objective measure of the minimum depth beneath the soil surface at which soil carbonate formed, so atmospheric influence on the $\delta^{13}\text{C}$ value of soil carbonate is possible. To test this, we calculated average $\delta^{13}\text{C}$ values for each soil, and fit an unweighted 3-point running average to this data series. For each soil, we calculated the difference between the measured soil average $\delta^{13}\text{C}$ value and the 3-point average for that level. These differences are plotted against preserved B-horizon thickness in Figure 3. If paleosols with thin preserved B-horizons had carbonate nodules that incorporated a large amount of atmospheric carbon, nodules from these soils should be systematically enriched in carbon-13 relative to those from adjacent thicker paleosols. Least-squares regression through the data in Figure 3 produces a best-fit line with a slope of -0.045% per meter, which is not significantly different from zero at the 95% confidence level. We therefore conclude that, on Polecat Bench, incorporation of atmospheric CO_2 does not disproportionately affect the ^{13}C of carbonate samples from paleosols with thin preserved B-horizons.

Diagenesis

The distribution of all micrite and spar measurements in $\delta^{13}\text{C}$ vs. $\delta^{18}\text{O}$ space is non-random (Fig. 4). Micrite values cluster in two groups, one characterized by $\delta^{13}\text{C}$ values of -16% to -12% and $\delta^{18}\text{O}$ values of -9.5% to -7.5% , and the other with $\delta^{13}\text{C}$ values of -10.5% to -8% and $\delta^{18}\text{O}$ values of -10% to -8% . These clusters correspond to stratigraphically-distinct por-

tions of the Polecat Bench composite section (Fig. 2), and represent P-E boundary isotope excursion values (first group) and pre- and post-excursion values (second group). Less numerous data scatter around these clusters, and it is notable that the $\delta^{18}\text{O}$ values of many of the samples are lower than those of the characteristic groups. Diagenetic spar from the carbonate nodules typically has $\delta^{18}\text{O}$ values less than -12% , and spans a wide range of $\delta^{13}\text{C}$ values (Table 3). The inadvertent incorporation of diagenetic spar in samples of paleosol micrite is problematic, since diagenetic fluids can contribute carbon from a variety of sources and potentially obscure the paleoatmospheric record preserved in the micrite.

While mixing of carbon sources can create diagenetic carbonate with widely varying carbon isotope compositions, there is a fundamental basis for expecting that the $\delta^{18}\text{O}$ value of diagenetic carbonate will be lower than that of soil-formed micrite, and this factor can be used to distinguish altered and unaltered samples. The fractionation of oxygen isotopes during calcite precipitation is strongly temperature dependent, such that a 2°C increase in the temperature of precipitation will produce a decrease in $\delta^{18}\text{O}$ value of ca. 1% (Friedman and O'Neil, 1977). Diagenetic calcite formed after any substantial amount of burial, then, should be notably depleted in $\delta^{18}\text{O}$ relative to soil-formed calcite. Analyses of secondary spar from Bighorn Basin soil carbonates (Koch et al., 1995; current study), and from fossil bone (Bao et al., 1998), show that the diagenetic phase is characterized by $\delta^{18}\text{O}$ values 3% to 10% lower than co-occurring micrite that formed in the soil environment.

In several cases we see evidence that our soil micrite samples are contaminated with a component of diagenetic calcite. Samples of nodules collected from the Purple-2 marker bed of Gingerich (this volume; 1519.3 to 1519.7 m) in three local sections show obvious evidence for contamination with diagenetic calcite (Fig. 5). The samples from this soil define a line in $\delta^{13}\text{C}$ vs. $\delta^{18}\text{O}$ space, one end of which lies within the region typical for P-E boundary excursion values. The other end of

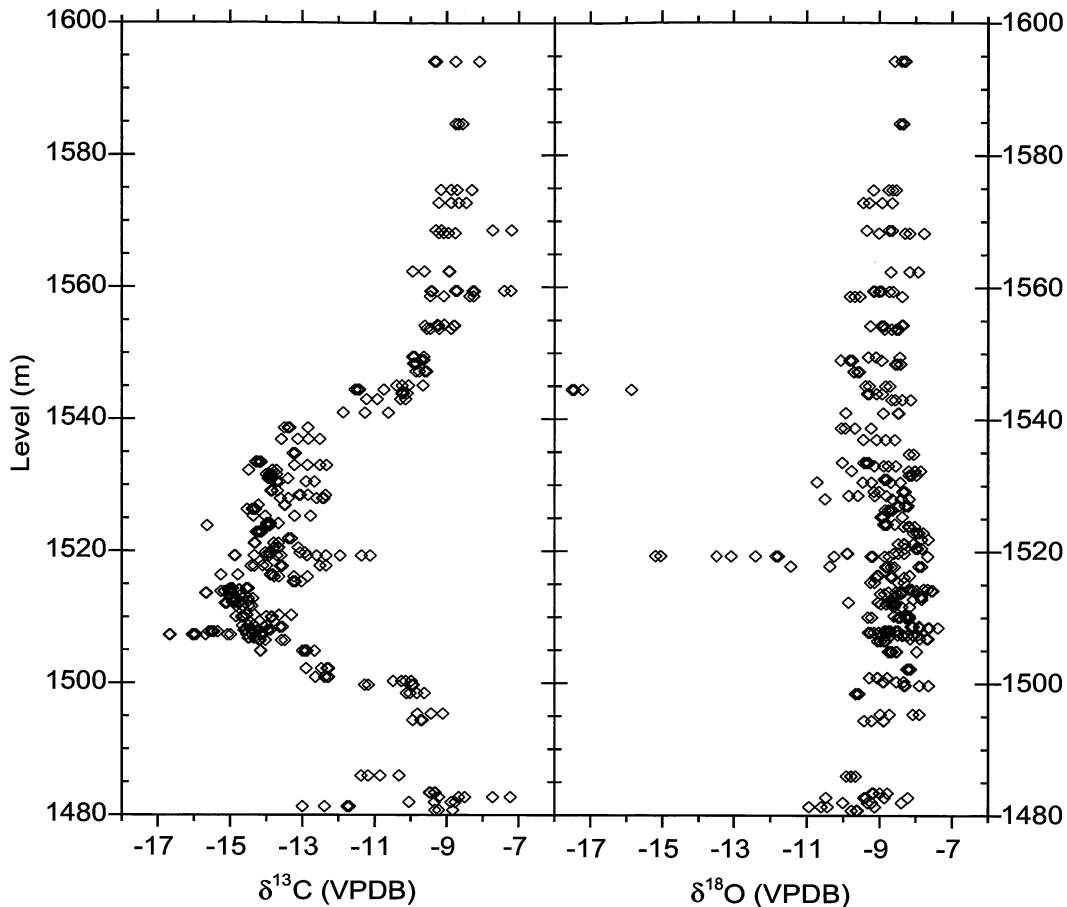


FIGURE 2 — All carbon and oxygen isotope measurements of Polecat Bench paleosol micrite plotted against stratigraphic level in the Polecat Bench composite section (Gingerich, this volume). Isotope measurements are listed in Table 1. Note fairly tight grouping (within ca. 1-3‰) of carbon and oxygen isotope values at most stratigraphic levels. Exceptions occur at the base of the section shown here, at the 1519 m level (carbon and oxygen), and at the 1544 m level (oxygen). Stratigraphic interval from 1500 m to 1540 m, with distinctly low $\delta^{13}\text{C}$ values, represents the Paleocene-Eocene boundary carbon isotope excursion.

this line lies within the broad region defined by our diagenetic spar samples, at $\delta^{13}\text{C} = -11\text{‰}$ and $\delta^{18}\text{O} = -16\text{‰}$ to -15‰ . We suggest that physical mixing of unaltered, pedogenic micrite with a diagenetic phase produces the large range of carbon and oxygen isotope values for nodules within this particular paleosol. Although our limited analyses of diagenetic spar produced no values that can be identified directly as this hypothetical diagenetic endmember, the more extensive analyses of Bao et al. (1998) produced several values that fall near the expected range.

Given the known potential for diagenetic contamination of paleosol carbonate and the recognition that some of our measurements may reflect such contamination, we filtered the dataset to identify and remove contaminated samples from subsequent analysis. Data were filtered based on their oxygen isotope composition only, according to two criteria: (1) Individual measurements were removed if repeated

analyses of the same nodule, or of nodules from the same horizon, consistently produced $\delta^{18}\text{O}$ values that were significantly (ca. 1‰ or more) different from the suspect value. (2) Multiple measurements from a single soil were excluded if they were dramatically depleted in $\delta^{18}\text{O}$ relative to nodules from surrounding soils (e.g., those data plotting outside of the "Normal Excursion Micrite" box in Fig. 5). Application of these criteria resulted in the culling of 24 of the 354 measurements in the data set (7%). Culled records are shown in italics in Table 1.

DISCUSSION

The composite carbon isotope stratigraphy spanning the Paleocene-Eocene boundary on Polecat Bench is shown in Figures 6 and 7. The first shows mean values of $\delta^{13}\text{C}$ for each paleosol in the composite section in relation to a composite

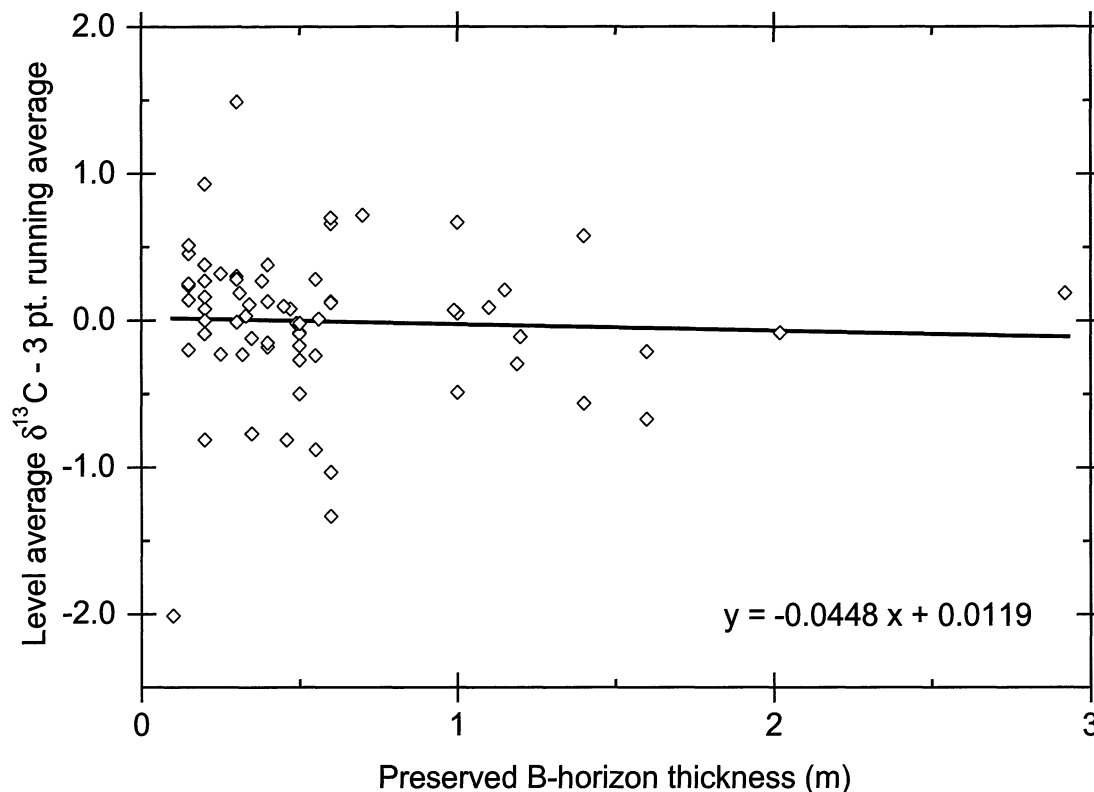


FIGURE 3 — Test for influence of atmospheric CO_2 on $\delta^{13}\text{C}$ values of paleosol carbonate sampled from thin paleosols on Polecat Bench. Differences between the mean $\delta^{13}\text{C}$ value for each soil and the unweighted 3-point average value for that level (both from Table 1) are plotted against preserved B-horizon thickness (Table 2). Least-squares regression yields a slope of -0.045% per meter B-horizon thickness, which is not significantly different from zero. Hence atmospheric CO_2 appears to have little effect on $\delta^{13}\text{C}$ of carbonate in paleosols with thin preserved B-horizons.

lithostratigraphic column and a detailed record of faunal change (Fig. 6), and the second shows mean values of $\delta^{13}\text{C}$ for each paleosol in each individual measured section in relation to oxygen isotope stratigraphy, a more generalized summary of faunal change, and a numerical estimate of geological age (Fig. 7). Individual measured sections are referred to by number here, with section 1 (open diamonds in Fig. 7) corresponding to the SC-343 section of Gingerich (this volume); section 2 (open squares in Fig. 7) corresponding to the SC-67 section; section 3 (open triangles in Fig. 7) corresponding to the SC-77 section; and section 4 (open circles in Fig. 7) corresponding to the SC-206 section.

The $\delta^{13}\text{C}$ Record on Polecat Bench

The most salient feature of the carbon isotope record shown in Figures 2, 6, and 7 is the negative excursion in values beginning at about the 1500 m level in the Polecat Bench composite section. Light $\delta^{13}\text{C}$ values persist for 40 m, and recovery to heavier values begins at about the 1540 m level. Carbon iso-

tope values vary widely in the lowest 10 m of the section studied here, with low ($<-10\%$) values observed at two distinct levels. Carbonate nodules were scarce and carbonate horizons poorly developed in paleosols below the 1485 meter level, and a substantial number of measurements from this interval appear to be affected by diagenetic contamination (Table 1). Further sampling of this stratigraphic interval will be necessary to verify the low carbon isotope values observed here. Most paleosols below the 1500 meter level have $\delta^{13}\text{C}$ values greater than -10% , within the range typical of pre-excursion soil carbonates (Koch et al., 1995).

Near the 1500 meter level $\delta^{13}\text{C}$ values begin to drop slightly; then they drop rapidly from -10% to -16% over a 7 m interval containing 6-7 soils. There is some suggestion here that the decrease occurs in a stepped manner, with two consecutive soils from section 1 (open diamonds in Fig. 7) producing intermediate values of about -12.5% . This observation is consistent with previously published high-resolution marine records from ODP site 690 and 1051 (Bains et al., 1999; Norris and Röhl, 1999; Bains et al., submitted). Taken together, all of the data appear

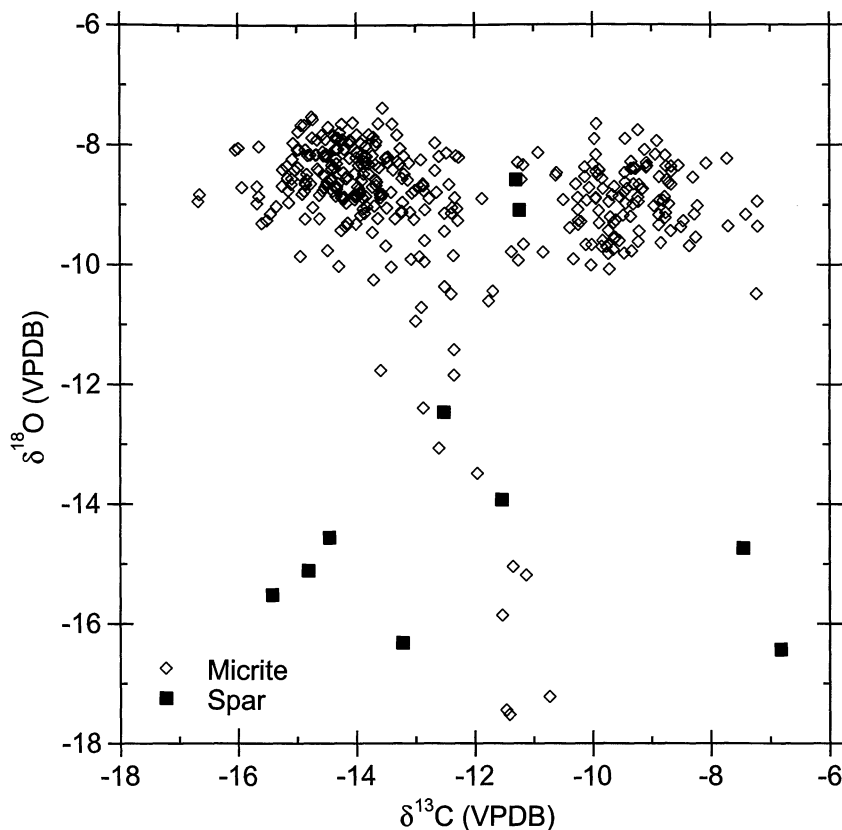


FIGURE 4 — Bivariate plot of carbon and oxygen isotope values for paleosol micrite on Polecat Bench (open diamonds; from Table 1), compared to carbon and oxygen isotope values for diagenetic spar (solid squares; Table 3). These cluster in two groups, one in the upper left quadrant (P-E boundary isotope excursion values) and one in the upper right quadrant (pre- and post-excursion values). Diagenetic spar from the carbonate nodules typically has $\delta^{18}\text{O}$ values less than -12‰ , and spans a wide range of $\delta^{13}\text{C}$ values.

to indicate a stepped onset of the carbon isotope excursion, plausibly caused by multiple pulses of methane release.

The total magnitude of the $\delta^{13}\text{C}$ excursion recorded on Polecat Bench is approximately 8‰ (from pre- and post-excursion $\delta^{13}\text{C}$ values of -8‰ to minimum excursion values of -16‰), meaning that the apparent amplitude of the atmospheric excursion is at least 3.5‰ greater than the maximum value observed in proxy records for the surface ocean (Kennett and Stott, 1991). Several factors could potentially contribute to this apparent decoupling of the atmospheric and oceanic carbon reservoirs, including loss of marine records due to dissolution, changes in soil properties that control the offset between atmospheric $\delta^{13}\text{C}$ values and those of soil carbonates, or repeated addition of small quantities of methane directly to the atmosphere. The cause of the apparent decoupling is unresolved, and this should be the focus of further study.

From a minimum at 1507 m, carbon isotope values rise abruptly by ca. 2‰ , and then begin to slowly and steadily increase through 30 meters of section. Superimposed on this

increase are several oscillations of 2‰ or less. We have no objective method for assessing potential changes in sedimentation rates within the Polecat Bench section, and thus have no objective age model for the Polecat Bench composite section (see discussion below). However, assuming roughly uniform rates of deposition, the portion of the record from 1507 to 1540 meters is not consistent with the modeled rebound of atmospheric and oceanic $\delta^{13}\text{C}$ values following a single, massive injection of methane (Dickens et al., 1997). Again, further work is required to bring carbon cycle models and observations into agreement.

Above the 1540 meter level of the Polecat Bench composite section, $\delta^{13}\text{C}$ values of soil carbonates rise rapidly and in a roughly exponential fashion, with complete rebound to typical non-excursion values (-9‰) by 1560 meters. Samples from two local sections (sections 2 and 4) track very closely through this interval and do not show the low magnitude oscillations characteristic of the previous 33 meters of section. The pattern observed here is similar to that predicted by Dickens et al. (1997)

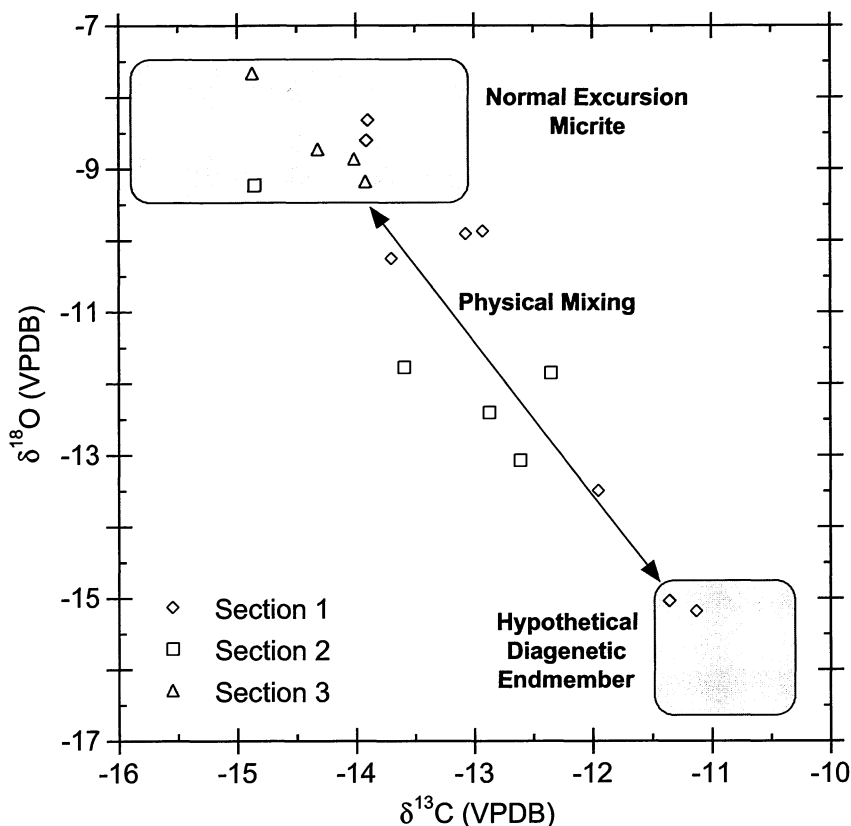


FIGURE 5—Bivariate plot of carbon and oxygen isotope values for paleosol micritic carbonate sampled from a single soil (Purple-2: 1519.3-1519.7 m interval) in three local sections on Polecat Bench. Section 1 (open diamonds) is the SC-343 section of Gingerich (this volume); section 2 (open squares) is the SC-67 section of Gingerich (this volume); and section 3 (open triangles) is the SC-77 section of Gingerich (this volume). Isotope values define a linear array here, suggesting that these samples include an admixture in varying proportions of primary carbonate and a diagenetic phase.

for the recovery of exogenic $\delta^{13}\text{C}$ values following methane injection. Above 1560 meters the carbon isotope composition of soil carbonates remains consistent to the top of Polecat Bench.

Biotic Change in Relation to Carbon Isotope Events

The Paleocene-Eocene boundary interval on Polecat Bench is marked by a dramatic reorganization of mammalian faunas (Clyde and Gingerich, 1998). This was first recognized as a boundary between the Clarkforkian and Wasatchian land-mammal ages, at the time archaic groups like *Champsosaurus*, *Plesiadapis*, *Probathyopsis*, and *Aletodon* disappeared, and new groups including the earliest representatives of Artiodactyla, Perissodactyla, Primates, and Hyaenodontidae appeared (Rose, 1981; Gingerich, 1983). As it became better known, a fauna within the boundary interval separating latest Clarkforkian zone Cf-3 from early Wasatchian zone Wa-1 was recognized to be distinctive (Gingerich, 1989). The new fauna is characterized by species of unusually small tooth and bone size,

and hence small body size. The presence of *Hyracotherium* and other representatives of modern orders indicates that the fauna is Wasatchian and thus it was designated Wa-0 to reflect its stratigraphic occurrence below Wa-1 and hence its greater age. The Wa-0 fauna is found at many places in the Clarks Fork Basin and on the eastern and western margins of the Bighorn Basin (Gingerich, 1989; Strait, this volume).

Shortly afterward, a broad survey of carbon and oxygen isotopes in soil nodules and fossil mammals, spanning the entire late Paleocene and early Eocene on Polecat Bench and adjacent Clarks Fork Basin, yielded a then-surprising negative $\delta^{13}\text{C}$ spike at locality SC-67 on the end of Polecat Bench (Koch et al., 1992, 1995), enabling correlation of Wa-0 to the deep sea isotope record (Kennett and Stott, 1991) and an important benthic foraminiferal extinction event (Thomas, 1991). Initial study suggested that the base of Wa-0 is correlative with the P-E boundary isotope excursion, perhaps indicating a causal link between climatic and biotic events near the boundary (Koch et

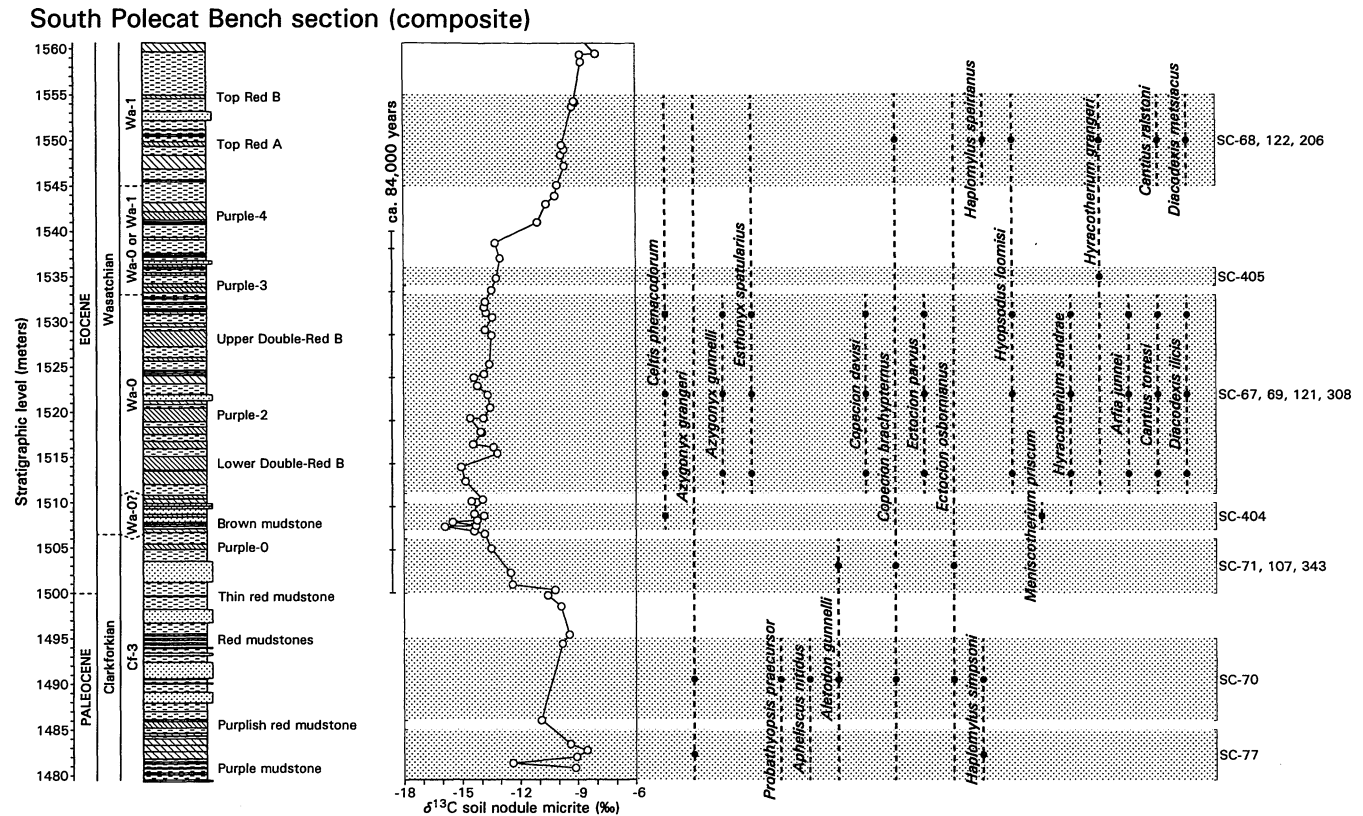


FIGURE 6 — Comparison of $\delta^{13}\text{C}$ isotope stratigraphy and biotic change at the south end of Polecat Bench. Lithostratigraphy and the ranges of *Celtis* and the principal mammalian taxa crossing the Paleocene-Eocene boundary are from Gingerich (this volume). Fourteen mammal-bearing fossil localities are known (SC-77, etc.), representing seven distinct stratigraphic intervals (shaded). These can be grouped into four time-successive associations based on their biota (Cf-3, Wa-0?, Wa-0, and Wa-1 on the ordinate). The interval labeled 'Wa-0 or Wa-1' on the ordinate is poorly-sampled and could be either Wa-0 or Wa-1 in age. The 84,000 year time scale shown here is consistent with an average rate of sediment accumulation of ca. 475 m/m.y. (Gingerich, 2000; Wing et al., 2000). Note that the beginning of the carbon isotope excursion is in the late Clarkforkian, overlapping the stratigraphic interval of localities SC-71, etc. The most negative $\delta^{13}\text{C}$ values are in the earliest zone of the Wasatchian (Wa-0?), represented by SC-404 with the first *Celtis* and *Meniscotherium*. The remainder of the carbon isotope excursion spans the interval of the classic dwarfed Wa-0 fauna with Perissodactyla, Artiodactyla, and Primates from localities SC-67, etc. Wasatchian mammals of standard size are known from localities SC-68, etc., in zone Wa-1 after carbon isotope values returned to normal (here ca. -9‰).

al., 1992). We are now able to improve this correlation by tying the Clarkforkian-Wasatchian faunal turnover directly to our new Polecat Bench carbon isotope stratigraphy.

Stratigraphic ranges for the dicot *Celtis phenacodorum* and 18 key mammalian taxa on Polecat Bench are shown in Figure 6. Specimens here were collected from 14 localities in seven successive stratigraphic intervals. The stratigraphic position of each locality and interval is well resolved, but each has a thickness (shown by stippling in Fig. 6), and fossils from a locality could have come from anywhere in the interval represented. Therefore, we take a conservative approach in representing species ranges, and show both constrained (solid circles) and unconstrained (dashed line) ranges in Figure 6. The base of a constrained range is placed in the middle of the stratigraphically lowest locality from which the taxon is known

(and the opposite is true for the top of a constrained range). Localities SC-67, SC-69, SC-121, and SC-308 have been so intensively collected that we are confident that ranges of taxa found there span virtually the full thickness of the Wa-0 interval.

Probathyopsis praecursor, *Apheliscus nitidus*, *Haplomylys simpsoni*, and *Aletodon gunnelli* are characteristically Clarkforkian species (Rose, 1981) that are not present in Wa-0 or subsequent faunas. The first three may range as high as the 1495 m level, and there is a record of *A. gunnelli* between 1500 and 1506 m. Hence all three of the lower stippled intervals in Figure 6 are late Clarkforkian or Cf-3 in age.

Three specimens of *Meniscotherium priscum* are known from the Bighorn Basin, one of which was collected on Polecat Bench in 2000 from the 1507-1510 m interval. The other two

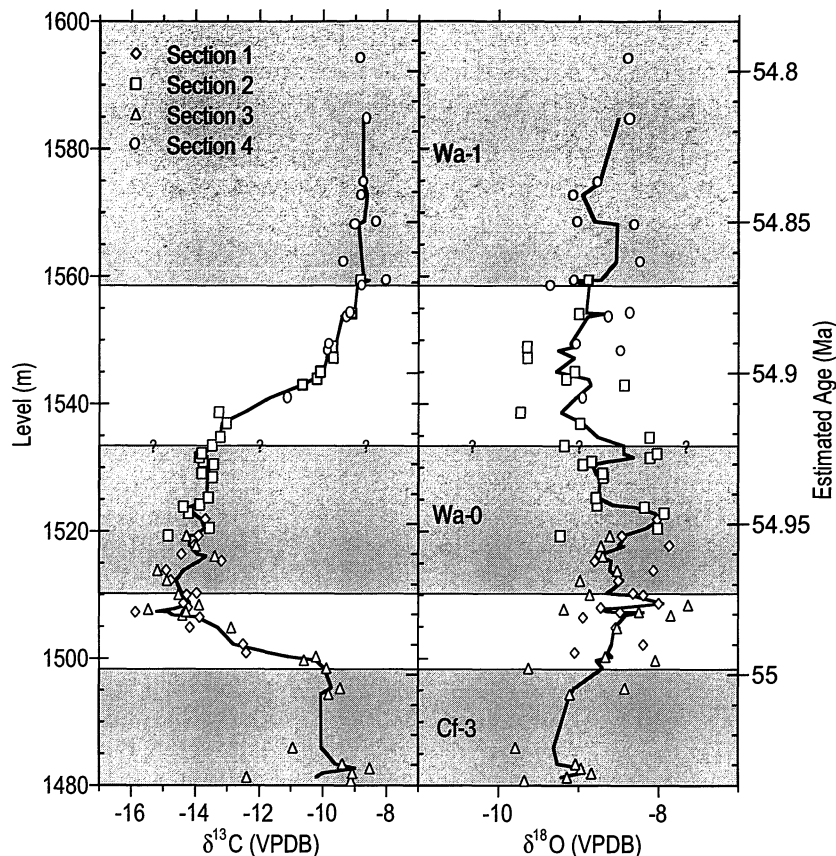


FIGURE 7 — Composite carbon and oxygen isotope records for the Polecat Bench section. Isotopic data plotted here are mean values for individual soils in each local section. Section 1 (open diamonds) = SC-343 section of Gingerich, this volume; section 2 (open squares) = SC-67; section 3 (open triangles) = SC-77 section; and section 4 (open circles) = SC-206. Isotopic records are plotted against meter level (left scale) and estimated age (right scale, see text). Bold lines are three-point running averages for $\delta^{13}\text{C}$ and $\delta^{18}\text{O}$, respectively, with each paleosol in the composite section represented only once. Subdivisions of the Clarkforkian and Wasatchian land-mammal ages are represented by grayscale shading, interpreted conservatively (see text and Fig. 6). The lower boundary for Wa-0 is placed at 1510, above the interval containing *Meniscotherium priscum*. The upper boundary for Wa-0 is placed at 1533 m, representing the upper limit of Wa-0 mammals recovered to date on Polecat Bench. Unshaded zones are intervals of faunal uncertainty that require further investigation.

specimens of *Meniscotherium priscum* both appear to be associated with a Wa-0 fauna or at least with endocarps of the dicot *Celtis phenacodorum*. Both *Meniscotherium* and *Celtis* occur in Wasatchian strata in the Bighorn Basin or elsewhere. Hence this zone is regarded as probably Wasatchian, and abbreviated Wa-0?

Faunas above the 1510 m level on Polecat Bench are dramatically different than those below and include many characteristically Eocene taxa. Wa-0 species, including *Copecion davisii*, *Ectocion parvus*, *Hyracotherium sandrae*, *Arfia junnei*, *Cantius torresi*, and *Diacodexis ilicis*, occur between 1510 and 1534 m. There is then a 10 m gap with no diagnostically Wa-

0 or Wa-1 taxa. Above the 1544 m level, mammalian faunas are dominated by Wa-1 taxa, including *Haplomylus speirianus*, *Cantius ralstoni*, and *Diacodexis metsiacus*.

Constrained taxonomic ranges were used to place conservative boundaries on the Cf-3 and Wa-1 faunal zones (Fig. 7). We place the lower boundary of Wa-0 at 1510 m, and tentatively place the top of Wa-0 at 1534 m. Unshaded intervals in Figure 7 represent intervals of uncertainty within which the boundaries between the three well-established faunal zones must lie. The transition from latest Paleocene (Cf-3) to earliest Eocene (Wa-0) occurs within the stratigraphic interval marked by the initial, dramatic decline in the $\delta^{13}\text{C}$ values of paleosol

carbonates. The window of uncertainty for this faunal transition, based on the age model described below, is approximately 25 k.y. Though less well constrained, the transition between the Wa-0 and Wa-1 faunal zones appears to be correlated with the exponential rebound in carbon isotope values. The window of uncertainty for the Wa-0 to Wa-1 transition here is about 50–60 k.y. The strength of the correlations between bio- and chemostratigraphic events as they stand at present is fortunate because this will allow comparison of the relative timings of biotic transitions worldwide (e.g., Bowen et al., 2000). It is of course possible, with further work, to make the correlations on Polecat Bench even more precise.

Age Model

The age model for the Polecat Bench–Sand Coulee master section is discussed in Gingerich (2000) and Wing et al. (2000). Briefly, the bottom of magnetochron 24R, dated at 55.90 Ma (Cande and Kent, 1995), lies at the 1070 m level in the Polecat Bench composite section (Butler et al., 1981; Gingerich, this volume: fig. 3). The top of chron 24R is higher stratigraphically than we have been able to obtain reliable magnetic polarities in this section. However, the highest locality in the section, SC-295, yields *Bunophorus* representing the base of biozone Wa-5. We derived an age estimate of 53.436 Ma for the base of Wa-5 in the nearby Foster Gulch–McCullough Peaks section (Clyde et al., 1994). Interpolation between the bottom of chron 24R and the base of zone Wa-5 yields an age for the base of the Wa-0 interval (1510 m) of 54.973 Ma, an age for the top of the Wa-0 interval (1533 m) of 54.925 Ma, and a duration for the Wa-0 interval of 0.048 m.y. or 48 k.y. Our estimates for the beginning and end of the carbon isotope excursion are 54.994 Ma and 54.925 Ma, respectively, and our inferred duration for the excursion event is 84 k.y.

Alternatively, the Paleocene-Eocene carbon isotope record on Polecat Bench can be correlated with the marine bulk carbonate records from ODP site 690 (Bains et al., 1999), for which an age model has been generated using astronomical calibration (Röhl et al., 2000). The correlation of marine and terrestrial records is described in detail in Bains et al. (submitted). Here we note that the core of the $\delta^{13}\text{C}$ excursion at site 690 (from the initial drop to the level where values begin to rebound) includes four complete precessional cycles, indicating a duration of ca. 84 k.y., identical to the duration estimated here by a completely independent method.

The $\delta^{18}\text{O}$ Record on Polecat Bench

The oxygen isotope record from the Polecat Bench section is also shown in Figure 7. Trends are apparent in the time series, especially when the record is displayed as a running average, but the magnitude of these fluctuations is similar to the scatter in the data. Mean $\delta^{18}\text{O}$ values are ca. -9.3‰ at the base of the section and increase by ca. 1‰ during the early stages of the carbon isotope excursion. Values rebound to ca. -9.3‰ by

the 1540 m level and remain nearly constant or increase slightly to the top of the section. Individual measurements were separated into excursion and non-excursion groups on the basis of their $\delta^{13}\text{C}$ values (excursion samples having $\delta^{13}\text{C} < -12\text{‰}$, non-excursion samples having $\delta^{13}\text{C} > -10\text{‰}$). Mean $\delta^{18}\text{O}$ values for these two groups are -8.5‰ ($n = 210$) and -8.9‰ ($n = 94$), respectively, and results of a two-sample Student's *t*-test indicate that these means are significantly different at a 95% confidence level ($p < 0.0001$).

Temporal variation in the oxygen isotopic composition of Polecat Bench paleosol carbonates may reflect changes in local mean annual temperature (after Dansgaard, 1964), precipitation/evaporation ratios (e.g., Quade et al., 1989), or large-scale atmospheric circulation patterns (e.g., Amundson et al., 1996). At this time it is not possible to constrain the potential contribution of the last of these factors to the patterns in the Polecat Bench record. First order considerations suggest that significant earth surface warming during the P-E boundary interval could have induced more intense hydrological circulation, producing generally "wetter" conditions in some places on land. The resulting increase in precipitation/evaporation ratios should lead to a decrease in the $\delta^{18}\text{O}$ value of paleosol carbonate, the opposite of the trend observed in the Polecat Bench record. Assuming that the source and transport of water vapor falling over the Bighorn Basin did not change significantly during the interval marked by the carbon isotope excursion, and that the modern, spatial relationship between precipitation $\delta^{18}\text{O}$ values and mean annual temperature is applicable to temporal changes in $\delta^{18}\text{O}$ values during the P-E boundary interval, we can apply the relationship of Dansgaard (1964) to estimate temperature change in the Bighorn Basin during this interval [it is worth noting that the Dansgaard relationship is based on temperate and polar climates for the most part—the curve is not well calibrated at high temperatures ($>15^\circ\text{C}$)]. Given these assumptions, the oxygen isotope record of Polecat Bench soil carbonates is consistent with a minimum of ca. 3° warming in local mean annual temperatures during the P-E boundary event.

Comparison of the faunal records to the Polecat Bench oxygen isotope record shows that the faunal zone boundaries are broadly correlative with the climatic changes reflected in the isotopic record. The Cf-3/Wa-0 boundary occurs within an interval marked by probable surface temperature warming, as indicated by increasing paleosol carbonate $\delta^{18}\text{O}$ values (Fig. 7). Previous work suggested that the first appearance of higher-order mammalian groups at the base of the Wasatchian NALMA was the result of migration across high-latitude land bridges (Gingerich, 1989), facilitated by methane-induced warming of high-latitude surface temperatures (e.g., Peters and Sloan, 2000). Our results provide strong support for such a mechanism by demonstrating the close correlation between carbon cycle, climatic, and biotic events. The transition from Wa-0 to Wa-1 faunas involved increases in species' body size (Gingerich, 1989; Clyde and Gingerich, 1998). Our record shows that this transition may also have been climate-related, as the boundary

between Wa-0 and Wa-1 faunal zones lies within or shortly following the decrease in oxygen isotope values from higher excursion values. This may indicate a cooling of local surface temperatures that favored larger body size in the derived Wa-1 species.

CONCLUSIONS

A new highly refined paleosol carbonate isotope stratigraphy across the Paleocene-Eocene boundary interval on Polecat Bench provides a detailed proxy record for the carbon isotopic composition of atmospheric CO₂. Tests of soil thickness and diagenesis were used to evaluate the reliability of the composite stratigraphy presented in Figure 7. The paleosol nodule record suggests that the δ¹³C of atmospheric CO₂ dropped by 8‰ during this interval, and then rebounded in two steps. Details of this record may prove useful in future work addressing the causes of and response to carbon cycle perturbation at the P-E boundary, but significant questions remain regarding the partitioning of time within the Polecat Bench section and the relationship between the magnitude of the δ¹³C shift of atmospheric CO₂ and that recorded in paleosol carbonates. Changes in the δ¹⁸O of paleosol carbonates are consistent with a significant increase in local mean annual temperature during the P-E boundary event. Comparison of the timing of carbon cycle and mammalian faunal events near the P-E boundary shows that faunal transitions are coincident with major features of the carbon isotope record to within ± 10-30 k.y. Comparison of oxygen isotope and mammalian taxonomic data suggests that the diminutive forms associated with the Wa-0 faunal zone dominated an interval of increased warmth during the P-E boundary event. These species were replaced by larger taxa following the return of temperatures to near pre-boundary levels.

LITERATURE CITED

- AMUNDSON, R. G., O. A. CHADWICK, C. KENDALL, Y. WANG, and M. J. DENIRO. 1996. Isotopic evidence for shifts in atmospheric circulation patterns during the late Quaternary in mid-North America. *Geology*, 24: 23-26.
- ARENS, N. C., A. H. JAHREN, and R. AMUNDSON. 2000. Can C3 plants faithfully record the carbon isotopic composition of atmospheric carbon dioxide? *Paleobiology*, 26: 137-164.
- BAINS, S., R. M. CORFIELD, and R. D. NORRIS. 1999. Mechanisms of climate warming at the end of the Paleocene. *Science*, 285: 724-727.
- BAO, H., P. L. KOCH, and R. P. HEPPLER. 1998. Hematite and calcite coatings on fossil vertebrates. *Journal of Sedimentary Research*, 68: 727-738.
- BEERLING, D. J. 2000. Increased terrestrial carbon storage across the Palaeocene-Eocene boundary. *Palaeogeography, Palaeoclimatology, Palaeoecology*, 161: 395-405.
- BEERLING, D. J. and D. W. JOLLEY. 1998. Fossil plants record an atmospheric ¹²C₂ and temperature spike across the Palaeocene-Eocene transition in NW Europe. *Journal of the Geological Society of London*, 155: 591-594.
- BOCHERENS, H., E. M. FRIIS, A. MARIOTTI, and K. R. PEDERSEN. 1993. Carbon isotopic abundances in Mesozoic and Cenozoic fossil plants; palaeoecological implications. *Lethaia*, 26: 347-358.
- BOWEN, G. J., P. L. KOCH, W. C. CLYDE, S. TING, Y. WANG, Y. WANG, and M. C. MCKENNA. 2000. East of Eden?: temporal constraints on the appearance of 'modern' mammalian orders in Asia. *Geological Society of America, Abstracts with Programs*, 32: 498.
- BOWN, T. M. and M. J. KRAUS. 1981. Lower Eocene alluvial Paleosols (Willwood Formation, northwest Wyoming, U.S.A.) and their significance for paleoecology, paleoclimatology, and basin analysis. *Palaeogeography, Palaeoclimatology, Palaeoecology*, 34: 1-30.
- BOWN, T. M. and M. J. KRAUS. 1987. Integration of channel and floodplain suites. I. Developmental sequence and lateral relations of alluvial Paleosols. *Journal of Sedimentary Petrology*, 57: 587-601.
- BOYLE, E. A. 1997. Cool tropical temperatures shift the global d¹⁸O-T relationship: an explanation for the ice core d¹⁸O-borehole thermometry conflict? *Geophysical Research Letters*, 24: 273-276.
- BUTLER, R. F., P. D. GINGERICH, and E. H. LINDSAY. 1981. Magnetic polarity stratigraphy and biostratigraphy of Paleocene and lower Eocene continental deposits, Clarks Fork Basin, Wyoming. *Journal of Geology*, 89: 299-316.
- CANDE, S. C. and D. V. KENT. 1995. Revised calibration of the geomagnetic polarity timescale for the Late Cretaceous and Cenozoic. *Journal of Geophysical Research*, 100: 6093-6095.
- CERLING, T. E. 1984. The stable isotopic composition of modern soil carbonate and its relationship to climate. *Earth and Planetary Science Letters*.
- CERLING, T. E., D. K. SOLOMON, J. QUADE, and J. R. BOWMAN. 1991. On the isotopic composition of carbon in soil carbon dioxide. *Geochimica et Cosmochimica Acta*, 55: 3403-3405.
- CLYDE, W. C. and P. D. GINGERICH. 1998. Mammalian community response to the latest Paleocene thermal maximum: an isotaphonomic study in the northern Bighorn Basin, Wyoming. *Geology*, 26: 1011-1014.
- CLYDE, W. C., J. STAMATAKOS, and P. D. GINGERICH. 1994. Chronology of the Wasatchian land-mammal age (early Eocene) magnetostratigraphic results from the McCullough Peaks section, northern Bighorn Basin, Wyoming. *Journal of Geology*, 102: 367-377.
- COJAN, I., M. G. MOREAU, and L. D. STOTT. 2000. Stable carbon isotope stratigraphy of the Paleogene pedogenic series of southern France as a basis for continental-marine correlation. *Geology*, 28: 259-262.
- DANSGAARD, W. 1964. Stable isotopes in precipitation. *Tellus*, 16: 436-468.
- DICKENS, G. R., M. M. CASTILLO, and J. C. G. WALKER. 1997. A blast of gas in the latest Paleocene; simulating first-order

- effects of massive dissociation of oceanic methane hydrate. *Geology*, 25: 259-262.
- FRICKE, H. C., W. C. CLYDE, J. R. O'NEIL, and P. D. GINGERICH. 1998. Evidence for rapid climate change in North America during the latest Paleocene thermal maximum: oxygen isotope compositions of biogenic phosphate from the Bighorn Basin (Wyoming). *Earth and Planetary Science Letters*, 160: 193-208.
- FRICKE, H. C., and J. R. O'NEIL. 1999. The correlation between $^{18}\text{O}/^{16}\text{O}$ ratios of meteoric water and surface temperature: its use in investigating terrestrial climate change over geologic time. *Earth and Planetary Science Letters*, 170: 181-196.
- FRIEDMAN, I., and J. R. O'NEIL. 1977. Data of geochemistry: compilation of stable isotope fractionation factors of geochemical interest. U.S. Geological Survey Professional Paper, 440KK: 1-12.
- GINGERICH, P. D. 1983. Paleocene-Eocene faunal zones and a preliminary analysis of Laramide structure deformation in the Clarks Fork Basin, Wyoming. *Wyoming Geological Association Guide Book*, 34: 185-195.
- GINGERICH, P. D. 1989. New earliest Wasatchian mammalian fauna from the Eocene of Northwestern Wyoming: Composition and diversity in a rarely sampled high-flood plain assemblage. *University of Michigan Papers on Paleontology*, 28: 1-97.
- GINGERICH, P. D. 2000. Paleocene-Eocene boundary and continental vertebrate faunas of Europe and North America. In B. Schmitz, B. Sundquist, and F. P. Andreasson (eds.), *Early Paleogene Warm Climates and Biosphere Dynamics*, GFF [Geologiska Föreningens Förhandlingar], Geological Society of Sweden, Uppsala, 122: 57-59.
- KATZ, M. E., D. K. PAK, G. R. DICKENS, and K. G. MILLER. 1999. The source and fate of massive carbon input during the latest Paleocene thermal maximum. *Science*, 286: 1531-1533.
- KENNETT, J. P. and L. D. STOTT. 1991. Abrupt deep-sea warming, palaeoceanographic changes and benthic extinctions at the end of the Palaeocene. *Nature*, 353: 225-229.
- KOCH, P. L., J. C. ZACHOS, and D. L. DETTMAN. 1995. Stable isotope stratigraphy and paleoclimatology of the Paleogene Bighorn Basin (Wyoming, USA). *Palaeogeography, Palaeoclimatology, Palaeoecology*, 115: 61-89.
- KOCH, P. L., J. C. ZACHOS, and P. D. GINGERICH. 1992. Correlation between isotope records in marine and continental carbon reservoirs near the Palaeocene-Eocene boundary. *Nature*, 358: 319-322.
- KRAUS, M. J. 1987. Integration of channel and floodplain suites. II. Vertical relations of alluvial Paleosols. *Journal of Sedimentary Petrology*, 57: 602-612.
- NORRIS, R. D. and U. RÖHL. 1999. Carbon cycling and chronology of climate warming during the Paleocene-Eocene transition. *Nature*, 401: 775-778.
- PETERS, R. B. and SLOAN, L.C. 2000. High concentrations of greenhouse gases and polar stratospheric clouds: a possible solution to high-latitude faunal migration at the latest Paleocene thermal maximum. *Geology*, 28: 979-982.
- QUADE, J., T. E. CERLING, and J. R. BOWMAN. 1989. Systematic variations in the carbon and oxygen isotopic composition of pedogenic carbonate along elevation transects in the southern Great Basin, United States. *Geological Society of America Bulletin*, 101: 464-475.
- RÖHL, U., T. J. BRALOWER, R. D. NORRIS, and G. WEFER. 2000. New chronology for the late Paleocene thermal maximum and its environmental implications. *Geology*, 28: 927-930.
- ROSE, K. D. 1981. The Clarkforkian land-mammal age and mammalian faunal composition across the Paleocene-Eocene boundary. *University of Michigan Papers on Paleontology*, 26: 1-197.
- THOMAS, E. 1991. The latest Paleocene mass extinction of deep sea benthic foraminifera: result of global climate change. *Geological Society of America Abstracts with Programs*, 23: A141.
- WING, S. L., H. BAO, and P. L. KOCH. 2000. An early Eocene cool period? Evidence for continental cooling during the warmest part of the Cenozoic. In: B. T. Huber, K. G. Macleod, and S. L. Wing (eds.), *Warm Climates in Earth History*. Cambridge University Press, Cambridge, UK, pp. 197-237.
- ZACHOS, J. C., K. C. LOHMANN, J. C. G. WALKER, and S. W. WISE. 1993. Abrupt climate changes and transient climates during the Paleogene: a marine perspective. *Journal of Geology*, 101: 191-213.

POLLEN ASSEMBLAGES AND PALEOCENE-EOCENE STRATIGRAPHY IN THE BIGHORN AND CLARKS FORK BASINS

GUY J. HARRINGTON

Department of Geology, National University of Ireland Cork, Cork, Ireland

Abstract.— Research on pollen and spore floras is limited in extent in the Bighorn and Clarks Fork basins. This is not due to unsuitable lithology, because there are many favorable environments for palynomorph preservation: these represent swamps and channel fills in both the upper Paleocene and lower Eocene. Pollen samples taken from mammalian fossil localities allow correlation of established pollen zones with land mammal ages. Data from the Bighorn Basin demonstrate that the boundary between pollen zones P6 and E is approximately at the Clarkforkian-Wasatchian North American land-mammal age (NALMA) boundary, which corresponds closely to the Paleocene-Eocene boundary. This is marked by changes in the abundances of long-ranging palynomorph taxa: *Caryapollenites* spp. and *Momipites* spp. are relatively less abundant in the Wasatchian, but *Alnipollenites*, *Eucommia*, *Sparganiaceapollenites*, and *Ulmipollenites* all become more abundant. *Platycarya* spp., *Intratropipollenites instructus* and *Punctatisporites* sp. are the only first-occurrences in the early Wasatchian. The early Eocene is notably more diverse than the late Paleocene, which, together with an increase in monocots and ferns, may indicate greater landscape openness in the Eocene.

INTRODUCTION

Pollen and spores are preserved in a wide range of sedimentary facies and can act as an excellent proxy for assessing past vegetation change. Palynomorph samples can also be taken at higher stratigraphic resolution than many other fossil groups, but in contrast to the megafloral (e.g., Wing, 1998), cold-blooded animal (e.g., Hutchison, 1998) and especially mammalian fossil records (e.g., Gingerich et al., 1980; Rose, 1981; Gingerich, 1989; Clyde and Gingerich, 1998), research into palynofloras from the late Paleocene to early Eocene has lagged well behind in the Bighorn Basin. Most pollen studies from Western Interior basins have stressed the stratigraphic potential of pollen and spores, which is the case

especially in the Powder River and Wind River Basins (Leffingwell, 1971; Spindel, 1975; Tschudy, 1976; Nichols and Ott, 1978; Pocknall 1986, 1987a, 1987b). In contrast, studies from the Bighorn Basin have tended to explore microfloral composition (e.g., Wilson and Webster, 1946), either as a result of taphonomic control (Farley, 1989, 1990; Farley and Traverse, 1990) or climate change (Wing, 1984a; Wing and Harrington, 2001).

A characteristic common to most pollen studies in the Western Interior basins is that results are generally poorly integrated with other fossil records. This is partly a function of lithological control, because lithologies that are conducive for pollen preservation are usually not those that preserve vertebrate remains. In addition, lithologies that yield the best preserved plant megafossils are usually too coarse-grained for successful sporomorph retrieval. However, good pollen-bearing strata are usually associated with carbonaceous, organic rich sediments that also yield satisfactory plant megafossils. A recent attempt to address the issue of

In: Paleocene-Eocene Stratigraphy and Biotic Change in the Bighorn and Clarks Fork Basins, Wyoming (P. D. Gingerich, ed.), University of Michigan Papers on Paleontology, 33: 89-96 (2001).

plant-pollen integration from the Bighorn Basin has provided, as expected, the most coherent record of floral change across the Paleocene-Eocene boundary from any known locality (Wing and Harrington, 2001).

In terms of the pollen record alone, there is still much to learn on three fronts that will potentially impact our understanding of early Paleogene plant communities: (1) compositional changes of the palynoflora in individual basins over time; (2) relationship of pollen floras to different depositional environments that characterize each basin; and, especially, (3) compositional differences between basins at a regional scale, and the importance that any such differences may have for assessing the geographic extent of vegetation types on various spatial scales.

The purpose of this contribution is to provide an overview of depositional settings in the Bighorn Basin where spores and pollen are commonly preserved, and of sporomorph stratigraphy in the late Paleocene to early Eocene. I use the Clarkforkian-Wasatchian NALMA boundary as an approximation of the Paleocene-Eocene boundary because this correlates with a negative carbon isotope excursion that is recognized globally and defined stratigraphically in the Bighorn Basin (Koch et al. 1992, 1995). A working group of the International Geological Correlation Program (IGCP project 308) recommended in 1998 that the Paleocene-Eocene boundary fall at the base of the carbon isotope excursion event. This isotope excursion is still under consideration as a global marker for the Paleocene-Eocene boundary.

DATA

The data below come from 87 samples collected in July 1997 from four main areas in the Bighorn and Clarks Fork basins: 12 samples from North Butte (T 45 N, R 89 W), 58 samples from the Antelope/Elk Creek section (AC/EC), 11 samples from the Contact Road section located next to the Otto-Basin highway (NE3, Section 18, T 51 N, R 93 W), and 6 samples from the Clarks Fork Basin (Saddle Mountain and Big Sand Coulee divide). The palynoflora of the late Paleocene to early Eocene yields 93 pollen and spore morphotypes, and is consistent with a warm-temperate to subtropical vegetation type. The first ca. 2 m.y. of the Eocene have 89 pollen and spore morphotypes, in contrast to the last 1.5 m.y. of the Paleocene that has 73 morphotypes. Data are lacking from the carbon isotope excursion interval because all these samples proved barren of palynomorphs.

DEPOSITIONAL ENVIRONMENTS

There are a number of different sedimentary facies in the Fort Union and Willwood formations of the Bighorn Basin (Bown, 1980; Kraus, 1996, 1997; Davies-Vollum and Wing, 1998), but only certain organic rich lithologies preserve palynomorphs. Pollen and spores are found in the drab mudstone facies described by Farley (1989, 1990), the

carbonaceous shale type II facies described by Wing (1984b), and the clay subunit underlying carbonaceous shales (Farley, 1990). Reduced floodplain environments are represented by drab mudstones, and wet, sub-swamp soils are represented by the clay subunit. Type II carbonaceous shales represent tabular backswamps that developed on stable floodplains (Wing, 1984b; Farley, 1990; Davies-Vollum and Wing, 1998). In addition, pollen and spores are found in channel fills and ponds that are representative of Wing's (1984b) type I carbonaceous shale facies. There are subtle differences in the characteristics of these environments that are expressed in the absolute abundance of palynomorphs preserved in each environment, and in terms of preservational quality (Table 1): of the 87 samples processed for pollen, only 60 samples yielded pollen and spores in significant quantities (>200 specimens). The sub-swamp soil has the worst sporomorph preservation potential, and the channel fills have the best preservation potential. Differences in preservation potential are related to variation in the level of the water table (Harrington, 1999), which affects the degree of oxidation of organic matter.

Palynological research focusing on the relationship of pollen floras to depositional environments shows that all environments preserve different compositions of pollen and spores (Farley, 1989, 1990; Farley and Traverse, 1990). However, Wing and Harrington (2001) show that this effect is not strong for pollen floras deposited in swamps (sub-swamp soil, backswamp, and reduced floodplain environments). Differences in preservation and representation of sporomorph abundance do not appear to affect the representation of pollen and spores in any depositional environment, with the exception of channel fills. These pond assemblages potentially have greater proportions of pollen transported long-distances than swamps, which tend to have a more local, autochthonous pollen spectrum (Farley, 1989, 1990).

In general, late Paleocene swamps have greater abundances of tree pollen of *Caryapollenites veripites* (Juglandaceae), *Cupressacites hiatipites* (Taxodiaceae), *Polyatriopollenites vermontensis* (Juglandaceae), and *Ulmipollenites* spp. (Ulmaceae) than late Paleocene ponds. Pond samples tend to have greater within-sample diversity (by ca. 16%), and a greater abundance of Betulaceae/Myricaceae pollen than do swamp deposits in both the late Paleocene and the early Eocene. The major distinction between swamps and ponds is the greater abundance of fern spores, Sparganiaceae, Platanaceae/Salicaceae (e.g., *Tricolpites hians*), and aroid pollen (e.g., *Pandaniidites typicus*) in ponds, as well as reduced quantities of Juglandaceae pollen both in the late Paleocene and early Eocene. However, taxa that have biostratigraphic value are present usually in all lithologies in similar quantities; the pollen of *Platycarya* spp. (Juglandaceae) is an exception because it is preferentially found in swamp deposits (Wing, 1984a; Farley, 1989, 1990). No single taxon is restricted to one environment, and some taxa, such as *Alnipollenites* (Betulaceae), can be numerically significant in ponds (Harrington, 1999) even though generally they are associated more strongly with swamps

TABLE 1 — Environmental characteristics based on sporomorph concentrations for all samples from the Bighorn and Clarks Fork basins. One lignite sample is not presented here because it lacks pollen concentration data. Pollen concentrations are calculated by addition of exotic spores to sample residues of known weight in the initial stages of processing. Abbreviations: Cf, Clarkforkian; Wa, Wasatchian.

Environment	Cf samples	Wa samples	Mean concentration (per gram)	Standard deviation (SD) concentration (per gram)	Percent difference SD : mean	Percent barren samples
Sub-swamp soil	3	3	13,305	26,279	49%	67%
Tabular swamp	11	14	67,866	111,633	39%	22%
Reduced floodplain	11	1	28,285	37,862	25%	15%
Channel fill	5	11	6,144	4,221	31%	0%

(Farley, 1990). Hence, the distinction between environments, and especially the various swamp soils, is not defined clearly (see Figure 3 in Wing and Harrington, 2001).

There are two lithologies that are notably barren of pollen and spores. First, soil profiles characterizing the Willwood Formation, which typify the Clarks Fork Basin, are barren of palynomorphs, although red, green/gray, and gray colored paleosols do contain variable quantities of black, amorphous organic matter. Paleosols in the Willwood Formation are oxidized intensely and contain no recognizable organic matter such as plant cuticle or fragmented palynomorphs. Second, the Wa-0 red bed sequence, that probably marks the position of the negative carbon isotope excursion in the central/southern Bighorn Basin (Wing, 1998; Wing et al., 2000), is similarly barren of palynomorphs. The only organic residue in red bed samples from the Otto-Basin road section is black, highly fragmented, and lacking structure.

STRATIGRAPHIC CHANGES IN POLLEN ASSEMBLAGES

The pollen stratigraphy of the late Paleocene to early Eocene in the Western Interior is unrefined in comparison to that of other fossil groups. Common to all published zonation schemes is the reliance on Juglandaceae pollen as stratigraphic markers and, to a lesser extent, on their characterization by changes in abundance of long-ranging taxa such as *Alnipollenites*, *Caryapollenites*, *Momipites*, and *Ulmipollenites* (Leffingwell, 1971; Tschudy, 1976; Nichols and Ott, 1978; Pocknall 1987a).

The most accepted pollen biozonation for the Bighorn Basin is that of Nichols and Ott (1978) because this scheme has been used for subdividing strata in the Bighorn Basin, Wind River Basin (where this model was established initially), as well as Powder River and Hanna Basins (Nichols, 1994, 1998). The entire Paleocene is divided into six zones by Nichols and Ott (1978), and the early Eocene is placed in a single pollen biozone. Two drawbacks with this scheme are: (1) this zonation

is based substantially on the assumed evolutionary changes in the Juglandaceae lineage; species within Juglandaceae form-genera *Caryapollenites* and *Momipites* can be difficult to recognize consistently because the morphological features that define a given species overlap greatly between other species constituent to both form-genera; and (2) pollen zones are correlated poorly with land mammal ages (Nichols, pers. comm., 1998). So far, there is one Tiffanian NALMA tie-point in the northern Powder River Basin between a mammalian fauna (Robinson and Honey, 1987) and zone P5 of Nichols and Ott (1978) (Pocknall and Nichols, 1996). There is also one tie point in the more southerly Great Divide Basin that again correlates at least the middle Tiffanian (Ti-2 - Ti-4) with Nichols and Ott's (1978) zone P5 (Gemmill and Johnson, 1997; Nichols pers. comm., 1998).

To improve the correlation between mammals and pollen, some samples from the Bighorn Basin have been taken at, or stratigraphically close to, known mammalian fossil localities (Table 2). Based on this information (Table 2), the Clarkforkian in the Bighorn Basin is totally contained within at least part of zone P6 of Nichols and Ott (1978). The pollen assemblages in the lower part of the Bighorn Basin pollen record (Fig. 1) are highly similar compositionally to those in the late Clarkforkian. Thus, P6 Zone probably extends down into at least the late Tiffanian. Unfortunately, there are no mammalian fossils to test whether these assemblages from the lower AC/EC section are Tiffanian except through stratigraphic extrapolation based on sediment accumulation rates in the central part of the Bighorn Basin (model 2 of Wing et al., 2000). Clearly, late Paleocene P5 and P6 biozones are long-ranging (>1.5 m.y.) in comparison to mammalian biozones, and there is presently little prospect of further subdividing zones P5 and P6 into robust pollen subzones.

The only pollen zone that is determined more by immigration than pollen morphology or species abundance changes is zone E of Nichols and Ott (1978). Based on data presented here (Table 2), the boundary between zones P6 and E appears

TABLE 2 — Correlation between pollen biozones of Nichols and Ott (1978) and mammalian stages in the Bighorn and Clarks Fork basins. Stratigraphic positions of samples are shown in Figure 2 of Wing and Harrington (2001). Abbreviations: *Cf*, Clarkforkian; *Wa*, Wasatchian; *AC/EC*, Antelope Creek/Elk Creek section; *BHB*, Bighorn Basin; *CFB*, Clarks Fork Basin; *NB*, North Butte.

Pollen sample(s)	Pollen zone	Location	NALMA	Comment
GH97-1.39	Zone E	BHB, AC/EC	Wa (Graybullian)	Sample lies at 58 m on the AC/EC section, 8 m above locality YPM-95 of Schankler (1980)
GH97-1.41	Zone E	BHB, AC/EC	Wa (Graybullian)	89 m on the AC/EC section, 9 m above locality YPM-200 of Schankler (1980)
PS02bsc, PS03bsc, PS05bsc	Zone E	CFB, Big Sand Coulee	Wa (Sandcouleean)	Samples lie 40 m above the large sand body that represents the Cf/Wa boundary (Gingerich et al., 1980)
PS946 and PS945	Zone P6	BHB, NB	Cf	Samples located 13 m and 20 m below localities with Wa-0 faunas and the distinctive red bed sequence
PS02sm and PS04sm	Zone P6	CFB, Saddle Mountain	Cf (Cf-3)	Samples located at 62 m below the large sand body that represents the Cf/Wa boundary (Gingerich et al., 1980); University of Michigan mammal localities SC-24 and SC-25 are more than 60 m below the sand body (Rose, 1981).
SC-216	Zone P6	CFB	Cf. (Cf-1)	1080 m level, University of Michigan locality SC-216 (Rose, 1981)

to correlate approximately with the Clarkforkian-Wasatchian NALMA boundary, forming the only distinct pollen event in the late Paleocene to early Eocene. This event is recognized primarily by the introduction of *Platycarya* spp., and *Tilia* type pollen (*Intratropipollenites instructus*) into the Western Interior. There is also a significant decline in the abundance of both *Caryapollenites* spp. and *Momipites* spp. commensurate with an increase in *Alnipollenites* spp., *Eucommia* sp., *Pandaniidites typicus*, *Sparganiaceapollenites* sp., and *Ulmipollenites* spp. (Figs. 1 and 2; Table 3). These changes are recognized in the Wind River (Nichols and Ott, 1978), Bighorn (Harrington, 2000; Wing and Harrington, 2001), and Powder River basins (Tschudy, 1976; Pocknall, 1987a). The top of zone E has not been defined, and there are no palynofloral immigration or turnover events between the Clarkforkian-Wasatchian boundary and the initiation of the later early Eocene thermal maximum, some 2 m.y. after the base of zone E. Hence, zone E, like pollen zone P6, spans at least 1.75 to 2 m.y.

COMPOSITION AND DIVERSITY CHANGES

Changes at the Clarkforkian-Wasatchian boundary are subtly expressed, but represent a modification in palynofloral com-

position. This can best be illustrated by detrended correspondence analysis [DCA] (Fig. 1). The prime influence on DCA sample scores is unrelated to extinction, which is minimal; there are probably only four last occurrences in the Clarkforkian of numerically insignificant taxa (less than 3 specimens each in the whole Paleocene count of 11,653 pollen and spores). However, the regional extinction of *Cingulatisporites*, *Ericipites*, *Platycaryapollenites* sp. B, and *Porocolpopollenites* sp. cannot be linked directly to the Paleocene-Eocene boundary events (Wing and Harrington, 2001). Pocknall (1987a) documents the last occurrences of both *Aquilapollenites spinulosus* and *Insulapollenites rugulatus* in the late Paleocene, but in the Bighorn Basin both these species are present in swamp deposits in the early Wasatchian. Therefore, 94% of taxa found in the Paleocene are also found in the Eocene.

First occurrences are also low across the Clarkforkian-Wasatchian boundary, and numerically significant taxa are represented only by *Intratropipollenites instructus* (4.09% of the Eocene count), the shrub/small tree *Platycarya* (0.27%), and the fern *Punctatisporites* (0.42%). Other potential immigrants into the Bighorn Basin include *Aesculiidites circumstriatus* and *Ilexpollenites*, but these are each represented by two specimens so there is great uncertainty establishing their

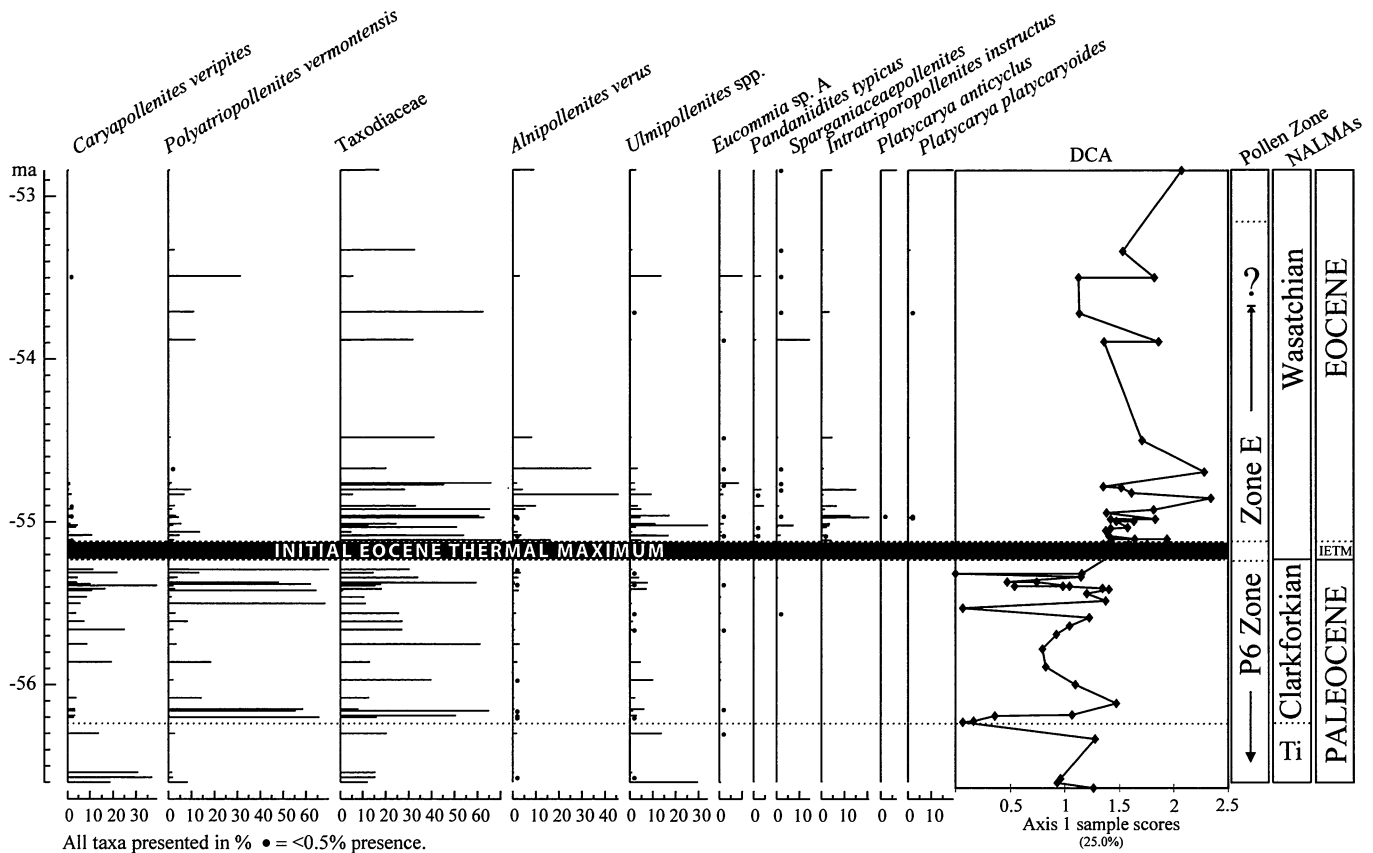


FIGURE 1 — Summary pollen diagram of taxa with numerical or stratigraphic significance plotted against time. The time-scale is that of Wing et al. (2000), and the pollen zones are those of Nichols and Ott (1978). Detrended correspondence analysis [DCA] was undertaken on percentage data, and rare taxa (those present in <20% of samples) were downweighted during ordination. *Platyacarya* is first found 38 m above the red bed sequence in the AC/EC section.

first occurrence. The changed relative abundance of pollen and spore morphotypes is the major factor that therefore controls the shift in distribution of DCA sample scores across the Paleocene-Eocene boundary (Figs. 1 and 2; Table 3). This is expressed in the ranked twenty most-abundant taxonomic groups (Table 3) with 70% of taxa shared by the late Paleocene and early Eocene in these top rankings.

The mean abundance of taxa also changes across the Paleocene-Eocene boundary because in the Paleocene the mean abundance of a taxon is 1.69% of count size, compared to 1.85% for the Eocene. Changes in rank abundance are not associated strongly with changes in the evenness component of diversity as measured by the Shannon-Wiener index because there is no significant change in the evenness of pollen assemblages across the Paleocene-Eocene boundary (Wing and Harrington, 2001). There are within- and among-sample diversity differences in the Eocene, which is more diverse than the Paleocene; there are 22% more species in the Eocene than the Paleocene and, on average, Eocene samples are 17% more diverse (Wing and Harrington, 2001). This is contrary to the earliest Eocene

megafloral record of Wing (1998) and Wing et al. (2000), which shows a long-ranging decline in plant diversity from the middle Clarkforkian through to the middle or late Wasatchian (Lysitean subage).

A plausible explanation for this discrepancy between the pollen and megafloral records could be the presence of greater landscape openness in the earliest Eocene. An established correlation, from modern pollen studies, is the relationship between the diversity of palynofloral assemblages and the size of the pollen source area (e.g., Jacobson and Bradshaw, 1981; Jackson and Lyford, 1999). This can be influenced by the openness of the landscape. Thus, high sample diversity in Holocene pollen records can be equated with greater vegetational disturbance and landscape openness (Birks and Line, 1992). In the context of the Bighorn Basin in the late Paleocene to early Eocene, the difference in vegetation structure that may support an argument for greater landscape openness is that understory taxa, as represented by pteridophyte spores, become relatively more abundant in the Eocene (48% more abundant, $p = 0.008$) (Table 3) together with monocots (increase by 92%, $p = 0.104$)

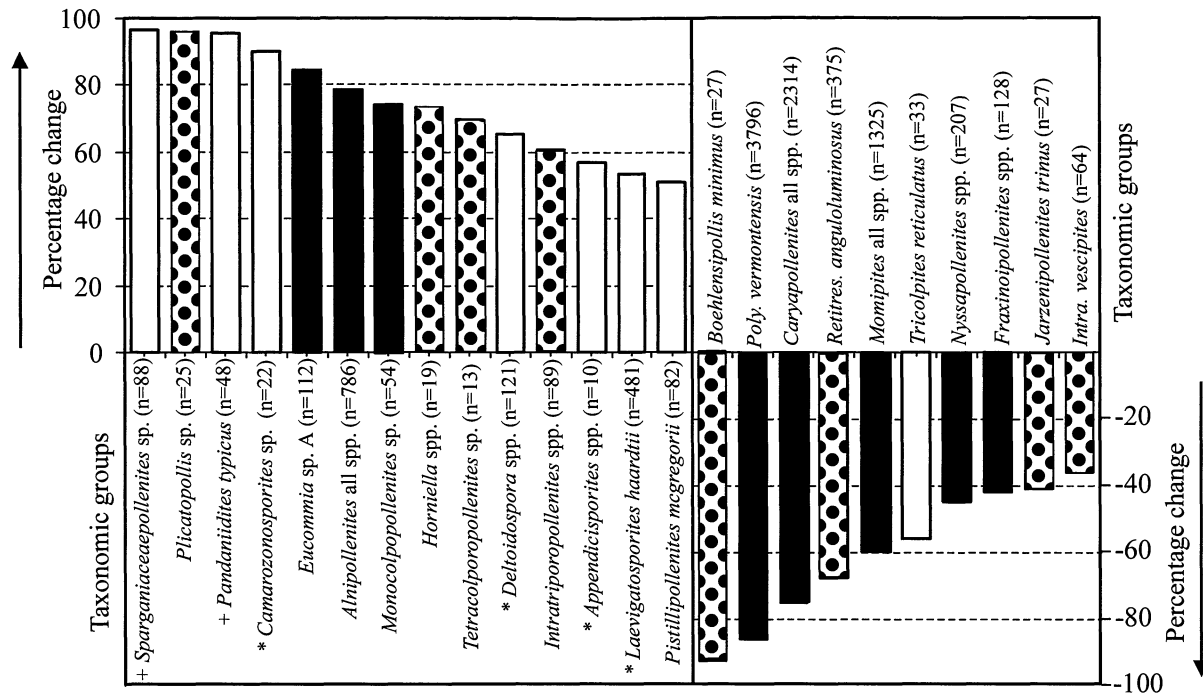


FIGURE 2 — Relative percentage change of numerically significant (≥ 10 specimens) taxonomic groups across the Paleocene-Eocene boundary. The aggregate number of specimens in both epochs is provided in brackets after the taxon name. Symbols: + = monocot pollen, * = pteridophyte spores. Potential habit, based on probable botanical affinity, is indicated by bar shading (this is highly tentative). White, probable understory taxa (e.g., ferns, herbs, shrubs); black, probable overstory taxa (e.g., small trees, canopy trees); black dots, unknown.

that generally have an herbaceous habit (Fig. 2). These changes are noted in all environments, and not just in channel fills. Essentially, plants at the faster end of the growth spectrum, and those growing under the forest canopy, are favored. This may signify that the Eocene vegetation was more successional than the Paleocene, or that there was greater moisture in the early Eocene. There is no evidence currently to support a wetter early Eocene, but there are more channel fill samples in the Wasatchian relative to the Eocene (Table 1), which may account for the apparent increase in ferns. However, ferns and monocots also increased in abundance on the U.S. Gulf Coast (Harrington, 2001), from a different set of depositional environments, so this vegetation dynamic is not unique to the Bighorn Basin.

ACKNOWLEDGEMENTS

I thank Scott Wing for his considerable help in collecting samples from the Bighorn Basin in July 1997 and for providing details on sampling localities. Pollen processing and identification was undertaken under tenure of NERC award GT5/95/281/E at the University of Sheffield, UK. I acknowledge funding from Enterprise Ireland award SC/00/045. I thank an anonymous reviewer for improving the quality of this paper.

LITERATURE CITED

- BIRKS, H. J. B. and J. M. LINE. 1992. The use of rarefaction analysis for estimating palynological richness from Quaternary pollen-analytical data. *The Holocene*, 2: 1-10.
- BOWN, T. M. 1980. Summary of latest Cretaceous and Cenozoic sedimentary, tectonic, and erosional events, Bighorn Basin, Wyoming. In: P. D. Gingerich (ed.), *Early Cenozoic Paleontology and Stratigraphy of the Bighorn Basin, Wyoming*. University of Michigan Papers in Paleontology, 24: 25-32.
- CLYDE, W. C. and P. D. GINGERICH. 1998. Mammalian community response to the latest Paleocene thermal maximum: an isotaphonomic study in the northern Bighorn Basin, Wyoming. *Geology*, 26:1011-1014.
- DAVIES-VOLLUM, K. S. and S. L. WING. 1998. Sedimentological, taphonomic, and climatic aspects of Eocene swamp deposits (Willwood Formation, Bighorn Basin, Wyoming.). *Palaios*, 13: 28-40.
- FARLEY, M. B. 1989. Palynological facies fossils in nonmarine environments in the Paleogene of the Bighorn Basin. *Palaios*, 4: 565-573.
- FARLEY, M. B. 1990. Vegetation distribution across the Early Eocene depositional landscape from palynological analysis. *Palaeogeography, Palaeoclimatology, Palaeoecology*, 79: 11-27.

TABLE 3 — Rank abundance comparison of the twenty most abundant Paleocene and Eocene taxa. Asterisk indicates Pteridophytes. Some taxa in this table have been grouped, for example Betulaceae/Myricaceae includes all species of *Triatriopollenites* and *Tripoporollenites* that have a betulaceous affinity.

PALEOCENE			EOCENE		
Taxonomic group	Specimens	Percent	Taxonomic group	Specimens	Percent
<i>Polyatriopollenites vermontensis</i>	3355	28.89	Taxodiaceae	3084	40.91
Taxodiaceae	2580	22.22	Betulaceae/Myricaceae	705	9.35
<i>Caryapollenites</i> spp. (all)	1852	15.95	<i>Alnipollenites</i> spp. (all)	583	7.73
<i>Momipites</i> spp. (all)	947	8.15	<i>Ulmipollenites</i> spp. (all)	435	5.77
Betulaceae/Myricaceae	725	6.24	<i>Caryapollenites</i> spp. (all)	407	5.39
<i>Ulmipollenites</i> spp. (all)	359	3.09	<i>Momipites</i> spp. all	320	4.24
<i>Retitrescolpites anguloluminosus</i>	286	2.46	<i>Intratripoporollenites instructus</i>	309	4.09
* <i>Laevigatosporites</i>	153	1.31	* <i>Laevigatosporites</i>	265	3.51
<i>I. sp. cf. Tilia tetraforaminipites</i>	150	1.29	<i>Polyatriopollenites vermontensis</i>	230	3.05
Bisaccate group	148	1.27	Bisaccate group	98	1.30
<i>Alnipollenites</i> spp. (all)	139	1.19	* <i>Cyathidites</i>	88	1.16
<i>Nyssapollenites</i> spp.	134	1.15	* <i>Gleicheniidites</i>	88	1.16
* <i>Cyathidites</i>	99	0.85	* <i>Deltoidospora</i>	80	1.06
<i>Tricolpites hians</i>	95	0.81	<i>I. sp. cf. Tilia tetraforaminipites</i>	75	0.99
* <i>Gleicheniidites</i>	92	0.79	<i>Rousea sp.</i>	71	0.94
<i>Fraxinoipollenites</i> spp.	81	0.69	<i>Tricolpites hians</i>	71	0.94
<i>Rousea sp.</i>	57	0.49	<i>Eucommia sp. A</i>	60	0.79
<i>Intratripoporollenites vescipites</i>	39	0.33	<i>Retitrescolpites anguloluminosus</i>	59	0.78
* <i>Deltoidospora</i>	31	0.26	<i>Nyssapollenites</i> spp.	58	0.76
<i>Pistillipollenites mcgregorii</i>	27	0.23	<i>Intratripoporollenites</i> spp.	54	0.71

- FARLEY, M. B. and A. TRAVERSE. 1990. Usefulness of palynomorph concentrations in distinguishing Paleogene depositional environments in Wyoming (U.S.A.). Review of Palaeobotany and Palynology, 64: 325-329.
- GEMMILL, C. E. C. and K. R. JOHNSON. 1997. Paleocology of a late Paleocene (Tiffanian) megafloora from the Northern Great Divide Basin, Wyoming. Palaios, 12: 439-448.
- GINGERICH, P. D. 1989. New earliest Wasatchian mammalian fauna from the Eocene of northwestern Wyoming: Composition and diversity in a rarely sampled high-floodplain assemblage. University of Michigan Papers in Paleontology, 28: 1-97.
- GINGERICH, P. D., K. D. ROSE, and D. W. KRAUSE. 1980. Early Cenozoic Mammalian faunas of the Clark's Fork Basin-Polecat Bench area, northwestern Bighorn Basin. In: P. D. Gingerich (ed.), Early Cenozoic Paleontology and Stratigraphy of the Bighorn Basin, Wyoming. University of Michigan Papers in Paleontology, 24: 51-68.
- HARRINGTON, G. J. 1999. North American palynofloral dynamics in the late Palaeocene to early Eocene. Unpublished Ph. D. thesis, University of Sheffield, pp. 321.
- HARRINGTON, G. J. 2000. Palynofloral dynamics of the late Palaeocene to early Eocene from the Bighorn Basin, northwest Wyoming, USA. In: B. Schmitz, B. Sundquist, and F. P. Andreasson (eds.), Early Paleogene Warm Climates and Biosphere Dynamics. GFF, 122: 67-68.
- HARRINGTON, G. J. 2001. Impact of Paleocene/Eocene greenhouse warming on North American paratropical forests. Palaios, in press.
- HUTCHISON, J. H. 1998. Turtles across the Paleocene/Eocene epoch boundary in west-central North America. In: M.-P. Aubry, S. G. Lucas, and W. A. Berggren (eds.), Late Paleocene-Early Eocene Climatic and Biotic Events in the Marine and Terrestrial Records. University of Columbia Press, New York. p. 401-408.
- JACKSON, S. T. and M. E. LYFORD. 1999. Pollen dispersal models in Quaternary plant ecology: assumptions, parameters, and prescriptions. The Botanical Review, 65: 39-75.
- JACOBSON, G. L. and R. H. W. BRADSHAW. 1981. The selection of sites for paleovegetational studies. Quaternary Research, 16: 80-96.
- KOCH, P. L., J. C. ZACHOS, and P. D. GINGERICH. 1992. Correlation between isotope records in marine and continental carbon reservoirs near the Palaeocene/Eocene boundary. Nature, 358: 319-322.
- KOCH, P. L., J. C. ZACHOS, and D. L. DETTMANN. 1995. Stable isotope stratigraphy and paleoclimatology of the Paleogene Bighorn Basin (Wyoming, U.S.A.). Palaeogeography, Palaeoclimatology, Palaeoecology, 115: 61-89.
- KRAUS, M. J. 1996. Avulsion deposits in lower Eocene alluvial rocks, Bighorn Basin, Wyoming. Journal of Sedimentary Research, 66(2): 354-363.

- KRAUS, M. J. 1997. Lower Eocene alluvial paleosols: Pedogenic development, stratigraphic relationships, and paleosol/landscape associations. *Palaeogeography, Palaeoclimatology, Palaeoecology*, 129: 387-406.
- LEFFINGWELL, H. A. 1971. Palynology of the Lance (Late Cretaceous) and Fort Union (Paleocene) Formations of the type Lance area, Wyoming. *In: R. M. Kosanke, and A. T. Cross (eds.), Symposium on Palynology of the Late Cretaceous and Early Tertiary. Geological Society of America Special Paper*, 127: 1-64.
- NICHOLS, D. J. 1994. Palynostratigraphic correlation of Paleocene rocks in the Wind River, Bighorn, and Powder River Basins, Wyoming. *In: R. M. Flores, K. T. Mehring, R. M. Jones, and T. L. Beck (eds.), Organics and the Rockies Field Guide. Wyoming State Geological Survey Public Information Circular*, 33: 17-29.
- NICHOLS, D. J. 1998. Palynological age determinations of selected outcrop samples from the Lance and Fort Union Formations in the Bighorn Basin, Montana and Wyoming. *In: W. R. Keefer and J. E. Goolsby (eds.), Cretaceous and lower Tertiary Rocks of the Bighorn Basin, Wyoming and Montana. Wyoming Geological Association Guidebook*, 49: 117-129.
- NICHOLS, D. J. and H. L. OTT. 1978. Biostratigraphy and evolution of the Momipites-Caryapollenites lineage in the early Tertiary in the Wind River Basin, Wyoming. *Palynology*, 2: 37-48.
- POCKNALL, D. T. 1986. Palynological data from the Fort Union and Wasatch Formations, Powder River Basin, Wyoming and Montana. *United States Geological Survey Open-File Report*, 86-117: 1-58.
- POCKNALL, D. T. 1987a. Palynomorph biozones for the Fort Union and Wasatch Formations (upper Paleocene-lower Eocene), Powder River Basin, Wyoming and Montana, U.S.A. *Palynology*, 11: 23-35.
- POCKNALL, D. T. 1987b. Paleoenvironments and age of the Wasatch Formation (Eocene), Powder River Basin, Wyoming. *Palaaios*, 2: 368-376.
- POCKNALL, D. T. and D. J. NICHOLS. 1996. Palynology of coal zones of the Tongue River Member (upper Paleocene) of the Fort Union Formation, Powder River Basin, Montana and Wyoming. *American Association of Stratigraphic Palynologists Contributions Series*, 32: 1-58.
- ROBINSON, L. N. and J. G. HONEY 1987. Geologic setting of a new Paleocene mammal locality in the northern Powder River Basin, Montana. *Palaaios*, 2: 87-90.
- ROSE, K. D. 1981. The Clarkforkian land-mammal age and mammalian faunal change across the Paleocene-Eocene boundary. *University of Michigan Papers in Paleontology*, 26: 1-196.
- SCHANKLER, D. M. 1980. Faunal zonation of the Willwood Formation in the central Bighorn Basin, Wyoming. *In: P. D. Gingerich (ed.), Early Cenozoic Paleontology and Stratigraphy of the Bighorn Basin, Wyoming. University of Michigan Papers in Paleontology*, 24: 99-114.
- SPINDEL, S. 1975. Palynological determination of the Paleocene-Eocene boundary between the Tongue River Member and Wasatch Formation, southeastern Montana. *North West Geology*, 4: 38-45.
- TSCHUDY, R. H. 1976. Pollen changes near the Fort Union-Wasatch boundary, Powder River Basin. *Wyoming Geological Society Guidebook, Annual Field Conference*, 28: 73-81.
- WILSON, L. R. and R. M. WEBSTER. 1946. Plant microfossils from the Fort Union coal of Montana. *American Journal of Botany*, 33: 271-278.
- WING, S. L. 1984a. A new basis for recognizing the Paleocene/Eocene boundary in western interior North America. *Science*, 226: 439-441.
- WING, S. L. 1984b. Relation of paleovegetation to geometry and cyclicity of some fluvial carbonaceous deposits. *Journal of Sedimentary Petrology*, 54: 52-66.
- WING, S. L. 1998. Late Paleocene-Early Eocene floral and climatic change in the Bighorn Basin, Wyoming. *In: M.-P. Aubry, S. G. Lucas, and W. A. Berggren (eds.), Late Paleocene-Early Eocene Climatic and Biotic Events in the Marine and Terrestrial Records. University of Columbia Press, New York. p. 380-400.*
- WING, S. L. and G. J. HARRINGTON. 2001. Floral response to rapid warming at the Paleocene/Eocene boundary and implications for concurrent faunal change. *Paleobiology*, in press.
- WING, S. L., H. BAO, and P. L. KOCH. 2000. An early Eocene cool period? Evidence for continental cooling during the warmest part of the Cenozoic. *In: B.T. Huber, K. G. MacCleod, and S. L. Wing (eds.), Warm Climates in Earth History. Cambridge University Press, Cambridge, pp. 197-237.*

TURTLE DIVERSITY AND ABUNDANCE THROUGH THE LOWER EOCENE WILLWOOD FORMATION OF THE SOUTHERN BIGHORN BASIN

PATRICIA A. HOLROYD¹, J. HOWARD HUTCHISON¹, AND SUZANNE G. STRAIT²

¹*Museum of Paleontology, University of California, Berkeley, California 94720*

²*Department of Biological Sciences, Marshall University, Huntington, West Virginia 25755*

Abstract.— The early Eocene is a period of significant change in the composition of North American turtle faunas. Over the first 2.2 million years of the Eocene, the fossil record documents several immigrations into depositional basins of the Western Interior and an expansion in the ecological niches of turtles toward herbivory. Focusing on the Willwood Formation, we document change in generic and species richness in greater detail than previously available and place this in a better-constrained temporal framework, confirming that the two major episodes of change in the turtle faunas coincide with the appearance of Wasatchian mammals and with an interval of climate change at biohorizon B-C within the Wasatchian land-mammal age. We report changes in relative abundances of turtles and discuss possible explanations for these changes. Climate change (at least as estimated by proxies for mean annual rainfall or temperature) does not provide an adequate explanation for the observed changes. Rather, we think that changes in habitat heterogeneity may be a better explanation and that changes in the turtle fauna can best be understood by examining how change in climate, in combination with effects of local tectonic controls on floodplain development, affected the availability and preservation of diverse habitats.

INTRODUCTION

The mammalian portion of the terrestrial early Eocene vertebrate fauna has attracted much attention, but an understanding of the herpetofauna (amphibians and reptiles) is essential for evaluating and testing scenarios of coevolution of early Eocene climates and biotas. Testudines are the best represented order of the ancient herpetofauna. Turtles are preserved in great numbers in a variety of lithologies and depositional settings, and even isolated elements of the shell are readily recognizable and identifiable. The Bighorn Basin record of turtles studied here (Fig. 1), is significant in being one of the longest (approximately 2.2 million years) and most complete records of a local fauna in the Western Interior and because it is currently

the only record of faunal change that can be correlated with similarly detailed studies of local changes in other aspects of the fauna (e. g., Gunnell, 1998; Hartman and Roth, 1998), climate (Wing et al., 2000) and hydrology (Bown and Kraus, 1993).

The Bighorn Basin testudine record was originally and preliminarily summarized by Hutchison (1980), who first recognized this major reorganization of the ecologic and taxonomic composition of turtle fauna. Subsequently, Hutchison (1982, 1992) explored the relationship between reptile diversity and climate change through the Paleogene, identifying the linked roles that climate and hydrology have in affecting changes in diversity and herpetofaunal composition. Systematic work on Bighorn Basin turtles in the last twenty years is somewhat more limited. Gingerich (1989) reported the earliest records of the immigrant *Echmatemys* from Wa-0 localities in the Clarks Fork Basin. Hutchison (1991) described the Kinosternidae (mud turtles) of the Bighorn Basin. Hutchison (1998) summarized

In: Paleocene-Eocene Stratigraphy and Biotic Change in the Bighorn and Clarks Fork Basins, Wyoming (P. D. Gingerich, ed.), University of Michigan Papers on Paleontology, 33: 97-107 (2001).

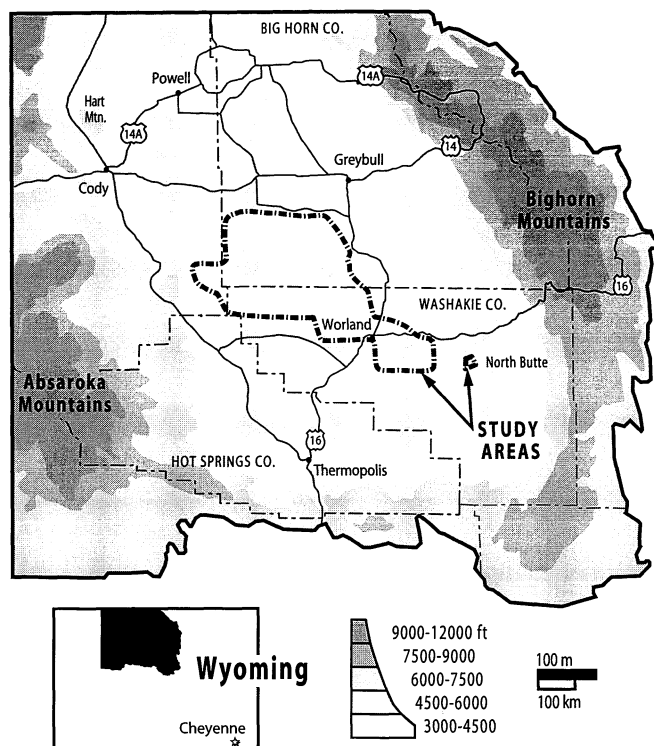


FIGURE 1 — Map of the Bighorn Basin, Wyoming, showing the distribution of turtle-bearing localities considered here.

the Paleocene-Eocene record of turtles in North America on a regional scale, observing two general patterns:

1. Across the Clarkforkian to Wasatchian North American Land-Mammal Age (NALMA) boundary, Clarkforkian taxa persist, and several new taxa appear (two genera of Kinosternidae, *Echmatemys* and Emydid P). These immigrants are relatively small in body size, represent both carnivores and omnivores, and are a mix of Asian and southern North American immigrants. Their first appearances are essentially synchronous across basins and correlate with mammalian immigrations (Hutchison, 1980; Holroyd and Hutchison, 2000).
2. A second major rearrangement of turtle faunas occurs in the mid-Wasatchian with the appearance and comparatively rapid increase in abundance of testudinids and dermatemydids (both large herbivorous turtles). This event is coincident with much increased warming, the local appearance of “megathermal” flora (Wing, 1998), and within a period of mammalian turnover called “Biohorizon B-C” (see Schankler, 1980; Bown et al., 1994). The late Wasatchian (late early Eocene) is marked by the last occurrences in the northern Rockies of the most common

Paleocene taxa (Emydid C and *Planetocheleys*) as well as the smallest emydid (Emydid P). In the case of Emydid C and Emydid P, these are their last known occurrences anywhere; *Planetocheleys* or a form similar to it appears to persist into the Uintan of Texas (Hutchison, unpubl. data).

Holroyd and Hutchison (2000), based on preliminary analysis of records of local faunas from several Wyoming basins, observed that taxonomic turnover during the Eocene is concentrated in the omnivorous to herbivorous turtles, both aquatic and terrestrial. Among the omnivore-herbivores, first appearances across basins are essentially synchronous, but last appearances (local extinctions) are not correlated across or within basins and are not readily correlatable to global climate trends, suggesting a different or more complex set of controls on their presence-absence. Carnivorous turtles, exclusively aquatic during this time, show no marked turnover at the regional scale, but do evince increasing diversity with the addition of kinosternids at the beginning of the Eocene and the local first appearance of additional trionychid genera in the mid-Wasatchian. However, the late Paleocene to early Eocene record of carnivorous turtles (particularly trionychids and baenids) is also more difficult to interpret than that of herbivorous taxa. Because many parts of the trionychid shell are morphologically conservative, isolated trionychid elements are difficult to assign below family level. Similarly, baenids (comparatively rare in any case) can only be assigned to genus when certain diagnostic elements are recovered. Consequently, it is very difficult to examine genus-level diversity patterns in these two groups in the absence of a more complete record. The problem is compounded in the Bighorn Basin record because only a handful of localities have produced sufficiently complete representatives of these groups to enable identification to genus. Thus, significant patterns of change may exist among carnivorous turtles through this interval, but they are still masked by an inadequate record of the groups.

Here we provide an updated summary of the Wasatchian Willwood Fm. turtle record based on more than 300 localities in the southern Bighorn Basin composite stratigraphic section (Bown et al., 1994), detail changes in the omnivorous-herbivorous turtle fauna, and examine how these relate to changes in climate and landscape through the period of greatest change, the early and middle early Eocene (basal to mid-Wasatchian).

THE TESTUDINE FAUNA

Thirteen genera in eight families are currently known from the Wasatchian of the Willwood Formation (Table 1). The number of species represented is still under study, but most genera appear to be monotypic through the Willwood Formation. An exception is the batagurid *Echmatemys*, which may show species changes through the section and include more than one lineage (Hutchison, pers. obs.). In terms of species richness, the numbers of species found throughout Willwood time are comparable to those observed in modern tropical to warm

TABLE 1 — Testudines of the Willwood Formation, with voucher specimens documenting the stratigraphic range of each genus in the southern Bighorn Basin stratigraphic sections. All specimens and localities are University of California Museum of Paleontology (UCMP). Locality equivalencies to US Geological Survey or Yale localities are noted as appropriate.

Baenidae

- Baena*, 364 m, V81093: 173699
Chisternon, 546 m, V96102 [=USGS D1212]: 173530
Palatobaena, 364 m, V81093: 173700

Chelydridae

- Protochelydra*, 343 m, V81071 [=Yale 135]: 136099; 481 m, V81170: 173526

Dermatemydidae

- Baptemys*, ca. 420 m, V98097 [10 m below Yale 271]: 173815; 601 m, V96073 [=Yale 33]: 173529

Bataguridae

- Echmatemys*, < 30 m, V99019 [=USGS D2018]: 212845; 601 m, V96073: 173713

Emydidae

- Emydid C, 30 m, V96118 [=USGS D1296]: 173533; 511 m, V81178: 126466
 Emydid P, 30 m, V96118 [=USGS D1296]: 173531; 435 m, V82201: 170567 and V82200: 170555

Family incertae sedis

- Planetochelys*, 34 m, V97014: 173534; 446 m, V96190: 173761; 516 m, V96124: 173812

Kinosternidae

- Baltemys*, 34 m, V97014: 173542; 546 m, V81182 [=Yale 192]: 127249

Testudinidae

- Hadrianus*, 392 m, V82346 [=USGS D1413]: 154505; 636 m, V96148 [=USGS D1651]: 173695

Trionychidae

- Plastomenus*, 380 m, V81043 [=Yale 67]: 154122; 505 m, V96045 [=USGS D1609]: 170351; cf.
Plastomenus, 559 m, V99207 [=USGS D1622]: 173716
Aspiderites (not shown), 465 m, V96159 [=USGS D1737]: 156078
-

temperate turtle faunas in much of Asia, the Amazon, or the southeastern United States. Generic richness of Bighorn Basin turtles, however, is greater than in many of these faunas. Despite its high diversity, the Willwood turtle fauna is still less rich than the most diverse modern faunas found in the Ganges River drainage (Iverson, 1992) or than in the latest Cretaceous to early Paleocene of North America (Hutchison and Archibald, 1986).

Turtles of the Willwood Formation display a wide range of shell shapes and sizes (Fig. 2), indicating the range of aquatic and terrestrial habitats they occupied. Baenidae is an extinct group of bottom-walking turtles that appear to have preferred river channels. Here Baenidae includes *Baena*, *Palatobaena*, and *Chisternon*. *Palatobaena* and *Chisternon* have not previously been reported from the Willwood Formation, but constitute the youngest known record of *Palatobaena* and the oldest

known record of *Chisternon* (Hutchison, 1998). For Chelydridae (snapping turtles), *Protochelydra* is the only described Wasatchian taxon, although another genus may be present (Hutchison, pers. obs.). Similarly, *Baptemys* is the sole early Eocene representative of the family Dermatemydidae, a family of large aquatic turtles endemic to North America.

Pond turtles of the Emydidae *sensu lato* (including both the Bataguridae and Emydidae *sensu stricto*) are the most diverse group of Willwood turtles, with a minimum of three genera. Records of "Emydidae indet." are probably poorly-preserved or pathologic *Echmatemys* specimens, but some may document another, undescribed genus ("Emydid E" of Hutchison, 1992, table 23.2). *Planetochelys*, of unclear phylogenetic affinities, is a highly specialized box turtle, possibly related to trionychoids (Hutchison, 1998). *Planetochelys* superficially resembles emydids and was originally discussed as a member of that family

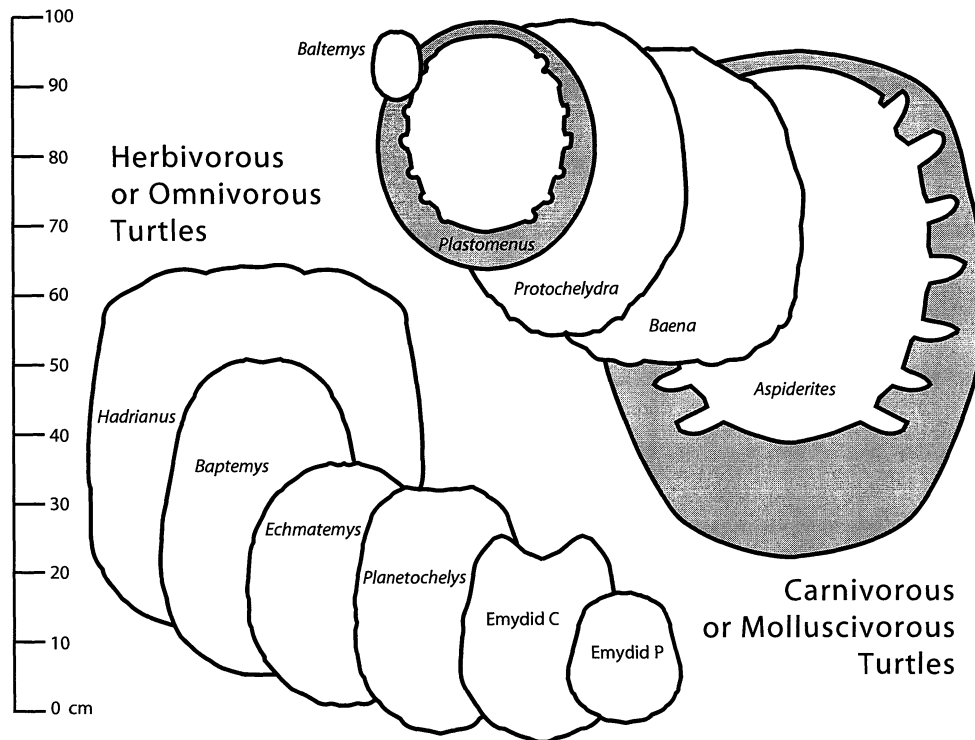


FIGURE 2 — Diagram showing maximum known shell size for representative Wasatchian turtles. Black outlines indicate the limits of the bony carapace; approximate extent of fleshy carapace of trionychids shown in gray.

(Emydid K of Hutchison, 1980). *Baltemys* is the sole representative of kinosternids (mud turtles) in the Willwood Fm, although *Xenochelys* is known from contemporaneous strata in the Wind River and Greater Green River Basins (Hutchison, 1991) where the two co-occur. Testudinidae (tortoises) are represented by *Hadrianus*, a large turtle of Old World origin. Trionychids (soft-shelled turtles) are common as fossils in the upper part of the Willwood Formation and two subfamilies, Trionychinae and Plastomeninae, are present. Unfortunately, fragmentary trionychids are difficult to classify and specimens identified only as Trionychinae may represent records of *Apalone* or the form-genus *Aspiderites*, which is also known from the Clarkforkian (Hutchison, 1998).

Ecologically, the majority of Willwood taxa are aquatic; only *Planetochelys* and *Hadrianus* show morphological features associated with terrestrial habits (Hutchison, 1998) and can be regarded as being at least partially terrestrial. *Planetochelys* is unique among early Eocene turtles in possessing a kinetic plastron similar to that of the extant emydoids *Cuora*, *Terrapene*, and *Emydoidea*. Specifically, the suture between the hyo- and hypoplastra remains unfused and is modified as a hinge that allows the anterior and posterior halves of the plastron to be closed to protect the head and tail when retracted. Among aquatic turtles, trionychids and baenids appear to favor chan-

nels, particularly those with sandy substrates. In the case of trionychids, we can make this inference based on analogy with modern taxa; in the case of baenids, we draw this inference from the disproportionate representation of complete specimens in channel deposits (Hutchison, 1984). By contrast, modern dermatemydids prefer more quiet, open water such as that found in large rivers, lakes, and ponds. Emydids sensu lato appear to be more catholic in their use of aquatic habitats, a fact reflected in their widespread distribution in many types of sediments. Dietarily, testudine diversity is fairly evenly split between carnivorous taxa and herbivorous to omnivorous taxa, and Willwood turtles show a considerable range of variation in adult body size among both carnivorous and herbivorous turtles (Fig. 2). Carnivorous turtles (based on cranial morphology and by analogy with modern relatives) displayed a range of habits from ambush predators (trionychids, chelydrids) to molluscivory (baenids, kinosternids).

The rise of a diverse herbivorous turtle fauna in North America is one of the hallmarks of the early Eocene and represents a significant shift in the ecological niche that turtles occupied in Western Interior faunas. Throughout the Cretaceous most of the turtles are inferred to be aquatic carnivores. Only one terrestrial herbivore (*Basilemys*) and two aquatic omnivore-herbivores (*Adocus*, and a macrobaenid), are present in

the eastern Rocky Mountain areas at the end of the Cretaceous. *Basilemys* became extinct at the end of the Cretaceous, although the two aquatic omnivore-herbivores persist into the Paleocene (Hutchison and Archibald, 1986). *Adocus* persists into the Torrejonian of northern areas (Montana, Wyoming, Colorado) and Clarkforkian of Texas (Hutchison, 1998), but is unreported in the Tiffanian or Clarkforkian of the northern Rockies. Macrobaenids are rare through the Paleocene (McKenna et al., 1987) and are last known in the Clarkforkian of Wyoming (Hutchison, unpubl. data). The first Paleogene probable omnivore may be Emydid C, which makes its appearance in the Torrejonian (e. g., in the upper Nacimiento Formation and in the Lebo Formation of Montana, Hutchison, pers. obs.), becomes the most common turtle in the Tiffanian and Clarkforkian (based on UCMP collections from Bison Basin and Greater Green River Basin), and persists into the Wasatchian in Wyoming. [Estes (1975) noted the presence of the European emydid *Ptychogaster* in the Tiffanian of the Clarks Fork Basin. As reported by Bartels (1980), this identification is suspect, and we now recognize these specimens and others from the Tiffanian of the Clarks Fork Basin to be Emydid C.] The jaws possess triturating surfaces (ridges associated with shearing surfaces on the overlying keratinous covering) that are relatively simple-suggesting a mixed diet.

The omnivorous-herbivorous family Dermatemydidae first appears in the Tiffanian of Texas in the form of a genus closely-related or ancestral to *Baptemys* (Hutchison, 1998), but representatives of this family do not appear in the northern Rockies until the mid-Wasatchian when *Baptemys garmanii* appears (Hutchison, 1980). The peculiar eastern Paleocene genus *Planetocheilus* (Weems, 1988, Hutchison and Weems, 1999), appears in the Clarkforkian and persists into the Wasatchian of Wyoming (Lysitean or Wa-6). Although absent from Wyoming thereafter, it persists into the middle Eocene (Uintan NALMA) in Texas (Hutchison, pers. obs.). The simple triturating apparatus suggests an omnivorous diet as in the other terrestrial or semi-terrestrial box turtles.

At the beginning of the Wasatchian, other omnivorous to herbivorous turtles begin to appear, all part of the testudinoid clade. The first is the batagurid *Echmatemys* which appears at the beginning of the Wasatchian land-mammal age (Wa-0; Gingerich, 1989), persists throughout the Eocene, and is generally the most common turtle. *Echmatemys*' dietary preference based on the simple construction of the triturating surfaces of the jaws (resembling the extant *Clemmys*, *Terrapene*, *Emydoidea*), was omnivorous or more likely herbivorous. Emydid P first appears shortly after *Echmatemys* and appears to be related to the Emydidae *sensu stricto*, generally resembling the extant omnivorous *Clemmys* and *Chrysemys picta* in shell shape. The jaw morphology of this form is unknown but its otherwise strong resemblance and probable relationship to the latter modern taxa suggests an omnivorous diet. One of the last but significant appearances of herbivorous turtles is the arrival of the tortoises (Testudinidae) of the genus *Hadrianus*. Based on the complexity of its triturating surfaces, it is the most herbivorous of the Willwood turtles.

LOCALITIES AND STRATIGRAPHIC SETTING

Our data set expands on the record of Wasatchian age turtles from the Willwood Formation in the southern Bighorn Basin (Hutchison, 1980). In discussion of their biostratigraphic context, both Schankler's (1980) range zone scheme and Gingerich's (1983, 1989) numbered interval scheme will be used to the extent that this is possible. Assignment to Wasatchian range zones (Schankler, 1980) is based on stratigraphic position as discussed in Bown et al. (1994) and Wing et al. (2000). Gingerich's (1983, 1989) Wa-0 through Wa-7 biozones are temporally more refined than Schankler's (1980) biostratigraphic scheme, but have not yet been adequately tested in the lower part of the Willwood section in the southern Bighorn Basin. The use of the numbered Wasatchian subzones in this paper is based on the correlations between Schankler's (1980) and Gingerich's (1983, 1989) zones as suggested in Clyde et al. (1994), Clyde (1997), and Wing et al. (2000; see also Gingerich, 1991, 2000).

In addition to numerous additional collections that fill gaps and stratigraphically refine the record of early and mid-Wasatchian turtles, a significant expansion of the data set is the incorporation of southern Bighorn Basin localities from the base of the Willwood Formation that are assigned to the Wa-0 biozone (see Wing, 1998; Strait, this volume). Since 1992, collecting in the Wa-0 interval in the southern Bighorn Basin has concentrated on localities in the North Butte area (Fig. 3). Here earliest Wasatchian vertebrates have been recovered from a number of localities that occur within an approximately 40 meter thick interval containing one or two bright red, deeply weathered paleosols called the 'Wa-0 red bed' (Wing, 1998). Isotopic studies of carbonates from this interval record a negative carbon excursion (Koch et al., 1992, 1995, Wing et al., 2000). Several localities (in sections 30 and 31, T46N, R98W, Washakie County, Wyoming) occur within these red beds (Wing, 1998). Localities in section 18, T46N, R98W (see Wing, 1998, Sec. 94-5), occur approximately 11 meters below the 'Wa-0 red bed' (Wing, written comm., 2000). The latter local section has not yet been analyzed isotopically, so the position of these localities relative to the Wa-0 carbon isotope excursion is not known. None of the localities from the North Butte area are tied to the Willwood Formation section of Bown et al. (1994). However, all North Butte localities are stratigraphically lower than the lowest localities (at the 30 m level in exposures east of Worland) in the southern Bighorn Basin composite section. For the purposes of this paper, localities from the North Butte Wa-0 interval are treated as less than 30 meters without further refinement.

The turtle record of the Willwood Formation in the central Bighorn Basin is based on more than 300 localities in measured sections in the southern Bighorn Basin. Stratigraphic levels for these localities are documented by Bown et al. (1994) or estimated based on topographic position and proximity to localities in the Bown et al. composite section. All localities taken together span the interval from earliest Wasatchian (Wa-0) through the middle Wasatchian (Lysitean or Wa-6), and record

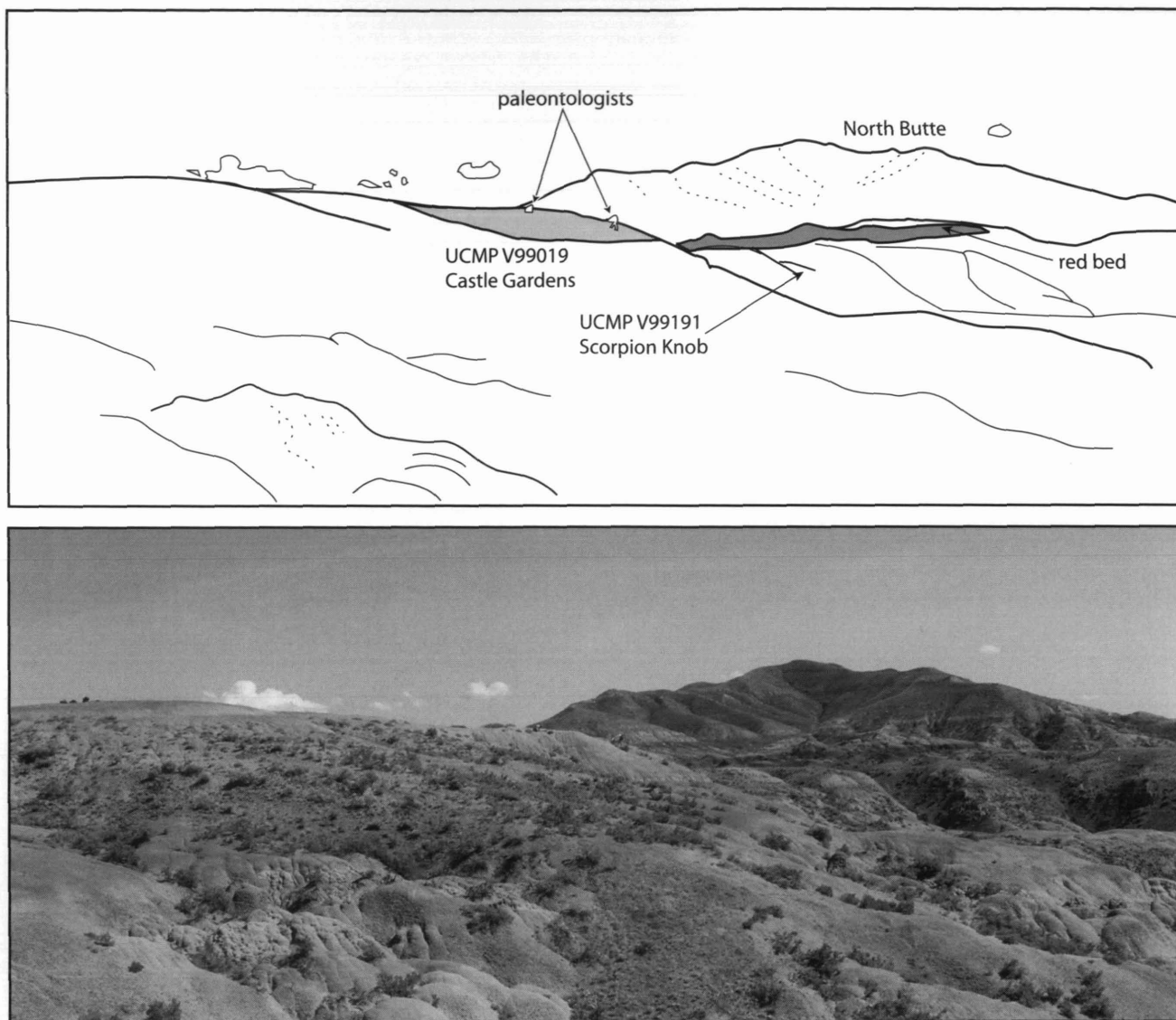


FIGURE 3 — Photograph looking southward toward North Butte, showing the position of the bed containing UCMP localities V99019 (Castle Gardens) and V99119 (Scorpion Knob). Although UCMP V99019 forms the cap of the small hill in the foreground, the bed can be traced laterally to a point where it is overlain by the “Wa-0 red bed” (Wing, 1998), a bright red, deeply-weathered paleosol.

changes in the fauna through several important climatic changes: the Wa-0 warm interval (Koch et al., 1992, 1995; Clyde and Gingerich, 1998), the ‘early Eocene cool period’ (Wing et al., 2000), and renewed warming coincident with a period of mammalian faunal turnover at “Biohorizon B-C” (approximately equal to Wa-5 or the *Bunophorus* interval zone; Schankler, 1980; Bown et al., 1994; Wing, 1999). Sampling through the section is uneven. This is in part due to depositional biases, and, to a lesser extent, to artifacts of post-1980 collecting efforts.

CHANGES IN THE TESTUDINE FAUNA THROUGH THE WILLWOOD FORMATION

The Wa-0 North Butte localities have to date produced an abundance of the batagurid turtle *Echmatemys* (UCMP V94082: 173506; V94083: 173501; V99019: 212835-212846, 212853, 212857; UCMP V99207: 173724-25), and less common and more fragmentary trionychids (UCMP V94083: 173502, 173507; V99019: 212847-212848, 212854, 212858; UCMP

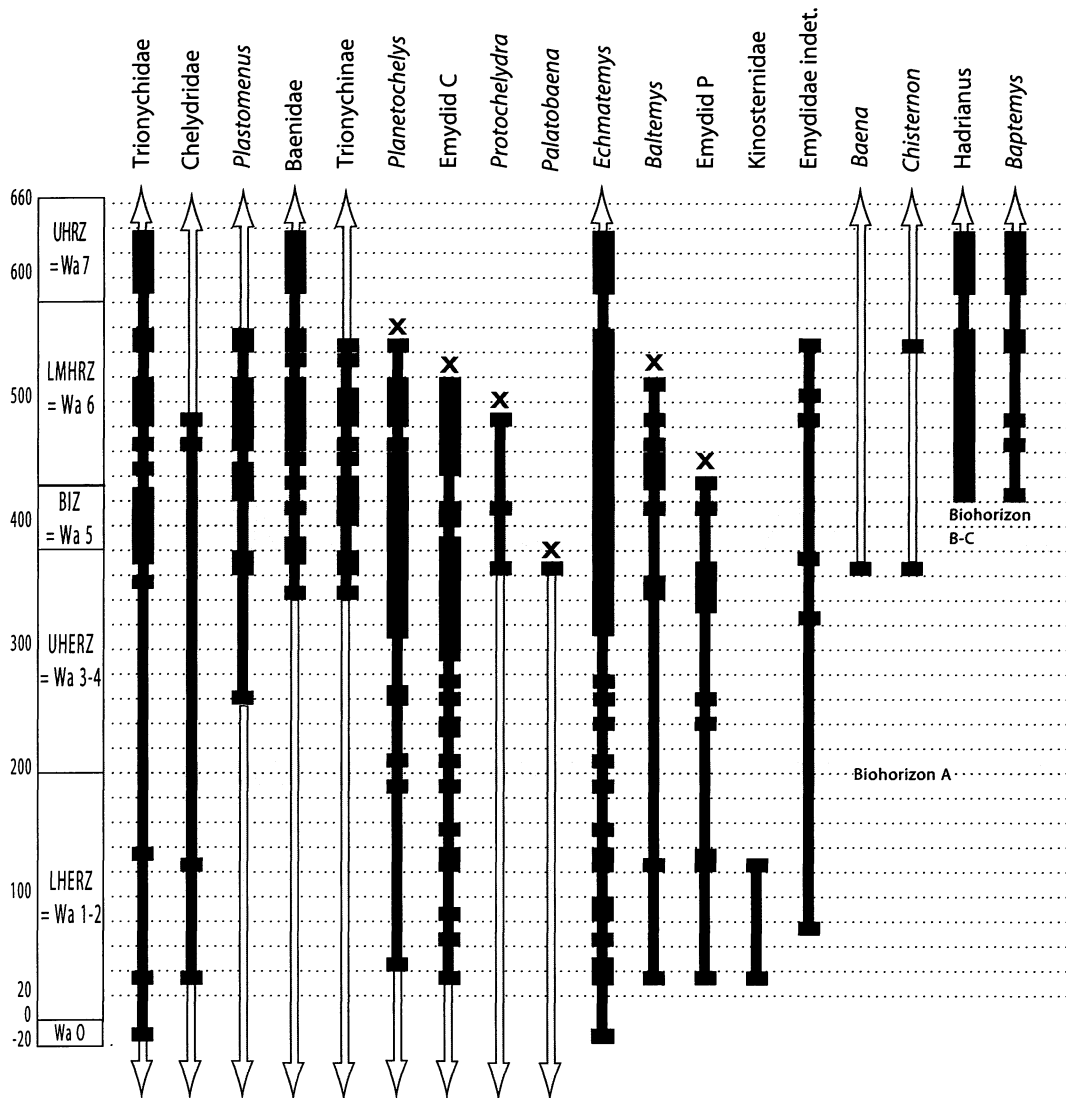


FIGURE 4 — Stratigraphic occurrences of turtle taxa in the Willwood Formation. Black bars indicate occurrences; narrower gray lines indicate ghost lineages; x indicates that the last occurrence shown represents a local last appearance. Abbreviations of biozones as follows: LHERZ, lower Haplomylus-Ectocion Range Zone; UHERZ, upper Haplomylus-Ectocion Range Zone; BIZ-Bunophorus Interval Zone; LMHRZ, Lower and Middle Heptodon Range Zone; UHRZ, Upper Heptodon Range Zone.

V99207: 173726). The only other reptiles recovered from these localities are sparse crocodylian bones representing the alligatoroid *Borealosuchus* (UCMP V94082: 173504; V94084: 173510; V99019: 212850), and osteoderms of glyptosaurine iguanid lizards (UCMP V94084: 173512). The abundance of *Echmatemys* in Wa-0 localities marks a dramatic change from older Clarkforkian faunas in the Bighorn Basin (documented in the University of Michigan collections), which are dominated by *Planetochelys* and Emydid C, with *Echmatemys* being absent. The reptile fauna is not particularly diverse, in contrast to the high diversity reported for the mammalian fauna

(Gingerich, 1989; Clyde and Gingerich, 1998; Strait, this volume). The low reptile diversity reflects, at least in part, sampling bias. Relatively few localities are known from the Wa-0 biozone. On average, a locality in the Willwood Formation produces only two turtle taxa; hence, in the absence of more localities or those with exceptional preservation, we should expect few taxa. Ghost lineages inferred for taxa known above and below but not in the Wa-0 interval in the Bighorn Basin would lead us to expect that at least one genus each of Baenidae and Chelydridae, plus *Planetochelys* and Emydid C, might have been present in the basin through Wa-0. However, even with

TABLE 2 — Counts of locality occurrences for the most common omnivorous-herbivorous turtle taxa, showing changes in relative abundance through time as depicted in Figure 5. Conversion of meter levels to absolute ages follows Wing et al., 2000: Age Model 1. Each stratigraphic grouping equals approximately 250,000 years. Localities provides the total number of localities present in the interval.

Meter level	<i>Platanochelys</i>	<i>Hadrianus</i>	<i>Baptemys</i>	Emydid P	<i>Echmatemys</i>	Emydid C	Locs.
480-590	10	36	7	0	53	8	75
375-480	36	33	4	4	69	18	114
310-375	29	0	0	6	24	36	56
250-310	4	0	0	2	14	12	18
190-250	1	0	0	0	3	6	8
120-190	2	0	0	2	10	18	16
60-120	0	0	0	0	3	4	7
< 60	1	0	0	1	7	1	10

the addition of these ghost lineages, testudine diversity is not as high in Wa-0 as it is throughout the remainder of Willwood time.

As the stratigraphic record shows (Fig. 4), preserved turtle diversity is at its lowest during Wa-0 time and increases approximately 50% in the early Wasatchian (at 30 meters in the composite section) with the first appearances of *Baptemys* and Emydid P. There is no substantial change in diversity until the interval represented by the 343 to 430 meter interval, during which several taxa make local first appearances (*Baena*, *Palatobaena*, *Hadrianus*, *Baptemys*, *Chisternon*) and disappearances (Emydid P). This interval corresponds to that termed Biohorizon B-C, during which there is marked turnover in the mammalian fauna (Schankler, 1980; Bown and Kraus, 1993; Bown et al., 1994). The episode of mammalian faunal turnover in the lower Willwood Formation termed Biohorizon A (Schankler, 1980) does not appear to have a corresponding turnover in the turtle fauna.

Analysis of occurrences (presence vs. absence) reveals that although the taxonomic composition is homogeneous within the study area, there are differences in relative abundance within the local stratigraphic sequence (Table 2; Fig. 5). Hutchison (1998) and Holroyd and Hutchison (2000) suggested that through the early Eocene, Paleocene holdover taxa slowly diminish in abundance as the abundance of immigrants rises. While this is true on a broad, regional scale (particularly when the Lostcabinian or Wa-7 is considered and the data are analysed based on biozones), the more detailed analysis presented here shows that while Emydid C and *Platanochelys* are somewhat reduced in abundance after the arrival of *Echmatemys* and Emydid P, both taxa persisted as a significant portion of the Willwood fauna. Both of these Paleocene holdovers (as well as Emydid P) only disappeared from the record after *Baptemys* and *Hadrianus* appeared. The possibility that immigrant taxa may have resulted in competitive displacement of endemic taxa

is really only suggested by the inverse correlation seen between the relative abundance of *Platanochelys* and *Hadrianus*.

An alternative climatic hypothesis may better explain observed changes in diversity and the demise of *Platanochelys* and Emydid C. The greatest abundance of the latter taxa during Willwood Formation time occurs during the 'early Eocene cool period.' At this time, climatic conditions most closely approximate those of the late Paleocene, when both of these taxa flourished. Renewed warming in the mid-Wasatchian may have been an important factor in their local disappearance; farther south in the Washakie Basin (where conditions were presumably somewhat warmer; Wilf, 2000), both taxa disappeared from the record at least 0.75 million years earlier than in the Bighorn Basin (Holroyd and Hutchison, unpubl. data).

Clear explanations for the observed changes in local richness and relative abundance are difficult to provide, in part because little is known about the climatic and ecologic correlates of these diversity measures in modern turtle populations. Of many temperature and rainfall variables, species richness in extant turtles is only significantly correlated with total annual rainfall and driest month rainfall (Iverson, 1992). However, paleobotanical measures of mean annual rainfall indicate that mean annual rainfall decreased through the early Eocene (Wilf, 2000), while turtle diversity increased through the same interval. Thus, rainfall amount alone is not an adequate explanation for observed patterns. The manner in which rainfall affects floodplain and wetland environments may be more critical for determining diversity. Bodie et al. (2000) identified a number of wetland characteristics that correlate with high species richness. They identified low annual duration of drying as the most important feature, and other additional variables affected relative abundance of turtle taxa. In their study, high abundance of species that preferred slow-moving aquatic environments correlated with connectedness of scours and frequent flooding while species preferring faster moving aquatic

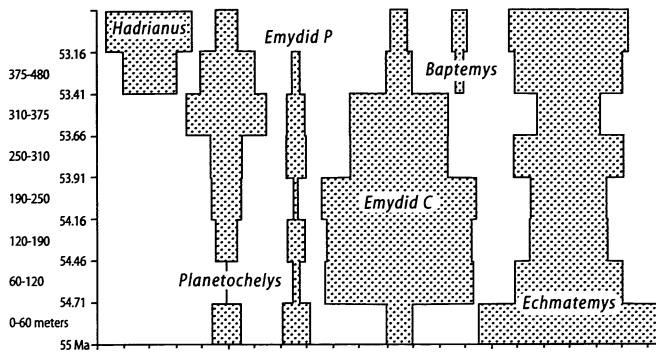


FIGURE 5 — Spindle diagram of omnivorous-herbivorous turtle occurrences, showing changes in the relative abundance as approximated by the number of locality occurrences. The width of each spindle represents the proportion of all localities within each interval at which the taxon has been recorded.

environments were more abundant in turbid wetlands close to the river. High regional diversity is apparently best achieved when heterogeneous, favorable habitats are present.

Changes in habitat heterogeneity through time is a possible, and plausible, explanation for the changes in generic and species richness seen through Willwood Formation time. Certainly, the absence of baenids and the comparative rarity of trionychids, both of which appear to favor riverine areas with sand bottoms, below approximately 350 meters elevation, is an indication of the absence of suitable habitats present (or at least preserved) in the basin. As has been noted by Bown (1979) and Bown and Kraus (1993), the lower part of the Willwood Formation in the southern Bighorn Basin is dominated by mature paleosols that developed in distal floodplain settings. A greater variety of architectural elements is only present in the upper Willwood Formation, with increasing seasonality and the possible development of monsoonal conditions (Bown and Kraus, 1981; Kraus and Bown, 1993). The possibility of seasonally more arid conditions (Bown and Kraus, 1981) as a cause for changes in mammalian faunas at Biohorizon B-C coincides with the highest diversity of aquatic turtles, so we find it unlikely that drying *per se* was responsible for the changes in the vertebrate fauna.

Differences in relative abundance within omnivorous-herbivorous turtles may reflect floral abundances or facies differences, reflective of local habitat differences. Certainly, among extant turtle taxa, many exhibit distinct habitat preferences that have been anecdotally related to numerous factors such as water depth, turbidity, and availability of basking or nesting areas. Unfortunately, floral data through the lower part of the section are not as refined as that of the vertebrate record, so the possible role of local habitat differences cannot be evaluated in a direct fashion. Based on the available botanical evidence, Wing et al. (1995) and Davies-Vollum and Wing (1998) suggested that the Willwood Formation possessed a mosaic of conditions in the wet floodplain backswamp. Changes in sedi-

mentological regime through the Willwood Formation, particularly with respect to soil wetness (as reflected by hydromorphic paleosols) and floodplain instability (reflected in channel and paleosol development), have been investigated in some detail (Bown and Kraus, 1981, 1993; Kraus and Bown, 1986, 1993; Wing and Bown, 1985). These changes are not yet tied directly to vertebrate localities throughout the section but should prove a fertile avenue for future inquiry.

In sum, the analysis of occurrences of Willwood turtles shows marked changes in the early Eocene turtle fauna, changes that are reflective of several episodes of faunal reorganization through a period of significant climatic change. However, attempts to unravel the causes and correlates of these changes in community structure highlight how little we know about the interaction of climate and biota effecting the changes, and how these are expressed in the preserved fossil record. For the most part, we have sought simple explanations for change, highlighting temperature (e. g., Rea et al., 1990; Wing et al., 1995), the rapidity of climate change (Wing et al., 2000), or seasonality (Bown and Kraus, 1981). However, these simple explanations are seemingly unsatisfactory, not only for the early Eocene, but for broader studies as well (e.g., Alroy et al., 2000). Understanding how climate has affected vertebrate diversity on the time scales considered here clearly requires a more complex explanation. In order to find that explanation, it will require a better understanding of how climatic factors affect modern diversity as well as a better idea of how local conditions affect our recovery of that record of change.

ACKNOWLEDGMENTS

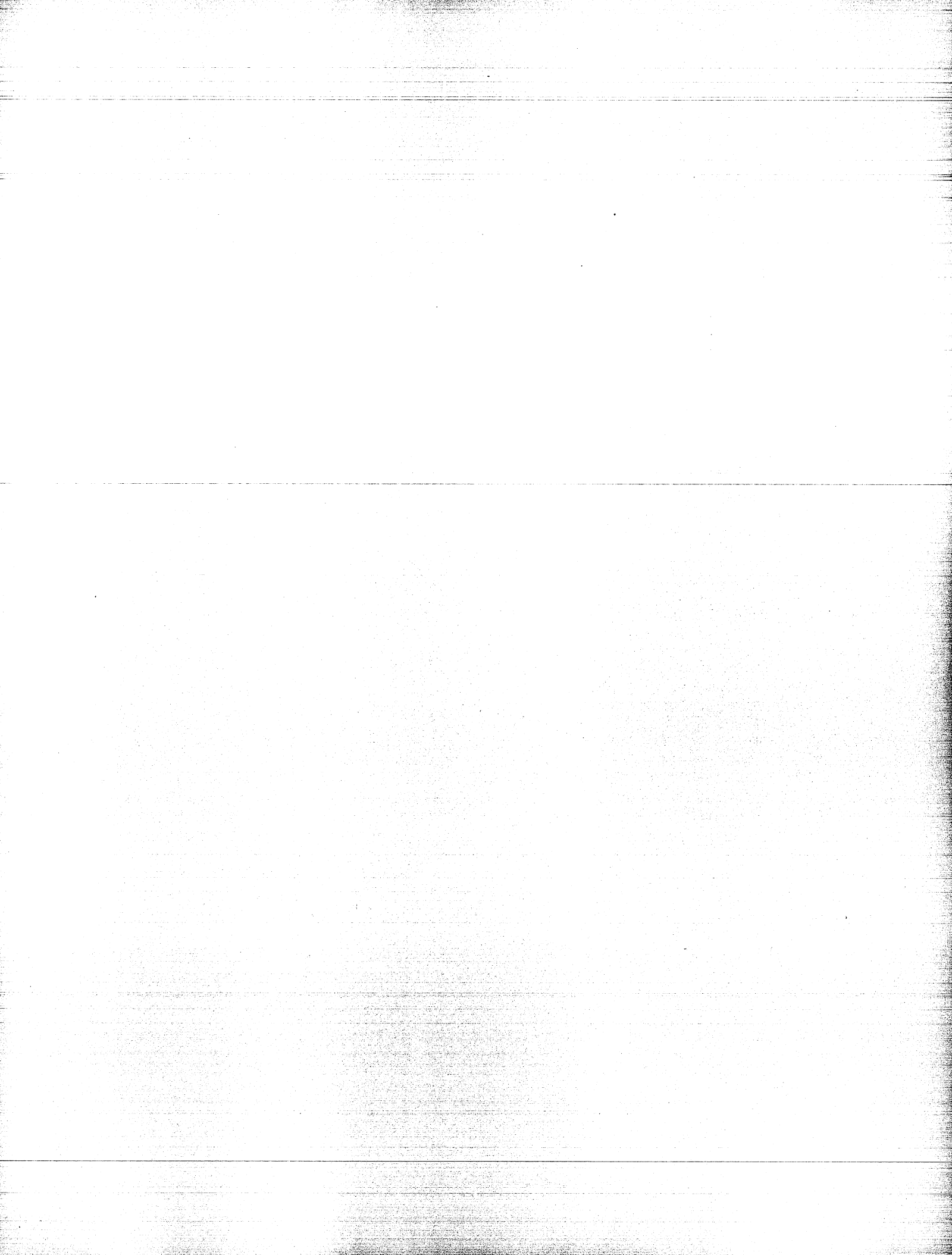
We are deeply grateful to Thomas M. Bown and Kenneth D. Rose, who contributed substantially to the collections described here and to our fieldwork in the Bighorn Basin. This study was funded by the Annie M. Alexander Endowment to JHH and PAH, and grants from Marshall University, West Virginia Women in Sciences, and NASA to SGS. Many colleagues graciously made collections available for study: Eugene Gaffney (American Museum of Natural History), Philip Gingerich and Gregg Gunnell (University of Michigan Museum of Paleontology), Jay Lillegraven and Michael Cassiliano (University of Wyoming). Specimens were collected under a series of permits from the Bureau of Land Management, and we gratefully acknowledge their cooperation.

LITERATURE CITED

- ALROY, J., P. L. KOCH, and J. C. ZACHOS. 2000. Global climate change and North American mammalian evolution. *In* D. H. Erwin and S. L. Wing (eds.) *Deep time: Paleobiology's Perspective*. *Paleobiology*, 26 (suppl. to no. 4): 259-288.
- BARTELS, W. S. 1980. Early Cenozoic reptiles and birds from the Bighorn Basin, Wyoming. *University of Michigan Papers on Paleontology*, 24: 73-80.
- BODIE, J. R., R. D. SEMLITSCH, and R. B. RENKEN. 2000. Diversity and structure of turtle assemblages: associations with

- wetland characters across a floodplain landscape. *Ecography*, 23: 444-456.
- BOWN, T. M. 1979. Geology and mammalian paleontology of the Sand Creek facies, lower Willwood Formation (lower Eocene), Washakie County, Wyoming. *Geological Survey of Wyoming, Memoir*, 2: 1-151.
- BOWN, T. M., and M. J. KRAUS. 1981. Lower Eocene alluvial paleosols (Willwood Formation, northwest Wyoming, U.S.A.) and their significance for paleoecology, paleoclimatology, and basin analysis. *Palaeogeography, Palaeoclimatology, Palaeoecology*, 34: 1-30.
- BOWN, T. M., and M. J. KRAUS. 1993. Time-stratigraphic reconstruction and integration of paleopedologic, sedimentologic, and biotic events (Willwood Formation, lower Eocene, northwest Wyoming, U.S.A.). *Palaios*, 8: 68-80.
- BOWN, T. M., K. D. ROSE, E. L. SIMONS and S. L. WING. 1994. Distribution and stratigraphic correlation of upper Paleocene and lower Eocene fossil mammal and plant localities of the Fort Union, Willwood and Tatman Formations, southern Bighorn Basin, Wyoming. U.S. Geological Survey Professional Paper, 1540: 1-103.
- CLYDE, W. C., 1997. Stratigraphy and mammalian paleontology of the McCullough Peaks, Northern Bighorn Basin, Wyoming: Implications for Biochronology, Basin Development, and Community Reorganization across the Paleocene-Eocene boundary. Ph.D. thesis, Geological Sciences, University of Michigan, Ann Arbor, 271 pp.
- CLYDE, W. C., and P. D. GINGERICH. 1998. Mammalian community response to the latest Paleocene thermal maximum: an isotaphonomic study in the northern Bighorn Basin, Wyoming. *Geology*, 26: 1011-1014.
- CLYDE, W. C., J. STAMATAKOS, and P. D. GINGERICH. 1994. Chronology of the Wasatchian land-mammal age (early Eocene): magnetostratigraphic results from the McCullough Peaks sections, northern Bighorn Basin, Wyoming. *Journal of Geology*, 102: 367-377.
- DAVIES-VOLLUM, K.S., and S. L. WING. 1998. Sedimentological, taphonomic, and climatic aspects of Eocene swamp deposits (Willwood Formation, Bighorn Basin, Wyoming). *Palaios* 13: 28-40.
- ESTES, R. 1975. Lower vertebrates from the Fort Union Formation, late Paleocene, Big Horn Basin, Wyoming. *Herpetologica*, 31: 365-385.
- GINGERICH, P. D. 1983. Paleocene-Eocene faunal zones and a preliminary analysis of Laramide structural deformation in the Clarks Fork Basin, Wyoming. *Wyoming Geological Association Annual Field Conference Guidebook*, 34: 185-195.
- GINGERICH, P. D. 1989. New earliest Wasatchian mammalian fauna from the Eocene of northwestern Wyoming: Composition and diversity in a rarely sampled high-floodplain assemblage. *University of Michigan Papers on Paleontology*, 28: 1-97.
- GINGERICH, P. D. 1991. Systematics and evolution of early Eocene *Perissodactyla* (Mammalia) in the Clarks Fork Basin, Wyoming. *Contributions from the Museum of Paleontology, University of Michigan*, 28: 181-213.
- GINGERICH, P. D. 2000. Paleocene-Eocene boundary and continental vertebrate faunas of Europe and North America. In B. Schmitz, B. Sundquist, and F. P. Andreasson (eds.), *Early Paleogene Warm Climates and Biosphere Dynamics*, Uppsala, Geological Society of Sweden, GFF, 122: 57-59.
- GUNNELL, G. F. 1998. Mammalian faunal composition and the Paleocene/Eocene Epoch/Series boundary: evidence from the northern Bighorn Basin, Wyoming. In M.-P. Aubry, S. G. Lucas and W. A. Berggren (eds.), *Late Paleocene-Early Eocene Climatic and Biotic Events in the Marine and Terrestrial Records*, Princeton University Press, Princeton, pp. 409-427.
- HARTMAN, J. H., and ROTH, B. 1998. Late Paleocene and early Eocene nonmarine molluscan faunal change in the Bighorn Basin, northwestern Wyoming and south-central Montana. In M.-P. Aubry, S. G. Lucas and W. A. Berggren (eds.), *Late Paleocene-Early Eocene Climatic and Biotic Events in the Marine and Terrestrial Records*, Princeton University Press, Princeton, pp. 401-408.
- HOLROYD, P. A., and J. H. HUTCHISON. 2000. Proximate causes for changes in vertebrate diversity in the early Paleogene: an example from turtles in the Western Interior of North America. In B. Schmitz, B. Sundquist, and F. P. Andreasson (eds.), *Early Paleogene Warm Climates and Biosphere Dynamics*, Uppsala, Geological Society of Sweden, GFF, 122: 75-76.
- HUTCHISON, J. H. 1980. Turtle stratigraphy of the Willwood Formation, Wyoming: preliminary results. *University of Michigan Papers on Paleontology*, 24: 115-118.
- HUTCHISON, J. H. 1982. Turtle, crocodylian, and champsosaur diversity changes in the Cenozoic of the north-central region of western United States. *Palaeogeography, Palaeoclimatology, Palaeoecology*, 37: 147-164.
- HUTCHISON, J. H. 1984. Determinate growth in the Baenidae (Testudines); taxonomic, ecologic and stratigraphic significance. *Journal of Vertebrate Paleontology*, 3:148-151.
- HUTCHISON, J. H. 1991. Early Kinosterninae (Reptilia: Testudines) and their phylogenetic significance. *Journal of Vertebrate Paleontology*, 11: 145-167.
- HUTCHISON, J. H. 1992. Western North American reptile and amphibian record across the Eocene/Oligocene boundary and its climatic implications. In D. R. Prothero and W. A. Berggren (eds.), *Eocene-Oligocene Climatic and Biotic Evolution*. Princeton University Press, Princeton, pp. 451-463.
- HUTCHISON, J. H. 1998. Turtles across the Paleocene/Eocene epoch boundary in west-central North America. In M.-P. Aubry, S. G. Lucas and W. A. Berggren (eds.), *Late Paleocene-Early Eocene Climatic and Biotic Events in the Marine and Terrestrial Records*, Princeton University Press, Princeton, pp. 401-408.
- HUTCHISON, J. H., and J. D. ARCHIBALD. 1986. Diversity of turtles across the Cretaceous/Tertiary boundary in northeastern Montana. *Palaeogeography, Palaeoclimatology, Palaeoecology*, 55: 1-22.
- HUTCHISON, J. H., and WEEMS, R. 1999. Paleocene turtle remains from South Carolina. In Sanders, A.E. (ed.), *Paleobiology of the Williamsburg Formation (Black Mingo Group; Paleocene)*

- of South Carolina, U.S.A. *Transactions of the American Philo-
sophical Society*, 88: 165-195.
- IVERSON, J. B. 1992. Global correlates of species richness in turtles. *Herpetological Journal*, 2: 77-81.
- KOCH, P. L., J. C. ZACHOS, and P. D. GINGERICH. 1992. Correlation between isotope records in marine and continental carbon reservoirs near the Palaeocene/Eocene boundary. *Nature*, 358: 319-322.
- KOCH, P. L., J. C. ZACHOS and D. L. DETTMAN. 1995. Stable isotope stratigraphy and paleoclimatology of the Paleogene Bighorn Basin (Wyoming, USA). *Palaeogeography, Palaeoclimatology, Palaeoecology*, 115: 61-89.
- KRAUS, M. J., and T. M. BOWN. 1986. Paleosols and time resolution in alluvial stratigraphy. *In* P. V. Wright (ed.), *Paleosols: Their Recognition and Interpretation*, Blackwell, London, pp. 180-207.
- KRAUS, M. J., and T. M. BOWN. 1993. Short-term sediment accumulation rates determined from Eocene alluvial paleosols. *Geology*, 21: 743-746.
- MCKENNA, M. C., J. H. HUTCHISON, and J. H. HARTMAN. 1987. Paleocene vertebrates and nonmarine Mollusca from the Goler Formation, California. *In* B. F. Cox (ed.) *Basin Analysis and Paleontology of the Paleocene and Eocene Goler Formation, El Paso Mountains, California*. Society of Economic Paleontologists and Mineralogists, Pacific Section, Los Angeles, California, pp. 31-41.
- REA, D. K., ZACHOS, J. C., OWEN, R. M., and GINGERICH, P. D. 1990. Global change at the Paleocene-Eocene boundary; climatic and evolutionary consequences of tectonic events. *Palaeogeography, Palaeoclimatology, Palaeoecology*, 79: 117-128.
- SCHANKLER, D. M. 1980. Faunal zonation of the Willwood Formation in the central Bighorn Basin, Wyoming. *University of Michigan Papers on Paleontology*, 24: 99-114.
- WEEMS, R. E. 1988. Paleocene turtles from Aquia and Brightseat Formations, with a discussion of their bearing on sea turtle evolution and phylogeny. *Proceedings of the Biological Society of Washington*, 10: 109-145.
- WILF, P. 2000. Late Paleocene-early Eocene climate changes in southwestern Wyoming: Paleobotanical analysis. *Geological Society of America Bulletin*, 112: 292-307.
- WING, S.L. 1998. Late Paleocene-early Eocene floral and climatic change in the Bighorn Basin, Wyoming. *In* M.-P. Aubry, S. G. Lucas, and W. A. Berggren (eds.), *Late Paleocene-Early Eocene Climatic and Biotic Events in the Marine and Terrestrial Records*. Princeton University Press, Princeton, pp. 380-400.
- WING, S. L., J. ALROY, and L. J. HICKEY. 1995. Plant and mammal diversity in the Paleocene to early Eocene of the Bighorn Basin. *Palaeogeography, Palaeoclimatology, Palaeoecology*, 115:117-155.
- WING, S. L., H. BAO, and P. L. KOCH. 2000. An early Eocene cool period? Evidence for continental cooling during the warmest part of the Cenozoic. *In* B. T. Huber, K. G. MacLeod and S. L. Wing (eds.), *Warm Climates in Earth History*. Cambridge University Press, pp. 137-238.
- WING, S. L., and T. M. BOWN. 1985. Fine scale reconstruction of Late Paleocene-early Eocene paleogeography in the Bighorn Basin of Northern Wyoming. *In* R. M. Flores and S. S. Kaplan (eds.), *Cenozoic Paleogeography of West-Central United States*. Rocky Mountain Section- SEPM, pp. 93-105.



MAMMALIAN BIOSTRATIGRAPHY OF THE McCULLOUGH PEAKS AREA IN THE NORTHERN BIGHORN BASIN

WILLIAM C. CLYDE

Department of Earth Sciences, University of New Hampshire, Durham, New Hampshire 03824-3589

Abstract.— The McCullough Peaks area of the north-central Bighorn Basin, Wyoming, preserves a thick (ca. 2700 m) sequence of highly fossiliferous upper Paleocene (Fort Union Formation) to lower Eocene (Willwood Formation) fluvial strata. A total of 407 fossil localities are known from this area and 255 of these have been correlated to measured stratigraphic sections. These provide a biostratigraphic framework for McCullough Peaks sections and indicate that mammalian faunal zones Ti-3 (Tiffanian land-mammal age) to Wa-7 (Wasatchian land-mammal age) are preserved in superpositional relationship in this area. Comparison of faunal zone thicknesses from different parts of the basin indicate that the McCullough Peaks had sediment accumulation rates similar to those of the Clarks Fork Basin, but exhibited significantly higher rates of accumulation than the southern Bighorn Basin. Magnetostratigraphic polarities from faunally well-sampled sections in the northern Bighorn Basin are used to develop a detailed geochronology for Paleocene and early Eocene mammalian faunal zones.

INTRODUCTION

The North American Land-Mammal Age (NALMA) framework was set up in 1941 by a seven-person committee to provide a common biostratigraphic framework for correlation among local mammal-bearing stratigraphic sections in North America (Wood et al., 1941). Although this framework has been consistently updated and revised since its formation, the basic structure remains largely unchanged (Woodburne, 1987). The nineteen land-mammal ages recognized today for North America are only slightly different, in name and meaning, from the “provincial ages” proposed by the Wood committee. Much of the biostratigraphic work that has taken place since the Wood committee report has been dedicated to developing useful zonations within these mammal ages in order to further refine biostratigraphic correlations. These finer-scale mammalian zonations are critical for making detailed geological and paleontological comparisons within and between different depositional basins in North America. Improvements in

geochronological techniques over the last two decades have also led to important advances in correlating the NALMA framework to the global geological time scale (Berggren et al., 1995) so patterns of mammalian turnover from North America can be compared to climatic and biotic records in other geological settings (Woodburne and Swisher, 1995). This has been particularly important in the Paleogene part of the NALMA record where several episodes of global climate change have been linked to NALMA boundaries (Koch et al., 1992; Clyde et al., 2001).

The Bighorn Basin has played a key role in developing the early Paleogene part of the NALMA framework. The combination of extensive exposure of fossiliferous deposits of Paleocene and early Eocene age and a consistent succession of field-based research programs has made the Bighorn Basin one of the best-documented biostratigraphic sequences in the North American mammalian fossil record (Gingerich, 1980). Mammalian assemblages of Puercan, Torrejonian, Tiffanian, Clarkforkian, and Wasatchian land-mammal ages have been recovered in superpositional relationship in various parts of the basin. The internal zonation for the early Paleogene part of the NALMA framework is largely the result of detailed sampling of this sequence.

In: Paleocene-Eocene Stratigraphy and Biotic Change in the Bighorn and Clarks Fork Basins, Wyoming (P. D. Gingerich, ed.), University of Michigan Papers on Paleontology, 33: 109-126 (2001).

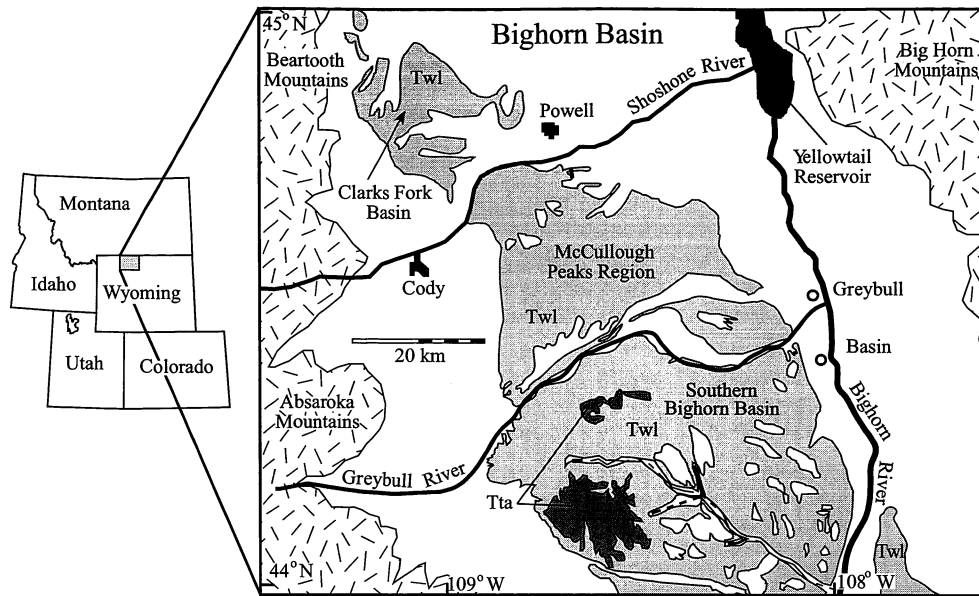


FIGURE 1 — Map showing the location of the McCullough Peaks field area in relation to the Clarks Fork Basin-Polecat Bench region to the north and southern Bighorn Basin area to the south. Light grey color outlines the lower Eocene Willwood Formation and dark grey outlines the lower-middle Eocene Tatman Formation.

The McCullough Peaks area represents an important part of the Bighorn Basin record for several reasons. It lies geographically and stratigraphically between the already well-sampled areas to the north (Clarks Fork Basin-Polecat Bench area; Gingerich, 1976, 1989; Rose, 1981) and south (southern Bighorn Basin area; Bown, 1979; Bown et al., 1994; Wing, 1980, 1998), providing a natural and much needed link between many previous Bighorn Basin studies. It preserves an essentially uninterrupted stratigraphic record from the Tiffanian through the late Wasatchian (Lostcabinian) making it rather unique in its continuity. Ongoing magnetostratigraphic research in this area has proven important in developing a refined geochronology for the early Paleogene part of the NALMA framework (Clyde et al., 1994). The Bighorn Basin provides a unique opportunity to develop a spatially complete picture of a terrestrial ecosystem through an important period of global climatic change and the McCullough Peaks will play a central role in piecing together this multi-dimensional puzzle.

GEOLOGICAL SETTING

The McCullough Peaks study area lies between the Shoshone River and Greybull River in the north-central part of the Bighorn Basin and spans almost the entire width of the basin (Fig. 1). The study area has been split into three laterally adjacent composite sections (Fig. 2). The southeast composite section is separated from the central composite

section by a fairly substantial region of poor sampling which was difficult to correlate across due to lateral changes in bed thicknesses. The central composite section is separated from the northwest composite section by a fault of unknown displacement. Fossil localities within each of these areas were measured into local stratigraphic sections, and those sections were correlated to one another to form the composite section for the region. By having three separate composite sections within the study area, it was possible to evaluate both temporal and lateral variability simultaneously. To have collapsed the entire McCullough Peaks study area into a single composite section would have been difficult, if not impossible, given the complex three-dimensional architecture of the Bighorn Basin's asymmetric fluvial deposits.

Two geologic formations are exposed in the McCullough Peaks area: the Paleocene Fort Union Formation and the lower Eocene Willwood Formation (Fig. 2). These formations represent the greatest volume of sedimentary rocks filling the Bighorn Basin and their distinct lithologies suggest important differences in the depositional systems responsible for their origin. The Fort Union Formation is dominated by drab sandstones, grey mudstones, and brown-to-black lignites that indicate a poorly drained fluvial-lacustrine system with numerous backwater paludal environments. The Willwood Formation is dominated by pedogenically altered, grey/red mudstones and channel sands that indicate a better drained fluvial system with numerous tributary channels and broad,

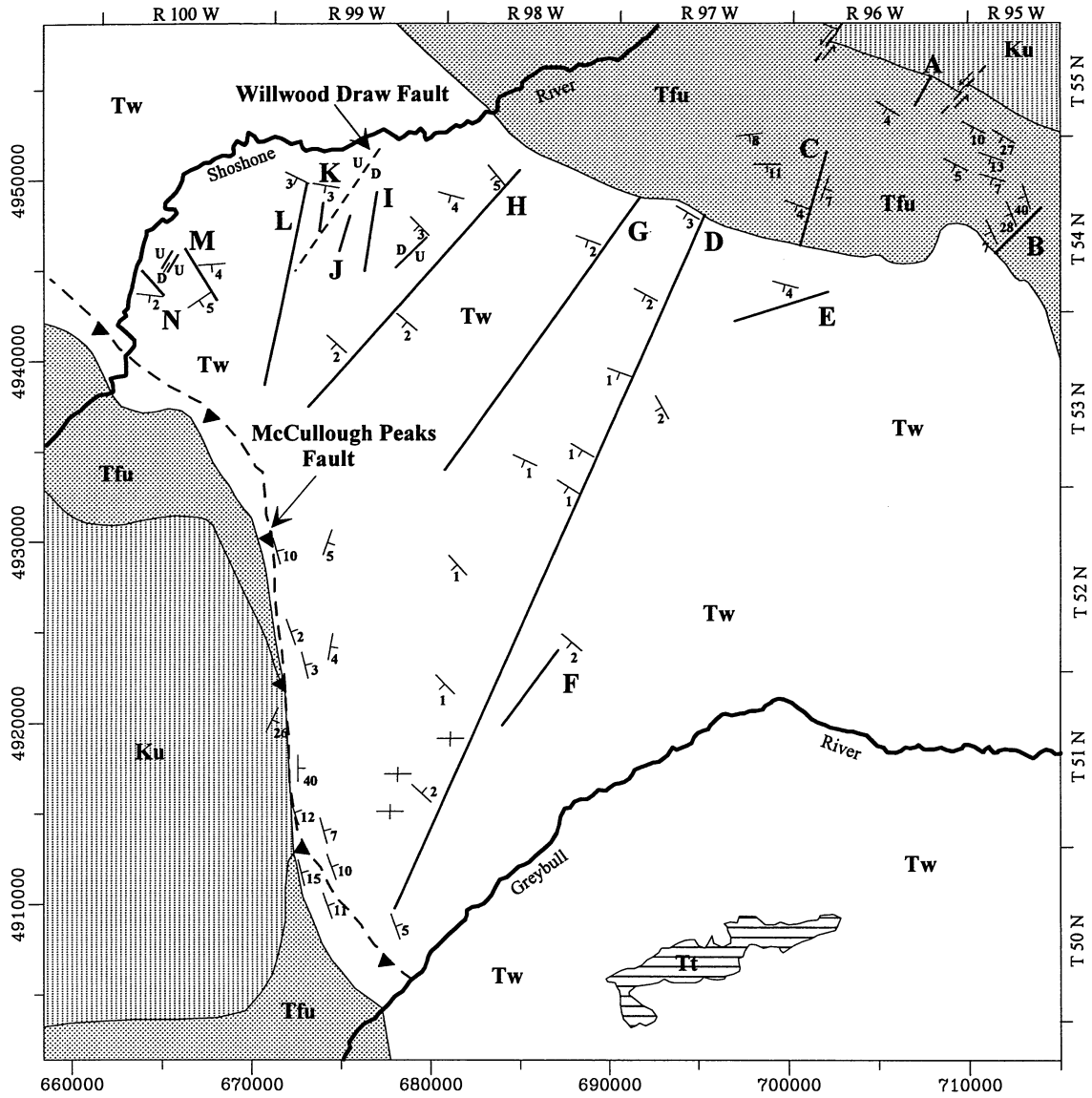


FIGURE 2 — Geological map for the McCullough Peaks area showing location of measured sections. *Ku* (dark grey) represents Cretaceous rocks (e.g., Lance Formation); *Tfu* (medium grey) is the Paleocene Fort Union Formation; *Tw* (light grey) is the Eocene Willwood Formation; and *Tt* (striped) is the Eocene Tatman Formation. Faults are shown with dashed lines. Local stratigraphic sections are labeled as follows: A, Cedar Point Section; B, South Foster Gulch Section; C, Jack Horner Reservoir Section; D, Foster Gulch-YU Bench Section; E, Coon Creek Section; F, East YU Bench Section; G, West Whistle Creek Section; H, Roan Wash Section; I, Lower Peerless Coulee Section; J, Willwood Draw Section; K, Willwood Draw North Section; L, Deer Creek Section; M, Vocation Section; N, Shoshone River Section. The McCullough Peaks southeast composite section is composed of local sections A-G; the McCullough Peaks central composite section is composed of local sections H-J; and the McCullough Peaks north-west composite section is composed of local sections K-N.

relatively dry, floodplains. The underlying cause of the transition from Fort Union to Willwood-type deposition is not entirely clear, but a similar transition is observed in many Laramide basins suggesting that it relates to tectonic and/or

climatic changes across the Paleocene-Eocene boundary that facilitated better drainage of the floodplains.

Despite relatively poor exposure, the Fort Union-Willwood transition is distinct in the Foster Gulch part of the study area.

The transition is marked by a series of thick, well-developed red beds, interpreted to represent very mature paleosol horizons. Gingerich (1989) first documented the anomalously mature paleosols at this level along the Polecat Bench section in the northern part of the basin (although they do not coincide with the Fort Union-Willwood contact there) and interpreted them to represent a distal floodplain environment. However, similarly mature paleosols have been observed at this level throughout the entire basin (Gingerich, 1989; Bown and Kraus, 1993; Wing, 1998), suggesting a more regional depositional phenomenon. The presence of such mature paleosols at the same time throughout the entire basin suggests that there was either a period of generally slower sediment accumulation or a period of generally higher rates of pedogenesis. Whereas low sediment accumulation rates could be driven by local climatic and/or tectonic variables, increased rates of pedogenesis are best explained by changes in climate. The fact that these mature paleosols correlate precisely with a well-documented carbon and oxygen isotope excursion (Koch et al., 1992; Fricke et al., 1998) and the anomalous Wa-0 fauna (Gingerich, 1989) provides compelling circumstantial evidence for a climatic role in this sedimentological anomaly. If true, similar depositional settings in other Laramide basins (e.g., Powder River Basin) should record a sedimentological anomaly at the same time. Unfortunately, this interval is presently not well-documented from other Laramide basins.

Beds in the McCullough Peaks area generally strike northwest-southeast (bearing 135°) and dips change gradually from approximately 40° SW at the Fort Union-Lance Formation contact (in the northeasternmost part of the study area) to horizontal in the middle to upper Willwood (Fig. 2). Local variations in this general pattern are common, with small-scale faulting and warping of beds increasing to the west. There is an abrupt change in bedding attitude in the Fort Union Formation in the Foster Gulch region (T54N, R96W). Here, relatively steeply dipping beds, striking approximately 160°, fold to shallower dips and a strike of about 110°. The far western edge of the field area is bounded by the McCullough Peaks fault, a major high-angle reverse fault associated with the Beartooth uplift. Only one major fault was identified within the field area (Willwood Draw fault). The magnitude of movement along this normal fault is unclear based on lithological evidence, although abundant fault gouge present along the fault plane indicates significant displacement. The Willwood Draw fault marks the boundary between the central and northwest composite sections, since without a good estimate of displacement in the field, it was impossible to accurately correlate beds across the area. Interestingly, the fault seems to dissect only part of the overlying section, with undisturbed Willwood deposition above it. Such synsedimentary faults reflect structural activity during deposition. By analyzing LANDSAT images of the basin, Kraus (1992) suggested that major east-west trending lineaments observed in adjacent Laramide mountain ranges extended into the basin and affected subsidence to the point of controlling local depositional environments. The fault along Willwood draw may be associated with one of these lineaments and

provides support for significant synsedimentary structural activity extending well into the basin center.

BIOSTRATIGRAPHIC NOMENCLATURE

The North American Land-mammal Age framework remains largely informal in its organization. Despite efforts to formalize this system into chronostratigraphic units using the guidelines set forth in the North American Stratigraphic Code (North American Commission on Stratigraphic Nomenclature, 1983), the NALMA framework continues to be a loose hierarchical network of biostratigraphic zones pieced together from geographically separate but temporally overlapping stratigraphic sequences throughout North America. Although in many cases sampling is now detailed enough to formalize the link between mammalian biostratigraphic units (e.g., biozones) and chronostratigraphic units (e.g., chronozones) in certain areas, the usefulness and stability of many of these biostratigraphic zonations outside their "type" areas has not been demonstrated, leaving many workers content to use biostratigraphic units as informal chronostratigraphic units until their broader context is better understood. This informality remains functional so long as the number and complexity of individual stratigraphic sections associated with a given biostratigraphic unit are not overwhelming, and pairwise comparisons between most (if not all) relevant stratigraphic sections can be made effectively. This remains true for most of the finer-scale biostratigraphies of the NALMA framework.

Unfortunately, most traditional stratigraphic terms have been given a formal stratigraphic meaning, so it is difficult to distinguish informal and formal units based solely on nomenclature. However, as long as these terms are applied consistently, whether formally designated or not, the distinction is not critical. Some authors prefer to put all informal stratigraphic terms in quotes (e.g., North American Land-mammal "Ages"; see Prothero, 1995). Since most of the NALMA framework remains informal, I will refrain from this practice for purposes of space and clarity.

The nomenclature associated with biostratigraphic zonation of Bighorn Basin deposits has changed significantly since Granger's original attempts in 1914 (Granger, 1914), although the zonation itself has changed very little (see Schankler, 1980; Gingerich, 1983; and Clyde et al., 1994, for comparisons). The biostratigraphic zonation used here follows those of Gingerich (1976, 1983), Rose (1981), and Archibald et al. (1987) for the Tiffanian and Clarkforkian land-mammal ages, and of Gingerich (1983, 1991) for the Wasatchian land-mammal age. These represent the most recent zonations proposed for these land-mammal ages and are in wide use. Figure 3 shows this framework and lists the principal first-occurring taxon that serves to define each zone. Most of these zones are based on the first appearance of a single taxon, an approach espoused by many biostratigraphers (Woodburne, 1987). However, other characteristic taxa are often used to augment correlations when sampling is poor. These auxiliary taxa are listed in the references noted above.

	NALMA Zone	First Appearing Taxon
Wasatchian	Wa-7	<i>Lambdaotherium popoagicum</i>
	Wa-6	<i>Heptodon calciculus</i>
	Wa-5	<i>Bunophorus etsagicus</i>
	Wa-4	<i>Hyracotherium pernix</i>
	Wa-3	<i>Homogalax protapirinus</i>
	Wa-2	<i>Arfia shoshoniensis</i>
	Wa-1	<i>Cardiolphus radinskyi</i>
	Wa-0	<i>Hyracotherium sandrae</i>
Clark-forkian	Cf-3	<i>Phenacodus - Ectocion Range Zone*</i>
	Cf-2	<i>Plesiadapis cookei</i>
	Cf-1	Rodentia
Tiffanian	Ti-6	<i>Plesiadapis gingerichi</i>
	Ti-5	<i>Plesiadapis simonsi</i>
	Ti-4	<i>Plesiadapis churchilli</i>
	Ti-3	<i>Plesiadapis rex</i>
	Ti-2	<i>Plesiadapis anceps</i>
	Ti-1	<i>Plesiadapis praecursor</i>

FIGURE 3 — Faunal zone framework used in this study. Zones are based on Gingerich (1983, 1991) and Archibald et al. (1987). NALMA: North American Land-mammal Age. **Phenacodus-Ectocion* Range zone is not based on the first appearance of a taxon but on the abundance of *Phenacodus* and *Ectocion* and the absence of *Plesiadapis cookei* and *Hyracotherium* spp.

SAMPLING AND TAPHONOMY

There are 407 University of Michigan fossil localities in the McCullough Peaks study area and 255 of them have been correlated to measured stratigraphic sections (Fig. 4). The fossils from these localities provide a biostratigraphic framework to correlate McCullough Peak stratigraphic sections to other sections in the Bighorn Basin and elsewhere. The sampling strategy and taphonomic regime of these localities are similar to those described from other parts of the basin (Badgley et al., 1995). McCullough Peaks' fossil localities are generally from 1,000 to 5,000 square meters in area, and encompass approximately 10 meters of vertical section. Lithologically, most localities preserve fossils in mudstone overbank deposits. In the Willwood Formation, the most fossiliferous facies is the A horizon of paleosols. Very few fossils are recovered from channel sandstones in the Willwood, although

this facies is variably productive in the Fort Union. Other more subtle lithological changes through the section (e.g., paleosol maturity) may also affect taphonomic conditions, although these are harder to document.

Geographically, localities are spread throughout the entire area, although local clusters of localities occur in especially well-exposed and/or accessible drainages. Localities that were not correlated to a stratigraphic section (shown as open symbols in Fig. 4) were either too distant from local sections to make correlation reliable, or were so unfossiliferous as to make the correlation irrelevant. The southeast composite section has far more geographic and vertical coverage of localities than the other two composite sections (Fig. 4). The vast majority of fossils recovered from McCullough Peaks localities were collected by University of Michigan field parties between the years of 1987 and 1992. Additional specimens were recovered by the author during the years 1993-1994 during geological field work in the region. All specimens are conserved in the Museum of Paleontology at the University of Michigan. Most localities have been collected between one and three times, with a few especially productive localities having as many as 10 collecting dates associated with them.

Generally, fossils are partially or wholly disarticulated when they are recovered, but not extensively water-worn, suggesting low to moderate transport before burial. In both Fort Union and Willwood deposits, dental fragments and isolated teeth are by far the most common and most easily identified elements. Most localities were collected by surface prospecting. A few localities have been quarried in areas where material is highly concentrated, especially in the Fort Union Formation, where large multistory sheet sandstones sometimes preserve lag concentrations of fossil material (e.g., Divide Quarry [FG046]). Screen-washing techniques have also been used on occasion, especially for small concentrations of fossil material in Willwood paleosols (e.g., FG016). Although surface, quarry, and wash collections represent different taphonomic modes and thus should be treated as different classes of samples in any faunal analysis (e.g., Clyde and Gingerich, 1998), all records are used irrespective of their taphonomic mode for purposes of documenting the biostratigraphy of these McCullough Peaks sections. Since biostratigraphy is based on presence/absence information, it is important to include all faunal information that is correlated to a stratigraphic section, no matter what its taphonomic history (unless, of course, the taphonomic history suggests that fossils are reworked or otherwise misplaced in the local stratigraphy, which is not the case here).

PROCEDURE

All fossil mammal material from each of the 255 correlated localities was examined and documented by the author in the following manner. Locality collections were inspected one by one, beginning with those in the southeast composite section and ending with those in the northwest composite section. Previously catalogued material from each locality as well as

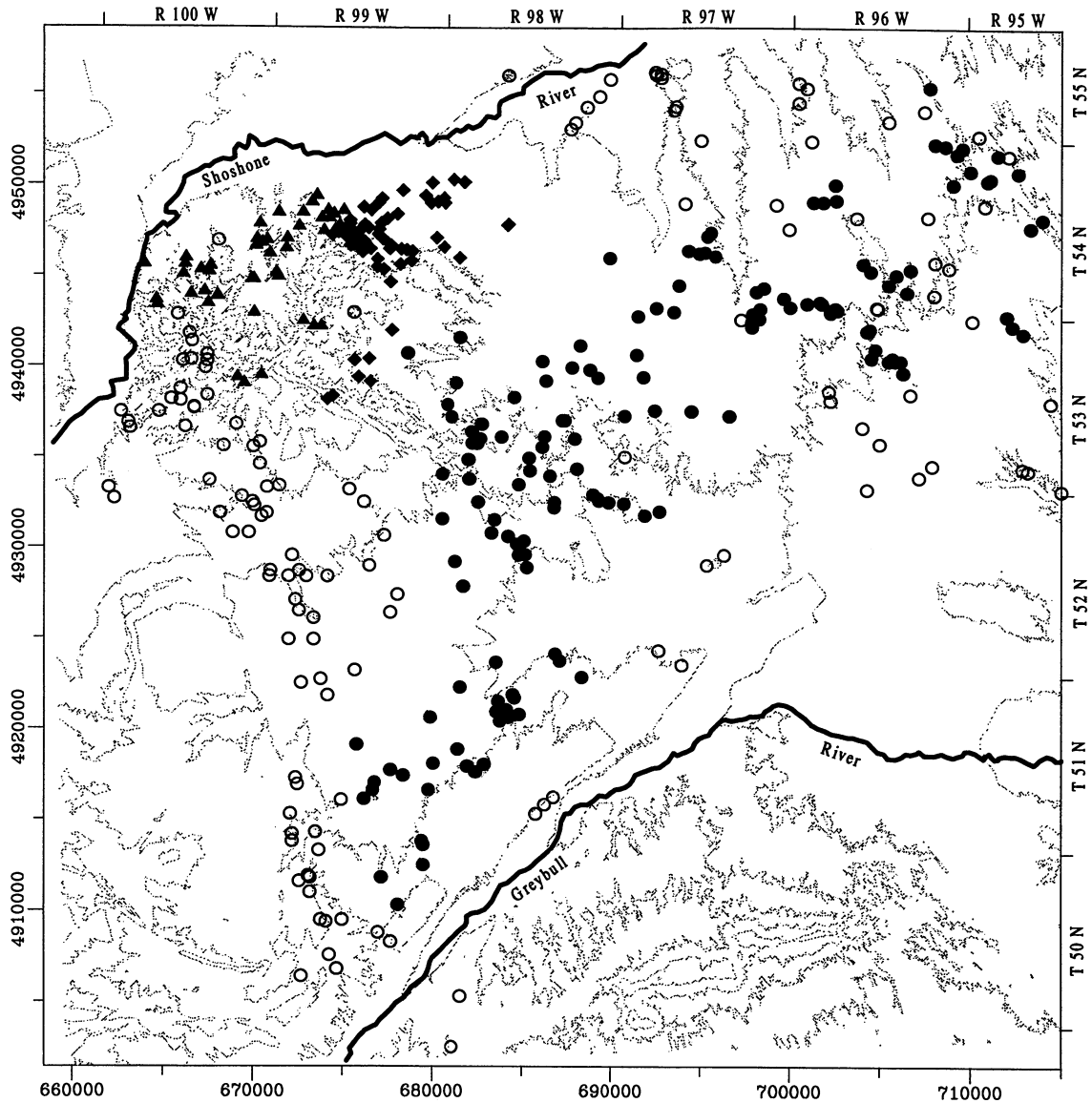


FIGURE 4 — Fossil locality map of McCullough Peaks field area. Open circles represent localities that have not been correlated to a stratigraphic section. Filled symbols represent localities that have been correlated to a stratigraphic section. Filled circles are localities correlated to the southeast composite section, filled diamonds are localities correlated to the central composite section, and filled triangles are localities correlated to the northwest composite section.

all isolated elements catalogued as “miscellaneous” were examined and measured using digital calipers. Isolated “miscellaneous” elements were identified through comparison with reference casts and specimens from the University of Michigan Museum of Paleontology collection. The identification of catalogued specimens was also checked and revised as needed. Each specimen was saved as a single record in a relational database that also included information on localities (stratigraphic level, location, formation, etc.) and taxa

(body mass, diet, systematics, etc.). Three localities (Cedar Point Quarry, Divide Quarry [FG046], and Croc Tooth Quarry [FG028]) that were correlated to stratigraphic sections were not examined, since much of this material is unavailable for study (on loan and/or generally dispersed from the collection) and requires a degree of attention beyond the scope of this study. These localities, however, have been well characterized elsewhere (Rose, 1981; Gingerich, unpublished data) so their faunal-zone identifications were used here. When catalogued

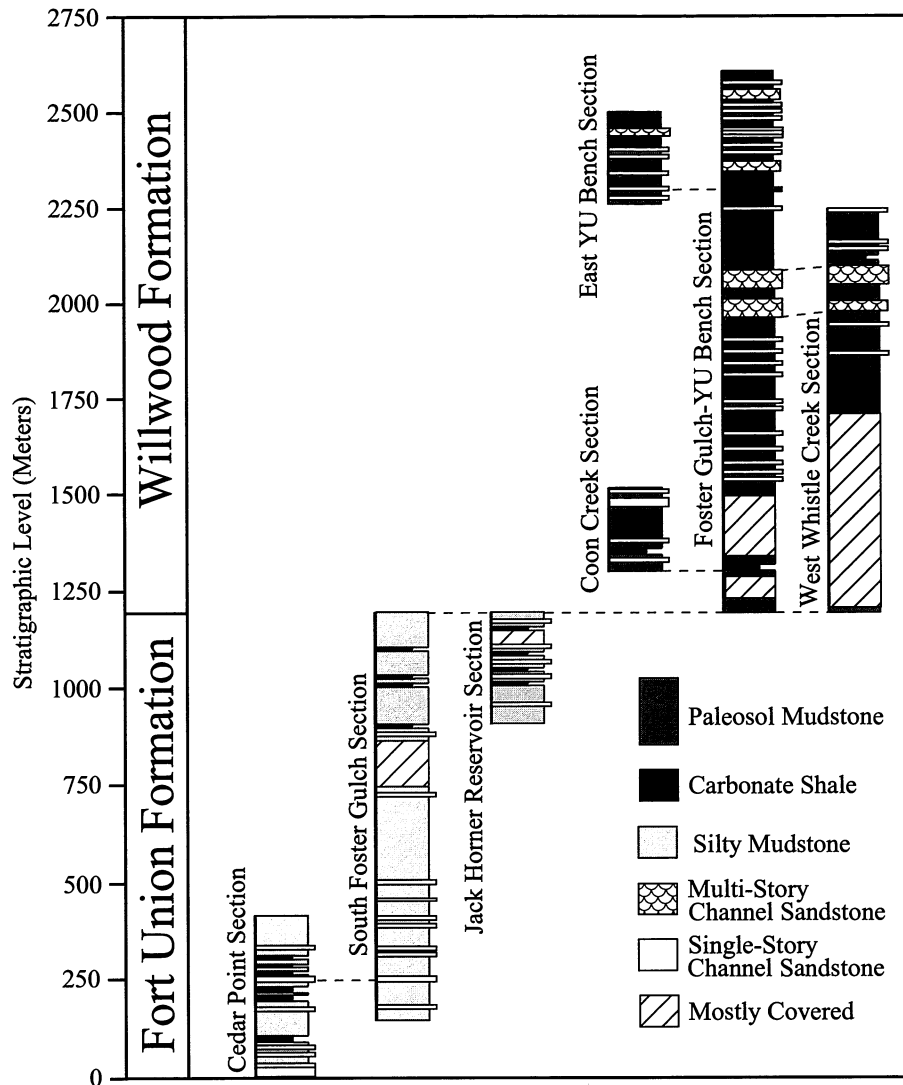


FIGURE 5 — Generalized lithology of local stratigraphic sections measured in the McCullough Peaks southeast composite section. Locations of sections are shown in Figure 2.

specimens were missing from the collection (e.g., on loan), the identification of that specimen in the University of Michigan Museum of Paleontology database was used and no measurements were recorded.

The taxonomy of many groups of fossil mammals is in a constant state of revision, making consistent identification among researchers difficult when dealing with whole assemblages of fossil taxa. Care was taken to use the most recent revision of taxonomic groups, especially when those revisions explicitly incorporated Bighorn Basin fossils. The long history of detailed systematic studies of Bighorn Basin fossil mammals has created an important network of taxonomic information conducive to rapid identification and naming of individual specimens. Without this network, and the laborious

research that went into developing it, a project like the one undertaken here would not have been possible.

RESULTS

Southeast Composite Section

The southeast composite section is the longest and most thoroughly sampled composite section in the study area. It consists of seven local stratigraphic sections that were measured, described and lithostratigraphically correlated to one another in the field (Fig. 5). A total of 151 fossil localities (with 8,364 fossil elements) have been correlated to these sections, representing 106 different stratigraphic levels. This

composite section spans the middle Tiffanian (Ti-3) through the late Wasatchian (Wa-7), making it one of the longest continuous Paleogene sections in the western interior of North America. Despite significant intervals of no exposure, all but one biostratigraphic zone between Ti-3 and Wa-7 are represented by at least some fossil material. Figure 6 shows a range chart of the southeast composite section and Table 1 provides the names for taxa numbered across the bottom of the figure. Constraints on the upper and lower bounds of different zones in this section are variable, with certain zonal boundaries poorly constrained to lie within a 250-meter interval (e.g., Ti-4 - Ti-5) and other zonal boundaries well constrained to lie within a 10-meter interval (e.g., Wa-2 - Wa-3).

Central Composite Section

The central composite section consists of three local stratigraphic sections and is entirely of Wasatchian age (Fig. 7). It preserves faunal zones Wa-1 through Wa-6, although no localities of Wa-5 are yet known. The lower part of the central composite section (Wa-1 through Wa-3) is well constrained biostratigraphically (i.e., many informative stratigraphic levels) whereas the upper part of the section (Wa-4 through Wa-6) is poorly resolved. A total of 61 localities has been correlated to this section (with 2,595 fossil elements), representing 38 stratigraphic levels. A range chart showing the stratigraphic distribution of all taxa known from the central composite section is shown in Figure 8 (see also Table 1).

Northwest Composite Section

The northwest composite section consists of 4 local stratigraphic sections and preserves sediments of Wa-2 through Wa-6 age (Fig. 7). Localities are known from each zone, although the lower half of the northwest composite section (Wa-2 to Wa-4) is better sampled than the upper half (Wa-5 to Wa-6). A total of 46 localities (preserving 2,213 fossil elements) from 30 stratigraphic levels has been correlated to this section. A range chart for this composite section is shown in Figure 9 (see also Table 1).

DISCUSSION

Comparison Between Sections

Boundaries between faunal zones represent the most practical fine-scale time lines available to correlate between sections. Lithologic correlation is very difficult over large distances in an asymmetric foreland basin like the Bighorn Basin, and magnetostratigraphic reversals during this part of

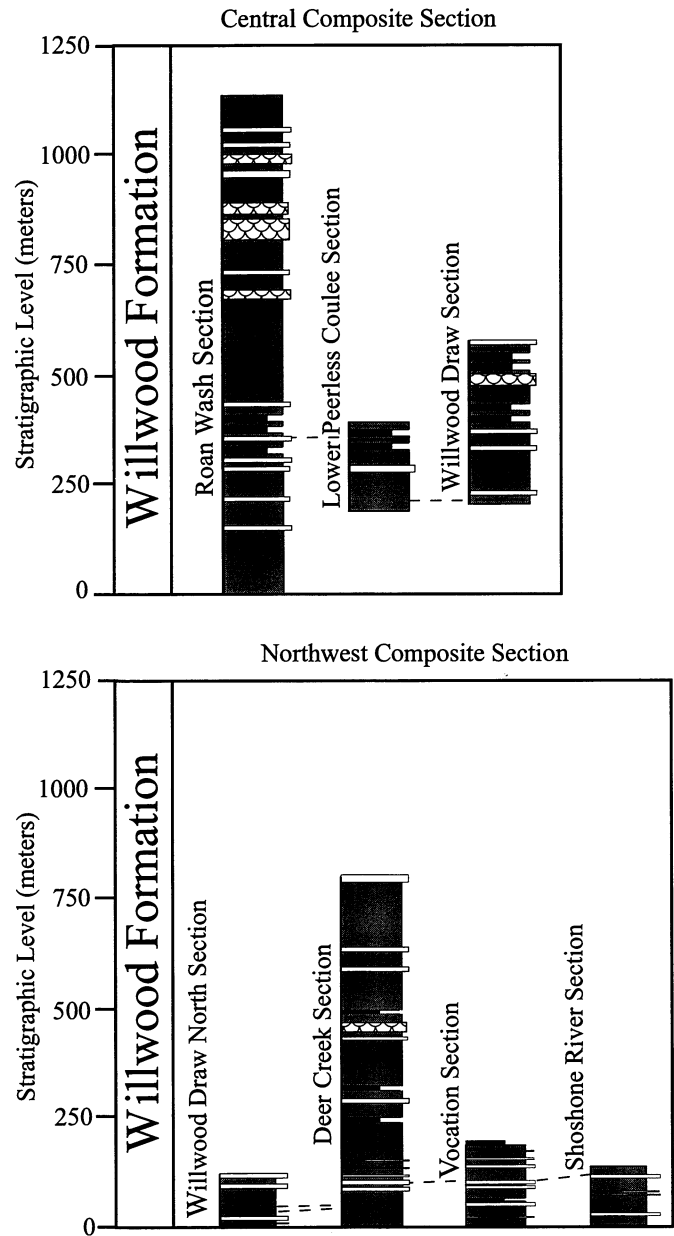


FIGURE 7 — Generalized lithology of local stratigraphic sections measured in the McCullough Peaks central (above) and northwest (below) composite sections. Legend is the same as Figure 5. Locations of sections are shown in Figure 2.

FIGURE 6 — Stratigraphic ranges of mammalian species from the southeast composite section of the McCullough Peaks. Open symbols indicate uncertain identification. Zone boundaries are interpolated between observed zone limits. Magnetostratigraphy is from Clyde et al. (1994, Clyde 1997). List of species and associated ID numbers are given in Table 1.

the time scale are generally less frequently distributed than faunal zone boundaries (Clyde et al., 1994). Using biostratigraphic events as time lines assumes that rates of dispersal outpace rates of sediment accumulation for the relevant taxa over the distance being considered. This assumption should always be tested by independent means, but it is generally accepted on the scale of a single basin.

Presently there are two well-documented lower Paleogene composite stratigraphic sections in the Bighorn Basin in addition to the ones discussed here. The first lies in the northernmost part of the Bighorn Basin and the adjacent Clarks Fork Basin (Gingerich, 1983, 1991, 2000, this volume). This 2,240-meter section begins in the Puercan land-mammal age (Pu-1; atop a locally conformable Cretaceous-Tertiary boundary) and extends up into the middle Wasatchian land-mammal age (Wa-5). Fossil assemblages are known from all intervening land mammal zones except Pu-2, Pu-3, To-1, To-2, and To-3. The second well-documented composite section lies south of the Greybull River, in the central and southern parts of the Bighorn Basin (Bown et al., 1994). Here, much of the section lies far from the basin axis, resulting in a condensed section. Faunally, however, this section is extremely well-sampled and well-documented (Bown et al., 1994). Although Paleocene sediments are present in this region, few mammalian fossil localities have been found in them. The composite section in this region spans the earliest Wasatchian (Wa-0) through the late Wasatchian (Wa-7).

Given the difficulty in making detailed lithostratigraphic correlations between distant sections in a highly asymmetric depositional settings like that of the Bighorn Basin, the zone boundaries represent a powerful tool for making intrabasinal stratigraphic comparisons. Figure 10 shows a fence diagram of the various composite sections from different parts of the Bighorn Basin. The most profound difference in zone thicknesses occurs between the southern Bighorn Basin section and those to the north. Interpolated zone thicknesses between the four northern Bighorn Basin sections are fairly consistent with one another, and are significantly greater than those in the southern Bighorn Basin. Stratigraphic levels of all zone boundaries are not available for the southern section because no review of perissodactyls has been published for this area. However, based on the boundaries that can be correlated, there is a clear thickening of zones to the north and west across the basin. The isopachous map of Bighorn Basin Tertiary deposits (Parker and Jones, 1986), shows this SE-NW thickening trend also, indicating a strong asymmetry in the depositional basin during this time. Gingerich (1983) documented a strong asymmetry in the Clark's Fork Basin, and the results presented here extend those observations to the rest of the Bighorn Basin.

Figure 11 shows graphic correlations between the McCullough Peaks southeast composite section and the other composite sections throughout the basin. All axes in these figures are shown to the same scale, so slopes greater than 1.0 indicate higher sediment accumulation rates in the local section compared to the reference section, and slopes less than 1.0 indicate lower sediment accumulation rates in the local section. Comparison between the Clarks Fork Basin section and the McCullough Peaks southeast composite section (MPSE) shows proportionally consistent zone thicknesses (i.e., little variation in slope). The slope here is also quite close to 1.0, suggesting very similar rates of sediment accumulation between

these sections. The comparison between the southern Bighorn Basin section and the MPSE section shows proportionally consistent zone thicknesses, but quite different average sediment accumulation rates. In this comparison, the slope is well below 1.0, indicating lower average sediment accumulation rates in the southern basin compared to the MPSE section. This further illustrates the depositional asymmetry present in the Bighorn Basin, with thinning of basin fill from northwest to southeast.

Comparing the McCullough Peaks central and northwest composite sections with the MPSE section, the central composite section seems to have the highest average sediment accumulation rates (Fig. 11). This would suggest that the basin axis during lower to middle Wasatchian time was slightly east of its present far western position, although the degree of measurement error involved here makes such a conclusion somewhat tenuous. Gingerich (1983) suggested that the structural axis of the Clarks Fork Basin moved rapidly westward during the Tiffanian and Clarkforkian. It is not clear how coupled the Clarks Fork Basin and Bighorn Basin structural centers were during this period, and it is possible that the timing and rate of westward axial migration in the Bighorn Basin proper was significantly different from that in the Clarks Fork Basin.

Detailed comparisons between the four northern Bighorn Basin sections show very consistent zone thicknesses during Tiffanian and Clarkforkian deposition, with slightly more variation in Wasatchian zone thicknesses (Fig. 10). Much of this variation can be attributed to interpolation error since, in many cases, zone boundaries are being interpolated over substantial vertical thicknesses (especially in the McCullough Peaks sections). However, this up-section increase in zone thickness variability could also be the result of changes in depositional style occurring at this time. For example, the transition from Fort Union to Willwood deposition may represent a change in the balance between sediment accumulation and basin subsidence. During Fort Union deposition, basin subsidence outpaced sediment flux, creating poorly drained depositional environments, and organic-rich, reduced sediments. As rates of sedimentation surpassed rates of subsidence during Willwood time, the fluvial system began to aggrade, floodplains became better drained, and sediments became more oxidized. This new aggradational system would impose greater variability in the geometry and availability of local depositional centers (through stream avulsion) than was present in the previous subsidence-dominated regime. Such variability in depositional geometry would be apparent in variable faunal-zone thicknesses and would result in more local stratigraphic discontinuities. Although further work will be required to more fully-constrain zone thicknesses from different parts of the basin, these preliminary results suggest that the lithological transition at the Fort Union-Willwood boundary reflects an important change in depositional style that has important implications for stratigraphic geometry and temporal completeness.

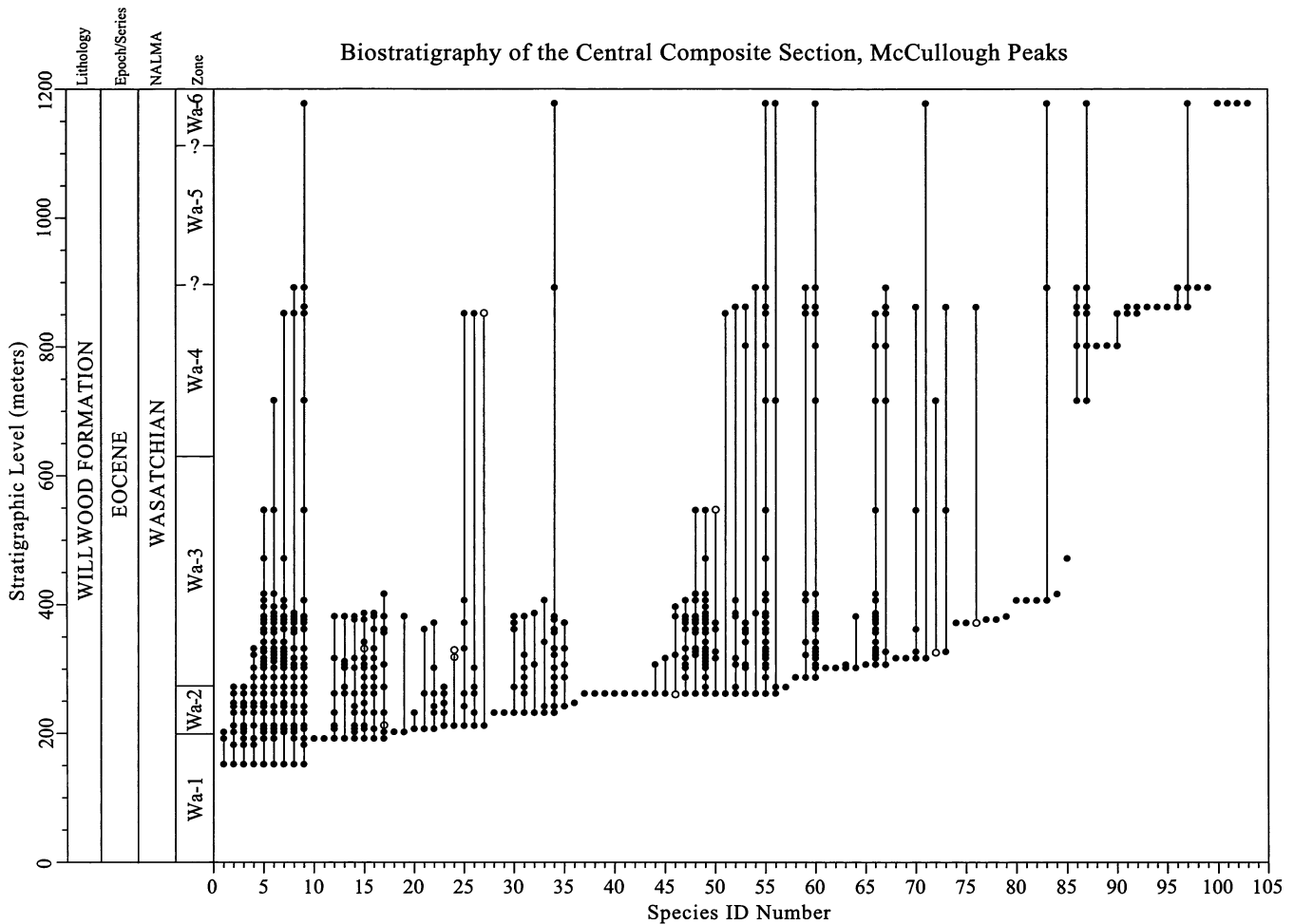


FIGURE 8 — Stratigraphic ranges of mammalian species from the central composite section of the McCullough Peaks. Open symbols indicate uncertain identification. Zone boundaries are interpolated between observed zone limits. List of species and associated ID numbers are given in Table 1.

Geochronology

Clyde et al (1994; see also Clyde, 1997) developed a magnetostratigraphic record for the Wasatchian part of the McCullough Peaks southeast composite section and proposed a correlation of this record to the Geomagnetic Polarity Time Scale (GPTS). More recently Wing et al. (2000) summarized existing geochronological constraints and developed two different age models for Bighorn Basin composite sections. Age model 1 from that study used the interpolated age estimates for paleomagnetic reversals from the most recent GPTS (Cande and Kent, 1995) as well as a 54.96 Ma age for the carbon isotope excursion (see Wing et al., 2000 for discussion of their age calculation for the carbon isotope excursion). Age model 2 used recalibrated age estimates for relevant paleomagnetic

reversals (by replacing the original 55.0 Ma age for Chron C24r[0.66] in Cande and Kent [1995] with an age of 52.8 for the base of Chron C24n.1n from Wing et al [1991]) and an age of 55.23 Ma for the carbon isotope excursion. Although there are stratigraphic uncertainties associated with each model, age model 2 has the advantage of being independent of the marine based GPTS timescale which is likely to be miscalibrated for this interval (Berggren and Aubry, 1998; Norris and Röhl, 1999; Wing et al. 2000). Using these age models in conjunction with the known levels of biostratigraphic zones from the McCullough Peaks southeast composite section and the Polecat Bench composite section (Gingerich, this volume), age estimates for faunal zone boundaries (Ti-2 through Wa-7) are possible (Tables 2 and 3). These age estimates will represent important geochronological reference points as we expand our detailed

TABLE 1 — List of species and corresponding identification numbers for the range charts presented in Figures 6, 8, 9. MPSE: McCullough Peaks southeast composite section (Fig. 6), MPC: McCullough Peaks central composite section (Fig. 8), MPNW: McCullough Peaks northwest composite section (Fig. 9).

Taxon	Section			Taxon	Section		
	MPSE	MPC	MPNW		MPSE	MPC	MPNW
<i>Aaptoryctes ivyi</i>	1			<i>Dipsalidictis transiens</i>	30		34
<i>Absarokius</i> sp.	140		90	<i>Dissacus longaevus</i>	23		
<i>Absarokius metoecus</i>	141	71		<i>Dissacus praenuntius</i>		38	73
<i>Absarokius abbotti</i>	158		95	<i>Dissacus</i> sp.		61	
<i>Absarokius noctivagus</i>	163			<i>Ectocion osbornianus</i>	5	8	5
<i>Acarictis?</i> sp.			77	<i>Ectocion parvus</i>	19		
<i>Acritoparamys atwateri</i>	26	35	56	<i>Ectoganus</i> sp.	18		
<i>Acritoparamys atavus</i>	61	37		<i>Ectoganus gliriformes</i>	87		66
<i>Alocodontulum atopum</i>	120			<i>Ectypodus tardus</i>	92		
<i>Anacodon ursidens</i>	136			<i>Esthonyx spatularius</i>	34	2	10
<i>Apatemys</i> sp.	135	77	42	<i>Esthonyx bisulcatus</i>	91	60	60
<i>Apatemys bellus?</i>	160			<i>Esthonyx grangeri</i>			32
<i>Apheliscus</i> sp.	10			<i>Galecyon? mordax</i>		65	
<i>Apheliscus chydaeus</i>	60	22	21	<i>Hapalodectes leptognathus</i>			17
<i>Apheliscus wapitiensis</i>	62	44		<i>Haplomylus speirianus</i>	44	5	6
<i>Apheliscus insidiosus</i>	110	91	74	<i>Haplomylus scottianus</i>	98	90	
<i>Arctodontomys wilsoni</i>	52		43	<i>Heptodon calciculus</i>	151		101
<i>Arfia zeke</i>	32	18		<i>Homogalax protapirinus</i>	90	55	38
<i>Arfia shoshoniensis</i>	53	23	23	<i>Hyopsodus loomisi</i>	36	6	7
<i>Arfia opisthotoma</i>	94	48		<i>Hyopsodus paucillus</i>	84	88	64
<i>Arfia</i> sp.			39	<i>Hyopsodus latidens</i>	96	67	
<i>Azygonyx</i> n. sp.	31			<i>Hyopsodus simplex</i>	124		84
<i>Bunophorus etsagicus</i>	128			<i>Hyopsodus powellianus</i>	134		103
<i>Bunophorus large</i> sp.	142		96	<i>Hyopsodus miticulus</i>	139		93
<i>Cantius ralstoni</i>	24	1		<i>Hyopsodus minor</i>	152	102	94
<i>Cantius mckennai</i>	71	7	14	<i>Hyopsodus lysitensis</i>	153	101	102
<i>Cantius trigonodus</i>	97	86		<i>Hyopsodus</i> sp.	154		
<i>Cantius abditus</i>	127	100	86	<i>Hyracotherium sandrae</i>	20		
<i>Cantius frugivorus</i>	159			<i>Hyracotherium grangeri</i>	22	3	1
<i>Cardiolphus radinskyi</i>	35	15	13	<i>Hyracotherium aemulor</i>	88	49	57
<i>Cardiolphus semihians</i>	126	83	97	<i>Hyracotherium cristatum</i>	101	97	91
<i>Carpolestes nigridentis</i>	8			<i>Hyracotherium pernix</i>	102	87	81
<i>Chriacus gallinae</i>	133		98	<i>Hyracotherium</i> sp.	105	56	
<i>Copecion brachypternus</i>	76	54	58	<i>Ignacius graybullianus</i>	75	19	12
<i>Copelemur feretutus</i>	162		99	<i>Labidolemur kayi</i>	43	39	
<i>Coryphodon eocaenus</i>	21	4	16	<i>Labidolemur</i> sp.	93	80	
<i>Coryphodon radians</i>	95	66		<i>Lambdotherium popoagicum</i>	164		
<i>Coryphodon</i> sp.		96	87	<i>Labidolemur serus</i>		84	78
<i>Coryphodon lobatus</i>	115	98	100	<i>Leipsanolestes siegfriedti</i>	122		31
<i>Coryphodon armatus</i>	118		85	<i>Leptacodon?</i> sp.	63		
<i>Diacodexis metsiacus</i>	42	9	8	<i>Miacis exiguus</i>	77	21	65
<i>Diacodexis robustus</i>	89	30	71	<i>Miacis deuschi</i>	85	40	20
<i>Didelphodus absarokae</i>	103	57	40	<i>Miacis</i> sp.	117	24	
<i>Didymictis leptomytus</i>	15		53	<i>Miacis petilus</i>	146		104
<i>Didymictis protenus</i>	47	59	28	<i>Miacis winkleri</i>		76	11
<i>Didymictis</i> sp.	116			<i>Microparamys cheradius</i>	123	28	

TABLE 1 (cont) — List of species and corresponding identification numbers for the range charts presented in Figures 6, 8, 9. MPSE: McCullough Peaks southeast composite section (Fig. 6), MPC: McCullough Peaks central composite section (Fig. 8), MPNW: McCullough Peaks northwest composite section (Fig. 9).

Taxon	Section			Taxon	Section		
	MPSE	MPC	MPNW		MPSE	MPC	MPNW
<i>Microparamys hunterae</i>	143			<i>Phenacodus intermedius</i>	16	34	15
<i>Microparamys</i> sp.	147	81		<i>Phenacodus trilobatus</i>	86	73	59
<i>Microsyops angustidens</i>	113	78	88	<i>Phenacolemur pagei</i>	3		
<i>Microsyops cardiorestes</i>	129			<i>Phenacolemur praecox</i>	33		
<i>Microsyops</i> sp.	137			<i>Phenacolemur simonsi</i>	45	75	79
<i>Microsyops latidens</i>	149		105	<i>Phenacolemur</i> sp.	46	50	45
<i>Microsyops knightensis</i>	165			<i>Phenacolemur citatus</i>	144		
<i>Neoliotomus ultimus</i>	17	20		<i>Plagiomene multicuspis</i>	106	70	80
<i>Niptomomys doreenae</i>	70			<i>Plesiadapis simonsi</i>	4		
<i>Niptomomys</i> sp.	78	58		<i>Plesiadapis gingerichi</i>	9		
<i>Niptomomys thelmae</i>	148			<i>Plesiadapis dubius</i>	13		
<i>Oxyaena gulo</i>	54	17	2	<i>Probathyopsis harrisorum</i>	10		
<i>Oxyaena intermedia</i>	99	32	44	<i>Probathyopsis praecursor</i>	14		
<i>Oxyaena forcipata</i>	100	99	106	<i>Prodiacodon</i> sp.	66		
<i>Oxyaena</i> sp.	104	12	30	<i>Prodiacodon tauricinerei</i>	67		
<i>Pachyaena ossifraga</i>	50	51	33	<i>Prolimnocyon atavus</i>	121	45	89
<i>Pachyaena gracilis</i>	55	64	49	<i>Prolimnocyon</i> sp.		68	
<i>Pachyaena gigantea</i>	130	41	48	<i>Prolimnocyon antiquus</i>	161		
<i>Pachyaena?</i> sp.	27	46	75	<i>Protictis</i> sp.		62	
<i>Palaeonodon</i> sp.	81		92	<i>Prototomus phobos</i>	37	13	52
<i>Palaeonodon nievelti</i>	112		25	<i>Prototomus deimos</i>	59		
<i>Palaeonodon ignavus</i>	125	52	22	<i>Prototomus martis</i>	72		54
<i>Palaeictops bicuspis</i>	58	63	72	<i>Prototomus robustus</i>	111	94	76
<i>Palaeonictis occidentalis</i>	38	36	36	<i>Prototomus secundarius</i>	131	103	108
<i>Palaeoryctes</i> sp.			9	<i>Prototomus</i> sp.	157	69	50
<i>Palaeosinopa incerta</i>	28	29	26	<i>Pseudotetonius ambiguus</i>	119		
<i>Palaeosinopa lutreola</i>	73	42		<i>Pyrocyon?</i> sp.		85	82
<i>Palaeosinopa</i> sp.	80	82	3	<i>Teilhardina americana</i>	74	33	55
<i>Palaeosinopa veterrima</i>	114	89	27	<i>Teilhardina tenuicula</i>	82		63
<i>Paramys taurus</i>	29	25	18	<i>Teilhardina crassidens</i>	109	43	67
<i>Paramys copei</i>	39	53	29	<i>Teilhardina?</i> sp.	138		51
<i>Paramys pycnus</i>	51			<i>Tetonius matthewi</i>	83	47	46
<i>Paramys large</i> sp.	57			<i>Thryptacodon antiquus</i>	25	14	24
<i>Paramys</i> sp.	79	31	61	<i>Tinimomys graybullensis</i>	68		
<i>Paramys</i> v. <i>large</i> sp.	132		107	<i>Tricentes</i> sp.	12		
<i>Paramys?</i> v. <i>large</i> sp.	155			<i>Tritemnodon strenuus</i>	145		
<i>Paramys delicatus?</i>		93		<i>Uintacyon rudis</i>	40		41
<i>Parectypodus lunatus</i>	64			<i>Vassacyon promicrodon</i>	107	92	68
<i>Parectypodus</i> sp.		74		<i>Viverravus politus</i>	49	11	35
<i>Parectypodus simpsoni</i>	108			<i>Viverravus acutus</i>	56	16	37
<i>Peradectes chesteri</i>	65			<i>Viverravus bowni</i>			69
<i>Peratherium marsupium</i>	156			<i>Viverravus rosei</i>	69	95	62
<i>Phenacodaptes</i> sp.	11			<i>Vulpavus australis</i>	41	27	47
<i>Phenacodus grangeri</i>	2			<i>Vulpavus canavus</i>			109
<i>Phenacodus</i> sp.	6	72	4	<i>Vulpavus</i> sp.			83
<i>Phenacodus vortmani</i>	7	26	19	<i>Vulpavus simplex</i>	150		
				<i>Wyolestes apheles</i>	48	79	70

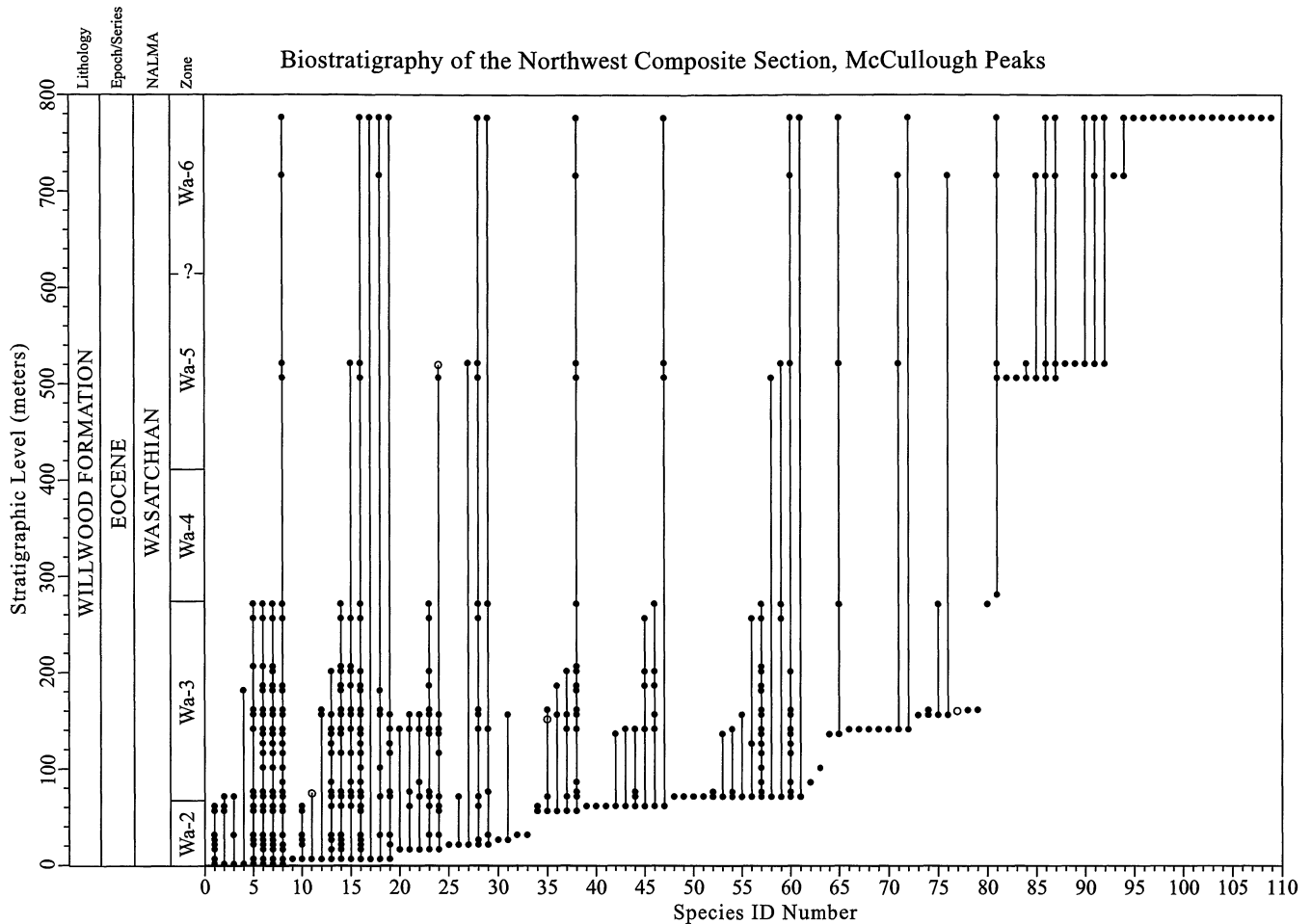


FIGURE 9 — Stratigraphic ranges of mammalian species from the northwest composite section of the McCullough Peaks. Open symbols indicate uncertain identification. Zone boundaries are interpolated between observed zone limits. List of species and associated ID numbers are given in Table 1.

understanding of Paleogene mammalian faunas to other continents.

SUMMARY

A total of 255 fossil localities preserving approximately 14,000 identifiable fossil mammal specimens from over 100 different stratigraphic levels provides a biostratigraphic framework for the McCullough Peaks area. Middle Tiffanian (Zone Ti-3) through late Wasatchian (Zone Wa-7) assemblages are preserved in superpositional relationship, making the McCullough Peaks one of the longest continuous stratigraphic sections in the North American Paleogene terrestrial record. The three composite sections in the study area vary in their degree of biostratigraphic precision. Comparison of

interpolated zone thicknesses show McCullough Peaks zones to be comparable in thickness to those in the Clarks Fork Basin, and significantly thicker than those in the southern Bighorn Basin. Zone thicknesses seem to be more variable during Willwood deposition, possibly due to geometric changes in accommodation space from the onset of the Willwood aggradational depositional regime. Magnetostratigraphic constraints on the biostratigraphic record from the McCullough Peaks and Polecat Bench provide absolute age estimates for Tiffanian (Paleocene) through Wasatchian (Eocene) faunal zones. This geochronological framework will be important for future intercontinental comparisons of the timing and magnitude of faunal turnover during this important period of earth history.

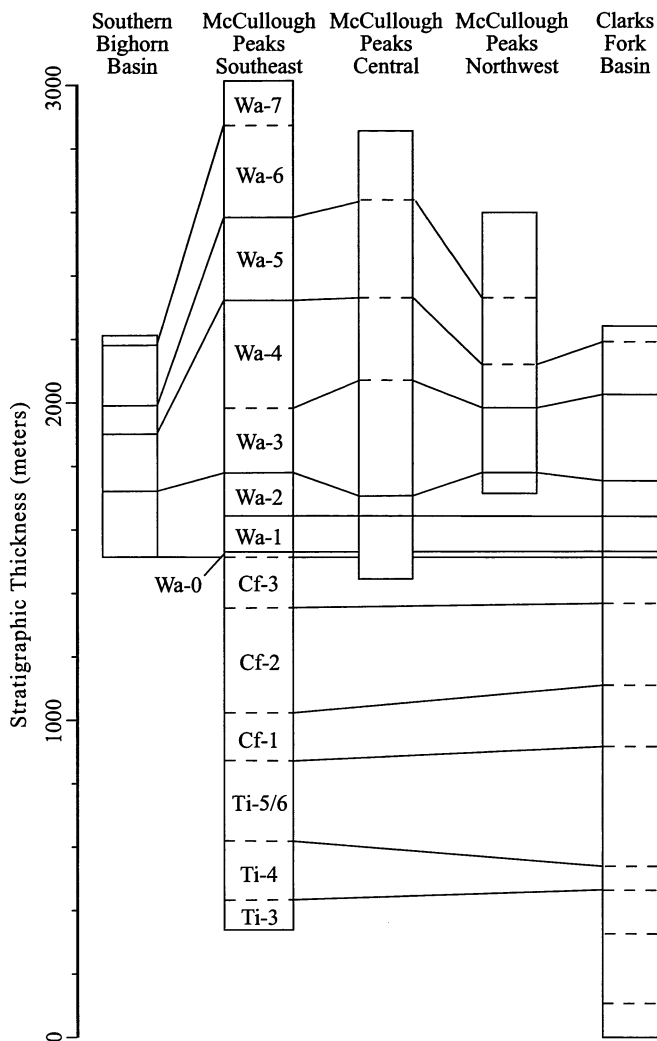


FIGURE 10 — Fence diagram showing thickness of biostratigraphic zones from different composite sections in the Bighorn Basin. Dashed lines at zone boundaries indicate relatively poor biostratigraphic control. Clarks Fork Basin stratigraphy is from Butler et al. (1981) and Gingerich (1991, this volume). Southern Bighorn Basin stratigraphy is from Bown and Rose (1987) and Bown et al. (1994). Notice the increase in zone thickness variability in the Wasatchian suggesting changes in depositional style during Willwood time compared to previous Fort Union time.

ACKNOWLEDGMENTS

Most of this research was carried out as part of my Ph.D. dissertation at the University of Michigan under the supervision of P. D. Gingerich. Thanks to G. F. Gunnell, J. I. Bloch, P. L. Koch, K. D. Rose, S. L. Wing for helpful feedback on various aspects of Bighorn Basin stratigraphy. I am indebted

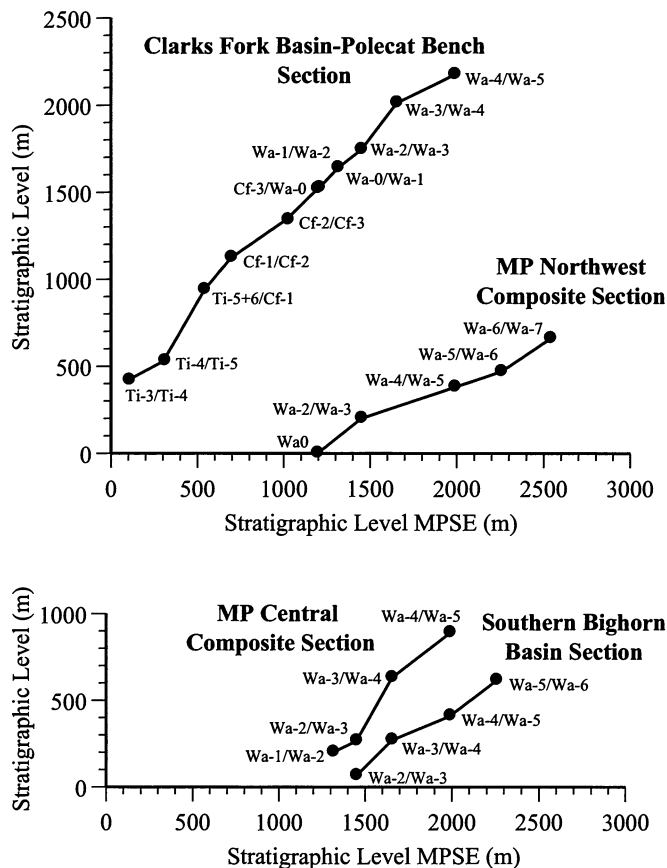


FIGURE 11 — *Top*: Graphic correlation comparing biostratigraphic boundaries of the Clarks Fork Basin-Polecat Bench section and Southern Bighorn Basin to the McCullough Peaks southeast composite section. Notice a slope of ~ 1 for the Clarks Fork Basin-Polecat Bench section (similar accumulation rates to the McCullough Peaks) but a slope significantly lower than 1 for the southern Bighorn Basin section (lower accumulation rates than McCullough Peaks). *Bottom*: Graphic correlation comparing McCullough Peaks central composite section and McCullough Peaks northwest composite section to the McCullough Peaks southeast composite section. Notice slopes close to 1 in each case indicating similar accumulation rates in all McCullough Peaks sections.

to Tom Churchill and his family for providing logistical support for field work. This research was supported by a Turner Award from the University of Michigan Department of Geological Sciences, a Geological Society of America Research Grant, a Grant-in-Aid from the Society of Sigma Xi, and a J. David Love Fellowship from the Wyoming Geological Association.

TABLE 2 — Calibration points for age models used here to estimate absolute ages of biostratigraphic zone boundaries. Age model 1 uses magnetic polarity reversal ages from Cande and Kent (1997) and an estimated age for the carbon isotope excursion from Norris and Rohl (1999) and Wing et al. (2000). Age model 2 uses recalibrated ages from Wing et al. (2000).

Calibration Point	Section	Level	Age Model 1	Age Model 2
Chron C24N.1r/C24N.2n	MPSE	2510	52.76	52.91
Chron C24N.2n/C24N.2r	MPSE	2445	52.80	52.96
Chron C24N.2r/C24N.3n	MPSE	2410	52.90	53.07
Chron C24N.3n/C24R	MPSE	2100	53.35	53.56
Carbon Isotope Excursion	MPSE /CFB	1195/1520	54.96	55.23
Chron C24R/C25N	CFB	1059	55.90	56.22
Chron C25N/C25R	CFB	830	56.39	56.69
Chron C25R/C26N	CFB	489	57.55	57.79
Chron C26N/C26R	CFB	400	57.91	58.13

TABLE 3 — Estimated absolute ages for faunal zones Ti-2 to Wa-7. Age model 1 and 2 use different calibration points (see Table 2 and Wing et al., 2000). Stratigraphic levels are from this paper and from Gingerich (2000; see also this volume) and are interpolated between sampling gaps.

Faunal Zone	Levels	Section	Age Model 1	Age Model 2
Wa-7	2540 - ?	MPSE	52.71 - ?	52.71 - ?
Wa-6	2257 - 2540	MPSE	53.12 - 52.71	53.32 - 52.86
Wa-5	2000 - 2257	MPSE	53.53 - 53.12	53.75 - 53.32
Wa-4	1655 - 2000	MPSE	54.14 - 53.53	54.39 - 53.75
Wa-3	1450 - 1655	MPSE	54.51 - 54.14	54.76 - 54.39
Wa-2	1315 - 1450	MPSE	54.75 - 54.51	55.01 - 54.76
Wa-1	1205 - 1315	MPSE	54.94 - 54.75	55.22 - 55.01
Wa-0	1195-1205/1515-1525	MPSE /CFB	54.96 - 54.94	55.23 - 55.22
Cf-3	1335 - 1515	CFB	55.34 - 54.96	55.63 - 55.23
Cf-2	1140 - 1335	CFB	55.74 - 55.34	56.04 - 55.63
Cf-1	935 - 1140	CFB	56.17 - 55.74	56.47 - 56.04
Ti-6	815 - 935	CFB	56.42 - 56.17	56.72 - 56.47
Ti-5	510 - 815	CFB	57.48 - 56.42	57.72 - 56.72
Ti-4	425 - 510	CFB	57.81 - 57.48	58.03 - 57.72
Ti-3	280 - 425	CFB	58.39 - 57.81	58.58 - 58.03
Ti-2	290 - 280	CFB	? - 58.39	? - 58.58

LITERATURE CITED

- ARCHIBALD, J. D., P. D. GINGERICH, E. H. LINDSAY, W. A. CLEMENS, D. W. KRAUSE, and K. D. ROSE. 1987. First North American Land-mammal Ages in the Cenozoic Era. *In*: M. O., Woodburne (ed.), *Cenozoic mammals of North America: geochronology and biostratigraphy*. University of California Press, Berkeley, pp. 24-76.
- BADGLEY, C., W. S. BARTELS, M. E. MORGAN, A. K. BEHRENSMEYER, and S. M. RAZA. 1995. Taphonomy of vertebrate assemblages from the Paleogene of northwestern Wyoming and the Neogene of northern Pakistan. *Palaeogeography, Palaeoclimatology, Palaeoecology*, 115: 157-180.
- BERGGREN, W. A. and M.-P. AUBRY. 1998. The Paleocene-Eocene Epoch/Series Boundary: Chronostratigraphic Framework and Estimated Geochronology. *In*: M.-P. Aubry, S. G. Lucas, and W.

- A. Berggren (eds.), Late Paleocene-Early Eocene Climatic and Biotic Events in the Marine and Terrestrial Records, Columbia University Press, New York, pp. 18-36.
- BERGGREN, W. A., D. V. KENT, C. C. SWISHER, and M.-P. AUBRY. 1995. A revised Cenozoic geochronology and chronostratigraphy. *In*: W. A. Berggren, D. V. Kent, M.-P. Aubry, and J. Hardenbol (eds.), Geochronology, time scales and global stratigraphic correlation, SEPM (Society for Sedimentary Geology) Special Publication, 54: 129-212.
- BOWN, T. M. 1979. Geology and mammalian paleontology of the Sand Creek facies, lower Willwood Formation (lower Eocene), Washakie County, Wyoming. Geological Survey of Wyoming Memoir, 2: 1-151.
- BOWN, T. M. and M. J. KRAUS. 1993. Time-stratigraphic reconstruction and integration of paleopedologic, sedimentologic, and biotic events (Willwood Formation, lower Eocene, northwest Wyoming, U.S.A.). *Palaios*, 8: 68-80.
- BOWN, T. M. and K. D. ROSE. 1987. Patterns of dental evolution in early Eocene Anaptomorphine Primates (Omomyidae) from the Bighorn Basin, Wyoming. *Journal of Paleontology*, Memoir, 23: 1-162.
- BOWN, T. M., K. D. ROSE, E. L. SIMONS, and S. L. WING. 1994. Distribution and stratigraphic correlation of upper Paleocene and lower Eocene fossil mammal and plant localities of the Fort Union, Willwood, and Tatman formations, southern Bighorn Basin, Wyoming. U.S. Geological Survey Professional Paper, 1540: 1-103.
- BUTLER, R. F., P. D. GINGERICH, and E. H. LINDSAY. 1981. Magnetic polarity stratigraphy and biostratigraphy of Paleocene and lower Eocene continental deposits, Clarks Fork Basin, Wyoming. *Journal of Geology*, 89: 299-316.
- CANDE, S. C. and D. V. KENT. 1995. Revised calibration of the geomagnetic polarity time scale for the Late Cretaceous and Cenozoic. *Journal of Geophysical Research*, 100: 6093-6095.
- CLYDE, W. C. 1997. Stratigraphy and mammalian paleontology of the McCullough Peaks, northern Bighorn Basin, Wyoming: Implications for biochronology, basin development, and community reorganization across the Paleocene-Eocene boundary. Ph.D. Dissertation. University of Michigan, 256 pp.
- CLYDE, W. C. and P. D. GINGERICH. 1998. Mammalian community response to the latest Paleocene thermal maximum: An isotaphonomic study in the northern Bighorn Basin, Wyoming. *Geology*, 26: 1011-1014.
- CLYDE, W. C., N. D. SHELDON, P. L. KOCH, G. F. GUNNELL, and W. S. BARTELS. 2001. Linking the Wasatchian-Bridgerian boundary to the Cenozoic Global Climate Optimum: new magnetostratigraphic and isotopic results from South Pass, Wyoming. *Palaeogeography, Palaeoclimatology, Palaeoecology*, 167:175-199.
- CLYDE, W. C., J. STAMATAKOS, and P. D. GINGERICH. 1994. Chronology of the Wasatchian Land-Mammal Age (early Eocene): Magnetostratigraphic results from the McCullough Peaks section, northern Bighorn Basin, Wyoming. *Journal of Geology*, 102: 367-377.
- FRICKE, H. C., W. C. CLYDE, J. R. O'NEIL, and P. D. GINGERICH. 1998. Evidence for rapid climatic change in North America during the latest Paleocene thermal maximum: oxygen isotope compositions of biogenic phosphate from the Bighorn Basin (Wyoming). *Earth and Planetary Science Letters*, 160: 193-208.
- GINGERICH, P. D. 1976. Cranial anatomy and evolution of early Tertiary Plesiadapidae (Mammalia, Primates). *University of Michigan Papers on Paleontology*, 15: 1-141.
- GINGERICH, P. D. 1980. History of early Cenozoic vertebrate paleontology in the Bighorn Basin. *In*: P. D. Gingerich (ed.), Early Cenozoic paleontology and stratigraphy of the Bighorn Basin, Wyoming. *University of Michigan Papers on Paleontology*, 24: 7-24.
- GINGERICH, P. D. 1983. Paleocene-Eocene faunal zones and a preliminary analysis of Laramide structural deformation in the Clark's Fork Basin, Wyoming. Thirty-Fourth Annual Field Conference, Wyoming Geological Association Guidebook, 34: 185-195.
- GINGERICH, P. D. 1991. Systematics and evolution of early Eocene Perissodactyla (Mammalia) in the Clarks Fork Basin, Wyoming. *Contributions from the Museum of Paleontology, University of Michigan*, 28: 181-213.
- GINGERICH, P. D. 1989. New earliest Wasatchian mammalian fauna from the Eocene of northwestern Wyoming: Composition and diversity in a rarely sampled high-floodplain assemblage. *University of Michigan Papers on Paleontology*, 28: 1-97.
- GINGERICH, P. D. 2000. Paleocene-Eocene boundary and continental vertebrate faunas of Europe and North America. *GFF*, 122: 57-59.
- GRANGER, W. 1914. On the names of lower Eocene faunal horizons of Wyoming and New Mexico. *Bulletin of the American Museum of Natural History*, 33: 201-207.
- KOCH, P. L., J. C. ZACHOS, and P. D. GINGERICH. 1992. Correlation between isotope records in marine and continental carbon reservoirs near the Palaeocene-Eocene boundary. *Nature*, 358: 319-322.
- KRAUS, M. J. 1992. Alluvial response to differential subsidence: sedimentological analysis aided by remote sensing, Willwood Formation (Eocene), Bighorn Basin, Wyoming, USA. *Sedimentology*, 39: 455-470.
- NORRIS, R. D. and U. RÖHL. 1999. Carbon cycling and chronology of climate warming during the Palaeocene-Eocene transition. *Nature*, 401: 775-778.
- NORTH AMERICAN COMMISSION ON STRATIGRAPHIC NOMENCLATURE (1982). 1983. North American stratigraphic code. *Bulletin of the American Association for Petroleum Geologists*, 65: 841-875.
- PARKER, S. E. and R. W. JONES. 1986. Isopachous map of Tertiary overburden above latest Cretaceous Lance Formation, Bighorn Basin, Wyoming. Geological Survey of Wyoming Open File Report, 86-8.
- PROTHERO, D. R. 1995. Geochronology and Magnetostratigraphy of Paleogene North American land mammal "ages". *In*: W. A. Berggren, D. V. Kent, M.-P. Aubry, and J. Hardenbol, Geochronology, time scales and global stratigraphic correlation. SEPM (Society of Sedimentary Geologists), Tulsa, OK, pp. 295-315.
- ROSE, K. D. 1981. The Clarkforkian land-mammal age and mammalian faunal composition across the Paleocene-Eocene boundary. *University of Michigan Papers on Paleontology*, 26: 1-196.

- SCHANKLER, D. M. 1980. Faunal zonation of the Willwood Formation in the central Bighorn Basin, Wyoming. *In*: P. D. Gingerich (ed.), Early Cenozoic paleontology and stratigraphy of the Bighorn Basin, Wyoming. University of Michigan Papers on Paleontology, 24:99-114.
- WING, S. L. 1980. Fossil floras and plant-bearing beds of the central Bighorn Basin. *In*: P. D. Gingerich (ed.), Early Cenozoic Paleontology and Stratigraphy of the Bighorn Basin, Wyoming. University of Michigan Papers on Paleontology, 24:119-125.
- WING S. L. 1998. Paleocene-Eocene floral change in the Bighorn Basin, Wyoming. *In*: M.-P. Aubry, S. Lucas, and W.A. Berggren (eds.), Late Paleocene-early Eocene climatic and biotic evolution. Columbia University Press, New York, pp. 380-400.
- WING, S. L., H. BAO, and P. L. KOCH. 2000. An early Eocene cool period? Evidence for continental cooling during the warmest part of the Cenozoic. *In*: B. T. Huber, K. MacCleod, and S. L. Wing, Warm Climates in Earth History, Cambridge University Press, Cambridge, pp. 197-237.
- WING, S. L., T. M. BOWN, and J. D. OBRADOVICH. 1991. Early Eocene biotic and climatic change in interior western North America. *Geology*, 19: 1189-1192.
- WOOD, H. E., R. W. CHANEY, J. CLARK, E. H. COLBERT, G. L. JEPSSEN, J. B. REESIDE, and C. STOCK. 1941. Nomenclature and correlation of the North American continental Tertiary. *Geological Society of America Bulletin*, 52:1-48.
- WOODBURNE, M. O. (ed.). 1987. Cenozoic Mammals of North America; Geochronology and Biostratigraphy. University of California Press, Berkeley, 336 pp.
- WOODBURNE, M. O. and C. C. SWISHER. 1995. Land mammal high-resolution geochronology, intercontinental overland dispersals, sea level, climate, and vicariance. *In*: W.A. Berggren, D. V. Kent, M.-P. Aubry, and J. Hardenbol, Geochronology, Time Scales and Global Stratigraphic Correlation. SEPM (Society of Sedimentary Geologists), Tulsa, OK, pp. 335-364.

NEW WA-0 MAMMALIAN FAUNA FROM CASTLE GARDENS IN THE SOUTHEASTERN BIGHORN BASIN

SUZANNE G. STRAIT

Department of Biological Sciences, Marshall University, Huntington, West Virginia 25755

Abstract.— An important new Wa-0 locality, Castle Gardens, was discovered in 1992 in the Honeycombs area of the southeastern Bighorn Basin of Wyoming. This is the first Wa-0 site that has proven amenable to screen-washing, and is unique among sites of this age in yielding a more diverse representation of smaller mammalian species. The 314 mammalian specimens from Castle Gardens reported here represent 27 genera and 29 species, including one new species of *Niptomomys*.

INTRODUCTION

The earliest Wasatchian was a time of great evolutionary and climatic change. This period, either associated or correlated with the Paleocene-Eocene boundary, has been recognized as contemporaneous with the most significant climatic event of the Cenozoic (see volumes edited by Aubry et al., 1998, and Schmitz et al., 2000). Warming resulted in global changes in both marine and terrestrial biotas (Bujak and Brinkhius, 1998; Dockery, 1998; Gunnell, 1998; Hutchison, 1998; Wing, 1998; Boyd, 2000; Holroyd and Hutchison, 2000). Among mammals it was a time of substantial faunal change due to both dispersal and evolution (Rose, 1981; Gingerich, 1989, 2000; Maas et al., 1995; Gunnell, 1998; Hooker, 1998; Lucas, 1998). For example, the beginning of the Wasatchian land-mammal age marks the first appearance of several modern mammalian ordinal-level groups in North America (e.g., Artiodactyla, hyaenodontid Creodonta, Perissodactyla, and Primates) that probably dispersed here from other regions. Other mammals of modern aspect, including rodents, chiropterans, marsupials, carnivorans, and lipotyphlans, are also known from the Wasatchian. Nearly all the orders of mammals found later in North America's Cenozoic history appeared on the continent by this time.

The earliest mammal-bearing stratigraphic level of the Wasatchian, referred to as Wa-0, is known from several areas

in the Bighorn Basin (Gingerich, 1989, this volume; Wing, 1998; K. D. Rose and T. M. Bown, pers. comm.), and from the southern Powder River Basin (Thewissen, 1990; Robinson and Williams, 1997). However, the relatively small number of localities found to date and low fossil concentrations within most of these, mean that much remains to be learned about this crucial interval in mammalian evolution. In 1992, while exploring Paleocene-Eocene sediments in the Honeycombs area of the southeastern Bighorn Basin, Wyoming, a new Wa-0 locality was discovered (here called Castle Gardens, UCMP locality V99019 or USGS locality D2018).

Fossils at Castle Gardens were recovered from a ca. 10 meter thick layer of light gray mudstone with drab orange mottling in the SW¼, Section 18, Township 46 North, Range 89 West, Washakie County, Wyoming (Fig. 1). Wa-0 fossils have been found at adjacent localities, laterally equivalent and to the east of Castle Gardens: Scorpion Knob, UCMP V99191; and Coryphodon Place, UCMP V99192 (see Fig. 2 in Holroyd et al., this volume). These do not have the substantial concentrations of fossils found at the main locality.

In the southeastern Bighorn Basin the base of the Willwood Formation is distinguished from the underlying Fort Union Formation by the first conspicuous and persistent red mudstones (Bown, 1979). All prior Wa-0 mammalian specimens from the southeastern Bighorn Basin were collected from this distinctive stratigraphic interval (Gingerich, 1989; Wing et al., 1991; Wing, 1998). Castle Gardens is in the Fort Union Formation just below this contact, and therefore appears to be stratigraphically lower than other Wa-0 localities in the area.

In: Paleocene-Eocene Stratigraphy and Biotic Change in the Bighorn and Clarks Fork Basins, Wyoming (P. D. Gingerich, ed.), *University of Michigan Papers on Paleontology*, 33: 127-143 (2001).

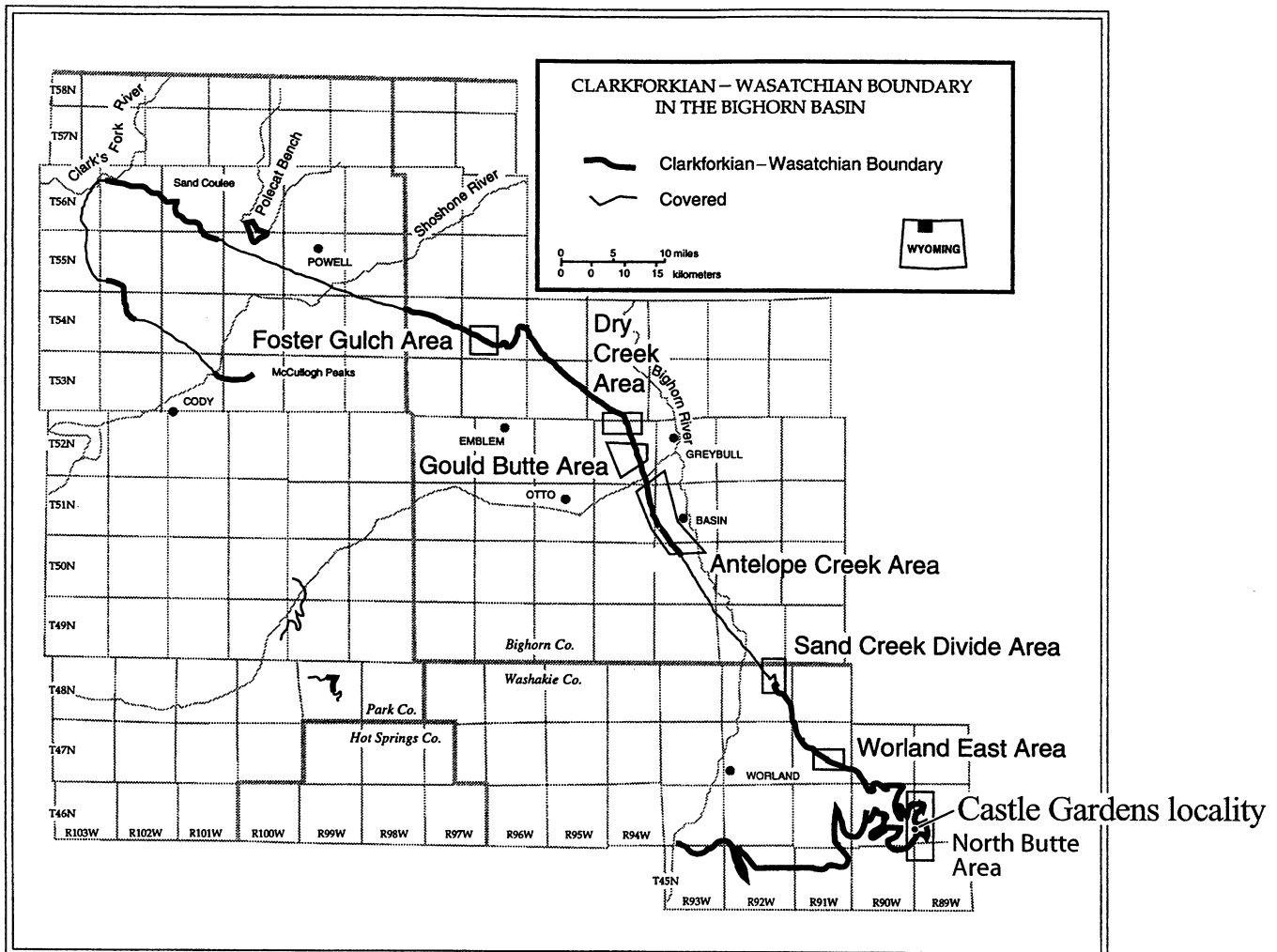


FIGURE 1 — Clarkforkian-Wasatchian boundary in the Bighorn Basin, showing the Castle Gardens locality. Redrawn from Gingerich (1989) and Wing (1998).

At the same time, it has typical Wasatchian first-appearance taxa such as *Hyracotherium* and hyaenodontids. The Wa-0 index fossil *Copecion davisii* is abundant. Several other rarer forms that are only known from Wa-0 localities (e.g., *Arfia junnei*, *Thryptacodon barae*, and *Chriacus badgleyi*) have also been found at Castle Gardens, further confirming a Wa-0 age for this site. It is worth noting that since the Castle Gardens locality is at the top of a ridge (Fig. 2), there is no possibility of contamination from higher layers, a concern with some localities in the northern Bighorn and Clarks Fork basins (Gingerich, 1989, and this volume).

Castle Gardens has been profitably surface collected, quarried, and screen-washed.

Thus far, a partial skeleton with associated maxilla of *Copecion davisii* has been removed intact from a quarry layer (K. D. Rose, this volume). Another fossiliferous layer appears to be conducive to screen-washing. Neither quarrying nor

screen-washing has been productive at other Wa-0 localities. Most Wa-0 fossils have been collected by surface-prospecting (Gingerich, 1989). Surface collections systematically under-represent small mammals. Missing from published Wa-0 accounts are many of the smallest mammals and other microvertebrates that are efficiently recovered through screen-washing (McKenna et al., 1994; Cifelli et al., 1996).

Gingerich (1989) screen-washed approximately one ton of sandstone in his most productive locality (SC-67) and recovered only 12 identifiable teeth or tooth fragments. The deposits at Castle Gardens are much more amenable to screen-washing techniques. During the summer of 1999 one ton of matrix from this locality was collected and screen-washed, yielding 175 identifiable dental specimens. Screen-washing was carried out using commercially-available window screen (18 mesh or 1 mm diameter openings). The original ton of matrix broke down to approximately 270 lbs. of



FIGURE 2 — Marshall University field crew collecting matrix for screen-washing from the top of the Castle Gardens locality (UCMP V99019; USGS D2018).

concentrate. This concentrate was sorted in the lab, and then rewashed through 10 (2.0 mm) and 35 (500 μm) mesh sieves.

Dental measurements and terminology follow Gingerich (1983), Gingerich and Winkler (1985), Krause (1982, 1987), Novacek (1976), and Thewissen (1990). Abbreviations used in the text include *L*, maximal anteroposterior length; *W*, maximal buccolingual width; *AW*, maximal buccolingual width across the trigonid; *PW*, maximal buccolingual width across the talonid. Higher-level taxonomy follows McKenna and Bell (1997).

Institutional abbreviations include: JHU— Johns Hopkins University, Baltimore; UCMP— University of California Museum of Paleontology, Berkeley; USGS— United States Geological Survey, Denver.

RESULTS

Sporadic collecting during 1992 and 1998, and a more concentrated effort by a Marshall University field crew during 1999 yielded a collection of over 300 Wa-0 specimens from Castle Gardens and vicinity. All specimens described below are from the main Castle Gardens locality, unless specifically noted (e.g., for *Ectoganus* and *Coryphodon*). A JHU/USGS field party also briefly visited Castle Gardens in 1994, but these specimens are not included in this paper. To date, 29 species from 27 genera

have been identified from dental remains (the postcrania have yet to be systematically examined). Non-vertebrate material from Castle Gardens is minimal. The only fossil plant material thus far recovered is a single *Celtis phenacodorum* seed, and no invertebrates have been found. Non-mammalian vertebrate fossils include fish (*Lepisosteus* sp. and *Amia* sp.), lizards, turtles (Holroyd et al., this volume), alligatorids (*Borealosuchus* sp.; J. H. Hutchison, pers. comm.), and the first frog known from the earliest Wasatchian.

SYSTEMATIC PALEONTOLOGY

Class MAMMALIA
Order MULTITUBERCULATA
Family PTILODONTIDAE
Subfamily NEOPLAGIAULACINAE

Ectypodus tardus (Jepsen, 1940)
Figure 3, Table 1

Referred specimens.— UCMP 212562, 212591, 212625, 212629, 212671, 212804, and tentatively 212449, 212508, 212539, 212573, 212587, 212589, 212735-212737, 212739, 212742, 212773, 212807, 212812.

Description.— This sample includes a total of 20 specimens, representing a minimum of eight individuals. Although the

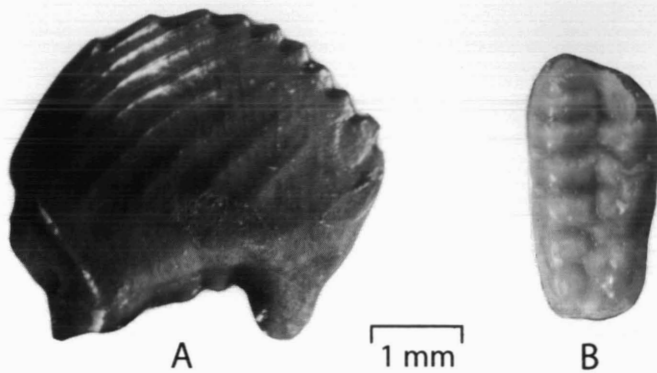


FIGURE 3 — Teeth of *Ectypodus tardus*. A, left P₄, UCMP 212591, in buccal view. B, right M₁, UCMP 212587, in occlusal view.

majority of these specimens were recovered from screen-washing ($n = 17$), some were surface collected, including the first tooth found at this locality (UCMP 212449). These specimens most closely match *Ectypodus tardus*, although it is often difficult to differentiate *E. tardus* from *Parectypodus lunatus* (Krause, 1982). *Ectypodus tardus* and *P. lunatus* are known to have lived sympatrically at some post-Wa-0 Wasatchian sites, and differentiation between the two taxa on isolated teeth other than lower fourth premolars must be considered tentative (Krause, 1982). In *E. tardus*, the lower fourth premolars are smaller and lower crowned. Taxonomic assignment of other tooth positions are based mainly on size (*E. tardus* is generally smaller), and are therefore less robust as there is much size overlap between the two species.

Of the thirteen P₄s known from the locality, only four were complete enough (UCMP 212562, 212591, 212629, 212671) for camera lucida drawing of labial profiles to be made (following Krause, 1982). There is no indication of bimodality in this sample, and all are relatively small and low crowned. Therefore they are allocated to *E. tardus*. Based on qualitative examinations of size and shape, all fragmentary plagiaulacoid blades are also provisionally allocated to *E. tardus*. Also known from the lower dentition are two complete M₁s (UCMP 212573, 212587). The size and cusp counts are within the typical range for both *E. tardus* and *P. lunatus*. The maxillary dentition is represented by isolated teeth from two tooth positions. Two complete M₁s have been recovered. One specimen (UCMP 21625) is smaller than any described *P. lunatus*, while the other (UCMP 212735) is within the range of either species. Based on size, a single P₄ (UCMP 212804) is allocated to *E. tardus*.

Discussion.— *Ectypodus tardus* is restricted to the Wasatchian (Krause, 1982) and has been previously described from another Wa-0 locality (SC-67; Gingerich, 1989). However, only P₄s have been previously known from this stratigraphic level. The screen washing at Castle Gardens has resulted in the first record of other tooth positions (i.e., M₁, P₄, M₁).

TABLE 1 — Measurements, serration counts, and cusp formulae for nine specimens of *Ectypodus tardus* from Castle Gardens. Abbreviations: C, cusp formula; L, crown length; S, serration count; W, crown width.

Tooth position		N	Range	Mean	Std. Dev.
<i>Upper dentition</i>					
P ₄	L	1	2.0	-	-
	W	1	0.9	-	-
	C	1	3:6	-	-
M ₁	L	2	2.0 - 2.4	2.20	-
	W	2	1.1 - 1.2	1.15	-
	C	2	7 : 8-9 : 4-7	7 : 8.5 : 5.5	-
<i>Lower dentition</i>					
P ₄	L	4	2.5 - 2.7	2.63	0.10
	W	4	0.9 - 1.0	0.93	0.05
	S	4	6 - 8	7.50	1.00
M ₁	L	2	1.9	1.90	-
	W	2	0.9 - 1.0	0.95	-
	C	2	7-7.5 : 4-4.5	7.25 : 4.25	-

Cf. *Parectypodus lunatus* Krause, 1982

Referred specimen.— UCMP 212780

Description.— An isolated P₃, UCMP 212780, has four cusps arranged in a 2:2 fashion. It is outside the size range of known *E. tardus* specimens, and identical in size ($L = 1.1$ mm, $W = 0.7$ mm) to the only known specimen at this tooth position from *P. lunatus*. UCMP 212780 is distally elongated, a characteristic apparently more typical of *P. lunatus*.

Discussion.— Although upper anterior premolars are not the ideal diagnostic teeth for multituberculate taxonomy, this specimen is suggestive of a second multituberculate species from Wa-0. UCMP 212780 may also represent the earliest appearance of this species in the fossil record.

Cohort MARSUPIALIA
Order DIDELPHIMORPHA
Family DIDELPHIDAE
Subfamily PERADECTINAE

Mimoperadectes labrus Bown and Rose, 1979

Figure 4, Table 2

Referred specimens.— UCMP 212441-212443, 212503, 212534, 212561, 212639, 212697, 212752, 212785.

Description.— Five isolated lower molars (UCMP 212441, 212443, 212561, 212639, 212752) of *Mimoperadectes labrus* have been recovered that closely resemble previously described specimens in both size and morphology (Bown and Rose, 1979;

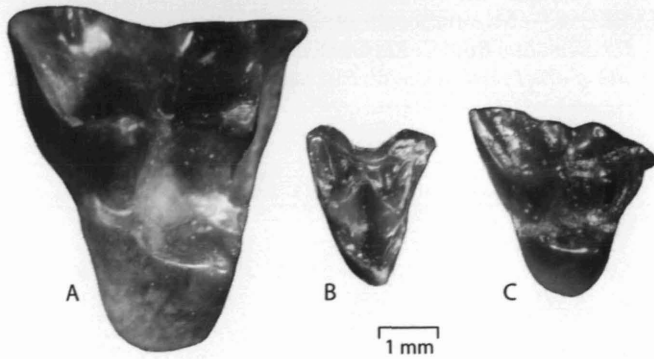


FIGURE 4 — Upper molars of marsupials, all in occlusal view. A, right M² of *Mimoperadectes labrus*, UCMP 212534. B, right M^{1/2} of *Peradectes protinnominatus*, UCMP 212776. C, right M^{1/2} of *Peratherium innominatum*, UCMP 212685.

Gingerich, 1989). Five isolated upper molars have also been collected from Castle Gardens. Prior to the Castle Gardens fauna, the upper molars for this taxon were only known from the holotype, a fragmentary maxilla. Based on the relative size and expansion of the parastylar and metastylar shelves, it appears that all four molar positions have been preserved in the new sample. Dental measurements are included in Table 2.

Discussion.— Only two specimens of the large didelphid *Mimoperadectes labrus* have been reported at other Wa-0 localities (Bown and Rose, 1979; Gingerich, 1989). There are ten specimens in the new collections, including the first complete crown of M¹ and an undamaged M².

Peradectes protinnominatus McKenna, 1960
Figure 4, Table 3

Referred specimens.— UCMP 212504, 212609, 212617, 212630, 212632, 212644, 212656, 212682, 212703, 212721, 212776, 212798.

Description.— *Peradectes protinnominatus* is very similar in size to a second marsupial that has been found at Castle Gardens, *Peratherium innominatum*. However, *Peradectes protinnominatus* can be distinguished on the bases of stylar cusp reduction, a more V-shaped protoconal base, twinned and subequal entoconid and hypoconulid, and in having a lower entoconid notch. A total of 12 teeth have been recovered including two single-tooth jaws. Measurements are summarized in Table 3.

Discussion.— The Clarkforkian-Wasatchian species, *Peradectes protinnominatus* is now known for the first time at a Wa-0 locality.

Subfamily HERPETOTHERIINAE

Peratherium innominatum Simpson, 1928
Figure 4, Table 4

TABLE 2 — Measurements of nine specimens of *Mimoperadectes labrus* from Castle Gardens. Abbreviations: AW, trigonid width; L, crown length; PW, talonid width; W, crown width.

Tooth position		N	Range	Mean	Std. Dev.
<i>Upper dentition</i>					
M ¹	L	1	2.9	-	-
	W	1	2.9	-	-
M ²	L	2	3.0	3.00	-
	W	1	3.7	-	-
M ³	L	1	2.9	-	-
	W	1	3.7	-	-
<i>Lower dentition</i>					
M _{1/2/3}	L	5	3.0 - 3.3	3.16	0.13
M _{1/2/3}	AW	5	1.3 - 1.8	1.54	0.18
M _{1/2/3}	PW	5	1.4 - 1.8	1.58	0.15

Referred specimens.— UCMP 212446, 212535, 212538, 212578, 212605, 212613, 212618, 212634, 212647, 212660, 212665, 212669, 212674, 212680, 212684, 212685, 212692, 212693, 212713, 212754, 212791, 212792, 212832.

Description.— *Peratherium innominatum* is the most common marsupial in the Castle Gardens fauna. All but one of the 23 specimens were found in the screen-washed matrix. The upper molars are typified by relatively short paracones, dilambodonty, and a posterior-lingual expansion of the protocone. Lower molars can be distinguished by a relatively low and posterior hypoconulid. Measurements are included in Table 4.

Discussion.— *Peratherium innominatum* is the smallest of the five species of *Peratherium* commonly recognized from the Eocene (Kristalka and Stucky, 1983a, b). The Castle Gardens sample represents the earliest appearance of this genus in North America.

Order CIMOLESTA
Family APATEMYIDAE

Apatemys sp.
Figure 5

Referred specimens.— UCMP 212606, 212621, 212683.

Description.— A RM₃ (UCMP 212606) is typified by the apatemyid pattern of a squared anterior trigonid formed where the preprotocristid joins the paracristid, coupled with a shallow talonid basin. Two similar-sized apatemyid species are known from the early Wasatchian of the Bighorn Basin, *Apatemys chardini* and *A. kayi*. *Apatemys chardini* differs from

TABLE 3 — Measurements of 12 specimens of *Peradectes protinnominatus* from Castle Gardens. Abbreviations: AW, trigonid width; L, crown length; PW, talonid width; W, crown width.

Tooth position	N	Range	Mean	Std. Dev.
<i>Upper dentition</i>				
M ^{1/2/3} L	5	1.3 - 1.5	1.44	0.09
W	5	1.6 - 1.8	1.76	0.09
<i>Lower dentition</i>				
M _{1/2/3} L	6	1.6 - 1.8	1.70	0.06
AW	6	0.8 - 1.1	0.98	0.12
PW	6	0.8 - 1.1	1.00	0.13
M ₄ L	1	1.5	-	-
AW	1	0.8	-	-
PW	1	0.7	-	-

A. kayi in being slightly smaller, having lost both P₂ and P₄, and in having relatively lower crowned molars (Gingerich, 1982). UCMP 212606 measures 1.6 mm in length, 0.9 mm in anterior width, and 1.0 mm in posterior width, being most consistent in size with *A. chardini* specimens. However, the ratio of relative crown height (RCH of Gingerich, 1982) for this specimen is 0.63 which is in the lower end of the range of the relatively higher crowned *A. kayi*.

Two hook-shaped cusps I¹s are also included in this apatemyid sample. They have large anterocones and posterocones, and small mediocones. They differ from most plesiadapiforms by the absence of a laterocone, and from forms such as *Tinimomys* by the absence of a lateroconule and a stronger posterocone (Rose et al., 1993). The average width of these specimens is 1.1 mm (length could not be accessed due to the fragmentary material). These specimens appear to be slightly smaller than described *A. kayi* specimens, however comparable I¹ data for *A. chardini* are unavailable (but presumably they are smaller). Because these taxa are so rare, comparative measurements and ratios are based on very limited samples, and intra-species variability has not been adequately documented. Therefore, species-level identification must await additional or more complete material.

Discussion.— These specimens represent the earliest record of apatemyids from the Wasatchian of North America.

Order TAENIODONTA
Family STYLINODONTIDAE

Ectoganus sp. Schoch, 1981
Figure 6

TABLE 4 — Measurements of 20 specimens of *Peratherium innominatum* from Castle Gardens. Abbreviations: AW, trigonid width; L, crown length; PW, talonid width; W, crown width.

Tooth position	N	Range	Mean	Std. Dev.
<i>Upper dentition</i>				
M ^{1/2/3} L	7	1.5 - 2.0	1.76	0.17
W	7	1.6 - 2.0	1.77	0.13
<i>Lower dentition</i>				
M _{1/2/3} L	13	1.5 - 1.9	1.64	0.13
AW	13	0.8 - 1.2	0.96	0.13
PW	13	0.7 - 1.3	0.97	0.18

Referred specimens.— UCMP 212457-212459, 212560 (Scorpion Knob, UCMP V99191).

Description.— The taeniodont *Ectoganus* sp. is well sampled. The collection includes three isolated teeth from Castle Gardens and five associated teeth and bone fragments from an isolated lateral locality (Scorpion Knob). The Castle Gardens teeth include LM¹? (UCMP 212458, L = 10.7 mm, W = 11.4 mm), a fragmented RM³ (UCMP 212457), and a newly erupted dP₄ (UCMP 212459, L = 10.1 mm, W = 8.0 mm). The associated teeth (UCMP 212560) include RC¹ (W = 15.1 mm), RM_{1/2} (L = 11.9 mm, W = 12.1 mm), LC¹ (W = 14.9 mm), LI³, LP²?, and LP³?

Discussion.— The relative small size of these specimens is comparable to either *E. bighornensis* or *E. copei* (Schoch, 1986; Gingerich, 1989), but no specific allocation is offered here. Further comparisons with museum collections are necessary to distinguish their relative degree of hyposodonty and premolar cusp development, which are the primary characters used to distinguish *E. bighornensis* from *E. copei*.

Order PANTODONTA
Family CORYPHODONTIDAE

Coryphodon sp.

Referred specimens.— UCMP 212489, 212492 (Coryphodon Place, UCMP V99192), 212506, 212528.

Description and discussion.— Specimens include fragmentary dental and postcranial remains of the cow-sized pantodont *Coryphodon* sp. The most complete material consists of very weathered cranial and postcranial fragments, including a lower molar and a canine (UCMP 212492) found associated at a laterally equivalent locality to Castle Gardens (Coryphodon Place). Since the most diagnostic teeth of this genus are M³ and M₃ (Lucas, 1984; Uhen and Gingerich, 1995), and they are not yet known from Castle Gardens, no specific allocation is offered.

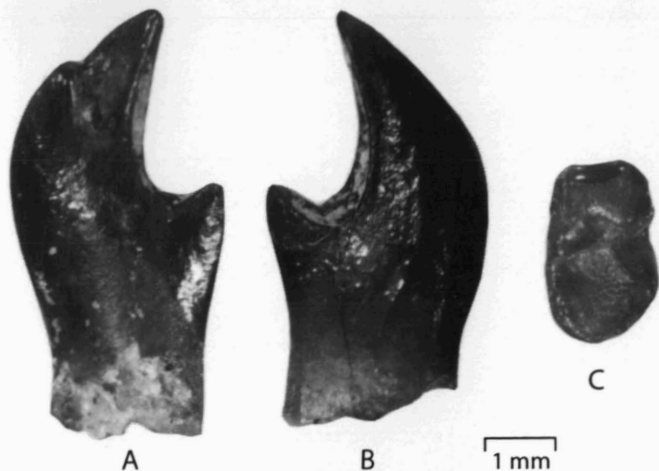


FIGURE 5 — Teeth of *Apatemys* sp. A and B, left I₁, UCMP 212621, in medial and lateral views. C, right M₃, UCMP 212606, in occlusal view.

Grandorder LIPOTYPHLA
Order ERINACEOMORPHA
Family AMPHILEMURIDAE

Macrocranium sp.
Figs. 7, 8, 9, Table 5

Referred specimens.— UCMP 212447, 212448, 212499, 212502, 212532, 212537, 212557, 212564-212567, 212571, 212572, 212574-212577, 212580, 212585, 212588, 212592, 212593, 212595, 212599, 212601, 212602, 212608, 212610, 212611, 212623, 212624, 212626-212628, 212643, 212645, 212651, 212652, 212658, 212659, 212663, 212664, 212676, 212679, 212690, 212695, 212696, 212705, 212706, 212710, 212712, 212715, 212724, 212725, 212729, 212732, 212747, 212750, 212751, 212759, 212778, 212782, 212783, 212789, 212790, 212793, 212794, 212796, 212797, 212799, 212800, 212805, 212809, 212811, 212816, 212817.

Description.— The Castle Gardens *Macrocranium* species is closely allied with *Macrocranium nitens* and *Macrocranium* cf. *M. nitens*, sharing with them a relatively large P₄, low trigonid, tall entoconids, and flat hypoconids (McKenna, 1960; Krishtalka, 1976; Bown and Schankler, 1982; Novacek et al., 1985). However, the Castle Gardens specimens differ in being significantly smaller (Fig. 8). Moreover, the P₄ metaconid is more posterior and the talonid basin is reduced. Upper molars are distinctive in the inferior placement and isolation of the hypocone. The M¹⁻² are less rectangular in outline, with a more concave buccal margin and more anteroposterior constriction across the conules. A more complete comparison of these specimens is in preparation as part of a larger study on *Macrocranium* (Smith et al., in prep.).

Discussion.— This species of *Macrocranium* is the most abundant small mammal recovered thus far from Castle Gardens. Seventy-six *Macrocranium* dental specimens have

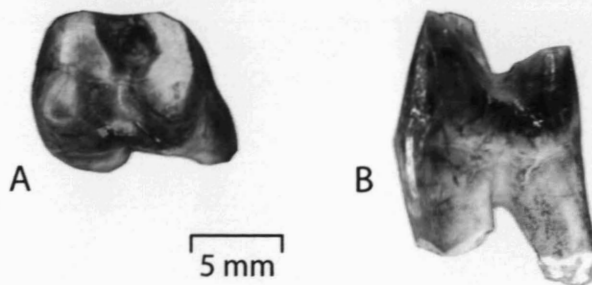


FIGURE 6 — Deciduous tooth of *Ectoganus* sp. A and B, left dP₄, UCMP 212459, in occlusal and lingual views.

been found, and the species accounts for over 40% of all specimens recovered from the screen-washed matrix. *Macrocranium* is one of the most common quarry species later in the Wasatchian (Silcox and Rose, in press), although, presumably because of its small size, it is rarely found on the surface.

Order SORICOMORPHA
Family NYCTITHERIIDAE

Plagiostenodon savagei Bown and Schankler, 1982
Figure 9

Referred specimens.— UCMP 212637, 212662.

Description.— A RP₄ has been found that represents the rare nyctitheriid *Plagiostenodon savagei*. This relatively large tooth is long and narrow ($L = 1.7$ mm, $W = 0.9$ mm), semimolariform, the paraconid is anteriorly projecting, and the talonid basin is relatively well-developed with a small cristid obliqua.

Moreover, an isolated I₂ with a scalloped dorsolateral margin and four well developed lobes has been recovered in the screen-washed material. This tooth is closest morphologically to the incisors of *Plagiostenodon krausae* and *Ceutholestes dolosus* (Rose and Gingerich, 1987), but it is almost twice the size ($L = 2.5$ mm, $W = 1.4$ mm). Based on its large size and morphology, this may be the first anterior tooth known for *P. savagei*.

Discussion.— *Plagiostenodon savagei* was described from a single specimen from the 140 meter level of the Bighorn Basin Willwood Formation (Bown and Schankler, 1982), and more recently Cf. *P. krausae* has been reported at several later Bighorn Basin quarries (Silcox and Rose, in press). The occurrence of this species in the Castle Gardens fauna marks its earliest appearance.

Order PRIMATES
Family MICROSYOPIDAE
Subfamily UINTASORICINAE

Niptomomys favorum, new species
Figure 10

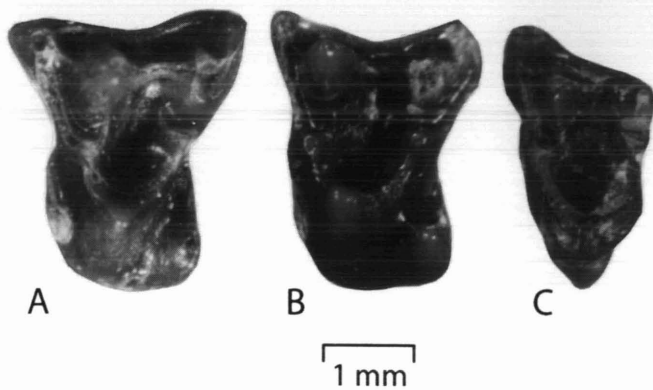


FIGURE 7 — Upper molars of *Macrocranion* sp. A, B, and C, left M¹ (UCMP 212611), M² (UCMP 212602) and M³ (UCMP 212593) in occlusal view.

Holotype.— UCMP 212635.

Diagnosis.— Resembles *Niptomomys* and differs from *Uintasorex* in having a smaller paracone and metacone and in having conules placed more buccally (Szalay, 1969). Upper molar here differs from those of *Niptomomys doreenae* (McKenna, 1960) and *N. thelmae* (Gunnell and Gingerich, 1981) in being substantially smaller and more squared in occlusal outline.

Description.— UCMP 21635 is an exceedingly small ($L = 0.7$ mm, $W = 0.8$ mm) upper molar. It is close to being square in occlusal outline. Like other uintasorcines, the new Wa-0 specimen lacks a hypocone.

Etymology.— From *favus*, Latin, honeycomb; referring to the provenance of the holotype in the Honeycombs area of the Bighorn Basin.

Discussion.— Even this limited material is sufficient to document a distinctively small new species of *Niptomomys*. Gingerich (1989) tentatively identified an edentulous dentary from the Wa-0 of the Clarks Fork Basin as Cf. *Niptomomys* sp. That mandibular fragment was described as being the same size as *N. doreenae* and larger than *Tinimomys graybullensis*. It is therefore much larger than the Castle Gardens *Niptomomys*, and is not considered conspecific with UCMP 212635.

Family MICROMOMYIDAE

Cf. *Tinimomys graybullensis* Szalay, 1974

Figure 10

Referred specimens.— UCMP 212691, 212757.

Description.— Two small lower molars (mean $L = 1.1$ mm, mean $W = 0.9$ mm) have been recovered. Although teeth at the most diagnostic position, P₄, are as yet unknown from Castle Gardens, the size and morphology of the molars are most suggestive of affinities with the Clarkforkian-Wasatchian form *Tinimomys graybullensis*.

Discussion.— These specimens are the first record of micromomyids from Wa-0.

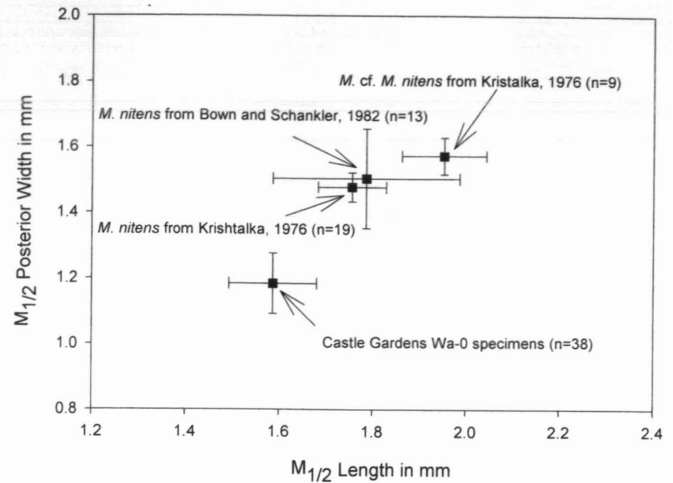


FIGURE 8 — Comparison of dental measurements of *Macrocranion*. Pooled first and second molar data demonstrating size distribution of published *Macrocranion* specimens and new sample from Castle Gardens. Data represented includes means (squares) and standard deviations (bidirectional error bars).

Order CREODONTA Family HYAENODONTIDAE

Acarictis ryani Gingerich and Deutsch, 1989

Referred specimen.— UCMP 212582.

Description.— A RM₁ recovered by screen-washing is attributed to *Acarictis ryani*. This specimen shows well developed and subequal paraconid and metaconid that are equidistant from an enlarged protoconid. Measurements for this specimen are: $L = 4.0$ mm, $AW = 2.0$ mm, and $PW = 1.7$ mm.

Discussion.— *Acarictis ryani* is the smallest of the early Wasatchian hyaenodontids and very rare. Prior to this Castle Gardens specimen, this taxon was only known from six specimens (Gingerich, 1989; Gingerich and Deutsch, 1989).

Cf. *Arfia junnei* Gingerich, 1989

Referred specimen.— UCMP 212615.

Description and discussion.— A trigonid from a lower molar suggests the presence of *Arfia junnei* in the Castle Gardens fauna.

Order CARNIVORA Family VIVERRAVIDAE

Didymictis sp.

Referred specimens.— UCMP 212468 and 212501, and questionably UCMP 212469 and 212616.

Description.— The largest carnivore in the Castle Gardens fauna is *Didymictis* sp. This species is represented by two

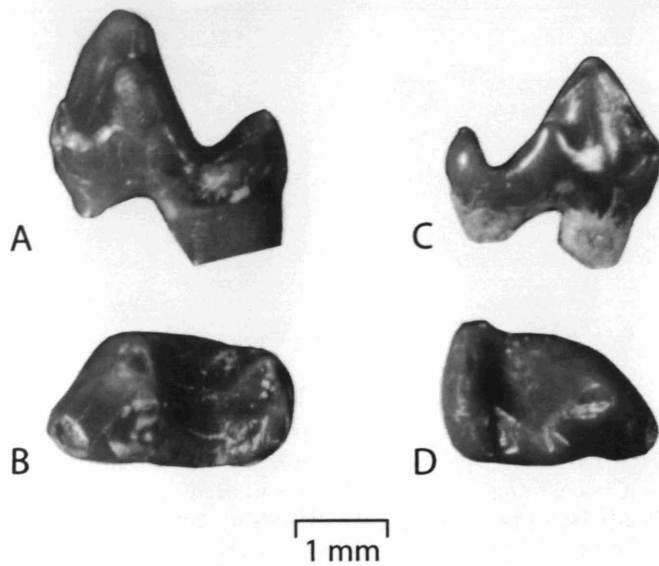


FIGURE 9 — Lower premolars of lipotyphlans. A and B, right P₄ of *Plagioctenodon savagei*, UCMP 212662, in lingual and occlusal views. C and D, left P₄ of *Macrocranion* sp., UCMP 212800, in lingual and occlusal views.

isolated teeth (RM₁ and RM₂) and possibly two fragmentary RP₄s. The lower molar (UCMP 212468) is much larger (fragmented but with *L* in excess of 9.0 mm, *AW* = 5.5 mm, *PW* 4.9 mm) than *D. proteus* from other Wa-0 localities, and within the size range of both late Clarkforkian (Cf-2 to Cf-3) *D. proteus* and early Wasatchian (Wa-1) *D. leptomytus* (Polly, 1997). The upper second molar (UCMP 212501) measures 3.6 mm in length and 6.8 mm in width, which is smaller than typical for either *D. proteus* or *D. leptomytus* (Polly, 1997).

Discussion.— More complete material is necessary to ascertain whether the Castle Gardens specimens are *D. proteus* or *D. leptomytus*.

Cf. *Viverravus politus*

Referred specimens.— UCMP 212555

Description.— An isolated upper fourth premolar may represent the large-sized *Viverravus politus*. This tooth measures 6.0 mm in length and 3.8 mm in width.

Discussion.— Gingerich (1989) reported two species of *Viverravus* from Wa-0, *V. boweni* and *V. politus*. The Castle Gardens specimen is larger than all *Viverravus* species except *V. politus*. Unfortunately, because very few P₄s are known for *V. politus*, its size variation is not well documented. Definitive species level designation for the Castle Gardens material must await the discovery of further specimens.

Family MIACIDAE

Miacis deutschii Gingerich, 1983

TABLE 5 — Measurements of 72 specimens of *Macrocranion* sp. from Castle Gardens. Abbreviations: *AW*, trigonid width; *L*, crown length; *PW*, talonid width; *W*, crown width.

Tooth position	N	Range	Mean	Std. Dev.	
<i>Upper dentition</i>					
M ¹	L	11	1.4 - 1.8	1.59	0.12
	W	11	1.8 - 2.3	2.01	0.15
M ²	L	12	1.4 - 1.8	1.66	0.12
	W	14	1.9 - 2.2	2.05	0.11
M ³	L	1	1.1	-	-
	W	1	1.7	-	-
<i>Lower dentition</i>					
P ₄	L	5	1.4 - 1.5	1.48	0.04
	W	5	0.8 - 1.0	0.92	0.08
M _{1/2}	L	38	1.3 - 1.7	1.59	0.09
	AW	38	0.9 - 1.3	1.11	0.09
	PW	40	0.9 - 1.3	1.19	0.09
M ₃	L	2	1.5	1.50	0.00
	AW	2	0.9	0.90	0.00
	PW	2	1.0	1.00	0.00

Referred specimens.— UCMP 212540.

Description.— An isolated RM₁ represents *Miacis deutschii*. This specimen differs from *M. winkleri* known at other Wa-0 localities (Gingerich, 1989) in that it is slightly larger (*L* = 4.9 mm, *AW* = 3.2 mm, *PW* = 2.9 mm) and has a lower trigonid (trigonid height, TH, of Gingerich, 1983 = 5.6 mm). Additionally, its trigonid height/crown ratio is 1.14, which is within the range of *M. deutschii* (1.07-1.18) and outside of the range of *M. winkleri* (1.27-1.40) (Gingerich, 1989).

Discussion.— This is the earliest occurrence of *M. deutschii*, as only *M. winkleri* has been reported from other Wa-0 localities.

Order PROCREODI
Family OXYCLAENIDAE

Chriacus badgleyi Gingerich, 1989
Figure 11

Referred specimens.— UCMP 212467, 212479.

Description.— Two isolated upper first or second molars of *Chriacus badgleyi* have been surface collected from Castle Gardens. This is the smallest species of *Chriacus* known, with

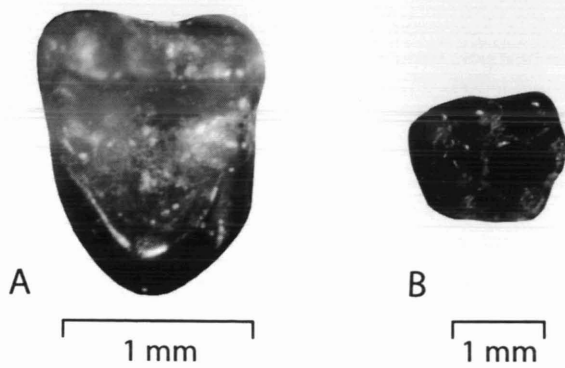


FIGURE 10 — Teeth of microsypids. A, left $M_{1/2}$ of *Niptomomys favorum*, new species, UCMP 212635 (holotype), in occlusal view. B, left $M_{1/2}$ of Cf. *Tinimomys graybullensis*, UCMP 212691, in occlusal view.

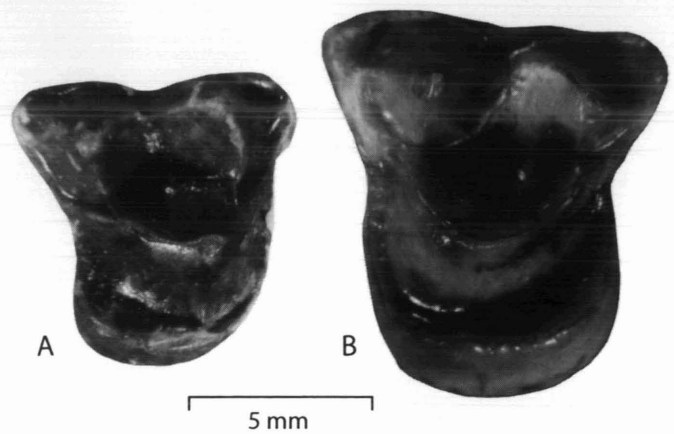


FIGURE 11 — Upper molars of *Chriacus*. A, right $M_{1/2}$ of *Chriacus bagleyi*, UCMP 212479, in occlusal view. B, left $M_{1/2}$ of *Chriacus* sp., UCMP 212466, in occlusal view.

UCMP 212467 measuring 5.3 mm in length and 5.7 mm in width, and UCMP 212479 measuring 5.3 mm in length and 5.5 mm in width. Like other *Chriacus* specimens, the Castle Gardens molars have a simple tritubercular crown and a well developed lingual cingulum.

Discussion.— UCMP 212467 and 212479 represent the first complete upper molars of *Chriacus badgleyi*.

Chriacus sp.
Figure 11

Referred specimen.— UCMP 212466.

Description.— An isolated first or second upper molar of larger species ($L = 6.2$ mm, $W = 7.2$ mm) of *Chriacus* is known from Castle Gardens. As is typical of the genus, this specimen displays a simple trigon and a continuous lingual cingulum (which is especially broad posterolingually).

Discussion.— Aside from *C. badgleyi*, *C. gallinae* is the only other species of *Chriacus* known from the Wasatchian (Matthew, 1915; McKenna, 1960; Delson, 1971). However, this specimen differs from *C. gallinae* of Matthew (1915) in having a much more developed lingual cingulum. UCMP 212466 also appears to differ from the Cf. "*Chriacus*" *gallinae* specimens described by Delson (1971) from the Almagre and Powder River local faunas in lacking a hypocone. Given the insufficient and contradictory published material concerning *Chriacus*, especially *C. gallinae*, no specific allocation is offered. Although *Chriacus* is typically a Torrejonian-Tiffanian form, UCMP 212466 demonstrates that two species of *Chriacus* lived sympatrically during the earliest Wasatchian.

Thryptacodon barae Gingerich, 1989

Referred specimens.— UCMP 212558.

Description.— A isolated LM_3 with an elongated hypoconulid and anteriorly placed paraconid represents

Thryptacodon barae. This M_3 is 5.4 mm in length, 3.4 mm in trigonid width, and 3.1 mm in talonid width.

Discussion.— This is only the third known specimen of this rare species.

Princetononia yalensis Gingerich, 1989
Figure 12

Referred specimens.— UCMP 212527.

Description.— An isolated first or second lower molar ($L = 5.6$ mm, $AW = 3.8$ mm, $PW = 3.9$) with a low trigonid, broadly basined talonid, and rounded cusps and crests represents an additional specimen of the rare *Princetononia yalensis*.

Discussion.— The majority of described *P. yalensis* specimens are from late Tiffanian through late Clarkforkian age. The holotype (YPM-PU 23629) was the only previously known Wa-0 specimen, and its locality data were not recorded precisely (Gingerich, 1989). This Castle Gardens specimen confirms the presence of *P. yalensis* in the Wasatchian.

Order CONDYLARTHRA
Family PHENACODONTIDAE

Phenacodus cf. *P. vortmani* (Cope, 1880)

Referred specimens.— UCMP 212430-212432, 212475, 212481, 212543.

Description.— Six dental specimens of *Phenacodus* cf. *P. vortmani* have been surface collected from the Castle Gardens locality. Most are very fragmentary, with few being complete enough for standard length and width measurements. The most complete specimen is UCMP 212431, an associated RP^{3-4} (P^3 : $L = 8.8$ mm, $W = 8.1$ mm; P^4 : $L = 9.3$ mm, $W = 10.3$ mm). The P^3 has a relatively small metacone, which is closely appressed to the larger paracone. The P^4 lacks a distinctive metaconule.



FIGURE 12 — Lower molar of *Princetonia yalensis*, UCMP 212527, left $M_{1/2}$ in occlusal view.

UCMP 212475 is a RM_3 talonid with a width of 7.4 mm. UCMP 212481 is a $LM_{2/3}$, and this tooth is approximately 11.2 mm in length, 10.0 in anterior width, and 9.0 mm in posterior width.

Discussion.— Previous interpretations of Wa-0 specimens have been ambiguous. Gingerich (1989) tentatively allocated the northern Bighorn Basin specimens to *Phenacodus* cf. *P. intermedius*. Thewissen (1990) reassessed this sample in his revision of Phenacodontidae. He found that six of the seven Wa-0 specimens from the northern Bighorn Basin clustered with *P. vortmani* in a principal components analysis, but noted that the P_4 was larger than any other *P. vortmani* and more comparable to *P. intermedius*.

This new contemporaneous material highlights the difficulty of allocating small, fragmented samples of *Phenacodus*. Based solely on size the Castle Gardens sample is most comparable to *P. intermedius* from the Lower *Haplomyilus-Ectocion* zone of the Bighorn Basin, and is much larger than *P. vortmani* (Thewissen, 1990). One of the most complete specimens from Castle Gardens (UCMP 212431) is a RP^4 , which is a diagnostic tooth for *Phenacodus* species-level distinctions (Thewissen, 1990). Thewissen found that P^4 width/length ratios were useful in *Phenacodus* taxonomic assessments. The Castle Gardens specimen has a ratio of 1.11, which is closer to *P. vortmani* at 1.12 and substantially higher than *P. intermedius* at 1.07. Finally, this tooth lacks a distinctive metaconule, a characteristic shared with *P. vortmani*. In summary, although this specimen is more similar in size to *P. intermedius*, it is tentatively allocated to *P. vortmani* based on the P^4 shape (W/L ratio) and the absence of the P^4 metaconule.

Copecion davisi Gingerich, 1989

Table 6

Referred specimens.— UCMP 212397, 212403, 212412-212418, 212422, 212423, 212425-212429, 212437, 212438, 212451, 212478, 212487, 212496, 212523, 212541, 212544, 212550, 212556, 212765, 212766 and questionable UCMP 212392, 212411, 212419, 212421, 212483, 212526, 212549.

Description.— Thirty-seven isolated teeth of *Copecion davisi* are known from Castle Gardens, of which only five speci-

TABLE 6 — Measurements of 34 specimens of *Copecion davisi* from Castle Gardens. Abbreviations: AW, trigonid width; L, crown length; PW, talonid width; W, crown width.

Tooth position		N	Range	Mean	Std. Dev.
<i>Upper dentition</i>					
P^3	L	2	4.5 - 4.7	4.6	0.14
	W	1	6.1	-	-
$M_{1/2}$	L	14	5.3 - 6.6	5.91	0.38
	W	14	6.0 - 7.0	6.65	0.31
M^3	L	3	3.9 - 4.3	4.07	0.21
	W	3	5.1 - 5.6	5.37	0.25
<i>Lower dentition</i>					
P_2	L	1	5.0	-	-
	W	1	2.4	-	-
P_4	L	4	6.6 - 7.0	6.80	0.18
	W	4	3.5 - 4.8	3.93	0.61
$M_{1/2}$	L	7	5.5 - 6.3	5.87	0.27
	AW	8	4.0 - 5.1	4.54	0.39
	PW	9	4.1 - 4.8	4.47	0.23
M_3	L	1	6.4	-	-
	AW	1	4.1	-	-
	PW	1	3.8	-	-

mens were recovered from screen-washing. Although *Copecion davisi* and *Ectocion parvus* differ only slightly in size (Tables 6, 7), Gingerich (1989) and Thewissen (1990) described numerous characteristics that can be used to distinguish between these two phenacodontids. The most distinctive dental element is the P_4 , however even isolated unworn molars can usually be identified to species. *Copecion davisi* has upper molars that tend to be more square, lack a lingual cingulum, and have a vertical furrow separating the protocone and hypocone. The lower molars can frequently be distinguished by a U-shaped paracristid connecting the protoconid and metaconid, a paracristid that ascends the metaconid, and a slightly smaller M^3 . Measurements of the Castle Gardens specimens are summarized in Table 6.

Discussion.— *Copecion davisi* is an important indicator taxon as it is restricted to Wa-0 and is only known from the Bighorn and Powder River Basins (Gingerich, 1989; Thewissen, 1990; Robinson and Williams, 1997). Because of its limited temporal and geographic range, *C. davisi* is not well known and this new sample from Castle Gardens nearly doubles the known number of specimens of this taxon.

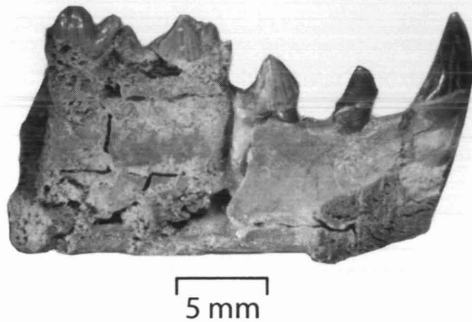


FIGURE 13 — Left dentary of *Ectocion parvus*, UCMP 212410, with C₁-P₄ in lingual view.

Ectocion parvus Granger, 1915
Figure 13, Table 7

Referred specimens.— UCMP 212386-212389, 212391, 212395, 212396, 212398-212400, 212404-212407, 212409, 212410, 212433-212436, 212439, 212440, 212450, 212464, 212490, 212493, 212494, 212498, 212510, 212514, 212520, 212525, 212529, 212536, 212546, 212548, 212551, 212559. UCMP 212390, 212393, 212394, 212401, 212402, 212408, 212488, 212491, 212497, 212509, 212518, 212531, 212553 may also belong to this species.

Description.— A total of 51 specimens of *Ectocion parvus* (MNI = 7) are known from Castle Gardens, including five dentaries with two or more teeth (UCMP 212386, 212387, 212409, 212410, and 212559) and a two-tooth maxilla (UCMP 212388). Gingerich (1989) and Thewissen (1990) provided detailed descriptions of this taxon. The Castle Gardens sample includes the most complete lower anterior dentition of this taxon. UCMP 212410 is a left dentary preserving C₁-P₄ found in association with mandibular fragments and a third lower molar (Fig. 13). Also recovered is the first deciduous tooth (dP₃, UCMP 212401) of *E. parvus*.

Discussion.— *Ectocion parvus* is known primarily from Wa-0 and during its brief appearance is quite abundant.

Order CETE
Family MESONYCHIDAE

Dissacus praenuntius Matthew, 1915
Figure 14

Referred specimens.— UCMP 212460 and tentatively UCMP 212470.

Description.— A medium-sized species of *Dissacus*, *D. praenuntius* is represented in this collection by two specimens. A lower first or second molar (UCMP 212460) measures *L* = 13.8 mm, *W* = 6.7 mm and an upper posterior premolar (UCMP 212470) measures *L* = 8.7 and *W* = 8.0.

Discussion.— These specimens, in addition to four collected by Gingerich (1989) at SC-67, are the only *Dissacus* specimens known from Wa-0.

TABLE 7 — Measurements of 44 specimens of *Ectocion parvus* from Castle Gardens. Abbreviations: AW, trigonid width; H, crown height; L, crown length; PW, talonid width; W, crown width.

Tooth position	N	Range	Mean	Std. Dev.	
<i>Upper dentition</i>					
P ³	L	1	4.5	-	-
	W	1	4.5	-	-
P ⁴	L	4	5.1 - 5.8	5.43	0.30
	W	5	4.9 - 5.8	5.34	0.33
M ¹	L	1	5.5	-	-
	W	1	7.1	-	-
M ²	L	1	5.8	-	-
	W	1	7.4	-	-
M ^{1/2}	L	7	5.3 - 6.2	5.74	0.27
	W	7	6.4 - 7.5	7.10	0.37
M ³	L	4	4.3 - 4.6	4.5	0.14
	W	4	5.4 - 5.8	5.68	0.19
<i>Lower dentition</i>					
dP ₃	L	1	4.4	-	-
	W	1	4.4	-	-
C ₁	L	1	3.5	-	-
	W	1	2.4	-	-
	H	1	5.8	-	-
P ₁	L	1	2.4	-	-
	W	1	1.4	-	-
P ₂	L	1	3.8	-	-
	W	1	2.1	-	-
P ₃	L	4	5.5 - 6.3	5.83	0.36
	W	4	2.7 - 3.2	3.00	0.22
P ₄	L	2	5.6 - 5.7	5.65	0.07
	AW	3	3.3 - 3.6	3.47	0.15
	PW	3	3.6 - 3.7	3.63	0.06
M ₁	L	3	5.0 - 5.9	5.43	0.45
	AW	4	4.2 - 4.4	4.28	0.10
	PW	3	4.2 - 4.4	4.30	0.10
M ₂	L	3	5.3 - 5.9	5.60	0.30
	AW	3	4.4 - 4.5	4.47	0.06
	PW	3	4.3 - 4.4	4.33	0.06
M _{1/2}	L	11	5.6 - 6.1	5.86	0.16
	AW	11	3.7 - 4.9	4.29	0.40
	PW	11	3.8 - 4.8	4.35	0.34
M ₃	L	6	5.8 - 6.3	6.03	0.19
	AW	6	3.5 - 4.1	3.70	0.25
	PW	7	3.2 - 3.8	3.44	0.19



FIGURE 14 — Lower molar of *Dissacus praenuntius*, UCMP 212460, left $M_{1/2}$ in buccal view.

Order RODENTIA
Family ISCHYROMYIDAE
Subfamily MICROPARAMYINAE

Acritoparamys atwateri
Figure 15, Table 8

Referred specimens.— UCMP 212453-212456, 212472, 212473, 212486, 212511-212513, 212521, 212530, 212545, 212547, 212563, 212568-212570, 212586, 212596, 212600, 212607, 212655, 212668, 212687, 212698, 212701, 212707, 212714, 212731, 212738, 212740, 212743, 212762, 212772, 212786, 212787, 212810, 212818.

Description.— The most common and smallest rodent is *Acritoparamys atwateri*. Thus far 39 dental specimens (not including incisors) have been recovered. More jaws have been found for this species ($n = 8$) than for any other taxon from Castle Gardens. The molars of this species are characterized by distinct hypoconulids, isolated entoconids, and relatively large hypocones. Measurements are summarized in Table 8 and are within the range of *A. atwateri* offered by Korth (1984) and Ivy (1990).

Discussion.— *Acritoparamys atwateri* is a common rodent from the Clarkforkian and Wasatchian, and has been identified at other Wa-0 localities (Gingerich, 1989).

Subfamily PARAMYINAE
Cf. *Paramys copei* Loomis, 1871

Referred specimens.— UCMP 212597.

Description.— A single large M_3 talonid fragment (width 3.5 mm) may represent *P. copei*.

Discussion.— There is some disagreement over the stratigraphic range of this taxon. Korth (1984) attributed

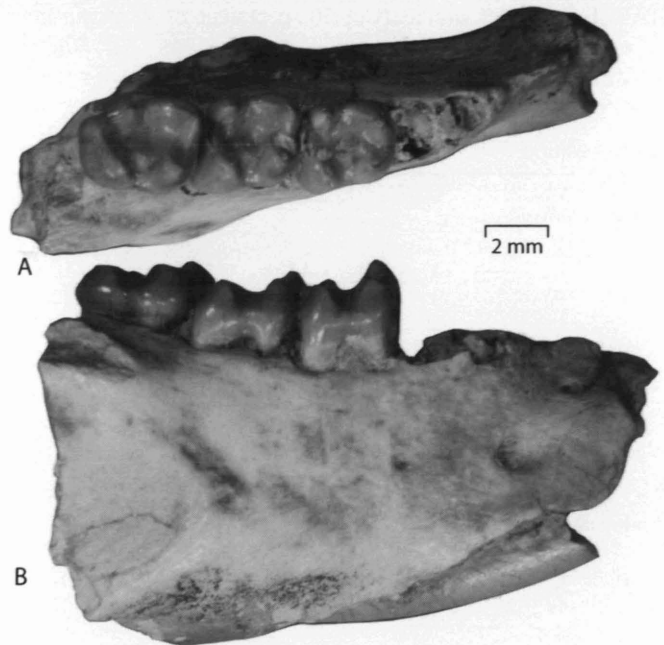


FIGURE 15 — Dentition of *Acritoparamys atwateri*. A and B, right $M_{1,3}$, UCMP 212472, in occlusal and buccal views.

several Clarkforkian isolated incisors to *P. copei*, however Ivy (1990) suggested that the first definitive specimens are known from the latest *C. ralstoni* zone of the Wasatchian. If this is the case, UCMP 212597 represents the earliest appearance of this large rodent.

Paramys taurus Wood, 1962

Referred specimens.— UCMP 212505.

Description.— *Paramys taurus* is represented in this fauna by an isolated LM_2 . This medium-sized rodent ($L = 2.9$ mm, $AW = 2.5$ mm, $PW = 2.5$ mm) has rhomboid-shaped molars, rounded cusps without prominent crests, a prominent mesoconid, a relatively small trigonid basin, and lacks a hypoconulid.

Discussion.— *Paramys taurus* has already been recognized at other Wa-0 localities (Gingerich, 1989), and is known to range from the Clarkforkian to the middle Wasatchian (Ivy, 1990).

Order PERISSODACTYLA
Family EQUIDAE

Hyacotherium grangeri Kitts, 1956

Referred specimens.— UCMP 212461-212463, 212474, 212480, 212519.

Description.— This species is represented by six specimens (all upper molars), including a two-tooth maxilla that was

TABLE 8 — Measurements of 36 specimens of *Acritoparamys atwateri* from Castle Gardens. Abbreviations: AW, trigonid width; L, crown length; PW, talonid width; W, crown width.

Tooth position		N	Range	Mean	Std. Dev.
<i>Upper dentition</i>					
P ⁴	L	3	1.9 - 2.1	2.00	0.10
	W	3	2.3 - 2.8	2.60	0.27
M ^{1/2}	L	12	2.0 - 2.6	2.83	0.18
	W	12	2.5 - 2.8	2.61	0.11
M ³	L	1	2.6	-	-
	W	1	2.5	-	-
<i>Lower dentition</i>					
P ₄	L	2	2.0 - 2.1	2.05	0.07
	W	2	1.5 - 1.6	1.55	0.07
M ₁	L	4	2.1 - 2.6	2.35	0.21
	AW	4	1.6 - 2.2	1.85	0.25
	PW	4	1.9 - 2.4	2.08	0.22
M ₂	L	6	2.2 - 2.6	2.40	0.14
	AW	4	1.8 - 2.0	1.93	0.10
	PW	5	2.0 - 2.2	2.12	0.08
M _{1/2}	L	7	2.1 - 2.8	2.46	0.22
	AW	8	1.7 - 2.4	2.06	0.21
	PW	7	2.0 - 2.6	2.29	0.19
M ₃	L	6	2.7 - 2.9	2.82	0.10
	AW	7	2.0 - 2.1	2.09	0.04
	PW	5	1.9 - 2.0	2.00	0.10

recovered during digging for screen-wash matrix. Measurements of the more complete specimens include: UCMP 212461 (LM²), *L* = 7.5 mm, *W* = 8.4 mm; UCMP 212462 (RM³), *L* = 7.3 mm, *W* = 8.3 mm; UCMP 212474 (LM¹), *L* = 7.1 mm, (LM²) *L* = 6.9 mm, *W* = 8.1 mm; UCMP 212480 (LM²), *L* = 6.9 mm, *W* = 8.2 mm.

Discussion.—Gingerich (1989) recognized two distinct species of *Hyracotherium* (*H. sandrae* and *H. grangeri*) from his Wa-0 localities. *Hyracotherium sandrae* was the fourth most abundant mammalian species in Gingerich's study. In contrast, all the *Hyracotherium* specimens recovered at Castle Gardens are too large to be included in this species, and are considered representatives of *H. grangeri*.

SUMMARY AND CONCLUSIONS

Work carried out to date at Castle Gardens has already substantially increased our knowledge of the diversity and

community structure of mammals from the earliest Wasatchian in North America. Over 300 new specimens have been recovered and identified. Of the 29 species thus far identified, 11 had not been previously reported at other Wa-0 localities (Table 9). The primary reason this diversity could be documented is the localization and density of the fossils at Castle Gardens, allowing the use of screen-washing in addition to traditional surface collecting techniques.

Although multituberculates are normally very rare in Wasatchian deposits, based on MNI data (Table 9) these primitive mammals comprise 13% of the Castle Gardens fauna. The high percentage of multituberculates in the Wasatchian is only exceeded by D-2037Q, a quarry locality at the 374 meter level of the Bighorn Basin (Silcox and Rose, in press). Another group that is relatively rare in Wasatchian faunas, but abundant at Castle Gardens, is Marsupialia. Three species have been identified, making up 10% of the total fauna in terms of MNI. A third group rarely well sampled because of their small size is Apatemyidae, which are now known for the first time from Wa-0. Aside from the 78 specimens of *Macrocranium* and *Plagioctenodon* described here, the only lipotyphlan known from Wa-0 is an undescribed maxilla of *Macrocranium* in the University of Michigan collection (Gingerich, 1989; Smith et al., in prep). Microsomyids are also known for the first time from Wa-0, including a new species of *Niptomomys*. Both the *Macrocranium* and *Niptomomys* species are considerably smaller than their congeners. This is notable as Gingerich (1989) reported that among his Wa-0 sample 28% of species with either Clarkforkian or later Wasatchian close relatives were relatively small. This "dwarfing" phenomenon that Gingerich noted among larger-bodied Wa-0 mammals appears to be true of some of the smaller-bodied sized Wa-0 mammals as well.

The creodont and carnivoran material thus far recovered is fragmentary, but still provides clear insights into the carnivore community during the earliest Wasatchian. Two hyaenodontids are known, *Acarictis ryani* and cf. *Arfia junnei*. Three carnivorans are also known, the largest carnivore at Castle Gardens is *Didymictis* sp. Cf. *Viverravus politus* and *Miacis deutschi* are also known. *Miacis deutschi* differs from *Miacis* at other Wa-0 localities, which represent the smaller species *M. winkleri* (Gingerich, 1983, 1989). Oxyclaenids (Procreodi) are not abundant, but several very rare species are represented (*Chriacus badgleyi*, *Chriacus* sp., *Thryptacodon barae*, and *Princetonina yalensis*). Condylarths are the most common larger-bodied mammals from Castle Gardens, and phenacodontids are very well represented (19% based on MNI). Other less common larger-bodied mammals found include *Ectoganus* sp., *Coryphodon* sp., *Dissacus praenuntius*, and *Hyracotherium grangeri*. Finally, rodents are well represented in the Castle Gardens fauna, with specimens of three species comprising 12% of the minimum number of individuals.

There are some notable absences from the Castle Gardens fauna. Surprisingly, the primate *Cantius torresi*, a relatively common element in Wa-0 faunas (Gingerich, 1986, 1989, 1995),

TABLE 9 — Mammalian faunal list for the Castle Gardens Wa-0 locality and vicinity, including abundance data (TNS, total number of specimens; MNI, minimum number of individuals). TNS from screen-washing is given in parentheses. Classification follows McKenna and Bell (1997). Asterisks denote species reported from Wa-0 for the first time.

Taxon	TNS	MNI	Taxon	TNS	MNI
Multituberculata			Creodonta		
Ptilodontidae			Hyaenodontidae		
<i>Ectypodus tardus</i>	20 (17)	8	<i>Acarictis ryani</i>	1 (1)	1
* <i>Cf. Parectypodus lunatus</i>	1 (1)	1	<i>Cf. Arfia junnei</i>	1 ()	1
Marsupialia			Carnivora		
Didelphidae			Viverravidae		
<i>Mimoperadectes labrus</i>	10 (5)	2	<i>Didymictis</i> sp.	4 (1)	2
* <i>Peradectes protinnominatus</i>	12 (12)	2	<i>Cf. Viverravus politus</i>	1 ()	1
* <i>Peratherium innominatum</i>	23 (22)	3	Miacidae		
Cimolesta			* <i>Miacis deutschi</i>	1 ()	1
Apatotheria			Procreodi		
Apatemyidae			Oxyclaenidae		
* <i>Apatemys</i> sp.	3 (3)	2	<i>Chriacus badgleyi</i>	2 ()	1
Taeniodonta			* <i>Chriacus</i> sp.	1 ()	1
Stylinodontidae			<i>Thryptacodon barae</i>	1 ()	1
<i>Ectoganus</i> sp.	4 ()	1	<i>Princetonia yalensis</i>	1 ()	1
Pantodonta			Condylarthra		
Coryphodontidae			Phenacodontidae		
<i>Coryphodon</i> sp.	4 ()	1	<i>Phenacodus</i> cf. <i>P. vortmani</i>	6 ()	1
Lipotyphla			<i>Copecion davisi</i>	37 (5)	5
Erinaceomorpha			<i>Ectocion parvus</i>	51 (1)	7
Amphilemuridae			Cete		
* <i>Macrocranion</i> sp.	76 (71)	11	Mesonychidae		
Soricomorpha			<i>Dissacus praenuntius</i>	2 ()	1
Nyctitheriidae			Rodentia		
* <i>Plagiostenodon savagei</i>	2 (2)	1	Ischyromyidae		
Primates			<i>Acritoparamys atwateri</i>	39 (27)	6
Microsyopidae			<i>Paramys taurus</i>	1 (1)	1
* <i>Niptomomys favorum</i>	1 (1)	1	* <i>Cf. Paramys copei</i>	1 (1)	1
Micromomyidae			Perissodactyla		
* <i>Cf. Tinimomys graybullensis</i>	2 (2)	1	Equidae		
			<i>Hyracotherium grangeri</i>	6 (2)	3
			Totals:	314 (175)	69

has not been recovered. The only other Wa-0 euprimate known, *Teilhardina brandti*, represented by a single specimen recovered from the northern Bighorn Basin (Gingerich, 1993), is also thus far unknown. However, continued collecting may rectify these deficiencies. In addition to primates, dental remains for several mammalian orders remain unknown from Castle Gardens, including: Tillodontia, Artiodactyla, and Edentata (Palaeonodonta). Hyopsodontids are absent as well. The most abundant species at most other Wa-0 localities, *Hyopsodus loomisi* (Gingerich, 1989), is conspicuously absent from the Castle Gardens fauna. As at other Wa-0 localities, *Haplomylys* is unknown (Gingerich, 1989; Robinson and Williams, 1997). Only further collecting will clarify whether

these absences are sampling artifacts, or whether this locality, for example, is sampling a different depositional or paleoenvironment.

ACKNOWLEDGMENTS

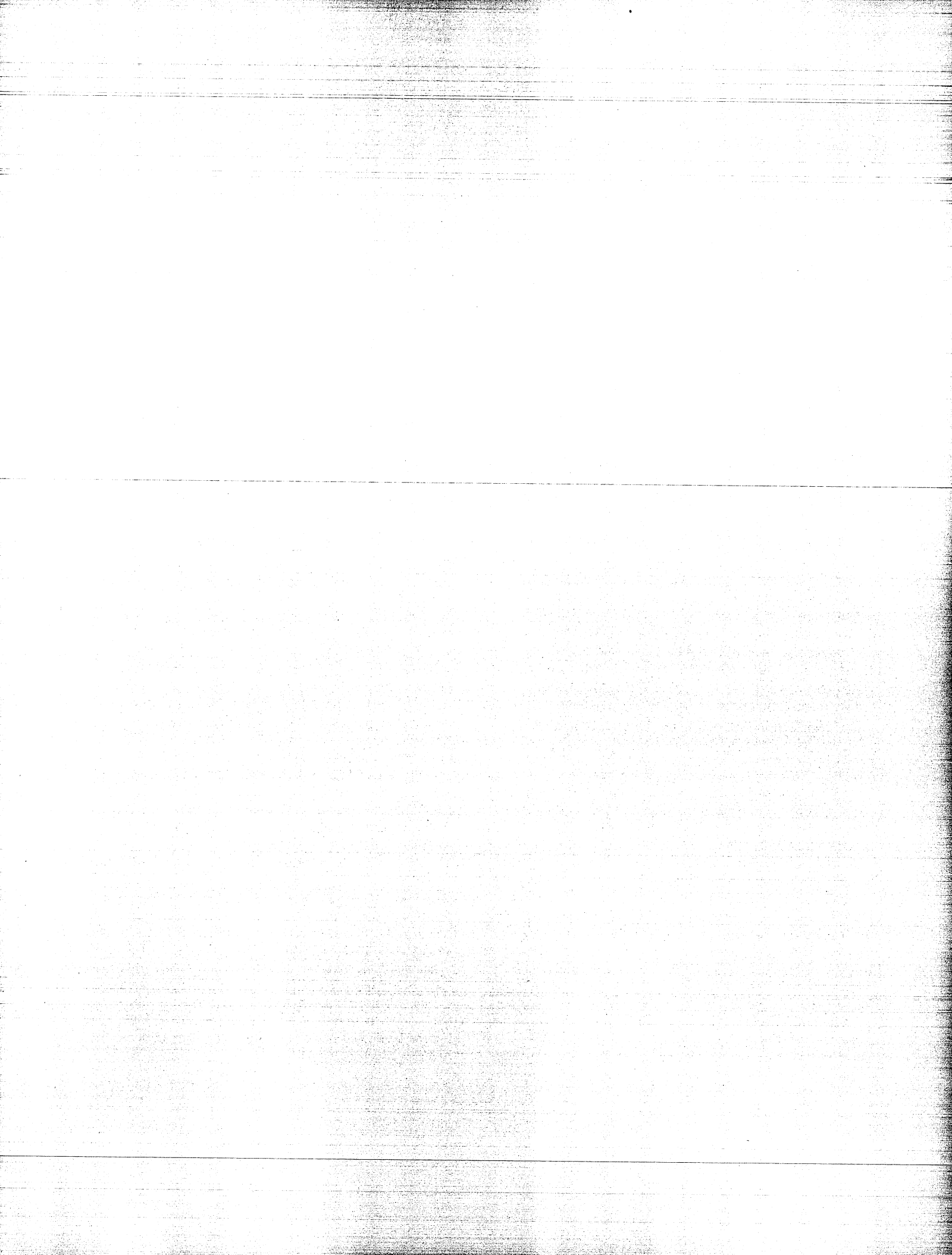
Field assistants from the 1999 season included Rose Ayoob, Liz Fet, Hadessa Frye, and Jean Perry. Phil Holman deserves special mention for his work over all three field seasons. Rose Ayoob, Jessica Lukacs, and Liz Fet are thanked for outstanding assistance in the lab. I would also like to thank the scientists at the following institutions for access to collections, stimulating discussions, and making casts available:

American Museum of Natural History (Mike Novacek and John Alexander); Carnegie Museum of Natural History (Chris Beard, Mary Dawson, and Alan Tabrum); Johns Hopkins University (Ken Rose); University of California Museum of Paleontology (Pat Holroyd); and University of Michigan Museum of Paleontology (Philip Gingerich, Gregg Gunnell, and Jon Bloch). The Bureau of Land Management is thanked for permits and logistical support. This work has been supported by grants from Marshall University, West Virginia Women in Sciences, and NASA.

LITERATURE CITED

- AUBRY, M.-P., S. G. LUCAS, W. A. BERGGREN (eds.). 1998. Late Paleocene-Early Eocene Climatic and Biotic Events in the Marine and Terrestrial Records. Columbia, New York, 513 pp.
- BOWN, T. M. 1979. Geology and mammalian paleontology of the Sand Creek facies, lower Willwood formation (Lower Eocene), Washakie County, Wyoming. Geological Survey of Wyoming Memoir, 2: 1-151.
- BOWN, T. M. and K. D. ROSE. 1979. *Mimoperadectes*, a new marsupial, and *Worlandia*, a new dermopter, from the lower part of the Willwood Formation (early Eocene), Bighorn Basin, Wyoming. Contributions from the Museum of Paleontology, University of Michigan, 25: 89-104.
- BOWN, T. M. and D. M. SCHANKLER. 1982. A review of the Proteuthera and Insectivora of the Willwood Formation (lower Eocene), Bighorn Basin, Wyoming. U.S. Geological Survey Bulletin, 1523: 1-79.
- BOYD, A. 2000. Paleogene paleoclimate of the North Atlantic Arctic as determined by vegetation. In B. Schmitz, B. Sundquist, and F. P. Andreasson (eds.), Early Paleogene Warm Climates and Biosphere Dynamics, Uppsala, Geological Society of Sweden, GFF [Geologiska Föreningens Förhandlingar], 122: 33.
- BUJAK, J. P. and H. BRINKHUIS. 1998. Global warming and dinocyst changes across the Paleocene-Eocene epoch boundary. In M.-P. Aubry, S. G. Lucas, and W. A. Berggren (eds.), Late Paleocene-Early Eocene Climatic and Biotic Events in the Marine and Terrestrial Records, Columbia University Press, New York, pp. 277-295.
- DELSON, E. 1971. Fossil mammals of the early Wasatchian Powder River local fauna, Eocene of northeast Wyoming. Bulletin of the American Museum of Natural History, 146: 305-364.
- DOCKERY, D. T. 1998. Molluscan faunas across the Paleocene-Eocene series boundary in the North American Coastal Plain. In M.-P. Aubry, S. G. Lucas, and W. A. Berggren (eds.), Late Paleocene-Early Eocene Climatic and Biotic Events in the Marine and Terrestrial Records, Columbia University Press, New York, pp. 296-322.
- GINGERICH, P. D. 1982. Studies on Paleocene and early Eocene Apatemyidae (Mammalia, Insectivora): Part II. *Labidolemur* and *Apatemys* from the early Wasatchian of the Clark's Fork Basin, Wyoming. Contributions from the Museum of Paleontology, University of Michigan, 26: 57-69.
- GINGERICH, P. D. 1983. Systematics of early Eocene Miacidae (Mammalia, Carnivora) in the Clark's Fork Basin, Wyoming. Contributions from the Museum of Paleontology, University of Michigan, 26: 197-225.
- GINGERICH, P. D. 1986. Early Eocene *Cantius torresi*— oldest primate of modern aspect from North America. Nature, 320: 319-321.
- GINGERICH, P. D. 1989. New earliest Wasatchian mammalian fauna from the Eocene of northwestern Wyoming: composition and diversity in a rarely sampled high-floodplain assemblage. University of Michigan Papers on Paleontology, 28: 1-97.
- GINGERICH, P. D. 1993. Early Eocene *Teilhardina brandti*: oldest omomyid primate from North America. Contributions from the Museum of Paleontology, University of Michigan, 28: 321-326.
- GINGERICH, P. D. 1995. Sexual dimorphism in earliest Eocene *Cantius torresi* (Mammalia, Primates, Adapoidea). Contributions from the Museum of Paleontology, University of Michigan, 29: 185-199.
- GINGERICH, P. D. 2000. Paleocene-Eocene boundary and continental vertebrate faunas of Europe and North America. In B. Schmitz, B. Sundquist, and F. P. Andreasson (eds.), Early Paleogene Warm Climates and Biosphere Dynamics, Uppsala, Geological Society of Sweden, GFF [Geologiska Föreningens Förhandlingar], 122 pp. 57-59.
- GINGERICH, P. D. and H. A. DEUTSCH. 1989. Systematics and evolution of early Eocene Hyaenodontidae (Mammalia, Creodonta) in the Clarks Fork Basin, Wyoming. Contributions from the Museum of Paleontology, University of Michigan, 27: 327-391.
- GINGERICH, P. D. and D. A. WINKLER. 1985. Systematics of Paleocene Viverravidae (Mammalia, Carnivora) in the Bighorn Basin and Clarks Fork Basin. Contributions from the Museum of Paleontology, University of Michigan, 27: 87-128.
- GUNNELL, G. F. 1998. Mammalian faunal composition and the Paleocene-Eocene epoch/series boundary: evidence from the northern Bighorn Basin, Wyoming. In M.-P. Aubry, S. G. Lucas, and W. A. Berggren (eds.), Late Paleocene-Early Eocene Climatic and Biotic Events in the Marine and Terrestrial Records, Columbia University Press, New York, pp. 409-427.
- GUNNELL, G. F. and P. D. GINGERICH. 1981. A new species of *Niptomomys* (Microsypidae) from the early Eocene of Wyoming. Folia Primatologica, 36: 128-137.
- HOLROYD, P. A. and J. H. HUTCHISON. 2000. Proximate causes for changes in vertebrate diversity in the early Paleogene: an example from turtles in the Western Interior of North America. In B. Schmitz, B. Sundquist, and F. P. Andreasson (eds.), Early Paleogene Warm Climates and Biosphere Dynamics, Uppsala, Geological Society of Sweden, GFF [Geologiska Föreningens Förhandlingar], 122 pp. 75-76.
- HOKKER, J. J. 1998. Mammalian faunal change across the Paleocene-Eocene transition in Europe. In M.-P. Aubry, S. G. Lucas, and W. A. Berggren (eds.), Late Paleocene-Early Eocene Climatic and Biotic Events in the Marine and Terrestrial Records, Columbia University Press, New York, pp. 428-450.
- HUTCHISON, J. H. 1998. Turtles across the Paleocene-Eocene epoch boundary in west-central North America. In M.-P. Aubry, S. G. Lucas, and W. A. Berggren (eds.), Late Paleocene-Early Eocene

- Climatic and Biotic Events in the Marine and Terrestrial Records, Columbia University Press, New York, pp. 401-408.
- IVY, L. D. 1990. Systematics of late Paleocene and early Eocene Rodentia (Mammalia) from the Clarks Fork Basin, Wyoming. Contributions from the Museum of Paleontology, University of Michigan, 28: 21-70.
- KORTH, W. W. 1984. Earliest Tertiary evolution and radiation of rodents in North America. Bulletin of Carnegie Museum of Natural History, 24: 1-71.
- KRAUSE, D. W. 1982. Multituberculates from the Wasatchian land-mammal age, early Eocene, of western North America. Journal of Paleontology, 56: 271-294.
- KRAUSE, D. W. 1987. *Baiotomeus*, a new ptilodontid multituberculate (Mammalia) from the middle Paleocene of western North America. Journal of Paleontology, 61: 595-603.
- KRISHTALKA, L. 1976. Early Tertiary Adapidae and Erinaceidae (Mammalia, Insectivora) of North America. Bulletin of Carnegie Museum of Natural History, 1: 1-40.
- KRISHTALKA, L. and R. K. STUCKY. 1983a. Revision of the Wind River Faunas, Early Eocene of central Wyoming. Part 3. Marsupialia. Annals of Carnegie Museum, 52: 205-227.
- KRISHTALKA, L. and R. K. STUCKY. 1983b. Paleocene and Eocene marsupials of North America. Annals of Carnegie Museum, 52: 229-263.
- LUCAS, S. G. 1984. Synopsis of the species of *Coryphodon* (Mammalia, Pantodonta). New Mexico Journal of Sciences, 24: 33-42.
- LUCAS, S. G. 1998. Fossil mammals and the Paleocene-Eocene series boundary in Europe, North America, and Europe. In M.-P. Aubry, S. G. Lucas, and W. A. Berggren (eds.), Late Paleocene-Early Eocene Climatic and Biotic Events in Marine and Terrestrial Records, Columbia University Press, New York, pp. 451-500.
- MAAS, M. C., M. R. L. ANTHONY, P. D. GINGERICH, G. F. GUNNELL, and D. W. KRAUSE. 1995. Mammalian generic diversity and turnover in the late Paleocene and early Eocene of the Bighorn and Crazy Mountains Basins, Wyoming and Montana (USA). Palaeogeography, Palaeoclimatology, Palaeoecology, 115: 181-207.
- MATTHEW, W. D. 1915. A revision of the lower Eocene Wasatch and Wind River faunas. Part I—Order Ferae (Carnivora). Suborder Creodonta. Bulletin of the American Museum of Natural History, 34: 4-103.
- MCKENNA, M. C. 1960. Fossil Mammalia from the early Wasatchian Four Mile fauna, Eocene of northwest Colorado. University of California Publications in Geological Sciences, 37: 1-130.
- MCKENNA, M. C. and S. K. BELL. 1997. Classification of Mammals Above the Species Level. Columbia University Press, New York, 631 pp.
- MCKENNA, M. C., A. R. BLEEFELD, and J. S. MELLETT. 1994. Microvertebrate collecting: large-scale wet sieving for fossil microvertebrates in the field. In P. Leiggi and P. May (eds.), Vertebrate Paleontological Techniques, Volume 1, Cambridge University Press, Cambridge, pp. 93-112.
- NOVACEK, M. J. 1976. Insectivora and Proteutheria of the later Eocene (Uintan) of San Diego County, California. Los Angeles County Museum Contributions in Science, 283: 1-52.
- NOVACEK, M. J., T. M. BOWN, and D. M. SCHANKLER. 1985. On the classification of the early Tertiary Erinaceomorpha (Insectivora, Mammalia). American Museum Novitates, 2813: 1-22.
- POLLY, P. D. 1997. Ancestry and species definition in paleontology: a stratocladistic analysis of Paleocene-Eocene Viverravidae (Mammalia, Carnivora) from Wyoming. Contributions from the Museum of Paleontology, University of Michigan, 30: 1-53.
- ROBINSON, P. and B. A. WILLIAMS. 1997. Species diversity, tooth size, and shape of *Haplomylys* (Condylarthra, Hyopsodontidae) from the Power River Basin, northeastern Wyoming. University of Wyoming Contributions to Geology, 31: 59-78.
- ROSE, K. D. 1981. The Clarkforkian land-mammal age and mammalian faunal composition across the Paleocene-Eocene boundary. University of Michigan Papers on Paleontology, 26: 1-197.
- ROSE, K. D., K. C. BEARD, and P. HOUE. 1993. Exceptional new dentitions of the diminutive plesiadapiforms *Tinimomys* and *Niptomomys* (Mammalia), with comments on the upper incisors of plesiadapiforms. Annals of Carnegie Museum, 62: 351-361.
- ROSE, K. D. and P. D. GINGERICH. 1987. A new insectivore from the Clarkforkian (earliest Eocene) of Wyoming. Journal of Mammalogy, 68: 17-27.
- SCHMITZ, BIRGER, B. SUNDQUIST, and F. P. ANDREASSON (eds.). 2000. Early Paleogene Warm Climates and Biosphere Dynamics, GFF [Geologiska Föreningens Förhandlingar], Geological Society of Sweden, Uppsala, 122: 1-192.
- SCHOCH, R. M. 1986. Systematics, functional morphology and macroevolution of the extinct mammalian order Taeniodonta. Bulletin of the Peabody Museum of Natural History, Yale University, 42: 1-307.
- SILCOX, M. T. and K. D. ROSE. 2001. Unusual vertebrate microfaunas from the Willwood Formation early Eocene of the Bighorn Basin, Wyoming. In G. F. Gunnell (ed.), Eocene Biodiversity: Unusual Occurrences and Rarely Sampled Habitats, Plenum Press, New York, in press.
- SZALAY, F. S. 1969. Uintasoricinae, a new subfamily of early Tertiary mammals (?Primates). American Museum Novitates, 2363: 1-36.
- THEWISSEN, J. G. M. 1990. Evolution of Paleocene and Eocene Phenacodontidae (Mammalia, Condylarthra). University of Michigan Papers on Paleontology, 29: 1-107.
- UHEN, M. D. and P. D. GINGERICH. 1995. Evolution of *Coryphodon* (Mammalia, Pantodonta) in the late Paleocene and early Eocene of northwestern Wyoming. Contributions from the Museum of Paleontology, University of Michigan, 29: 259-289.
- WING, S. L. 1998. Late Paleocene-early Eocene floral and climatic change in the Bighorn Basin, Wyoming. In M.-P. Aubry, S. G. Lucas, and W. A. Berggren (eds.), Late Paleocene-Early Eocene Climatic and Biotic Events in the Marine and Terrestrial Records, Columbia University Press, New York, pp. 380-400.
- WING, S. L., T. M. BOWN, and J. D. OBRADOVICH. 1991. Early Eocene biotic and climatic change in interior western North America. Geology, 19: 1189-1192.



BASIN-MARGIN VERTEBRATE FAUNAS ON THE WESTERN FLANK OF THE BIGHORN AND CLARKS FORK BASINS

GREGG F. GUNNELL¹ and WILLIAM S. BARTELS²

¹*Museum of Paleontology, The University of Michigan, Ann Arbor, Michigan 48109-1079*

²*Department of Geological Sciences, Albion College, Albion, Michigan 49224*

Abstract.— Examination of Paleocene-Eocene vertebrate assemblages from the western flanks of the Bighorn and Clarks Fork basins, adjacent to the Absaroka Volcanic Field and Beartooth Uplift, respectively, shows that some localities preserve faunal elements expected in a basin margin setting. Basin-margin faunas can be recognized by the presence of *distinctive taxa*, including those that are uniquely or frequently found in basin margin settings, and *anachronistic taxa*, including co-occurrences of within-lineage or clade taxa that do not overlap in basin-center assemblages. Wapiti Valley late Wasatchian (Wa-7) through middle Bridgerian (Br-2) faunas in the Willwood and Aycross formations west of Cody provide one of the best Bighorn Basin examples of a basin-margin assemblage. Owl Creek early to middle Bridgerian (Br-1 and Br-2) faunas in the Aycross Formation northwest of Thermopolis are another example. Two localities associated with the Beartooth Uplift, early Clarkforkian (Cf-1) Bear Creek and middle Clarkforkian (Cf-2) Paint Creek, contain faunal elements consistent with basin-margin settings, although both may represent, in part, unique environments not necessarily associated with marginal deposition.

INTRODUCTION

A series of North American Land-Mammal Ages (NALMAs) for the Paleocene and Eocene (and other epochs) has been developed (Wood *et al.*, 1941; Archibald *et al.*, 1987; Krishtalka *et al.*, 1987), based on study of terrestrial deposits in the Rocky Mountain Interior and their contained faunas. Paleocene and Eocene NALMAs include from oldest to youngest: Puercan, Torrejonian, Tiffanian, Clarkforkian, Wasatchian, Bridgerian, Uintan, Duchesnean, and Chadronian (Archibald *et al.*, 1987; Krishtalka *et al.*, 1987; Prothero and Swisher, 1992). In every case, the faunal samples used to define each of these ages are derived from richly fossiliferous sequences of fluvial rocks deposited in lowland areas near the centers of intermontane basins. These "type faunas" for each land-mammal age and

stratigraphic ranges of the contained taxa are based on sampling of a narrow range of depositional environments and habitats.

Black (1967) noted the presence of several middle Eocene archaic mammalian taxa thought to have become extinct in the earliest Eocene and suggested that known middle Eocene faunal samples were all derived from similar ecological circumstances that do not reflect the true diversity of mammals living during middle Eocene time. Black (1967, p. 62) further suggested that "faunas of different ecological aspect may be recovered from sediments along, and in, the mountain fronts of northwestern Wyoming."

Recent paleontological and geological fieldwork along the northeastern margin of the Green River Basin in southwestern Wyoming, the South Pass area, corroborates Black's suggestion, and indicates that vertebrate faunal samples derived from basin margins differ in composition from time-equivalent samples in basin-center depositional environments (Bartels and Gunnell, 1997; Gunnell and Bartels, 1997, 1998, 2001). Here

In: Paleocene-Eocene Stratigraphy and Biotic Change in the Bighorn and Clarks Fork Basins, Wyoming (P. D. Gingerich, ed.), University of Michigan Papers on Paleontology, 33: 145-155 (2001).

we present a brief overview of the characteristics of basin margins and their faunal assemblages, and then examine four areas along the western margin of the Bighorn and Clarks Fork basins where possible basin-margin samples are available. The impact of such samples for understanding early Cenozoic biotic diversity and local biostratigraphy warrants further discussion.

BASIN MARGINS

Basin margins can be defined by a set of geographic, physiographic, ecologic, geologic, and paleontologic components (Gunnell and Bartels, 2001). In the broadest sense, basin margins can be thought of as comparable to upland areas. Geographically, basin margins are located adjacent to mountainous areas and include mountain fronts and foothills. Physiographically, basin margins have much greater topographic relief than basin centers and, because of this increased topographic complexity, are ecologically diverse with a much wider variety of habitats and microhabitats than are generally available in basin centers. Geologically, basin margins are closer to source areas of basin fill than are basin centers and as such are characterized by higher energy depositional settings (alluvial fans and braided streams) with an abundance of coarser and less mature sediments. All of these features combine to offer vertebrates a more complex and more demanding environment than they generally encounter in the less topographically and climatologically complex, less ecologically diverse, and generally lower energy environments of basin centers.

Definitions

Based on studies of faunal samples from South Pass (Gunnell and Bartels, 2001), two general paleontological characteristics of vertebrate assemblages can be viewed as indicators of basin margin environments. These include the presence of *distinctive taxa*, and the presence of *anachronistic taxa*. Distinctive taxa are those that are absent or rare in basin center assemblages but abundant in basin margin samples. Anachronistic taxa are those that are found on a basin margin during times when they are not represented in the basin center. Most importantly, these include examples of taxa that do not co-occur in basin center assemblages but occur in the same localities or overlap stratigraphically in basin margin samples. Such co-occurrences often represent presumed ancestor-descendent pairs of taxa.

Basin Margin Samples from the Bighorn Basin

The Bighorn Basin is bordered by Laramide basement faults represented at the surface by folds, thrusts, and high-angle reverse faults (Fig. 1; Brown, 1993; Stone, 1993). The structural evolution of the basin is characterized by a series of late Laramide (Eocene) uplifts that severely reduce the potential for the preservation of basin margin deposits of early Paleogene age (Foose et al., 1961; Wise, 2000). This is particularly true of the eastern and southern margins of the basin (Foose,

1973). The western margin of the basin was only moderately deformed by late Laramide tectonism and provides a greater opportunity for the preservation and study of basin margin sediments and assemblages.

Minor Laramide structures such as the Dead Indian monocline, the Pat O'Hara horst (*Fpoh* in Fig. 1), and the Rattlesnake Mountain structure (*Frs* in Fig. 1) combined with relatively little late movement on the Beartooth Fault (*Fbt*) to conserve some basin-margin and near-margin areas (Lutz and Omar, 1996). Post-Laramide volcanic activity in the Absaroka Volcanic Field provided a renewed source area along the western and southwestern edges of the basin at the beginning of the middle Eocene and allowed for additional basin margin deposition and preservation.

Four vertebrate samples from potential basin margin settings are recognized in the Bighorn and Clarks Fork basins thus far, all located along the western margin (Fig. 1). These include one area south of the Beartooth Uplift in the Wapiti Valley along the north and south forks of the Shoshone River (Gunnell et al., 1992); one on the eastern flank of the southern Absaroka Range in the vicinity of Owl Creek (Bown, 1979, 1982); and two areas along the eastern flank of the Beartooth Mountains, the Bear Creek and Paint Creek localities (Rose, 1981). The Wapiti Valley localities span the later Wasatchian and early Bridgerian (Wa-7 to Br-2; early to middle Eocene), the Owl Creek samples represent the middle Bridgerian (Br-1 to Br-2; early middle Eocene), and the Bear Creek and Paint Creek samples represent the Clarkforkian (Cf-1 and Cf-2, respectively; latest Paleocene).

Wapiti Valley

The localities in Wapiti Valley are situated approximately 30 km west of Cody, Wyoming, near the juncture of the Beartooth and Absaroka ranges along the northwestern margin of the Bighorn Basin. In Wapiti Valley, the fluvial Willwood Formation rests unconformably on the marine Upper Cretaceous Cody Shale and is in turn unconformably overlain by volcanoclastic sediments of the Aycross Formation. This sequence is capped by Absaroka volcanics of the Wapiti Formation (Torres and Gingerich, 1983; Torres, 1985). Here again, the Willwood is characterized by generally fine-grained deposition despite relatively close proximity to its Beartooth source to the north. Aycross deposits are derived from more proximal Absaroka volcanic sources to the northwest and are decidedly coarser grained. They are characterized by a suite of basin margin depositional features such as conglomerates and sandy to conglomeratic mudrocks indicating distal fan mudflow and sheetwash deposits similar to those seen in the Owl Creek area (see below). Late Laramide deformation in this area (Rattlesnake Mountain; *Frs* in Fig. 1) occurred well basinward of the sequence, thereby enhancing its potential to survive later Cenozoic erosion.

The first fossil vertebrates from Wapiti Valley were discovered by Princeton University parties (Jepsen, 1939), with later work being done by Van Houten (1944), and more recently by the University of Michigan (Torres and Gingerich, 1983; Torres,

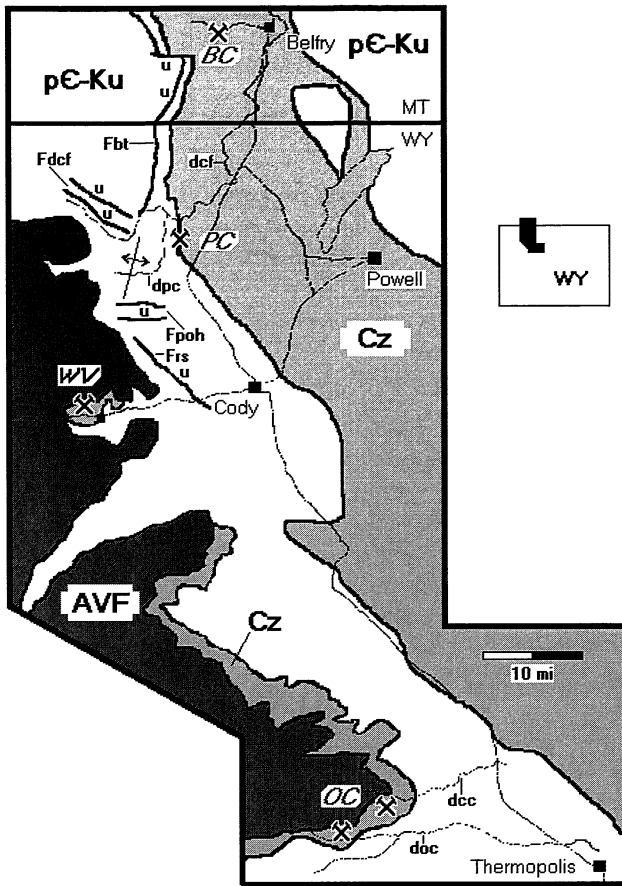


FIGURE 1 — Map of Bighorn Basin showing the location of Bear Creek (BC), Paint Creek (PC), Wapiti Valley (WV), and Owl Creek (OC) basin margin localities. Cenozoic outcrop belts (Cz) indicated by shading, vent and proximal facies of the Absaroka Volcanic Field (AVF) indicated by darker shade. Relevant faults are identified in the text and shown with upthrown side indicated (u). Drainages of the Clarks Fork River (dcf), Paint Creek (dpc), Cottonwood Creek (dcc) and Owl Creek (doc) are indicated. Major roadways are unlabelled. Modified from Love and Christiansen (1985).

1985; Gunnell et al., 1992). Localities range from the late early Wasatchian (Wa-7 or Lostcabinian) through early middle Bridgerian (Br-2), and represent one of only a few faunal sequences that document the Wasatchian-Bridgerian transition (Gunnell et al., 1992).

There are several distinctive taxa in the Wapiti Valley assemblage (Table 1). The ziphodont crocodylid *Pristichampsus vorax* is present at Lostcabinian and early Gardnerbuttean localities in Wapiti Valley. *Pristichampsus* is also a common element in basin margin samples from South Pass (Gunnell and Bartels, 2001) but is very rare from basin center assemblages (Gingerich, 1989; Gunnell and Bartels, 1994). Among mam-

mals *Elwynella oreas*, *Washakius laurae*, *Didymictis vanicleveae*, *Ectocion superstes*, and *Trogosus latidens* are all very rare taxa known only from a small number of places outside of Wapiti Valley. The omomyid primate *Loveina wapitiensis* is only known from Wapiti Valley and represents a unique occurrence.

Two cases of anachronism also are documented in Wapiti Valley. The brontotheriid *Eotitanops borealis* is an index taxon of the earliest Gardnerbuttean (Br-0) in the Wind River Basin (Stucky, 1984; Gunnell and Yarborough, 2000). In Wapiti Valley it occurs in the Lostcabinian (Wa-7) in association with the palaeotheriid *Lambdaotherium*, the most important index taxon of the Lostcabinian. Outside of Wapiti Valley there are few confirmed co-occurrences of *E. borealis* and *L. popoagicum* (Gunnell and Yarborough, 2000).

The other case of anachronism involves *Didymictis vanicleveae* and *Microsyops annectens*. Both of these taxa occur at Van Houten's B-1 locality along the South Fork of the Shoshone River. This locality cannot be tied into the local section so its relative stratigraphic position is unknown. However, outside of Wapiti Valley, *D. vanicleveae* is only known from the later Gardnerbuttean (Br-1a) at Huerfano Park in Colorado (Robinson, 1966), while *M. annectens* is only known from the late Bridgerian (Br-3) in Wyoming and possibly the Uintan in California (Gunnell, 1989). In either case, one of these two taxa represents an anachronism because they do not overlap in time outside of Wapiti Valley. Either the presence of *M. annectens* represents a precocious first appearance or the presence of *D. vanicleveae* represents a delayed last occurrence (or both). It will not be possible to determine which is the correct interpretation without further independent geochronologic evidence.

Owl Creek

The Owl Creek localities are situated along the southwestern margin of the Bighorn Basin on the flanks of the southern Absaroka Range in the Aycross Formation (Bown, 1982). The majority of the samples are derived from four localities (Vass, Clay Gall, Flattop, and 21 quarries) with a few specimens coming from other scattered localities in the Aycross Formation. The structural geology is complex in this area and it is not as yet possible to assign relative stratigraphic positions to any of the localities. However, the faunal constituents indicate that all Owl Creek localities represent the early to middle Bridgerian (Bown, 1979, 1982; Gunnell and Gingerich, 1996).

Locally the Aycross Formation consists of volcanoclastic conglomerates, conglomeratic to sandy mudrocks, sandstones, and shales. These sediments represent deposits characteristic of the medial facies (distal fan to fluvial) of the Absaroka volcanic field with vent and proximal facies to the northwest serving as the source area (Bown, 1982). These typical basin margin facies interfinger with finer lake margin deposits similar to those of the South Pass area (Bown, 1982). The finer deposits generally contain basin center faunal elements, while the coarser deposits, such as those found at 21 Quarry, are characterized by a more typical basin margin assemblage.

TABLE 1 — Vertebrate faunal list for the early to middle Eocene Wapiti Valley assemblage, late Wasatchian through middle Bridgerian (Wa-7 through Br-2; Gunnell et al., 1992). Wapiti local-faunal distribution is given in parentheses; A-4 and B-1 are Van Houten (1944) designations. Key: *, distinctive taxon; **, anachronistic taxon.

Class Osteichthyes	Order Condylarthra
Order Lepisosteiformes	Family Hyopsodontidae
Family Lepisosteidae	<i>Hyopsodus miticulus</i> (II)
<i>Lepisosteus</i> sp. (II, III, V)	<i>Hyopsodus paulus</i> (III)
Class Reptilia	<i>Hyopsodus minusculus</i> (V)
Order Testudines	Family Phenacodontidae
Family Trionychidae	<i>Ectocion</i> cf. <i>E. superstes</i> * (II)
Trionychid indet. (II, III, V)	<i>Phenacodus vortmani</i> (II)
Family Emydidae	<i>Phenacodus intermedius</i> (II)
Emydid indet. (II, III, V)	Order Pantodonta
Family Testudinidae	Family Coryphodontidae
<i>Hadrianus</i> sp. (II, III)	<i>Coryphodon</i> sp. (II)
Order Squamata	Order Tillodontia
Family Anguidae	Family Esthonychidae
<i>Xestops</i> sp. (II)	<i>Esthonyx</i> cf. <i>E. acutidens</i> (II)
Order Crocodylia	<i>Trogosus latidens</i> * (V, A-4)
Family Crocodylidae	<i>Trogosus</i> sp. (III)
Crocodylid indet. (II, V)	Order Rodentia
<i>Borealosuchus</i> sp. (II)	Family Paramyidae
<i>Pristichampsus vorax</i> * (II, III)	<i>Paramys copei</i> (II, V)
Family Alligatoridae	<i>Paramys delicatus</i> (III)
<i>Allognathosuchus</i> sp. (II, III)	<i>Pseudotomus</i> cf. <i>P. robustus</i> (V)
Class Mammalia	Reithroparamyine sp.* (V)
Order Erinaceomorpha	Family Sciuravidae
Family Sespedectidae	<i>Knightomys</i> cf. <i>K. huerfanensis</i> (V)
<i>Scenopagus curtidens</i> (II)	<i>Knightomys</i> cf. <i>K. depressus</i> (V)
Order Primates?	Order Perissodactyla
Family Microsyopidae	Family Equidae
<i>Microsyops scottianus</i> (II)	<i>Hyracotherium</i> sp. (I)
<i>Microsyops</i> cf. <i>M. elegans</i> (III)	<i>Hyracotherium</i> cf. <i>H. venticolum</i> (II)
<i>Microsyops</i> cf. <i>M. annectens</i> (? , B-1)	<i>Hyracotherium</i> cf. <i>H. craspedotum</i> (II)
Family Paromomyidae	<i>Orohippus pumilus</i> (III)
Cf. <i>Elwynella oreas</i> * (II)	Family Isectolophidae
Order Primates	Cf. <i>Cardiolphus semihians</i> (I)
Family Omomyidae	Family Helaletidae
<i>Loveina wapitiensis</i> * (II)	<i>Heptodon posticus</i> (II)
<i>Washakius laurae</i> * (V)	<i>Hyrachyus modestus</i> (III, V)
Family Notharctidae	Family Palaeotheriidae
<i>Smilodectes mcgrewi</i> (III)	<i>Lambdotherium popoagicum</i> (II)
<i>Smilodectes gracilis</i> (V)	Family Brontotheriidae
Order Carnivora	<i>Eotitanops borealis</i> (II)
Family Viverravidae	<i>Palaeosyops fontinalis</i> (III)
<i>Viverravus gracilis</i> (II)	Order Artiodactyla
<i>Didymictis</i> cf. <i>D. vanclaveae</i> * (? , B-1)	Family Dichobunidae
Family Miacidae	<i>Diacodexis</i> cf. <i>D. secans</i> (II)
<i>Vulpavus</i> cf. <i>V. australis</i> (II)	<i>Bunophorus sinclairi</i> (II)

While much of the fauna indicates early or middle Bridgerian affinities (Table 2), there are a number of unique taxa present in the Owl Creek localities. Among taxa that have been well studied, the picromomyid plesiadapiform *Alveojunctus minutus*,

TABLE 2 — Vertebrate faunal list for the middle Eocene Owl Creek assemblage (Bridgerian, Br-1 and Br-2; from Bown, 1982, with additions). Key: *, distinctive taxon; **, anachronistic taxon.

Class Reptilia	Family Aptemyidae	Family Oxyaenidae
Order Testudines	<i>Apatemys</i> cf. <i>A. bellus</i>	<i>Patriofelis</i> sp.
Family Trionychidae	<i>Apatemys</i> cf. <i>A. bellulus</i>	Order Carnivora
Trionychid indet.	Family Palaeoryctidae	Family Viverravidae
<i>Trionyx</i> sp.	<i>Didelphodus</i> sp.*	<i>Viverravus gracilis</i>
Cf. <i>Plastomenus</i> sp.	Order Erinaceomorpha	Viverravid indet.*
Family Emydidae	Family Sespedectidae	Family Miacidae
<i>Echmatemys</i> sp.	<i>Scenopagus curticens</i>	<i>Uintacyon</i> sp.*
Cf. <i>Echmatemys</i> sp.	<i>Scenopagus edenensis</i>	Order Mesonychia
Family Baenidae	<i>Scenopagus</i> cf. <i>S. priscus</i>	Family Mesonychidae
Cf. <i>Baena</i> sp.	Sespedectid indet.*	<i>Mesonyx obtusidens</i>
Family Carettochelyidae	Family Amphilemuridae	Family Hapalodectidae
<i>Anosteira ornata</i> *	Cf. <i>Macrocranium</i> sp.*	<i>Hapalorestes lovei</i> *
Family Dermatemnydidae	Order Soricomorpha	Order Condylarthra
Cf. <i>Baptemys</i> sp.	Family Geolabididae	Family Hyopsodontidae
<i>Baptemys</i> cf. <i>B. wyomingensis</i>	Cf. <i>Marsholestes</i> sp.*	<i>Hyopsodus</i> cf. <i>H. paulus</i>
Family Testudinidae	Family Nyctitheriidae	Order Tillodontia
<i>Hadrianus</i> sp.	<i>Nyctitherium serotinum</i>	Family Esthonychidae
Family Kinosternidae	Cf. <i>Nyctitherium</i> sp.	<i>Trogosus</i> sp.
Kinosternid indet.	Cf. <i>Pontifactor</i> sp.	Order Dinocerata
Order Squamata	Order Chiroptera	Family Uintatheriidae
Family Anguidae	Family Indet.	<i>Bathyopsis</i> sp.
<i>Xestops vagans</i>	Chiropteran indet.	Order Perissodactyla
<i>Glyptosaurus sylvestris</i>	Order Primates?	Family Equidae
Family Agamidae	Family Microsopidae	<i>Orohippus</i> sp.
<i>Tinosaurus</i> sp.*	<i>Microsops</i> cf. <i>M. elegans</i>	Family Brontotheriidae
Family Boidae	<i>Uintasorex parvulus</i>	<i>Eotitanops minimus</i> *
Boid indet.*	Family Picromomyidae	<i>Palaeosyops fontinalis</i>
Order Crocodylia	<i>Alveojunctus minutus</i> *	Family Helaletidae
Family Crocodylidae	Family Paromomyidae	Cf. <i>Helaletes nanus</i>
Crocodylid indet. (1)	Cf. <i>Phenacolemur</i> sp.	<i>Hyrachyus modestus</i>
Crocodylid indet. (2)	Order Primates	Order Artiodactyla
Family Alligatoridae	Family Omomyidae	Family Dichobunidae
<i>Allognathosuchus</i> sp.	<i>Omomys carteri</i>	<i>Antiacodon pygmaeus</i>
Class Mammalia	<i>Shoshonius bowni</i> *	Order Rodentia
Order Marsupialia	<i>Aycrossia lovei</i> *	Family Paramyidae
Family Didelphidae	<i>Gazinius amplus</i> *	Cf. <i>Leptomys</i> (2 species)
<i>Peradectes</i> cf. <i>P. innominatus</i>	<i>Strigorhysis rugosus</i> *	<i>Thisbemys corrugatus</i>
<i>Peratherium knighti</i>	<i>Strigorhysis bridgerensis</i> *	Cf. <i>Thisbemys</i> sp.
<i>Peratherium</i> cf. <i>P. marsupium</i>	Family Notharctidae	Cf. <i>Pseudotomus</i> sp.
Order Cimolesta	<i>Notharctus</i> sp.	<i>Reithroparamys</i> cf. <i>R. delicatissimus</i>
Family Leptictidae	Order Creodonta	<i>Microparamys</i> (2 species)
<i>Palaeictops</i> cf. <i>P. bridgeri</i>	Family Hyaenodontidae	Family Sciuravidae
	<i>Proviverroides piercei</i> *	<i>Taxymys cuspidatus</i> *

the omomyid primates *Shoshonius bowni* and *Strigorhysis rugosus*, the hyaenodontid creodont *Proviverroides piercei*, the hapalodectid mesonychian *Hapalorestes lovei*, and the sciuravid rodent *Taxymys cuspidatus*, all represent taxa unknown elsewhere. Other less well-studied or poorly represented taxa that may be unique include the geolabidid soricomorph

Marsholestes sp., the miacid carnivore *Uintacyon* sp., and an unidentified viverravid carnivore.

There are also a number of distinctive taxa present in the Owl Creek assemblage including the omomyid primates *Aycrossia lovei* (also possibly known from the Wind River Basin), *Gazinius amplus* (also poorly known from the early

TABLE 3 — Vertebrate faunal list for the late Paleocene Bear Creek assemblage (Clarkforkian, Cf-1; from Rose, 1981, with additions). Key: *, distinctive taxon; **, anachronistic taxon.

Class Reptilia	<i>Planetetherium mirabile*</i>
Order Testudines	Order ?Primates
Family Trionychidae	Family Plesiadapidae
Trionychid indet.	<i>Plesiadapis dubius</i>
<i>Plastomenus</i> sp.	<i>Chiromyoides potior</i>
Order Choristodera	Family Carpolestidae
Family Champsosauridae	<i>Carpolestes nigridentis</i>
<i>Champsosaurus gigas</i>	Family Paromomyidae
<i>Simodosaurus</i> sp.	<i>Phenacolemur pagei</i>
Order Crocodylia	Order Condylarthra
Family Crocodylidae	Family Arctocyoniidae
<i>Leidyosuchus</i> sp.	<i>Thryptacodon pseudarctos</i>
	Family Phenacodontidae
	<i>Phenacodus intermedius</i>
Class Mammalia	Family Hyopsodontidae
Order Marsupialia	<i>Haplomylys palustris*</i>
Family Didelphidae	Cf. <i>Phenacoptes sabulosus*</i>
Cf. <i>Peradectes</i> sp.	Order Mesonychia
Order Cimolesta	Family Mesonychidae
Family Cimolestidae	<i>Dissacus</i> sp.
<i>Protentomodon ursirivalis*</i>	Order Taeniodonta
Family Pantolestidae	Family Stylinodontidae
Cf. <i>Aphronorus</i> sp.*	<i>Lampadophorus lobbelli</i>
Cf. <i>Palaeosinopa</i> sp.	Order Carnivora
Family Apatemyidae	Family Viverravidae
<i>Labidolemur kayi</i>	<i>Viverravus</i> sp.
Order Erinaceomorpha	Order Rodentia
Family Erinaceidae	Family Paramyidae
<i>Leipsanolestes siegfreidti*</i>	<i>Acritoparamys atavus</i>
Order ?Dermoptera	
Family Plagiomenidae	

Bridgerian in the Green River Basin), and *Strigorhysis bridgerensis* (also represented by one or two specimens from the basin center in the Bighorn Basin), and the brontotheriid *Eotitanops minimus* (elsewhere known from Huerfano Park and South Pass). Among reptiles, distinctive taxa include the carettochelydrid turtle *Anosteira ornata*, the agamid lizard *Tinosaurus*, and an unusually high abundance of boid snakes.

Some unique morphological forms that may represent new species are also known from Owl Creek localities, including *Didelphodus* sp., *Macrocranium* sp., and an indeterminate sespedectid erinaceomorph. No apparent cases of anachronism have been documented as yet from the Owl Creek localities.

Bear Creek

The Bear Creek locality is situated in the Fort Union Formation along the Beartooth Front in southern Carbon County, south-central Montana, about 12 miles north of the Wyoming state line. The fauna is derived from an argillaceous layer in

the roof of the old Eagle Mine in the Red Lodge coal field (Simpson, 1928).

Poor exposure and limited access to proprietary mine information precludes a detailed consideration of the stratigraphy of the Bear Creek deposits, but they are clearly atypical of a basin margin setting. Although in relatively close proximity to the Beartooth thrust and Maurice tear faults, the deposits represent a paludal facies of the Fort Union Formation (Hickey, 1980). The deposition of fine-grained Paleocene and Eocene sequences close to the Beartooth Front was augmented by the predominance of mid-Paleozoic carbonate and mudrock units in the source area, which yielded sediments that exhibit a pronounced and rapid basinward fining. Although sedimentologically atypical of near-source deposits, the Bear Creek deposits formed close enough to the Beartooth Uplift to potentially contain remains of basin margin faunal elements.

The Bear Creek assemblage was first described by Simpson (1928), with updates provided by Simpson (1929a, b), Jepsen

TABLE 4 — Vertebrate faunal list for the late Paleocene Paint Creek assemblage (Clarkforkian, Cf-2; from Rose, 1981, with additions). Key: *, distinctive taxon; **, anachronistic taxon.

Class Reptilia	<i>Plesiadapis gingerichi</i> **
Order Testudines	<i>Chiromyoides major</i> *
Family Emydidae	Family Carpolestidae
Emydid sp. nov.	<i>Carpolestes nigridentis</i> **
Order Squamata	<i>Carpolestes simpsoni</i> **
Family Anguillidae	Family Paromomyidae
<i>Machaerosaurus torreonensis</i> **	<i>Ignacius</i> sp.
<i>Odaxosaurus piger</i> **	<i>Phenacolemur pagei</i>
<i>Proxestops</i> sp.	Order Condylarthra
<i>Xestops</i> sp.**	Family Hyopsodontidae
<i>Melanosaurus maximus</i>	<i>Aletodon gunnelli</i>
Order Crocodylia	<i>Apheliscus nitidus</i> *
Family Alligatoridae	Family Arctocyonidae
<i>Allognathosuchus</i> sp.	<i>Chriacus</i> sp.
Class Mammalia	<i>Thryptacodon antiquus</i>
Order Multituberculata	Family Phenacodontidae
Family Neoplagiulacidae	<i>Ectocion osbornianus</i>
<i>Ectypodus powelli</i>	<i>Phenacodus</i> sp.
<i>Parectypodus laytoni</i>	Order Carnivora
Family Eucosmodontidae	Family Viverravidae
<i>Microcosmodon rosei</i>	<i>Didymictis leptomytus</i>
Order Cimolesta	Order Mesonychia
Family Apatemyidae	Family Mesonychidae
<i>Labidolemur</i> sp.	<i>Dissacus</i> sp.
Order Soricomorpha	Order Dinocerata
Family Nyctitheriidae	Family Uintatheriidae
<i>Plagioctenodon</i> sp.	<i>Probathyopsis</i> sp.
<i>Pontifactor</i> sp.	Order Taeniodonta
Order Primates?	Family Stylinodontidae
Family Microsypidae	<i>Ectoganus</i> sp.
<i>Arctodontomys simplicidentis</i>	Order Palaeonodonta
Family Plesiadapidae	Family Metacheiromyidae
<i>Plesiadapis dubius</i>	<i>Palaeonodon</i> sp.
<i>Plesiadapis cookei</i> **	Order Rodentia
	Family Paramyidae
	Paramyid indet.

(1937), Van Valen and Sloan (1966), and Rose (1981). The fauna is clearly Clarkforkian, and the mutual occurrence of *Chiromyoides potior*, *Phenacodaptes sabulosus*, and *Paramys atavus*, and the absence of *Plesiadapis cookei*, indicates early Clarkforkian (Cf-1; Rose, 1981). This is supported by presence of a distinctive species of *Haplomytus*, *H. palustris* (Gingerich, 1994).

An examination of the faunal list (Table 3) points out the aberrant nature of the Bear Creek assemblage. Most of the mammals are of small to very small body size indicating that the sample has been taphonomically sorted. None-the-less, many oddities persist. Fully one-third of the total number of mammal specimens represent *Planetetherium mirabile* (Fig. 2B), an otherwise almost unknown taxon (only two other

specimens are known from localities other than Bear Creek). *Protentomodon ursirivalis* is only known from Bear Creek, as is the *Aphronorus*-like pentacodontid. *Leipsanolestes siegfriedti*, while known from other localities, is never as common as it is at Bear Creek. The reptiles preserved at Bear Creek represent a typical late Paleocene assemblages of large aquatic taxa. The geographic position of the Bear Creek locality and the unusual nature of its mammalian faunal assemblage argue for at least partial derivation from a basin margin setting.

Paint Creek

The Paint Creek locality is situated to the southeast of the Beartooth Uplift approximately 3 km west of Wyoming High-

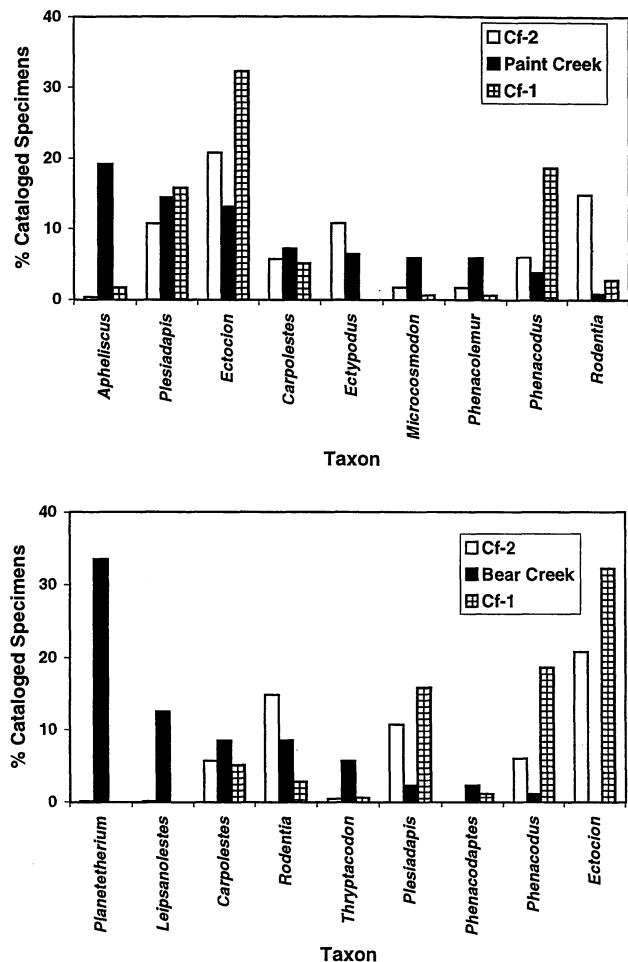


FIGURE 2 — Comparisons of Paint Creek (A) and Bear Creek (B) mammalian faunal assemblages with those of Clarkforkian biochronological zones Cf-1 and Cf-2 as percentages of mammalian samples. Clarkforkian samples are compiled from the five richest UM localities representing each zone in the northwestern Bighorn Basin. Paint Creek and Bear Creek samples are compiled from Rose (1981) and University of Michigan collections. Total mammals represented: Paint Creek, 236 specimens; Bear Creek, 176 specimens; Cf-1, 177 specimens; and Cf-2, 704 specimens.

way 120 at an elevation of 1555 m, about 150 meters above the floor of the Clarks Fork Basin (Rose, 1981) in fine grained overbank sediments of the Willwood Formation.

The locality is on the eastward facing limb of the Dead Indian monocline, a late Laramide ramp produced by a basinward tilted fault block (Foose et al., 1961; Wise, 2000). Here the Willwood deposits rest unconformably on the Upper Cretaceous Mesa Verde and Meeteetse formations at a low angle. The entire sequence was tilted after local deposition and the

Willwood now dips approximately 70° to the east and the Cretaceous units are almost vertical. Since most of the deformation on the monocline and the nearby Pat O'Hara Mountain was post-depositional, there was no significant nearby upland at the time of deposition. Basin margin elements in the fauna would have been derived from the Beartooth Uplift in the vicinity of the Dillworth and Clarks Fork faults some 10 km to the northwest (*Fdcf* in Fig. 1). Again, the mid-Paleozoic carbonate and mudrock dominated source area allowed for the deposition of very fine grained sediments in a geographic basin margin setting.

The Paint Creek assemblage (Table 4) has been interpreted as representing the middle Clarkforkian (Cf-2) because of the presence of *Plesiadapis cookei*, the main index taxon of Clarkforkian biochron Cf-2 (Gingerich, 1976; Rose, 1981; Bloch and Gingerich, 1998). However, recently Bloch and Gingerich (1998) described the first specimen of *Plesiadapis gingerichi* from Paint Creek, the presumed ancestor of *Plesiadapis cookei*, and also noted the presence of the presumed ancestor-descendant couplet of *Carpolestes nigridentis*-*Carpolestes simpsoni* at Paint Creek. The presence of these anachronistic taxa is not surprising given the expectations of basin margin faunal composition (Gunnell and Bartels, 2001).

Other evidence also supports interpretation of the Paint Creek faunal sample as representing a basin margin. The presence of *Chiromyoides major* is a distinctive occurrence, as this taxon is almost unknown from areas other than Paint Creek (four other specimens from the rest of the Bighorn Basin). Other distinctive taxa include *Apheliscus nitidus* and *Microcosmodon rosei*, both of which are very common at Paint Creek but relatively rare from basin center Cf-1 and Cf-2 samples (Fig. 2A). The common basin center Cf-1 and Cf-2 taxa *Ectocion* and *Phenacodus* are relatively rare at Paint Creek, as are rodents (also relatively rare in Cf-1, but more common in Cf-2). The anachronistic assemblage of lizards also indicates sampling of a basin margin fauna. Typically earlier Paleocene elements *Machaerosaurus torrejonensis* and *Odaxosaurus piger* are present, along with *Xestops vagans*, which does not appear in basin center faunas until the Wasatchian.

Summary

Characteristic elements of basin-margin faunal assemblages can be recognized in the vertebrates sampled at Wapiti Valley, Owl Creek, Bear Creek, and Paint Creek. Each contains some combination of distinctive and/or anachronistic taxa (despite their occurrence in atypical basin margin sequences at Bear Creek and Paint Creek). While Bear Creek is clearly a mixed assemblage of typical basin center and basin margin taxa, the other three localities preserve more characteristic basin-margin faunal elements.

As discussed above, the potential for studying basin margin faunas in the Bighorn Basin is somewhat limited by late Laramide uplifts and the weathering instability of the source rocks available in the Beartooth Uplift during the Paleocene

and Eocene. Of the areas treated here, the Owl Creek sequence holds the greatest potential for further examination of basin margin faunas in the Bighorn Basin.

IMPLICATIONS FOR BIODIVERSITY AND BIOSTRATIGRAPHY

Fossil vertebrates derived from basin margins represent assemblages from habitats not commonly sampled in the fossil record. It is evident from Bighorn Basin and other marginal assemblages that such samples can and do impact both biodiversity and local biostratigraphy. Western North American early Cenozoic fossil assemblages have normally been collected from a limited number of depositional environments, representing a small number of all available paleohabitats. It has always been tacitly understood that this reliance on commonly sampled paleohabitats necessarily underestimates total paleobiodiversity. Evidence presently available from basin margins provides confirmation of this underestimation. Certain vertebrate taxa lived away from the centers of deposition either by choice, or because of competition between taxa for limited resources. Many taxa apparently never lived in commonly sampled environments, while others rarely occupied such areas as part of their home ranges or were rarely introduced post-mortem by taphonomic processes. Basin margins and other unique depositional settings (Gingerich, 1987, 1989; Bloch and Gingerich, 1998; Bloch and Bowen, 2001; Silcox and Rose, 2001) provide otherwise overlooked evidence of vertebrate biodiversity and suggest that there is a great deal yet to be learned about the geographic distribution of paleohabitats and paleomicrohabitats and the consequences of habitat preference among vertebrates. The effects of these factors on the distribution and biodiversity of early Cenozoic vertebrates have yet to be evaluated at scales necessary to enable a full understanding of paleocommunity structure.

In the same sense, the understanding of the stratigraphic distribution of vertebrates is also impacted by studies of non-traditional paleohabitats. Anachronistic taxa in basin margins call into question the reliance on assemblages from limited paleohabitats to construct general biostratigraphic taxonomic range charts. It remains to be seen how study of marginal assemblages and the requisite changes in local biostratigraphic sections produced by such studies will impact regional biochronologies.

Studies of basin margins and other unique or rarely sampled habitats are just beginning. Much more effort is required before the full effects of these studies will be appreciated. However, enough is known to demonstrate that the work is worth pursuing.

ACKNOWLEDGMENTS

We thank J. I. Bloch and P. D. Gingerich for reading and improving the manuscript. Many colleagues and students have worked with us in the field in Wyoming. Special thanks go to

G. H. Junne, C. G. Childress, R. J. Walker, J.-P. Zonneveld, J. I. Bloch, J. A. Trapani, E. R. Miller, and K. M. Muldoon. Finally, we wish to thank the Churchill family for 25 years of friendship.

LITERATURE CITED

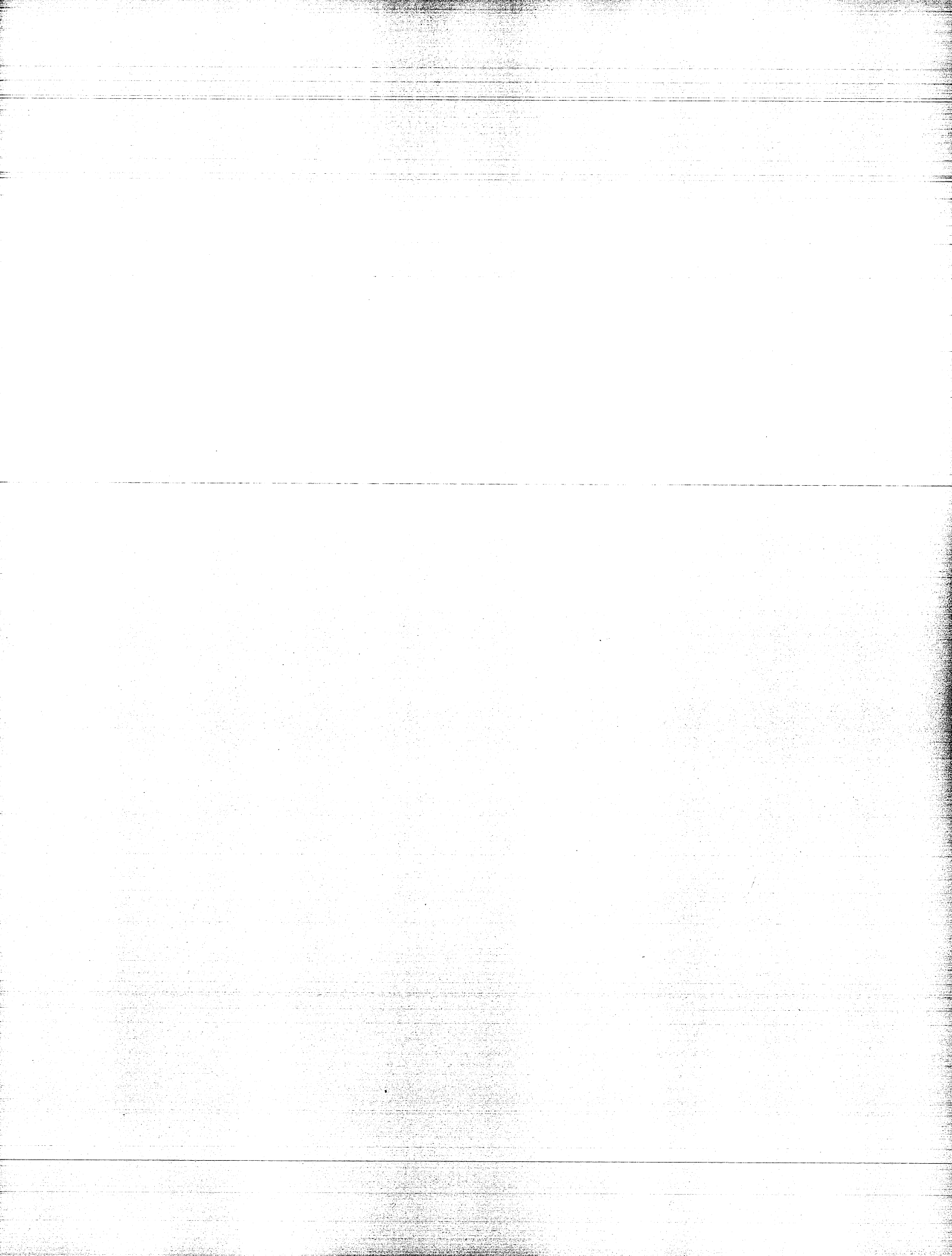
- ARCHIBALD, J. D., W. A. CLEMENS, P. D. GINGERICH, D. W. KRAUSE, E. H. LINDSAY, and K. D. ROSE. 1987. First North American land mammal ages of the Cenozoic era. In M. O. Woodburne (ed.), *Cenozoic Mammals of North America: Geochronology and Biostratigraphy*, University of California Press, Berkeley, pp. 24-76.
- BARTELS, W. S. and G. F. GUNNELL. 1997. Basin margin faunas and the origin of North American Land Mammal Age faunal turnover (abstract). *Journal of Vertebrate Paleontology*, 17: 31A.
- BLACK, C. C. 1967. Middle and late Eocene communities: a major discrepancy. *Science*, 156: 62-64.
- BLOCH, J. I. and G. J. BOWEN. 2001. Paleocene-Eocene microvertebrates in freshwater limestones of the Willwood Formation, Clarks Fork Basin, Wyoming. In G. F. Gunnell (ed.), *Eocene Biodiversity: Unusual Occurrences and Rarely Sampled Habitats*, Plenum Publishing Corporation, New York, in press.
- BLOCH, J. I. and P. D. GINGERICH. 1998. *Carpolestes simpsoni*, new species (Mammalia, Proprimates) from the late Paleocene of the Clarks Fork Basin, Wyoming. *Contributions from the Museum of Paleontology, University of Michigan*, 30: 131-162.
- BOWN, T. M. 1979. New omomyid primates (Haplorhini, Tarsiiformes) from the middle Eocene rocks of west-central Hot Springs County, Wyoming. *Folia Primatologica*, 31: 48-73.
- BOWN, T. M. 1982. Geology, paleontology, and correlation of Eocene volcanoclastic rocks, southeast Absaroka range, Hot Springs County, Wyoming. U.S. Geological Survey Professional Paper, 1201A: 1-75.
- BROWN, W. G. 1993. Structural style of Laramide basement-cored uplifts and associated folds. *Geological Society of America, Memoir*, 5: 312-371.
- FOOSE, R. M. 1973. Vertical tectonism and gravity in the Bighorn Basin and surrounding ranges of the middle Rocky Mountains. In K. A. De Jong and R. Scholten (eds.), *Gravity and Tectonics*, John Wiley and Sons, New York, pp. 433-455.
- FOOSE, R. M., D. U. WISE, and G. GARBARINI. 1961. Structural geology of the Beartooth Mountains, Montana and Wyoming. *Geological Society of America Bulletin*, 72: 1143-1172.
- GINGERICH, P. D. 1976. Cranial anatomy and evolution of early Tertiary Plesiadapidae (Mammalia, Primates). *University of Michigan Papers on Paleontology*, 15: 1-140.
- GINGERICH, P. D. 1987. Early Eocene bats (Mammalia, Chiroptera) and other vertebrates in freshwater limestones of the Willwood Formation, Clarks Fork Basin, Wyoming. *Contributions from the Museum of Paleontology, University of Michigan*, 27: 275-320.
- GINGERICH, P. D. 1989. New earliest Wasatchian mammalian fauna from the Eocene of northwestern Wyoming: composition and diversity in a rarely sampled high-floodplain assemblage. *University of Michigan Papers on Paleontology*, 28: 1-97.

- GINGERICH, P. D. 1994. New species of *Apheliscus*, *Haplomyilus*, and *Hyopsodus* (Mammalia, Condylarthra) from the late Paleocene of southern Montana and early Eocene of northwestern Wyoming. *Contributions from the Museum of Paleontology, University of Michigan*, 29: 119-134.
- GUNNELL, G. F. 1989. Evolutionary history of Microsypoidea (Mammalia, ?Primates) and the relationship between Plesiadapiformes and Primates. *University of Michigan Papers on Paleontology*, 27: 1-157.
- GUNNELL, G. F. and W. S. BARTELS. 1994. Early Bridgerian (middle Eocene) vertebrate paleontology and paleoecology of the southern Green River Basin, Wyoming. *University of Wyoming Contributions to Geology*, 30: 57-70.
- GUNNELL, G. F. and W. S. BARTELS. 1997. Basin-margin mammalian assemblages from the Wasatch Formation (Bridgerian) of the northeastern Green River Basin, Wyoming— anachronistic taxa and the origin of new genera (abstract). *Journal of Vertebrate Paleontology*, 17: 51A.
- GUNNELL, G. F. and W. S. BARTELS. 1998. Basin margins and morphologic divergence: paleontologic documentation of cladogenesis and evolutionary innovation (abstract). *Journal of Vertebrate Paleontology*, 18: 47A.
- GUNNELL, G. F. and W. S. BARTELS. 2001. Basin margins, biodiversity, evolutionary innovation, and the origin of new taxa. In G. F. Gunnell (ed.), *Eocene Biodiversity: Unusual Occurrences and Rarely Sampled Habitats*, Plenum Publishing Corporation, New York, in press.
- GUNNELL, G. F., W. S. BARTELS, P. D. GINGERICH, and V. TORRES-ROLDAN. 1992. Wapiti Valley faunas: early and middle Eocene fossil vertebrates from the North Fork of the Shoshone River, Park County, Wyoming. *Contributions from the Museum of Paleontology, University of Michigan*, 28: 247-287.
- GUNNELL, G. F. and P. D. GINGERICH. 1996. New hapalodectid *Hapalorestes lovei* (Mammalia, Mesonychia) from the early middle Eocene of northwestern Wyoming. *Contributions from the Museum of Paleontology, University of Michigan*, 29: 413-418.
- GUNNELL, G. F. and V. L. YARBOROUGH. 2000. Brontotheriidae (Perissodactyla) from the late early and middle Eocene (Bridgerian), Wasatch and Bridger Formations, southern Green River Basin, southwestern Wyoming. *Journal of Vertebrate Paleontology*, 20: 349-368.
- HICKEY, L. J. 1980. Paleocene stratigraphy and flora of the Clarks Fork basin. In P. D. Gingerich (ed.), *Early Cenozoic Paleontology and Stratigraphy of the Bighorn Basin, Wyoming*, University of Michigan Papers on Paleontology, 24 pp. 33-49.
- JEPSEN, G. L. 1937. A Paleocene rodent, *Paramys atavus*. *Proceedings of the American Philosophical Society*, 78: 291-301.
- JEPSEN, G. L. 1939. Dating Absaroka volcanic rocks by vertebrate fossils. *Geological Society of America, Abstracts with Programs*, 50: 1914.
- KRISHTALKA, L., R. M. WEST, C. C. BLACK, M. R. DAWSON, J. J. FLYNN, W. D. TURNBULL, R. K. STUCKY, M. C. MCKENNA, T. M. BOWN, D. J. GOLZ, and J. A. LILLE-GRAVEN. 1987. Eocene (Wasatchian through Duchesnean) biochronology of North America. In M. O. Woodburne (ed.), *Cenozoic Mammals of North America: Geochronology and Biostratigraphy*, University of California Press, Berkeley, pp. 77-117.
- LOVE, J. D. and A. C. CHRISTIANSEN. 1985. Geologic map of Wyoming. U.S. Geological Survey, 1 sheet.
- LUTZ, T. M. and G. I. OMAR. 1996. Variations in denudation and geothermal gradient in the Beartooth Mountains uplift based on refined interpretation of apatite fission track data. *Geological Society of America, Abstracts with Programs*, 28: 373.
- PROTHERO, D. R. and C. C. SWISHER. 1992. Magnetostratigraphy and geochronology of the terrestrial Eocene-Oligocene transition in North America. In D. R. Prothero and W. A. Berggren (eds.), *Eocene-Oligocene Climatic and Biotic Evolution*, Princeton University Press, Princeton, pp. 47-73.
- ROBINSON, P. 1966. Fossil Mammalia of the Huerfano Formation, Eocene, of Colorado. *Yale University Peabody Museum of Natural History Bulletin*, 21: 1-95.
- ROSE, K. D. 1981. The Clarkforkian land-mammal age and mammalian faunal composition across the Paleocene-Eocene boundary. *University of Michigan Papers on Paleontology*, 26: 1-197.
- SILCOX, M. T. and K. D. ROSE. 2001. Unusual vertebrate microfaunas from the Willwood Formation, early Eocene of the Bighorn Basin, Wyoming. In G. F. Gunnell (ed.), *Eocene Biodiversity: Unusual Occurrences and Rarely Sampled Habitats*, Plenum Publishing Corporation, New York, in press.
- SIMPSON, G. G. 1928. A new mammalian fauna from the Fort Union of southern Montana. *American Museum Novitates*, 297: 1-15.
- SIMPSON, G. G. 1929a. A collection of Paleocene mammals from Bear Creek, Montana. *Annals of Carnegie Museum*, 19: 115-122.
- SIMPSON, G. G. 1929b. Third contribution to the Fort Union fauna at Bear Creek, Montana. *American Museum Novitates*, 345: 1-12.
- STONE, D. S. 1993. Basement-involved thrust-generated folds as seismically imaged in the subsurface of the central Rocky Mountain Foreland. *Geological Society of America, Special Paper*, 280: 271-318.
- STUCKY, R. K. 1984. The Wasatchian-Bridgerian land mammal age boundary (early to middle Eocene) in western North America. *Annals of Carnegie Museum*, 53: 347-382.
- TORRES, V. 1985. Stratigraphy of the Eocene Willwood, Aycross, and Wapiti formations along the North Fork of the Shoshone River, north-central. *Contributions to Geology, University of Wyoming*, 23: 83-97.
- TORRES, V. and P. D. GINGERICH. 1983. Summary of Eocene stratigraphy at the base of Jim Mountain, North Fork of the Shoshone River, northwestern Wyoming. *Wyoming Geological Association Guidebook*, 34: 205-208.
- VAN HOUTEN, F. B. 1944. Stratigraphy of the Willwood and Tatman Formations in northwestern Wyoming. *Geological Society of America Bulletin*, 55: 165-210.

VAN VALEN, L. M. and R. E. SLOAN. 1966. The extinction of the multituberculates. *Systematic Zoology*, 15: 261-278.

WISE, D. U. 2000. Laramide structures in basement and cover of the Beartooth Uplift near Red Lodge, Montana. *American Association of Petroleum Geologists Bulletin*, 84: 360-375.

WOOD, H. E., R. W. CHANEY, J. CLARK, E. H. COLBERT, G. L. JEPSEN, J. B. REESIDE, and C. STOCK. 1941. Nomenclature and correlation of the North American continental Tertiary. *Bulletin of the Geological Society of America*, 52: 1-48.



COMPENDIUM OF WASATCHIAN MAMMAL POSTCRANIA FROM THE WILLWOOD FORMATION OF THE BIGHORN BASIN

KENNETH D. ROSE

*Department of Cell Biology and Anatomy, Johns Hopkins University School of Medicine
Baltimore, Maryland 21205*

Abstract.— Postcranial remains are now known from almost half of the ca. 100 genera and a third of the ca. 200 species of mammals reported from the Wasatchian (early Eocene) part of the Willwood Formation in the Bighorn Basin. For many early Eocene genera Willwood specimens are the best or only known postcranial remains. The Willwood Formation has produced the oldest known skeletons of primates, artiodactyls, perissodactyls, carnivorans, creodonts, and rodents. This review summarizes additions to our knowledge of Willwood mammalian postcranial anatomy over the last decade.

INTRODUCTION

The Willwood Formation of the Bighorn Basin has produced more early Eocene mammalian fossils than anywhere else in the world. It is the principal source of information on the postcranial anatomy of early Eocene mammals, having provided such data on a much greater diversity of mammals than any other site. The only or most complete known skeletons for most early Eocene mammal genera come from this basin. These include the oldest known primates (*Cantius*), artiodactyls (*Diacodexis*), perissodactyls (*Hyracotherium* and *Homogalax*), rodents (paramyids), carnivorans (a diversity of miacids and viverravids), and creodonts (hyaenodontids and oxyaenids). A decade ago I summarized what was then known of the postcranial skeleton of Willwood mammals (Rose, 1990). The present contribution is an attempt to update the status of our knowledge of early Eocene mammalian postcrania, following another decade of intensive collecting. It is not intended to be a comprehensive review, but rather a synopsis listing new literature and highlighting significant anatomical features, primarily at the generic or family level. Details on functional anatomy of particular taxa can be found in the literature cited. An appendix following the review lists significant postcranial

associations that are new since the list published in 1990 (Rose, 1990: table 1).

The focus of this report is the collection accumulated from the southern half of the Bighorn Basin by the Johns Hopkins and U.S. Geological Survey–Johns Hopkins collaborative projects. All specimens were deposited initially in the paleontological collection of the USGS–Denver, but were transferred to the Department of Paleobiology, National Museum of Natural History (Smithsonian Institution), in 1996, following major changes at the USGS. Since 1996 specimens have been catalogued directly into the Smithsonian collection. Many earlier specimens have been recatalogued with Smithsonian (USNM) numbers, but the majority still have USGS catalogue numbers (although the intention is ultimately to convert all to USNM numbers). Also mentioned in this report are other important postcranial specimens described from the Wasatchian of the Bighorn Basin over the last decade or so, but I have not attempted to be comprehensive in listing all postcranial specimens in other collections, particularly the important University of Michigan collection.

More than 200 mammalian species in over 100 genera are currently recognized from the Wasatchian part of the Willwood Formation (e.g., Bown, 1979; Gingerich, 1989; Badgley, 1990; Bown et al., 1994; Clyde, 1997). Of these, there is now confidently attributed postcranial evidence for almost half of the genera and a third of the species. Approximately 300

In: Paleocene-Eocene Stratigraphy and Biotic Change in the Bighorn and Clarks Fork Basins, Wyoming (P. D. Gingerich, ed.), *University of Michigan Papers on Paleontology*, 33: 157-183 (2001).

significant skeletal associations, ranging from multiple associated bones to virtually complete skeletons, have been collected by JHU and USGS-JHU field parties, nearly two-thirds of them since the 1990 report. Many have been described or are currently under study, while others have been instrumental in broader studies of the comparative and functional anatomy or phylogenetic relationships of Wasatchian taxa. The latter include analyses of the skeleton in Plesiadapiformes (Beard, 1989), Phenacodontidae (Otts, 1991), Miacoidea (Heinrich, 1995), and Hyaenodontidae (Egi, 1999), and eigenshape analysis of the radial head and ungual phalanges as a tool for inferring locomotor behavior in a broad spectrum of fossil mammals (MacLeod and Rose, 1993; 1997). Nevertheless, a large number of these skeletons remains to be studied in detail. Besides these partial skeletons, we have also collected thousands of isolated postcranial elements, most ascribable to genus or species by comparison with more complete, dentally-associated remains. These isolated specimens are not discussed here unless they constitute the only known postcrania for a taxon. Nonetheless, they are important for illustrating intraspecific variation in postcranial anatomy, and in some cases they preserve anatomical details better than do more complete skeletons.

Although skeletal associations are known from throughout the Willwood Formation, it will be apparent from the list in the Appendix that the majority of postcranial associations from the southern Bighorn Basin come from the upper half of the Willwood Formation, above 350 m (i.e., mostly from zones Wa-5 and Wa-6 of Gingerich, 1991). This is a reflection of the prevalence of immature paleosols, associated with higher rates of sedimentation, in the upper part of the formation (Bown and Kraus, 1993). Associated skeletal remains are more common in immature paleosols, presumably because of the greater probability of rapid burial during frequent periods of deposition.

Institutional acronyms used are as follows: AMNH—Department of Vertebrate Paleontology, American Museum of Natural History, New York; DPC—Duke University Primate Center, Durham, North Carolina; UCM—University of Colorado Museum, Boulder, Colorado; UM—University of Michigan Museum of Paleontology, Ann Arbor, Michigan; USGS—U.S. Geological Survey, Denver, Colorado (collections now at USNM); USNM—Department of Paleobiology, National Museum of Natural History, Smithsonian Institution, Washington, D.C.; YPM-PU—Princeton University collection, now at Peabody Museum of Natural History, Yale University, New Haven, Connecticut.

SYNOPSIS OF WILLWOOD MAMMALIAN POSTCRANIAL ANATOMY

Leptictida

Although two leptictid postcranial specimens were reported in 1990, several important new specimens were discovered

during the last decade. Ten partial skeletons are now known, representing at least two genera, *Prodiacodon* and *Palaeictops* (Fig. 1). Significant postcranial differences between the two genera are not yet apparent from the limited material. These specimens indicate that Wasatchian leptictids were small terrestrial mammals with short, generalized forelimbs, and much longer, slender hind limbs (Rose, 1999). The intermembral index was about 60. The keeled manubrium and moderately robust humerus resemble those of the ground squirrel *Spermophilus*, and, together with prominent extensor tuberosities on metacarpals II and III, suggest that leptictids used their forelimbs for digging. The tibia is perhaps slightly longer than the femur (articular length), and is completely fused with the delicate fibula for the distal half of their length, as in *Leptictis*. This contrasts with Torrejonian *Prodiacodon*, in which fusion is only present far distally. These features, together with the rather deeply grooved astragalus, slightly elongated tarsals, and elongate metatarsals, suggest that leptictids were terrestrial quadrupeds, progressing by occasional running and hopping (but probably not habitually saltatorial), much like present-day elephant-shrews.

Pantolestia

Pantolestids are relatively rare constituents of Wasatchian faunas. Our collection includes only two postcranial specimens of pantolestids, both referable to *Palaeosinopa*. Each consists of just two or three useful associated elements, which serve primarily to demonstrate that these Wasatchian pantolestids resemble Bridgerian *Pantolestes* in form of the astragalus and calcaneus.

Palaeanodonta

Considerable new Willwood palaeanodont material has been collected since the 1990 report (see Appendix), representing several species of *Palaeanodon* and *Alocodontulum* (probably = *Tubulodon*). More than 20 new skeletal associations have been discovered, including a nearly complete skeleton of *Alocodontulum* collected by G.F. Gunnell of the University of Michigan, and excellent specimens of *Palaeanodon*, making these among the best known Willwood genera postcranially. Palaeanodonts were the most fossorially adapted small mammals of the early Eocene.

New material of *Palaeanodon* (Metacheiromyidae) reveals a considerable size range, unknown until recently. The skeleton of *Dasyypus*-sized *P. ignavus* (Fig. 2) is now relatively well known, but limited postcrania are known for the diminutive earliest Wasatchian *P. nievelti* as well (Appendix; Gingerich, 1989). The skeleton of *Alocodontulum* (Epoicotheriidae) is best known from UM 93740 (Figs. 3 and 4), which is the most complete known epoicotheriid skeleton (Rose et al., 1992). This and other specimens indicate that *Alocodontulum* was somewhat smaller than its contemporary *P. ignavus*. It further confirms that *Alocodontulum* was more

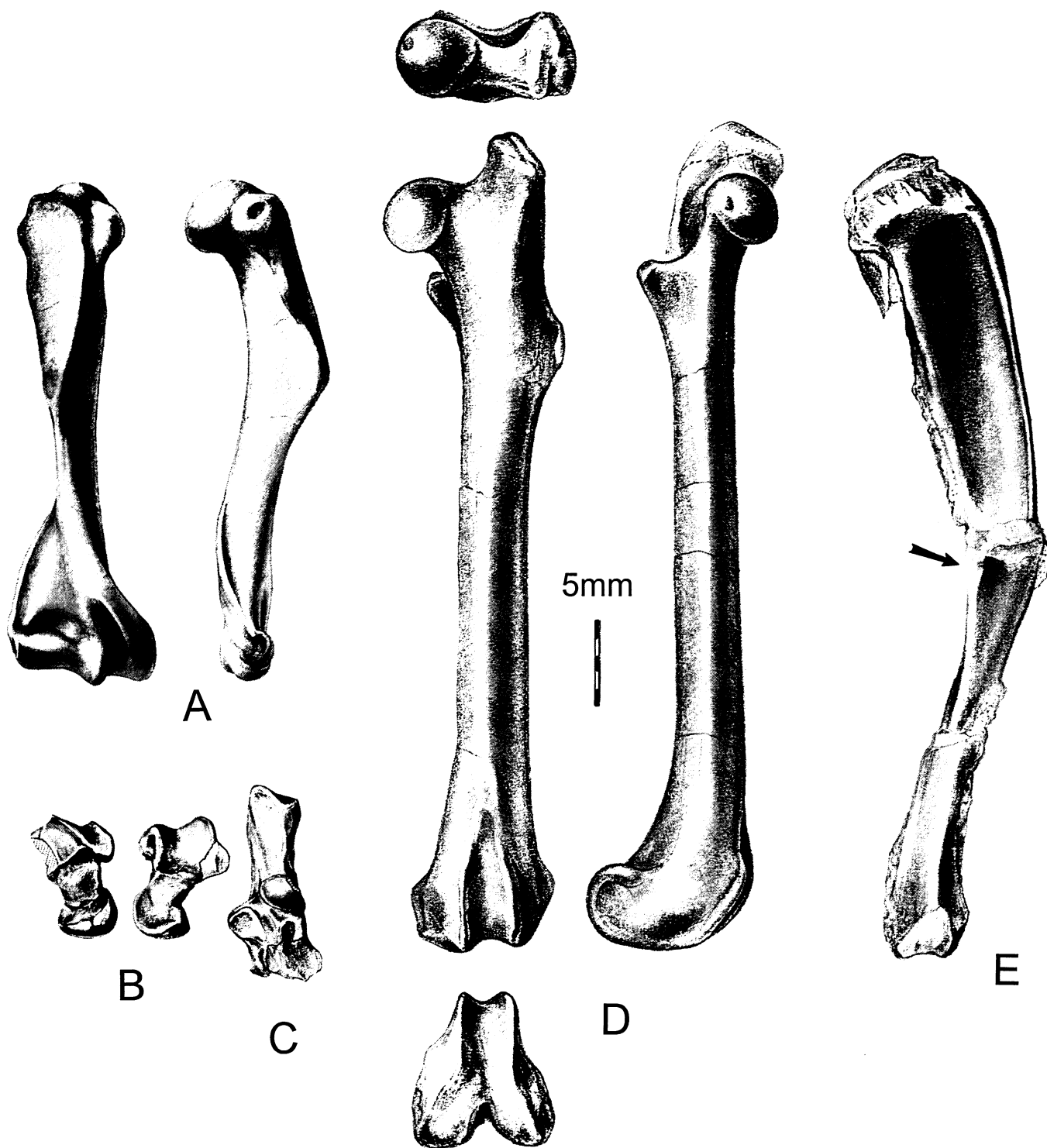


FIGURE 1 — Postcrania of Willwood leptictids. A, right humerus; B, left astragalus; C, left calcaneus; D, left femur; E, right tibia, with arrow showing level of fibular fusion. A and D are referred to *cf. Prodiacodon tauricineri* (UM 88105). B and C are identified as *cf. Palaeictops* sp. (USNM 495152). E is from an unidentified leptictid (UM 66021). From Rose (1999).

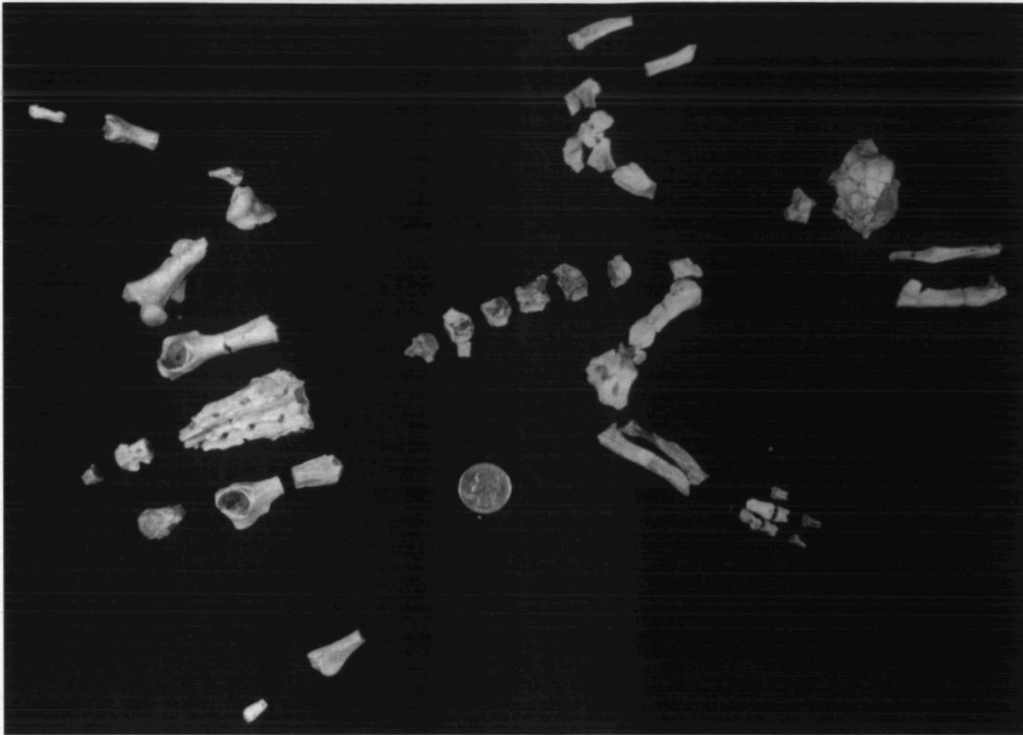


FIGURE 2 — Partial skeleton of *Palaeonodon ignavus*, USGS 21876. Coin is 2.4 cm in diameter.

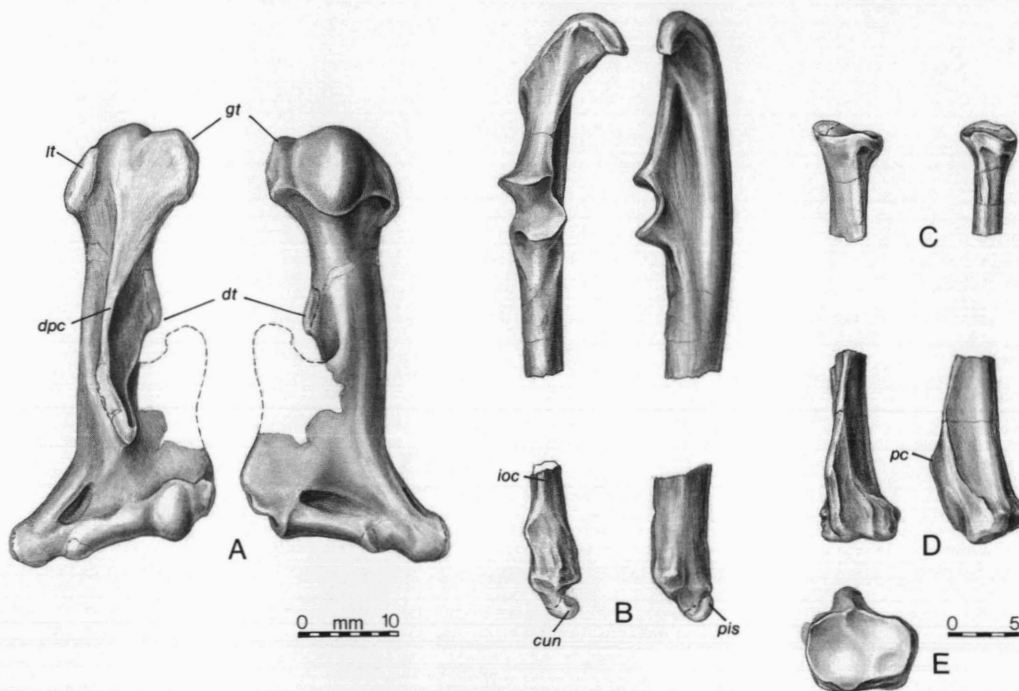


FIGURE 3 — Forelimb elements of *Allocodontulum atopum*, UM 93740. A, left humerus; B, right ulna; C-E, right radius (C, proximal; D-E, distal). Abbreviations: *cun*, cuneiform facet; *dpc*, deltopectoral crest; *dt*, deltoid tubercle; *gt*, greater tubercle; *ioc*, interosseous crest; *lt*, lesser tubercle; *pc*, pronator crest; *pis*, pisiform facet. From Rose et al. (1992).

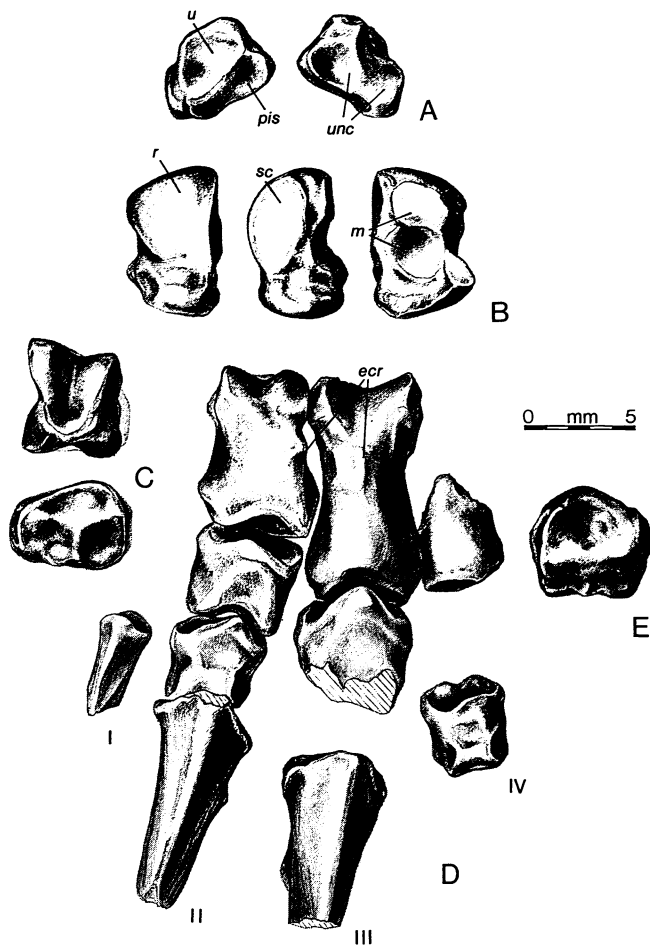


FIGURE 4 — Left carpus and manus of *Allocodontulum atopum*, UM 93740. A, cuneiform in proximal and distal views; B, lunar in proximal, medial, and distal views; C, metacarpal II in proximal and distal views; D, manus; E, distal view of metacarpal III. Abbreviations: *ecr*, tubercles for insertion of extensor carpi radialis tendons; *m*, facets for magnum; *pis*, facet for pisiform; *r*, facet for radius; *sc*, facet for scaphoid; *u*, facet for ulnar styloid process; *unc*, facet for unciform. From Rose et al. (1992).

specialized for digging than was *Palaeonodon*, as evidenced by generally shorter, more robust limb elements; a relatively longer deltopectoral crest, more distal teres tubercle, and longer olecranon process; relatively shorter manus elements, especially metacarpals; a shorter, flatter astragalus, and a distally short calcaneus with a prominent, very distal peroneal process.

Taeniodonta

A single new postcranial specimen of this rare group was recovered since the last report. It represents *Ectoganus* and includes intermediate and ungual phalanges of the manus, which serve to reinforce the extraordinary fossorial specialization of

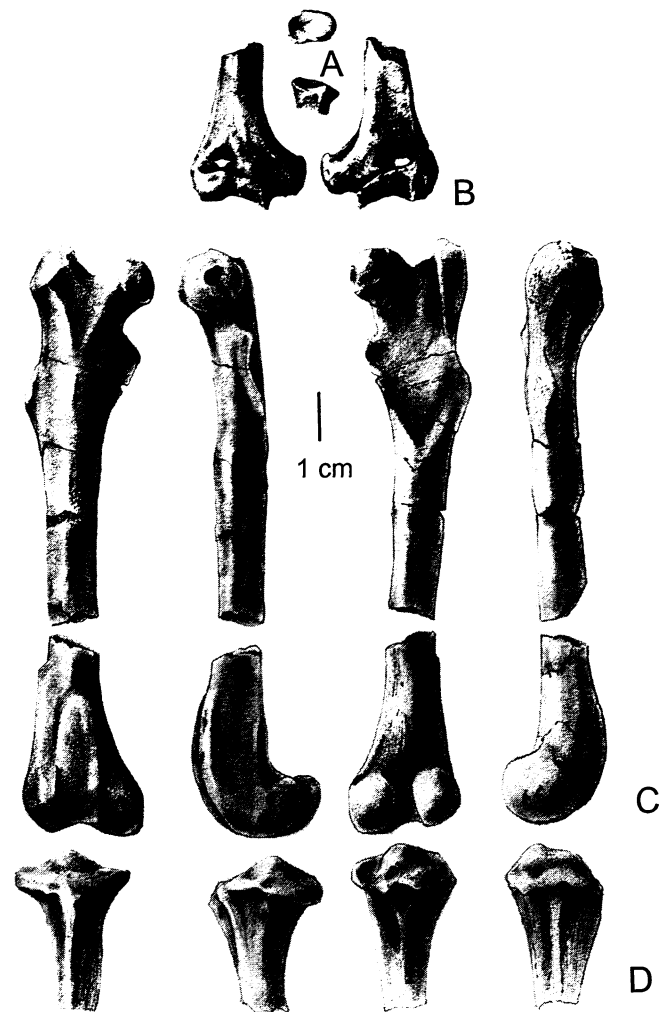


FIGURE 5 — Postcrania of the tillodont *Esthonyx bisulcatus*, USNM 487889. A, proximal right radius; B, distal right humerus; C, right femur; D, proximal right tibia.

these animals. So far as known, this is only the fifth postcranial specimen of *Ectoganus* known from the Willwood Formation, and only the third to consist of more than a single element (Schoch, 1986; Rose, 1990). Although it is a relatively small individual (judging from the associated dentary), the curved and laterally-compressed ungual phalanx exceeds 50 mm in length, whereas the intermediate phalanx is exceptionally short, only 10 mm long. Thus *Ectoganus* had the largest ungual phalanges of any Willwood mammal.

Tillodontia

The postcranial skeleton of Wasatchian tillodonts remains poorly known. Half a dozen postcranial associations can be added to the two reported a decade ago. Gingerich (1989) described and illustrated fragmentary remains of *Azygonyx*, the

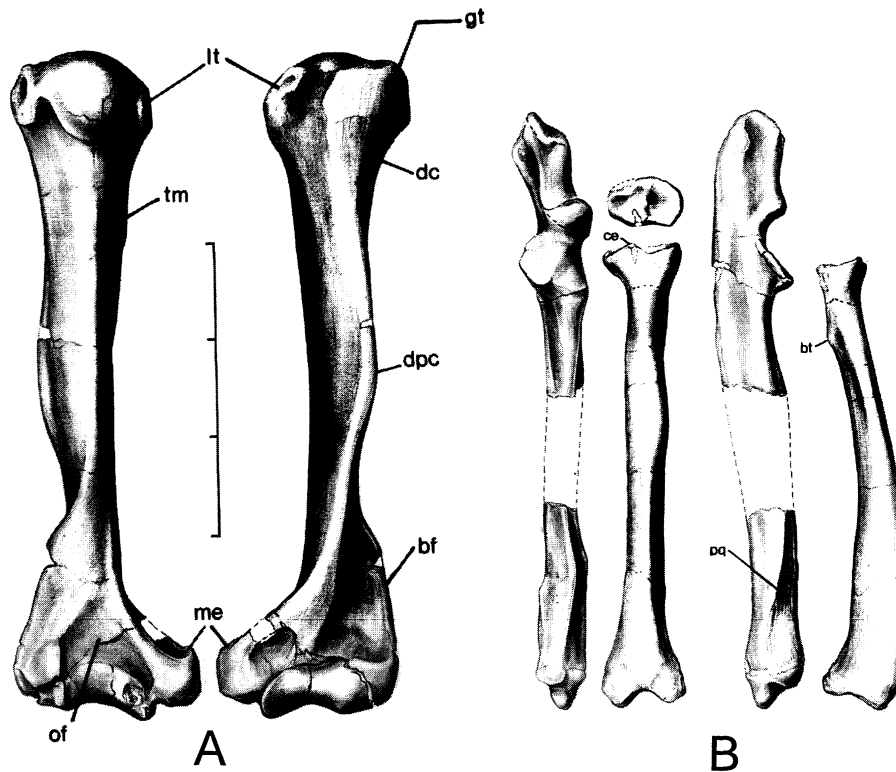


FIGURE 6 — Forelimb elements of the creodont *Prolimnocyon atavus*, DPC 5364. A, Left humerus; B, left ulna and radius. Abbreviations: *bf*, brachial flange (= supinator crest); *bt*, bicipital tuberosity; *ce*, capitulum; *dc*, deltoid crest; *dpc*, deltopectoral crest; *me*, medial epicondyle; *of*, olecranon fossa; *pq*, pronator quadratus crest; *tm*, teres major crest. Scale = 3 cm. From Gebo and Rose (1993).

oldest North American genus, remarking on its relatively round radial head, dorsoventrally flattened astragalar head, broad and shallow astragalar trochlea, high astragalar foramen, and prominent calcaneal tuber. From these limited remains he inferred that *Azygonyx* was capable of antebrachial supination and had a plantigrade foot posture with limited crurotalar mobility. He concluded that it “was probably more bearlike than piglike in locomotor pattern” (Gingerich, 1989: 27).

Several new specimens of *Esthonyx* (Fig. 5) provide additional information on the skeleton of these obscure mammals, and confirm the association of elements in USGS 7551 (reported by Rose, 1990) as *Esthonyx*, despite their close resemblance also to the arctocyonid *Chriacus*. Although analysis is still in progress, some preliminary remarks may be offered. Most of the preserved elements are, indeed, similar in size and morphology to those of *Chriacus*, though several important distinctions can be noted. For example, the supinator crest is weaker, the radial head relatively wider mediolaterally, and the distal femur deeper anteroposteriorly with a more elevated, narrower, and somewhat deeper patellar groove. The calcaneus is slightly narrower, with a distally placed peroneal process (not opposite or slightly proximal to the sustentaculum tali as in *Chriacus*), but it lacks the expanded

tuber calcanei of *Azygonyx* and apparently lacks the prominent fibular contact present in *Chriacus*. While the resemblances to *Chriacus* suggest climbing ability (and possible relationship to arctocyonids, as suggested by Van Valen, 1963), the differences point to more terrestrial habits than in the arctocyonid. Thus *Esthonyx* may have been rather generalized in substrate preference, being capable of both terrestrial and scansorial habits.

Pantodonta

Many new skeletal specimens of *Coryphodon* add to the already extensive sample of postcrania known for this common mammal, the largest Willwood herbivore, but they have not yet been studied in any detail. Previous authors have suggested that *Coryphodon* was a ponderous, tapir- to cow-sized, graviportal animal, perhaps semiaquatic and hippopotamus-like in general habits (e.g., Simons, 1960); however, this is based more on subjective assessment than on any detailed functional analysis. Writing more than half a century ago, Patterson (1939: 97) observed that “... *Coryphodon* might be supposed to be one of the best known of the early Tertiary mammals. Unfortunately, however, this is far from true. No

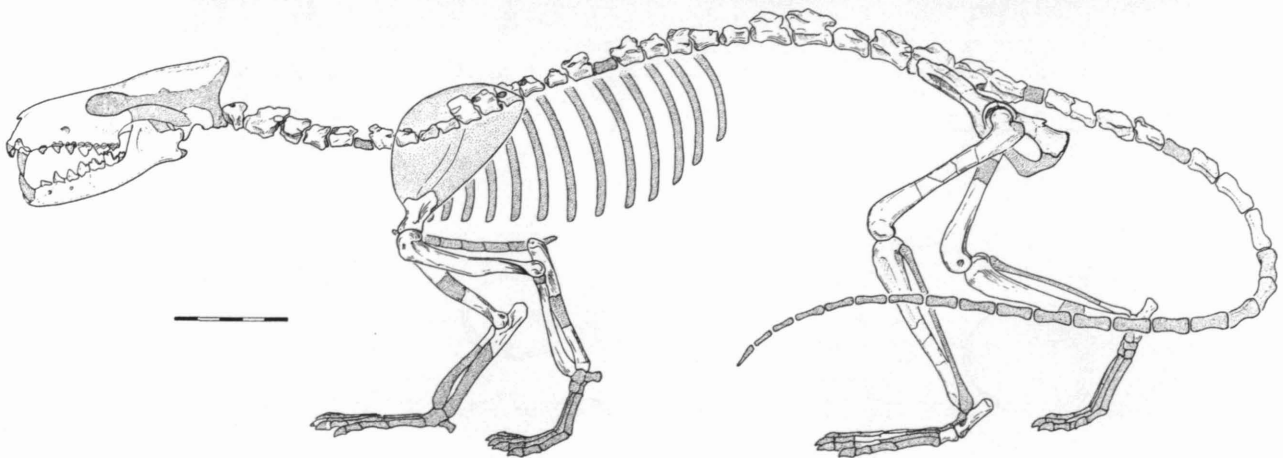
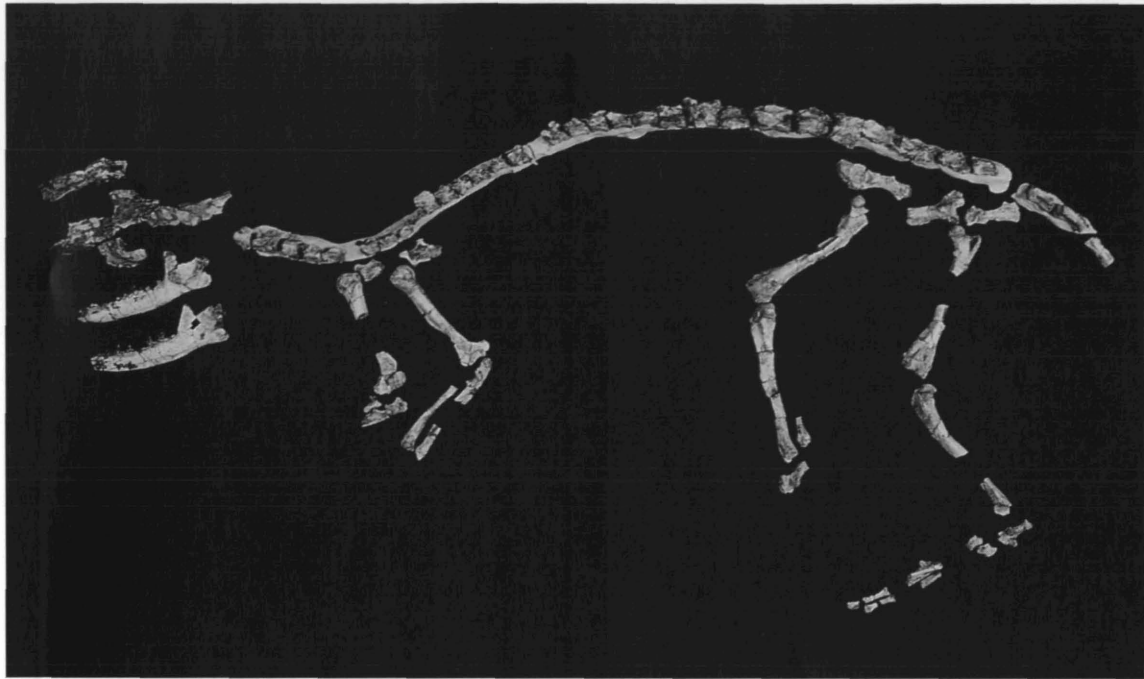


FIGURE 7 — Skeleton of *Prolimmocyon atavus*, DPC 5364. Scale = 5 cm. Restoration from Gebo and Rose (1993).

thorough account of the osteology is available.” Surprisingly, this statement still applies. In view of persistent questions about its general habits, limb posture, body size, and sexual dimorphism, careful study of the skeleton of *Coryphodon* is long overdue.

Creodonta

Oxyaenidae

Oxyaenids were the most common large carnivorous mammals of the Wasatchian. The skeleton of *Oxyaena* has been known for a century; its skeletal characteristics have been enumerated elsewhere (e.g., Denison, 1938; Rose, 1990, and

references therein). The combination of features seen in *Oxyaena* has no close parallel among extant mammals, hence its habits and locomotor behavior have proven difficult to infer and remain enigmatic. Gunnell and Gingerich (1991; Gingerich, 1989) illustrated a few elements and reported briefly on some postcrania of Wasatchian oxyaenids, including *Oxyaena forcipata*, *Dipsalidictis platypus*, and *D. transiens*. They found that *Dipsalidictis* was a smaller, more gracile animal than *Oxyaena*, with a rounder radial head and more flexible ankle. Based on these differences, they concluded that *Dipsalidictis* was probably scansorial, whereas *Oxyaena* was “an ambulatory terrestrial predator” (Gunnell and Gingerich, 1991: 169). Some features of *Oxyaena* that are consistent with

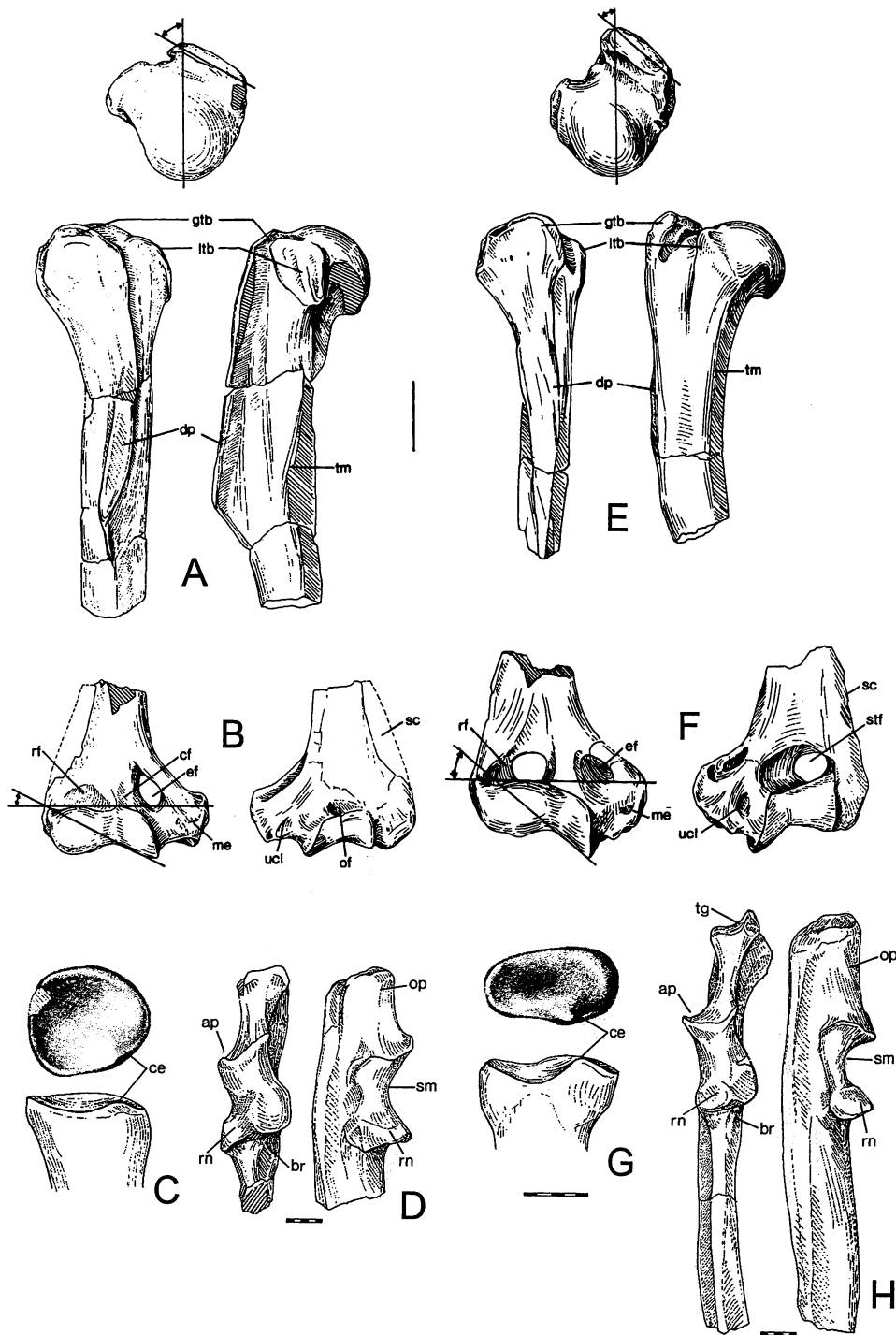


FIGURE 8 — Right forelimb elements of Willwood miacids (A-D) and a viverravid (E-H). A, proximal humerus of *Vulpavus*, USGS 25219; B, distal humerus of *Uintacyon*, USGS 21910; C, proximal radius of *Vulpavus*, USGS 5025; D, proximal ulna of *Vulpavus*, USGS 25219; E, proximal humerus of *Didymictis*, USGS 5024; F, distal humerus of *Didymictis*, USGS 27585; G, proximal radius of *Didymictis*, USGS 21836; H, proximal ulna of *Didymictis*, USGS 5024. Abbreviations: *ap*, anconeal process; *br*, brachialis insertion site; *ce*, capitular eminence; *cf*, coronoid fossa; *dp*, deltopectoral crest; *ef*, entepicondylar foramen; *gtb*, greater tuberosity; *ltb*, lesser tuberosity; *me*, medial epicondyle; *of*, olecranon fossa; *op*, olecranon process; *rf*, radial fossa; *rn*, radial notch; *sc*, supinator crest; *sm*, semilunar notch; *stf*, supratrochlear foramen; *tg*, groove for triceps insertion; *tm*, teres major tubercle; *ucl*, pit for ulnar collateral ligament. From Heinrich and Rose (1997).

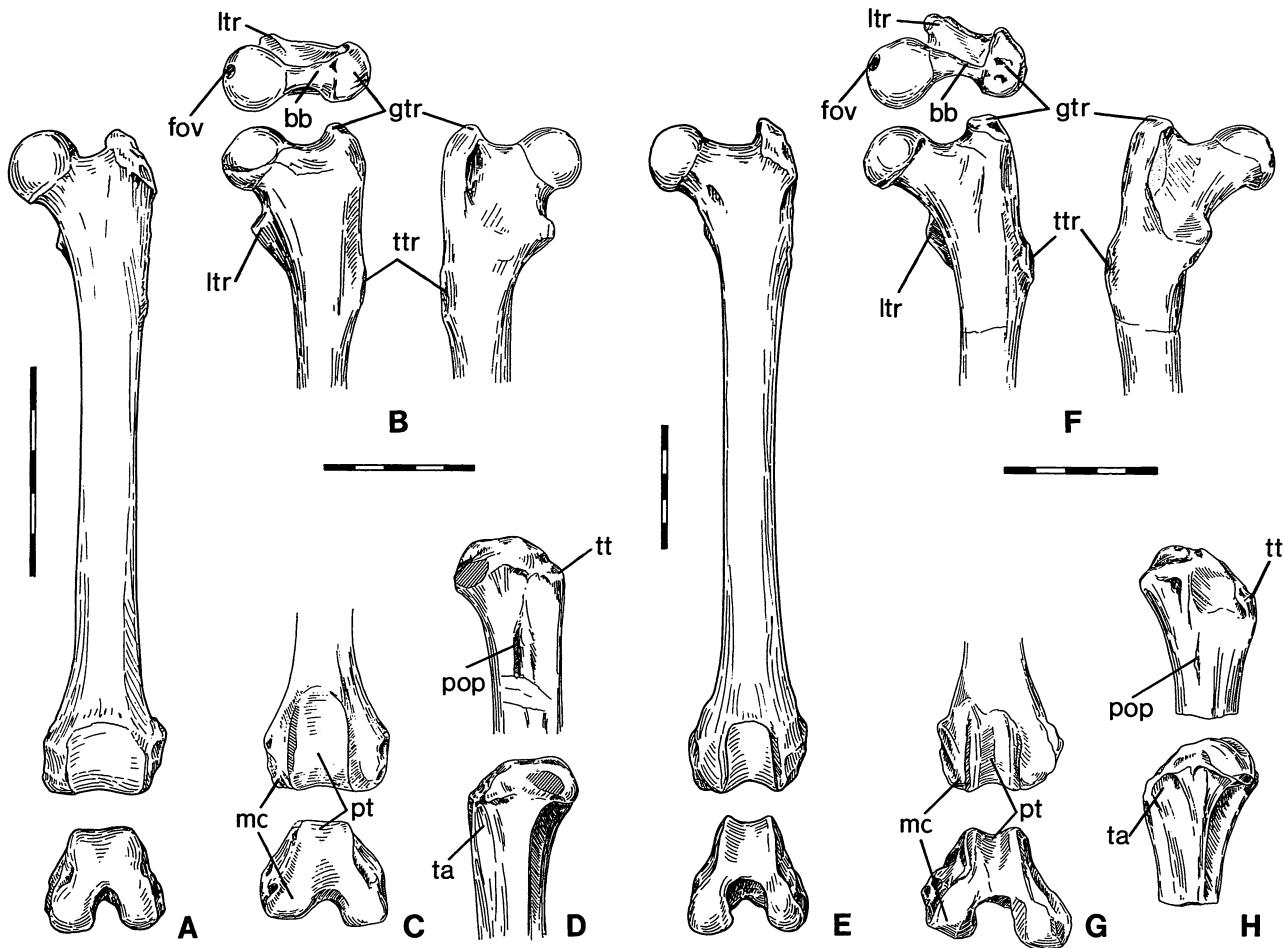


FIGURE 9 — Left hind limb elements of the miacid *Vulpavus* (B-D) compared with the femur of the extant arboreal viverrid *Paradoxurus* (A), and of the viverravid *Didymictis* (F-H) compared with the femur of the terrestrial viverrid *Viverra zibetha* (E). B, proximal femur, USGS 7143; C, distal femur, USGS 7143; D, proximal tibia, USNM 362847; F, proximal femur, USGS 6087; G, distal femur, USGS 25040; H, proximal tibia, USGS 5024. D is from the Bridger; all others are from the Willwood Formation. Abbreviations: *bb*, bone bridge; *fov*, fovea capitis; *gtr*, greater trochanter; *ltr*, lesser trochanter; *mc*, medial condyle; *pop*, popliteus insertion site; *pt*, patellar trochlea; *ta*, tibialis anterior fossa; *tt*, tibial tuberosity; *ttr*, third trochanter. From Heinrich and Rose (1997).

scansorial habits (e.g., humeral morphology, somewhat divergent first digits, and a relatively flexible cruroastragalar joint) may simply be primitive retentions (Denison, 1938). *Oxyaena*'s ungual phalanges are short, curved, and proximally deep, as in most climbing mammals, but unlike the latter they are distally fissured and mediolaterally broader (MacLeod and Rose, 1993). These and other features—such as a well-developed, medially inflected olecranon process, oblique tibioastragalar joint, and robust metapodials—are equally consistent with semifossorial habits (Heinrich and Rose, 1993). Like diggers, *Oxyaena* had relatively short, stout limbs, and low crural and brachial indices (well below 100; Rose, 1990). It seems that we cannot improve much on Matthew's (1909) interpretation that oxyaenids were the mustelid equivalent of the Eocene. *Oxyaena* was probably somewhat analogous to

living badgers, preying in part on other semifossorial mammals (Heinrich and Rose, 1993), or to wolverines, which are more generalized and retain the ability to climb.

Hyaenodontidae

Except for a partial skeleton of *Sinopa hians* (= *Tritemnodon? strenuus*) figured and briefly described by Matthew (1915: fig. 70), virtually nothing was known of the postcranial skeleton of Wasatchian hyaenodontids until the last decade or so. Gingerich and Deutsch (1989) described fragmentary material of early Wasatchian *Arfia*, which exhibits a curious combination of cursorial and scansorial features. The relatively gracile humerus with high greater tuberosity, low deltopectoral crest, reduced supinator crest, and supratrochlear foramen, and the prominent greater trochanter and narrow,

elevated patellar groove of the femur, are features typical of cursors or incipient cursors. At the same time, *Arfia* has a very flexible ankle, which, according to these authors, may have allowed some degree of hind foot reversal. From this they inferred that *Arfia* was partly arboreal. Other Willwood hyaenodontids also show features, especially of the femur (high greater trochanter, posteriorly-directed lesser trochanter, anteroposteriorly deep distal femur) that suggest terrestrial habits, but differ from *Arfia* in having a long, more elevated deltopectoral crest, broader distal humerus, and shallower olecranon fossa, all of which are suggestive of scansorial habits (Rose, 1990). The specimens on which this inference was based were allocated to *Prototomus* and *Tritemnodon* by Rose (1990), but all are now thought to belong to either *Tritemnodon* or *Pyrocyon*. Several skeletal specimens more likely to represent *Prototomus* are now known, including a nearly complete skeleton of *P. secundarius* (USGS 25296), and they suggest more frequent scansorial habits, based on such traits as a more medially directed lesser trochanter, broader and shallower patellar groove, and flexible ankle.

The first significant skeletal remains of *Prolimnocyon* (Figs. 6 and 7) also show a seemingly paradoxical combination of traits (Gebo and Rose, 1993). In particular, the low greater tubercle, long and sharp deltopectoral crest, prominent entepicondyle and supinator crest, medially directed lesser trochanter, and shallow astragalar trochlea, resemble those of scansorial carnivorans. However, some features of the femur (relatively high greater trochanter, torsion of shaft, depth of distal end, and well-defined patellar groove), as well as the slightly broader and less curved ungual phalanges, are more compatible with terrestrial habits. *Prolimnocyon* had an elongate body form and relatively short limbs and, like most other Wasatchian hyaenodontids, probably was reasonably facile in the trees as well as on the ground.

Carnivora

Many new carnivoran postcranial associations have been found since the last report, and these and previously collected specimens were the focus of detailed study by Heinrich (1995) and Heinrich and Rose (1995, 1997). These studies contrasted the anatomical characteristics of the viverravid *Didymictis*, the largest Willwood carnivoran, with those of the miacids *Vulpavus*, *Miacis*, and *Uintacyon*. They confirmed preliminary interpretations (Rose, 1990), as well as the much earlier conclusions of Matthew (1909), which had been based on Bridgerian taxa.

Specifically, *Didymictis* was a primarily terrestrial carnivore, incipiently cursorial, judging from such features as the prominent, high greater tuberosity of the humerus, reduced deltopectoral crest, deep olecranon fossa and supratrochlear foramen, sharply angled medial trochlear ridge, widely ovoid radial head with an almost flat articular surface for the ulna, tightly curved semilunar notch, weak ischial spine, posteriorly directed lesser trochanter, relatively elevated and deep patellar

groove, narrow and elongate calcaneus, and moderately grooved astragalar trochlea (Figs. 8 and 9). Most of these modifications are associated with reducing flexibility at limb joints in favor of increasing stability, speed, and stride-length. Although Lostcabinian *Didymictis altidens* had relatively long, shallow, ungual phalanges like those of extant diggers and terrestrial mammals (Matthew, 1915), ungual phalanges of Wasatchian *D. protenus* were shorter and deeper, as in scansorial mammals.

In contrast, miacids, particularly *Vulpavus*, were arboreally adapted, maximizing mobility at most limb joints. This is evident from the reduced greater tuberosity, sharp and elevated deltopectoral crest, shallow humeral trochlea and olecranon fossa, more open semilunar notch, nearly circular radial head (conveying extensive supinatory ability), prominent and caudally placed ischial spine, medially directed lesser trochanter, broad and flat patellar groove, flat astragalar trochlea, and short, broad calcaneus with proximally positioned peroneal tubercle (Figs. 8 and 9). The proximally deep and laterally compressed ungual phalanges of *Vulpavus* closely correspond in shape to those of the most arboreal extant carnivores (MacLeod and Rose, 1993). The scaphoid and lunar, fused in extant Carnivora, are separate in both *Didymictis* and *Vulpavus*.

Lipotyphla

Lipotyphlan insectivores represent one of the most poorly understood groups in the Wasatchian. With increased emphasis on quarrying, screen-washing, and acid preparation of bone-bearing nodules (e.g., Bloch et al., 1998; Silcox and Rose, in press), considerable diverse and well-preserved jaw and dental material has accumulated over the last 10-20 years, although much of it is still undescribed. Wasatchian nodules from the Clarks Fork Basin have produced as yet undescribed nyctitheriid postcranial associations (J. I. Bloch, pers. comm.). Matthew (1918) reported the only described Willwood postcrania ascribed to lipotyphlans, very fragmentary remains representing *Creotarsus lepidus* and "*Nyctitherium celatum*" (probably = *Pontifactor*). To this we can add two specimens of tibiofibulae, the two elements fused at midshaft, which are believed to belong to *Macrocranium* or a similar lipotyphlan. They are smaller than the comparable elements in leptictids and resemble in size and morphology tibiofibulae in *Macrocranium* from Messel, Germany (Maier, 1979), but detailed comparisons have not yet been made.

Primates

Significant euprimate postcrania from the Willwood are currently known only for the adapiform *Cantius*, which is among the most common taxa known from jaws, being represented by several thousand dentaries and maxillary fragments (Gingerich and Simons, 1977; O'Leary, 1996). Despite its apparent abundance, skeletal associations remain

very scarce and only a few fragmentary partial skeletons have been found, none of which can be characterized as anywhere near complete. The only significant new skeletal association we have unearthed in the last decade is a partial foot of *Cantius mckennai*, the first postcranial association for this species. Many parts of the skeleton of *Cantius* are very distinctive, however, and hundreds of isolated elements have been identified (e.g., Gebo, 1987; Gebo et al., 1991). Although these specimens represent several time-successive species of *Cantius*, as well as *Copelemur feretutus*, morphometric analyses of the most common elements—tali and calcanei—indicate that they differ primarily in size rather than other aspects of morphology. Thus postcranial anatomy, or at least the tarsus, remained relatively conservative through the Wasatchian, whereas dental anatomy changed substantially.

The known postcranial elements of *Cantius* (Fig. 10) resemble those of various extant Malagasy lemurs, strikingly so for bones such as the femur (Rose and Walker, 1985). Despite differences in certain details of pedal anatomy, the rather close overall correspondence indicates that *Cantius* can be interpreted as an active, hind-limb dominated arboreal quadruped.

In a series of papers, Beard (1989, 1990, 1991, 1993a,b) has described postcranial material of Wasatchian Paromomyidae and Micromomyidae, placed variously in the Dermoptera or the Plesiadapiformes. Although their precise higher relationships are controversial, these families are widely considered to be related to primates. Most of Beard's specimens are isolated elements lacking direct association with teeth, however two dentally-associated partial skeletons of Wasatchian *Phenacolemur*, representing *Phenacolemur* cf. *jepseni* (USGS 17847; Rose, 1990) and *P. praecox*, support their allocation to these families. Beard assigned the isolated Wasatchian elements to the paromomyids *Phenacolemur simonsi* and *Ignacius graybullianus*, and the micromomyids to *Tinimomys graybulliensis* and *Chalicomomys antelucanus*. These paromomyid and micromomyid postcrania are characterized by low humeral tuberosities; a sharp, elevated deltopectoral crest; broad distal humerus with large entepicondyle and spherical capitulum; flaring supinator crest (paromomyids only); relatively round radial head; ulnar shaft convex posteriorly with olecranon angled craniad; large, medially projecting lesser trochanter; broad, shallow patellar groove; shallow astragalar trochlea; and laterally compressed and proximally deep, curved ungual phalanges. For the most part, these are features typical of arboreal mammals. Beard considered the anatomy of the manus and pes to be of special significance, citing particularly the slender, elongate phalanges (with intermediate phalanges apparently longer than proximal ones), and specializations of the carpus and tarsus, as evidence of relationship to extant dermopterans and the probable presence, at least in paromomyids, of a patagium for gliding. The proper attribution and functional interpretation of these postcrania has been controversial (e.g., Krause, 1991; Runestad and Ruff, 1995; Hamrick et al., 1999); nonetheless, there is general agreement



FIGURE 10 — Partial skeleton of the primate *Cantius trigonodus*, USGS 5900 (see Rose and Walker, 1985). Skull and mandible are of *C. abditus*, USNM 494881 (see Rose et al., 1999).

that both paromomyids and micromomyids were arboreally adapted mammals, perhaps similar in lifestyle to extant petaurid marsupials (sugar gliders).

Condylarthra

It is a conundrum that significant postcranial material of *Hyopsodus*, by far the most common Wasatchian mammal in the Bighorn Basin, remains unknown or unrecognized from the Willwood Formation. Nevertheless, considerable skeletal

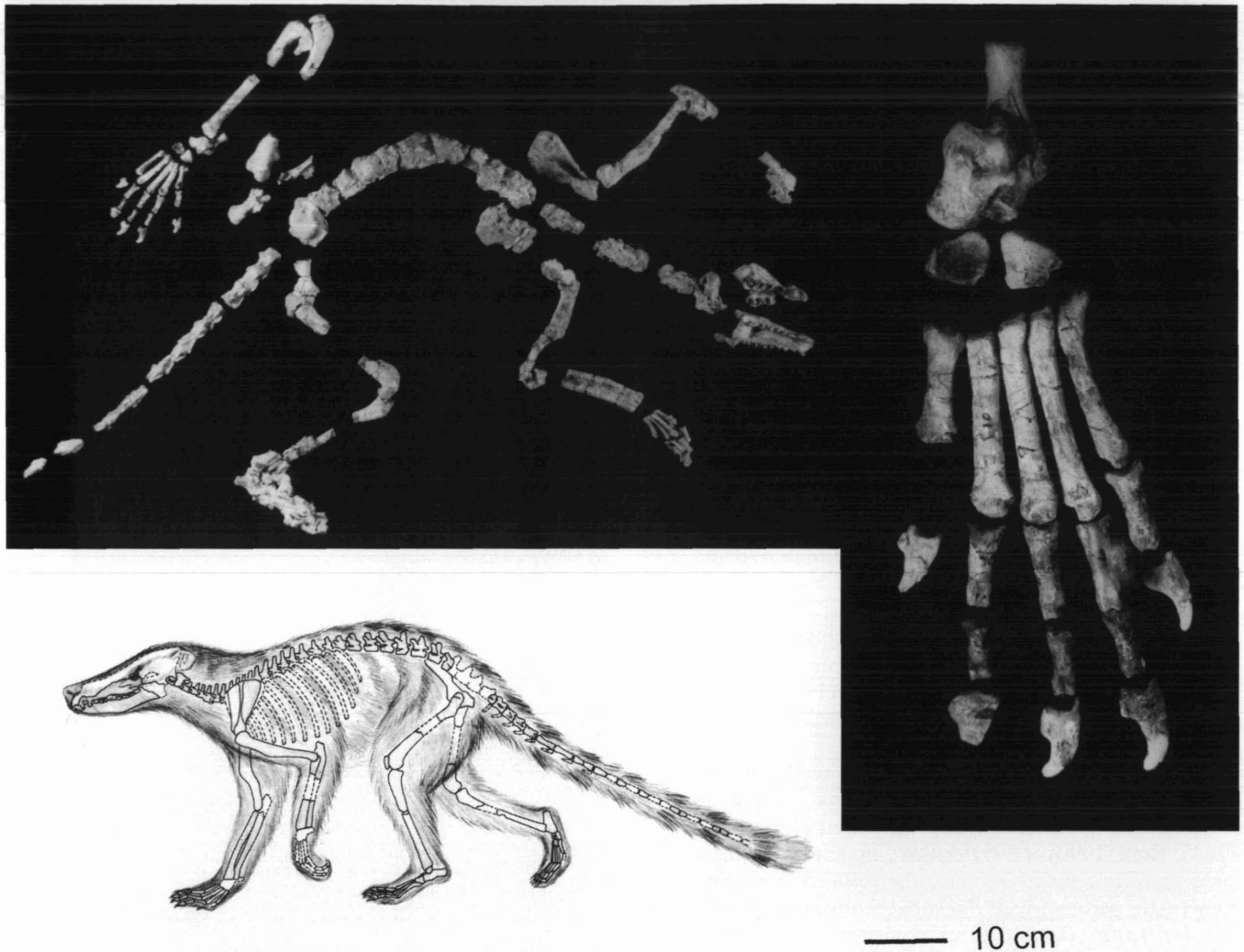


FIGURE 11 — Skeleton and restoration of the arctocyonid *Chriacus*, USGS 2353, with close-up of left pes (ungual tips restored). Restoration by Elaine Kasmer. Scale applies to restoration.

material of other condylarths has been recovered, making them some of the best known Willwood mammals.

Arctocyonidae

Arctocyonids are generally rare elements of Wasatchian faunas, but curiously, their postcrania are much more common than would be expected based on the occurrence of jaws and teeth. Several new partial skeletons of both *Chriacus* and *Anacodon* have been unearthed in the last decade, bringing the total to ten for each genus. Most of the skeleton is now known for both of them, but for the most part they have not yet been studied in detail. I previously described numerous anatomical traits of Wasatchian *Chriacus* (Fig. 11) that indicate adaptation to arboreal life (Rose, 1987). These include specializations that probably facilitated hind-foot reversal, as occurs, for example, in tree squirrels and kinkajous, allowing them to descend trees headfirst (Jenkins and McClearn, 1984). Some

Torrejonian remains attributed to *Chriacus* corroborate these arboreal modifications, including a derived, highly flexible ankle (Szalay and Lucas, 1996). MacLeod and Rose (1993) included ungual phalanges and radial heads of both *Chriacus* and *Anacodon* in an eigenshape analysis of these elements in Paleogene mammals. The elements of *Chriacus* plotted within the field for arboreal and scansorial extant mammals, whereas those of *Anacodon* were inconclusive as to locomotor habit. As noted previously (Rose, 1990), *Anacodon* had massive forelimbs, suggestive of digging capability, and a very unusual tarsal structure. Pending further study, the best living analogues for these arctocyonids are probably procyonids and ursids, respectively.

The arboreal adaptations of *Chriacus* were taken by Rose (1987) as evidence against Van Valen's (1978) hypothesis that this genus lay close to the origin of Artiodactyla. At least one Torrejonian species of *Chriacus*, however, is now known to

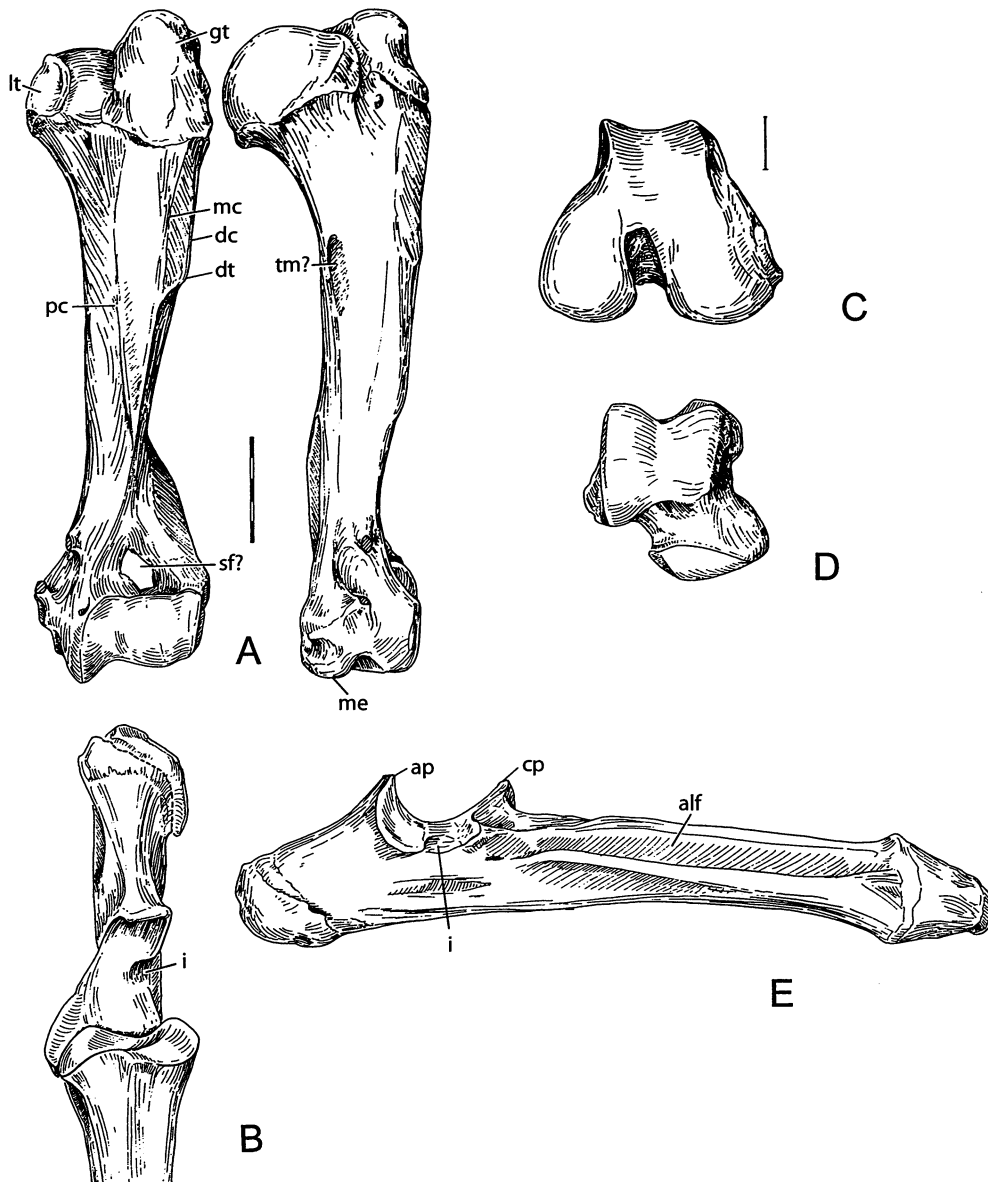


FIGURE 12 — Limb elements of the mesonychian *Pachyaena*. A, B, and E, *P. gigantea*, USNM 14915; C and D, *P. gracilis*. A, left humerus; B, proximal left ulna and radius; E, right ulna. C, distal end of left femur of USGS 25280; D, right astragalus of AMNH 16968 supplemented by AMNH 2959A. Abbreviations: *alf*, anterolateral fossa; *ap*, anconeal process; *cp*, coronoid process; *dc*, deltoid crest; *dt*, deltoid tuberosity; *gt*, greater tuberosity; *i*, incisure in trochlear notch; *lt*, lesser tuberosity; *mc*, median crest; *me*, medial epicondyle; *pc*, pectoral crest; *sf?*, supratrochlear foramen?; *tm?*, teres major tubercle?. Scale for A, B, and E = 5 cm; scale for C and D = 1 cm. From O'Leary and Rose (1995).

show certain hind limb features foreshadowing the cursorial specializations of basal artiodactyls like *Diacodexis* (Rose, 1996a). It thus seems premature to rule out Arctocyoniidae as a possible source or sister-taxon of Artiodactyla.

Phenacodontidae

Skeletal remains of phenacodontids are among the most common postcrania from the Willwood Formation. The USGS-JHU collection includes about 30 partial skeletons and skeletal

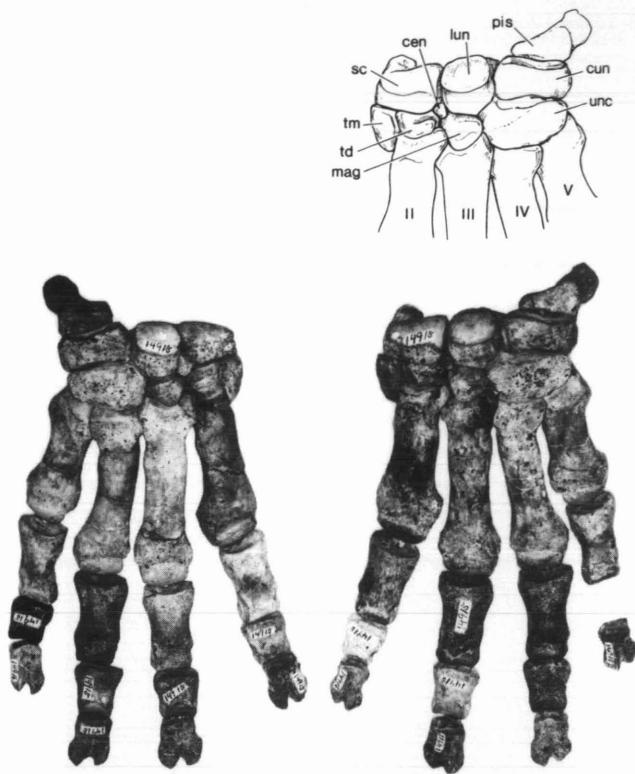


FIGURE 13 — Manus of *Pachyaena gigantea*, USNM 14915. Abbreviations: *cen*, centrale; *cun*, cuneiform; *lun*, lunate; *mag*, magnum; *pis*, pisiform; *sc*, scaphoid; *td*, trapezoid; *tm*, trapezium; *unc*, unciform. Scale = 5 cm. From Rose and O'Leary (1995).

associations, primarily representing *Phenacodus*, two-thirds of them new since the last report. The larger specimens of *Phenacodus* are here assigned to either *P. trilobatus* or the somewhat smaller *P. intermedius* based on size (both have usually been subsumed under the name *P. primaevus*), following Thewissen (1990), and still smaller ones to *P. vortmani*. Post-cranial remains of *P. intermedius* are much less frequent than those of the other two species, and are from stratigraphically lower than the others, consistent with Thewissen's (1990) observation that *P. intermedius* is particularly common in the lower part of the Wasatchian section.

As shown by previous workers (e.g., Radinsky, 1966; Otts, 1991), *Phenacodus* was digitigrade and incipiently cursorial, based on numerous modifications of the limb skeleton to lengthen stride and limit motion mainly to a parasagittal plane. Cursorial features that foreshadow the anatomy of early perissodactyls include: a prominent greater tuberosity, reduced deltoid and supinator crests, and a supratrochlear foramen on the humerus; broad, uneven radial head positioned anterior to the ulna; distal radius with paired carpal facets; ulna concave posteriorly; high greater trochanter and elevated, well-defined patellar groove on the femur; deeply grooved tibiotalar joint; and mesaxonic manus and pes with reduced lateral digits and

broad, flat, hoof-like ungual phalanges. These features made *Phenacodus* better adapted for cursorial habits than most other early Eocene mammals. It was, however, less specialized in this regard than Willwood perissodactyls or artiodactyls (for example, limb elements are neither as elongate nor as gracile as in the modern ungulates, there is no fusion or loss of limb elements, and the clavicle was retained; Thewissen, 1990), and slightly less cursorial than contemporary mesonychians.

Ectocion is one of the most abundant late Paleocene-early Eocene mammals from the Willwood Formation, but its post-cranial skeleton remains very poorly known. Thewissen (1990) observed minor differences from *Phenacodus* (smaller greater tubercle, weaker deltopectoral crest, and long, narrow patellar trochlea), from which he inferred that *Ectocion* was slightly more cursorially adapted.

Thewissen (1990) figured and briefly described a partial skeleton of *Copecion brachypternus* (UM 64179), including substantial parts of the limbs. Like *Ectocion*, it differs from *Phenacodus* in having a weaker deltopectoral crest and lacking an astragalar foramen, again suggesting slightly more progressive cursorial adaptation. (Although Thewissen reported the astragalar foramen to be present in all four *Phenacodus* astragali he studied, it is variable in our sample. The foramen is present in three specimens of *P. trilobatus*, and absent in three; it is present in one *P. intermedius* and absent in one; and a small foramen appears to be present in two specimens of *P. vortmani*.)

USGS 38074, from the base of the Eocene in the southern Bighorn Basin, is the first significant partial skeleton known for *Copecion davisi*. It is the smallest known phenacodontid, about two-thirds the linear dimensions of *C. brachypternus*, and just slightly larger than the artiodactyl *Diacodexis*. Compared to *C. brachypternus*, the deltopectoral crest is sharper and slightly stronger, and the posterior calcaneal facet is more transverse. The ulna is convex posteriorly, even more so than in *Phenacodus vortmani*, both species contrasting in this regard with *P. trilobatus*, in which the ulnar shaft is distinctly concave posteriorly (as in cursors generally; see O'Leary and Rose, 1995: fig. 7). The radial notch of the ulna is set off from the trochlear notch at a sharp angle, as in *P. trilobatus*. This differs from *P. vortmani*, in which the angle of the radial notch is less, suggesting a more mobile humeroulnar joint. As in *C. brachypternus* and *Ectocion*, the cuboid facet of the calcaneus is more sharply angled than in *Phenacodus*. The astragalar trochlea is deeply grooved, there is no astragalar foramen, and the astragalar neck is relatively longer than in other phenacodontids. While most of these features suggest slightly more cursorial specialization than in the larger *Phenacodus* species, the ulnar profile and stronger deltopectoral crest do not. This specimen is currently under study and will be analyzed more fully elsewhere.

Mesonychia

Several new skeletal specimens of *Pachyaena ossifraga* and *P. gracilis*, as well as a previously undescribed partial skeleton of *P. gigantea* (USNM 14915), were the focus of study by

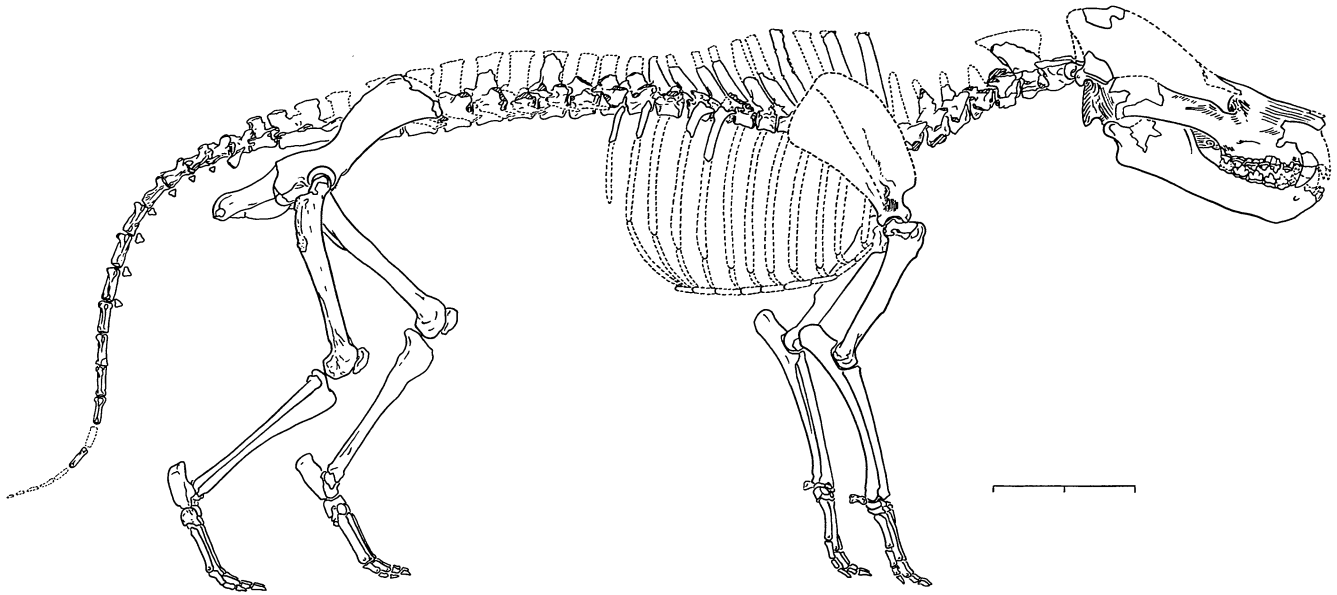


FIGURE 14 — Reconstruction of the skeleton of *Pachyaena ossifraga*, based primarily on UM 95074. From Zhou et al. (1992).

O'Leary and Rose (1995; Rose and O'Leary, 1995). The three species, ranging from wolf- to bear-sized, were the largest Wasatchian mammalian carnivores, some reaching weights of several hundred kilograms. They differ primarily in size and robustness. The skeleton of *Pachyaena* exhibits a variety of cursorial specializations that variously resemble those seen in present-day artiodactyls, perissodactyls, and carnivorans. The limb joints in *Pachyaena*, unlike those of arctocyonids (the probable progenitor of Mesonychia), are modified to restrict motion largely to flexion and extension in a parasagittal plane. Cursorial traits of *Pachyaena* that are widespread among mammalian runners include a broad, caudally projecting humeral head, high greater tuberosity, relatively low deltopectoral crest and proximal deltoid tuberosity, reduced humeral epicondyles, narrow humeral articular surface with steep medial trochlear ridge, deep or perforate olecranon fossa, posteriorly concave ulnar shaft, deep distal femur with elevated and well-defined patellar groove, and a deeply grooved astragalar trochlea (Fig. 12). The proximal radial articulation, like those of modern ungulates, is broad, uneven, and mostly anterior rather than lateral to the ulna. The manus and pes are paraxonic, like those of artiodactyls, but have vestigial pollex and hallux, and the digits are terminated by slightly fissured ungulate-like hoofs (Fig. 13). *Pachyaena* had an alternating arrangement of carpal and tarsal bones, the latter somewhat resembling the condition in artiodactyls and some perissodactyls (e.g., *Tapirus*). The vertebral column of *Pachyaena* was also modified for cursorial locomotion, with specializations of the distal thoracic and lumbar vertebrae that made the lower back relatively rigid, as in modern dorsostable ungulates and scavenging carnivores such as hyenas (Zhou et al., 1992).

Despite its obvious cursorial specializations, *Pachyaena* had comparatively short limbs, especially the distal segments (Fig.

14). This indicates that it was not a particularly swift runner (though probably faster than most other Wasatchian mammals), and it was more likely adapted for endurance rather than speed. *Pachyaena* seems most likely to have been a scavenger or an active predator, but its diet and precise lifestyle remain enigmatic.

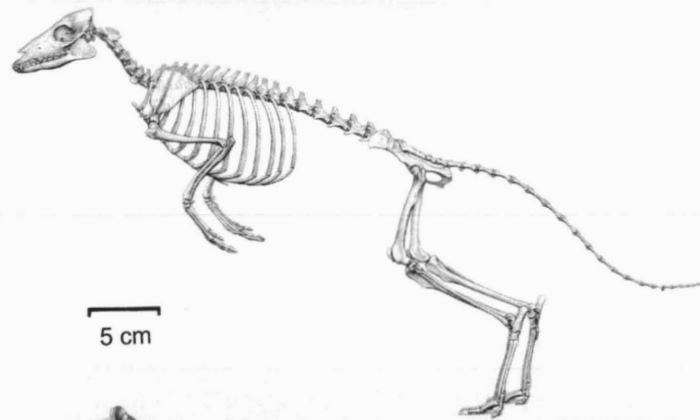
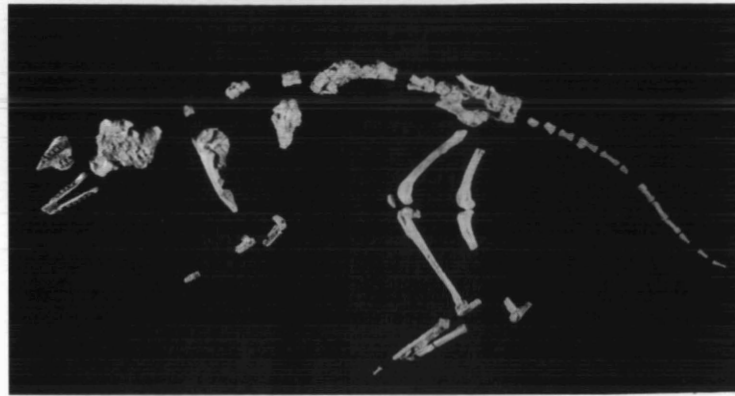
Artiodactyla

The basal artiodactyl *Diacodexis* is one of the most common Willwood mammals, represented by thousands of jaws, but skeletal associations are very rare. Only a single very fragmentary association was added to our collection over the last decade. The substantially complete skeleton of *Diacodexis* found over 20 years ago by M. J. Kraus (USGS 2352, Fig. 15; Rose, 1982, 1985) is still by far the best skeleton known for the genus. It demonstrates that *Diacodexis*, with its gracile, elongate hind limbs, was the most specialized small runner/umper in the Willwood mammal fauna.

Postcrania of *Bunophorus* are rarer still, and nothing that can be called a partial skeleton has been found in the Bighorn Basin. However, a couple of skeletal associations, both of which preserve comparable tarsal elements, represent two species of substantially different size. Known elements resemble those of *Diacodexis* except for being larger and somewhat more robust.

Perissodactyla

More than 20 additional partial skeletons of perissodactyls, representing the equoid *Hyracotherium (sensu lato)*, and the tapiroids *Homogalax* and *Heptodon*, were collected by JHU and USGS field parties over the last decade. In addition to the



© 1993 J. H. Matternes



© 1993 J. H. Matternes



© 1993 J. H. Matternes

FIGURE 15 — Skeleton and restoration of the artiodactyl *Diacodexis metsiacus*, USGS 2352. Restorations by Jay H. Matternes ©1993; published by permission of Jay H. Matternes.

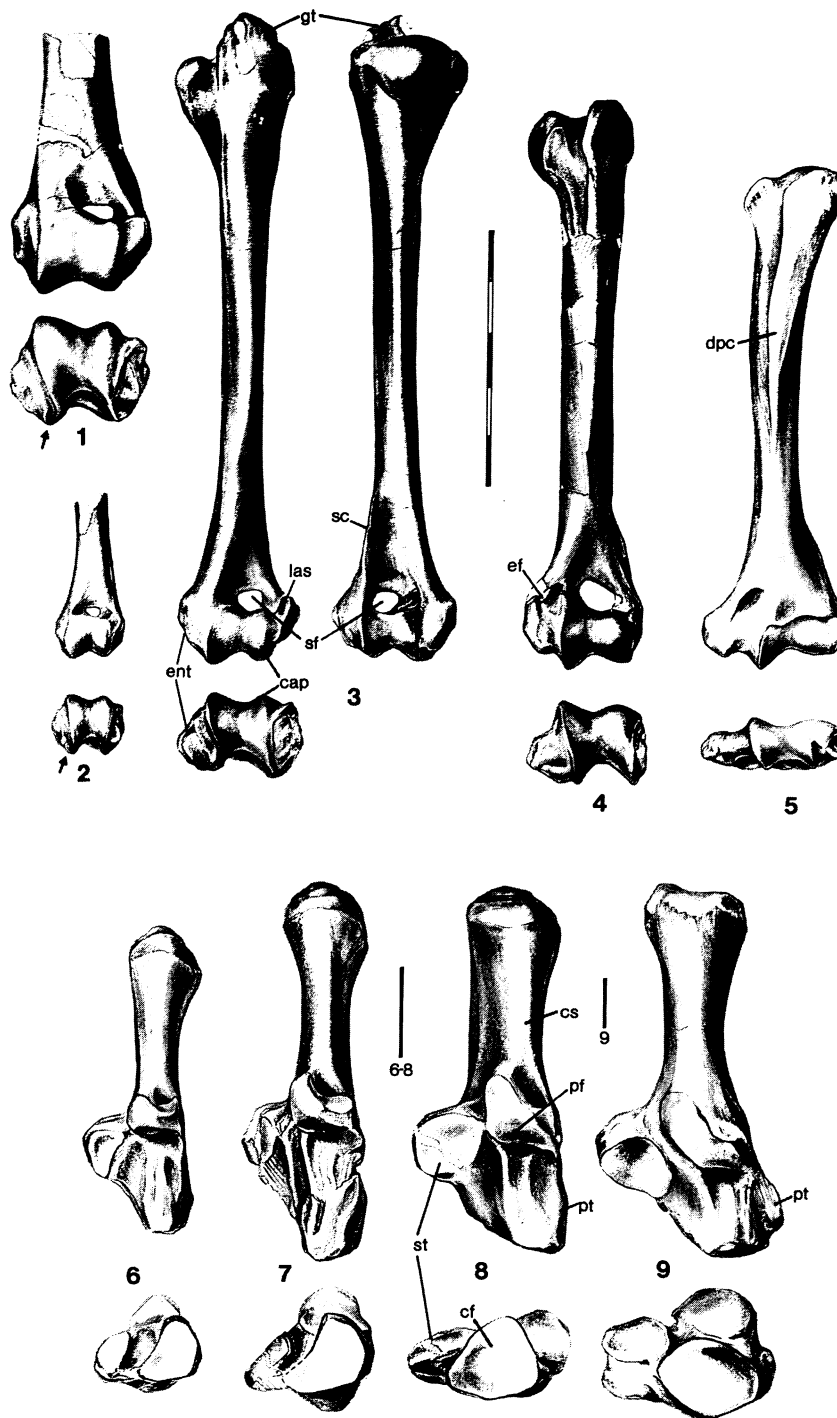


FIGURE 16 — Left humeri and calcanei of Willwood tapiroids (1, 3, 7, 8) compared with those of some other Willwood ungulates. 1, *Heptodon* sp., USGS 25333; 2, *Hyracotherium* sp., USGS 25105; 3, *Homogalax protapirinus*, USGS 25032; 4, *Phenacodus vortmani*, USGS 7159; 5, *Chriacus* sp., USGS 2353 supplemented by USGS 15404 and USGS 21907; 6, *Hyracotherium* sp., USGS 38039; 7, *Cardiolphus radinskyi*?, UM 80318; 8, *Homogalax protapirinus*, USGS 25032; 9, *Phenacodus trilobatus*, USGS 7146. Abbreviations: *cap*, capitulum; *cf*, cuboid facet; *cs*, calcaneal shaft; *dpc*, deltopectoral crest; *ef*, entepicondylar foramen; *ent*, entepicondyle; *gt*, greater tuberosity; *las*, lateral articular shelf; *pf*, proximal facet of calcaneus; *pt*, peroneal tubercle; *sc*, supinator crest; *sf*, supratrochlear foramen; *st*, sustentaculum tali. Arrows in 1 and 2 indicate caudally projecting entepicondyle. Top scale = 5 cm, lower scales = 1 cm. From Rose (1996b).

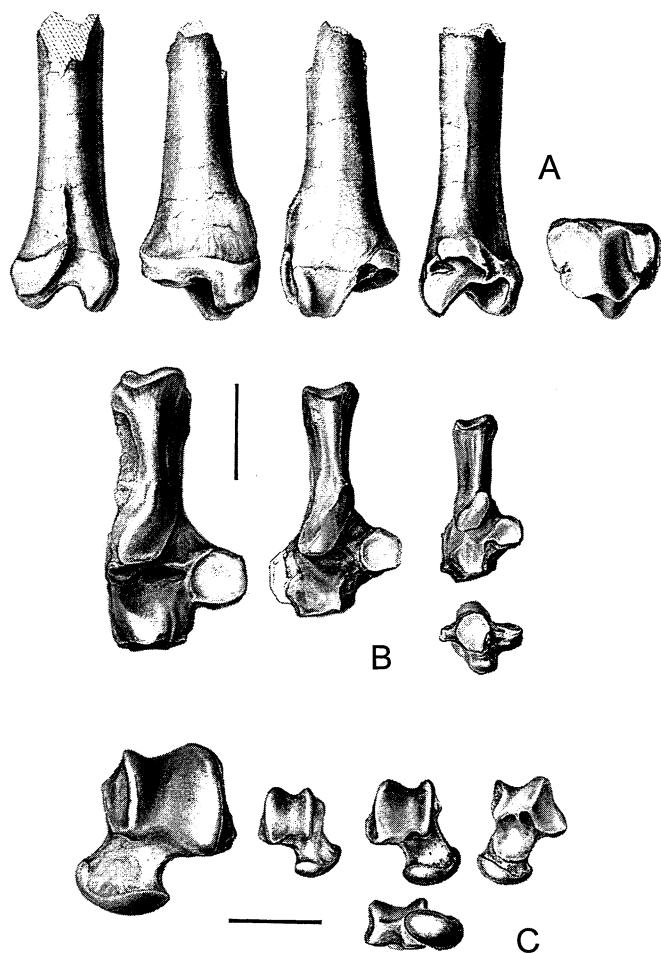


FIGURE 17 — Hind limb elements of Willwood paramyid rodents. A, Distal right tibia of cf. *Paramys wortmani*, USNM 491864, in medial, anterior, posterior, lateral, and distal views. B, Right calcanei of three different paramyids: left to right, cf. *Leptotomus* sp. (USNM 491959), cf. *Paramys wortmani* (USNM 491864), *Paramys taurus* (USNM 491855). C, Astragali of three different paramyids: left to right, left astragalus of cf. *Leptotomus* sp. (USNM 491959), right astragalus of *Paramys taurus* (USNM 491856), right astragalus of *Paramys* sp. (USNM 491851) in three views. Scales = 1 cm.

specimens listed in the appendix, it can be noted that a concentration of *Hyracotherium* including substantial parts of the skeleton of at least four individuals was found at locality WW-57 in 2000. Perissodactyls were among the most cursorially specialized Wasatchian mammals.

New skeletal material of *Homogalax* and *Cardiophus* (the latter collected by the University of Michigan) confirmed preliminary inferences that basal tapiroids were more plesiomorphic in several postcranial traits than *Hyracotherium* (Rose, 1996b). Particularly, in the tapiroids the distal humerus,

tarsus, and metapodials are relatively more robust, and the posterior calcaneoastragalar joint is less restrictive. In all these aspects *Homogalax* is structurally intermediate between phenacodontids and *Hyracotherium* (Fig. 16). On the other hand, *Homogalax* seems to have been more derived than *Hyracotherium* in having a more reduced fifth metacarpal. New skeletal remains of *Hyracotherium* and *Heptodon* have not yet been studied except to compare with *Homogalax*.

Rodentia

Our collection contains considerable postcranial material of Wasatchian rodents (about 25 partial skeletons), most apparently representing the genus *Paramys*; a few specimens are assigned tentatively to *Thisbemys*, *Leptotomus*, and the sciuravid *Knightomys*. The paramyids ranged from about the size of the living tree squirrel *Sciurus* to larger than the ground-hog *Marmota*, whereas *Knightomys* (known so far from only a single distal tibia) was among the smallest rodents in the Willwood fauna, about the size of the chipmunk *Tamias*. Wasatchian paramyids compare closely with extant sciurids in many features of the postcranial skeleton (Chinnery and Rose, 2000), showing a mixture of arboreal and terrestrial traits, often within the same element.

The forelimb elements in most specimens resemble those of tree squirrels in having a relatively round humeral head, low tuberosities, an oval or almost circular radial head, an open semilunar notch, and a radial notch offset at a low angle from the trochlear notch. At the same time, many show a laterally-directed deltopectoral crest, a wide radial notch, and a pronator quadratus crest similar to those present in ground squirrels (e.g., Thorington et al., 1998). The humeri referred to *Leptotomus* are more robust, with more prominent tuberosities comparable in development to those of *Marmota*. Most features of the hind limb are more like those of terrestrial squirrels. These include a posteromedially-directed lesser trochanter, well-defined patellar trochlea, a very prominent tibial malleolus, a distally placed peroneal process on the calcaneus, and astragalar trochlear ridges of roughly equal dimension (Fig. 17). Comparative osteological evidence indicates that paramyids were very generalized rodents, more terrestrially adapted than *Sciurus*, but probably proficient climbers as well, apparently better adapted for tree-climbing than extant ground squirrels like *Spermophilus* and *Marmota*.

DISCUSSION

The Wasatchian mammal assemblage of the Willwood Formation lived in a humid, forested, subtropical-to-tropical lowland floodplain, which has been compared to present-day tropical forests of southeast Asia (Morgan et al., 1995). During this warmest interval of the Cenozoic, the Bighorn Basin flora included palms, cycads, and ferns, as well as sycamore, walnut, hickory, ginkgo, and dawn redwood (Wing et al., 1991; Wing, 2001, and personal communication). At first glance, the mammalian assemblage would have appeared

alien to a present-day observer. Many constituents of the Wasatchian mammal fauna, such as tillodonts, taeniodonts, mesonychids, and phenacodontids, have no close modern analogues. Others, however, would seem familiar: arboreal primates, arboreal and terrestrial carnivorans and creodonts that resembled extant viverrids and mustelids to various degrees, squirrel-like rodents, diminutive chevrotain-like artiodactyls, small tapiroids and miniature horses, armadillo-like diggers, saltatorial and other ground-dwelling insectivores, and raccoon- and bear-like arctocyonids (Rose, 2001). Although closer inspection shows that most of these mammals differ substantially from their present-day counterparts, many of them occupied ecological niches more or less similar to those in tropical mammal communities today. Just as dietary specialization was greater in Wasatchian faunas than earlier (Gunnell et al., 1995), postcranial specializations also were more diverse.

Many of the postcranial specializations of Wasatchian mammals were innovations not present in Paleocene mammals. The most important anatomical innovations seen in Wasatchian mammals are those of the oldest known members (or the oldest known postcranial remains) of many mammalian orders that survive today, including primates, artiodactyls, perissodactyls, carnivorans, and rodents. Early Eocene carnivorans included incipiently cursorial forms, as well as some of the most arboreally adapted placentals known up to that time. Most early Eocene rodents, on the other hand, appear to have been generalists, equally adept on the ground and in the trees. Artiodactyls and perissodactyls independently achieved unique new modifications for cursorial locomotion, each with their own distinctive tarsal morphology, and associated, respectively, with paraxonic and mesaxonic foot symmetry. Early euprimates evolved grasp-leaping arboreal specializations, including elongate hind limbs, an opposable hallux, and nail-bearing digits. Such varied postcranial adaptations were instrumental in the early success of these orders, eventually leading them to become the dominant terrestrial mammals of the post-Eocene world.

ACKNOWLEDGMENTS

I thank Dr. Philip Gingerich for inviting me to present this review, and Amy Chew, Shawn Zack, and Dr. Gregg Gunnell for providing information for the appendix. Much of the field work that produced the skeletons reported here was conducted jointly with my friend and colleague Tom Bown. I am indebted to the dozens of students and colleagues whose countless hours of searching the badland outcrops have resulted in the collections summarized here. In addition to those listed in the acknowledgments in Bown et al. (1994), Amy Chew, Don Kron, Jay Mussell, and Mary Silcox deserve special mention. The illustrations in this review, mostly reproduced from previous works, are primarily the work of Elaine Kasmer, to whom I am particularly grateful. I thank Jay Matternes for permission to use his restorations of *Diacodexis* (Fig. 15), Mary Ellen Didion for Figure 5, and Norman Barker for the photographs of

Willwood skeletons. Support for our field work and research on Willwood mammal postcrania from the National Science Foundation (including grants BSR-8801037, DEB-8918755, IBN-9419776, and SBR-9815884 during the last decade or so), and from the Bureau of Land Management, especially the Worland District Office, is gratefully acknowledged.

LITERATURE CITED

- BADGLEY, C. 1990. A statistical assessment of last appearances in the Eocene record of mammals. *In*: T.M. Bown and K.D. Rose (eds.), Dawn of the Age of Mammals in the Northern Part of the Rocky Mountain Interior. Geological Society of America Special Paper, 243: 153-167.
- BEARD, K. C. 1989. Postcranial anatomy, locomotor adaptations, and paleoecology of early Cenozoic Plesiadapidae, Paromomyidae, and Micromomyidae (Eutheria, Dermoptera). Unpublished Ph.D. Dissertation, Johns Hopkins University, 661 pp.
- BEARD, K. C. 1990. Gliding behaviour and palaeoecology of the alleged primate family Paromomyidae (Mammalia, Dermoptera). *Nature*, 345: 340-341.
- BEARD, K. C. 1991. Vertical postures and climbing in the morphotype of Primatomorpha: implications for locomotor evolution in primate history. *In*: Y. Coppens and B. Senut (eds.), Origines de la Bipédie chez les Homínidés. Paris, Editions de CNRS (Cahiers de Paléanthropologie), pp. 79-87.
- BEARD, K. C. 1993a. Phylogenetic systematics of the Primatomorpha, with special reference to Dermoptera. *In*: F.S. Szalay, M.J. Novacek, and M.C. McKenna (eds.), Mammal Phylogeny: Placentals. New York, Springer-Verlag, pp. 129-150.
- BEARD, K. C. 1993b. Origin and evolution of gliding in early Cenozoic Dermoptera (Mammalia, Primatomorpha). *In*: R.D.E. MacPhee (ed.), Primates and Their Relatives in Phylogenetic Perspective. New York, Plenum Press, pp. 63-90.
- BLOCH, J. I., K. D. ROSE, and P. D. GINGERICH. 1998. New species of *Batodonoides* (Lipotyphla, Geolabididae) from the early Eocene of Wyoming: smallest known mammal? *Journal of Mammalogy*, 79: 804-827.
- BOWN, T. M. 1979. Geology and mammalian paleontology of the Sand Creek facies, lower Willwood Formation (lower Eocene), Washakie County, Wyoming. Geological Survey of Wyoming Memoir, 2: 1-151.
- BOWN, T. M. and M. J. KRAUS. 1993. Time-stratigraphic reconstruction and integration of paleopedologic, sedimentologic, and biotic events (Willwood Formation, lower Eocene, northwest Wyoming, U.S.A.). *Palaios*, 8: 68-80.
- BOWN, T. M., K. D. ROSE, E. L. SIMONS, and S. L. WING. 1994. Distribution and stratigraphic correlation of fossil mammal and plant localities of the Fort Union, Willwood, and Tatman formations (upper Paleocene-lower Eocene), central and southern Bighorn Basin, Wyoming. U.S. Geological Survey Professional Paper, 1540: 1-103.
- CHINNERY, B. J. and K. D. ROSE. 2000. Early Eocene rodent postcrania from the Willwood Formation, Bighorn Basin, Wyoming. *Journal of Vertebrate Paleontology*, 20, supplement to no.3: 35A.

- CLYDE, W. C. 1997. Stratigraphy and mammalian paleontology of the McCullough Peaks, northern Bighorn Basin, Wyoming: implications for biochronology, basin development, and community reorganization across the Paleocene-Eocene boundary. Unpublished Ph.D. Dissertation, University of Michigan, 256 pp.
- DENISON, R. H. 1938. The broad-skulled Pseudocreoedi. *Annals of the New York Academy of Sciences*, 37: 163-256.
- EGI, N. 1999. Functional morphology of the limb bones in recent carnivores and its application to North American hyaenodontid Creodonta. Unpublished Ph.D. Dissertation, Johns Hopkins University, 476 pp.
- GEBO, D. L. 1987. Humeral morphology of *Cantius*, an early Eocene adapid. *Folia Primatologica*, 49: 52-56.
- GEBO, D. L. and K. D. ROSE. 1993. Skeletal morphology and locomotor adaptation in *Prolimnocyon atavus*, an early Eocene hyaenodontid creodont. *Journal of Vertebrate Paleontology*, 13: 125-144.
- GEBO, D. L., M. DAGOSTO, and K. D. ROSE. 1991. Foot morphology and evolution in early Eocene *Cantius*. *American Journal of Physical Anthropology*, 86: 51-73.
- GINGERICH, P. D. 1989. New earliest Wasatchian mammalian fauna from the Eocene of northwestern Wyoming: composition and diversity in a rarely sampled high-floodplain assemblage. *University of Michigan Papers on Paleontology*, 28: 1-97.
- GINGERICH, P. D. 1991. Systematics and evolution of early Eocene Perissodactyla (Mammalia) in the Clarks Fork Basin, Wyoming. *Contributions from the Museum of Paleontology, University of Michigan*, 28: 181-213.
- GINGERICH, P. D. and H. A. DEUTSCH. 1989. Systematics and evolution of early Eocene Hyaenodontidae (Mammalia, Creodonta) in the Clarks Fork Basin, Wyoming. *Contributions from the Museum of Paleontology, University of Michigan*, 27: 327-391.
- GINGERICH, P. D. and E. L. SIMONS. 1977. Systematics, phylogeny, and evolution of early Eocene Adapidae (Mammalia, Primates) in North America. *Contributions from the Museum of Paleontology, University of Michigan*, 24: 245-279.
- GUNNELL, G. F., and P. D. GINGERICH. 1991. Systematics and evolution of late Paleocene and early Eocene Oxyaenidae (Mammalia, Creodonta) in the Clarks Fork Basin, Wyoming. *Contributions from the Museum of Paleontology, University of Michigan*, 28: 141-180.
- GUNNELL, G. F., M. E. MORGAN, M. C. MAAS, and P. D. GINGERICH. 1995. Comparative paleoecology of Paleogene and Neogene mammalian faunas: trophic structure and composition. *Palaeogeography, Palaeoclimatology, Palaeoecology*, 115: 265-286.
- HAMRICK, M. W., B. A. ROSENMAN, and J. A. BRUSH. 1999. Phalangeal morphology of the Paromomyidae (?Primates, Plesiadapiformes): the evidence for gliding behavior reconsidered. *American Journal of Physical Anthropology*, 109: 397-413.
- HEINRICH, R. E. 1995. Functional morphology and body size of Early Tertiary Miacoidea (Mammalia, Carnivora). Unpublished Ph.D. Dissertation, Johns Hopkins University, 241 pp.
- HEINRICH, R. E. and K. D. ROSE. 1993. *Oxyaena* (order Creodonta): locomotor adaptations and paleobiology revisited. *Journal of Vertebrate Paleontology*, supplement to no. 3: 41A.
- HEINRICH, R. E. and K. D. ROSE. 1995. Partial skeleton of the primitive carnivoran *Miacis petilus* from the early Eocene of Wyoming. *Journal of Mammalogy*, 76: 148-162.
- HEINRICH, R. E. and K. D. ROSE. 1997. Postcranial morphology and locomotor behaviour of two early Eocene miacoid carnivorans, *Vulpavus* and *Didymictis*. *Palaeontology*, 40: 279-305.
- JENKINS, F. A. and D. MCCLEARN. 1984. Mechanisms of hind foot reversal in climbing mammals. *Journal of Morphology*, 182: 197-219.
- KRAUSE, D. W. 1991. Were paromomyids gliders? Maybe, maybe not. *Journal of Human Evolution*, 21: 177-188.
- MACLEOD, N. and K. D. ROSE. 1993. Inferring locomotor behavior in Paleogene mammals via eigenshape analysis. *American Journal of Science*, 293A: 300-355.
- MACLEOD, N. and K. D. ROSE. 1997. 3-D morphometric-functional analysis of modern and Paleogene mammalian radial heads. *Journal of Vertebrate Paleontology*, 17, supplement to no 3: 61A.
- MAIER, W. 1979. *Macrocranion tupaiodon*, an adapisoricid (?) insectivore from the Eocene of "Grube Messel" (western Germany). *Paläontologische Zeitschrift*, 53: 38-62.
- MATTHEW, W. D. 1909. The Carnivora and Insectivora of the Bridger Basin, middle Eocene. *Memoirs of the American Museum of Natural History*, 9: 289-567.
- MATTHEW, W. D. 1915. A revision of the lower Eocene Wasatch and Wind River faunas. Part 1. Order Ferae (Carnivora). *Suborder Creodonta*. *Bulletin of the American Museum of Natural History*, 34: 4-103.
- MATTHEW, W. D. 1918. A revision of the lower Eocene Wasatch and Wind River faunas. Part 5. Insectivora (continued), Glires, Edentata. *Bulletin of the American Museum of Natural History*, 38: 565-657.
- MORGAN, M. E., C. BADGLEY, G. F. GUNNELL, P. D. GINGERICH, J. W. KAPPELMAN, and M. C. MAAS. 1995. Comparative paleoecology of Paleogene and Neogene mammalian faunas: body-size structure. *Palaeogeography, Palaeoclimatology, Palaeoecology*, 115: 287-317.
- O'LEARY, M. A. 1996. Dental evolution in the early Eocene Notharctinae (Primates, Adapiformes) from the Bighorn Basin, Wyoming: documentation of gradual evolution in the oldest true primates. Unpublished Ph.D. Dissertation, Johns Hopkins University, 398 pp.
- O'LEARY, M. A. and K. D. ROSE. 1995. Postcranial skeleton of the early Eocene mesonychid *Pachyaena* (Mammalia: Mesonychia). *Journal of Vertebrate Paleontology*, 15: 401-430.
- OTTS, C. 1991. Postural and locomotor capabilities in the phenacodontid condylarths (Mammalia). Unpublished Ph.D. Dissertation, University of Arizona, 566 pp.
- PATTERSON, B. 1939. A skeleton of *Coryphodon*. *Proceedings of the New England Zoological Club*, 17: 97-110.
- RADINSKY, L. 1966. The adaptive radiation of phenacodontid condylarths and the origin of the Perissodactyla. *Evolution*, 20: 408-417.

- ROSE, K. D. 1982. Skeleton of *Diacodexis*, oldest known artiodactyl. *Science* 216: 621-623.
- ROSE, K. D. 1985. Comparative osteology of North American dichobunid artiodactyls. *Journal of Paleontology*, 59: 1203-1226.
- ROSE, K. D. 1987. Climbing adaptations in the early Eocene mammal *Chriacus* and the origin of Artiodactyla. *Science*, 236: 314-316.
- ROSE, K. D. 1990. Postcranial skeletal remains and adaptations in early Eocene mammals from the Willwood Formation, Bighorn Basin, Wyoming. In: T.M. Bown and K.D. Rose (eds.), Dawn of the Age of Mammals in the Northern Part of the Rocky Mountain Interior. Geological Society of America Special Paper, 243: 107-133.
- ROSE, K. D. 1996a. On the origin of the order Artiodactyla. *Proceedings of the National Academy of Sciences, USA*, 93: 1705-1709.
- ROSE, K. D. 1996b. Skeleton of early Eocene *Homogalax* and the origin of Perissodactyla. *Palaeovertebrata*, 25: 243-260.
- ROSE, K. D. 1999. Postcranial skeleton of Eocene Leptictidae (Mammalia), and its implications for behavior and relationships. *Journal of Vertebrate Paleontology*, 19: 355-372.
- ROSE, K. D. 2001. Wyoming's Garden of Eden. *Natural History*, 110(3), April: 55-59.
- ROSE, K. D. and M. A. O'LEARY. 1995. The manus of *Pachyaena gigantea* (Mammalia: Mesonychia). *Journal of Vertebrate Paleontology*, 14: 855-859.
- ROSE, K. D. and A. WALKER. 1985. The skeleton of early Eocene *Cantius*, oldest lemuriform primate. *American Journal of Physical Anthropology*, 66: 73-89.
- ROSE, K. D., R. J. EMRY, and P. D. GINGERICH. 1992. Skeleton of *Alocodontulum atopum*, an early Eocene epiacanthid (Mammalia, Palaeodonta) from the Bighorn Basin, Wyoming. *Contributions from the Museum of Paleontology, University of Michigan*, 28: 221-245.
- ROSE, K. D., R. D. E. MacPHEE, and J. P. ALEXANDER. 1999. Skull of early Eocene *Cantius abditus* (Primates: Adapiformes) and its phylogenetic implications, with a reevaluation of "*Hesperolemur*" *actius*. *American Journal of Physical Anthropology*, 109: 523-539.
- RUNESTAD, J. A., and C. B. RUFF. 1995. Structural adaptations for gliding in mammals with implications for locomotor behavior in paromomyids. *American Journal of Physical Anthropology*, 98: 101-119.
- SCHOCH, R. M. 1986. Systematics, functional morphology, and macroevolution of the extinct mammalian order Taeniodonta. *Peabody Museum Bulletin*, 42: 1-307.
- SILCOX, M. T. and K. D. ROSE. in press. Unusual vertebrate microfaunas from the Willwood Formation, early Eocene of the Bighorn Basin, Wyoming. In: G.F. Gunnell (ed.), *Eocene Vertebrates: Unusual Occurrences and Rarely Sampled Habitats*. New York, Plenum, pp. 131-164.
- SIMONS, E. L. 1960. The Paleocene Pantodonta. *Transactions of the American Philosophical Society, new series*, 50(6): 1-99.
- SZALAY, F. S., and S. LUCAS. 1996. The postcranial morphology of Paleocene *Chriacus* and *Mixodectes* and the phylogenetic relationships of archontan mammals. *New Mexico Museum of Natural History and Science Bulletin*, 7: 1-47.
- THEWISSEN, J. G. M. 1990. Evolution of Paleocene and Eocene Phenacodontidae (Mammalia, Condylarthra). *University of Michigan Papers on Paleontology* 29: 1-107.
- THORINGTON, R. W., A. M. L. MILLER, and C. G. ANDERSON. 1998. Arboreality in tree squirrels (Sciuridae). In: M. A. Steele, J. F. Merritt, and D. A. Zegers (eds.), *Ecology and Evolutionary Biology of Tree Squirrels*. Virginia Museum of Natural History Special Publication, 6: 119-130.
- VAN VALEN, L. 1963. The origin and status of the mammalian order Tillodontia. *Journal of Mammalogy*, 44: 364-373.
- VAN VALEN, L. 1978. The beginning of the Age of Mammals. *Evolutionary Theory*, 4: 45-80.
- WING, S. L. 2001. Hot times in the Bighorn Basin. *Natural History*, 110(3), April: 48-54.
- WING, S. L. T. M. BOWN, and J. D. OBRADOVICH. 1991. Early Eocene biotic and climatic change in interior western North America. *Geology*, 19: 1189-1192.
- ZHOU, X., W. J. SANDERS, and P. D. GINGERICH. 1992. Functional and behavioral implications of vertebral structure in *Pachyaena ossifraga* (Mammalia, Mesonychia). *Contributions from the Museum of Paleontology, University of Michigan*, 28: 289-319.

APPENDIX

Postcranial associations from the Wasatchian part of the Willwood Formation collected, identified, or described since the last review (Rose, 1990). Locality number and stratigraphic level or faunal zone follows the specimen number and identification (meters from base of Willwood Formation in the southern Bighorn Basin, after Bown et al., 1994; Wasatchian faunal zone for northern Bighorn and Clarks Fork basins, after Gingerich, 1991). Listings for UM collection are incomplete. Principal elements are listed here; most specimens include additional associated fragments.

Geologic sections of the Willwood Formation in the northern and southern parts of the Bighorn Basin differ in thickness and have not been precisely correlated. Consequently, it is difficult to apply Gingerich's faunal zonation, which was developed in the Clarks Fork Basin, to the southern sections. The following approximations provide an estimate of comparable intervals. Wa-0 faunas come from approximately -20 m through +10 m in the southern Bighorn Basin. Wa-1 and Wa-2 occur in the succeeding interval up to about 200 m (Biohorizon A), which represents about half of Willwood time in the southern Bighorn Basin (Bown and Kraus, 1993). Wa-3 and Wa-4 occupy the interval from ca. 200 m to 400 m. Precise levels of the Wa-1/Wa-2 and Wa-3/Wa-4 boundaries are uncertain. *Bunophorus etsagicus*, whose first appearance marks the beginning of Wa-5 in the Clarks Fork Basin, first occurs at ca. 400 m in the southern basin. The lower boundary of Wa-6

(essentially equivalent to the "Lysitean" subage) coincides with the first appearances of *Heptodon* and *Absarokius*, which occur at 425-430 m (Bown et al., 1994). Wa-7 (equivalent to the "Lostcabinian") begins at about 590-600 m, based on first occurrence of *Lambdaotherium* (though this taxon is relatively uncommon).

LEPTICTIDA

Leptictidae

Prodiacodon

UM 88105, cf. *P. tauricinerei* (locality MP-29, Wa-6): maxilla, dentary, and associated skeleton including manubrium sterni, both humeri, left ilium, left femur, proximal and distal left tibia, distal right tibiofibula with articulated tarsus in concretion, right metatarsals and phalanges, left metatarsals, articulated vertebrae, ribs

Palaeictops

USNM 495150 (formerly USGS 25166), cf. *P. bicuspis* (D-1310, 442 m): partial skull, partial femora, pelvis, proximal tibia

USNM 495152 (formerly USGS 16493), cf. *Palaeictops* sp. (D-1198=Y-45, 470 m): heavily worn lower dentition, and partial skeleton including incomplete humeri, ulna, proximal and distal femora and right tibia, most of left tibiofibula, astragali, calcaneus

USNM 495153 (formerly USGS 16492), *Palaeictops* sp. (D-1612, 505 m): left maxilla and right dentary, pelvis, femur, and vertebrae in matrix

USNM 495154 (formerly USGS 27235), *Palaeictops* sp. (D-1968, ca. 500 m): articulated skull and mandible with deciduous and unerupted premolars, and partial skeleton in matrix, including vertebrae, distal humerus, left femur, ?metatarsals

USNM 495155 (formerly USGS 25115), *Palaeictops* sp. (D-1517, ca. 400-500 m): partial skull, right maxilla and dentary, distal ulna and radius, phalanx, pelvic fragments, proximal femur, distal femora, proximal right tibia, distal tibiofibulae, vertebrae

Leptictidae (indeterminate or unassigned)

UM 66021 (Y-45S, 470 m): most of both femora, right tibiofibula, proximal left tibia, right ilium, a few vertebrae

USNM 491972 (D-1827, ca. 350-400 m?): associated hind limb elements including ilia, proximal right femur, distal femora, proximal and distal right tibia, most of left tibiofibula

USNM 491973 (D-1781, 556 m): associated bones including right scapula, distal left humerus, complete right femur, distal left femur, proximal left tibia

USNM 495151 (formerly USGS 26496) (locality D-1198=Y-45, 470 m): crushed skull with associated bones in matrix, including partial right humerus articulated with radius and

ulna, incomplete right femur and tibiofibula, astragalus, metapodials, phalanx, ribs

PANTOLESTA

Palaeosinopa

USGS 25138, cf. *P. didelphoides* (D-1873, m-level uncertain, probably 150-200 m): dentaries, proximal ulna, astragalus, and associated fragments

USNM 495265, *Palaeosinopa* sp. (D-1762Q, 414m): astragalus and calcaneus

PALAEANODONTA

Palaeanodon

UM 87335, *P. nievelti* (SC-67, Wa-0): braincase, dentary, humerus, proximal ulna, vertebrae, sacrum

USNM 495066, cf. *P. nievelti* (Y-104, 140 m): dentary, distal humerus, metacarpals, phalanx

UCM 75161, *P. ignavus* (locality unknown): scapulae, proximal humeri, mc III, distal femur, partial tibiae, astragalus

USGS 21876, *P. ignavus* (D-1776, 463 m): braincase, dentaries, and partial skeleton including scapula, humeri, radii, ulna, mc III, pelvis, proximal femur, distal tibia and fibula, phalanges, vertebrae, sacrum

USGS 25087, *P. ignavus* subadult (D-1538, 405 m): dentary, partial scapula, humerus, and ulna, femur, calcaneus

USGS 25106, *P. ignavus* (D-1421, 380 m): proximal humerus, proximal and distal femur, distal tibia

USGS 25160, *P. ignavus* (D-1964, 370 m): partial humerus and ulna, proximal and distal femur, distal tibia and fibula, vertebrae, sacrum

USGS 25260, *P. ignavus* (D-1779, 412 m): fragments of femur, radius, and ulna, mc III, vertebrae

USGS 25315, *P. ignavus* (D-1946, 422 m): radius, ulna, ungual phalanx, partial femur, distal tibia

USGS 27233, *P. ignavus* (Y-350, 290 m): dentary, distal radius, phalanx, distal tibia, vertebrae

USGS 27605, *P. ignavus* (D-1514, 380 m): scapula, distal ulna, phalanx, proximal and distal tibia, astragalus

USGS 38072, *P. ignavus* (D-1454, 409 m): proximal radius, femur, distal tibiae, astragalus

USGS 38485, *P. ignavus* (Y-289, 280 m): partial humerus, pelvis, proximal and distal femur

USNM 495061, *P. ignavus* (Y-131, 346 m): partial pelvis and femur, distal tibiae, partial astragalus and calcaneus

USNM 510876, *P. ignavus* (D-1532, 485 m): pelvis, femur, metatarsal, vertebrae

USGS 21930, *Palaeanodon* sp. (D-1776, 463 m): partial humerus, proximal and distal femur, distal tibia, vertebrae, sacrum

Alocodontulum

UM 93740, *A. atopum* (MP-152, Wa-5): fragments of skull, dentaries, and nearly complete skeleton

- USGS 25093, *A. atopum* (D-1326, 425 m): partial pelvis, femur, and distal tibia
 USNM 487877, *A. atopum* (D-1782, 496 m): scapula, distal humeri, proximal ulna, pelvis, caudal vertebrae
 USNM 487881, *A. atopum* (D-1583, 551 m): distal femur, distal tibia, astragali, calcaneus
 USNM 491828, *A. atopum* (D-1782, 496 m): proximal humerus, metacarpals, phalanges
 USNM 491955, *A. atopum* (D-1382, 430 m): humerus, distal radius, distal femur, distal tibia, vertebrae
 USNM 495064, *A. atopum* (D-1334, 360 m): dentary, partial humerus, proximal and distal ulna, distal radius, ungual phalanx, pelvis, proximal femur, axis vertebra
 UCM 75175, *Alocodontulum* sp. (Y-420, ca. 350-400 m): distal radius, pelvis, femur, tibia, astragalus

TAENIODONTA

Ectoganus sp.

- USNM 487884 (Y-18B, 521 m): dentary and associated intermediate and ungual phalanges of manus

TILLODONTIA

Azygonyx

- UM 83874, *A. gunnelli* (SC-351, Wa-0): cranial fragments, dentaries, and upper teeth, proximal radius and ulna, carpals and tarsals including astragalus, calcaneus, navicular, and cuboid, metapodials and phalanges (Gingerich, 1989)
 UM 66616, *Azygonyx* sp. (SC-67, Wa-0): astragalus, calcaneus, navicular, phalanges (Gingerich, 1989)

Esthonyx bisulcatus

- USNM 487889 (D-1994, 482 m): dentaries, distal humerus, proximal radius, pelvis, femora, proximal tibia, distal fibula, phalanx, vertebrae
 USNM 490653 (Y-45S, 470 m): dentary, proximal humerus, proximal tibia, metapodials, vertebra
 USNM 510865 (D-1699, 463 m): dentaries, maxillae, and associated hind limbs including pelvis, proximal and distal femur and tibiae, distal fibula, calcaneus, vertebrae
 USNM 510880 (D-1782, 496 m): canine, carpals, fragments of metapodials and phalanges

PANTODONTA

Coryphodon sp.

- USGS 21887 (D-1767, 475 m): carpus and manus
 USGS 21892 (D-1537, 449 m): tarsals and metatarsals
 USGS 21936 (D-1429, 446 m): proximal radius, femur, proximal and distal tibia, distal fibula
 USGS 21946 (D-1778, 474 m): scapula, distal femur, tibia, fibula
 USGS 25286 (D-1800, ?m): proximal radius and carpals

- USGS 25287 (D-1824, 406 m): scapula, proximal and distal humerus, distal tibia, fibula
 USGS 27590 (D-1959, ?m): distal humerus, radius, ulnae, femur, patella, proximal tibia, astragali, phalanges
 USGS 38467 (D-2032, ?m): canine, proximal radius, carpals, patella, metapodials, phalanges, axis vertebra
 USGS 510893 (D-1797, ?m): distal humerus, distal femur, proximal and distal tibia, calcaneus
 USGS 510894 (D-1693, 438 m): dentary fragment, proximal ulnae, distal femur, distal tibia, calcaneus
 USGS 510895 (D-1427, ?m): dentary fragments, distal humerus, radius, ulna, pelvis, tibia
 USGS 510896 (D-1454, 409 m): distal humeri, ulnae, proximal radius, pelvic fragment, proximal and distal femur and tibiae
 USGS 510897 (WW-58, ?m): pelvic fragments, distal femur, proximal and distal tibia, calcaneus, astragalus, phalanges

CREODONTA

Hyaenodontidae

Arfia

- UM 69474, *A. shoshoniensis* (SC-207, Wa-2): humeri, pelvis, proximal and distal femur, patella, tibia, astragali, calcaneus, partial metapodials, vertebrae

Pyrocyon

- UM 94757, *P. dioctetus* (MP-193, Wa-5): maxilla, dentary, humerus and other parts of fore and hind limbs, vertebrae
 USGS 27236, *Pyrocyon* sp. (D-1960, ca. 400-450 m): skull and dentaries, humeri, proximal radii, distal tibiae and fibula, calcanei, astragalus, partial metapodial

Prototomus

- [Note: The four specimens attributed to *Prototomus* by Rose (1990)—USGS 1824, 6111, 7157, and 16475—are here considered to represent either *Tritemnodon* or *Pyrocyon*.]
 USNM 509700, cf. *P. martis* (Y-290, 210 m): dentary, humeral fragments, femur, distal tibia and fibula, astragalus, cuboid, ungual phalanx, vertebrae
 USGS 25296, *P. secundarius* (D-1595, probably >500 m): dentaries and maxilla, and most of the skeleton, including scapulae, humeri, ulna, proximal and distal radius, carpals, pelves, femur, tibia, fibula, tarsals, metapodials, phalanges, and most of vertebral column
 USNM 510864, *P. secundarius?* (D-1160, 470 m): dentary, humerus, proximal ulna
 USGS 25021, *Prototomus* sp. (D-1691, ca. 380 m): dentary and maxilla, proximal humerus, proximal radius and ulna, proximal and distal femur, proximal and distal tibia, vertebrae
 USGS 25128, *Prototomus* sp.? (D-1866, 423 m): dentary and maxilla, scapula, proximal ulna, pelvis, proximal and distal femur, metapodials, vertebrae

- USGS 25275, *Prototomus* sp. (Y-81, 360 m): dentary and maxilla, distal humeri, pelvic fragment, proximal femora
 USGS 38460, *Prototomus* sp.? (D-2004, 336 m): tooth, partial ulna, proximal femur, distal tibia and fibula, calcaneus, cuboid, metapodials, phalanges
 USNM 510870, *Prototomus* sp. (D-1204, 438-444 m): maxillae, proximal femur, ulnae

Galecyon sp.

- USNM 487920 (Y-314, 511 m): dentaries and maxilla, scapula, distal humerus, proximal ulna, proximal femur, distal tibia

Prolimmocyon

- DPC 5364, *P. atavus* (D-1601, ?m): partial skull and dentaries and most of a skeleton, including scapulae, humeri, radii, proximal and distal ulnae, pelves, femora, tibiae, partial fibula and astragalus, calcanei, cuboid, fragmentary metapodials and phalanges, most of vertebral column
 USGS 25056, *P. atavus* (D-1676, 464 m): dentaries and proximal radius

Oxyaenidae

Oxyaena

- UM 64037, *O. forcipata* (Y-420, ca. 350-400 m): dentary, hind limb elements, ribs, vertebrae (Gunnell and Gingerich, 1991)
 UM 94269, *O. forcipata* (MP-173, Wa-5): dentaries, humeri, radii, ulna, carpals, ribs (Gunnell and Gingerich, 1991)
 USGS 25278, *O. gulo* (D-1843, 528 m): jaw fragments, proximal humerus, distal radius, pelvis, proximal and distal femur, patella, distal tibiae, partial calcanei, vertebrae
 USGS 25386, *Oxyaena* sp. (D-1946, 422 m): ulna, radius, carpus, metapodials, phalanges, proximal tibia, fibula, calcaneus, vertebrae
 USNM 510881, *Oxyaena* sp. (D-1583, 551 m): canine, proximal and distal radius, carpals, metapodials, phalanges

Dipsalidictis

- UM 66137, *D. platypus* (SC-67, Wa-0): dentary and maxilla, calcanei, astragali, and pedal elements including ungual phalanges (Gingerich, 1989)

CARNIVORA

Miacidae

Miacis

- USGS 25171, *Miacis petilus* (D-1204, 438-444 m): scapula, proximal and distal humerus, femur, and tibia, vertebrae
 USGS 27584, *Miacis* sp. (Y-175, 531 m): humerus, proximal ulna, proximal and distal radius, proximal tibia, distal fibula, calcaneus, astragalus, vertebrae (2 individuals)

Uintacyon sp.

- USGS 27586 (D-1672, 495 m): maxilla, proximal ulna, proximal femora, proximal and distal tibia, calcaneus, vertebrae

Vulpavus

- USGS 16491, *Vulpavus* sp.? (D-1534, 536 m): scapula, proximal ulna, distal femur, proximal and distal tibiae, metapodials, phalanx, vertebrae
 USGS 25186, *Vulpavus australis* (D-1473, 556 m): scapula, proximal ulna, proximal femur, distal tibia, cuboid, metapodials, vertebrae
 USGS 25219, *Vulpavus* sp. (D-1828, 546 m): proximal and distal humerus, distal radius, proximal femur, vertebrae
 USGS 25330, *Vulpavus* sp. (D-1310, 442 m): dentary, scapula, proximal humerus, proximal and distal femur, proximal tibiae, calcanei, astragali, articulated metapodials, vertebrae
 USNM 510879, *Vulpavus* sp.? (D-1686, 591 m): scapula, proximal radius, pelvic fragment, distal tibiae, calcaneus, astragalus, metapodial fragments
 USNM 510891, *Vulpavus* sp. (D-1174, 501 m): maxilla, dentary fragments, distal humerus, distal radius, femoral fragments, proximal and distal tibiae, distal fibula, astragalus, vertebrae

Viverravidae

Didymictis

- USGS 21928, *D. protenus* (D-1799, ?m): dentary fragments, humerus, pelvic fragments, proximal femur, proximal tibia
 USGS 25038, *D. protenus* (D-1843, 528 m): dentary fragments, scapula, proximal humerus, proximal and distal femur, proximal tibia, articulated partial tarsus and pes, vertebrae
 USGS 25039, *D. protenus* (D-1833, 463 m): dentaries and maxillae, humerus, proximal and distal ulna, distal radii, scaphoid, femora, proximal and distal tibia, distal fibula, cuboid, metapodials, vertebrae
 USGS 25040, *D. protenus* (D-1737, 463-469 m): partial skull and dentaries, humeri, proximal and distal radii, proximal ulnae, articulated partial carpus and manus, femur, proximal tibia
 USGS 25117, *D. protenus* (D-1517, ?m): maxilla, partial humerus, proximal ulna, partial femur, proximal tibia, vertebrae
 USGS 25144, *D. protenus* (D-1341, 384 m): dentary, distal humerus, proximal ulna and radius, calcaneus
 USGS 25195, *D. protenus* (D-1694, 435 m): proximal humerus, proximal radius, pelvis, proximal femur, distal tibia, astragalus, vertebrae
 USGS 25258, *D. protenus* (D-1845, ca. 450-500 m): proximal humerus, proximal and distal femur and tibia, vertebrae
 USGS 27585, *D. protenus* (D-1994, 482 m): dentary, scapula, proximal and distal humeri and radius, proximal and distal femur and tibiae, astragali, cuboid, metapodials, phalanges, vertebrae

LIPOTYPHLA

?*Macrocranium* sp.

- USNM 491971 (D-2035Q, 397 m), tibiofibula
 USNM 495051 (D-2035Q, 397 m), tibiofibula

PRIMATES

Plesiadapiformes

Phenacolemur

- UM 66440 and UM 86352, *P. praecox* (SC-46, Wa-2): dentaries, proximal ulna, pelvic fragments, femur, calcanei, astragalus, cuboids, metapodials, phalanges, vertebrae (believed to belong to one individual according to Beard, 1989, 1990)
 USGS 17847, cf. *P. jepseni* (D-1651, 636 m): dentaries, upper teeth, fragments of scapula, distal humerus, proximal radii, proximal and distal ulna, triquetrum, proximal first metacarpal, pelvic fragments, proximal and distal femora, proximal tibia, proximal and distal fibula, tarsals, metapodials, and phalanges

Euprimates

Cantius

- USGS 25029, *C. mckennai* (D-1872, 213 m): associated foot skeleton including calcanei, astragalus, navicular, metapodials

CONDYLARTHRA

Arctocyoniidae

Chriacus sp.

- USGS 21907 (D-1785, ca. 400-450 m): proximal and distal humeri, femur, proximal tibia, distal fibula, calcaneus, vertebrae
 USGS 21918 (D-1789, ca. 500 m): maxilla, scapula, distal humerus, proximal radius, proximal tibia, vertebrae
 USGS 25113 (D-1545, 430 m): proximal and distal humerus, distal tibia, calcaneus, astragalus, phalanges, vertebrae
 USGS 25118 (D-1326, 425 m): partial humerus, ulna, and tibia, pelvis, calcaneus, astragalus
 USGS 25163 (D-1833, 463 m): humeri, proximal radius and ulna, pelvis, distal femur, distal tibiae, calcaneus, astragalus, ungual phalanx, vertebrae
 USGS 25221 (D-1833, 463 m): molar, humerus, ulna, tarsals

Anacodon

- USGS 25034 (D-1833, 463 m): dentary and maxilla, ulna, tibia, nearly complete tarsus and pedal skeleton, vertebrae
 USNM 487950 (WW-12, 417 m): partial skull and mandible, and nearly complete skeleton (two individuals)
 USNM 495292 (D-1699, 463 m): maxillae, partial humerus, radius, ulna, pelvis, femur, tibiae
 Phenacodontidae

Phenacodus

- UM 82241, *P. trilobatus* (SC-54, Wa-2): partial skeleton (Thewissen, 1990)
 UM 94050, *P. trilobatus* (MP-166, Wa-5): partial skeleton (Thewissen, 1990)

- UM 94232, *P. trilobatus* (MP-172, Wa-5): partial skeleton (Thewissen, 1990)
 UM 94330, *P. trilobatus* (MP-175, Wa-4): partial skeleton (Thewissen, 1990)
 USGS 9135, *P. trilobatus* (D-1427, ?m): dentary, fragments of scapula, humerus, and ulna, proximal radius, pelvis, proximal tibia, metapodials
 USGS 25169, *P. trilobatus* (D-1955, ?m): dentary, humeri, carpals, metapodials, phalanges, distal tibiae and fibula, calcaneus, astragalus, vertebrae
 USGS 25295, *P. trilobatus* (D-1924, 357 m): articulated vertebral column, pelvis, and hind limbs
 USGS 27589, *P. trilobatus* (D-1460, 409 m): dentary, pelvis, vertebrae
 USNM 494926, *P. trilobatus* (D-2037Q, 347m): dentaries, maxillae, scapulae, fragments of humerus, ulna, carpals, metapodials, phalanges, calcaneus (>1 individual)
 USNM 510866, *P. trilobatus* (WW-59, ?m): fragments of dentary, maxillae, and most of skeleton
 USNM 510867, *P. trilobatus* (WW-60, ?m): dP4 and manus skeleton
 USNM 510868, *P. trilobatus* (D-1872, 213 m): fragments of distal humerus, proximal ulna, femur, metapodials, phalanges, vertebrae
 USGS 25036, *P. intermedius* (D-1228, 81 m): distal tibia and astragalus
 USGS 27595, *P. intermedius* (D-2038, ?m): pedal skeleton
 USNM 510874, *P. intermedius* (D-1447, 113 m): scapula, proximal ulna and radius, distal femur, distal tibia, calcaneus, vertebrae
 UM 75286, *P. vortmani* (GR-9, Wa-5): partial skeleton (Thewissen, 1990)
 USGS 813, *P. vortmani* (D-1160, 470 m): dentaries, scapula, proximal humeri, femur, vertebrae
 USGS 21878, *P. vortmani* (D-1799, ?m): fragments of dentary and maxilla, scapulae, proximal and distal radius, partial ulna, distal tibia and fibula, astragalus, metapodials, phalanges
 USGS 21929, *P. vortmani* (D-1785, ca. 400-450m): dentaries, maxilla, proximal femur, proximal tibia, calcaneus, phalanges, vertebrae
 USGS 25023, *P. vortmani* (D-1588, 442 m): dentary, maxillae, scapulae, ulna, proximal tibia, metapodials, phalanges
 USGS 25299, *P. vortmani* (D-1934, ca. 480 m): proximal and distal radius, distal fibula, calcaneus, cuboid, metapodials, phalanges
 USNM 487929, *P. vortmani* (D-1983, 488 m): distal humerus, distal tibia and fibula and articulated tarsus
 USNM 491806, *P. vortmani* (D-1754, 511 m): femur, distal tibia, calcaneus, astragalus, fragments of metapodials, vertebrae

Copecion

- USGS 38074, *C. davisi* (D-2018, -20 m [Wa-0]): maxilla, scapula, humerus, ulna, radius, femur, tibia, tarsals, phalanges, and articulated section of vertebral column with ribs and pelvis

UM 64179, *C. brachypternus* (Y-421, 390 m): dentaries, scapula, humeri, proximal radius and ulnae, femur, patella, tibiae, proximal fibula, tarsals, metapodials, phalanx, vertebrae including sacrum (Thewissen, 1990)

USGS 25302, *C. brachypternus* (D-1206, 438 m): proximal humerus, distal tibiae, calcaneus, metapodials, vertebrae

Ectocion

UM 83100, *E. osbornianus* (SC-210, Wa-1): teeth, proximal humerus, proximal radius, proximal and distal ulna, pelvic fragments, proximal and distal femur, tibia, calcaneus, phalanges (Thewissen, 1990)

MESONYCHIA

Pachyaena

USNM 14915, *P. gigantea* ("Upper Graybull beds, 5 miles south of Otto"): mandible, nearly complete forelimbs, pelvis, vertebrae

USGS 25280, *P. gracilis* (D-1798, ca. 400±50 m): partial humerus, radius, ulna, femur, tibia, fibula, tarsus, pes, vertebrae, sternebrae, and ribs

USGS 27587, cf. *P. gracilis* (D-1454, 409 m): canine fragments, proximal and distal humeri, distal radius, distal femur, proximal tibiae, cuboid, metapodial fragments, ungual phalanx, vertebrae

UM 94783, *P. ossifraga* (MP-195, zone unknown): skull, limbs, vertebrae (Zhou et al., 1992)

UM 95074, *P. ossifraga* (MP-201, Wa-3): teeth, limb elements, and nearly complete vertebral column (Zhou et al., 1992)

USGS 21945, *P. ossifraga* (D-1411, 412 m), edentulous mandible, proximal humeri, vertebrae

USGS 25292, *P. ossifraga* (D-1924, 357 m): teeth and dentary fragments, scapulae, humeri, radius, ulna, carpals, femora, tibiae, nearly complete tarsi, metapodials, phalanges, vertebrae, ribs

USNM 491807, *P. ossifraga* (D-2049, ca. 180 m): partial dentary, distal radius, pisiform, tarsus, phalanges, vertebrae

YPM-PU 14708, *P. ossifraga* (locality uncertain): lower dentition, pelvis, limbs, carpals, tarsals, vertebral column, sacrum (Zhou et al., 1992)

ARTIODACTYLA

Diacodexis

USGS 25251, *D. metsiacus* (D-1829, 501 m): femur, tibia, calcaneus, astragalus

Bunophorus

USNM 510877, cf. *B. grangeri* (D-1965, ca. 560m): distal tibia, calcaneus, astragalus

USGS 25266, *B. macropternus* (Y-185, 531 m): dentaries and maxilla, pelvis, proximal tibia, calcaneus, astragali

PERISSODACTYLA

Hyracotherium

UM 79889, *H. sandrae* (SC-67, Wa-0): dentaries, maxillae, and partial skeleton including partial scapula, humeri,

proximal radii and ulnae, femora, tibiae, astragalus, calcaneus, metapodial fragments, phalanx, vertebrae

USGS 25140, cf. *H. sandrae* (D-1888, 3m): teeth, fragments of ulna and pelvis, astragalus, vertebrae

USGS 21877, *Hyracotherium* sp. (D-1693, 438 m): dentaries, proximal radius and ulna, pelvis, astragalus, calcaneus

USGS 21926, *Hyracotherium* sp. (D-1766, ?m): dentaries, pelvic fragments, femur, distal tibia, vertebrae

USGS 21977, *Hyracotherium* sp. (D-1708, ca. 500-600 m): pelvic fragments, tibia, calcaneus, cuboid

USGS 25255, *Hyracotherium* sp. (D-1842, ca. 400-500 m): dentary, distal humerus, proximal femur, distal tibia, astragalus, vertebrae

USNM 487873, *Hyracotherium* sp. (D-1936, 463 m): dentaries, maxillae, proximal and distal humerus, proximal and distal radius and ulna, pelvic fragments, distal femora, distal tibiae, metapodials, vertebrae including axis and sacrum (≥2 individuals)

USNM 510883, *Hyracotherium* sp. (D-1454, 409 m): distal humerus, proximal ulna, partial femora, tibiae, sacrum

Cardiolphus

UM 80318, *C. radinskyi*? (SC-2, Wa-2): distal tibia, calcaneus, astragalus, phalanges

Homogalax

UM 87027, *H. protapirinus* (FG-091, zone unknown): palate and jaw fragments, humeri, proximal ulna, proximal and distal radius, most of manus, femur, proximal and distal tibia, pedal fragments, vertebrae

USGS 25032, *H. protapirinus* (D-1838, 400-500 m): maxillae and premaxillae, complete mandible, humeri, pelvis, femur, tibia, patella, distal fibula, nearly complete tarsus, metatarsals, phalanges, vertebrae

USNM 510882, *H. protapirinus* (D-1641, ca. 450-500 m): maxillae, dentary, distal humerus, distal femur

UM 90987, *Homogalax* sp. (SC-128, Wa-3): fragments of humerus, ulna, radius, femur, calcaneus, astragalus

USGS 21913, *Homogalax* sp. (D-1407, 442 m): scapula, distal humerus, proximal and distal radius, proximal ulna

USGS 21958, *Homogalax* sp. (D-1931, 315 m): tibia, calcaneus, astragalus

USGS 38040, *Homogalax* sp. (D-1577, 311 m): proximal tibia, astragalus, cuboid, distal metapodials

Heptodon sp.

USGS 25149 (D-1477, ca. 500-600 m): distal tibia and fibula, calcaneus, navicular, metapodial

USGS 25158 (D-1534, 536 m): scapula, proximal radius and ulna

USGS 25252 (D-1833, 463 m): tibia, distal fibula, calcaneus, astragalus

USGS 25269 (D-1814, ca. 500-600 m): femur, distal fibula, navicular, metapodials

USGS 25333 (D-1940, ?m): scapula, distal humerus, proximal ulna, pelvis, proximal tibia, astragalus, vertebrae, sacrum

USGS 38469 (D-1214, ca. 450-550m): scapula, distal humerus, femur, tibia, calcaneus, astragalus, metapodial

USNM 510878 (D-2056, 531 m): lower molars, distal humerus, proximal radius

Unidentified Perissodactyl

USGS 25308 (D-1943, ?m): distal tibia, astragalus, metatarsals

RODENTIA

Paramys

USNM 491852, *P. copei* (D-1528, 414 m): dentary, proximal ulna, pelvic and femoral fragments, distal tibia

USNM 491869, *P. copei* (D-1862, ?m): dentaries, ischium, femoral heads, astragalus, caudal vertebrae

USNM 491966, *P. copei* (D-1690, ca. 350-450 m): proximal and distal humerus, proximal and distal tibia, metapodial fragments, vertebrae (2 individuals)

USNM 509702, *P. copei* (-1686, 591 m): edentulous dentary, pelvic fragment, distal femur, proximal and distal tibia, calcanei, astragalus, navicular, vertebrae

USNM 491861, cf. *P. copei* (D-1473, 556 m): dentary, premaxillae, maxilla, distal femur, cuboid, metapodial fragments, vertebrae

USNM 491853, *P. taurus* (D-1830, 501 m): distal humerus, distal tibiae, astragalus

USNM 491855, *P. taurus* (D-1454, 409 m): maxilla, pelvic fragments, proximal and distal femora, proximal and distal tibiae, calcaneus, sacrum

USNM 491862, *P. taurus* (D-1893, ca. 400-450 m): dentary, proximal and distal humerus, proximal ulna, pelvic fragments, proximal femur, proximal tibiae, calcaneus, cuboid, vertebrae

USNM 491866, *P. taurus* (D-1699, 463 m): edentulous dentaries, proximal tibia, calcaneus

USNM 491963, *P. taurus* (D-1507, 494 m): dentary, maxillae, proximal humerus, proximal and distal femur, proximal tibia, calcaneus, vertebrae

USNM 491854, cf. *P. wortmani* (D-1799, ca. 400-500m): teeth, distal tibia, astragalus

USNM 491864, cf. *P. wortmani* (D-1951, 402 m): dentary, proximal ulna, pelvic and femoral fragments, distal tibia, calcaneus

USNM 491868, cf. *P. wortmani* (D-1558L, 556 m): distal tibia, astragalus

USNM 491961, cf. *P. wortmani* (D-1311, 442 m): dentaries, proximal ulna, proximal femora, distal tibiae, calcaneus

USNM 487893, *Paramys* sp. (Y-18B, 521 m): edentulous dentaries, proximal and distal humerus, distal radius, pelvic fragments, proximal and distal femur, proximal tibia, vertebrae

USNM 491859, *Paramys* sp. (D-1341, 384 m): edentulous dentary, proximal femur, distal tibia, astragalus, vertebrae

USNM 491860, *Paramys* sp. (D-1206, 438 m): proximal and distal humerus, proximal ulna, pelvic fragments, femoral head, distal femur, distal tibia

USNM 491871, *Paramys* sp. (Y-18B, 521 m): edentulous dentaries, premaxillae, scapula, proximal and distal humerus, proximal and distal femur, proximal and distal tibia, calcaneal fragments, vertebrae

USNM 491957, *Paramys* sp. (Y-192S, 546 m): upper molar, proximal humerus, distal femur, distal tibia, vertebrae

USNM 491968, *Paramys* sp. (D-1571, 435 m): edentulous dentaries and maxilla, premaxillae, proximal and distal humerus, pelvic fragment, proximal and distal femur, proximal tibia, vertebrae

USNM 491969, *Paramys* sp. (D-1992, 492 m): upper molars, pelvis, proximal and distal femur, proximal and distal tibia, distal fibula

USNM 491970, *Paramys* sp. (D-1415, 354 m): partial humeri, questionably associated proximal radius, pelvic fragments, partial femur

cf. *Thisbemys* sp.

USNM 491965 (D-1625, 516 m): partial skull, dentary, pelvic fragment, femur, distal tibia

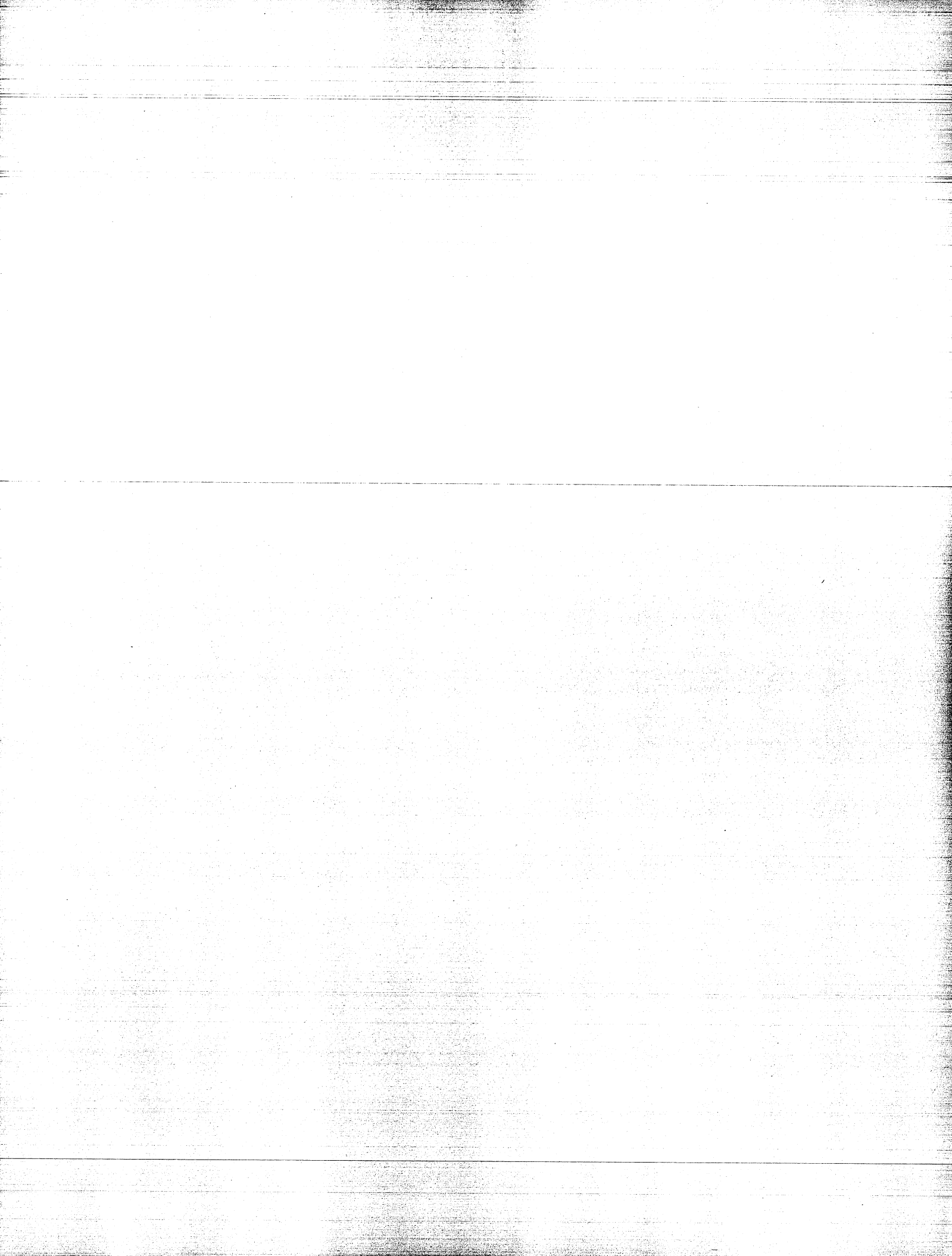
cf. *Leptotomus* sp.

USNM 491863 (D-1605, 478 m): dentary fragment, proximal humerus, femoral fragments, distal tibia, partial astragalus, calcaneus, and metapodials, vertebrae

USNM 491959 (D-1829, 501 m): dentary, proximal humerus, proximal tibia, calcaneus, astragalus

Knightomys sp.

USNM 509716 (D-1460Q, 411 m): distal tibia



TAPHONOMY OF SMALL MAMMALS IN FRESHWATER LIMESTONES FROM THE PALEOCENE OF THE CLARKS FORK BASIN

JONATHAN I. BLOCH and DOUG M. BOYER

Department of Geological Sciences and Museum of Paleontology, The University of Michigan, Ann Arbor, MI 48109-1079

Abstract.— Freshwater limestones in the Fort Union and Willwood formations of the Clarks Fork Basin, Wyoming, preserve unusually complete skeletons of Paleocene and early Eocene micromammals. Here we describe a method of documenting postcranial-dental associations and apply this to skeletons removed from two blocks of limestone from the Clarkforkian land-mammal age (late Paleocene). One block from the middle Clarkforkian (Cf-2) yielded a total of 414 identifiable mammal bones from skeletons of 13 individuals (skeletons range from ca. 1 to 52% complete). These were found in two distinct layers within the limestone. A second block from the late Clarkforkian (Cf-3), as yet only partially prepared, has yielded 11 individuals (ca. 80 to 100% complete). Skeletal-element frequencies in the limestones are close to those expected for a generalized mammal, indicating that each individual entered the assemblage as an articulated partial or complete skeleton. Limestones accumulated in depressions on a Paleocene floodplain, and it is likely that these acted as natural pit-traps. Predation and normal attritional processes contributed bone to each assemblage as well. Results to date include: (1) the most complete paromomyid skeleton yet discovered, (2) the only known carpolestid skeleton, (3) the only known nyctitheriid skeleton, and (4) the earliest known rodent skeleton from North America. A diversity of mammals, many new, has been documented from Clarkforkian and Wasatchian limestones. Rigorous sampling of small mammals from this rarely-sampled habitat is resulting in range extensions. These include: (1) the earliest occurrences of *Tinimomys* (Cf-1) and *Batodonoides* (Wa-4), and (2) the latest occurrences of *Alagomys* (Wa-4), *Wyonycteris* (Wa-4), and *Plesiadapis gingerichi* (Cf-2).

INTRODUCTION

The Bighorn Basin and contiguous Clarks Fork Basin of northwestern Wyoming have been, for the past 120 years, among the most important areas for recovering Paleogene vertebrate fossils and for studying late Paleocene and early Eocene mammalian evolution. Fossils preserved in fluvial sediments of the Fort Union and Willwood formations document a radiation of archaic mammals; presence of the extant orders Marsupialia, Carnivora, and Lipotyphla in the Paleocene; and the first appearance of Rodentia in North America in the late Paleocene (Rose, 1981). They further document the earliest records of

In: Paleocene-Eocene Stratigraphy and Biotic Change in the Bighorn and Clarks Fork Basins, Wyoming (P. D. Gingerich, ed.), University of Michigan Papers on Paleontology, 33: 185-198 (2001).

Artiodactyla, hyaenodontid Creodonta, Perissodactyla, and Primates in the earliest Eocene (Gingerich, 1989).

In 1975, a partial dentary of a new species of the plesiadapiform *Carpolestes* was discovered in a late Paleocene freshwater limestone in the Willwood Formation of the Clarks Fork Basin (Gingerich, 1987; Bloch and Gingerich, 1998). Following this discovery, University of Michigan field parties have collected over 100 fossiliferous limestones from 30 localities in the Clarks Fork Basin (Figs. 1 and 2). The limestones occur as isolated masses within incipient and poorly developed paleosols (stages 0-1 of Bown and Kraus, 1987) and levee deposits of the Fort Union and Willwood Formations (Gingerich, 1987; Kraus, 1988). The limestones occur in local abundance at particular stratigraphic levels, where they form distinctive, laterally extensive bands (Fig. 3A). Limestones

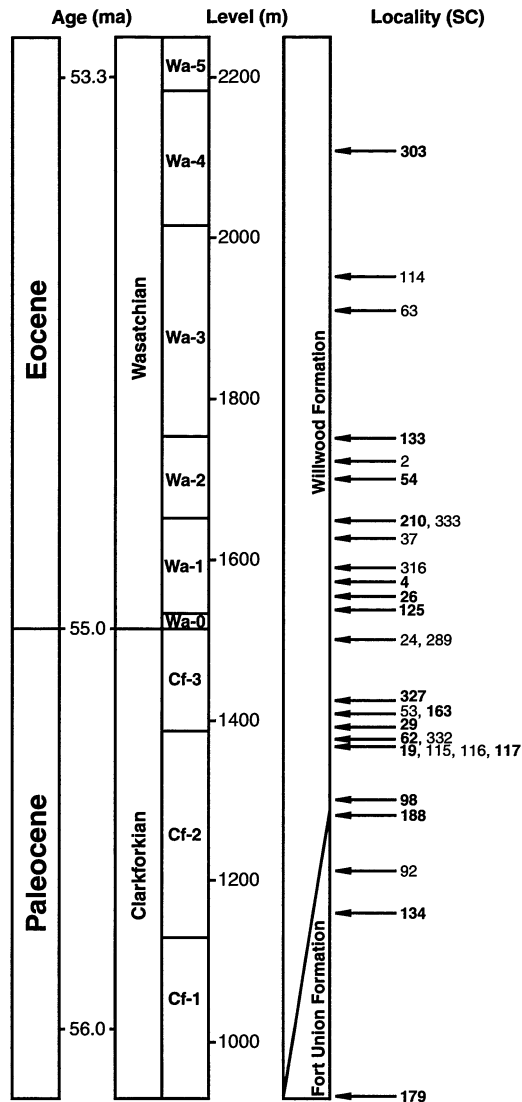


FIGURE 2 — Stratigraphic section in Clarks Fork Basin. Limestone-bearing localities are shown to the right of the section. Localities producing limestones sampled in this study are in bold type. The Fort Union-Willwood contact is gradational and occurs approximately at the top of the Cf-1 subdivision of the Clarkforkian North American Land Mammal Age. Ages are assigned to meter levels using paleomagnetic calibrations (55.9 mya and 53.4 mya) and the carbon isotope excursion at the Paleocene-Eocene boundary (model 1 of Wing et al., 1999). All limestone localities sampled here are within the Willwood Formation except SC-179 (Cf-1) which is in the Fort Union Formation. Other fossiliferous limestones from lower in the Fort Union (latest Tiffanian Land Mammal Age) are also known (Secord, personal communication) but are not included in this study. Figure modified from Bloch and Bowen (2001: fig. 2).

superimposed on avulsion-belt and overbank deposits (Bown and Kraus, 1981; Winkler, 1983; Bown and Beard, 1990;

Badgley et al., 1995), and on certain channel sandstone quarry deposits (e.g., Alexander, 1982; Bartels, 1987). Here we characterize the taphonomy of the limestone faunal assemblage and compare it to taphonomies previously described for paleosol and quarry deposits.

DOCUMENTING ASSOCIATION AND ARTICULATION

Limestones are usually chosen for study based upon surficial visibility of identifiable fossils, particularly teeth and skull fragments. Each limestone exhibits different degrees of bioturbation and related disarticulation of skeletons. Preparation of limestones with distinct bone horizons facilitates documentation of skeletal associations and in some cases recovery of articulated skeletons.

Once a limestone block has been selected, it is prepared such that it will be stable and maneuverable throughout the etching process. A single surface of the block is coated with a thin layer of epoxy. The surface should be roughly parallel to any bone horizons in the limestone, and have a minimal number of bones exposed. A minimum of three epoxy cylinders attached to this surface serve as 'legs' upon which the block will rest. If the block is less than 5 kilograms, holes drilled through the epoxy cylinders allow the block to be suspended from narrow rods or wire. The block is then etched by lowering it into a tub of dilute formic acid. Using this method, we can easily control the amount of limestone exposed to acid. Less limestone is exposed (the acid level is kept lower) when the bones are fairly concentrated in order to be able to remove bones in a sequential bottom-to-top process. Blocks larger than five kilograms are placed in a tub, resting on their 'legs,' and are submerged in acid. In this case, only by regulating the degree to which we coat the 'bottom' surface with epoxy can we control the amount of limestone exposed during the etching process.

For the most part, we follow the methods outlined by Rutzky et al. (1994) for use of organic acids to dissolve carbonate from bone. Exposed bone is coated with polyvinylacetate (PVA) to protect the bone against etching and breaking. Limestones are dissolved with 7% formic acid buffered with calcium phosphate tribasic. Each etching session lasts for 1 to 3 hours, and is followed by a rinse period of 2 to 6 hours. During rinsing, blocks are submerged in water that is constantly circulated and replenished. The blocks are then allowed to dry. Both acid and rinse water are strained through a fine-meshed screen to catch fossils. Once dry, the block is carefully examined under a dissecting microscope. Sediment and glue are scraped away and cleaned, using carbide picks and acetone. Newly exposed bone is again coated with PVA. Finally, any newly propagated fractures or fissures are filled with Paleobond® brand glue, which is resistant to acid and semi-resistant to acetone. At this point, the block is ready for another etching session.

Documentation of skeletal association occurs via preservation of articulation in some cases and by careful mapping of bone distributions in others. In cases where bones are articulated, we try to preserve articulation by gluing adjacent surfaces together as the bones are being exposed. Using this method to preserve associations and articulations for as long as

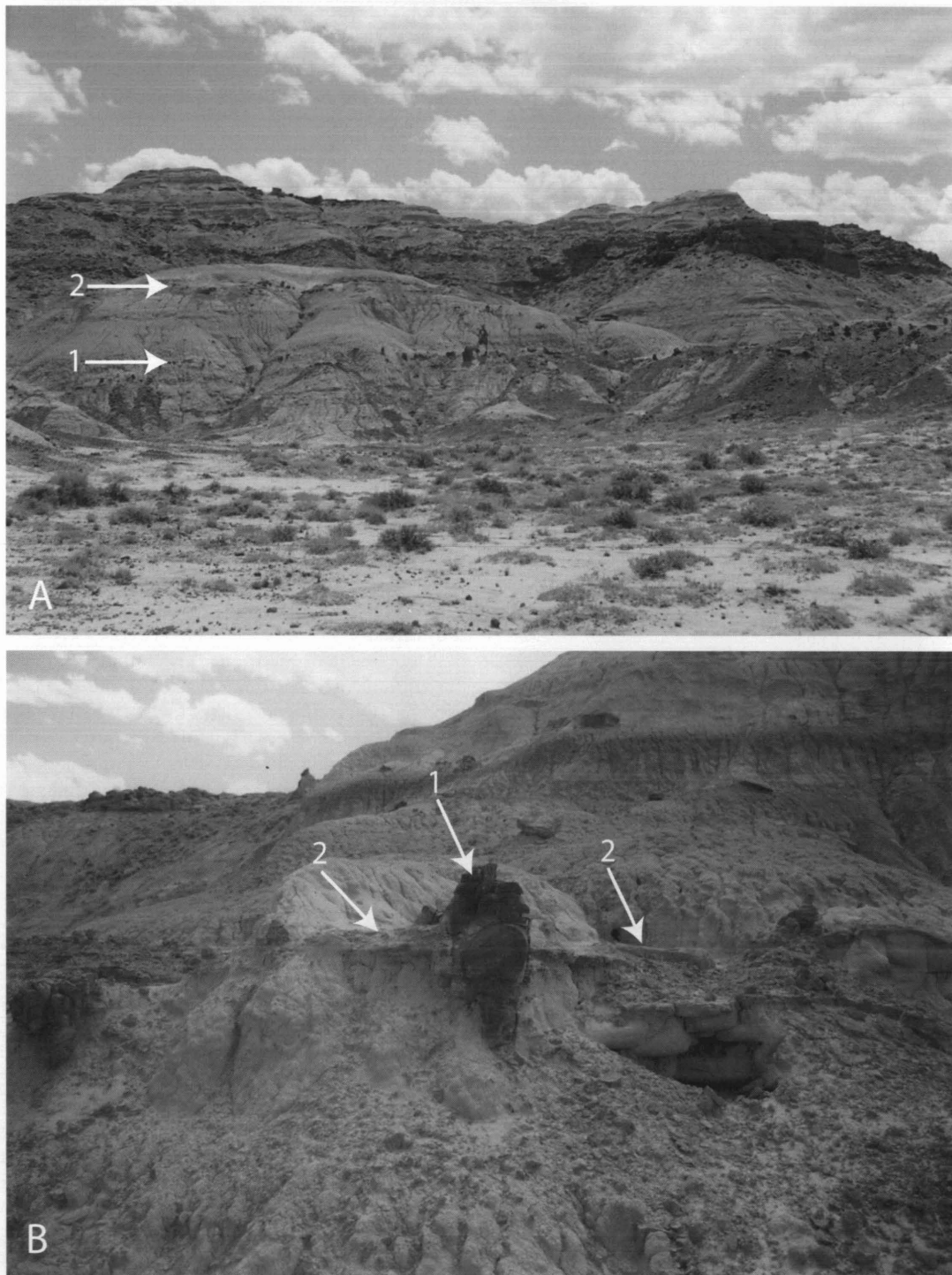


FIGURE 3 — Photograph of limestone-bearing locality SC-19 (Cf-2). A, landscape view. Numbered arrows indicate two distinct, laterally extensive, limestone layers at this locality. Collector in the middle of the photograph (at layer 1) for scale. B, cylindrical (type 1) and flat-lying (type 2) limestones from SC-29 (Cf-3). Note that both morphologies are found in direct association here. Hammer hanging on the right side of the type 1 limestone indicates scale.

Faunal Zone	Cf-1	Cf-2	Cf-2	Cf-2	Cf-2	Cf-2	Cf-2	Cf-3	Cf-3	Cf-3	Wa-0	Wa-1	Wa-1	Wa-1	Wa-1	Wa-2	Wa-2	Wa-3	Wa-4	
Sand Coulee Locality	179	134	188	98	19	117	62	29	163	327		125	26	4	210	54	133		303	
<i>Aphelsicus nitidus</i>	x																			
<i>Diacocherus n. sp.</i>	x																			
<i>Leptacodon rosei</i>	x				x	x	x	x		x				x	x		x			
<i>Neoliotomus conventus</i>	x																			
<i>Acritoparamys n. sp.</i>	x																			
<i>Peradectes protinnominatus</i>	x	x	x		x	x	x	x	x	x										
<i>Plesiadapis dubius</i>	x																			
<i>Tinimomys graybulliensis</i>	x					x	x	x		x			x	x	x					
<i>Ignacius n. sp.</i>		x				x	x													
<i>Plesiadapis cookei</i>			x	x	x	x														
<i>Plesiadapis gingrichi</i>					x															
<i>Arctostylops staini</i>					x															
<i>Chalicomomys n. sp.</i>					x					x										
<i>Chriacus n. sp.</i>					x															
<i>Paramys excavatus</i>					x															
<i>Worldia inusitata</i>					x			x												
<i>Wyonycteris chaix</i>					x			x												
<i>Carpolestes simpsoni</i>						x	x		x											
<i>Ectypodus powelli</i>						x		x												
<i>Haplomyilus simpsoni</i>						x														
<i>Leptacodon n. sp. A</i>						x	x							x						
<i>Microparamys cheradius</i>						x														x
<i>Prodiacodon sp.</i>						x								x						
<i>Thryptacodon antiquus</i>						x								x						x
<i>Uintacyon rudis</i>						x														
<i>Ceutholestes dolosus</i>							x													
<i>paramomyid n.gen.,n.sp.</i>							x													
<i>cf. Leptacodon sp.</i>							x		x											
<i>Palaoryctes punctatus</i>							x													
<i>Paramys sp.A</i>							x		x	x										
<i>Paramys sp.B</i>							x													
<i>Paramys sp.C</i>							x													
<i>Cf. Plagioctenodon krausae</i>							x													
<i>Erinaceomorph n.gen.,n.sp.</i>								x												
<i>Ectocion osbornianus</i>								x												
<i>Cf. Icaronycteris sp.</i>								x												
<i>Limaconyssus habrus</i>								x												
<i>Macrocranium n. sp.</i>								x												
<i>Viverravus acutus</i>								x						x	x					
<i>Wyonycteris n. sp. A</i>								x						x						
<i>Didymictis sp.</i>									x											
<i>Phenacodus sp.</i>									x											
<i>Labidolemur kayi</i>										x					x					
<i>Prolimnocyon sp.</i>										x										
<i>Viverravus rosei</i>										x										x
<i>Ignacius graybullianus</i>												x		x			x			
<i>Peradectes chesteri</i>												x		x	x	x	x			
<i>Acarictis ryani</i>														x						
<i>Haplomyilus speirianus</i>														x						
<i>Hyopsodus latidens</i>														x	x					
<i>Chalicomomys antelucanus</i>														x						
<i>Niptomomys doreanae</i>														x	x					
<i>Acritoparamys atwateri</i>														x						
<i>Paramys taurus</i>														x						x
<i>Phenacolemur simonsi</i>														x						
<i>Plagiomene cf. P. accola</i>														x						
<i>Ectypodus tardus</i>														x						
<i>Hyracotherium grangeri</i>															x		x			
<i>Phenacolemur praecox</i>															x					
<i>Diacodexis metsiacus</i>															x		x			
<i>Prototomus phobos</i>																x				
<i>Aphelsicus insidiosus</i>																		x		x
<i>Arctodontomys wilsoni</i>																		x		x
<i>Cantius</i>																		x		x
<i>Centetodon</i>																		x		x
<i>Mimoperadectes n. sp.</i>																		x		x
<i>Microparamys hunterae</i>																		x		x
<i>Prototomus deimos</i>																		x		x
<i>Uintacyon sp.</i>																		x		x
<i>Alagomys n.sp.</i>																				x
<i>Batodonoides vanhouteni</i>																				x
<i>cf. Reithroparamys</i>																				x
<i>Leptacodon n. sp. B</i>																				x
<i>Leptacodon n. sp. C</i>																				x
<i>Leptacodon n. sp. D</i>																				x
<i>Leptacodon n. sp. E</i>																				x
<i>Leptacodon n. sp. F</i>																				x
<i>Macrocranium nitens</i>																				x
<i>Palaoryctes sp.</i>																				x
<i>Peratherium sp.</i>																				x
<i>Plagioctenodon n. sp.</i>																				x
<i>Wyonycteris n. sp. B</i>																				x
<i>Wyonycteris n. sp. C</i>																				x
<i>small multituberculate</i>																				x

FIGURE 4 — Mammalian faunas from Clarkforkian and early Wasatchian limestones. Presence in a limestone is indicated by x. Shading marks intervals where fossiliferous limestones have not been found.

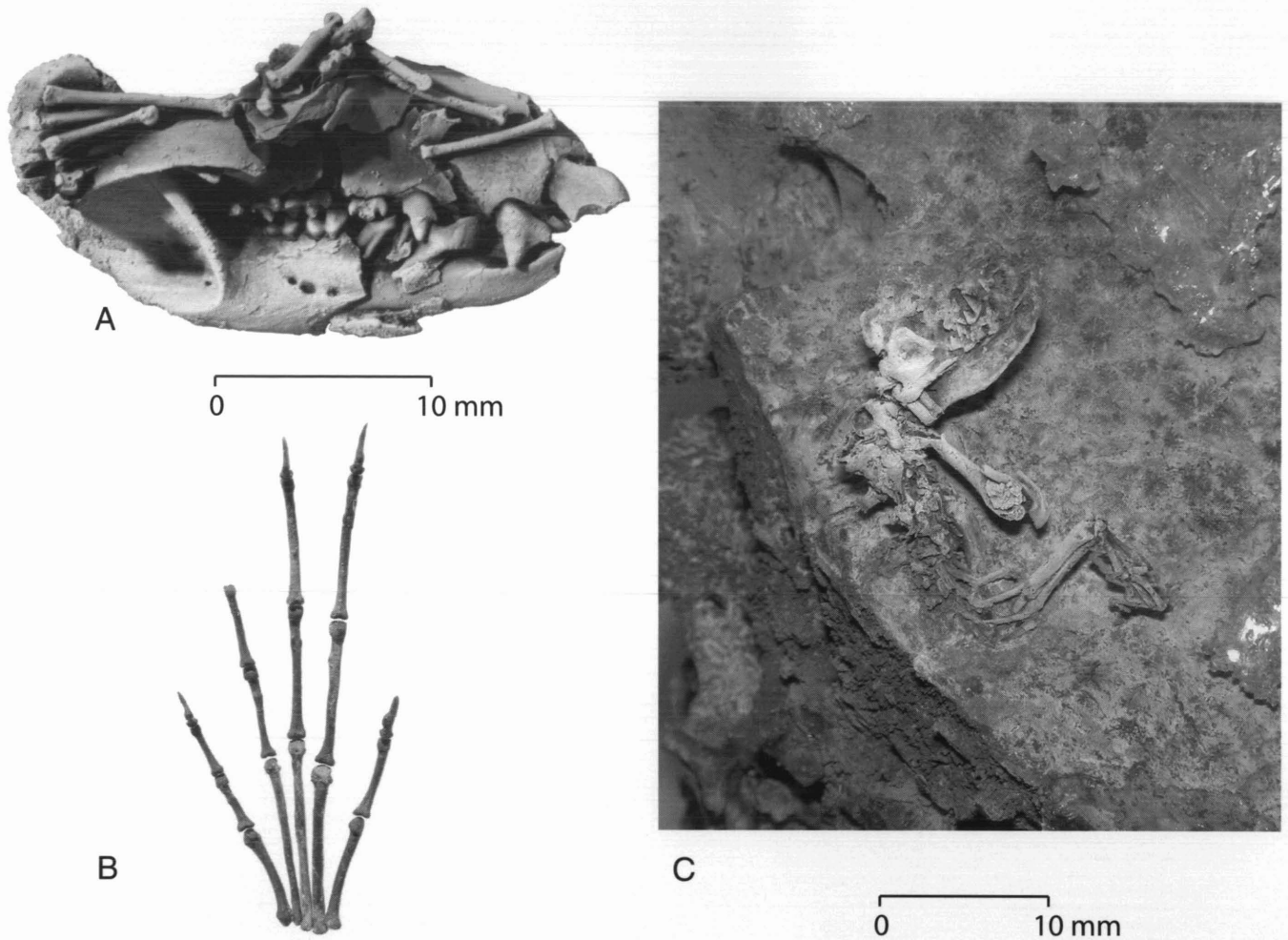


FIGURE 5 — Partial skeletons of apatemyid *Labidolemur kayi* and nyctitheriid *Leptacodon rosei*. A, skull and jaws of *Labidolemur kayi* from the SC-327 limestone (Cf-3). Specimen was preserved with a semiarticulated hand pressed onto its right side. This includes metacarpals I-V, proximal phalanges I-V and distal phalanges I, II, III and V. Bones were kept in their original positions with respect to the skull, as depicted here, by applying small amounts of glue to adjacent surfaces of bone as limestone matrix was dissolved away. B, assembled hand of *Labidolemur kayi*. Preserving the hand in original orientation until dissolution of limestone allowed direct observation of articular relationships. C, articulated skeleton of nyctitheriid insectivore *Leptacodon rosei* from the SC-327 limestone (Cf-3). This is also being prepared by gluing bones in situ. Scales are in mm.

possible during the etching process reveals patterns in the distributions of skeletons that would otherwise be lost (Fig. 5).

Bone orientations and positions within blocks are documented in detail during preparation, using photographs and drawings. A digital camera is particularly useful for photographic documentation. Bones exposed when photos are taken are numbered and recorded in a database. As a new bone is exposed it is given a unique number and also included in a database. Photographs are overlain with tracing paper and each bone is labeled on the photograph. Newly exposed bones are drawn on the tracing paper in their correct positions and labeled with their numbers. After exhumation, bones are stored with their numbers so that they can be re-associated using photographs and sketches. Photographs are taken periodically,

when distributions of bones are particularly informative or become too difficult to illustrate accurately by hand. When dissolution is complete, photographs and sketches are compiled to produce maps of how the bones were distributed in the nodule (Fig. 6).

TAPHONOMIC CHARACTERIZATION AND FAUNAL COMPOSITION

Previous Work

Gingerich (1987) dissolved most of a limestone lens from a late Clarkforkian fossil locality (University of Michigan locality SC-29), and interpreted the gastropod fauna as suggestive of a humid microenvironment including decaying wood or

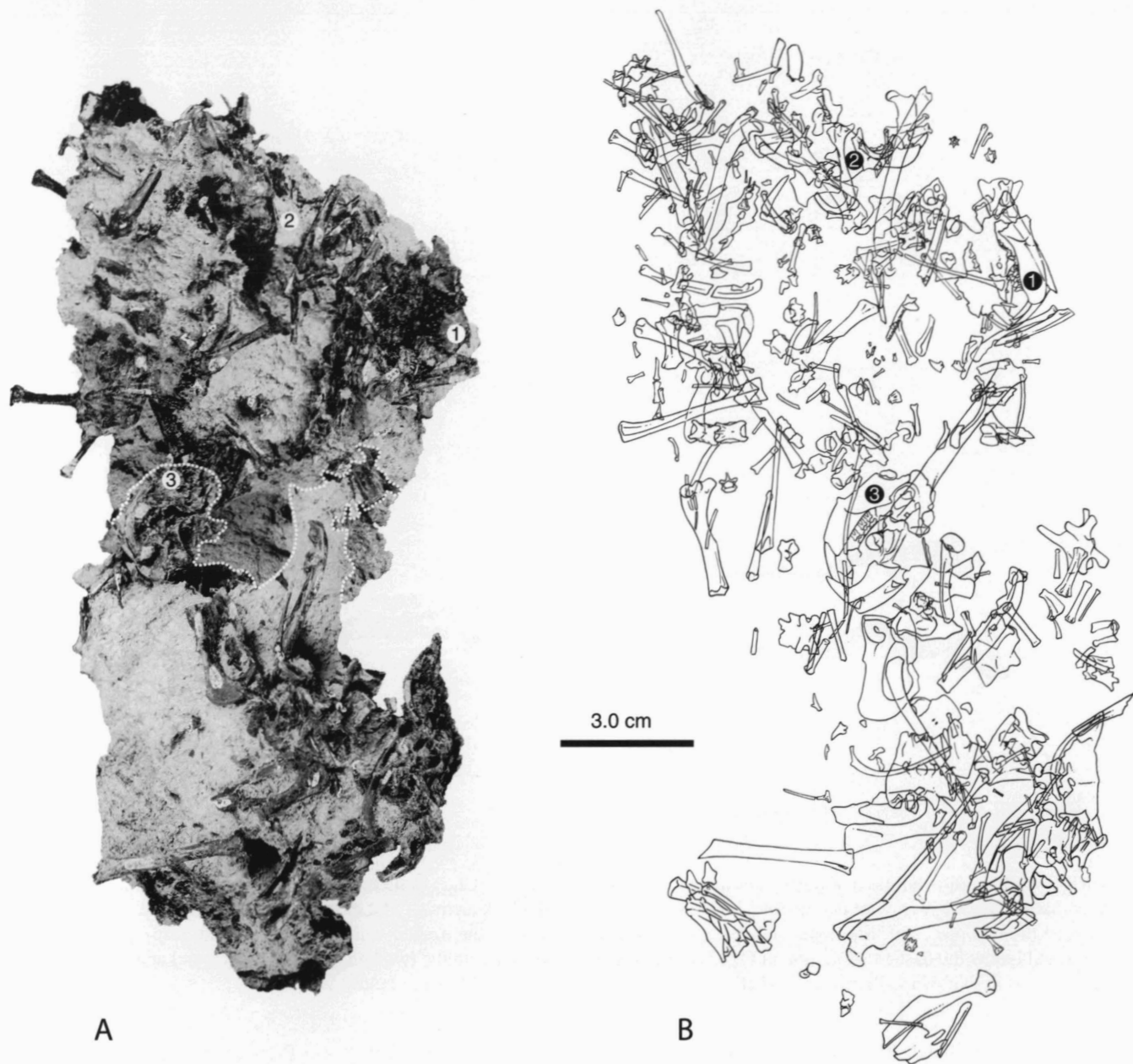


FIGURE 6 — Map showing distribution of all bones in a freshwater limestone block from SC-62 (Cf-2). A, composite photograph of block in what is interpreted as top view. Black objects are bone and white matrix is limestone. The block was prepared in two pieces (as collected in the field). The first piece (above the dashed white line) is shown here from what is interpreted as the top. The second piece (below the dashed white line) is shown from the bottom, inverted as if it were on top. B, interpretive drawing. Jaws of a new paromyid plesiadapiform (1), a carpolestid plesiadapiform (2), and a rodent (3) are labeled. Scale is in cm.

leaves. The amphibians and reptiles indicated proximity to leaf litter, and were consistent with a habitat favorable to the gastropods. Gingerich noted that some of the mammalian jaws showed signs of reflection without disassociation, suggesting predation or scavenging as an explanation. He also described punctures on some specimens that he interpreted as bite marks

(Gingerich, 1987: fig. 24). Broken eggshell, possibly avian in origin, was also preserved throughout the lens.

Houde (1988), and Houde and Olsen (1989, 1992) described the avifaunas from several Clarks Fork Basin limestones. Most differed considerably from the avifauna of stratigraphically contiguous mudstones. Houde noted that birds preserved in

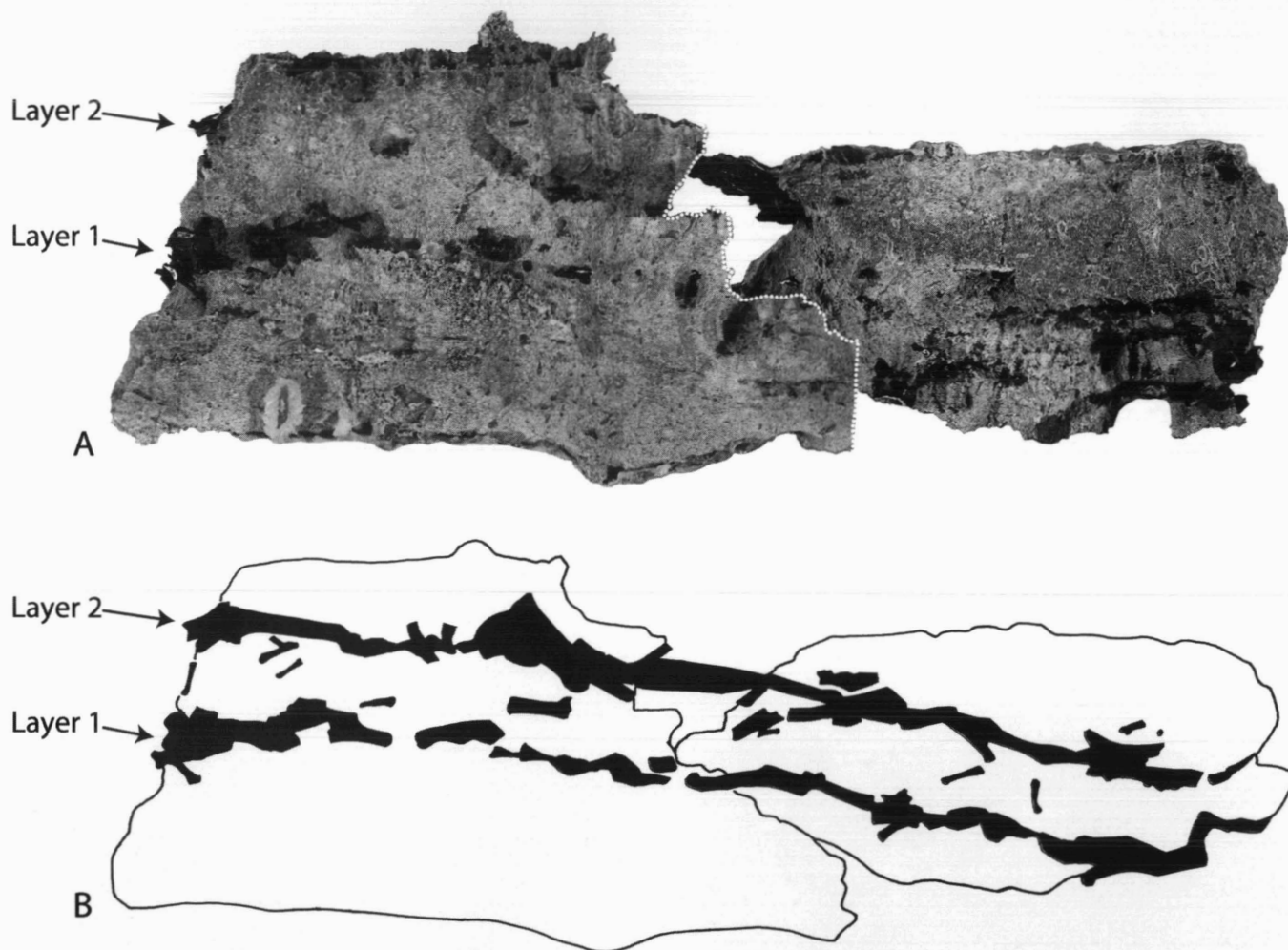


FIGURE 7 — Bone distribution in a freshwater limestone block from SC-62 (Cf-2; same block as in Fig. 6), here shown in side view. A, composite photograph with two distinct bone layers indicated by black arrows. The dashed white line indicates the separation between the two pieces of limestone. The pieces to the left and right of the dashed white line correspond, respectively, to those above and below the dashed white line in Figure 6. B, composite sketch with the two bone layers in black and again identified by arrows. It is not known with certainty whether layer 1 here was originally above or below layer 2.

the limestone assemblage (lithornithids) were not predators; thus, the co-occurrence of small vertebrates with eggshell accumulations might indicate transportation and concentration. He concluded that eggshell within a single limestone represented the contents of a single lithornithid bird nest that had been transported a short distance.

This Study

We prepared a block of exceptionally fossiliferous limestone from the middle zone of the Clarkforkian land-mammal age (Cf-2, locality SC-62; Figs. 1 and 2) using the above methods. Fossils occurred at two distinct layers in the limestone block (Fig. 7). Although skeletons are mostly disarticulated as a result of bioturbation, many original associations and orienta-

tions are preserved (Fig. 8). Parts of several of the skeletons were semi-articulated and associated with crania. A total of 414 identifiable mammal bones were prepared from the two layers in the Cf-2 limestone block. Badgley (1995) summarized skeletal-element frequencies in a Fort Union channel sandstone (Alexander, 1982) and a Willwood paleosol (Bown and Kraus, 1981), and compared them to values for a generalized whole mammal. Skeletal-element frequencies from the block are compared to those found in a generalized mammal, a channel-sandstone locality, and a paleosol locality in Table 1. In general, skeletal-element frequencies in the limestone are close to those expected for an average mammal: frequencies in limestones are much closer to expectation than are skeletal assemblages from traditionally sampled mudstone and sandstone deposits.



FIGURE 8 — Maps separating the distributions of bones in layers 1 and 2 of the freshwater limestone block from SC-62 (Cf-2; same block as in Figs. 6 and 7). A, bones in layer 1. Those thought to represent a single individual are coded by the same shading pattern. In the case of the paromomyid, two individuals (juveniles at different ontogenetic stages) are shaded the same. All of the paromomyid postcranials are thought to be associated with the individual represented by the skull and jaws (number 1 of Fig. 6). B, bones in layer 2. Here again bones thought to represent the same individuals are shaded the same.

A second limestone, from the late Clarkforkian land-mammal age (Cf-3, locality SC-327; Figs. 1 and 2), differs from the Cf-2 block just described in that all of the exposed skeletons, representing 11 individuals, were articulated (ca. 80 to 100% complete; Fig. 5C). Thus, although skeletons were mostly disarticulated in the Cf-2 block, each individual probably entered the deposit as a complete skeleton with little or no subsequent transport. Disarticulation of some specimens after burial resulted from disturbance by plant roots and invertebrate burrows (Bowen and Bloch, 2001).

In this analysis we found that the vertebrate fauna in Clarkforkian limestones is composed predominantly of mammals and lizards (96% of total specimens), with amphibians and birds rarely preserved. Aquatic vertebrates such as crocodiles, turtles, and fish are absent (Table 2). This composition contrasts starkly with paleosols, whose fauna is composed of up to 10% fish, and with sandstones, whose fauna is composed

of up to 24% crocodiles. Both paleosols and sandstones preserve turtles and rarely preserve amphibians and birds.

In Table 3 we summarize the mammalian faunal composition from limestone and mudstone samples of Clarkforkian localities in the Willwood Formation of the Clarks Fork Basin. As noted by previous authors (Rose 1981, Bloch and Bowen, 2001), paleosols are dominated by condylarths (53%). In contrast, limestones are dominated by lipotyphlan insectivores (45%), with condylarths making up only a very minor component of the fauna (1%). Another notable difference is that while marsupials make up less than 1% of the mammalian component in paleosols, they represent up to 14% of individuals in limestones. Both limestones and mudstones contain a high percentage of plesiadapiformes (20-21%), but different genera are preserved in the two lithologies (e.g., in Cf-2 limestones most specimens are *Carpolestes*, while in mudstones most are *Plesiadapis*; Bloch and Bowen, 2001: table 1, p.106).

TABLE 1 — Skeletal-element proportions (in percent) for mammalian fossil assemblages from different depositional environments, compared to values for the average whole mammal (table modified from Badgley et al., 1995). Abbreviations in order of appearance: *MDX*, mandible + maxilla; *T*, isolated teeth; *SK*, skull; *S/P*, scapula or pelvis; *LB*, limb; *MP*, metapodial, or metapodial + podial; *POD*, podial; *PH*, phalanx; *VT*, vertebra; *RIB*, ribs and other elements; *n*, number of specimens. Significance: +, observed double or more expectation; -, observed half or less expectation; ±, observed more or less equal to expectation.

	Skeletal part(s)									
	MDX	T	SK	S/P	LB	MP	POD	PH	VT	RIB
Average whole mammal (<i>n</i> = 210: Badgley et al., 1995)	2	17	0.5	2	6	6	12	19	21	14.5
Willwood limestone (<i>n</i> = 414: UM locality SC-62; this study)	3	1.5	2	3	14	11	14	27	19	6
<i>Significance</i>	±	-	+	±	+	±	±	±	±	-
Fort Union channel sandstone (<i>n</i> = 516: quarried and screen-washed; Alexander, 1982)	5	82	0.2	0	3	2		5	3	1
<i>Significance</i>	+	+	-	-	-	-		-	-	-
Willwood paleosol (<i>n</i> = 13,248: nine mudstones in 46 localities; Bown and Kraus, 1981)	22	66	0.1	0.3	4	3		3	2	0.1
<i>Significance</i>	+	+	-	-	±	-		-	-	±

As illustrated in Figure 9A, the surface-collected paleosol sample from the Clarkforkian is biased against collection of the small-mammal component of the fauna, with most specimens representing species 3-22 kg in body mass. In contrast, most specimens in the limestones represent small taxa (species 7-55 g in body mass). Thus, the limestones yield a proportionally larger sample of small mammals than the mudstones (Bloch and Bowen, 2001). While the number of small mammal specimens is much higher in the limestones than the mudstones, the number of small mammal genera represented is not notably different (Fig. 9B; Bloch and Bowen, 2001).

PROCESSES OF ACCUMULATION

Bowen and Bloch (2001) suggested that morphological and petrographical features of the limestones are most similar to those of ponded-water carbonate crusts and palustrine deposits. This implies that micrite precipitated from ponded water (in a low-energy environment) in microtopographic soil-surface depressions. These depressions were probably episodically flooded, and the ponded-water was ephemeral, as no characteristically aquatic fossils are preserved in the limestones. The carbonate content of the limestones ranges from 80 to 95% (wt % CaCO₃), with a very low siliciclastic

component (Bowen and Bloch, 2001). Occasional preservation of complete bird eggs, together with the observation that most of the bone in the faunal assemblages lacks signs of weathering or transport, indicates fairly rapid burial with a high rate of sediment accumulation.

One of the interesting taphonomic biases of the limestone assemblages is that many of the mammals represent juveniles with replacement of teeth in progress (e.g., Bloch et al., 1998; Bloch et al., 2001). In their description of the smallest known mammal, *Batodonoides vanhouteni*, from an Eocene limestone, Bloch et al. (1998) suggested that the type specimen probably represented a juvenile at about the age of dispersal from the nest. The process of becoming independent and dispersing to new foraging and nesting sites represents a time of high mortality in extant juvenile insectivores (Churchfield, 1990). It is possible that the microtopographic lows in which the limestones accumulated acted as natural 'pit-traps,' catching juvenile mammals as they left the nest. This would also be a natural age for a high rate of predation. Further evidence for predators contributing to concentration of bone in the assemblage includes missing ends to long bones and bite marks (Fig. 10). It is likely that predation or scavenging, pit-trapping, and normal attritional processes all contributed to concentration of bone in the limestone assemblage.

TABLE 2 — Faunal proportions (in percent) of vertebrates in different depositional environments (table modified from Badgley et al., 1995: table 5a, p. 172). Numbers in bold represent the vertebrate groups that are the most abundant in the specified facies.

	Vertebrate group						
	Mammal	Crocodile	Turtle	Fish	Lizard	Amphibian	Aves
Fort Union Formation channel deposit (<i>n</i> = 864: Alexander, 1982)	60	24	5	0	11	0.3	0
Willwood Formation paleosol (<i>n</i> = 249: SC-67; Gingerich, 1989)	81	3	2	10	3	0	0
Willwood Formation limestone (<i>n</i> = 65: SC-29; Gingerich, 1987)	82	0	0	0	14	3	2

TABLE 3 — Faunal composition (in percent) of mammalian orders from a sample of Clarkforkian localities in the Willwood Formation of the Clarks Fork Basin. The limestone and mudstone faunas were compiled from the same localities. Data from University of Michigan Museum of Paleontology vertebrate collections (J. I. Bloch; P. D. Gingerich; unpublished data), and from Bloch and Bowen (2001). Numbers in bold represent the mammal groups that are the most abundant in the specified facies.

Mammalian Order	Limestone (<i>n</i> = 370)	Mudstone (<i>n</i> = 446)
Carnivora	2	6
Chiroptera (?)	0.8	0
Condylarthra	1	53
Creodonta	0.3	2
Dermoptera (?)	1	2
Dinocerata	0	2
Lipotyphla	45	1
Marsupialia	14	0.7
Multituberculata	7	0.7
Notoungulata	1	0.5
Palaeonodonta	0	0.2
Pantodonta	0	5
Proprimates (Plesiadapiformes)	20	21
Proteutheria	1	0.7
Rodentia	7	2
Tillodontia	0	3

A diversity of mammals, many new, has been documented from the limestones (Fig. 4). Intensive sampling of small mammals, possibly from a rarely sampled habitat, is resulting in range extensions. These include the earliest occurrences of *Tinimomys* (Cf-1) and *Batodonoides* (Wa-4), and the latest occurrences of *Alagomys* (Wa-4), *Wyonycteris* (Wa-4), and *Plesiadapis gingerichi* (Cf-2). It is likely that further work on limestone faunal assemblages will contribute towards a more

refined understanding of biostratigraphy and biogeography of the North American late Paleocene and early Eocene.

CONCLUSIONS

Skeletal-element frequencies, and the fact that some limestones preserve articulated skeletons (Fig. 5), indicate that many of the mammal fossils in the freshwater limestones entered the

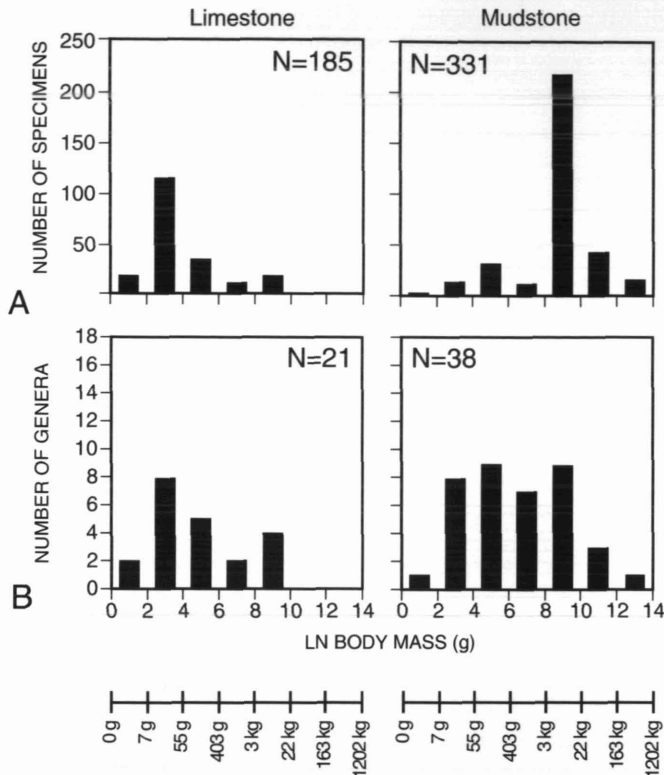


FIGURE 9 — Histograms representing body size distributions of mammalian specimens and genera from the Clarkforkian in both the limestones and mudstones. Limestones are plotted in the left column and mudstones in the right. The x-axis represents body size categories in log units. A, y-axis represents number of specimens. B, y-axis represents number of genera.

assemblage as complete skeletons. This was probably true to a lesser extent for individuals in which predation played a role. Limestones with skeletons that were subsequently partly or completely disarticulated (Fig. 6) may reflect differential rates of sediment accumulation and degrees of bioturbation between limestone assemblages. In cases of disarticulation it is still possible to document associations of postcrania-crania through careful mapping of bone elements (Fig. 8). Information regarding anatomical position is often retrieved using this methodology.

An abundance of individuals, representing a considerable diversity of mammals of similar age and body sizes, is preserved in the limestone assemblage. Without the type of documentation discussed here it is difficult to associate postcrania with crania confidently, leading to potentially inaccurate phylogenetic and morphologic interpretations (see Krause, 1991).

Our initial study, motivated by the need to develop a technique for more accurately documenting postcranial-cranial associations, produced several fairly complete skeletons of late



FIGURE 10 — Damaged proximal humerus of *Ignacius* n. sp. from a freshwater limestone from UM locality SC-62 (Cf-2). Arrows indicate bite marks possibly made by a small mammalian carnivore.

Paleocene mammals (Fig. 11). These include: (1) the most complete paromomyid plesiadapiform skeleton yet discovered; (2) the only known skeleton of a carpolestid plesiadapiform; (3) the only known skeleton of a nyctitheriid insectivore; and (4) the earliest known rodent skeleton known from North America. Further work on limestones using similar techniques promises to produce additional skeletons of poorly known Paleocene-Eocene mammals.

ACKNOWLEDGMENTS

We thank C. Badgley, D. Fisher, P. Gingerich, G. Gunnell, P. Houde, K. Rose, W. Sanders, and R. Secord for helpful discussions. We thank C. Badgley, P. Gingerich, J. Groenke, G. Gunnell, R. Secord, J. Trapani, and P. Wilf for improvements to the manuscript. W. Sanders assisted in all limestone preparation, and B. Miljour assisted in preparation of all figures. Field and laboratory research was supported by grants from the National Science Foundation to Philip D. Gingerich (most

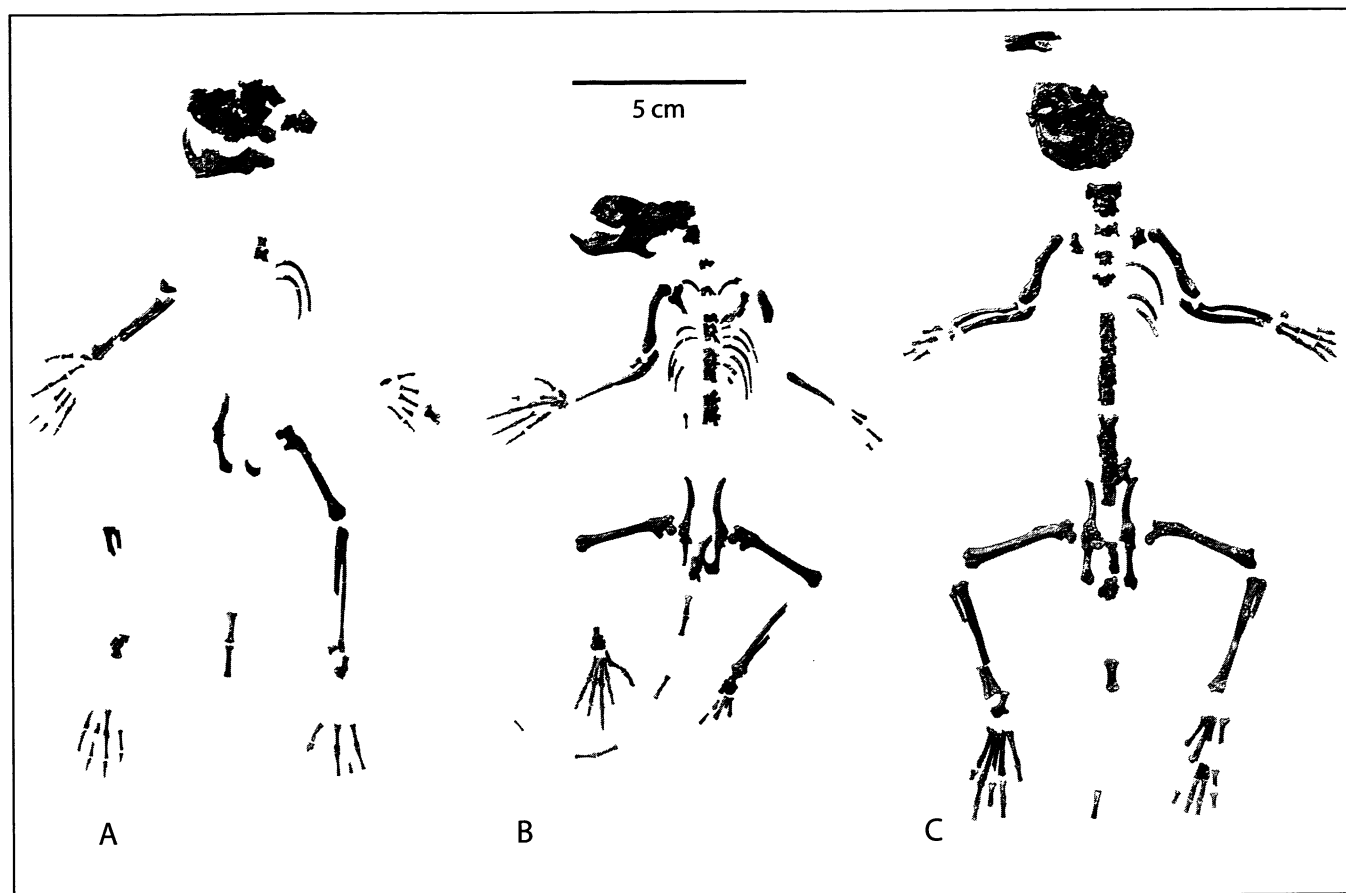


FIGURE 11 — Partial skeletons of mammals in freshwater limestone block from UM locality SC-62 (Cf-2). A, photo of juvenile paromomyid n. gen., n. sp. (Bloch et al., 2001). B, photo of adult *Carpolestes simpsoni*. C, photo of juvenile rodent (“Rodent 1” of Fig. 8A).

recently EAR-9105147), and from the Scott Turner Fund, Department of Geological Sciences, University of Michigan, to J. I. B.

LITERATURE CITED

- ALEXANDER, A. J. 1982. Sedimentology and taphonomy of a middle Clarkforkian (early Eocene) fossil vertebrate locality, Fort Union Formation, Bighorn Basin, Wyoming. M. S. dissertation, University of Michigan, Ann Arbor, 112 pp.
- BADGLEY, C., W. S. BARTELS, M. E. MORGAN, A. K. BEHRENSMEYER, and S. MRAZA. 1995. Taphonomy of vertebrate assemblages from the Paleogene of northwestern Wyoming and the Neogene of northern Pakistan. *Palaeogeography, Palaeoclimatology, Palaeoecology*, 115: 157-180.
- BARTELS, W. S. 1987. Fossil reptile assemblages and depositional environments of selected early Tertiary vertebrate bone concentration, Bighorn Basin, Wyoming. Unpublished Ph.D. thesis, University of Michigan, Ann Arbor, 617 pp.
- BEARD, K. C. and P. HOUDE. 1989. An unusual assemblage of diminutive plesiadapiformes (Mammalia, ?Primates) from the early Eocene of the Clarks Fork Basin, Wyoming. *Journal of Vertebrate Paleontology*, 9: 388-399.
- BLOCH, J. I. and G. J. BOWEN. 2001. Paleocene-Eocene microvertebrates in freshwater limestones of the Willwood Formation, Clarks Fork Basin, Wyoming. *In*: G. F. Gunnell (ed.), *Eocene Biodiversity: Unusual Occurrences and Rarely Sampled Habitats*. Plenum Press, New York, 95-129.
- BLOCH, J. I., D. M. BOYER, P. D. GINGERICH, and G. F. GUNNELL. 2001. New primitive paromomyid from the Clarkforkian of Wyoming and dental eruption in Plesiadapiformes. *Journal of Vertebrate Paleontology*, in press.
- BLOCH, J. I. and P. D. GINGERICH. 1998. *Carpolestes simpsoni*, new species (Mammalia, Proprimates) from the late Paleocene of the Clarks Fork Basin, Wyoming. *Contributions from the Museum of Paleontology, University of Michigan*, 30: 131-162.
- BLOCH, J. I., K. D. ROSE, and P. D. GINGERICH. 1998. New species of *Batodonoides* (Lipotyphla, Geolabididae) from the early Eocene of Wyoming: smallest known mammal? *Journal of Mammalogy*, 79: 804-827.
- BOWEN, G. J. and J. I. BLOCH. 2001. Petrography and geochemistry of freshwater limestones from the Bighorn Basin, Wyoming:

- constraining carbonate deposition and fossil accumulation on early Tertiary floodplain soils. *Journal of Sedimentary Research*, in press.
- BOWN, T. M. and K. C. BEARD. 1990. Systematic lateral variation in the distribution of fossil mammals in alluvial paleosols, lower Eocene Willwood Formation, Wyoming. *In*: T. M. Bown, and K. D. Rose (eds), *Dawn of the Age of Mammals in the northern part of the Rocky Mountain Interior*. Geological Society of America Special Paper, 243: 135-151.
- BOWN, T. M. and M. J. KRAUS. 1981. Vertebrate fossil-bearing paleosol units (Willwood Formation, lower Eocene, northwest Wyoming, U.S.A.): Implications for taphonomy, biostratigraphy, and assemblage analysis. *Palaeogeography, Palaeoclimatology, Palaeoecology*, 34: 31-56.
- BOWN, T. M. and M. J. KRAUS. 1987. Integration of channel and floodplain suites, 1. Developmental sequence and lateral relations of alluvial paleosols. *Journal of Sedimentary Petrology*, 57: 587-601.
- CHURCHFIELD, S. 1990. *The natural history of shrews*. Comstock Publishing Associates, Ithaca, 178 pp.
- GINGERICH, P. D. 1987. Early Eocene bats (Mammalia, Chiroptera) and other vertebrates in freshwater limestones of the Willwood Formation, Clarks Fork Basin, Wyoming. *Contributions from the Museum of Paleontology, University of Michigan*, 27: 275-320.
- GINGERICH, P. D. 1989. New earliest Wasatchian mammalian fauna from the Eocene of northwestern Wyoming: Composition and diversity in a rarely sampled high-floodplain assemblage. *University of Michigan Papers on Paleontology*, 28: 1-97.
- HOUDE, P. 1986. Ostrich ancestors found in the northern hemisphere suggest new hypothesis of ratite origins. *Nature*, 324: 563-565.
- HOUDE, P. 1987. Histological evidence for the systematic position of *Hesperornis* (Odontornithes: Hesperornithiformes). *Auk*, 104: 125-129.
- HOUDE, P. 1988. Paleognathous birds from the early Tertiary of the northern hemisphere. *Nuttall Ornithological Club, Cambridge, Massachusetts*, 22: 1-148.
- HOUDE, P. and S. L. OLSEN. 1989. Small arboreal nonpasserine birds from the early Tertiary of western North America. *In*: H. Ouellet (ed.), *Acta XIX Congressus Internationalis Ornithologici*. University of Ottawa Press, Ottawa, pp. 2030-2036.
- HOUDE, P. and S. L. OLSON. 1992. A radiation of coly-like birds from the Eocene of North America (Aves; Sandcoleiformes new order). *Natural History Museum of Los Angeles County, Science Series*, 36: 137-160.
- KRAUS, M. J. 1987. Integration of channel and floodplain suites. II. Vertical relations of alluvial paleosols. *Journal of Sedimentary Petrology*, 57: 602-612.
- KRAUS, M. J. 1988. Nodular remains of early Tertiary Forests, Bighorn Basin, Wyoming. *Journal of Sedimentary Petrology*, 58: 888-893.
- KRAUSE, D. W. 1991. Were paromomyids gliders? Maybe, maybe not. *Journal of Human Evolution*, 21: 177-188.
- ROSE, K. D. 1981. The Clarkforkian land-mammal age and faunal composition across the Paleocene-Eocene boundary. *University of Michigan Papers on Paleontology*, 26: 1-196.
- ROSE, K. D. and P. D. GINGERICH. 1987. A new insectivore from the Clarkforkian (earliest Eocene) of Wyoming. *Journal of Mammalogy*, 68: 17-27.
- RUTZKY, I. S., W. B. ELVERS, J. G. MAISEY, and A. W. A. KELLNER. 1994. Chemical preparation techniques. *In*: P. Leiggi and P. May (eds.), *Vertebrate paleontological techniques, Volume 1*. Cambridge University Press, Cambridge, pp. 155-186.
- THEWISSEN, J. G. M. and P. D. GINGERICH, P. D. 1989. Skull and endocranial cast of *Eoryctes melanus*, a new palaeoryctid (Mammalia: Insectivora) from the early Eocene of western North America. *Journal of Vertebrate Paleontology*, 9: 459-470.
- WING, S.L., H. BAO, and P.L. KOCH. 1999. An early Eocene cool period? Evidence for continental cooling during the warmest part of the Cenozoic. *In*: B. T. Hubert, K. MacCleod, and S. L. Wing (eds.), *Warm Climates in Earth History*. Cambridge University Press, Cambridge, pp. 197-237.
- WINKLER, D. A. 1983. Paleocology of an early Eocene mammalian fauna from the paleosols in the Clarks Fork Basin, northwestern Wyoming. *Palaeogeography, Palaeoclimatology, Palaeoecology*, 43: 261-298.

